CIVIL ENGINEERING STUDY
STRUCTURAL SERIES 88-6-1

SAFETY-BASED OPTIMUM DESIGN OF NONDETERMINISTIC STRUCTURES SUBJECTED TO VARIOUS TYPES OF SEISMIC LOADS

by Franklin Y. Cheng
Curators' Professor

Chein-Chi Chang
Graduate Assistant

Department of Civil Engineering
University of Missouri-Rolla
Rolla, MO 65401-0249
1988

Report Series
Prepared for the National Science Foundation
Under Grant No. NSF CEE 8403875

GENERAL DISCLAIMER

This document may have problems that one or more of the following disclaimer statements refer to:

- This document has been reproduced from the best copy furnished by the sponsoring agency. It is being released in the interest of making available as much information as possible.
- This document may contain data which exceeds the sheet parameters. It was furnished in this condition by the sponsoring agency and is the best copy available.
- This document may contain tone-on-tone or color graphs, charts and/or pictures which have been reproduced in black and white.
- The document is paginated as submitted by the original source.
- Portions of this document are not fully legible due to the historical nature of some of the material. However, it is the best reproduction available from the original submission.

CIVIL ENGINEERING STUDY
STRUCTURAL SERIES 88-6-1

SAFETY-BASED OPTIMUM DESIGN OF NONDETERMINISTIC STRUCTURES SUBJECTED TO VARIOUS TYPES OF SEISMIC LOADS

by
Franklin Y. Cheng
Curators' Professor

Chein-Chi Chang
Graduate Assistant

Department of Civil Engineering
University of Missouri-Rolla
Rolla, MO 65401
1988

Report Series
Prepared for the National Science Foundation Under Grant No.
NSF CEE 8403875

ABSTRACT

Reliability-based optimization techniques are developed for steel structures subjected to various seismic loadings of static equivalent load, dynamic response spectra, and stationary process with seismic spectra. The static equivalent load is based on Uniform Building Code; the dynamic response spectra are based on Newmark's nondeterministic response approach which uses a statistical technique to estimate the response amplification factors; and the seismic spectra of stationary process are related to white noise, filter white noise, or modified white noise. The optimization techniques are derived from the optimality criterion method and the penalty function method, which have proven to be efficient for nondeterministic structural design. Reliability is based on two mathematical models of normal and lognormal distribution with two different variance approaches.

The structural formulation is derived on the basis of the matrix displacement method and the lumped mass model. The objective function can be either minimum weight or minimum total cost. The cost function includes initial construction costs of structural and nonstructural elements and expected costs of failure at various safety levels. The constraints include the reliability considerations for displacement and internal forces of individual members as well as a system.

Several numerical examples are provided to illustrate the application and parameter study of reliability-based optimum design for various types of seismic loadings. Observations of numerical studies demonstrate: 1) for dead and live load case, the model of Great Britain requires heavier design than the models of the U.S.; 2) the optimum design is very sensitive to high variation of UBC seismic load and the peak ground acceleration, especially with lognormal distribution; 3) at high reliability criteria, the lognormal distribution requires a heavier design than normal distribution; 4) the second variance approach demands a heavier design than the first variance approach; 5) the effect of vertical ground acceleration can noticeably affect the optimum solutions; 6) the optimum design results of modified white noise spectrum are close to those of the filter white noise spectrum; 7) the optimum design for first passage equation is conservative among the various failure probability expressions; 8) for different ratios of initial

cost to member cost, the design yields similar member cross sections but different final costs; 9) the optimum cost is not sensitive to the ratio of expected failure cost to initial cost at high reliability; and 10) at high reliability level, the difference between maximum and minimum bound of system failure probability is very small.

ACKNOWLEDGMENTS

This is one of a series of reports on optimum design of structural systems with parametric multicomponent seismic excitations and code provisions sponsored by the National Science Foundation under the grant no. CEE 8403875. Supports for this study are gratefully acknowledged. The authors also wish to thank the Civil Engineering Department for providing facilities and substantial amount of computer time for this work.

TABLE OF CONTENTS

LIST OF ILLUSTRATIONS

LIST OF TABLES

LIST OF SYMBOLS

A = area

A_I = influence area

$\{a\}$ = ground acceleration matrix

$[A]_m^T$ = transpose of a member static matrix

$[C]$ = damping matrix

C_D = an influence coefficient which tranforms dead load intensity D into the desired load effect (displacement or internal force)

C_L = an influence coefficient which tranforms live load intensity L into the desired load effect (displacement or internal force)

C_E = an influence coefficient which tranforms earthquake load intensity E into the desired load effect (displacement or internal force)

C_I = initial construction cost

C_p = a percentage constant of C_S

C_T = total structural cost

C_S = influence coefficient of structural response

D = dead load intensity

E = earthquake load intensity which may be the shear force at the structural base in Uniform Building Code

E_m = elastic modulus

EUDL = the uniform distributed load

f_1 = yielding failure in column failure

f_2 = bending instability in column failure

f_3 = lateral torsional buckling in column failure

f_4 = buckling about weak axis in column failure

$F_{E_{ux}}$ = lateral force applied to level x due to a unit seismic load intensity

F_{E_x} = lateral force applied to level x

$\{F\}_m$ = the internal forces in a member

F_{tu} = the concentrated force at the top due to a unit seismic load intensity

F_y = yield strength of material

G_0 = the constant spectral density value

g_j = jth constraint

$G_a(\omega)$ = excitation spectrum

G_s = shear modulus

$G_s(\omega)$ = response spectrum

$G(\omega)$ = the spectral density function

$H(\omega)$ = the transfer function of a structural system

I = moment of inertia

$[K]$ = stiffness matrix

$[K]^{-1}$ = inversion of stiffness matrix

$[K]_G$ = geometric stiffness matrix

KL = effective length

$[K]_S$ = linear elastic stiffness matrix

L = live load intensity

L_f = expected failure cost

$[m]$ = mass matrix

$\overline{M}$ = mean of applied moment

σ^2_M = variance of applied moment

V_M = coefficient of variation of applied moment

M_{cr} = critical moment

$\overline{M}_{cr}$ = mean critical moment

$\sigma^2_{M_{cr}}$ = variance of critical moment

$V_{M_{cr}}$ = coefficient of variation of critical moment

M_y = yield moment

$\overline{M}_y$ = mean yield moment

$\sigma^2_{M_y}$ = variance of yield moment

V_{M_y} = coefficient of variation of yield moment

$O(\ )$ = objective function

$P(\ )$ = penalty function

P_{cr} = axial load capacity of columns

$\overline{P}_{cr}$ = mean critical load

$\sigma^2_{P_{cr}}$ = variance of critical load

$V_{P_{cr}}$ = coefficient of variation of critical load

$P_d(R)$ = probability density of structural resistance

$P_d(S)$ = probability density of structural response

P_E = Euler buckling load

$\overline{P}_E$ = mean Euler buckling load

$\sigma^2_{P_E}$ = variance of Euler buckling load

V_{P_E} = coefficient of variation of Euler buckling load

P_f = probability of failure

P_{fT} = system probability of failure

$PN(\ )$ = the standard cumulative normal function

P_r = reliability

P_y = yield load

$\overline{P}_y$ = mean yield load

$\sigma^2_{P_y}$ = variance of yield load

V_{P_y} = coefficient of variation of yield load

Q = the function in terms of R and S

$\overline{Q}, \sigma_Q$ = the mean and standard deviation of Q

q' = the load intensity

r = random parameters

R = structural resistance

$\overline{R}$ = mean structural resistance

σ_R = standard deviation of structural resistance

V_R = coefficient of variation of structural resistance

r_g = the radius of gyration

r_p^k = a penalty value

S = structural response

S_c = elastic section modulus

S_D = dead load effect

S_E = earthquake load effect

S_L = live load effect

$[S]_m$ = a member stiffness matrix

$\bar{s}_{max}$ = the mean of peak response

$s(t)$ = a stationary process

T = structural fundamental peroid

T_i = recurrence equation

T_0 = a given time interval

u = structural displacement

$\dot{u}$ = structural velocity

$\ddot{u}$ = structural acceleration

u_D = displacement due to dead load intensity

u_E = displacement due to earthquake load intensity

u_L = displacement due to live load intensity

$\{u\}_m$ = the corresponding external displacements in a member

V_D = coefficient of variation of dead load intensity

V_E = coefficient of variation of earthquake load intensity

V_L = coefficient of variation of live load intensity

W = weight

x^k = design variables

x^* = the optimal solution

Y_n = generalized coordinate

y_{ω_n} = spectral displacement

α = a relaxation constant

β = safety factor

ρ = correlation coefficient

σ_{smax} = standard deviation of peak response

Λ = scaling factor

λ_j = jth Lagrangian multiplier

λ_{sk} = moments of response

ζ_g = filter damping ratio

ζ_n = critical damping ratio coefficient for nth mode

Γ_n = participation factor for nth mode

ω_g = filter fundamental frequency

ω_n = structural natural frequency for nth mode

$\{\Phi\}_n$ = nth mode shape matrix

ν_a^+ = an expected frequency of crossing the given level

I. INTRODUCTION

A. LITERATURE REVIEW

Because of recent advances in electronics, engineers and scientists are on the threshold of a new era in structural analysis and design. Most of their research efforts are based on the development of sophisticated computer programs for the analysis of complex structures. [67, 68] Currently, when these programs are used to design structures, the relative stiffnesses of a structure's constituent members must be assumed. If the preliminary stiffnesses are misjudged, repeated analyses, regardless of a program's sophistication, will usually not yield an improved design. The programs that are presently used are actually based on conventional designs, and their application in reality is an art rather than a science.

The optimum design concept has been recognized as being more rational and reliable than those that require the conventional trial and error process. [71,92] It is because for a given set of constraints, such as allowable stresses, displacements, drifts, frequencies, upper and lower bounds of member sizes, and given seismic loads, such as equivalent forces in the code provisions, spectra, or time-histories, the stiffnesses of members are automatically selected through the mathematical logic (structural synthesis) written in the computer program. Consequently, the strengths of the constitutent members are uniformly distributed, and the rigidity of every component can uniquely satisfy the demands of the external loads and the code requirements, such as displacements and drifts. By using an optimum design computer program, one can conduct a project schedule at a high speed and thus increase the benefit because of the time that is saved. [61] An optimum design program can also be used for parametric studies to identify which structural system is more economical and serviceable than the other and assess the principles of various building code provisions as to whether they are as logical as they are intended to be. [24,33]

In the structural optimization field, all the optimization techniques and the computer programs are generally developed on the premise that the design variables, resistances, responses, and loadings are deterministic. [21,47,48,89,90,91] The reasons for the lack of research

advancement with regard to structural optimization of nondeterministic systems may be that 1) the modern structural optimization algorithms rely on the various techniques of sensitivity analysis [6,27,87] (rate of change of response quantities with respect to design variables), which can become a pyramidical task in nondeterministic cases, and 2) it is too difficult to establish the objective function involving risk analysis of expected damage costs suitable for an individual structural design at a particular site. [49,51,78]

In recognition of the random nature of seismic structural problems and the advances that have been made in reliability analyses of structures, the research project was subsequently developed for optimum design of nondeterministic structures subjected to seismic excitations. The study has taken into consideration the safety levels of a system with respect to its various failure modes, uncertainties in the dead and live loads as well as seismic forces, and random parameters in responses and resistances. The cost function includes initial construction costs of structural and nonstructural elements and expected costs of failure at various safety levels. The structural members are designed on the basis of the global optimum decision, namely, when an increase of the initial cost is balanced by a reduction in the expected cost of failure times the risk.

1. Optimum Structural Design in General. In the past decade, a considerable amount of literature has been published on the subject of optimum structural design. The increasing number of publications corresponds closely to the rapid demand for economical and reliable structural designs in virtually all fields of endeavor. Optimum designs have been extensively used in aircraft structural engineering, [91,92] and more recently they have been widely applied in the automobile industry. [12,17]

Various optimization techniques of linear, nonlinear, and dynamic programming have been developed for different types of static and dynamic structures. [13,14,20–22,47,48,57,61] In general, most of the techniques have some limitations and are best suited for certain classes of problems. The technique based on energy distribution as the optimality criterion has been proven to be effective for large structural systems in aerospace engineering. [71,91,92] Venkayya and Cheng [90] extended the optimization algorithm for civil engineering structures subject to

general dynamic loads. The method, however, is approximate for the multiple constraint case. Further studies by Venkayya, Khot, Fleury, Cheng, and others have led to some modern optimizations, which are efficient for large structural systems and multiple constraints. Cheng and associates have further extended the modern optimization algorithms to direct optimality criteria for steel and reinforced concrete building systems. [27,31]

The development of the optimality criteria method may be considered to be a great contribution in the field of engineering optimization in that it offers a major improvement over any other optimizations currently in vogue. The significant advantage of the method is that the number of iterations required to converge on an optimum (or pseudo-optimum) design is largely independent of the number of variables in the problem. The optimality mehtod has been traditionally used for deterministic structures, which is now further developed for nondeterministic structures in this research.

2. Optimum Design in Earthquake Structural Engineering. Previous studies of optimum seismic structural design were mostly based on the linearization technique and static equivalent seismic forces for simple structures and shear buildings. [57,61,84] Cheng and Botkin [20,22] studied the feasible direction technique for the design of tall buildings and large frameworks. This included the geometric nonlinearity of the P - Δ effect. The technique was also studied by Ray et al. [73,74] and Walker and Pister [93] for optimal elastic design. Cheng and his associates later studied the energy distribution criteria and the direct optimality criteria for various seismic structural designs. [23,25,26,29,33] The above briefly cited references among others mainly deal with feasible seismic structural design of sizing the constituent members for which the feasible domain is an expression of the standards of code requirements; however, another distinct branch in seismic resistant design is associated with the policy decisions of minimizing the total cost with a design, that is maximization of the total benefit minus the total cost; the merit function includes the building cost and the expected damage. [16,62,63,78,79,80] This is emphasized on decision models but not for the complete design of structural systems with code requirements.

The computer-aided interactive design has also been introduced in earthquake structural design. The algorithm falls in with the mathematical programming of feasible direction. Sample

problems deal with minimum weight, minimum cost, and minimum or maximum response (for energy-absorbing device at supports) for deterministic systems. [8–11,69]

It may be concluded that a great deal of research interest has been developed in connection with optimization models for making policy decisions and structural optimizations for deterministic systems. The structural optimization of nondeterministic structures subjected to seismic excitations is still in infant stage and has recently been studied by Cheng and Chang, [28,30,32] and others. [42,58] The reliability-based structural design may be found in Reference 41 for dynamic loads and Reference 72 for random loads.

3. Reliability Analysis of Earthquake Structures. Ever since Cornell published his classic paper on seismic risk analysis, [36] a great deal of work has been done on a variety of analytical models. [82] Major efforts have been put forth to develop models for determining seismic hazards (probability of seismic intensity), vulnerability (probability of damage for a specified level of seismic intensity), and seismic risk (probability of loss). For instance, the seismic hazard studies have been based on various models, such as point source, line and / or area source, and fault-rupture length. [59]

Evaluating the safety of a seismic structure in the past consisted of analyzing the system to find the probable failure level (risk level) of its individual members of which the sizes are given. Reliability models have been studied by Ang and others. [2–4, 35, 70] Other notable works with strong socioeconomic implications for seismic engineering systems have been written by Whitman et al., [94] Blume and Monroe, [15] Liu and Neghabat, [62] and Shinozuka and Tan. [83] These works are related to life-line problems. The seismic structural design, which is based on a given set of risk levels and provides optimum components, has yet to be explored.

B. OBJECTIVE AND SCOPE

1. Seismic Loadings - UBC, NNSRS, Stationary Process. In order to achieve a broader observation of parameter studies through the structural optimization, three types of practical and commonly used loading models are employed in this study. The first type is the UBC codified seismic load. The second is the Newmark's nondeterministic seismic response spectrum (NNSRS) including the statistical response results of actual horizontal or vertical earthquake records. The third is a Gaussian random process with a constant or varied seismic spectrum which has been commonly used to represent the seismic random load in civil engineering community.

2. Parameter Study in Reliability-Based Optimum Design Subjected to Various Seismic Loads. The parameter study for UBC is to investigate the sensitivity of some parameters and to compare the formulations in reliability-based optimum models. The parameters studied are the coefficient of variation of column resistance parameters and coefficient of variation for UBC. The formulations compared are the probability distributions of response and resistance, the variance approaches, and the zone coefficients in UBC. The parameters and formulations are also studied for NNSRS such as variations of column resistance, peak ground acceleration, and different variance approaches. For the stationary seismic loads, the formulations for various stationary seismic spectra and failure probability expressions are compared in the optimal solutions. Further parameter studies are due to the difficulty to assess the nonstructural and expected failure cost, some coefficients to represent different magnitudes of these costs are studied to show their influences on the optimum design results. In the past, four live load models of ANSI (American National Standard Institute), NBS (National Bureau of Standards), UK (United Kingdom), and UNREDUCED (actual) models were proposed. However, no comparison has been performed to show if there is any difference among these models. In this study the comparison of four live load models is investigated.

C. CONTENTS OF THE STUDY

This report consists of tweleve chapters. Chapter 1 includes the literature review and the objective of the study. Chapter 2 presents the reliability concepts. Chapters 3, 4, and 5 include structural analysis with reliability consideration respectively associated with static and static equivalent load, nondeterministic response spectrum, and stationary seismic process. The problem formulations and optimization algorithms for the design are presented in Chapter 6. Comparisons of ANSI, NBS, UK, and UNREDUCED live load models are given in Chapter 7. The application of optimality criterion method and comparison results with penalty function method are included in Chapter 8. Chapters 9, 10, and 11 contain studies of the sensitivities and comparisons of some parameters for UBC, NNSRS, and stationary seismic process. Chapter 12 is the conclusion including observations of the numerical studies.

II. RELIABILITY CONCEPTS

A. RELIABILITY AND PROBABILITY OF FAILURE

Reliability is a measure of the probability of structural survival during a structure's lifetime. Thus reliability is a probabilistic measure of the safety for the structure concerned. The probability of failure, which is the opposite of reliability, can also be adopted to represent the safety problem in an alternative way. In a classical formulation, reliability and probability of failure are defined as

$$P_r(R \geq S) = \int_{-\infty}^{\infty} P_d(S)[\int_S^{\infty} P_d(R)\, dR]dS \tag{2.1}$$

$$P_f(R < S) = 1 - P_r(R \geq S) \tag{2.2}$$

where R, S = structural resistance and response; $P_d(S)$, $P_d(R)$ = probability density function of structural response and resistance, respectively. Hereafter the reliability and probability of failure will also be represented as P_r and P_f .

Since in practice, the complete knowledge of exact distributions of resistance and response is impossible to determine, two approximate expressions to the reliability or failure probability have been used in many studies. One is a first-order second-moment expression that estimates reliability and probability of failure through a safety factor formulation. The other is a first passage expression that estimates the probability of crossing the specified barrier during the vibration time interval.

B. A FIRST-ORDER SECOND-MOMENT EXPRESSION

1. Probability Distribution of Response and Resistance. In 1969, Cornell [37] proposed a simple approximation model called a first-order second-moment expression, which involves the evaluation of the mean and variance of the structural resistance and response, and represents either reliability or probability of failure. Along with this expression two probability distributions of structural resistance and response considered in this study are normal and lognormal distributions.

a. Normal Distribution. Since R and S are independent normally distributed variables, a linear function Q of R and S, where Q = R-S, is also normally distributed and thus, $(Q - \overline{Q}) / \sigma_Q$ is the standard normal variable with zero mean and unit variance. Let P_f be probability of failure and be given by

$$P_f = P_f(R - S \leq 0) = PN(\frac{0 - \overline{Q}}{\sigma_Q}) = PN(\frac{-\overline{Q}}{\sigma_Q}) = 1 - PN(\frac{\overline{Q}}{\sigma_Q}) \tag{2.3}$$

where PN( ) is the standard cumulative normal distribution function, $\overline{Q} = \overline{R} - \overline{S}$, $\sigma_Q = (\sigma_R^2 + \sigma_S^2)^{1/2}$, and $\overline{R}, \overline{S}, \sigma_R^2, \sigma_S^2$ = the mean and variance of structural resistance, R, and response, S, respectively.

If a safety factor (or safety index), β , is defined as the ratio $\overline{Q}/\sigma_Q$, then probability of failure,

$$P_f = 1 - PN(\beta) \tag{2.4}$$

reliability,

$$P_r = PN(\beta) \tag{2.5}$$

where

$$\beta = (\overline{R} - \overline{S}) / (\sigma_R^2 + \sigma_S^2)^{1/2} \tag{2.6}$$

b. Lognormal Distribution. If R and S are both lognormally distributed, the function Q = lnR-lnS is normally distributed. Thus analogous to the normal distribution case, the probability of failure and the reliability are given as follows.

Since

$$P_f = P_f(\ln R - \ln S \le 0) = PN(\frac{Q - \overline{Q}}{\sigma_Q}) = PN(\frac{-\overline{Q}}{\sigma_Q}) = 1 - PN(\frac{\overline{Q}}{\sigma_Q}) \tag{2.7}$$

then

$$P_f = 1 - PN(\frac{\overline{Q}}{\sigma_Q}) \tag{2.8}$$

and

$$P_r = PN(\frac{\overline{Q}}{\sigma_Q}) = PN(\frac{\overline{\ln R} - \overline{\ln S}}{(\sigma^2_{\ln R} + \sigma^2_{\ln S})^{1/2}}) \tag{2.9}$$

where the mean and variance of lnR and lnS are

$$\overline{\ln R} = \ln\overline{R} + (\frac{-1}{2}\sigma^2_{\ln R}), \quad \sigma^2_{\ln R} = \ln(V_R^2 + 1) \tag{2.10}$$

$$\overline{\ln S} = \ln\overline{S} + (\frac{-1}{2}\sigma^2_{\ln S}), \quad \sigma^2_{\ln S} = \ln(V_S^2 + 1) \tag{2.11}$$

where

$$V_R^2 = \frac{\sigma_R^2}{\overline{R}^2} \quad , \quad V_S^2 = \frac{\sigma_S^2}{\overline{S}^2} \tag{2.12}$$

The derivation of Equations (2.10) and (2.11) are given in Appendix A.

The mean and variance of Q are obtained as

$$\overline{Q} = \overline{\ln R} - \overline{\ln S} = \ln[(\frac{\overline{R}}{\overline{S}})(\frac{1 + V_S^2}{1 + V_R^2})^{1/2}] \tag{2.13}$$

$$\sigma_Q^2 = \sigma_{\ln R}^2 + \sigma_{\ln S}^2 = \ln(V_R^2 + 1) + \ln(V_S^2 + 1) = \ln[(1 + V_R^2)(1 + V_S^2)] \tag{2.14}$$

Hence the safety factor, $\beta = \frac{\overline{Q}}{\sigma_Q}$, is of the form

$$\beta = \frac{\ln[(\overline{R} - \overline{S})\sqrt{\frac{1 + V_S^2}{1 + V_R^2}}\,]}{\sqrt{\ln[(1 + V_R^2)(1 + V_S^2)]}} \tag{2.15}$$

2. Uncertainty Formulations of Response and Resistance. According to Equations (2.6) and (2.15), finding the safety factor formulation is equivalent to calculating the means and coefficients of variation of structural resistance and response. Since determining uncertainties of structural response and resistance is impossible, a first-order approximation is employed to approximate the uncertainties in terms of their parameter uncertainties. The approximation of the means and variances of structural response and resistance can be derived as :

mean,

$$\begin{aligned}\overline{S(\bar{r})} &= E[S(\bar{r}) + \sum_i (\frac{\partial S}{\partial r_i})_{\bar{r}}(r_i - \bar{r}_i)] \\ &= S(\bar{r}) + \sum_i (\frac{\partial S}{\partial r_i})_{\bar{r}} E[r_i - \bar{r}_i] \\ &= S(\bar{r}) + \sum_i (\frac{\partial S}{\partial r_i})_{\bar{r}}(\bar{r}_i - \bar{r}_i) \\ &= S(\bar{r})\end{aligned} \tag{2.16}$$

$$\begin{aligned}\overline{R(\bar{r}')} &= E[R(\bar{r}') + \sum_{i'} (\frac{\partial R}{\partial r_{i'}})_{\bar{r}'}(r'_{i'} - \bar{r}'_{i'})] \\ &= R(\bar{r}')\end{aligned} \tag{2.17}$$

variance,

$$\sigma_S^2 = E[(S - \overline{S})(S - \overline{S})]$$

$$= E[(S(\bar{r}) + \sum_i (\frac{\partial S}{\partial r_i})_{\bar{r}}(r_i - \bar{r}_i) - \bar{S})(S(\bar{r}) + \sum_j (\frac{\partial S}{\partial r_j})_{\bar{r}}(r_j - \bar{r}_j) - \bar{S})]$$

$$= E[(\sum_i (\frac{\partial S}{\partial r_i})_{\bar{r}}(r_i - \bar{r}_i))(\sum_j (\frac{\partial S}{\partial r_i})_{\bar{r}}(r_j - \bar{r}_j))]$$

$$= \sum_i \sum_j (\frac{\partial S}{\partial r_i})_{\bar{r}}(\frac{\partial S}{\partial r_j})_{\bar{r}} \rho_{r_i r_j} V_{r_i} V_{r_j} \bar{r}_i \bar{r}_j \tag{2.18}$$

$$\sigma_R^2 = E[(R - \bar{R})(R - \bar{R})]$$

$$= \sum_{i'} \sum_{j'} (\frac{\partial R}{\partial r'_{i'}})_{\bar{r}'}(\frac{\partial R}{\partial r'_{j'}})_{\bar{r}'} \rho_{r'_{i'} r'_{j'}} V_{r'_{i'}} V_{r'_{j'}} \bar{r}'_{i'} \bar{r}'_{j'} \tag{2.19}$$

where r_i , r_j , r'_i , r'_j = ith, jth random parameters of response and resistance; $\rho_{r_i r_j}$, $\rho_{r'_{i'} r'_{j'}}$ = the correlation coefficients of r_i and r_j , $r'_{i'}$ and $r'_{j'}$; V_{r_i} , V_{r_j} , $V_{r'_{i'}}$, $V_{r'_{j'}}$ = the coefficints of variation of r_i , r_j , $r'_{i'}$, $r'_{j'}$; $\bar{r}_i$, $\bar{r}_j$, $\bar{r}'_{i'}$, $\bar{r}'_{j'}$ = the means of r_i , r_j , $r'_{i'}$, $r'_{j'}$; $\bar{r}$, $\bar{r}'$ = all mean random parameter values of response and resistance.

A structural response S such as a displacement and an internal force can be determined by

$$S = C_S q' \tag{2.20}$$

where C_S = an influence coefficient that transforms the load intensity (q') into the desired response; q' = the load intensity which may be dead, live, or earthquake load.

Two approaches for finding the variance of a response are suggested in the following.

a. A Variance Approach to Be Called 1st Variance Approach Hereforth. If the random parameters involved in a response are known, the variance of a response is found to be

$$\sigma_S^2 = \sum_i \sum_j (\frac{\partial S}{\partial r_i})_{\bar{r}}(\frac{\partial S}{\partial r_j})_{\bar{r}} \rho_{r_i r_j} V_{r_i} V_{r_j} \bar{r}_i \bar{r}_j$$

$$= \sum_i \sum_j [(\frac{\partial C_S}{\partial r_i})_{\bar{r}}(\frac{\partial C_S}{\partial r_j})_{\bar{r}} \bar{q}'^2 + (\frac{\partial q'}{\partial r_i})_{\bar{r}}(\frac{\partial q'}{\partial r_j})_{\bar{r}} \bar{C}_S^2] \rho_{r_i r_j} V_{r_i} V_{r_j} \bar{r}_i \bar{r}_j \tag{2.21}$$

Once the uncertainties of each random parameter are determined, the variance of a response can be obtained through the Equation (2.21). [40,41,42]

b. A Variance Approach to Be Called 2nd Variance Approach Hereafter. In many practical situations, finding the means and coefficients of variation of random parameters in a response is difficult. Therefore, the variance of the structural response can be calculated based on the square of some percentage of the mean value of the influence coefficient $(\bar{C}_S)$ by [44,70]

$$\sigma_S^2 = (C_p\bar{C}_S)^2\bar{q'}^2 + (\bar{C}_S)^2V_{q'}^2\bar{q'}^2 \tag{2.22}$$

where C_p is a percentage constant of $\bar{C}_S$ and $V_{q'}$ is a coefficient of variation of load intensity, q'.

Comparing with Equations (2.21) with (2.22), the two equations will be the same if the following terms are equal.

$$\sum_i\sum_j[(\frac{\partial C_S}{\partial r_i})_{\bar{r}}(\frac{\partial C_S}{\partial r_j})_{\bar{r}}\bar{q'}^2]\rho_{r_ir_j}V_{r_i}V_{r_j}\bar{r}_i\bar{r}_j = (C_p\bar{C}_S)^2\bar{q'}^2 \tag{2.23}$$

and

$$\sum_i\sum_j[(\frac{\partial q'}{\partial r_i})_{\bar{r}}(\frac{\partial q'}{\partial r_j})_{\bar{r}}\bar{C}_S^2]\rho_{r_ir_j}V_{r_i}V_{r_j}\bar{r}_i\bar{r}_j = (\bar{C}_S)^2V_{q'}^2\bar{q'}^2 \tag{2.24}$$

C. A FIRST PASSAGE EXPRESSION

For a random vibration problem, the probability of failure may be the probability that a stationary response will fail in a prescribed bound during the system operating time. This probability called the first passage equation has the following form.

Let s(t) be a stationary process, and ν_a^+ be an expected frequency of crossing the constant level $s = \tilde{a}$ with a positive slope, which is described in Appendix B, then

$$\nu_a^+ = \int_0^\infty \dot{s}\, P_d(\tilde{a}, \dot{s})\, d\dot{s} \tag{2.25}$$

where $\dot{s}$ = the derivative of s; $P_d(\tilde{a}, \dot{s})$ = joint probability density function of $\tilde{a}$ and $\dot{s}$.

If s(t) is a stationary Gaussian process with zero mean, this implies that the joint probability density of s and $\dot{s}$ takes the following form:

$$P_d(s,\dot{s}) = \frac{1}{2\pi\sigma_s\sigma_{\dot{s}}} \exp\left(\frac{-1}{2}\left(\frac{s^2}{\sigma_s^2} + \frac{\dot{s}^2}{\sigma_{\dot{s}}^2}\right)\right) \tag{2.26}$$

where σ_s and $\sigma_{\dot{s}}$ are the standard deviations of s and $\dot{s}$, respectively.

Substituting Equation (2.26) into Equation (2.25), We find

$$\nu_a^+ = \int_0^\infty \frac{\dot{s}}{2\pi\sigma_s\sigma_{\dot{s}}} \exp\left(\frac{-1}{2}\left(\frac{\tilde{a}^2}{\sigma_s^2} + \frac{\dot{s}^2}{\sigma_{\dot{s}}^2}\right)\right) d\dot{s}$$

$$= \frac{1}{2\pi\sigma_s\sigma_{\dot{s}}} \exp\left(\frac{-\tilde{a}}{2\sigma_s^2}\right) \int_0^\infty \dot{s} \exp\left(\frac{\dot{s}^2}{\sigma_{\dot{s}}^2}\right) d\dot{s}$$

$$= \frac{\sigma_{\dot{s}}}{2\pi\sigma_s} \exp\left(\frac{-\tilde{a}^2}{2\sigma_s^2}\right) \tag{2.27}$$

For a double barrier case, $|s| < \tilde{a}$, shown in Figure 1, the expected frequency of crossing the level $|s| = \tilde{a}$ becomes

$$\nu_a = 2\nu_a^+ = \frac{\sigma_{\dot{s}}}{\pi\sigma_s} \exp\left(\frac{-\tilde{a}^2}{2\sigma_s^2}\right) \tag{2.28}$$

When the crossings of the level $|s| = \tilde{a}$ constitute a Poisson process, the first-passage probability density $P_d(t)$ has the form

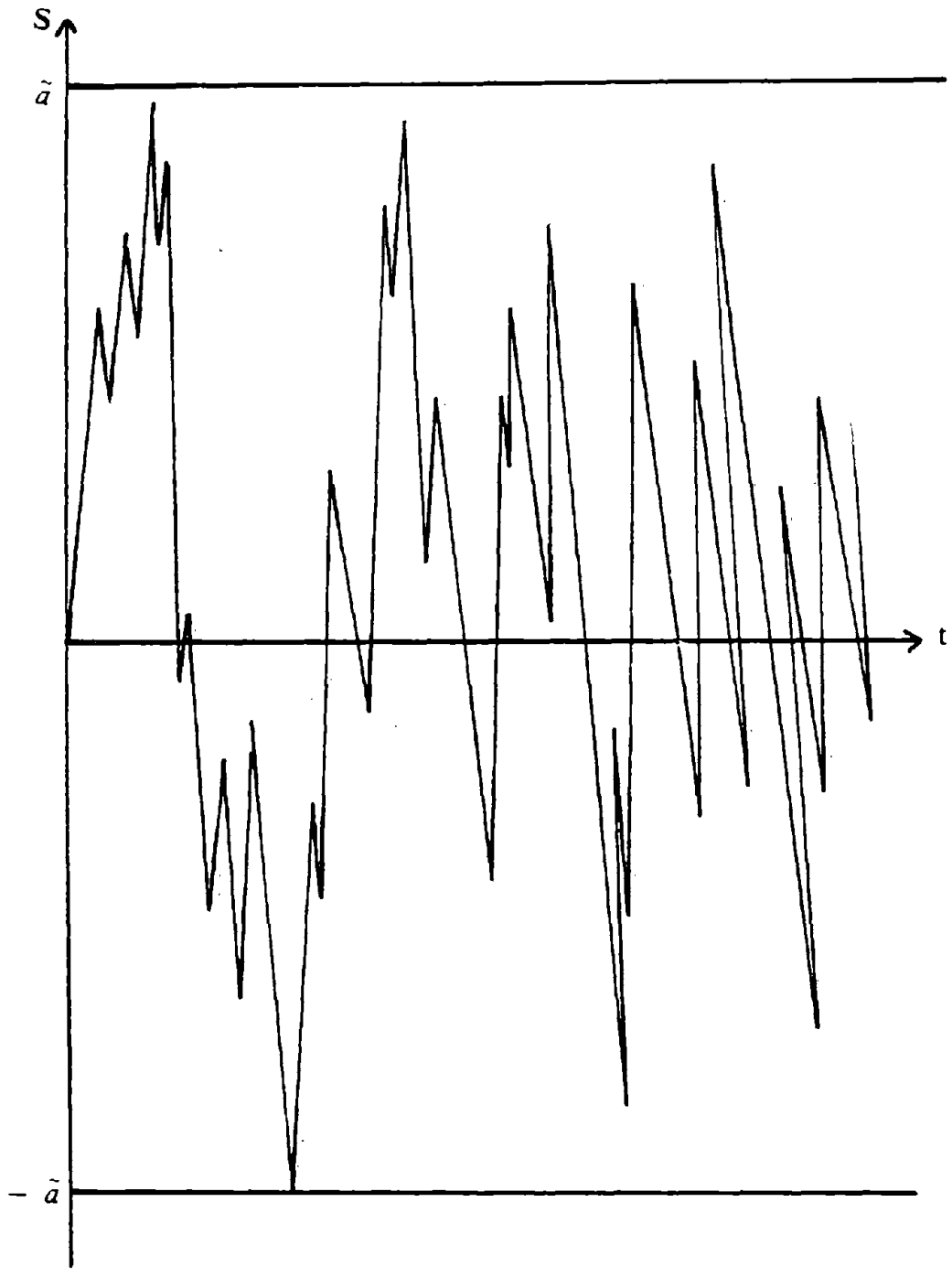

Figure 1. A Double Barrier for A Random Process s(t).

$$P_d(t) = \nu_a \exp(-\nu_a t) \tag{2.29}$$

where t is a time parameter.

Therefore reliability (P_r) and probability of failure (P_f) on time interval $0 < t < T_0$ are given by

$$P_f = P_f(T_0) = \int_0^{T_0} P_d(t)dt = 1 - \exp(-\nu_a T_0) \tag{2.30}$$

$$P_r = P_r(T_0) = 1 - P_f(T_0) = \exp(-\nu_a T_0) \tag{2.31}$$

D. RELIABILITY OF STRUCTURAL SYSTEM

In Section A, the derivations of reliability and probability of failure are based on a single failure mode with a single structural response and resistance case. However, a structural system may have many failure modes. Hence the system reliability or probability of failure may also be the desired quantity for considering the structural safety problem.

There are two fundamental types of systems, namely, a series system and a parallel system. A system is a series system if it is in a state of failure whenever any of its elements fails. Such a system is also called a weakest-link system. For a parallel system, failure in a single mode will not always result in failure of the total system, because the structural capacity may be able to sustain external loads.

In this study, the structural system is considered to be a series system, which means that the structure fails when any safety criterion is not satisfied. The probability of failure for this system, P_{fT} , may have the form

$$P_{fT}(R < S) = 1 - P_r(R > S) = 1 - P_r(R_1 > S_1 \cap R_2 > S_2 \cap .....) \tag{2.32}$$

where R_1, R_2, S_1, S_2..... are the resistances and responses of each failure mode for a structural system.

The determination of the exact value of Equation (2.32) is very difficult since the relationship among failure modes is too complicated. Nevertheless, two extreme bounds can be determined on the basis of the following conditions. [4, 35]

Perfectly correlated among failure modes

From Equation (2.32), the system probability of failure, P_{fT}, may be expressed as

$$P_{fT} = 1 - P_r(R_j > S_j) = 1 - (1 - P_f(R_j < S_j)) = P_f(R_j < S_j) \tag{2.33}$$

Therefore, using the maximum value of all failure probability modes yields the system failure probability as

$$P_{fT} = \max(P_{f_j}) \tag{2.34}$$

Perfectly uncorrelated among failure modes

$$P_{fT} = 1 - P_r(R_1 > S_1)P_r(R_2 > S_2) \ldots P_r(R_j > S_j) = 1 - \Pi(1 - P_f(R_j \le S_j))$$

$$= 1 - 1 + \sum_j P_{f_j} + \sum_i \sum_j P_{f_i} P_{f_j} \tag{2.35}$$

$$= \sum_j P_{f_j} \tag{2.36}$$

where P_{f_j} = the component failure probability of a structural system.

E. APPROXIMATION FORMULA FOR CUMULATIVE NORMAL DISTRIBUTION

From previous sections, the reliability and probability of failure are calculated through the cumulative normal distribution. However, finding the exact value of this distribution is very complicated and difficult. Therefore, some approximation formulae have to be used to approximate this function. In this study the formula in Reference 38 is used. The formula has two equations in two different ranges of safety factor. They are

Formula (1), $\beta \le 1.6$

$$P_r = (\beta - \frac{\beta^3}{6} + \frac{\beta^5}{40})\frac{1}{\sqrt{2\pi}} + 0.5 \tag{2.37}$$

$$P_f = 1 - P_r \tag{2.38}$$

$1.5 > \beta > 1.6$

$$P_r = 0.5[1 - (1 - \frac{1}{\beta^2} + \frac{3}{\beta^4})e^{-\frac{\beta^2}{2}}\sqrt{\frac{2}{\pi}}\ /\beta] + 0.5 \tag{2.39}$$

$$P_f = 1 - P_r \tag{2.40}$$

Formula (2), $\beta \geq 1$

$$P_f = \frac{1 + \beta^2}{2 + \beta^2}\ \frac{P_n(\beta)}{\beta} \tag{2.41}$$

where

$P_n(\beta)$ = standard normal density function

$$= \frac{1}{\sqrt{2\pi}} e^{-\beta^2/2} \tag{2.42}$$

Formula (3),

$$P_f = (\frac{\underline{A}\,\underline{B}}{1 + 2\underline{y}} + \frac{1}{1 + \underline{B}\beta + \underline{C}\underline{y} + \underline{D}\underline{y}\beta + \underline{x} + \underline{E}\,\underline{x}\beta})/2e^{\underline{y}} \tag{2.43}$$

where $\underline{A} = (\frac{2}{\pi})^{1/2}$; $\underline{B} = 1.604$; $\underline{C} = 3.91$; $\underline{D} = 4.45$; $\underline{E} = 0.73$; $\underline{y} = \frac{\beta^2}{2}$; $\underline{x} = 2.93\,\underline{y}^2$.

Comparing Formula (1) with Formulae (2) and (3) yields the results shown in Figure 2 from which one may observe that the results are very close except in the range of safety factor between 1.4 and 1.8. Therefore Formula (1) is used in this study excluding the safety factor between 1.4 and 1.8. The Formulae (2) and (3) are given in Reference 81.

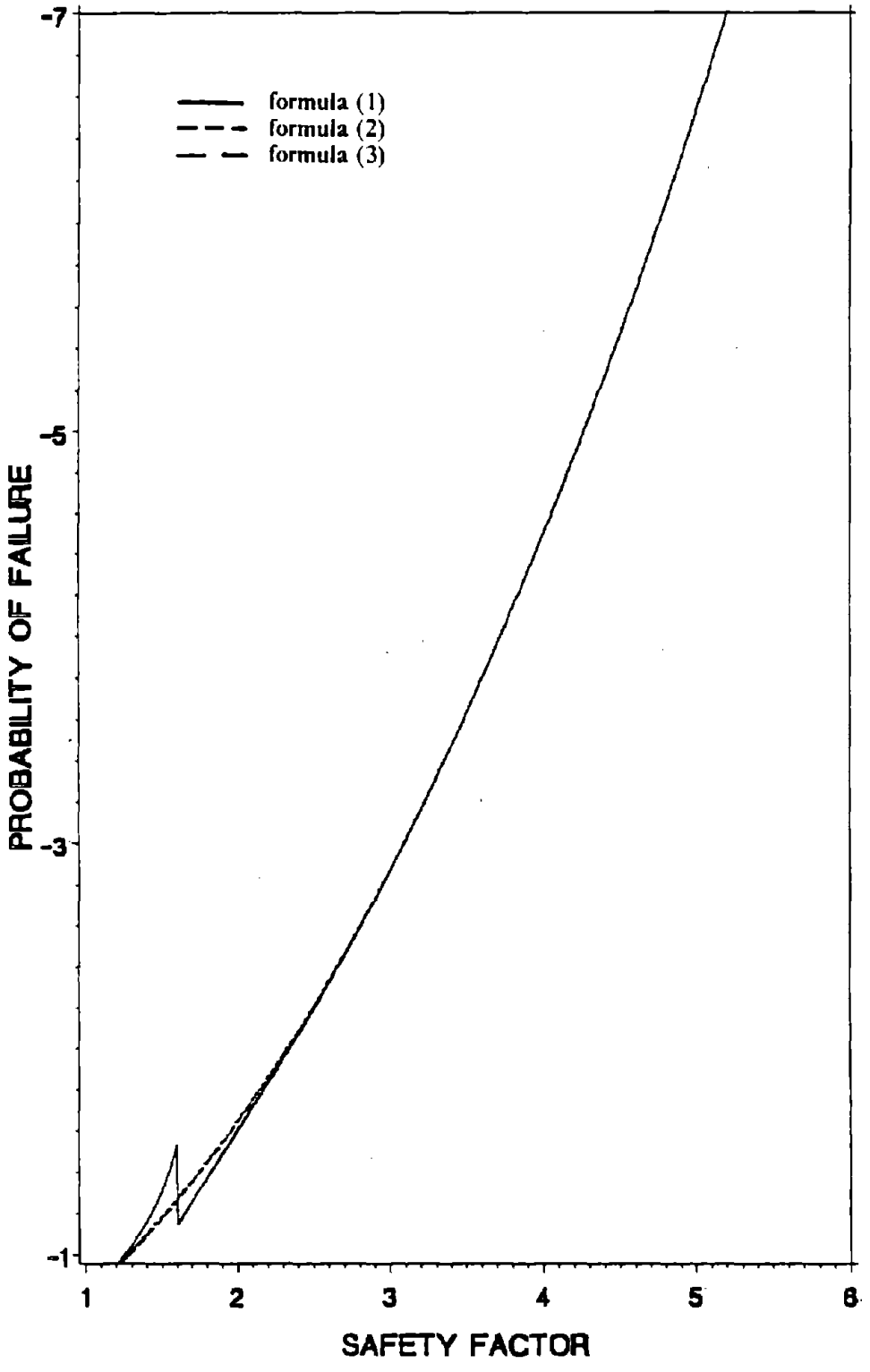

Figure 2. Various Approximate Equations for Standard Cumulative Normal Distribution.

III. STRUCTURAL SYSTEM TO STATIC AND EQUIVALENT SEISMIC LOAD

A. LOADING.

Structures may be subjected to the dead loads due to the weights of the structures and permanent fixtures; the live loads due to maximum total loads of occupancy and movable furniture; and the static equivalent lateral loads due to earthquakes. In what follows, the models for dead, live, and static equivalent lateral (UBC) seismic loads are discussed.

1. Dead Load. The dead load on a structure consists of the weight of the structure and permanent installations. The weight of a structure can be obtained from its geometry and the unit weight of the elements and their dimensions.

The mean value of a dead load is assumed to be the constituent of all its mean component values. The coefficient of variation of a dead load may be caused by the coefficient of variation of the weight of steel members which is 0.05 and the coefficient of variation due to the weight of non-structural elements, which is estimated as 0.1. [44] By using the above values the coefficient of variation for the dead load can be obtained as

$$V_D = \sqrt{(0.05)^2 + (0.1)^2} = 0.12 \tag{3.1}$$

2. Live Load. Live loads are loads arising from movable equipments and fixtures, vehicles and stored goods, and other non-permanent loads. Some live loads may be practically permanent, and others may be highly transient. They vary with both time and space, and can be idealized as being composed of two parts, the sustained live loads and the transient live loads.

The sustained live loads exist on the floor for a relatively long time and include furniture and normal working personnel. The changes in the sustained live loads may occur due to tenancy changes in the use of the floor area.

The transient live loads occur infrequently but with a relatively high intensity and short duration. The transient live loads may be due to people gathering in a room in large numbers for a special occasion, due to stocking some goods in a room for a short time, or due to the concentration of furniture during remodeling.

The probabilistic model for live loads may be assumed to be

$$L(x,y) = L_y + \varepsilon(x,y) \tag{3.2}$$

where $L(x,y)$ = the live load intensity, in pound per square foot at (x,y); L_y = a random variable modeling the average unit load on the floor; $\varepsilon(x,y)$ = a stochastic process with zero mean describing the deviations from the average.

The equivalent uniform distributed load (EUDL), which is the uniform distributed load and produces the same load effect as the actual set of loads, is our desired model and has the following meaning :

$$EUDL = \frac{\int\int L(x,y)I(x,y)dxdy}{\int\int I(x,y)dxdy} \tag{3.3}$$

where $I(x,y)$ = an influence surface coefficient.

The mean and variance of EUDL can be determined as follows

mean,

$$E[EUDL] = E[\frac{\int\int (L_y + \varepsilon(x,y))I(x,y)dA_I}{\int\int I(x,y)dA_I}]$$

$$= \frac{\bar{L}_y A_I \int_0^l \int_0^l I(x,y)dxdy}{A_I \int_0^l \int_0^l I(x,y)dxdy} = \bar{L}_y \tag{3.4}$$

variance,

$$\sigma^2_{EUDL} = \sigma_r^2 + \frac{\sigma_t^2}{A_I} K_L \tag{3.5}$$

where $K_L = \int_0^1\int_0^1 I^2(x,y)dxdy \; / \; (\int_0^1\int_0^1 I(x,y)dxdy)^2$; σ_r^2, σ_t^2 = empirical constants to fit the data from a live load survey; A_I = the influence area which covers the influence surface. $K_L, \sigma_r^2, \sigma_t^2$ can be determined from live load survey.

Statistical information on live loads is obtained from the live load surveys. [45,64,66] These surveys gave the instantaneous values of the live loads on the particular building at the time at which the survey was conducted.

The lifetime maximum total live load, which is the maximum value of the live load (sustained plus transient) over the whole lifetime of the structure and is described in Appendix C, is considered in this study. For the purpose of simplicity, the four lifetime maximum total live load models of office building structure which are independent on time are described and used. The statistics of these four models are :

(1) ANSI 1980 recommendation (L1) [66]

The load subcommittee of American National Standard Committee A58 recommended a 1980 version of a live load model. The statistics of this model were given as

mean,

$$\overline{L1} = 50(0.25 + 15 / \sqrt{A_I}) \quad \text{psf} \tag{3.6}$$

coefficient of variation,

$$V_{L1} = 0.14 \tag{3.7}$$

(2) NBS survey (L2) [45]

The National Bureau of Standard (NBS) published the load survey results for office buildings in the United States. The statistics of this live load model were given as

mean,

$$\overline{L2} = 18.7 + 520 / \sqrt{A_I} \quad \text{psf} \tag{3.8}$$

coefficient of variation,

$$V_{L2} = (14.2 + 18900/A_I) / \overline{L2} \tag{3.9}$$

(3) United Kingdom survey (L3) [64]

Mitchall and Woodgate proposed a live load model according to the survey results for office buildings in the United Kingdom. The analysis resulted in

mean,

$$\overline{L3} = 14.9 + 763 / \sqrt{A_I} \quad \text{psf} \tag{3.10}$$

coefficient of variation,

$$V_{L3} = (11.3 + 15000 / A_I) / \overline{L3} \tag{3.11}$$

(4) UNREDUCED live load (L4) [66]

This live load model is a fixed value which does not relate to any space parameters. The statistics of this model are

mean,

$$\overline{L4} = 50 \quad \text{psf} \tag{3.12}$$

coefficient of variation,

$$V_{L4} = 0.14 \tag{3.13}$$

In the above models, the influence area parameter A_I is the area that contributes the load determination, and the unit 1 psf (pounds per square foot) equals 992.16 kPa.

3. UBC Seismic Load. The seismic load may be represented as the static equivalent lateral load that is constructed in code specifications such as ATC [5] or UBC [55]. In these codes the earthquake is first expressed as the ground base shear force and then distributed to the desired location. The earthquake load expression in the Uniform Building Code [55] is used in this study.

$$E = ZI_E K_E C_E S_E W \tag{3.14}$$

where

E = the shear force at the base;

Z = numerical coefficient depends on the zone that the structure is located, for zones I, II, III, IV; Z = 3/16, 3/8, 3/4, 1, respectively;

I_E = occupancy importance factor;

K_E = numerical coefficient;

C_E = $\frac{1}{(15\sqrt{T})}$, the value need not exceed 0.12;

T = structural fundamental period;

S_E = numerical coefficient for site-structure resonance, when characteristic site period is not properly established, the value of S shall be 1.5;

W = the total dead load.

The structural fundamental period, T, can be calculated in the formula

$$T = 2\pi \sqrt{(\sum_{i=1}^{n} W_i u_i^2)} / \sqrt{(g \sum_i F_{Ei} u_i)}$$

Because the calculation of this period involves structural analysis which is not known in the beginning, the approximate period $T = 0.05h_n/\sqrt{D_n}$ is needed first (Where D_n = the dimension of the structure in parallel with applied force direction; h_n = the height of the highest level; W_i = the weight of ith level; u_i = the deflection of ith level; F_{Ei} = the lateral force applied at level i).

After the force E is determined, E shall be distributed over the height of the structure in the following formula:

$$F_{Ex} = [(1 - F_{tu}) W_x \frac{h_x}{\sum_i W_i h_i}] E = F_{E_{ux}} E \tag{3.15}$$

where F_{Ex} = lateral force applied to level x; $F_{E_{ux}}$ = lateral force applied to level x due to a unit seismic load intensity; F_{tu} = the concentrated force at the top due to a unit seismic load intensity = 0.07T; W_i , W_x = the portion of W which is located at or is assigned to level i or x, respectively; h_i , h_x = the height of i or x th level.

The statistics of the UBC seismic load may be determined as:

mean,

$$\bar{E} = \bar{Z}\,\bar{I}_E\,\bar{K}_E\,\bar{C}_E\,\bar{S}_E\,\bar{W} \tag{3.16}$$

The coefficient of variation of earthquake may be assumed to follow a Type II extreme value distribution [36] which is described in Appendix D and has a probability distribution of

$$E'(e_1) = e^{(\frac{-e_1}{u1})-K1} \tag{3.17}$$

where E' = earthquake random variable; e_1 = a value of E'; u1 , K1 = parameters which are determined from seismological data survey.

For this type of distribution, the coefficient of variation of earthquake, V_E , is

$$V_E = \sqrt{\frac{\Gamma(1-\frac{2}{K1})}{\Gamma^2(1-\frac{1}{K1})}-1} \tag{3.18}$$

where $\Gamma(\ )$ is a Gamma function.

Since the phenomina of earthquake is highly complicated and unpredicable, the exact value of K1 is impossible to determine. However, many values of K1 and coefficient of variation of earthquake have been proposed in the past decade. Within them the value of K1, 2.3, which corresponds to coefficient of variation, 1.38, is reported in National Bureau of Standards Special Publication No. 577 [66] and has been used for some seismic designs. The value of K1, 2.7, which corresponds to coefficient of variation, 0.85, is recommended for the nuclear power plant design. [54]

B. STRUCTURAL RESPONSE

The desired load effects for a structure subjected to dead, live, or seismic load may be the structural displacements or members' internal forces. The total load effects may be due to the combination of these loads. In the following the general response formulations for dead, live, and UBC seismic loads are described.

1. Dead Load Effect. The dead load effect, S_D , can be obtained by

$$S_D = C_D D \tag{3.19}$$

where C_D is an influence coefficient which transforms the dead load intensity D into the desired load effect (displacement or internal force) through structural analysis.

The mean ($\bar{S}_D$) and the variance ($\sigma^2_{S_D}$) are

$$\bar{S}_D = \bar{C}_D \bar{D} \tag{3.20}$$

(a) 1st variance approach,

$$\begin{aligned}\sigma^2_{S_D} &= \sum_i \sum_j \left(\frac{\partial S_D}{\partial r_i}\right)_{\bar{r}} \left(\frac{\partial S_D}{\partial r_j}\right)_{\bar{r}} \rho_{r_i r_j} V_{r_i} V_{r_j} \bar{r}_i \bar{r}_j \\ &= \sum_i \sum_j \left(\frac{\partial C_D}{\partial r_i} D\right)_{\bar{r}} \left(\frac{\partial C_D}{\partial r_j} D\right)_{\bar{r}} \rho_{r_i r_j} V_{r_i} V_{r_j} \bar{r}_i \bar{r}_j \\ &\quad + \sum_i \sum_j \left(\frac{\partial D}{\partial r_i} C_D\right)_{\bar{r}} \left(\frac{\partial D}{\partial r_j} C_D\right)_{\bar{r}} \rho_{r_i r_j} V_{r_i} V_{r_j} \bar{r}_i \bar{r}_j\end{aligned} \tag{3.21}$$

(b) 2nd variance approach,

$$\sigma^2_{S_D} = (\bar{S}_D)^2 [(0.1)^2 + V_D^2] \tag{3.22}$$

where 0.1 is the assumed value to describe the static analysis error [44]; V_D = the coefficient of variation of dead load intensity which is assumed to be 0.12 in Equation (3.1).

2. Live Load Effect. The live load effect is obtained as

$$S_L = C_L L \tag{3.23}$$

where C_L is an influence coefficient that transforms the live load intensity L into the desired load effect.

The mean ($\bar{S}_L$) and the variance ($\sigma^2_{S_L}$) are

$$\bar{S}_L = \bar{C}_L \bar{L} \tag{3.24}$$

(a) 1st variance approach,

$$\begin{aligned}\sigma^2_{S_L} &= \sum_i \sum_j \left(\frac{\partial S_L}{\partial r_i}\right)_{\bar{r}} \left(\frac{\partial S_L}{\partial r_j}\right)_{\bar{r}} \rho_{r_i r_j} V_{r_i} V_{r_j} \bar{r}_i \bar{r}_j \\ &= \sum_i \sum_j \left(\frac{\partial C_L}{\partial r_i} L\right)_{\bar{r}} \left(\frac{\partial C_L}{\partial r_j} L\right)_{\bar{r}} \rho_{r_i r_j} V_{r_i} V_{r_j} \bar{r}_i \bar{r}_j \\ &\quad + \sum_i \sum_j \left(\frac{\partial L}{\partial r_i} C_L\right)_{\bar{r}} \left(\frac{\partial L}{\partial r_j} C_L\right)_{\bar{r}} \rho_{r_i r_j} V_{r_i} V_{r_j} \bar{r}_i \bar{r}_j\end{aligned} \tag{3.25}$$

(b) 2nd variance approach,

$$\sigma^2_{S_L} = (\bar{S}_L)^2 [(0.1)^2 + V_L^2] \tag{3.26}$$

where 0.1 is the assumed value to describe the static analysis error [44]; V_L = the coefficient of variation of live load intensity which is assumed to be the value in Equations (3.7), (3.9), (3.11), or (3.13).

3. UBC Seismic Load Effect. The UBC seismic load effect is obtained as

$$S_E = C_E E \tag{3.27}$$

where C_E is an influence coefficient that transforms the earthquake load intensity E into the desired load effect .

The mean ($\bar{S}_E$) and the variance ($\sigma^2_{S_E}$) are

$$\bar{S}_E = \bar{C}_E \bar{E} \tag{3.28}$$

(a) 1st variance approach,

$$\begin{aligned}\sigma^2_{S_E} &= \sum_i \sum_j \left(\frac{\partial S_E}{\partial r_i}\right)_{\bar{r}} \left(\frac{\partial S_E}{\partial r_j}\right)_{\bar{r}} \rho_{r_i r_j} V_{r_i} V_{r_j} \bar{r}_i \bar{r}_j \\ &= \sum_i \sum_j \left(\frac{\partial C_E}{\partial r_i} E\right)_{\bar{r}} \left(\frac{\partial C_E}{\partial r_j} E\right)_{\bar{r}} \rho_{r_i r_j} V_{r_i} V_{r_j} \bar{r}_i \bar{r}_j \\ &+ \sum_i \sum_j \left(\frac{\partial E}{\partial r_i} C_E\right)_{\bar{r}} \left(\frac{\partial E}{\partial r_j} C_E\right)_{\bar{r}} \rho_{r_i r_j} V_{r_i} V_{r_j} \bar{r}_i \bar{r}_j\end{aligned} \tag{3.29}$$

(b) 2nd variance approach,

$$\sigma^2_{S_E} = (\bar{S}_E)^2 [(0.1)^2 + V_E^2] \tag{3.30}$$

where 0.1 is the assumed value to describe the static analysis error [44]; V_E = the coefficient of variation of earthquake load intensity which is assumed to be the value in Equation (3.18).

4. Combined Load Effect.

The total load effect due to the combined action of dead, live, and UBC load is

$$S = S_D + S_L + S_E \tag{3.31}$$

The mean ($\bar{S}$) and variance (σ^2_S) of total load effect are

$$\bar{S} = \bar{S}_D + \bar{S}_L + \bar{S}_E \tag{3.32}$$

(a) 1st variance approach,

$$\sigma^2_S = \sum_i \sum_j \left(\frac{\partial S}{\partial r_i}\right)_{\bar{r}} \left(\frac{\partial S}{\partial r_j}\right)_{\bar{r}} \rho_{r_i r_j} V_{r_i} V_{r_j} \bar{r}_i \bar{r}_j$$

$$= \sum_{i1}\sum_{j1}\left(\frac{\partial C_D}{\partial r_{i1}}D + \frac{\partial C_L}{\partial r_{i1}}L + \frac{\partial C_E}{\partial r_{i1}}E\right)_{\bar{r}}\left(\frac{\partial C_D}{\partial r_{j1}}D + \frac{\partial C_L}{\partial r_{j1}}L + \frac{\partial C_E}{\partial r_{j1}}E\right)_{\bar{r}}\rho_{r_{i1}r_{j1}}V_{r_{i1}}V_{r_{j1}}\bar{r}_{i1}\bar{r}_{j1}$$

$$+ (\bar{C}_D\bar{D})^2V_D^2 + (\bar{C}_L\bar{L})^2V_L^2 + (\bar{C}_E\bar{E})^2V_E^2 \qquad (3.33)$$

where i1 and j1 are random parameters related to structural analysis.

(b) 2nd variance approach,

$$\sigma_S^2 = \sigma_{S_D}^2 + \sigma_{S_L}^2 + \sigma_{S_E}^2 + 2(0.1)^2(\bar{S}_D\bar{S}_L + \bar{S}_D\bar{S}_E + \bar{S}_L\bar{S}_E)$$

$$= \bar{C}_D^2\bar{D}^2((0.1)^2+V_D^2) + \bar{C}_L^2\bar{L}^2((0.1)^2+V_L^2) + \bar{C}_E^2\bar{E}^2((0.1)^2 + V_E^2)$$

$$+ 2(0.1)^2(\bar{S}_D\bar{S}_L + \bar{S}_D\bar{S}_E + \bar{S}_L\bar{S}_E)$$

$$= (0.1)^2[\bar{C}_D^2\bar{D}^2 + \bar{C}_L^2\bar{L}^2 + \bar{C}_E^2\bar{E}^2 + 2\bar{C}_D\bar{D}\,\bar{C}_L\bar{L} + 2\bar{C}_D\bar{D}\,\bar{C}_E\bar{E} + 2\bar{C}_L\bar{L}\,\bar{C}_E\bar{E}]$$

$$+ (\bar{C}_D\bar{D})^2V_D^2 + (\bar{C}_L\bar{L})^2V_L^2 + (\bar{C}_E\bar{E})^2V_E^2 \qquad (3.34)$$

C. COMPUTATION OF STRUCTURAL RESPONSE

In this section the computations of structural response which may be displacement or internal force can be performed as follows:

1. Displacement. The displacement may be calculated as:

$$\{u\} = \{C_S\}q' = [K]^{-1}\{q\}q' \qquad (3.35)$$

where $\{u\}$ = displacement matrix; $[K]^{-1}$ = inverse of global stiffness matrix; q = the applied load matrix due to a unit dead, live, or UBC seismic load intensity; and q' = the load intensity which may be the dead, live, or UBC seismic load intensity.

By using the above equation the uncertainties of load effects for dead load, live load, UBC seismic load, and combination of these loads are given :

a. Dead Load Effect. The mean and variance of dead load effect can be expressed as mean,

$$\{\bar{u}_D\} = \{\bar{C}_D\}\bar{D} = ([\bar{K}]^{-1}\{q_D\})\bar{D} \tag{3.36}$$

(a) 1st variance approach,

$$\sigma^2_{\{u_D\}} = \sum_{i1}\sum_{j1}\left(\frac{\partial\{u_D\}}{\partial r_{i1}}\right)_{\bar{r}}\left(\frac{\partial\{u_D\}}{\partial r_{j1}}\right)_{\bar{r}}\rho_{r_{i1}r_{j1}}V_{r_{i1}}V_{r_{j1}}\bar{r}_{i1}\bar{r}_{j1} + \{\bar{u}^2_D\}V^2_D \tag{3.37}$$

where i1 and j1 are the random parameters related to structural analysis; and Equation (3.37) is derived from Equation (3.21) as

$$\begin{aligned}\sigma^2_{\{u_D\}} &= \sum_{i1}\sum_{j1}\left(\frac{\partial\{u_D\}}{\partial r_{i1}}\right)_{\bar{r}}\left(\frac{\partial\{u_D\}}{\partial r_{j1}}\right)_{\bar{r}}\rho_{r_{i1}r_{j1}}V_{r_{i1}}V_{r_{j1}}\bar{r}_{i1}\bar{r}_{j1} + \left(\frac{\partial D}{\partial D}C_D\right)^2_{\bar{r}}\bar{D}^2V^2_D \\ &= \sum_{i1}\sum_{j1}\left(\frac{\partial\{u_D\}}{\partial r_{i1}}\right)_{\bar{r}}\left(\frac{\partial\{u_D\}}{\partial r_{j1}}\right)_{\bar{r}}\rho_{r_{i1}r_{j1}}V_{r_{i1}}V_{r_{j1}}\bar{r}_{i1}\bar{r}_{j1} + \{C^2_D\}\bar{D}^2V^2_D\end{aligned} \tag{3.38}$$

The derivative of displacement with respect to i1th or j1th random variable of r can be derived as follows: Since $\{q_D\}D = [K]\{u_D\}$, the derivative of this equation with respect to random parameter r_{i1} is

$$\frac{\partial(\{q_D\}D)}{\partial r_{i1}} = \frac{\partial[K]}{\partial r_{i1}}\{u_D\} + [K]\frac{\partial\{u_D\}}{\partial r_{i1}} \tag{3.39}$$

Rearranging Equation (3.39), it can be found in

$$\frac{\partial\{u_D\}}{\partial r_{i1}} = [K]^{-1}\left(\frac{\partial(\{q_D\}D)}{\partial r_{i1}} - \frac{\partial[K]}{\partial r_{i1}}\{u_D\}\right) \tag{3.40}$$

Similary we can have

$$\frac{\partial\{u_D\}}{\partial r_{j1}} = [K]^{-1}\left(\frac{\partial(\{q_D\}D)}{\partial r_{j1}} - \frac{\partial[K]}{\partial r_{j1}}\{u_D\}\right) \tag{3.41}$$

(b) 2nd variance approach,

$$\sigma^2_{\{u_D\}} = \{\bar{u}^2_D\}((0.1)^2 + V^2_D) \tag{3.42}$$

which is based on Equation (3.22).

b. Live Load Effect. The mean and variance of live load effect can be expressed as mean,

$$\{\bar{u}_L\} = \{\bar{C}_L\}\bar{L} = ([\bar{K}]^{-1}\{q_L\})\bar{L} \tag{3.43}$$

(a) 1st variance approach,

$$\sigma^2_{\{u_L\}} = \sum_{i}\sum_{j}\left(\frac{\partial\{u_L\}}{\partial r_{i1}}\right)_{\bar{r}}\left(\frac{\partial\{u_L\}}{\partial r_{j1}}\right)_{\bar{r}}\rho_{r_{i1}r_{j1}}V_{r_{i1}}V_{r_{j1}}\bar{r}_{i1}\bar{r}_{j1} + \{\bar{u}^2_L\}V^2_L \tag{3.44}$$

The derivation of Equation (3.44) is similar to Equation (3.37); and the sensitivity analysis of the displacement may be expressed as

$$\frac{\partial\{u_L\}}{\partial r_{i1}} = [K]^{-1}\left(\frac{\partial(\{q_L\}L)}{\partial r_{i1}} - \frac{\partial[K]}{\partial r_{i1}}\{u_L\}\right) \tag{3.45}$$

$$\frac{\partial\{u_L\}}{\partial r_{j1}} = [K]^{-1}\left(\frac{\partial(\{q_L\}L)}{\partial r_{j1}} - \frac{\partial[K]}{\partial r_{j1}}\{u_L\}\right) \tag{3.46}$$

(b) 2nd variance approach,

$$\sigma^2_{\{u_L\}} = \{\bar{u}^2_L\}((0.1)^2 + V^2_L) \tag{3.47}$$

c. UBC Seismic Load Effect. The mean and variance of UBC load effect can be expressed as

mean,

$$\{\bar{u}_E\} = \{\bar{C}_E\}\bar{E} = ([\bar{K}]^{-1}\{q_E\})\bar{E} \tag{3.48}$$

Here q_E has the same meaning as $F_{E_{ux}}$ in Equation (3.15).

(a) 1st variance approach,

$$\sigma^2_{\{u_E\}} = \sum\sum_{i1j1}\left(\frac{\partial\{u_E\}}{\partial r_{i1}}\right)_{\bar{r}}\left(\frac{\partial\{u_E\}}{\partial r_{j1}}\right)_{\bar{r}}\rho_{r_{i1}r_{j1}}V_{r_{i1}}V_{r_{j1}}\bar{r}_{i1}\bar{r}_{j1} + \{u^2_E\}V^2_E \tag{3.49}$$

The derivation of Equation (3.49) is similar to Equation (3.38); and the sensitivity analysis of the displacement may be expressed as

$$\frac{\partial\{u_E\}}{\partial r_{i1}} = [K]^{-1}\left(\frac{\partial(\{q_E\}E)}{\partial r_{i1}} - \frac{\partial[K]}{\partial r_{i1}}\{u_L\}\right) \tag{3.50}$$

$$\frac{\partial\{u_E\}}{\partial r_{j1}} = [K]^{-1}\left(\frac{\partial(\{q_E\}E)}{\partial r_{j1}} - \frac{\partial[K]}{\partial r_{j1}}\{u_E\}\right) \tag{3.51}$$

(b) 2nd variance approach,

$$\sigma^2_{\{u_E\}} = \{\bar{u}^2_E\}((0.1)^2 + V^2_E)$$

$$= ([\bar{K}]^{-1}\{q_E\}\bar{E})^2((0.1)^2 + V^2_E) \tag{3.52}$$

d. Combined Load Effect.

mean,

$$\{\bar{u}\} = \{\bar{u}_D\} + \{\bar{u}_L\} + \{\bar{u}_E\}$$

$$= [\bar{K}]^{-1}\{q_D\}\bar{D} + [\bar{K}]^{-1}\{q_L\}\bar{L} + [\bar{K}]^{-1}\{q_E\}\bar{E} \tag{3.53}$$

(a) 1st variance approach,

$$\sigma^2_{\{u\}} = \sum\sum_{i1j1}\left(\frac{\partial\{u_D\}}{\partial r_{i1}} + \frac{\partial\{u_L\}}{\partial r_{i1}} + \frac{\partial\{u_E\}}{\partial r_{i1}}\right)_{\bar{r}}\left(\frac{\partial\{u_D\}}{\partial r_{j1}} + \frac{\partial\{u_L\}}{\partial r_{j1}} + \frac{\partial\{u_E\}}{\partial r_{j1}}\right)_{\bar{r}}\rho_{r_{i1}r_{j1}}V_{r_{i1}}V_{r_{j1}}\bar{r}_{i1}\bar{r}_{j1}$$

$$+ \{\bar{u}^2_D\}V^2_D + \{\bar{u}^2_L\}V^2_L + \{\bar{u}^2_E\}V^2_E \tag{3.54}$$

(b) 2nd variance approach,

$$\sigma^2_{\{u\}} = \{\bar{u}^2_D\}((0.1)^2+V^2_D) + \{\bar{u}^2_L\}((0.1)^2 + V^2_L) + \{\bar{u}^2_E\}((0.1)^2 + V^2_E)$$

$$+ 2(0.1)^2(\{\bar{u}_D\bar{u}_L + \bar{u}_D\bar{u}_E + \bar{u}_L\bar{u}_E\}) \quad (3.55)$$

The derviations of Equations (3.54) and (3.55) are similar to Equations (3.33) and (3.34).

For displacement failure mode, substituting Equations (3.53), (3.54), (3.55) into Equations (2.6) or (2.15), then the probability of failure in Equations (2.4) or (2.8) can be determined if the statistics of allowable displacement are given.

2. Internal Force. The internal forces in a structrual member which may be axial forces or bending moments are given by

$$\{F\}_m = [S]_m[A]^T_m\{u\}_m \quad (3.56)$$

where $\{F\}_m$ = the internal forces in a member; $[S]_m$ = a member stiffness matrix; $[A]^T_m$ = transpose of a member's static matrix; $\{u\}_m$ = the corresponding external displacements in a member.

The uncertainties of load effects due to dead, live, and earthquake load are

a. Dead Load Effect.

mean,

$$\{\bar{F}_D\}_m = [\bar{S}]_m[A]^T_m\{\bar{u}_D\}_m \quad (3.57)$$

(a) 1st variance approach,

$$\sigma^2_{\{F_D\}_m} = \sum_{i1}\sum_{j1}\left(\frac{\partial\{F_D\}_m}{\partial r_{i1}}\right)_{\bar{r}}\left(\frac{\partial\{F_D\}_m}{\partial r_{j1}}\right)_{\bar{r}}\rho_{r_{i1}r_{j1}}V_{r_{i1}}V_{r_{j1}}\bar{r}_{i1}\bar{r}_{j1} + ((\bar{F}^2_D)V^2_D) \quad (3.58)$$

where i1 and j1 are random parameters related to structural analysis; and for which the derivation may be obtained as

$$\sigma^2_{\{F_D\}_m} = \sum_{i1}\sum_{j1}\left(\frac{\partial\{F_D\}_m}{\partial r_{i1}}\right)_{\bar{r}}\left(\frac{\partial\{F_D\}_m}{\partial r_{j1}}\right)_{\bar{r}}\rho_{r_{i1}r_{j1}}V_{r_{i1}}V_{r_{j1}}\bar{r}_{i1}\bar{r}_{j1} + \left(\frac{\partial\{F_D\}_m}{\partial D}\right)^2_{\bar{r}}V_D^2 \tag{3.59}$$

In Equation (3.58) we have

$$\frac{\partial\{F_D\}_m}{\partial r_{i1}} = \frac{\partial[S]_m}{\partial r_{i1}}[A]^T_m\{u_D\}_m + [S]_m[A]^T_m\frac{\partial\{u_D\}_m}{\partial r_{i1}} \tag{3.60}$$

$$\frac{\partial\{F_D\}_m}{\partial r_{j1}} = \frac{\partial[S]_m}{\partial r_{j1}}[A]^T_m\{u_D\}_m + [S]_m[A]^T_m\frac{\partial\{u_D\}_m}{\partial r_{j1}} \tag{3.61}$$

(b) 2nd variance approach,

$$\sigma^2_{\{F_D\}_m} = \{\bar{F}^2_D\}_m((0.1)^2 + V_D^2) \tag{3.62}$$

b. Live Load Effect.

mean,

$$\{\bar{F}_L\} = [\bar{S}]_m[A]^T_m\{\bar{u}_L\}_m \tag{3.63}$$

(a) 1st variance approach,

$$\sigma^2_{\{F_L\}_m} = \sum_{i1}\sum_{j1}\left(\frac{\partial\{F_L\}_m}{\partial r_{i1}}\right)_{\bar{r}}\left(\frac{\partial\{F_L\}_m}{\partial r_{j1}}\right)_{\bar{r}}\rho_{r_{i1}r_{j1}}V_{r_{i1}}V_{r_{j1}}\bar{r}_{i1}\bar{r}_{j1} + \{\bar{F}^2_L\}_m V_L^2 \tag{3.64}$$

The derivation of Equation (3.64) is similar to Equation (3.58); and the sensitivity analysis of internal force may be expressed as

$$\frac{\partial\{F_L\}_m}{\partial r_{i1}} = \frac{\partial[S]_m}{\partial r_{i1}}[A]^T_m\{u_L\}_m + [S]_m[A]^T_m\frac{\partial\{u_L\}_m}{\partial r_{i1}} \tag{3.65}$$

$$\frac{\partial\{F_L\}_m}{\partial r_{j1}} = \frac{\partial[S]_m}{\partial r_{j1}}[A]^T_m\{u_L\}_m + [S]_m[A]^T_m\frac{\partial\{u_L\}_m}{\partial r_{j1}} \tag{3.66}$$

(b) 2nd variance approach,

$$\sigma^2_{\{F_L\}_m} = \{\bar{F}^2_L\}_m((0.1)^2 + V^2_L) \tag{3.67}$$

c. UBC Load Effect.

mean,

$$\{\bar{F}_E\} = [\bar{S}]_m[A]^T_m\{\bar{u}_E\}_m \tag{3.68}$$

(a) 1st variance approach,

$$\sigma^2_{\{F_E\}_m} = \sum_{i1}\sum_{j1}\left(\frac{\partial\{F_E\}_m}{\partial r_{i1}}\right)_{\bar{r}}\left(\frac{\partial\{F_E\}_m}{\partial r_{j1}}\right)_{\bar{r}}\rho_{r_{i1}r_{j1}}V_{r_{i1}}V_{r_{j1}}\bar{r}_{i1}\bar{r}_{j1} + \{\bar{F}^2_E\}_m V^2_E \tag{3.69}$$

The derivation of Equation (3.69) is similar to Equation (3.58); and the sensitivity analysis of internal force may be expressed as

$$\frac{\partial\{F_E\}_m}{\partial r_{i1}} = \frac{\partial[S]_m}{\partial r_{i1}}[A]^T_m\{u_E\}_m + [S]_m[A]^T_m\frac{\partial\{u_E\}_m}{\partial r_{i1}} \tag{3.70}$$

$$\frac{\partial\{F_E\}_m}{\partial r_{j1}} = \frac{\partial[S]_m}{\partial r_{j1}}[A]^T_m\{u_E\}_m + [S]_m[A]^T_m\frac{\partial\{u_E\}_m}{\partial r_{j1}} \tag{3.71}$$

(b) 2nd variance approach,

$$\sigma^2_{\{F_E\}_m} = \{\bar{F}^2_E\}_m((0.1)^2 + V^2_E) \tag{3.72}$$

d. Combined Load Effect.

$$\{\bar{F}\}_m = \{\bar{F}_D\}_m + \{\bar{F}_L\}_m + \{\bar{F}_E\}_m \tag{3.73}$$

(a) 1st variance approach,

$$\sigma^2_{\{F\}_m} = \sum_{i1}\sum_{j1}\left(\frac{\partial\{F\}_m}{\partial r_{i1}}\right)_{\bar{r}}\left(\frac{\partial\{F\}_m}{\partial r_{j1}}\right)_{\bar{r}}\rho_{r_{i1}r_{j1}}V_{r_{i1}}V_{r_{j1}}\bar{r}_{i1}\bar{r}_{j1}$$

$$+ \{\bar{F}_D^2\}_m V_D^2 + \{\bar{F}_L^2\}_m V_L^2 + \{\bar{F}_E^2\}_m V_E^2 \tag{3.74}$$

The derivation of Equation (3.74) is

$$\sigma^2_{\{F\}_m} = \sum_{i1}\sum_{j1}\left(\frac{\partial\{F\}_m}{\partial r_{i1}}\right)_{\bar{r}}\left(\frac{\partial\{F\}_m}{\partial r_{j1}}\right)_{\bar{r}}\rho_{r_{i1}r_{j1}} V_{r_{i1}} V_{r_{j1}} \bar{r}_{i1}\bar{r}_{j1}$$

$$+ \left(\frac{\partial\{F\}_m}{\partial D}\right)^2_{\bar{r}} V_D^2 \bar{D}^2 + \left(\frac{\partial\{F\}_m}{\partial L}\right)^2_{\bar{r}} V_L^2 \bar{L}^2 + \left(\frac{\partial\{F\}_m}{\partial E}\right)^2_{\bar{r}} V_E^2 \bar{E}^2 \tag{3.75}$$

The sensitivity analysis of internal force may be expressed as

$$\frac{\partial\{F\}_m}{\partial r_{i1}} = \frac{\partial\{F_D\}_m}{\partial r_{i1}} + \frac{\partial\{F_L\}_m}{\partial r_{i1}} + \frac{\partial\{F_E\}_m}{\partial r_{i1}} \tag{3.76}$$

$$\frac{\partial\{F\}_m}{\partial r_{j1}} = \frac{\partial\{F_D\}_m}{\partial r_{j1}} + \frac{\partial\{F_L\}_m}{\partial r_{j1}} + \frac{\partial\{F_E\}_m}{\partial r_{j1}} \tag{3.77}$$

(b) 2nd variance approach,

$$\sigma^2_{\{F\}_m} = \sigma^2_{\{F_D\}_m} + \sigma^2_{\{F_L\}_m} + \sigma^2_{\{F_E\}_m}$$

$$+ 2(0.1)^2(\{\bar{F}_D\bar{F}_L + \bar{F}_D\bar{F}_E + \bar{F}_L\bar{F}_E\}_m) \tag{3.78}$$

For column failure modes sustituting Equations (3.73), (3.74), and (3.78) which may be the uncertainties of applied axial loads (P) or moments (M) into Equations (6.10), (6.12), (6.16), (6.17), (6.21), (6.22), (6.25), and (6.26) yields the means and variances of interaction equations. Substituting these statistics, the safety factors in Equations (2.6) or (2.15), then the probabilities of failure in Equations (2.4) or (2.8) can be determined if the statistics of allowable values of interaction equations are given.

D. STRUCTURAL RESISTANCE

In Equations (2.6) and (2.15) they were shown that the uncertainties of structural resistance are required in calculating the safety factor. The steel member resistances considered are

1. Yield Moment. The yield moment, M_y, is $F_y S_c$; where F_y = yield strength of material; S_c = elastic section modulus.

The mean and variance of yield moment are

mean,

$$\overline{M}_y = \overline{F}_y \overline{S}_c \tag{3.79}$$

variance,

$$\sigma^2_{M_y} = \overline{M}_y^2 \overline{V}^2_{M_y} \tag{3.80}$$

where V_{M_y} is the coefficient of variation of yield moment that equals 0.12 and is assumed to be a sum of square of the prediction error, elastic section modulus, and yield strength of a steel member (The coefficients of variation of F_y, S_c, and the predicted behavior error are assumed to be 0.1, 0.04, and 0.05, respectively [76]); i.e.

$$V_{M_y} = \sqrt{(0.1)^2 + (0.04)^2 + (0.05)^2} = 0.12 \tag{3.81}$$

2. Euler Buckling Load. For a long column the capacity of the column is governed by the Euler bucking load and may be expressed as

$$P_E = \frac{\pi^2 E_m I}{(KL)^2} \tag{3.82}$$

where E_m = elastic modulus ; I = moment of inertia; KL = effective length. The mean and variance of P_E are

mean,

$$\overline{P}_E = \frac{\pi^2 \overline{E}_m \overline{I}}{\overline{(KL)}^2} \tag{3.83}$$

variance,

$$\sigma^2_{P_E} = V^2_{P_E} \overline{P}^2_E \tag{3.84}$$

where V_{P_E} is the coefficient of variation of P_E, which equals to 0.3 and involves the uncertainties of prediction, elastic modulus , moment of inertia, and effective length factor. [76]

3. Axial Load Capacity. The axial load capacity, P_{cr}, is

$$P_{cr} = [1 - \frac{(KL/r_g)^2}{2C_c^2}]F_y A_c, \qquad \text{for } KL/r_g < C_c \tag{3.85}$$

or

$$P_{cr} = P_E, \qquad \text{for } KL/r_g > C_c \tag{3.86}$$

in which $C_c^2 = 2\pi^2 E_m / F_y$; P_E = Euler buckling load; r_g = the radius of gyration; A_c = cross sectional area.

The mean and variance of P_{cr} are

mean,

$$\overline{P}_{cr} = (1 - \overline{\lambda}^2/4)\overline{F}_y \overline{A}_c, \qquad \text{for } KL/r_g < C_c \tag{3.87}$$

or

$$\overline{P}_{cr} = \overline{P}_E, \qquad \text{for } KL/r_g > C_c \tag{3.88}$$

variance,

$$\sigma^2_{P_{cr}} = V^2_{P_{cr}} \bar{P}^2_{cr} \tag{3.89}$$

In Equations (3.87) and (3.89),

$$\bar{\lambda} = \frac{\overline{KL}}{\bar{r}_g} \frac{1}{\pi} \sqrt{\frac{\bar{F}_y}{\bar{E}_m}} \tag{3.90}$$

where $V_{P_{cr}}$ may vary from 0.14 to 0.31 and are considered to be the uncertainties of steel member area and elastic modulus. [76]

4. Yield Load. The yield load is given by

$$P_y = F_y A_c \tag{3.91}$$

The mean and variance of P_y are

mean,

$$\bar{P}_y = \bar{F}_y \bar{A}_c \tag{3.92}$$

variance,

$$\sigma^2_{P_y} = V^2_{P_y} \bar{P}^2_y \tag{3.93}$$

where V_{P_y} is the coefficient of variation of P_y, which is assumed to be 0.14 and includes the uncertainties of yield strength and a steel member area. [76]

5. Critical Moment. The critical moment, i.e., the moment at which lateral torsional buckling occurs is

$$M_{cr} = \{[\frac{C_b \pi E_m I_y}{K_y L}][\frac{G_s J}{E_m} + \frac{\pi^2 C_w}{(K_z L)^2}]\}^2 \tag{3.94}$$

where K_y and K_z are effective length factors which account for the effects of end restraints to lateral deflection and twist, respectively; C_b is a coefficient which depends on the variation in moment along the span; the shear modulus, G_s, is assumed to be $0.385 E_m$; I_y is the moment of inertia of weak axis; J = the polar moment of inertia; and C_w is a warping torsional coefficient.

The mean and variance of M_{cr} are

mean,

$$\overline{M}_{cr} = \{[\overline{C}_b \pi \frac{\overline{E}_m \overline{I}_y}{\overline{K}_y \overline{L}}][\frac{\overline{G}_s \overline{J}}{\overline{E}_m} + \frac{\pi^2 \overline{C}_w}{(\overline{K}_z \overline{L})^2}]\}^2 \tag{3.95}$$

variance,

$$\sigma^2_{M_{cr}} = V^2_{M_{cr}} \overline{M}^2_{cr} \tag{3.96}$$

where coefficient of variation $V_{M_{cr}}$ may be from 0.15 to 0.20 and contains the uncertainties of moment of inertia, elastic modulus, and shear modulus. [76]

IV. NONDETERMINISTIC SEISMIC RESPONSE SPECTRUM ANALYSIS.

A. LOADING

The earthquake load in this chapter is considered as a dynamic load which varies with time. This load will be the ground acceleration at the support of a structure which may be assumed along the directions of coordinate axes either in horizontal or/and vertical directions. The structural responses subjected to the ground acceleration may be derived from the time-history or response spectrum method. The use of time-history to evaluate the statistics of response requires repeated analysis for many earthquake records. This will cause an excessive amount of computation, and thus will not be applicable for the analysis. On the other hand, the response spectrum method is a simple scheme to calculate the dynamic load effects such as displacements or internal forces from a seismic response spectrum and a peak ground acceleration. Although many response spectra have been proposed in the past, most of them are considered only in horizontal ground acceleration and deterministic spectral responses values. They are, however, not suitable for the purpose of reliability design. Therefore, Newmark's Nondeterministic Seismic Responce Spectrum (NNSRS), [65] which uses the statistical technique to estimate the horizontal or vertical ground spectrum from actual earthquake accelerograms, is adopted for the study. The seismic response spectrum suggested by Newmark was based on 14 earthquakes which had 28 horizontal components and 14 vertical components. By utilizing these earthquake acceleration records, the statistics of spectral displacements, velocities, and accelerations for maximum ground acceleration were obtained and used to estimate the structural displacements and internal forces.

B. DYNAMIC EQUILIBRIUM FORMULATION FOR EARTHQUAKE EXCITATIONS.

The equation of motion for multi-degree structural system can be formulated as follows:

$$[m]\{\ddot{u}\} + [C]\{\dot{u}\} + [K]\{u\} = \{P\} \tag{4.1}$$

where $[m]$ = mass matrix; $[C]$ = damping matrix; $[K]$ = stiffness matrix; $\{P\}$ = external force matrix; $\{u\}$, $\{\dot{u}\}$, $\{\ddot{u}\}$ = structural displacement, velocity, acceleration, respectively.

If the applied external forces are the ground accelerations, Equation (4.1) becomes

$$[m]\{\ddot{u}_E\} + [C]\{\dot{u}_E\} + [K]\{u_E\} = -[m]\{a\} \tag{4.2}$$

where $\{a\}$ = the ground acceleration matrix which may include horizontal or/and vertical ground accelations; $\{u_E\}$, $\{\dot{u}_E\}$, $\{\ddot{u}_E\}$ = structural displacements, velocities, accelerations due to earthquake excitations, respectively.

The structural displacements may be expressed as a sum of a linear combination of the undamped free vibration mode shapes and the spectral displacements which is

$$\{u_E\} = \sum_n \{\Phi\}_n Y_n \tag{4.3}$$

where the nth mode shape matrix $\{\Phi\}_n$ is used to transform from a generalized coordinate Y_n to a geometric coordinate u_E at nth mode, and the generalized coordinate Y_n which is the modal magnitude is called normal coordinate.

Since the mode shapes have orthogonal properties,

$$\{\Phi\}_m^T[m]\{\Phi\}_n = 0, \quad \{\Phi\}_m^T[C]\{\Phi\}_n = 0, \quad \{\Phi\}_m^T[K]\{\Phi\}_n = 0, \ m \neq n. \tag{4.4}$$

Equation (4.2) can be transformed into the single degree equation of motion

$$M_n\ddot{Y}_n + 2\zeta_n\omega_n M_n\dot{Y}_n + M_n\omega_n^2 Y_n = -\{\Phi\}_n^T[m]\{1\}a \qquad (4.5)$$

where

$M_n = \{\Phi\}_n^T[m]\{\Phi\}_n$; $2\zeta_n\omega_n M_n = \{\Phi\}_n^T[C]\{\Phi\}_n$;

ω_n = structural natural frequency for nth mode

$= (\{\Phi\}_n^T[K]\{\Phi\}_n / M_n)^{1/2}$;

ζ_n = critical damping ratio coefficient for nth mode.

If the orthonormal mode in which M_n equals one is used, Equation (4.5) is given by

$$\ddot{Y}_n + 2\zeta_n\omega_n\dot{Y}_n + \omega_n^2 Y_n = -\Gamma_n a \qquad (4.6)$$

where Γ_n = participation factor for nth mode $= -\{\Phi\}_n^T[m]\{1\}$

When the second-order ($P - \Delta$) effect is considered, the stiffness matrix in Equation (4.2) becomes

$$[K] = [K]_S - [K]_G \qquad (4.7)$$

where $[K]_S$ = elastic stiffness matrix; $[K]_G$ = geometric stiffness matrix.

C. STRUCTURAL RESPONSE

The desired structural responses are displacements and internal forces. The estimation of uncertainties of these quantities can be obtained as follows:

1. Displacement.

a. Earthquake Load Effect. The normal coordinate at nth mode, Y_n , can be solved by the Duhamal integral

$$Y_n = \frac{\Gamma_n}{M_n\omega_{Dn}}\int_0^t ae^{-\zeta_n\omega_n(t-\tau)}\sin\omega_{Dn}(t-\tau)d\tau \qquad (4.8)$$

where $\omega_{Dn} = \omega_n\sqrt{1-\zeta_n^2}$; t = time; τ = a time difference.

For practical usage the commonly used spectral displacement, $y_{\omega n}$, which is the maximum value of Equation (4.8) has been chosen, that is

$$y_{\omega n} = [\frac{\Gamma_n}{M_n\omega_{Dn}}\int_0^t ae^{-\zeta_n\omega_n(t-\tau)}\sin\omega_{Dn}(t-\tau)d\tau]_{max} \tag{4.9}$$

In order to find the statistics of displacement, the mean, variance, and coefficient of variation of spectral displacement for each mode, $y_{\omega n}$, are needed and can be derived for different frequency ranges which are shown in Figure 3.

(i) in the constant displacement range : $\bar{\omega}_n / 2\pi < \bar{f}_{\omega 1}$

$$\bar{y}_{\omega n} = \bar{\alpha}_d\bar{d} = \bar{\alpha}_d(\overline{\frac{v^2}{v^2}\frac{a^2}{a^2}d}) = \bar{\alpha}_d(\overline{\frac{ad}{v^2}})(\overline{\frac{v}{a}})^2\bar{a} \tag{4.10}$$

$$\frac{\partial y_{\omega n}}{\partial r_i} = \frac{\partial[\alpha_d(\frac{ad}{v^2})(\frac{v}{a})^2 a]}{\partial r_i} \tag{4.11}$$

$$\sigma^2_{y_{\omega n}} = (\frac{\partial y_{\omega n}}{\partial\alpha_d})^2_f V^2_{\alpha_d}\bar{\alpha}^2_d + (\frac{\partial y_{\omega n}}{\partial(\frac{ad}{v^2})})^2_f V^2_{ad/v^2}(\overline{\frac{ad}{v^2}})^2 + (\frac{\partial y_{\omega n}}{\partial a})^2_f V^2_a\bar{a}^2 + (\frac{\partial y_{\omega n}}{\partial(\frac{v}{a})})^2_f V^2_{v/a}(\overline{\frac{v}{a}})^2$$

$$= [(\frac{ad}{v^2})(\frac{v}{a})^2 a]^2_f\bar{\alpha}^2_d V^2_{\alpha_d} + [\alpha_d(\frac{v}{a})^2 a]^2_f V^2_{ad/v^2}(\overline{\frac{ad}{v^2}})^2$$

$$+ [2\alpha_d(\frac{ad}{v^2})(\frac{v}{a})a]^2_f(\frac{v}{a})^2 V^2_{v/a} + [\alpha_d(\frac{ad}{v^2})(\frac{v}{a})^2]^2_f\bar{a}^2 V^2_a$$

$$= \bar{y}^2_{\omega n}V^2_{\alpha_d} + \bar{y}^2_{\omega n}V^2_{ad/v^2} + 4\bar{y}^2_{\omega n}V^2_{v/a} + \bar{y}^2_{\omega n}V^2_a \tag{4.12}$$

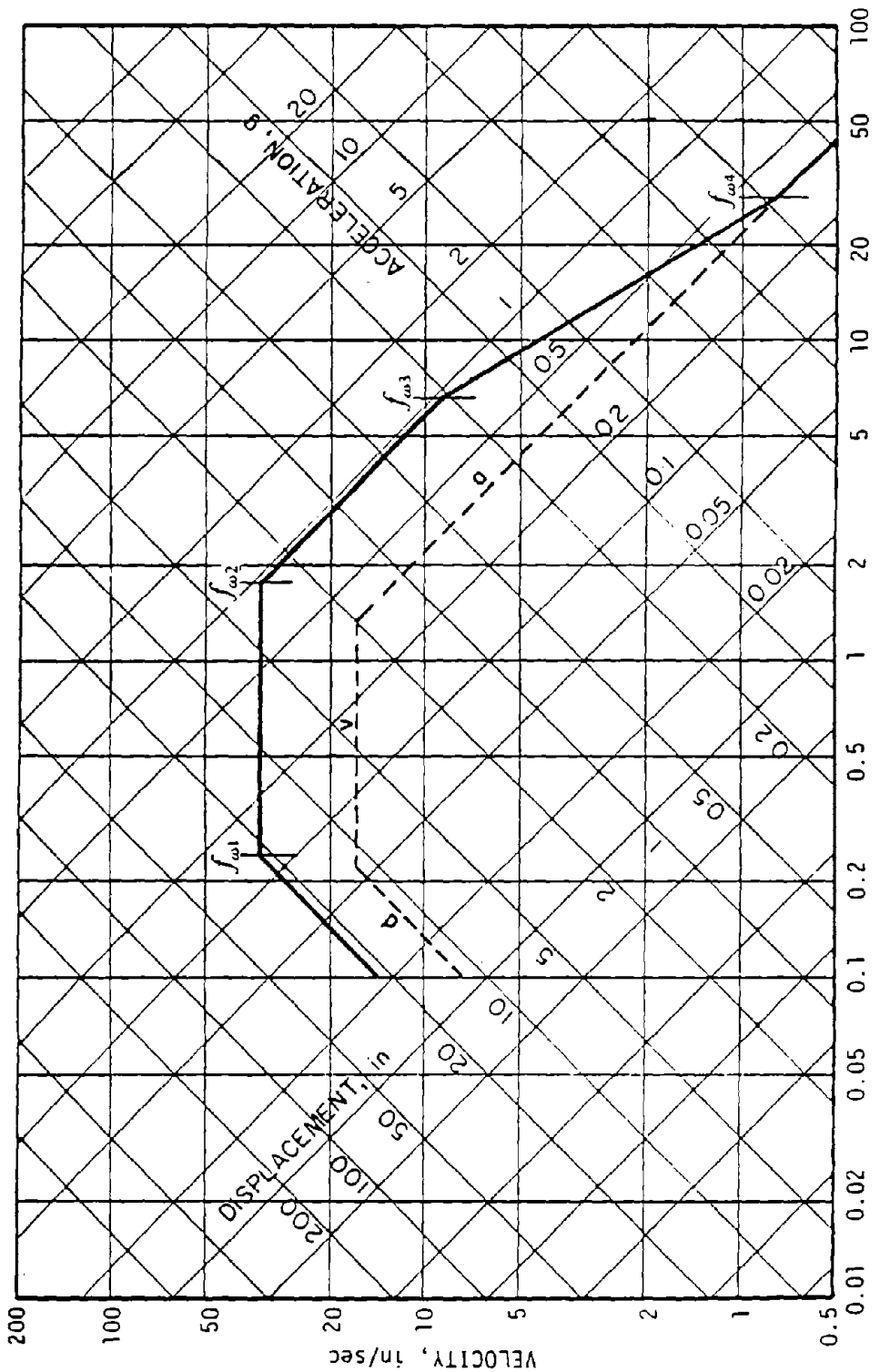

Figure 3. Newmark's Nondeterministic Response Spectrum.

$$V^2_{y_{\omega n}} = \frac{\sigma^2}{\bar{y}^2_{\omega n}} = V^2_{\alpha_d} + V^2_{ad/v^2} + 4V^2_{v/a} + V^2_a \tag{4.13}$$

where α_d , α_v , α_a = the amplification factors of spectral displacement, velocity, acceleration, respectively; d,v,a = the maximum ground displacement, velocity, acceleration, respectively; the bar over the parameters represents the mean of these parameters; the uppercase V represents the coefficient of variation for corresponding parameters; the σ is the standard deviation symbol. The statistics of α_d, α_v, α_a, v/a, and ad/v^2 can be found in Reference 65.

(ii) in the constant velocity range : $\bar{f}_{\omega 1} < \bar{\omega}_n / 2\pi < \bar{f}_{\omega 2}$;

$$\bar{y}_{\omega n} = \frac{\bar{\alpha}_v \bar{v}}{\bar{\omega}_n} = \frac{\bar{\alpha}_v}{\bar{\omega}_n}(\frac{\bar{v}}{\bar{a}})\bar{a} \tag{4.14}$$

$$\frac{\partial y_{\omega n}}{\partial r_i} = \frac{\partial[\frac{\alpha_v}{\omega_n}(\frac{v}{a})a]}{\partial r_i} \tag{4.15}$$

$$\sigma^2_{y_{\omega n}} = (\frac{\partial y_{\omega n}}{\partial \alpha_v})^2 V^2_{\bar{\alpha}_v}\bar{\alpha}^2_v + (\frac{\partial y_{\omega n}}{\partial(\frac{v}{a})})^2 V^2_{v/a}(\frac{\bar{v}}{\bar{a}})^2 + (\frac{\partial y_{\omega n}}{\partial \omega_n})^2 V^2_{\bar{\omega}_n}(\bar{\omega}_n)^2 + (\frac{\partial y_{\omega n}}{\partial a})^2 V^2_{\bar{a}}\bar{a}^2$$

$$= \bar{y}^2_{\omega n} V^2_{\alpha_v} + \bar{y}^2_{\omega n} V^2_{v/a} + \bar{y}^2_{\omega n} V^2_{\omega_n} + \bar{y}^2_{\omega n} V^2_a \tag{4.16}$$

$$V^2_{y_{\omega n}} = V^2_{\alpha_v} + V^2_{v/a} + V^2_a + V^2_{\omega_n} \tag{4.17}$$

where V_{ω_n} = the coefficient of variation of nth mode frequency.

(iii) in the constant acceleration range : $\bar{f}_{\omega 2} < \bar{\omega}_n / 2\pi < \bar{f}_{\omega 3}$

$$\bar{y}_{\omega n} = \frac{\bar{\alpha}_a \bar{a}}{\bar{\omega}^2_n} \tag{4.18}$$

$$\frac{\partial y_{\omega n}}{\partial r_i} = \frac{\partial[\frac{\alpha_a a}{\omega_n^2}]}{\partial r_i} \tag{4.19}$$

$$\sigma^2_{y_{\omega n}} = (\frac{\partial y_{\omega n}}{\partial \alpha_a})^2 V^2_{\alpha_a} \bar{\alpha}^2_a + (\frac{\partial y_{\omega_n}}{\partial \omega_n})^2 V^2_{\omega_n} (\bar{\omega}_n)^2 + (\frac{\partial y_{\omega_n}}{\partial a})^2 V^2_a \bar{a}^2$$

$$= \bar{y}^2_{\omega n} V^2_{\alpha_a} + 4\,\bar{y}^2_{\omega n} V^2_{\omega_n} + \bar{y}^2_{\omega n} V^2_a \tag{4.20}$$

$$V^2_{y_{\omega n}} = V^2_{\alpha_a} + V^2_a + 4V^2_{\omega_n} \tag{4.21}$$

(iv) in the transition range : $f_{\omega 3} < \omega_n / 2\pi < f_{\omega 4}$

$$\bar{y}_{\omega n} = \frac{\overline{\alpha_a(\omega) a}}{\bar{\omega}_n^2} = \exp[\frac{\ln \bar{\alpha}_a \ln(\bar{f}_{\omega 1}/\bar{f}_{\omega n})}{\ln(\bar{f}_{\omega 4}/\bar{f}_{\omega 3})}]\, \bar{a}/\bar{\omega}_n^2 \tag{4.22}$$

$$\frac{\partial y_{\omega n}}{\partial r_i} = \partial(\exp[\frac{\ln \alpha_a \ln(f_{\omega 1}/f_{\omega n})}{\ln(f_{\omega 4}/f_{\omega 3})}]\, a/\omega_n^2)/\partial r_i \tag{4.23}$$

$$\sigma^2_{y_{\omega n}} = (\frac{\partial y_{\omega n}}{\partial \alpha_a})^2 V^2_{\alpha_a} \bar{\alpha}^2_a + (\frac{\partial y_{\omega n}}{\partial(\omega_n)})^2 V^2_{\omega_n} (\bar{\omega}_n)^2 + (\frac{\partial y_{\omega n}}{\partial a})^2 V^2_a \bar{a}^2$$

$$= \bar{y}^2_{\omega n}[\frac{\ln(\bar{f}_{\omega 1}/\bar{f}_{\omega n})}{\ln(\bar{f}_{\omega 4}/\bar{f}_{\omega 3})}]^2 V^2_{\alpha_a} + \bar{y}^2_{\omega n}[\frac{\ln \bar{\alpha}_a}{\ln(\bar{f}_{\omega 4}/\bar{f}_{\omega 3})}]^2 V^2_{\omega_n}$$

$$+ 4\,\bar{y}^2_{\omega n} V^2_{\omega_n} + \bar{y}^2_{\omega n} V^2_a \tag{4.24}$$

$$V^2_{y_{\omega n}} = [\frac{\ln(\bar{f}_{\omega 1}/\bar{f}_{\omega n})}{\ln(\bar{f}_{\omega 4}/\bar{f}_{\omega 3})}]^2 V^2_{\alpha_a} + V^2_a + [\frac{\ln \bar{\alpha}_a}{\ln(\bar{f}_{\omega 4}/\bar{f}_{\omega 3})}]^2 V^2_{\omega_n} + 4V^2_{\omega_n} \tag{4.25}$$

(v) in the constant ground acceleration range : $\bar{f}_{\omega 4} < \bar{\omega}_n / 2\pi$

$$\bar{y}_{\omega n} = \frac{\bar{a}}{\bar{\omega}_n^2} \tag{4.26}$$

$$\frac{\partial y_{\omega n}}{\partial r_i} = \frac{\partial[\frac{a}{\omega_n^2}]}{\partial r_i} \tag{4.27}$$

$$\sigma^2_{y_{\omega n}} = (\frac{\partial y_{\omega n}}{\partial \omega_n})^2_{\bar{r}} V^2_{\omega_n} \bar{\omega}_n^2 + (\frac{\partial y_{\omega n}}{\partial (\omega_n)})^2_{\bar{r}} V^2_{\bar{a}} \bar{a}^2 = \bar{y}^2_{\omega n} V^2_a + \bar{y}^2_{\omega n} V^2_{\omega_n} \tag{4.28}$$

$$V^2_{y_{\omega n}} = V^2_a + 4V^2_{\omega_n} \tag{4.29}$$

Since displacements due to earthquake excitations can be assumed to be the sum of square of displacement for each mode, the statistics of displacements are determined as follows.

mean,

$$\{\bar{u}_E\} = [\sum_n (\{\bar{\Phi}\}_n \bar{\Gamma}_n \bar{y}_{\omega n})^2]^{1/2} \tag{4.30}$$

(a) 1st variance approach,

$$\sigma^2_{\{u_E\}} = \sum_i \sum_j (\frac{\partial \{u_E\}}{\partial r_i})_{\bar{r}} (\frac{\partial \{u_E\}}{\partial r_j})_{\bar{r}} \rho_{r_i r_j} V_{r_i} V_{r_j} \bar{r}_i \bar{r}_j \tag{4.31}$$

where

$$\frac{\partial \{u_E\}}{\partial r_i} = \frac{1}{u_E}[\sum_n (\{\Phi\}_n (\frac{\partial \{\Phi\}_n}{\partial r_i}) \Gamma^2_n y^2_{\omega n} + \{\Phi\}^2_n \Gamma_n (\frac{\partial \Gamma_n}{\partial r_i}) y^2_{\omega n} + \{\Phi\}^2_n \Gamma^2_n (\frac{\partial y_{\omega n}}{\partial r_i}) y_{\omega n})]$$

$$\frac{\partial \{u_E\}}{\partial r_j} = \frac{1}{u_E}[\sum_n (\{\Phi\}_n (\frac{\partial \{\Phi\}_n}{\partial r_j}) \Gamma^2_n y^2_{\omega n} + \{\Phi\}^2_n \Gamma_n (\frac{\partial \Gamma_n}{\partial r_j}) y^2_{\omega n} + \{\Phi\}^2_n \Gamma^2_n (\frac{\partial y_{\omega n}}{\partial r_j}) y_{\omega n})]$$

$\partial\{\Phi\}_n/\partial r_i$, $\partial\{\Phi\}_n/\partial r_j$ = the derivatives of mode shape matrices with respect to ith and jth random parameters; $\partial\Gamma_n/\partial r_i$, $\partial\Gamma_n/\partial r_j$ = the derivatives of participation factors with respect to ith and jth random parameters; $\partial y_{\omega n}/\partial r_i$, $\partial y_{\omega n}/\partial r_j$ = the derivatives of spectral displacements with respect to ith and jth random parameters.

If $\frac{\partial\{\Phi\}_n}{\partial r_i}$ is assumed to be a linear combination of mode shapes, i.e. $\frac{\partial\{\Phi\}_n}{\partial r_i} = \sum_k a_{nik}\{\Phi\}_k$, the determination of the scalar multiplier, a_{nik}, can be derived by two conditions. [22]

(1) $n \neq k$ case

Differentiating the undamped vibration equation with repect to random parameters, $([K] - \omega_n^2[m])\{\Phi\}_n = \{0\}$, it yields

$$(\frac{\partial[K]}{\partial r_i} - \frac{\partial\omega_n^2}{\partial r_i}[m] - \omega_n^2\frac{\partial[m]}{\partial r_i})\{\Phi\}_n + ([K] - \omega_n^2[m])\frac{\partial\{\Phi\}_n}{\partial r_i} = \{0\} \tag{4.32}$$

Substituting the linear combination of the mode shapes for $\frac{\partial\{\Phi\}_n}{\partial r_i}$ into the above equation and premultiplying by $\{\Phi\}_k^T$ for $k \neq n$ yields

$$\{\Phi\}_k^T(\frac{\partial[K]}{\partial r_i} - \frac{\partial\omega_n^2}{\partial r_i}[m] - \omega_n^2\frac{\partial[m]}{\partial r_i})\{\Phi\}_n$$

$$+ \{\Phi\}_k^T([K] - \omega_n^2[m])\sum_k a_{nik}\{\Phi\}_k = 0 \tag{4.33}$$

Because of mode shape orthogonal properties, Equation (4.33) becomes

$$\{\Phi\}_k^T(\frac{\partial[K]}{\partial r_i} - \frac{\partial\omega_n^2}{\partial r_i}[m] - \omega_n^2\frac{\partial[m]}{\partial r_i})\{\Phi\}_n$$

$$+ a_{nik}\{\Phi\}_k^T([K] - \omega_n^2[m])\{\Phi\}_k = 0 \tag{4.34}$$

If the mode shapes are orthonormal modes (i.e., $\{\Phi\}_k^T[m]\{\Phi\}_k = 1$), the term $\{\Phi\}_k^T[K]\{\Phi\}_k$ yields ω_k^2. Then the coefficients a_{nik} can be found from Equation (4.34) as

$$a_{nik} = \frac{\{\Phi\}_k^T\frac{\partial[K]}{\partial r_i}\{\Phi\}_n - \omega_n^2\{\Phi\}_k^T\frac{\partial[m]}{\partial r_i}\{\Phi\}_n}{\omega_n^2 - \omega_k^2} \tag{4.35}$$

(2) $n = k$ case

In Equation (4.35) a_{nik} approaches an infinitive value as ω_k equals to ω_n. As a result, it can not be used in n = k condition. For the orthonormal modes

$$\{\Phi\}_n^T[m]\{\Phi\}_n = 1 \tag{4.36}$$

Differentiating Equation (4.36) with respect to random parameters yields

$$2\{\Phi\}_n^T[m]\frac{\partial\{\Phi\}_n}{\partial r_i} + \{\Phi\}_n^T\frac{\partial[m]}{\partial r_i}\{\Phi\}_n = 0 \tag{4.37}$$

Now substituting $\frac{\partial\{\Phi\}_n}{\partial r_i}$ into Equation (4.37) solves the coefficient a_{nin} which is given by

$$a_{nin} = \frac{-\{\Phi\}_n^T\frac{\partial[m]}{\partial r_i}\{\Phi\}_n}{2} \tag{4.38}$$

The derivative of the natural frequency with respect to design variable, $\frac{\partial\omega_n^2}{\partial r_i}$, can also be derived as follows.

Differentiating the equation $\{\Phi\}_n^T([K]-\omega_n^2[m])\{\Phi\}_n = 0$, we have

$$\frac{\partial\{\Phi\}_n^T}{\partial r_i}([K]-\omega_n^2[m])\{\Phi\}_n + \{\Phi\}_n^T(\frac{\partial[K]}{\partial r_i} - \frac{\partial\omega_n^2}{\partial r_i}[m] - \omega_n^2\frac{\partial[m]}{\partial r_i})\{\Phi\}_n$$

$$+ \{\Phi\}_n^T([K]-\omega_n^2[m])\frac{\partial\{\Phi\}_n}{\partial r_i} = 0 \tag{4.39}$$

By observing the above equation in which the first and third terms are zero, Equation (4.34) becomes

$$\frac{\partial\omega_n^2}{\partial r_i} = \{\Phi\}_n^T(\frac{\partial[K]}{\partial r_i} - \omega_n^2\frac{\partial[m]}{\partial r_i})\{\Phi\}_n \tag{4.40}$$

The derivative of participation factor with respect to design variable, $\frac{\partial\Gamma_n}{\partial r_i}$, is

$$\frac{\partial\Gamma_n}{\partial r_i} = \frac{\partial\{\Phi\}_n^T}{\partial r_i}[m]\{1\} + \{\Phi\}_n^T\frac{\partial[m]}{\partial r_i}\{1\} \tag{4.41}$$

(b) 2nd variance approach,

$$\sigma^2_{\{u\}_E} = \sum_{n1}\sum_{n2}\left[\left(\frac{\partial\{u_E\}}{\partial y_{\omega n1}}\right)\bar{r}\left(\frac{\partial\{u_E\}}{\partial y_{\omega n2}}\right)\bar{r}\rho_{y_{\omega n1}y_{\omega n2}}V_{y_{\omega n1}}V_{y_{\omega n2}}\bar{y}_{\omega n1}\bar{y}_{\omega n2}\right] + (0.15)^2\{\bar{u}^2_E\} \quad (4.42)$$

where

$$\frac{\partial\{u_L\}}{\partial y_{\omega n1}} = \frac{1}{u_L}\left[\{\Phi\}^2_{n1}\Gamma^2_{n1}y_{\omega n1}\right]; \quad (4.43)$$

$$\frac{\partial\{u_E\}}{\partial y_{\omega n2}} = \frac{1}{u_E}\left[\{\Phi\}^2_{n2}\Gamma^2_{n2}y_{\omega n2}\right]; \quad (4.44)$$

and 0.15 is assumed to be the dynamic analysis error. [50]

b. Combined Load Effect. After the uncertainties of dead, live, and earthquake load effect are individually obtained from previous knowledge, the uncertainties of combination of these load effects may be given as

mean,

$$\{\bar{u}\} = \{\bar{u}_D\} + \{\bar{u}_L\} + \{\bar{u}_E\} \quad (4.45)$$

(a) 1st variance approach,

$$\sigma^2_{\{u\}} = \sum_i\sum_j\left(\frac{\partial\{u\}}{\partial r_i}\right)\bar{r}\left(\frac{\partial\{u\}}{\partial r_j}\right)\bar{r}\rho_{r_ir_j}V_{r_i}V_{r_j}\bar{r}_i\bar{r}_j \quad (4.46)$$

where

$$\frac{\partial\{u\}}{\partial r_i} = \frac{\partial\{u_D\}}{\partial r_i} + \frac{\partial\{u_L\}}{\partial r_i} + \frac{\partial\{u_E\}}{\partial r_i} \quad (4.47)$$

(b) 2nd variance approach,

$$\sigma^2_{\{u\}} = \sigma^2_{\{u_D\}} + \sigma^2_{\{u_I\}} + \sigma^2_{\{u_E\}} + 2(0.1)^2\{\bar{u}_D\}\{\bar{u}_I\} \tag{4.48}$$

where 0.1 is the static analysis error.

For displacement failure mode, substituting Equations (4.45), (4.46), and (4.48) into Equations (2.6) or (2.15), then the probabilities of failure in Equations (2.4) or (2.8) can be determined if the statistics of allowable displacement are given.

2. Internal Forces.

a. Earthquake Load Effect. The internal force fomulations for the dead and live load are the same as the previous chapter. However, the dynamic seismic load effect considered here has a little difference from that. That is

mean,

$$\{\bar{F}_E\}_m = [\sum_n([S]_m[A]^T_m\{u_E\}_{mn})^2]^{1/2} \tag{4.49}$$

where $[S]_m$, $[A]^T_m$ are the same notations used in Equation (3.56); $\{u_E\}_{mn}$ = the seismic displacements for nth mode corresponding to the mth member

(a) 1st variance approach,

$$\sigma^2_{\{F_E\}_m} = \sum_i\sum_j(\frac{\partial\{F_E\}_m}{\partial r_i})_{\bar{r}}(\frac{\partial\{F_E\}_m}{\partial r_j})_{\bar{r}}\rho_{r_i r_j}V_{r_i}V_{r_j}\bar{r}_i\bar{r}_j \tag{4.50}$$

where

$$\frac{\partial\{F_E\}_m}{\partial r_i} = \frac{1}{(F_E)_m}[\sum_n([S]_m[A]^T_m\{u_E\}_{mn})$$

$$(\frac{\partial[S]_m}{\partial r_i}[A]^T_m\{u_E\}_{mn} + [S]_m[A]^T_m\frac{\partial\{u_E\}_{mn}}{\partial r_i})] \tag{4.51}$$

$$\frac{\partial\{F_E\}_m}{\partial r_j} = \frac{1}{(F_E)_m}[\sum_n([S]_m[A]_m^T\{u_E\}_{mn})$$

$$(\frac{\partial[S]_m}{\partial r_j}[A]_m^T\{u_E\}_{mn} + [S]_m[A]_m^T\frac{\partial\{u_E\}_{mn}}{\partial r_j}) \quad (4.52)$$

(b) 2nd variance approach,

$$\sigma^2_{\{F_E\}_m} = \sum_{n1}\sum_{n2}[(\frac{\partial\{F_E\}_{mn}}{\partial y_{\omega n1}})_{\bar{r}}(\frac{\partial\{F_E\}_{mn}}{\partial y_{\omega n2}})_{\bar{r}}\rho_{y_{\omega n1}y_{\omega n2}}V_{y_{\omega n1}}V_{y_{\omega n2}}\bar{y}_{\omega n1}\bar{y}_{\omega n2}]$$

$$+ (0.15)^2\{\bar{F}^2_{Em}\} \quad (4.53)$$

where

$$\frac{\partial\{F_E\}_m}{\partial y_{\omega n1}} = \frac{1}{(F_E)_m}[\sum_n([S]_m[A]_m^T\{u_E\}_{mn})([S]_m[A]_m^T\frac{\partial\{u_E\}_{mn}}{\partial y_{\omega n1}})]; \quad (4.54)$$

$$\frac{\partial\{F_E\}_m}{\partial y_{\omega n2}} = \frac{1}{(F_E)_m}[\sum_n([S]_m[A]_m^T\{u_E\}_{mn})([S]_m[A]_m^T\frac{\partial\{u_E\}_{mn}}{\partial y_{\omega n2}})]; \quad (4.55)$$

and 0.15 is assumed to be the dynamic analysis error.

b. Combined Load Effect. The internal forces due to dead, live, and earthquake load are given as a combination in the following.

mean,

$$\{\bar{F}\}_m = \{\bar{F}_D\}_m + \{\bar{F}_L\}_m + \{\bar{F}_E\}_m \quad (4.56)$$

(a) 1st variance approach,

$$\sigma^2_{\{F\}_m} = \sum_i\sum_j(\frac{\partial\{F\}_m}{\partial r_i})_{\bar{r}}(\frac{\partial\{F\}_m}{\partial r_j})_{\bar{r}}\rho_{r_ir_j}V_{r_i}V_{r_j}\bar{r}_i\bar{r}_j \quad (4.57)$$

where

$$\frac{\partial\{F\}_m}{\partial r_i} = \frac{\partial\{F_D\}_m}{\partial r_i} + \frac{\partial\{F_L\}_m}{\partial r_i} + \frac{\partial\{F_E\}_m}{\partial r_i} \tag{4.58}$$

$$\frac{\partial\{F\}_m}{\partial r_i} = \frac{\partial\{F_D\}_m}{\partial r_j} + \frac{\partial\{F_L\}_m}{\partial r_j} + \frac{\partial\{F_E\}_m}{\partial r_j} \tag{4.59}$$

(b) 2nd variance approach,

$$\sigma^2_{\{F\}_m} = \sigma^2_{\{F_D\}_m} + \sigma^2_{\{F_L\}_m} + \sigma^2_{\{F_E\}_m} + 2(0.1)^2\{\bar{F}_D\}_m\{\bar{F}_L\}_m \tag{4.60}$$

where 0.1 is assumed to be the static analysis error.

For column failure modes, sustituting Equations (4.56), (4.57), and (4.60), which may be the uncertainties of applied axial loads (P) or moments (M) into Equations (6.10), (6.12), (6.16), (6.17), (6.21), (6.22), (6.25), and (6.26) yields the means and variances of interaction equations. Substituting these statistics, the safety factors in Equations (2.6) or (2.15), and then the probabilities of failure in Equations (2.4) or (2.8) can be determined if the statistics of allowable values of interaction equations are given.

D. STRUCTURAL RESISTANCE

The structural resistances are (1) yield moment, (2) Euler buckling load, (3) axial load capacity of columns, (4) yield load, and (5) critical moment. The means and variances of these resistances which are the same notations in Section IIID are summarized as follows.

1. Yield Moment.

mean,

$$\bar{M}_y = \bar{F}_y\bar{S}_c$$

variance,

$$\sigma^2_{M_y} = (0.12)^2\ \bar{M}_y^2$$

2. Euler Buckling Load.

mean,

$$\bar{P}_E = \frac{\pi^2 E_m \bar{I}}{\overline{(KL)^2}}$$

variance,

$$\sigma^2_{P_E} = (0.3)^2 \bar{P}^2_E$$

3. Axial Load Capacity.

mean,

$$\bar{P}_{cr} = (1 - \bar{\lambda}^2/4)\bar{F}_y\bar{A}_c, \qquad \text{for } KL/r_g < C_c$$

or

$$\bar{P}_{cr} = \bar{P}_E, \qquad \text{for } KL/r_g > C_c$$

variance,

$$\sigma^2_{P_{cr}} = (V_{P_{cr}})^2 \bar{P}^2_{cr}$$

where $V_{P_{cr}}$ varies from 0.14 to 0.31.

4. Yield Load.

mean,

$$\bar{P}_y = \bar{F}_y\bar{A}_c$$

variance,

$$\sigma^2_{P_y} = (0.14)^2 \bar{P}^2_y$$

5. Critical Moment.

mean,

$$\bar{M}_{cr} = \{[\bar{C}_b\pi\frac{\bar{E}_m\bar{I}_y}{\bar{K}_y\bar{L}}][\frac{\bar{G}_s\bar{J}}{\bar{E}_m} + \frac{\pi^2\bar{C}_w}{(\bar{K}_z\bar{L})^2}]\}^2$$

variance,

$$\sigma^2_{M_{cr}} = (V_{M_{cr}})^2 \bar{M}^2_{cr}$$

where $V_{M_{cr}}$ varies from 0.15 to 0.2.

V. STRUCTURAL SYSTEM TO STATIONARY SEISMIC RANDOM PROCESSES.

A. LOADING

In addition to static equivalent load and dynamic seismic load, earthquake can also be modeled as stationary seismic random process. In this chapter a stationary seismic random process is introduced to analyze earthquake's phenominon. A stationary seismic process is a process whose statistical properties do not change with time and can be characterized by three classes of noise process: white noise, filter white noise, and modified white noise. These three random processes can be used to model phenomina of earthquake induced by ground motion and are described as follows :

1. White Noise Processes. A stationary process with a constant power spectral density for all frequencies, $G(\omega) = G_0$, is known as a white noise process which is described in Appendix E. The validity of using white noise approximations to simulate strong-motion earthquakes was examined by Bycroft. [18] It is shown in his study that a white noise process representation yields velocity spectra that compares favorably with the average velocity spectra of Housner [34] for actual earthquakes. These results, therefore, justified applicability of white noise processes to model earthquake's motions.

2. Filter White Noise Processes. According to the existing strong motion accelerograms, the considered frequency spectra are not constant even over a limited band but somewhat oscillatory in character, and may have peaks at one or several frequencies and damp out with increasing frequencies. Thus a stationary filter white noise process characterized by its transfer function could be more suitable to actual ground accelerograms. Hence, a second order linear damped oscillator suggested by Kanai [56] and Tajimi [86] will be an appropriate filter which is specified by the filter fundamental frequency, ω_g , and damping ratio, ζ_g , so that the resulting filtered motion has a statistically correct frequency constant. The filter which is used to simulate earthquake's motions has the form:

$$G(\omega) = \frac{\omega_g^2 + 4\zeta_g^2\omega_g^2\omega^2}{(\omega_g^2 - \omega^2)^2 + 4\zeta_g^2\omega_g^2\omega^2} G_0 \tag{5.1}$$

where G_0 is the constant power spectral density value; ω = frequency.

In general, the parameters ω_g and ζ_g are affected by the ground layer rigidity, the epicentral distance, and the earthquake magnitude. In Reference 46, it gave three sets values of ω_g and ζ_g to represent three types of soil conditions as

Soil Type	I	II	III
ω_g	8π	5π	2.4π
ζ_g	0.6	0.6	0.85

I - Rock or stiff soil conditions

II - Deep cohesionless soils

III - Soft to medium clays and sands

3. Modified White Noise Processes. A modified white noise process has a constant spectrum which is obtained by substituting structural natural frequency, ω_n, into the Kanai-Tajimi filter. As a result, the constant spectrum is obtained to be

$$G(\omega_n) = \frac{\omega_g^4 + 4\zeta_g^2\omega_g^2\omega_n^2}{(\omega_g^2 - \omega_n^2)^2 + 4\zeta_g^2\omega_g^2\omega_n^2} G_0 \tag{5.2}$$

In Reference 53, Housner and Jennings proposed possible values of $\omega_g = 15.6$ rad/ sec , $\zeta_g = 0.64$, and $G_0 = 1.0$ in^2/sec^3 for firm gound condition, based on the shape of an average pseudo-velocity response spectrum for eight accelerograms (two component each for four earthquakes).

B. STRUCTURAL RESPONSE

When a structural system is subjected to dead, live, and stationary seismic load, the randomness of structural responses is primarily due to the randomness of stationary seismic processes. Therefore the effect due to a stationary seismic load which is a zero mean Gaussian process is considered here. The response for a single degree system is illustrated first and then is extended to a multi-degree system.

1. Single Degree Freedom System. Let s(t) represent the displacement response of a single degree, viscously damped, linear oscillator to a stationary earthquake excitation a(t); in random vibration theory, the random function s(t) may be represented by a continuous superposition of sinusoids in a Fourier integral form as

$$s(t) = \int_{-\infty}^{\infty} G_s(\omega) e^{i\omega t} d\omega \tag{5.3}$$

where $G_s(\omega)$ is the response spectrum which has the following relationship to the excitation spectrum $G_a(\omega)$

$$G_s(\omega) = H(\omega) G_a(\omega) \tag{5.4}$$

In Equation (5.4), $H(\omega)$ = the transfer function of a structural system = $-1 / (\omega_n^2 - \omega^2 + 2i\zeta\omega_n\omega)$; ω_n = the structural natural frequency for nth mode; $i = \sqrt{-1}$.

The transfer function $H(\omega)$ is derived as following. The structural design system which is similar to Equation (4.6) can be formulated as

$$\ddot{s}(t) + 2\zeta\omega_n\dot{s}(t) + \omega_n^2 s(t) = -a(t) \tag{5.5}$$

Let $a(t) = \exp(i\omega t)$ and $s(t) = H(\omega) \exp(i\omega t)$, Equation (5.5) becomes

$$H(\omega) \exp(i\omega t)[-\omega^2 + 2i\zeta\omega_n\omega + \omega_n^2] = -\exp(i\omega t) \tag{5.6}$$

then $H(\omega)$ can be determined from Equation (5.6) as given in Equation (5.4).

Similar to Equation (5.3), an excitation process can be transformed into the excitation spectrum; through the transfer function the response spectrum can be determined from Equation (5.4); then the response spectrum can be transformed into the response process. The relationship between excitation and response is shown in Figure 4.

If the ground acceleration is a Gaussian process with mean-zero, the response process of a linear deterministic structural system to this excitation is also a Gaussian process with mean zero. Since a Gaussian process is completely specified by its first two order statistics (i.e., its mean and variance), the statistical quantities of interest in structural design are the moments of responses, λ_{sk}, which the cases with k = 0 and k = 2 have the physical meanings of mean square of response and of time derivative of response, and are defined by

$$\lambda_{sk} = \int_{-\infty}^{\infty} \omega^k G_{ss}(\omega) d\omega \ , \quad k = 0,1,2 \tag{5.7}$$

where λ_{sk} = the kth moments of the power spectral density function of s(t) about the frequency origin; and $G_{ss}(\omega)$ is the spectral density of the mean square of s(t) which is determined to be

$$G_{ss}(\omega) = \frac{1}{2\pi}\int_{-\infty}^{\infty} R_{ss}(\tau) \exp(-i\omega\tau) d\tau$$

$$= \frac{1}{2\pi}\int_{-\infty}^{\infty} \exp(-i\omega\tau) \int_{-\infty}^{\infty}\int_{-\infty}^{\infty} R_{aa}(\tau + \theta_1 - \theta_2)\, h(\theta_1)\, h(\theta_2)\, d\theta_1\, d\theta_2 d\tau$$

$$= \int_{-\infty}^{\infty} h(\theta_1) \exp(i\omega\theta_1) d\theta_1 \int_{-\infty}^{\infty} h(\theta_2) \exp(-i\omega\theta_2) d\theta_2$$

$$\frac{1}{2\pi}\int_{-\infty}^{\infty} R_{aa}(\tau + \theta_1 - \theta_2) \exp(-i\omega(\tau + \theta_1 - \theta_2)) d\tau$$

$$= H(\omega)H(-\omega)G_{aa}(\omega) = |H(\omega)|^2 G_{aa}(\omega) \tag{5.8}$$

in which $h(\theta_1)$, $h(\theta_2)$ are unit impulse response functions; $G_{ss}(\omega)$ = spectral density function of s(t); $R_{ss}(\tau)$ = autocorrelation of s(t); $G_{aa}(\omega)$ = spectral density function of a(t); $R_{aa}(\tau)$ = autocorrelation of a(t); for k = 0 and 2, the moments, λ_{sk}, have physical meanings as:

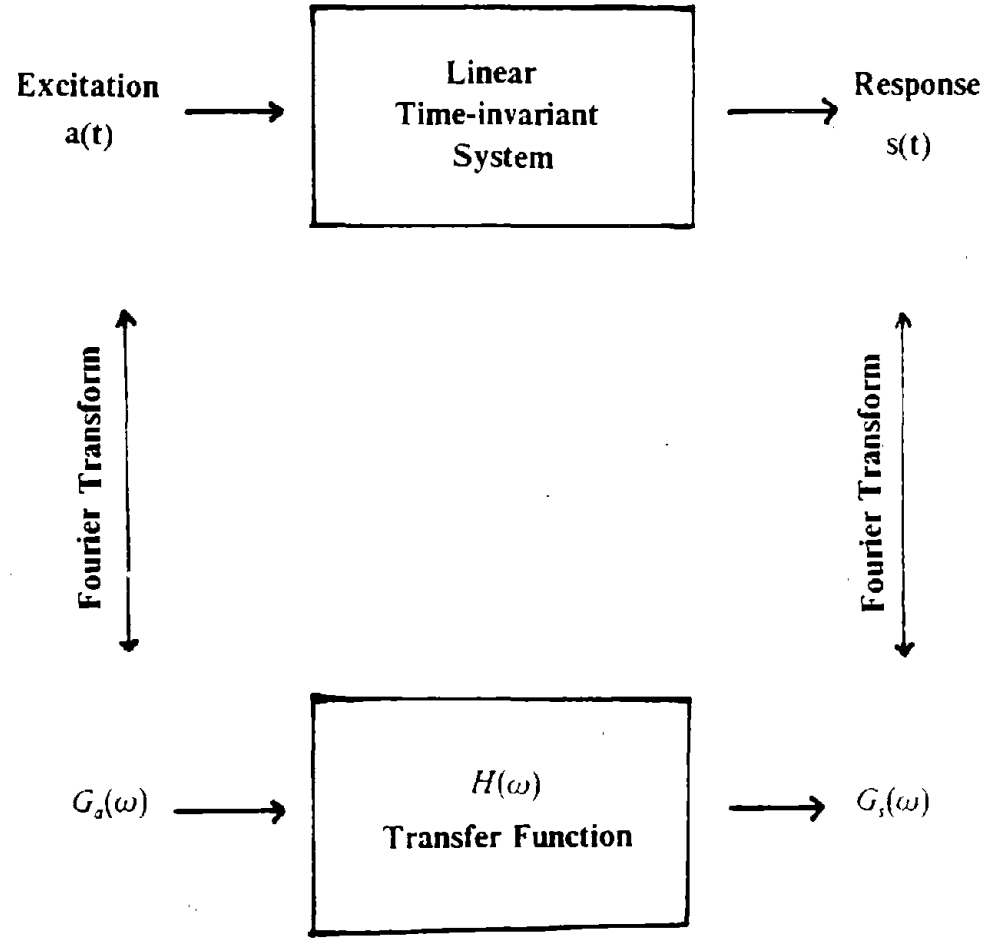

Figure 4. The Relationship Between Excitation Process And Response Process.

(i) k = 0,

$$\lambda_{s0} = \int_{-\infty}^{\infty} G_{ss}(\omega)d\omega \tag{5.9}$$

The autocorrelation of the response s(t) is

$$E[s(t)s(t+\tau)] = R_{ss}(\tau) = \int_{-\infty}^{\infty} G_{ss}(\omega)e^{i\omega\tau}d\omega \tag{5.10}$$

where τ = the time difference between two processes.

If τ is assumed to be a zero value, the above equation yields the variance

$$\sigma_s^2 = E[s^2(t)] = \int_{-\infty}^{\infty} G_{ss}(\omega)d\omega = \lambda_{s0} \tag{5.11}$$

Thus the zeroth moment of response, λ_{s0}, is the mean square value of response s(t).

(ii) k = 2,

$$\lambda_{s2} = \int_{-\infty}^{\infty} G_{ss}(\omega)\omega^2 d\omega \tag{5.12}$$

Since the first derivative of $R_{ss}(\tau)$ with respect to time difference gives

$$R'_{ss}(\tau) = \frac{dR_{ss}(\tau)}{d\tau} = E[\dot{s}(t)s(t-\tau)] , \tag{5.13}$$

taking the second derivative of $R_{ss}(\tau)$ with respect to τ yields

$$R''_{ss}(\tau) = -E[\dot{s}(t-\tau)\dot{s}(t)] = -R_{\dot{s}\dot{s}}(\tau) \tag{5.14}$$

From Equation (5.10), Equations (5.13) and (5.14) become

$$R'_{ss}(\tau) = \int_{-\infty}^{\infty} i\omega G_{ss}(\omega)\exp(i\omega\tau)d\omega \tag{5.15}$$

and

$$R''_{ss}(\tau) = \int_{-\infty}^{\infty} (i\omega)^2 G_{ss}(\omega) \exp(i\omega\tau) d\omega = \int_{-\infty}^{\infty} -\omega^2 G_{ss}(\omega) \exp(i\omega\tau) d\omega \tag{5.16}$$

If $\tau = 0$,

$$R_{\dot{s}\dot{s}}(0) = -R''_{ss}(0) = \int_{-\infty}^{\infty} \omega^2 G_{ss}(\omega) d\omega \tag{5.17}$$

Therefore the 2nd moment of response, λ_{s2}, is the mean square value of time derivative of the response.

After the relationship between response and earthquake excitation is determined, the displacements for a single degree system can be found as follows for three types of random seismic input spectra which are white noise spectrum, filter white noise spectrum, and modified white noise spectrum.

a. White Noise Processes. For a white noise seismic spectrum, the spectral density function $G(\omega)$ is a constsnt G_0. Then the spectral moments at nth mode are obtained as [60]

$$\lambda_{s0} = \int_{-\infty}^{\infty} G_{ss}(\omega) d\omega = \int_{-\infty}^{\infty} |H(\omega)|^2 G_{aa}(\omega) d\omega = G_0 \int_{-\infty}^{\infty} |H(\omega)|^2 d\omega$$

Substituting $H(\omega)$ which is seen in Equation (5.4) into the above equation yields

$$\lambda_{s0} = \frac{\pi G_0}{2\zeta\omega_n^3} \tag{5.18}$$

$$\lambda_{s1} = \int_{-\infty}^{\infty} \omega G_{ss}(\omega) d\omega = \int_{-\infty}^{\infty} \omega |H(\omega)|^2 G_{aa}(\omega) d\omega = G_0 \int_{-\infty}^{\infty} \omega |H(\omega)|^2 d\omega$$

$$= \left(\frac{\pi G_0}{2\zeta\omega_n^2}\right) \frac{1 - 2/\pi \tan^{-1}(\zeta/\sqrt{1-\zeta^2})}{\sqrt{1-\zeta^2}} \tag{5.19}$$

$$\lambda_{s2} = \int_{-\infty}^{\infty} \omega^2 G_{ss}(\omega) d\omega = \int_{-\infty}^{\infty} \omega^2 |H(\omega)|^2 G_{aa}(\omega) d\omega = G_0 \int_{-\infty}^{\infty} \omega^2 |H(\omega)|^2 d\omega$$

$$= \frac{\pi G_0}{2\zeta\omega_n} \tag{5.20}$$

b. Filter White Noise Processes.

In Reference 60 Kiureghian has derived the formulae for displacement moments for a filter white noise process. The moments of single degree displacements, λ_{s0}, λ_{s1}, λ_{s2} can be determined and used to find displacements and internal forces.

$$\lambda_{s0} = \int_{-\infty}^{\infty} G_{ss}(\omega)d\omega = \int_{-\infty}^{\infty} |H(\omega)|^2 G_{aa}(\omega)d\omega$$

$$= \int_{-\infty}^{\infty} \{(\omega_g^2 + 4\zeta_g^2\omega_g^2\omega^2)/[(\omega_g^2 - \omega^2)^2 + 4\zeta_g^2\omega_g^2\omega^2]G_0\}d\omega \tag{5.21}$$

$$\lambda_{s1} = \int_{-\infty}^{\infty} \omega G_{ss}(\omega)d\omega \tag{5.22}$$

$$\lambda_{s2} = \int_{-\infty}^{\infty} \omega^2 G_{ss}(\omega)d\omega \tag{5.23}$$

The integration results of λ_{s0}, λ_{s1}, λ_{s2} are given in Appendix F.

c. Modified White Noise Processes. Similar to white noise processes case, the moments of s(t) are obtained by a constant Kanai-Tajimi spectrum with the structural natural frequency.

$$\lambda_{s0} = \int_{-\infty}^{\infty} G_{ss}(\omega_n)d\omega = \int_{-\infty}^{\infty} |H(\omega)|^2 G_{aa}(\omega_n)d\omega$$

$$= \int_{-\infty}^{\infty} \{(\omega_g^2 + 4\zeta_g^2\omega_g^2\omega^2)/[(\omega_g^2 - \omega_n^2)^2 + 4\zeta_g^2\omega_g^2\omega_n^2]G_0\}d\omega$$

$$= \left(\frac{\pi G_0}{2\zeta\omega_n^3}\right)\left(\frac{\omega_g^4 + 4\zeta_g^2\omega_g^2\omega_n^2}{(\omega_g^2 - \omega_n^2)^2 + 4\zeta_g^2\omega_g^2\omega_n^2}\right) \tag{5.24}$$

$$\lambda_{s1} = \int_{-\infty}^{\infty} \omega G_{ss}(\omega_n) d\omega$$

$$= \left(\frac{\pi G_0}{2\zeta\omega_n^2}\right) \frac{1 - 2/\pi \tan^{-1}(\zeta/\sqrt{1-\zeta^2})}{\sqrt{1-\zeta^2}} \left(\frac{\omega_g^4 + 4\zeta_g^2\omega_g^2\omega_n^2}{(\omega_g^2 - \omega_n^2)^2 + 4\zeta_g^2\omega_g^2\omega_n^2}\right) \tag{5.25}$$

$$\lambda_{s2} = \int_{-\infty}^{\infty} \omega^2 G_{ss}(\omega_n) d\omega$$

$$= \left(\frac{\pi G_0}{2\zeta\omega_n}\right) \left(\frac{\omega_g^4 + 4\zeta_g^2\omega_g^2\omega_n^2}{(\omega_g^2 - \omega_n^2)^2 + 4\zeta_g^2\omega_g^2\omega_n^2}\right) \tag{5.26}$$

2. Multidegree Structural System. Based on normal mode method, the displacements and internal forces of a multidegree system can be obtained by the superposition of equations for a single degree system as follows:

a. Displacement. Let u(t) be the displacement matrix of multidegree system, then

$$\{u(t)\} = \sum_n \{\Phi\}_n \Gamma_n s_{\omega_n} \tag{5.27}$$

and the spectrum of u(t), $G_u(\omega)$, is expressed as

$$G_u(\omega) = \frac{1}{2\pi}\int_{-\infty}^{\infty} R_u(0) d\tau = \sum_n \{\Phi\}_n \Gamma_n \frac{1}{2\pi}\int_{-\infty}^{\infty} R_s(0) d\tau$$

$$= \sum_n \{\Phi\}_n \Gamma_n G_s(\omega) = \sum_n \{\Phi\}_n \Gamma_n H_n(\omega) G_a(\omega) \tag{5.28}$$

where $\{\Phi\}_n$ and Γ_n are the mode shape and the participation factor; s_{ω_n} = the displacement for a single degree system. The system transfer function $\{H_u(\omega)\}$ and the spectral density of displscement $\{G_{uu}(\omega)\}$[88] are given by

$$\{H_u(\omega)\} = \sum_n \{\Phi\}_n \Gamma_n H_n(\omega) \tag{5.29}$$

and

$$\{G_{uu}(\omega)\} = G_{aa}(\omega)H_u(\omega)H_{u'}(-\omega)$$

$$= G_{aa}(\omega)\sum_n\sum_{n'}\{\Phi\}_n\{\Phi\}_{n'}\Gamma_n\Gamma_{n'}H_n(\omega)H_n^*(\omega) \tag{5.30}$$

where $H_n(\omega)$ = the transfer function for the nth mode; $G_{aa}(\omega)$ = the spectral density of mean square earthquake excitation; H_n^* = the complex conjugate of $H_n(\omega)$. For lightly damped systems whose model frequencies are well separated, the terms of all cross-spectral contributions over $G_{uu}(\omega)$ may be negligible. The moments of displacements are determined as

$$\lambda_{u0} = \int_{-\infty}^{\infty} G_{uu}(\omega)d\omega = \sum_n\{\Phi^2\}_n\Gamma_n^2\int_{-\infty}^{\infty}|H_n(\omega)|^2G_{aa}(\omega)d\omega = \sum_n\{\Phi^2\}_n\Gamma_n^2\lambda_{s0} \tag{5.31}$$

$$\lambda_{u1} = \int_{-\infty}^{\infty}\omega G_{uu}(\omega)d\omega = \sum_n\{\Phi^2\}_n\Gamma_n^2\lambda_{s1} \tag{5.32}$$

$$\lambda_{u2} = \int_{-\infty}^{\infty}\omega^2 G_{uu}(\omega)d\omega = \sum_n\{\Phi^2\}_n\Gamma_n^2\lambda_{s2} \tag{5.33}$$

For displacement failure mode, substituting Equations (5.31) and (5.33) into Equation (2.28), and then the probability of failure in Equation (2.30) can be determined if deterministic allowable displacement is given.

b. Internal Force. Let $\{F\}_m$ be the forces matrix for mth member, these forces can be determined from the displacements by $\{F\}_m = [S]_m[A]_m^T\ \{u\}_m = [SAT]_m\ \{u\}_m$, where $[S]_m$, $[A]_m^T$, $\{u\}_m$ are the same notations in Chapter III, and $[SAT]_m = [S]_m[A]_m^T$. Since matrices $[S]_m$ and $[A]_m^T$ are the deterministic values, the moments of internal forces can be derived from the above relation by

$$\lambda_{0\{F\}_m} = \int_{-\infty}^{\infty} G_{FF}(\omega)d\omega = [SAT^2]\int_{-\infty}^{\infty} G_{uu}(\omega)d\omega$$

$$= [SAT^2]_m\lambda_{\{u0\}_m} \tag{5.34}$$

$$\lambda_{1\{F\}_m} = [SAT^2]_m\lambda_{\{u1\}_m} \tag{5.35}$$

$$\lambda_{2\{F\}_m} = [SAT^2]_m \lambda_{\{u2\}_m} \tag{5.36}$$

For column failure modes substituting Equations (5.34) and (5.36) which may be the applied axial load (P) or moment (M) into Equations (6.28), (6.30), (6.32), and (6.34), they yield the values of σ_s and $\sigma_{\dot{s}}$ for interaction equations. Substituting the standard deviations of s and ṡ into Equation (2.28), then the probabilities of can be determined from Equation (2.30) if the deterministic allowable values of interaction equations are known.

C. THE STATISTICS OF PEAK RESPONSES

If the uncertainties of peak responses for random loads can be found, the probability of failure for a first-order second moment expression can still be chosen for criterion. Two expressions to respresent the statistics of peak responses are given as follows. These statistics can be used to calculate the means and variances of responses in the safety factor expression. Therefore, the probability of failure can be determined.

1. Davenport's Expression. Davenport [39] derived the mean and standard deviation of the maximum absolute value of a stationary zero-mean Gaussian process s(t) over duration based on results obtained by Cartwright and Longuet- Higgins and Rice. [19,75]

mean,

$$\bar{s}_{max} = \int_{-\infty}^{\infty} s_{max} P_{smax}(s_{max})\, ds_{max} \tag{5.37}$$

standard deviation,

$$\sigma_{s_{max}} = [\overline{s^2_{max}} - \bar{s}^2_{max}]^{1/2} \tag{5.38}$$

In Reference 39, the values of $P_{smax}(s_{max})\, ds_{max}$ and s_{max} were given by

$$P_{smax}(s_{max})ds_{max} = \exp(-\xi)d\xi \tag{5.39}$$

and

$$s_{max} = \sqrt{(2\ln \nu T_0)} - \frac{\ln \xi}{\sqrt{2\ln \nu T_0}} - \frac{1}{2}\frac{\ln \xi}{\sqrt{2\ln \nu T_0}} + \ldots\ldots \tag{5.40}$$

where $\xi = \nu T_0 \exp(-s^2/2)$, T_0 = a duration, and $\nu = (\lambda_{s2}/\lambda_{s0})/\pi$. λ_{s0} is given in Equations (5.31) and (5.34) for displacements and internal forces and λ_{s2} is given in Equations (5.33) and (5.36) for displacements and internal forces. Thus, the mean square value of s_{max} is found to be

$$\overline{s_{max}^2} = \int_{-\infty}^{\infty} s_{max}^2 \exp(-\xi) d\xi \tag{5.41}$$

By substituting Equations (5.39), (5.40), and (5.41) into Equations (5.37) and (5.38), the uncertainties become

$$\bar{s}_{max} = (\sqrt{(2\ln \nu T_0)} + \frac{0.5772}{\sqrt{2 \ln \nu T_0}})\sigma_s \tag{5.42}$$

$$\sigma_{s_{max}} = [(\frac{\pi}{\sqrt{6}})(\frac{1}{\sqrt{2 \ln \nu T_0}})]\sigma_s \tag{5.43}$$

where σ_s is given in Equations (5.31) or (5.34) depending on the analysis of displacements or internal forces.

For displacement failure mode, substituting Equations (5.31) and (5.33) into Equations (5.42) and (5.43) yields the values of mean and standard deviation of s_{max}; then, the safety factors in Equations (2.6) or (2.15) or probabilities of failure in Equations (2.4) or (2.8) can be determined if the deterministic allowable displacements are given.

For column failure modes, substituting Equations (5.34) and (5.36) which may be applied axial loads (P) or applied moments (M) into Equations (5.42) and (5.43) yields the values of mean and standard deviation of s_{max}; then substituting these values into Equations (6.27) through (6.34), the safety factors in Equations (2.6) or (2.15) or probabilities of failure in

Equations (2.4) or (2.8) can be determined if the deterministic allowable values of interaction equations are known.

2. Kiureghian's Expression. By modifying Davenport's expression Kiureghian [60] derived the following empirical expressions for the uncertainties of peak reponses as follows.

mean,

$$\bar{s}_{max} = (\sqrt{(2\ln \nu_e T_0)} + \frac{0.5772}{\sqrt{2 \ln \nu_e T_0}})\sigma_s \tag{5.44}$$

standard deviation,

$$\sigma_{s_{max}} = [\frac{1.2}{\sqrt{2 \ln \nu_e T_0}} - \frac{5.4}{13 + (\sqrt{2 \ln \nu_e T_0})^{6.4}}]\sigma_s , \quad \nu_e T_0 > 2.1 \tag{5.45}$$

$$\sigma_{s_{max}} = 0.65\sigma_s , \quad \nu_e T_0 \leq 2.1 \tag{5.46}$$

where

$$\nu_e = (1.63q^{0.45} - 0.38)\nu , \quad q < 0.69 \tag{5.47}$$

$$q = \sqrt{1 - \lambda_{s1}^2/\lambda_{s0}\lambda_{s2}} , \quad q \geq 0.69 \tag{5.48}$$

For displacement failure mode, substituting Equations (5.31), (5.32), and (5.33) into Equations (5.45) and (5.46) yields the values of mean and standard deviation of s_{max}; then, the safety factors in Equations (2.6) or (2.15) or probabilities of failure in Equations (2.4) or (2.8) can be determined if the deterministic allowable displacements are given.

For column failure modes, substituting Equations (5.34), (5.35), and (5.36) which may be applied axial load (P) or applied moment (M) into Equations (5.44), (5.45) and (5.46) yields the values of mean and standard deviation of s_{max}; then substituting these values into Equations (6.27) through (6.34), the safety factors in Equations (2.6) or (2.15) or probabilities of failure in Equations (2.4) or (2.8) can be determined if the deterministic allowable values of interaction equations are given.

D. STRUCTURAL RESISTANCE

Since the structural system considered here is deterministic, the structural resistances are all deterministic values as well. The structural resistances which are the same notations in Section IIID are

1. Yield Moment.

$$M_y = F_y S_c$$

2. Euler Buckling Load.

$$P_E = \frac{\pi^2 E_m I}{(KL)^2}$$

3. Axial Load Capacity.

$$P_{cr} = (1 - \lambda^2/4) F_y A_c, \qquad \text{for } KL/r_g < C_c$$

or

$$P_{cr} = P_E, \qquad \text{for } KL/r_g > C_c$$

4. Yield Load.

$$P_y = F_y A_c$$

5. Critical Moment.

$$M_{cr} = \{[C_b \pi \frac{E_m I_y}{K_y L}][\frac{G_s J}{E_m} + \frac{\pi^2 C_w}{(K_z L)^2}]\}^2$$

VI. OPTIMIZATION FORMULATIONS AND ALGORITHMS

A. OPTIMIZATION FORMULATIONS

In engineering optimum design, the goal is to produce a best solution which provides not only a safety but also a best objective value. An optimum strurctural problem can be formulated as:

minimize objective function

subject to constraints

1. Objective Function. The objective function of a structural design problem may be weight or cost function which are

a. Weight. Weight (W) is the constituents of structural member weights and can be expressed as

$$W = \sum_i r_{di} \ell_i A_i \tag{6.1}$$

where r_{di}, ℓ_i, A_i = the mass density, length, and area of a member, respectively.

b. Cost. Total estimated structural cost (C_T) which is shown in Figure 5 consists of two parts: the initial construction cost (C_I) and the expected future failure loss ($L_f P_{fT}$); i.e.,

$$C_T = C_I + L_f P_{fT} \tag{6.2}$$

where L_f = expected failure cost; P_{fT} = system failure probability.

Initial construction cost C_I comprises of the structural material cost and the miscellaneous cost. The structural material cost is the cost of structural members. The miscellaneous cost may be the product of total unit floor price shown in Table I [43] and total area. The expected future loss has two components: the expected failure cost (L_f) and the system probability of failure (P_{fT}).

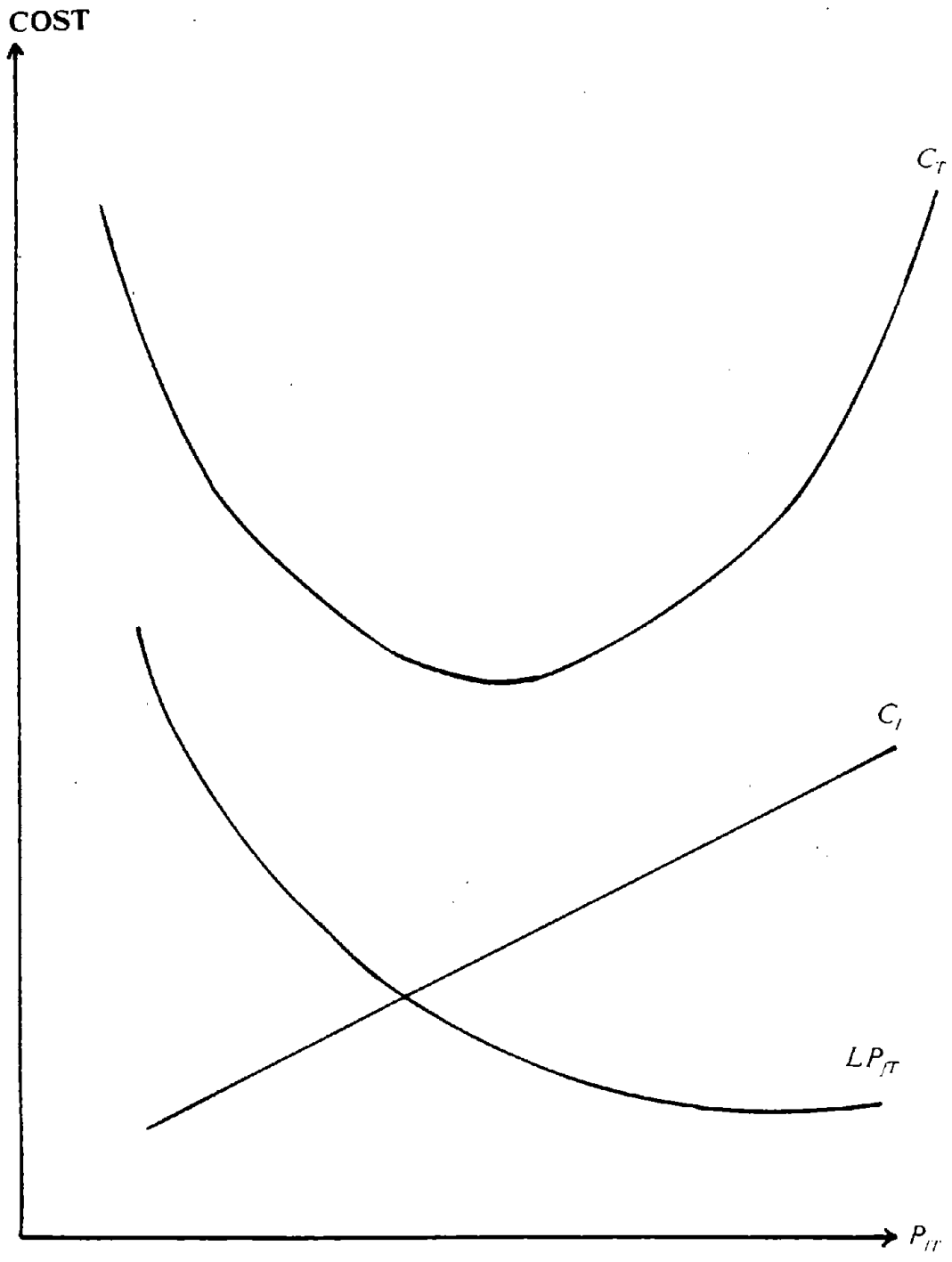

Figure 5. Cost vs System Probability of Failure.

Table I. UNIT FLOOR COST FOR OFFICE BUILDING

	Average $/SF
Foundation	2.27
Exterior walls	5.96
Partitions	3.07
Interior wall finishes	1.36
Floor finishes	1.22
Ceilings	0.99
Specialties	0.38
Conveying systems	0.56
Plumbing	2.13
Fire protection	0.27
HVAC	6.20
Electrical	3.99
General conditions	2.20
Equipment	0.69
Site work	2.00
total	33.29

The expected failure cost (L_f) is the total loss incurred in a structural failure state. This includes an additional replacement cost, damage to property, liabilities due to death and injury, and business interruption. They are estimated based on the following assumptions: The additional replacement cost is taken to be two times of initial structural cost. [77] The loss due to property damage in which no loss of expensive equipments is assumed as 50% of the initial construction cost.[52] Liabilities due to death and injury include only the people present in the building failure. Loss due to death is calculated based on an average death age of 30 and is the sum of the person's salary until he reaches the retirement age of 65 years. Thus, this loss is 35 times the average annual net income. [52] The loss due to serious injuries is assumed to be $350,000 per person. [77] The loss due to minor injury is $5,000 per person. Business interruption is estimated as the income of the employees during a 4-year reconstruction period. The loss due to legal service may be assumed to be 15 % of the failure loss.[85]

The estimation of a system failure probability is approximated by Equation (2.36) which is expressed as

$$P_{fT} = \sum_{i=1}^{nf} P_{fj} \tag{6.3}$$

where nf = the number of failure modes.

2. Constraints. In a structural design one requires the probabilities of desired response failures less than the the allowable probabilities of failures or the safety factors for those failures greater than the allowable values. These requirements become the constraints in optimum structural design problems. The desired response failures may be displacment failures, column failures, and beam failures which are described as follows. In addition to the above individual failure mode constraints, the system failure probability which is less than the allowable probability value can also be added to the constraints.

In the following the safety factor with normal distribution and probability of failure, which are Equations (2.6) and (2.4), respectively, are used to illustrate the formulations for various failure modes.

a. displacement failure. A structural failure due to an excessive displacement may be expresse as β_u or $P_f(\beta_u)$ which is the safety factor or probability of failure. The safety factor has the form

$$\beta_u = \frac{\bar{u} - \bar{u}_a}{\sqrt{\sigma_u^2 + \sigma_{ua}^2}} \tag{6.4}$$

where $\bar{u}, \sigma_u^2$ = the mean and variance of a displacement; $\bar{u}_a, \sigma_{ua}^2$ = the mean and variance of allowable displacement.

Thus, the probability of failure is

$$P_f(\beta_u) = 1 - PN(\beta_u) \tag{6.5}$$

b. beam failure. Beam may fail in a number of different modes. However it is assumed that the beam fails when the applied moment exceeds the flexural yield capacity of beam, i.e., β_M or $P_f(\beta_M)$. The safety factor is

$$\beta_M = \frac{\overline{M} - \overline{M}_y}{\sqrt{\sigma_M^2 + \sigma_{M_y}^2}} \tag{6.6}$$

where $\overline{M}, \sigma_{Mx}^2$ = the computed mean and variance of moment; $\overline{M}_y, \sigma_{M_y}^2$ = the mean and variance of allowable yielding moment.

c. column failure. Four cases may occur in column failure. The representations of them are

1) failure by yielding at the ends, f_1

The safety factor and probability of failure in this case may be expressed as β_{f_1} or $P_f(\beta_{f_1})$. Thus

$$\beta_{f_1} = \frac{1.0 - \bar{f}_1}{\sqrt{\sigma_{f_1}^2}} \tag{6.7}$$

$$P_{f_1} = 1 - PN(\beta_{f_1}) \tag{6.8}$$

where

$$f_1 = \frac{P}{P_y} + \frac{M}{M_y} \tag{6.9}$$

where P = applied axial load; M = applied moment at one end of the column; P_y = yield axial load; M_y = yield moment.

To determine the safety factor and probability of failure the mean and variance of f_1 are needed. These uncertainties can be determined from Equations (2.16) and (2.18). They are mean,

$$\bar{f}_1 = \frac{\bar{P}}{\bar{P}_y} + \frac{\bar{M}}{\bar{M}_y} \tag{6.10}$$

variance,

$$\sigma_{f_1}^2 = (\frac{\partial f_1}{\partial P})^2 V_P^2 \bar{P}^2 + (\frac{\partial f_1}{\partial P_y})^2 V_{P_y}^2 \bar{P}_y^2 + (\frac{\partial f_1}{\partial M})^2 V_M^2 \bar{M}^2$$

$$+ (\frac{\partial f_1}{\partial M_y})^2 V_{M_y}^2 \bar{M}_y^2 + 2(\frac{\partial f_1}{\partial P_y})(\frac{\partial f_1}{\partial M_y}) \rho_{P_y M_y} V_{M_y} V_{P_y} \bar{P}_y \bar{M}_y$$

$$= (\frac{1}{P_y})^2 V_P^2 \bar{P}^2 + (\frac{-P}{P_y^2})^2 V_{P_y}^2 P_y^2 + (\frac{1}{M_y})^2 V_M^2 \bar{M}^2 + (\frac{-M}{M_y^2})^2 V_{M_y}^2 M_y^2$$

$$+ 2(\frac{\bar{P}}{\bar{P}_y})(\frac{\bar{M}}{\bar{M}_y}) \rho_{P_y M_y} V_{P_y} V_{M_y} \tag{6.11}$$

$$= (\frac{\bar{P}}{\bar{P}_y})^2 (V_P^2 + V_{P_y}^2) + (\frac{\bar{M}}{\bar{M}_y})^2 (V_M^2 + V_{M_y}^2) + 2(\frac{\bar{P}}{\bar{P}_y})(\frac{\bar{M}}{\bar{M}_y}) \rho_{P_y M_y} V_{P_y} V_{M_y} \tag{6.12}$$

where $\bar{P}, \bar{P}_y, V_P, V_{P_y}$ = the means and coefficients of variation of P and P_y; $\rho_{P_y M_y}$ = the correlation coefficient of P_y and M_y; The value of $\rho_{P_y M_y}$ is assumed to be 0.70 in the study.

2) instability in the plane of bending, f_2

The safety factor and probability of failure may be expressed as β_{f_2}, $P_f(\beta_{f_2})$. Thus

$$\beta_{f_2} = \frac{1.0 - \bar{f}_2}{\sqrt{\sigma_{f_2}^2}} \tag{6.13}$$

$$P_f(\beta_{f_2}) = 1 - PN(\beta_{f_2}) \tag{6.14}$$

where

$$f_2 = \frac{P}{P_{cr}} + \frac{M}{M_y(1 - P/P_E)} \tag{6.15}$$

where P_{cr} = critical axial load; P_E = Euler buckling load.

The mean and variance of f_2 which can be determined from Equations (2.16) and (2.18) are

mean,

$$\bar{f}_2 = \frac{\bar{P}}{\bar{P}_{cr}} + \frac{\bar{M}}{(1 - \bar{P}/\bar{P}_E)\bar{M}_y} \tag{6.16}$$

variance,

$$\sigma_{f_2}^2 = \left(\frac{\bar{P}}{\bar{P}_{cr}} + \frac{\bar{M}}{(1 - \bar{P}/\bar{P}_E)^2\bar{M}_y}\frac{\bar{P}}{\bar{P}_E}\right)^2 V_P^2 + \left(\frac{\bar{P}}{\bar{P}_{cr}}\right)^2 V_{P_{cr}}^2 + \left(\frac{\bar{M}}{(1 - \bar{P}/\bar{P}_E)^2\bar{M}_y}\frac{\bar{P}}{\bar{P}_E}\right)^2 V_{P_E}^2$$

$$+ \left(\frac{\bar{M}}{(1 - \bar{P}/\bar{P}_E)\bar{M}_y}\right)^2 (V_{M_y} + V_M^2) + 2\left(\frac{\bar{P}}{\bar{P}_{cr}}\right)\left(\frac{\bar{M}}{(1 - \bar{P}/\bar{P}_E)^2\bar{M}_y}\frac{\bar{P}}{\bar{P}_E}\right)\rho_{P_{cr}P_E} V_{P_{cr}} V_{P_E}$$

$$+ 2\left(\frac{\bar{P}}{\bar{P}_{cr}}\right)\left(\frac{\bar{M}}{(1 - \bar{P}/\bar{P}_E)\bar{M}_y}\right)\rho_{P_{cr}M_y} V_{P_{cr}} V_{M_y}$$

$$+2\left(\frac{\overline{M}}{(1-\overline{P}/\overline{P}_E)\overline{M}_y}\right)\left(\frac{\overline{M}}{(1-\overline{P}/\overline{P}_E)^2\overline{M}_y}\frac{\overline{P}}{\overline{P}_E}\right)\rho_{P_{M_y}}P_E V_{M_y} V_{P_E} \tag{6.17}$$

where $\overline{P}_{cr}, \overline{P}_E, V_{P_{cr}}, V_{P_E}$ = the means and coefficients of variation of P_{cr} and P_E; $\rho_{P_{cr}P_E}$, $\rho_{P_{cr}M_y}, \rho_{P_E M_y}$ = the correlation coefficients of P_{cr} and P_E, P_{cr} and M_y, M_y and P_E.

3) lateral torsional buckling f_3

The safety factor and probability of failure may be expressed as β_{f_3} or $P_f(\beta_{f_3})$. Thus

$$\beta_{f_3} = \frac{1.0 - \bar{f}_3}{\sqrt{\sigma^2_{f_3}}} \tag{6.18}$$

$$P_{f_3} = 1 - PN(\beta_{f_3}) \tag{6.19}$$

and

$$f_3 = \frac{P}{P_{cr}} + \frac{M}{M_{cr}(1 - P/P_E)} \tag{6.20}$$

M_{cr} = critical moment.

The mean and variance of f_3 which can be determined from Equations (2,16) and (2,18) are

mean,

$$\bar{f}_3 = \frac{\overline{P}}{\overline{P}_{cr}} + \frac{\overline{M}}{\overline{M}_{cr}(1 - \overline{P}/\overline{P}_E)} \tag{6.21}$$

variance,

$$\sigma^2_{f_3} = \left(\frac{\overline{P}}{\overline{P}_{cr}} + \frac{\overline{M}}{(1-\overline{P}/\overline{P}_E)^2\overline{M}_{cr}}\frac{\overline{P}}{\overline{P}_E}\right)^2 V^2_P + \left(\frac{\overline{P}}{\overline{P}_{cr}}\right)^2 V^2_{P_{cr}} + \left(\frac{\overline{M}}{(1-\overline{P}/\overline{P}_E)^2\overline{M}_{cr}}\frac{\overline{P}}{\overline{P}_E}\right)^2 V^2_{P_E}$$

$$+ \left(\frac{\overline{M}}{(1-\overline{P}/\overline{P}_E)\overline{M}_{cr}}\right)^2 (V_{M_{cr}} + V^2_M) + 2\left(\frac{\overline{P}}{\overline{P}_{cr}}\right)\left(\frac{\overline{M}}{(1-\overline{P}/\overline{P}_E)^2\overline{M}_{cr}}\frac{\overline{P}}{\overline{P}_E}\right)\rho_{P_{cr}P_E} V_{P_{cr}} V_{P_E}$$

$$+2\left(\frac{\bar{P}}{\bar{P}_{cr}}\right)\left(\frac{\bar{M}}{(1-\bar{P}/\bar{P}_E)\bar{M}_{cr}}\right)\rho_{P_{cr}M_{cr}}V_{P_{cr}}V_{M_{cr}}$$

$$+2\left(\frac{\bar{M}}{(1-\bar{P}/\bar{P}_E)\bar{M}_{cr}}\right)\left(\frac{\bar{M}}{(1-\bar{P}/\bar{P}_E)^2\bar{M}_{cr}}\frac{\bar{P}}{\bar{P}_E}\right)\rho_{M_{cr}P_E}V_{M_{cr}}V_{P_E} \qquad (6.22)$$

where $\bar{M}_{cr}$, $V_{M_{cr}}$ = the mean and coefficient of variation of M_{cr}; $\rho_{P_{cr}P_E}$, $\rho_{P_{cr}M_{cr}}$, $\rho_{P_EM_{cr}}$ = the correlation coefficients of P_{cr} and P_E, P_{cr} and M_{cr}, M_{cr} and P_E.

4) bucking about the weak axis, f_4

The safety factor and probability of failure may be expressed as β_{f_4} and $P_f(\beta_{f_4})$. Thus

$$\beta_{f_4} = \frac{1.0-\bar{f}_4}{\sqrt{\sigma^2_{f_4}}} \qquad (6.23)$$

where

$$f_4 = \frac{P}{P_{cry}} \qquad (6.24)$$

where P_{cr_y} = the critical axial load capacity at weak axis.

The mean and variance of f_4 which can be determined from Equations (2.16) and (2.18) are

mean,

$$\bar{f}_4 = \frac{\bar{P}}{\bar{P}_{cry}} \qquad (6.25)$$

variance,

$$\sigma^2_{f_4} = \left(\frac{\bar{P}}{\bar{P}_{cr}}\right)^2(V_P^2 + V^2_{P_{cry}}) \qquad (6.26)$$

where $\bar{P}_{cry}$, $V_{P_{cry}}$ = the mean and coefficient of variation of P_{cry}.

In the random load cases, the structural resistances are deterministic. Thus the uncertainties of interaction equations for column members are only due to the uncertainties of structural responses which are

(1) f_1

mean,

$$\bar{f}_1 = \frac{\bar{P}}{P_y} + \frac{\bar{M}}{M_y} \tag{6.27}$$

variance,

$$\sigma^2_{f_1} = \frac{1}{P_y^2}\sigma^2_{\bar{P}} + \frac{1}{M_y^2}\sigma^2_{\bar{M}} \tag{6.28}$$

(2) f_2

mean,

$$\bar{f}_2 = \frac{\bar{P}}{P_{cr}} + \frac{\bar{M}}{(1 - \bar{P}/P_E)M_y} \tag{6.29}$$

variance,

$$\sigma^2_{f_2} = \left(\frac{1}{P_{cr}} + \frac{\bar{M}}{(1 - \bar{P}/P_E)^2 M_y}\frac{1}{P_E}\right)^2\sigma^2_{\bar{P}} + \left(\frac{1}{(1 - \bar{P}/P_E)^2 M_y}\right)^2\sigma^2_{\bar{M}} \tag{6.30}$$

(3) f_3

mean,

$$\bar{f}_3 = \frac{\bar{P}}{P_{cr}} + \frac{\bar{M}}{(1 - \bar{P}/P_E)M_{cr}} \tag{6.31}$$

variance,

$$\sigma^2_{f_3} = \left(\frac{1}{P_{cr}} + \frac{\bar{M}}{(1 - \bar{P}/P_E)^2 M_{cr}}\frac{1}{P_E}\right)^2\sigma^2_{\bar{P}} + \left(\frac{1}{(1 - \bar{P}/P_E)^2 M_{cr}}\right)^2\sigma^2_{\bar{M}} \tag{6.32}$$

(4) f_4

mean,

$$\bar{f}_4 = \frac{\bar{P}}{P_{cry}} \tag{6.33}$$

variance,

$$\sigma^2_{\bar{f}_4} = (\frac{1}{P_{cry}})^2 \sigma^2_{\bar{P}} \tag{6.34}$$

where P_y , M_y , P_{cr} , P_E , M_{cr} , P_{cr_y} are deterministic values; $\sigma^2_{\bar{P}}$ and $\sigma^2_{\bar{M}}$ are the variance of applied axial forces and moments.

After the objective function and constraints are decided, the next step is to use an optimization algorithm to solve the formulated problem. The optimization algorithm may be classified into two classes: mathematical programing method and optimality criterion method.

B. PENALTY FUNCTION METHOD

The penalty function method is one of the mathematical programming techniques which is used to search the best moving route of design variables and to reduce the objective functional value untill no objective functional value can further be minimized; the procedure is then terminated where an optimum solution is obtained. In this study, interior penalty function method is used.

Since objective function or constraints may be nonlinear, an optimum structural design becomes a nonlinear programming problem. There are many search techniques used in the nonlinear programming; among them penalty function is a procedure for approximating constrained optimization formulation by sequently unconstrained problem. The approximation is accomplished by adding to the objective function a term that prescribes a high penalty value for violation of constraints. Associated with this method is a penalty parameter, r_p, which determines the severity of the penalty and, consequently, the degree to which the unconstrained

formulation approximates the original constrained problem. As r_p approaches zero, the approximation increasingly approaches to a solution which is closer to the actual solution.

The method considered leads the intermediate solution during the search to lying in a feasible region and converging to the optimal solution from the interior of acceptable domain. The advantage is that one may stop the search at any time and ends up with a feasible and suboptimal but less critical design. A drawback is that the initial point should start in the feasible region which may be difficult to determine.

The formulation of the method can be defined as

$$P_p(X^k, r_p^k) = O(X^k) - r_p^k \sum_j 1/g_j^k , \qquad g_j^k \le 0 \tag{6.35}$$

where $P_p(X^k, r_p^k)$ = penalty function; $O(X^k)$ = objective function; X^k = design variables; r_p^k = a penalty value; g_j = jth constraint; k = the number of completed stages for the subsequent change of penalty values r_p^k.

At an interior point, the sum of the inversing constraints in penalty term is negative, and a positive r_p^k will result in a positive penalty term to be added to objective function. As a boundary of the feasible region is reached, some constraints will approach zero and the inverse of constraints will approach infinity. By successively reducing the parameter r_p^k, the optimal solution for the constrained problem will be found.

The process for finding a solution is as follows:

(1) The initial design variables X^0 are assumed to be in a feasible region and the penalty value r_p^0 is chosen; then the unconstrained optimization algorithm is used to find the minimum solution of penalty function $P_p(X^0, r_p^0)$.

(2) Reducing the r_p^k by using the rule $r_p^{k+1} = C_r r_p^k$, where $C_r < 1$, and finding the minimum of $P_p(X^{k+1}, r_p^{k+1})$.

(3) Check whether convergence criterion is satisfied, if not, repeat step (2); if yes, an optimal solution is obtained.

In order to solve the penalty function the unconstrained optimization algorithm is needed. An algorithm used in this study is based on the Powell's method with Goggin one-dimensional search technique which is described in Appendix H.

C. OPTIMALITY CRITERION METHOD

Optimality criterion method is an indirect method which utilizes iterative processes to find the optimum solution based on a criterion for optimality.

Let an optimum structural problem be formulated as:

minimize $O(X)$

subject to $g_j(X) \leq 0$, $j = 1, 2, 3, ..., nc$

where X = design variables; $O(X)$ = objective function; $g_j(X)$ = jth constraint; and nc = the number of constraints.

The criterion for optimality of the method may be expressed as :

$$(\frac{\partial O(X)}{\partial x_i})_{x^*} + \sum_{j=1}^{nc} \lambda_j (\frac{\partial g_j(X)}{\partial x_i})_{x^*} = 0 \text{ , and } \lambda_j \geq 0 \tag{6.36}$$

where x_i ith design variable; λ_j = jth Lagrangian multiplier; x^* = an optimal solution. Based on the above criterion, the design variables x_i^{v+1} at $v+1$th iteration can be expressed in terms of x_i^v at the vth iteration as

$$x_i^{v+1} = [\alpha + (1-\alpha)T_i]x_i^v \tag{6.37}$$

in which T_i is called the recurrence equation and can be written as

$$T_i = (-\sum_{j=1}^{act} \lambda_j (\frac{\partial g_j(X)}{\partial x_i}))/(\frac{\partial O(X)}{\partial x_i}) \tag{6.38}$$

α = a relaxation constant; and act = the number of active constraints. The partial derivative of constraints with respect to design variables, $\partial g_j/\partial x_i$, can be expressed in terms of safety factor, β_j, as

$$\frac{\partial g_j}{\partial x_i} = \frac{\partial(\beta_a - \beta)}{\partial x_i} = \frac{-\partial \beta_j}{\partial x_i} \tag{6.39}$$

or in terms of probability of failure as

$$\frac{\partial g_j}{\partial x_i} = \frac{\partial(P_f - P_{f_a})}{\partial x_i} = \frac{\partial P_f(\beta)}{\partial x_i} = \frac{-1}{\sqrt{2\pi}} \exp(\frac{-\beta_j^2(X)}{2}) \frac{\partial \beta_j(X)}{\partial x_i} \tag{6.40}$$

where β_a and P_{f_a} are allowable safety factor and probability of failure, respectively.

At each iteration one has to scale the initial design and to decide the active constraints for accelerating convergence before the value of Γ_i (Equation (6.38)) is found. For each constraint the scaling factor is computed by a linearized approximation to the allowable safety factor or probability of failure as follows:

$$\Delta\beta_j = \sum_{i=1}^{act} (\frac{\partial \beta_j}{\partial x_i}) \Delta x_i + \sum_{i'=1}^{passive} (\frac{\partial \beta_j}{\partial x_{i'}})(x_{i'\,min} - x_{i'}) \tag{6.41}$$

in which $x_{i'\,min}$ represents passive elements.

Substituting $\Delta x_i = x_i^{\nu+1} - x_i^{\nu} = \Lambda x_i^{\nu} - x_i^{\nu}$ into the above equation yields

$$\beta_a - \beta_j = \sum_{i=1}^{act} (\frac{\partial \beta_j}{\partial x_i})(\Lambda - 1)x_i + \sum_{i'=1}^{passive} (\frac{\partial \beta_j}{\partial x_{i'}})(x_{i'\,min} - x_{i'}) \tag{6.42}$$

Thus the scaling factor for safety factor can be calculated as follows:

$$\Lambda_j = \frac{(\beta_a - \beta_j) + \sum_{i=1}^{act} (\frac{\partial \beta_j}{\partial x_i}) x_i - \sum_{i'=1}^{passive} (\frac{\partial \beta_j}{\partial x_{i'}})(x_{i'\,min} - x_{i'})}{\sum_{i=1}^{act} (\frac{\partial \beta_j}{\partial x_i}) x_i} \tag{6.43}$$

For the probabilities of failure, the scaling factors become

$$\Lambda_j = \frac{(P_{f_a} - P_{f_j}) + \sum_{i=1}^{act} (\frac{\partial P_{f_j}}{\partial x_i}) x_i - \sum_{i'=1}^{passive} (\frac{\partial P_{f_j}}{\partial x_{i'}})(x_{i'\,min} - x_{i'})}{\sum_{i=1}^{act} (\frac{\partial P_{f_j}}{\partial x_i}) x_i} \tag{6.44}$$

In order to determine T_i, the active Lagrangian multipliers λ_p must be determined from the following simultaneous equations which are derived from linearized approximations to the zero constraint values:

$$\Delta g_j = g_j^{\nu+1} - g_j^{\nu} = \sum_{i=1}^{act} (\frac{\partial g_j}{\partial x_i}) \Delta x_i + \sum_{i'=1}^{passive} (\frac{\partial g_j}{\partial x_{i'}}) \Delta x_{i'}(P) \tag{6.45}$$

in which $\Delta x_{i'}(P)$ represents passive elements.

Let $g_j^{\nu+1} = 0$,

$$\Delta x_i = [\alpha + (1 - \alpha) T_i] x_i^{\nu} - x_i^{\nu}, \tag{6.46}$$

and

$$T_i = (- \sum_{j=1}^{act} \lambda_j (\frac{\partial g_j(x)}{\partial x_i})) / (\frac{\partial O(x)}{\partial x_i}) \tag{6.47}$$

then Equation (6.45) becomes

$$-g_j = \sum_{i=1}^{act} (\frac{\partial g_j}{\partial x_i}) \alpha x_i + (1 - \alpha) \sum_{i=1}^{act} \frac{(- \sum_{p}^{nc1} \lambda_p \frac{\partial g_j}{\partial x_i} \frac{\partial g_p}{\partial x_i})}{(\frac{\partial O}{\partial x_i})} x_i$$
$$- \sum_{i=1}^{act} \frac{\partial g_i}{\partial x_i} x_i + \sum_{i'=1}^{passive} \frac{\partial g_i}{\partial x_{x'}} \Delta x_{i'}(P) \tag{6.48}$$

in which ncl = the number of active constraints, g_p = the active constraints, λ_p = the Lagrangian multipliers of active constraints and can be found from the following simultaneous equations,

$$(1-\alpha)\sum_{p=1}^{nc}\left(\sum_{i=1}^{act}\left(\frac{\partial g_j}{\partial x_i}\right)\left(\frac{\partial g_p}{\partial x_i}\right)/\left(\frac{\partial O}{\partial x_i}\right)\lambda_p x_i\right)$$

$$= g_j + (\alpha-1)\sum_{i=1}^{act}\left(\frac{\partial g_j}{\partial x_i}\right)x_i + \sum_{i'=1}^{passive}\left(\frac{\partial g_j}{\partial x_{x'}}\right)\Delta x_{i'}(P) \qquad (6.49)$$

A flow chart of optimality criterion method solving constrained or unconstrained problems is shown in Appendix I. The recurrence equation, T_i, derived from $\frac{\partial C_T}{\partial x_i} = 0$ for cost function in the unconstrained algorithm has the following form

$$T_i = \frac{-L_f P_{fT}}{C_I} \qquad (6.50)$$

VII. STUDIES OF ANSI, NBS, UK, AND UNREDUCED MODELS

The two-story steel frame in Figure 6 is used to demonstrate the designs for four live load models. The optimal weight, moment of inertia of a member, and probability of failure are shown in the following figures. The notations in the figures are L1, L2, L3, and L4 which signify the live load models of ANSI, NBS, UK, UNREDUCED, respectively; 1st and 2nd represent the two variance approaches for two probability distributions; N and LN are corresponding to normal and lognormal, respectively; D + L signifies the dead load combined with live load; and D + L + E represents the load combination of dead load, live load, and UBC seismic force. The parameters used in the example are $A_I = 900$ ft^2 (274.32 m^2) $\overline{D}$ = 80 psf (3.82 kPa), $V_D = 0.12$, allowable individual failure probabilities = 0.0001, allowable joint rotations = 0.05 rad., allowable joint displacements = 0.5 in (1.27 cm), allowable variances of joint rotations and displacements are assumed to be zero, $\overline{F}_y$ = 36 ksi (2.448x10^5 kPa), $\overline{E}_m$ = 30000 ksi (2.067x10^8 kPa), $V_{M_y} = 0.12$, $V_{P_E} = 0.3$, $V_{P_{cr}} = 0.31$, $V_{P_y} = 0.14$, $V_{M_{cr}} = 0.20$, $V_{P_{cry}} = 0.3$, $\rho_{P_y M_y} = 0.8$, $\rho_{P_{cr} M_y} = 0.8$, $\rho_{P_{cr} P_E} = 0.8$ (= 1 if $P_{cr} = P_E$), $\rho_{P_E M_y} = 0.$, $\rho_{P_{cr} M_y} = 0.8$, $\rho_{P_y M_{cr}} = 0.15$, $\rho_{P_E M_{cr}} = 0.15$. The parameters for the seismic base shear in UBC are $Z = 3/8$, $I_E = 1.0$, $K_E = 1.0$, $S_E = 1.5$, hn = 27 ft (8.23 m) and Dn = 30 ft (9.14 m). The structural members are assumed to be rectangular sections and have the relationship area = $2\sqrt{2}$(moment of inertia)$^{1/2}$. The minimum moment of inertia of all the members is 50 in^4 (2081.16 cm^4).

A. DEAD AND LIVE LOAD CASE

The analytical results corresponding normal distribution are given in Figure 7 which shows the magnitude of optimum weight in which the British model (L3) demands a heavier structural deaign than the U.S. models (L1 and L2); ANSI (L1) demends heavier design than NBS (L2); UNREDUCED model (L4) demands the heaviest design simply because it does not reduce the live load in term of influence area A_I .The 2nd variance approach yields more weight than the first. The moments of inertia of a typical beam (I_1) and a column (I_4)

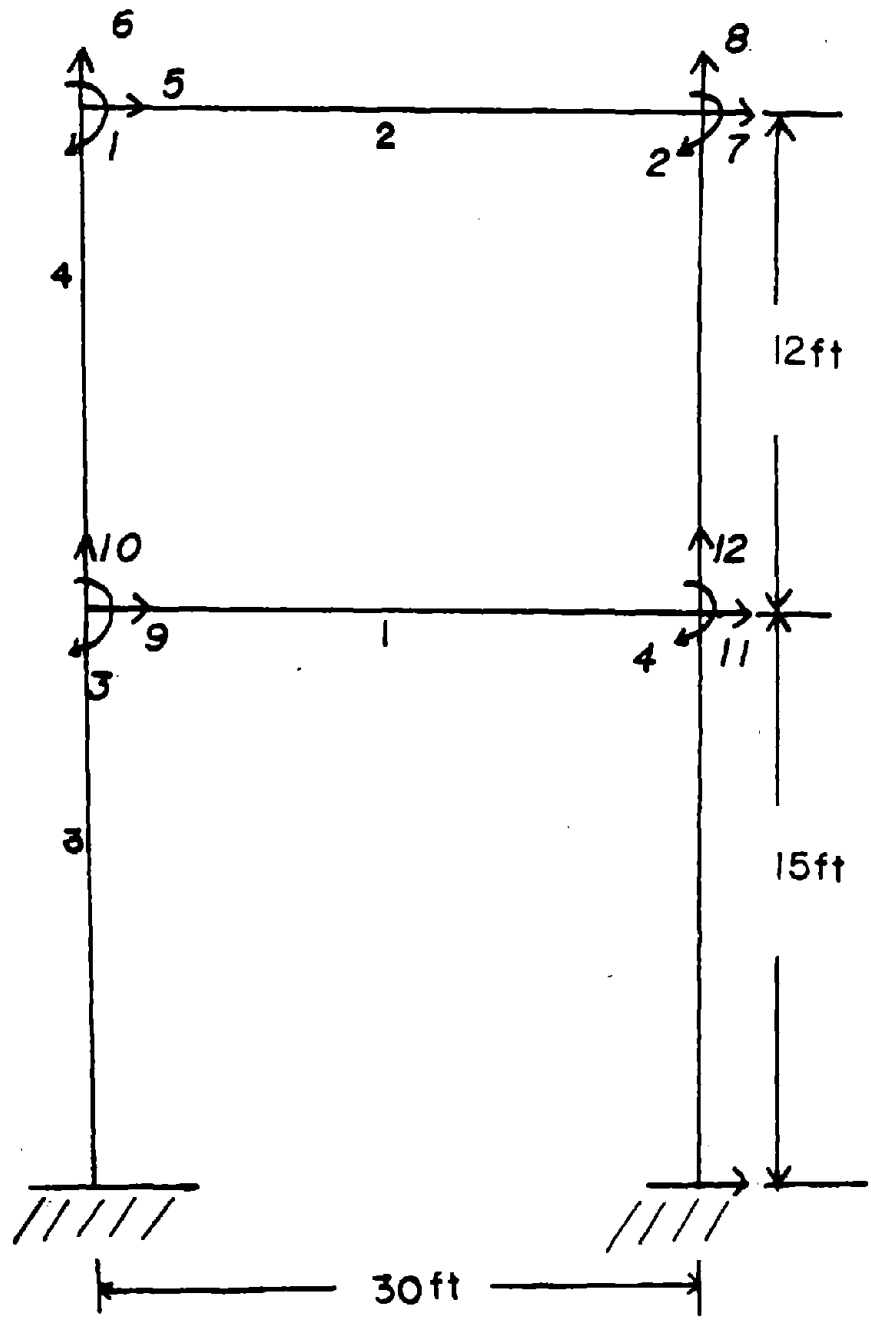

Figure 6. Two Story Building Structure (1 ft = 30.48 cm)

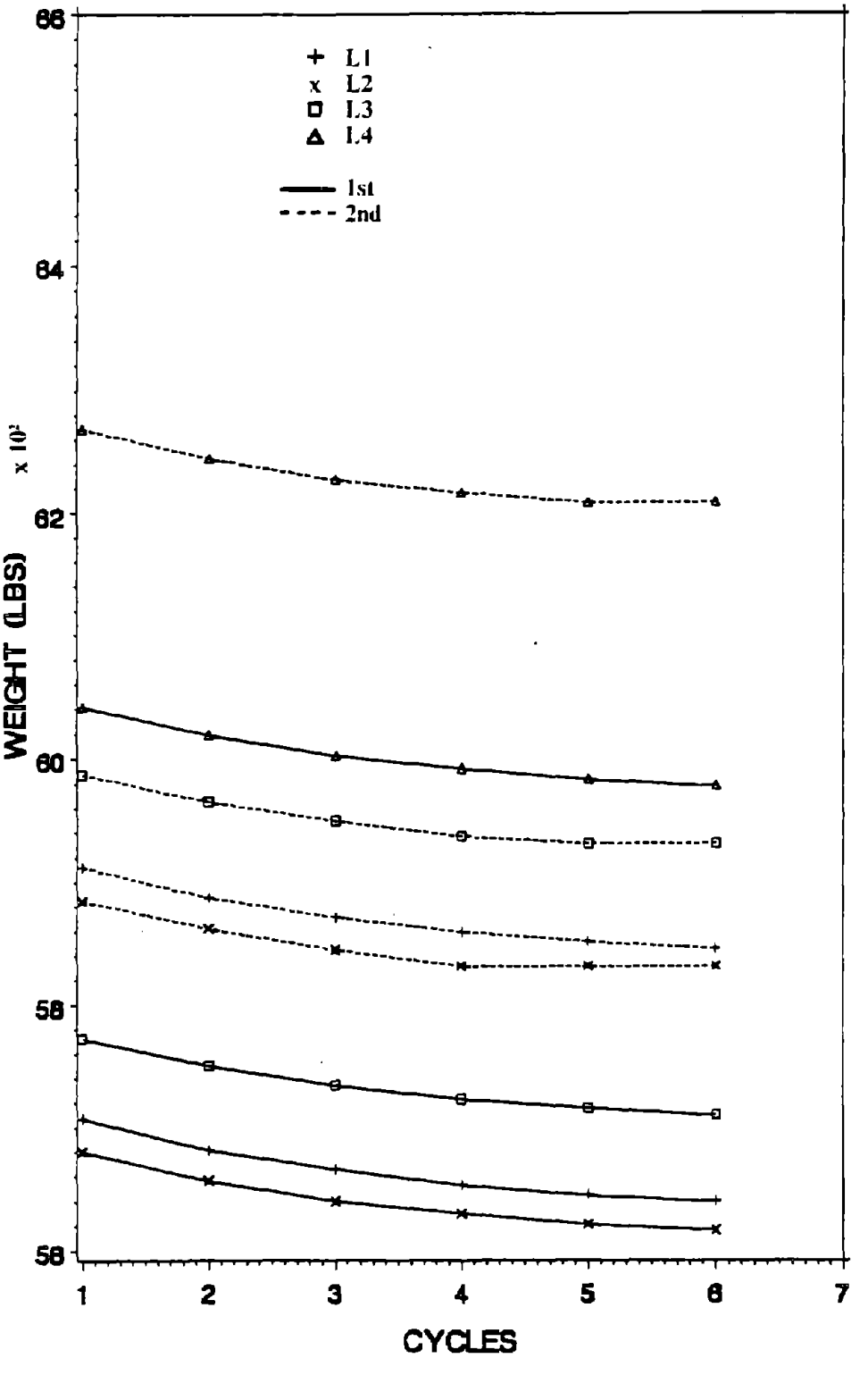

Figure 7. Optimum Weight for Various Live Load Models with N and D+L Case.(1 lb = 4.45 N)

are sketched in Figures 8 and 9, respectively. The effects of four live load models and the two variance formulations on the design are similar to the optimum weight in Figure 7. The probability of failures of the typical members are given in Figures 10 through 13 in which b_1 and b_2 are corresponding to the failures due to yielding moment given in Equation (6.6) of beams 1 and 2, respectively; and $(f_1)_4$ and $(f_2)_4$ represent the column failure (element 4) due to yielding at the member end (Equation (6.9)) and instability in the plane of bending (Equation (6.15)), respectively. The supporting column, member 3, reaches the minimum moment of inertia before any failure modes. The failure modes at the optimum solution are close to the allowable, 10×10^{-5}. The design was determined at the 6th cycle, because the next cycle could not further improve the optimum solution of the structural weight or the moment of inertia.

The optimum design parameters of weight, moments of inertia, and failure modes are also studied for lognormal distribution and are sketched in Figures 14 through 20. The effect of four live load models and that of two variance approaches on the optimum design results are similar to those observed on the bases of normal distribution.

Comparsion of the optimum solutions resulting from normal and lognormal distributions reveals that normal distribution requires a heavier structural design than the lognormal distribution for the first approach, but a lighter structural design for the second approach. The comparison may be observed from Figures 7 and 14. Similar observations may be conclued for moments of inertia.

As observed from the normal distribution case, the failure modes shown in Figures 17 through 20 indicate that the individual failure mode approaches the specified failure bound, $P_{f0} = 0.0001$, for four live load models and two probability distributions. The failure modes which approach the bound are the yielding failure of beams 1 and 2 (b1 and b2), and the yielding and bending instability failures of column 4 ($(f_1)_4$ and $(f_2)_4$) for both the 1st and 2nd variance approach.

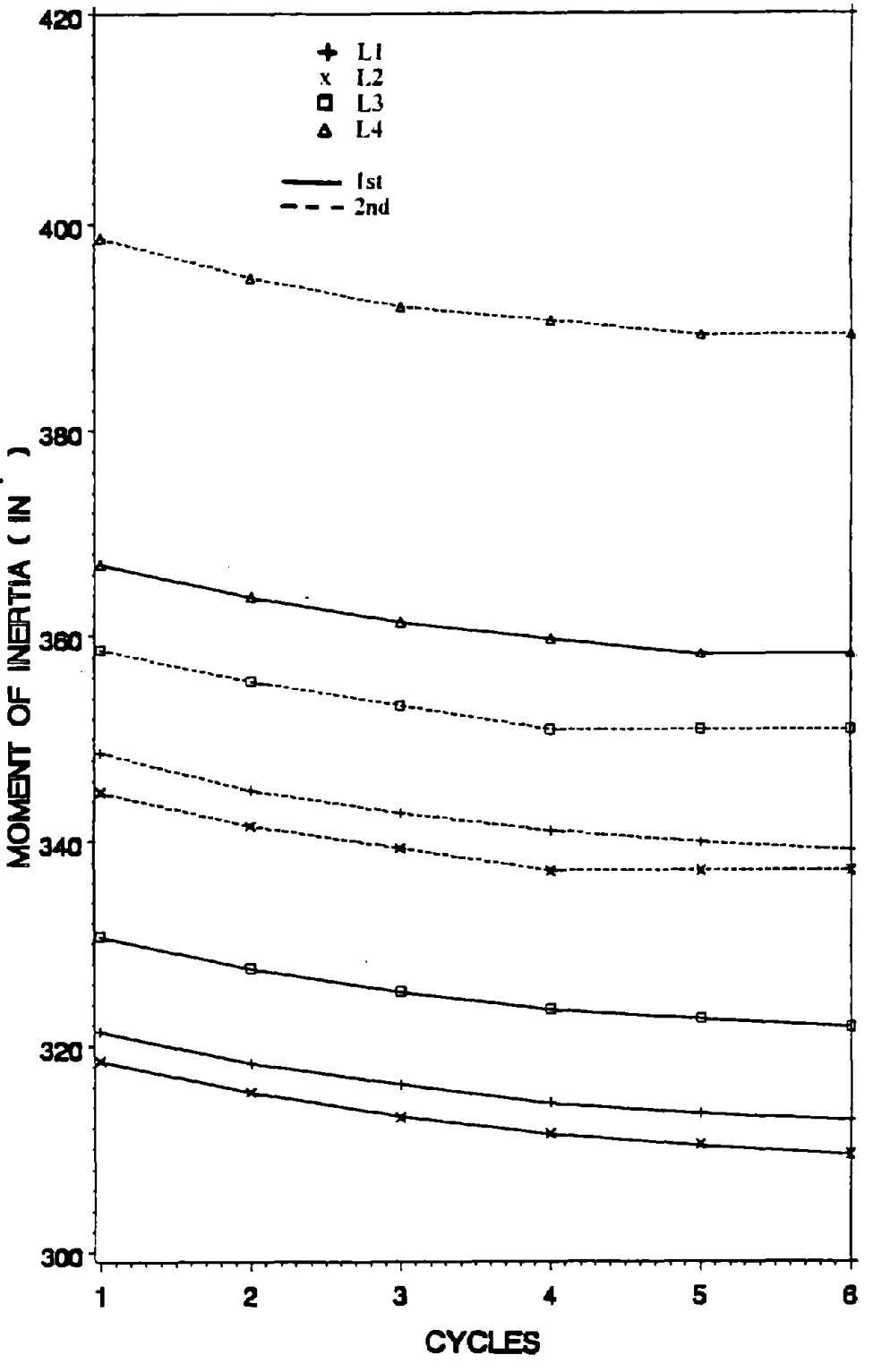

Figure 8. I_1 for Various Live Load Models with N and D+L Case.(1 in^4 = 41.62 cm^4)

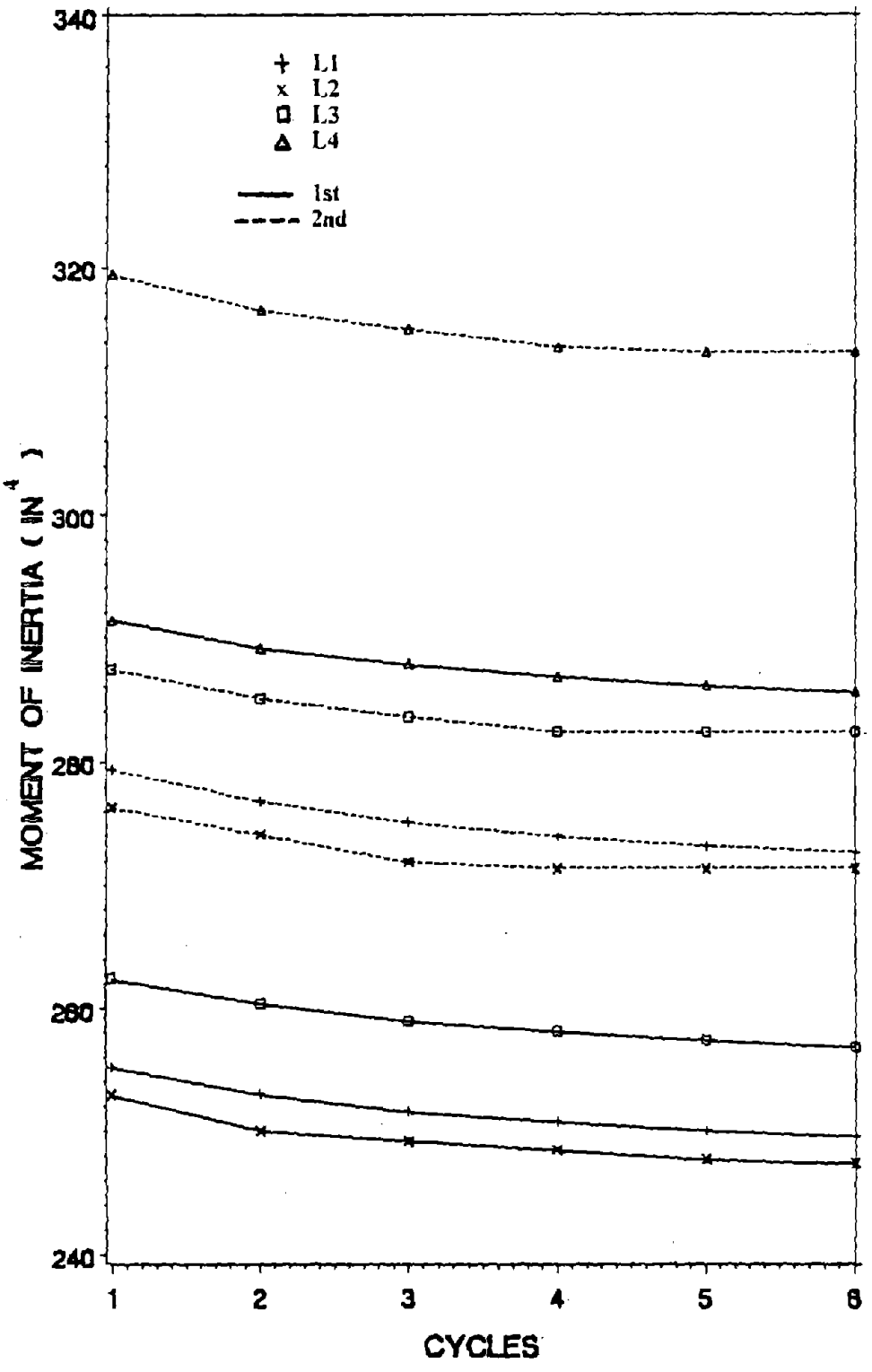

Figure 9. I_4 for Various Live Load Models with N and D + L Case.(1 in^4 = 41.62 cm^4)

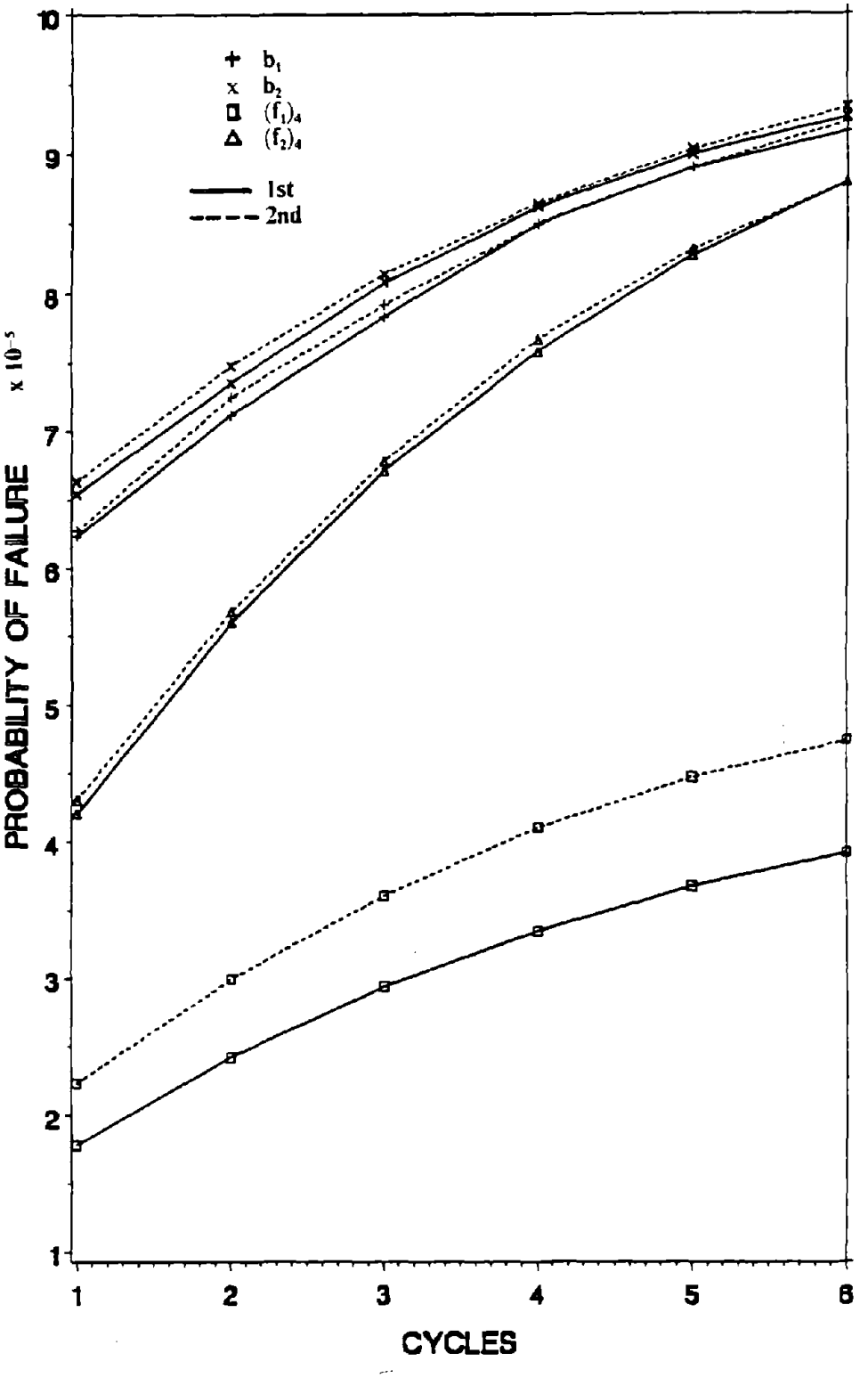

Figure 10. Probability of Failure for ANSI Live Load Model with N and D + L Case.

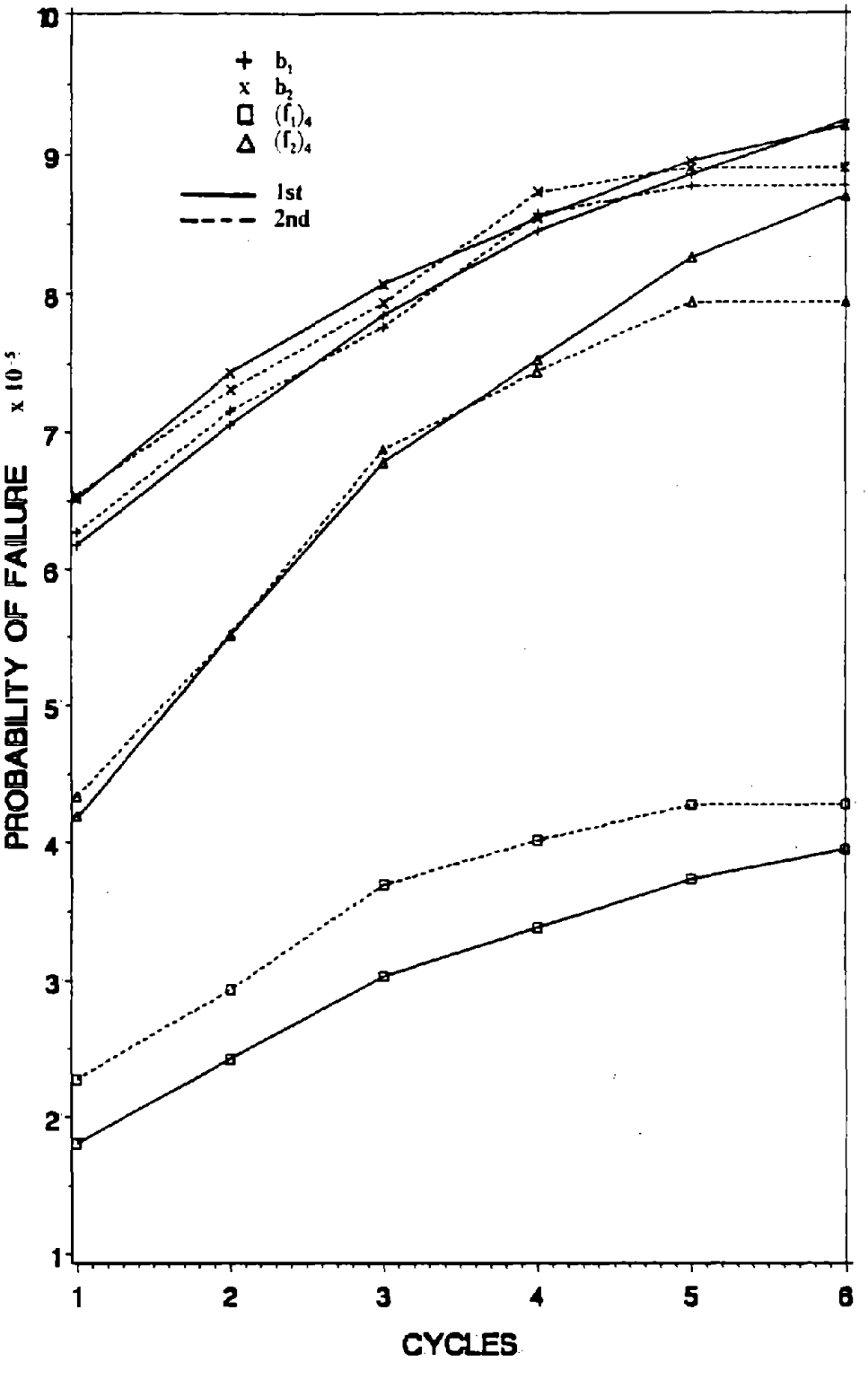

Figure 11. Probability of Failure for NBS Live Load Model with N and D + L Case.

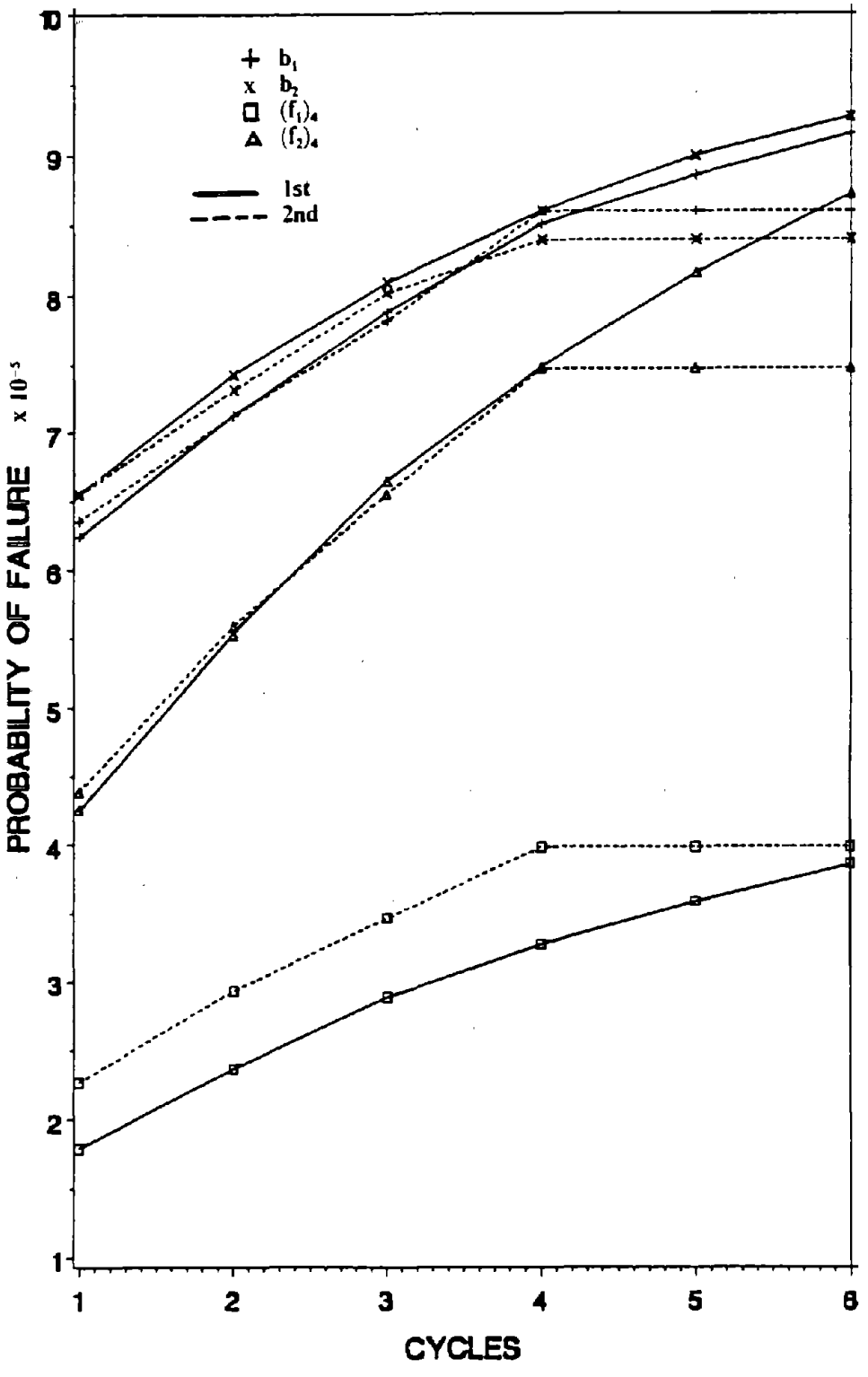

Figure 12. Probability of Failure for UK Live Load Model with N and D+L Case.

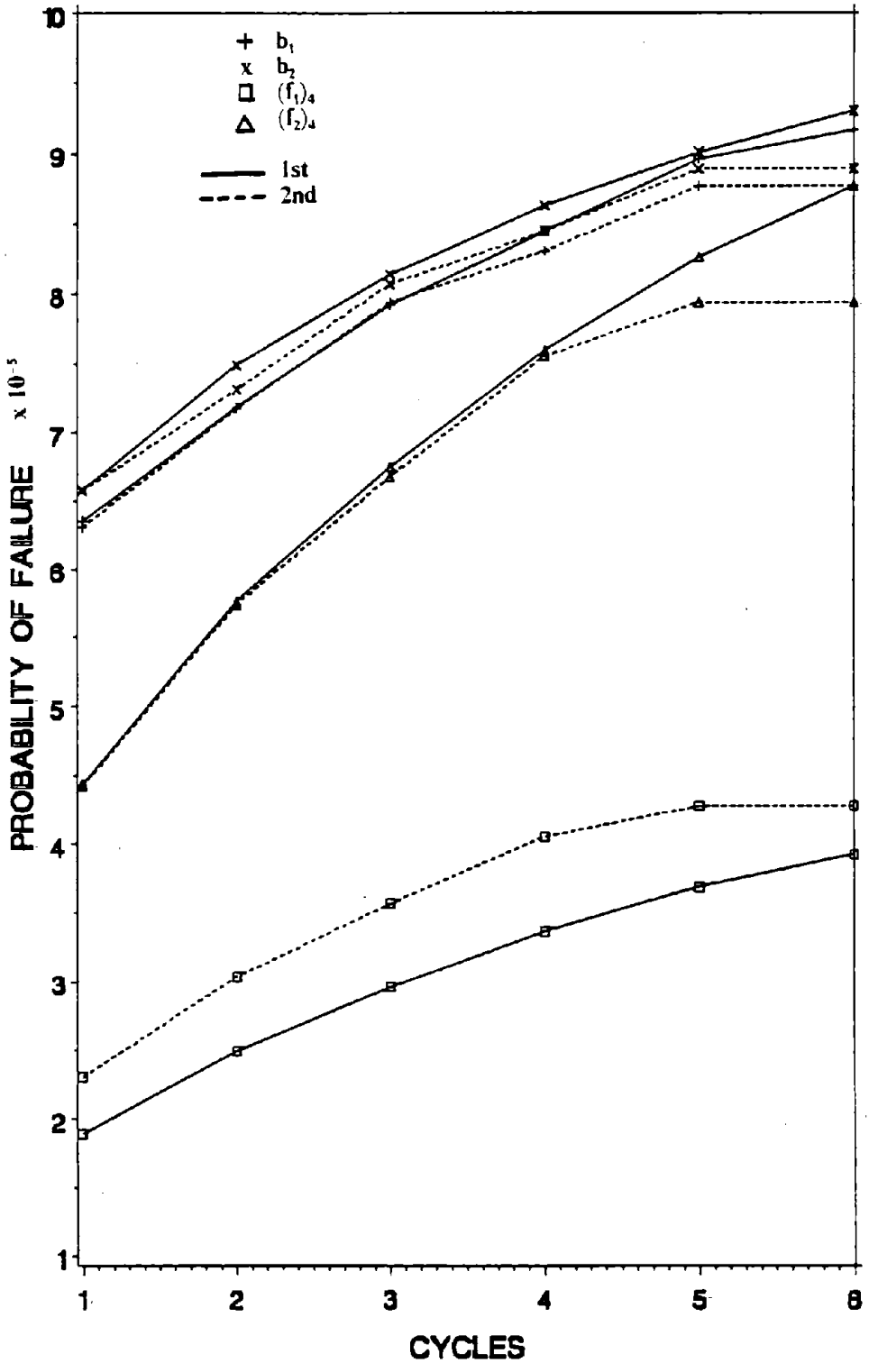

Figure 13. Probability of Failure for UNREDUCED Live Load Model with N and D+L Case.

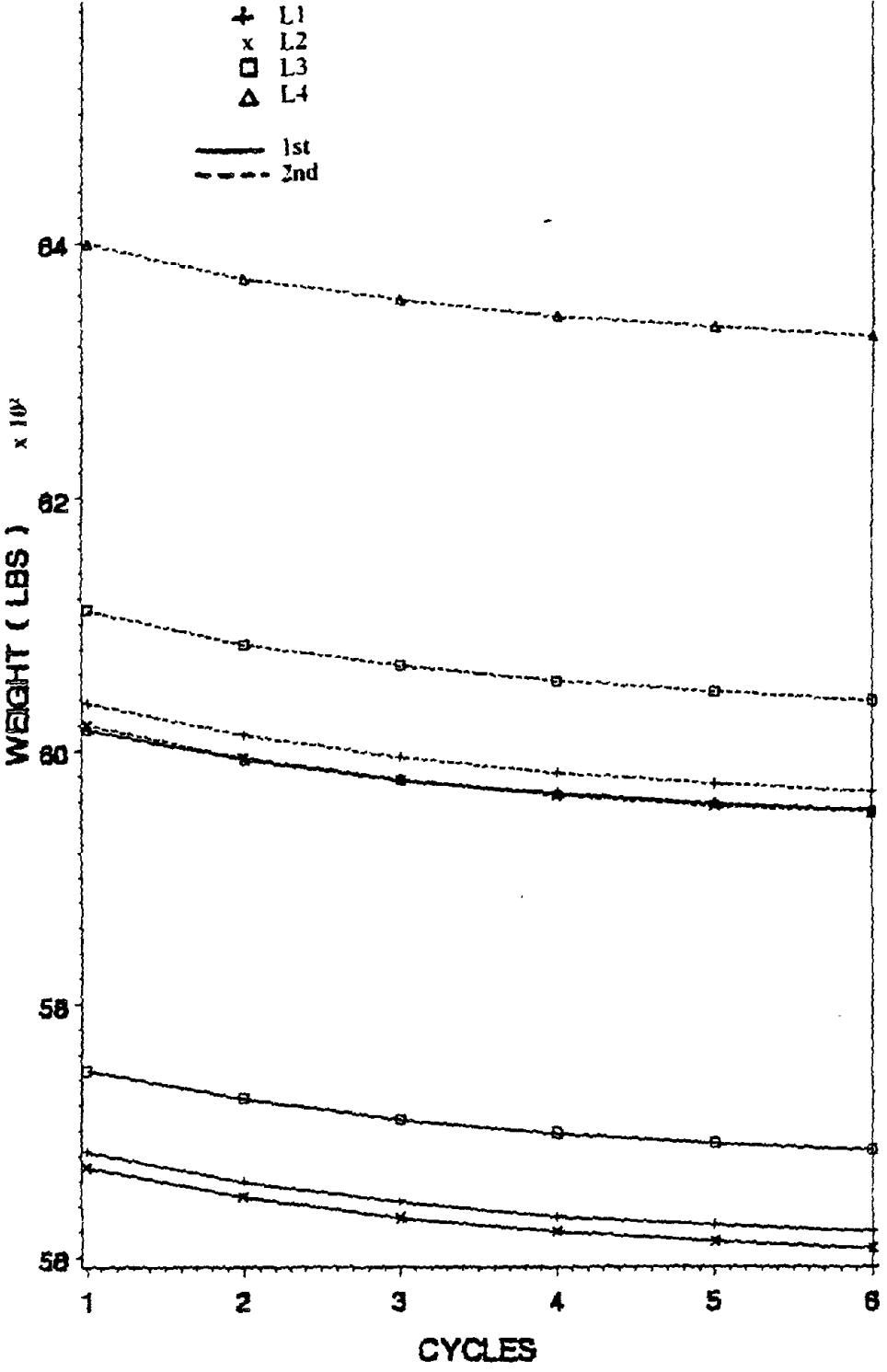

Figure 14. Optimum Weight for Various Live Load Models with LN and D+L Case
= 4.45 N)

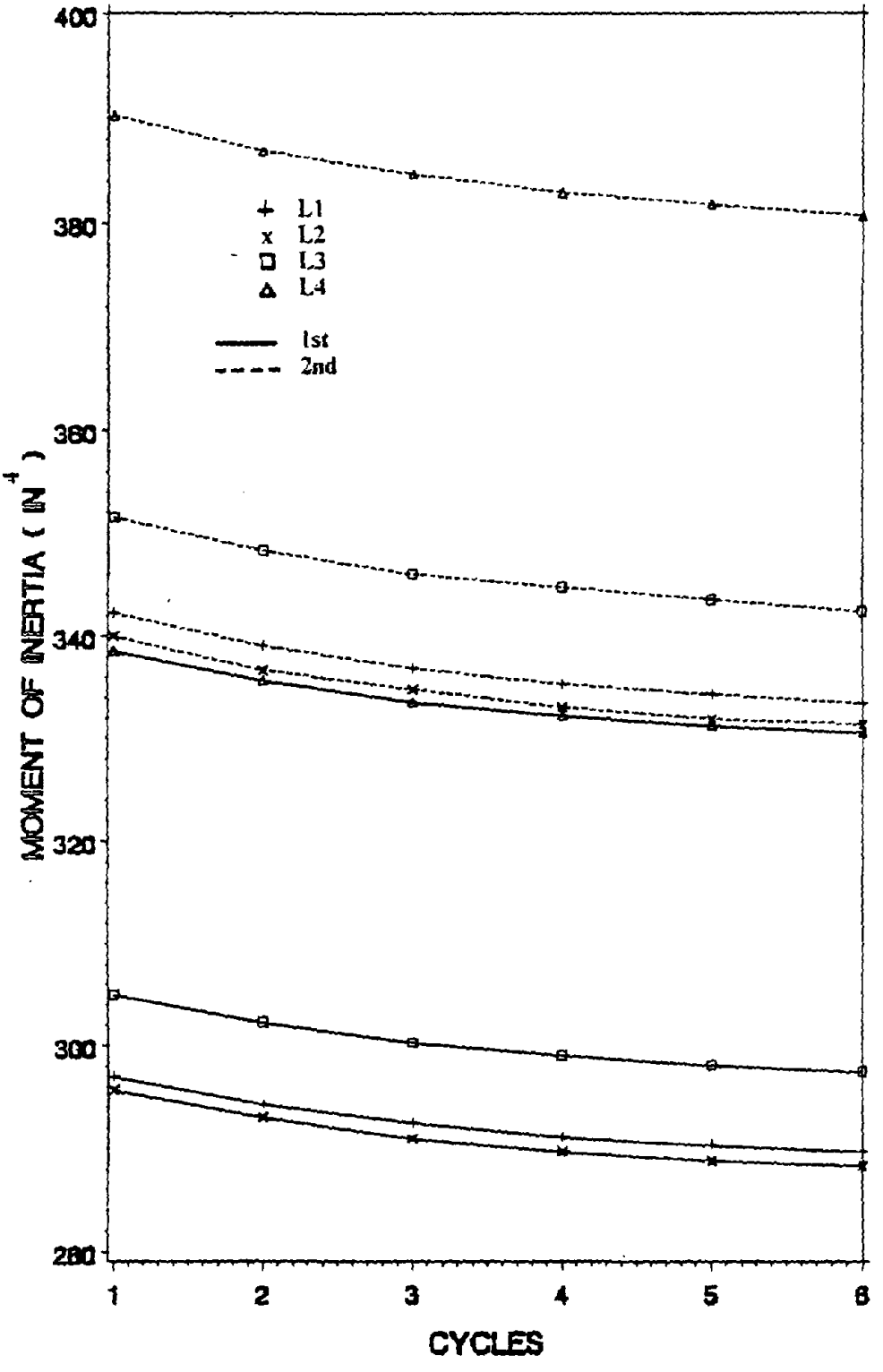

Figure 15. I_1 for Various Live Load Models with LN and D + L Case.(1 in^4 = 41.62 c

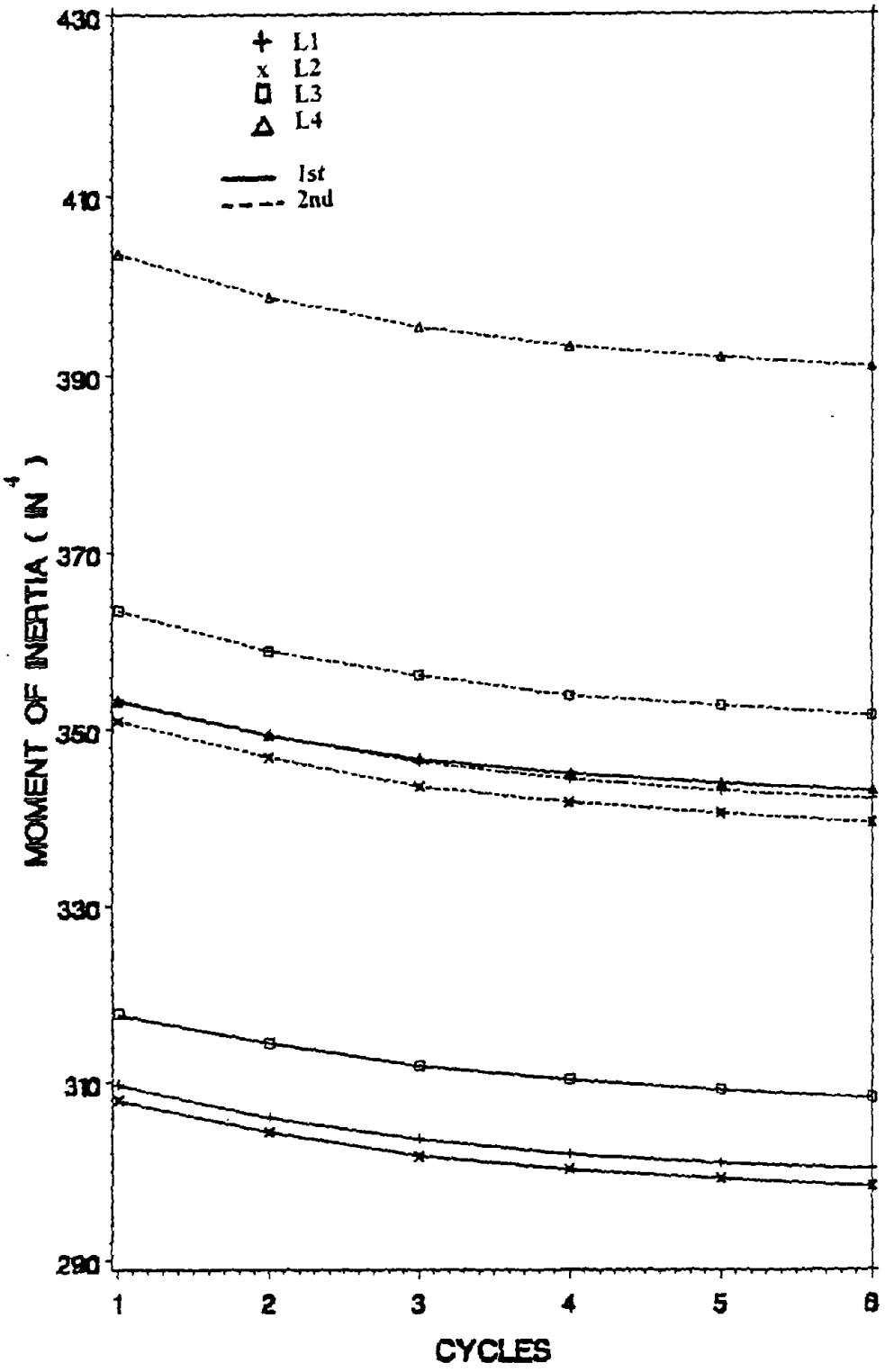

Figure 16. I_4 for Various Live Load Models with LN and D+L Case.(1 in^4 = 41.62 cm^4)

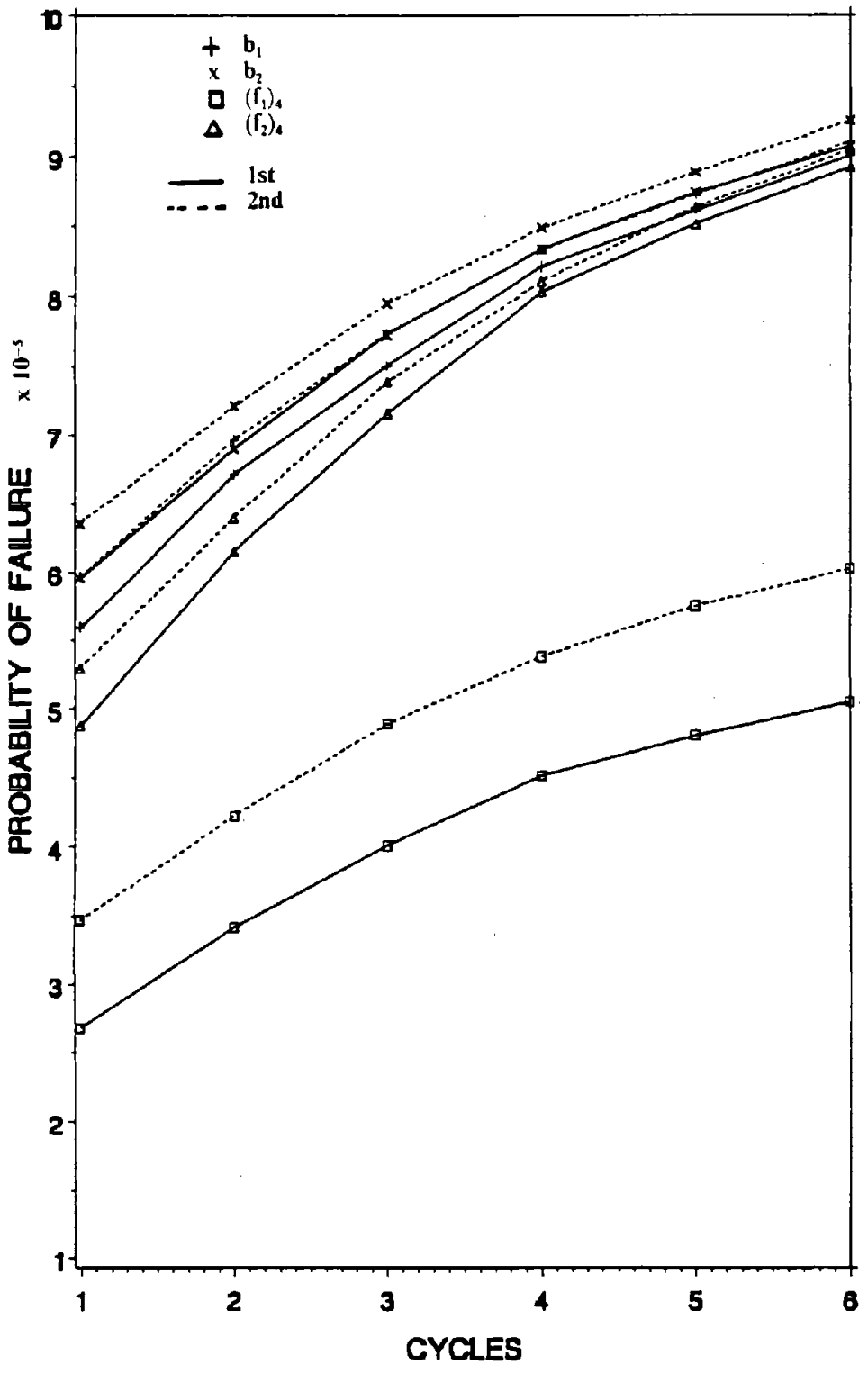

Figure 17. Probability of Failure for ANSI Live Load Model with LN and D + L Case.

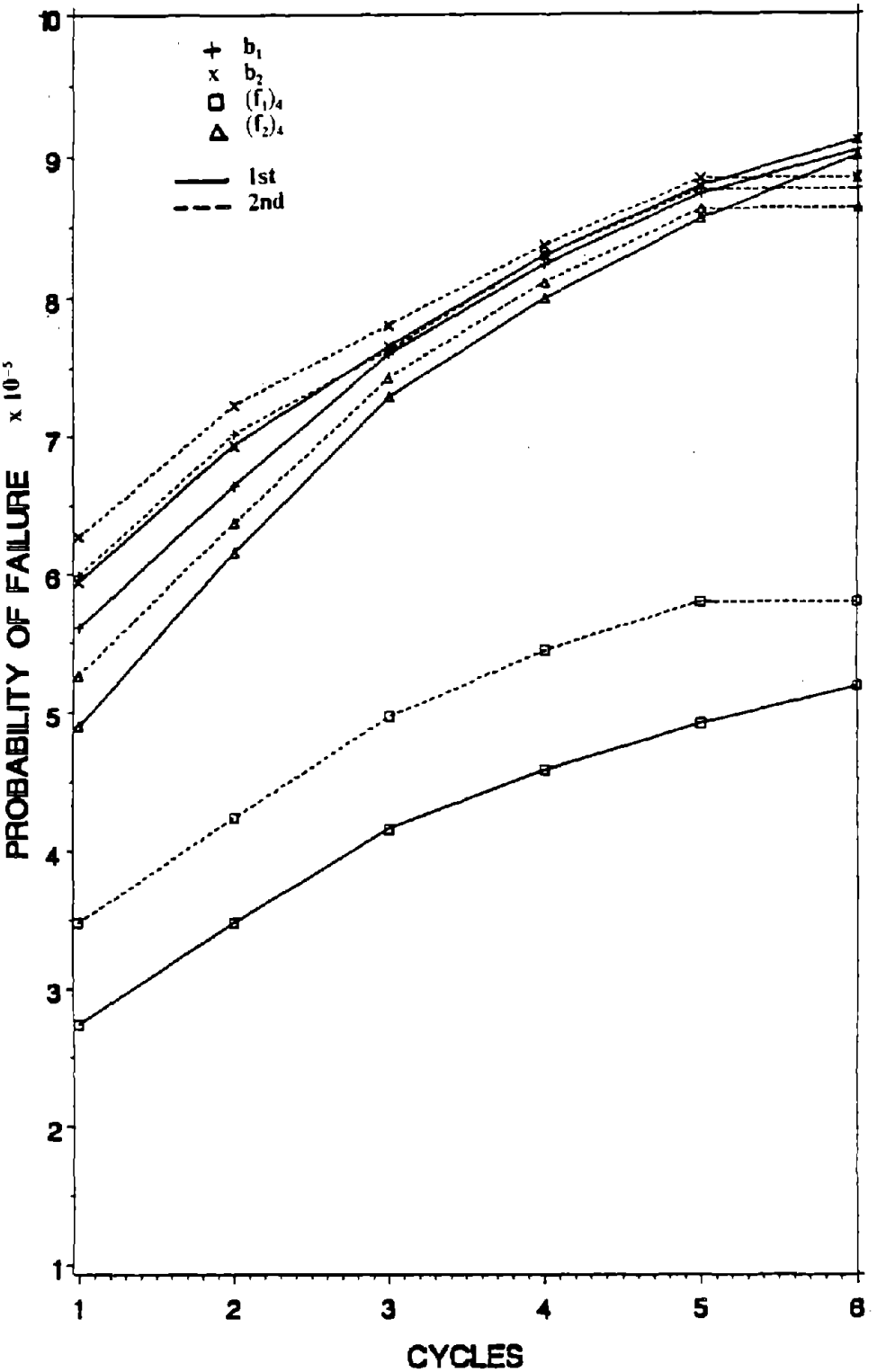

Figure 18. Probability of Failure for NBS Live Load Model with LN and D+L Case.

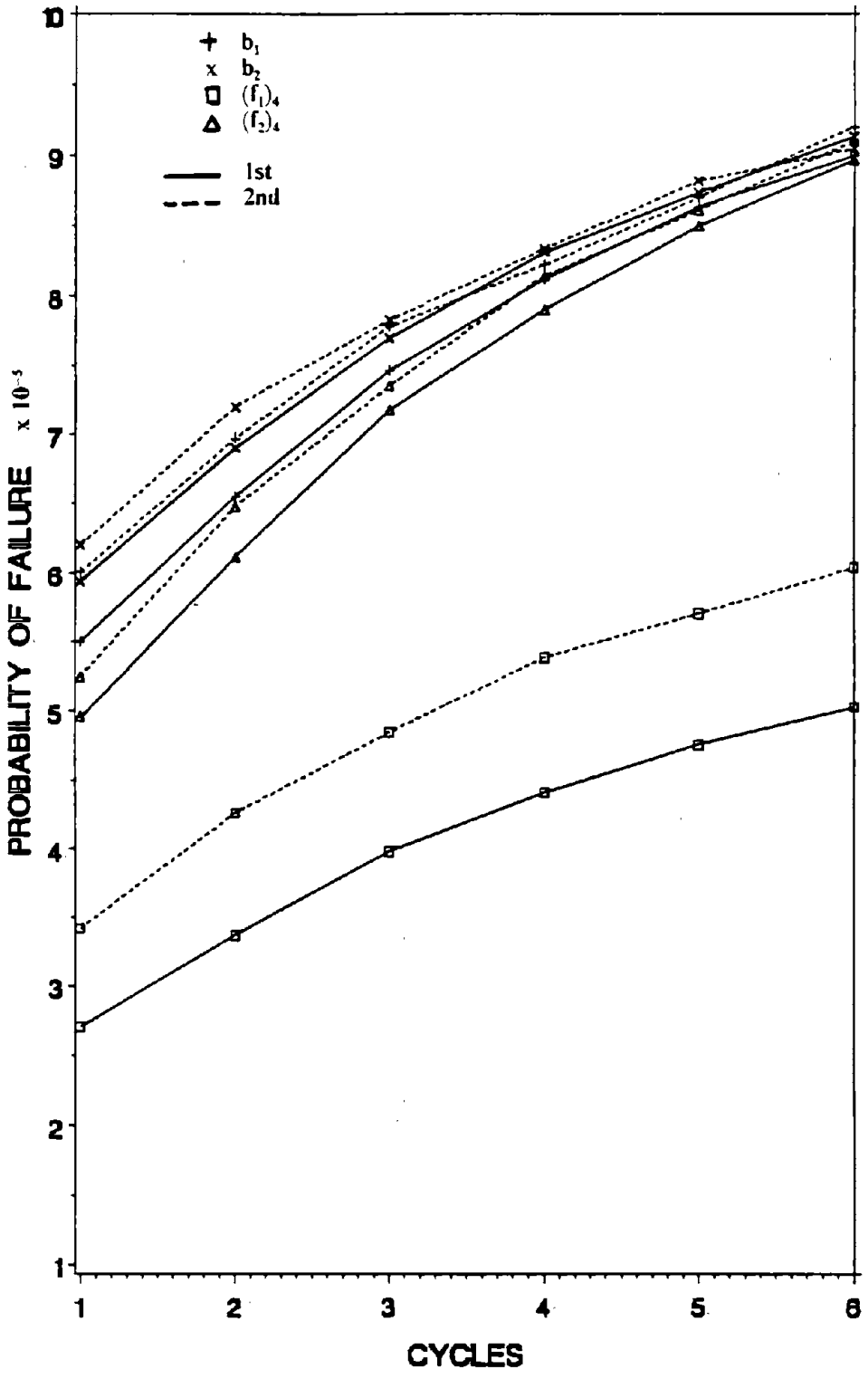

Figure 19. Probability of Failure for UK Live Load Model with LN and D + L Case.

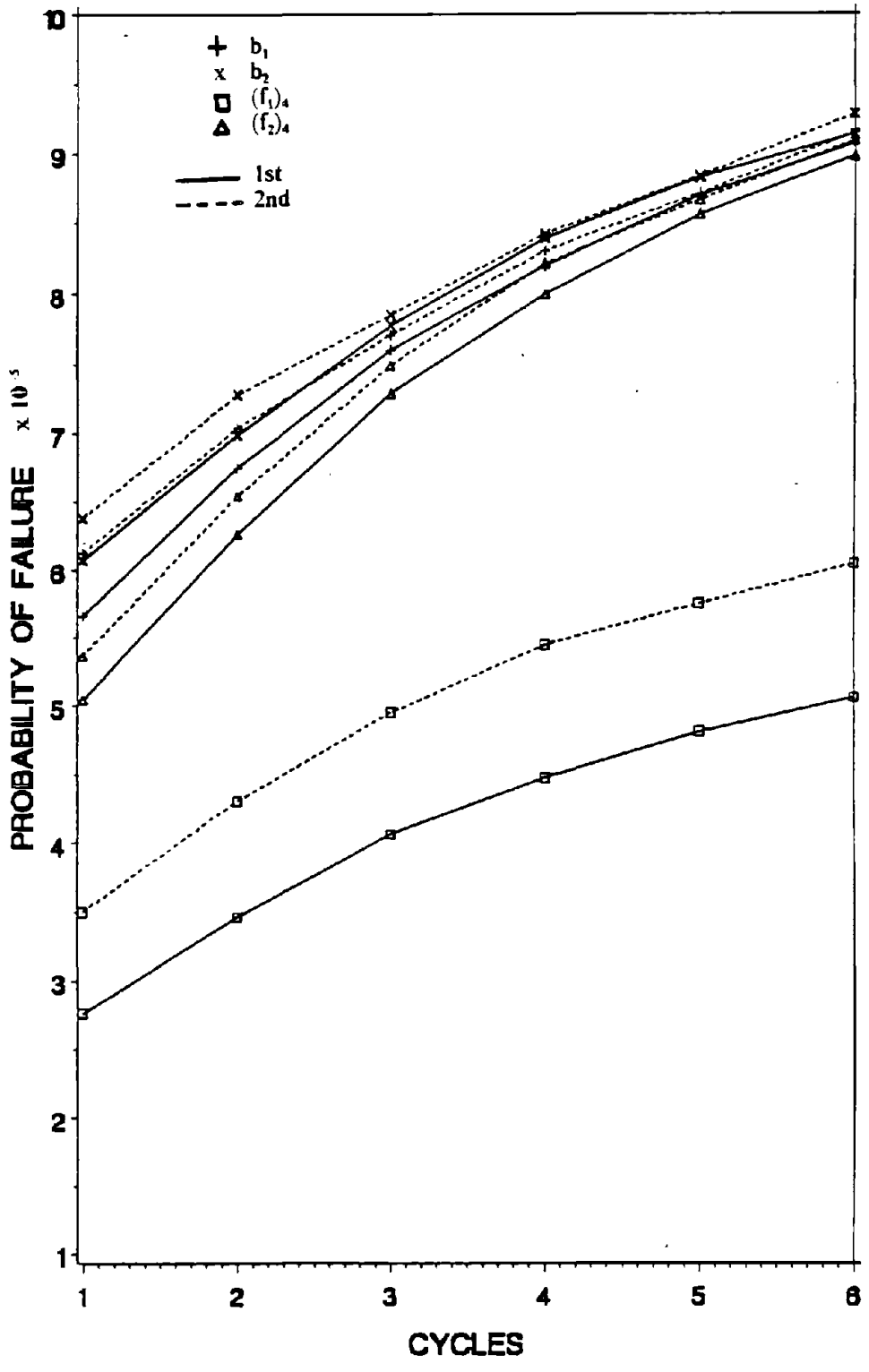

Figure 20. Probability of Failure for UNREDUCED Live Load Model with LN and D+L Case.

B. DEAD, LIVE, AND UBC LOAD CASE

As studied in the previous section, the interior penalty function algorithm is also used in this section. In general, an initial penalty value is first assumed which is then reduced for each cycle to approach the optimal solution. For optimization process different starting points may result significant differences of suboptimal solutions. Therefore the suboptimal solutions between two cycles may have large differences because of two different starting values. These differences can be seen in the study of ANSI and NBS live load models. In this section the UBC load, with the variation of 1.38 as recommended by NBS, combined with dead and live load (D + L + E) is used to study the effects of the live load models of ANSI (L1), NBS (L2), UK (L3), UNREDUCED (L4) on optimum design parameters. In Figures 21 and 24, the optimum weights affected by L1 through L4 are not quire consistent as shown in D + L case. According to the present study of normal distribution, the optimum weight varies from heavy to light in the sequence of UNREDUCED, UK, NBS, ANSI, for 1st variance approach and UNREDUCED, NBS, UK, ANSI, for 2nd variance approach; for the case of lognormal distribution, the sequence is UNREDUCED, NBS, UK, ANSI for the 1st variance approach, and UNREDUCED, NBS, ANSI, UK corresponding to the 2nd variance approach. The figures show that the case of D + L + E requires less design cycles than the case of D + L. It is quite consistent, however, that the lognormal distribution demands a heavier design than the normal distribution. From Figures 22, 23, 25, and 26, the design sections have the same conclusions as optimum weight. Figures 27 through 30 show that the failure bounds are mainly due to the lateral displacements of the top floor.

C. SUMMARIES

1. For the D + L case, the magnitude order of optimum weight from large to small is UNREDUCED, UK, ANSI, NBS for both normal and lognormal distributions.

2. For the D + L case, the lognormal distribution requires a heavier structural design than normal distribution for 2nd variance approach, but a lighter structural design for the 1st variance approach.

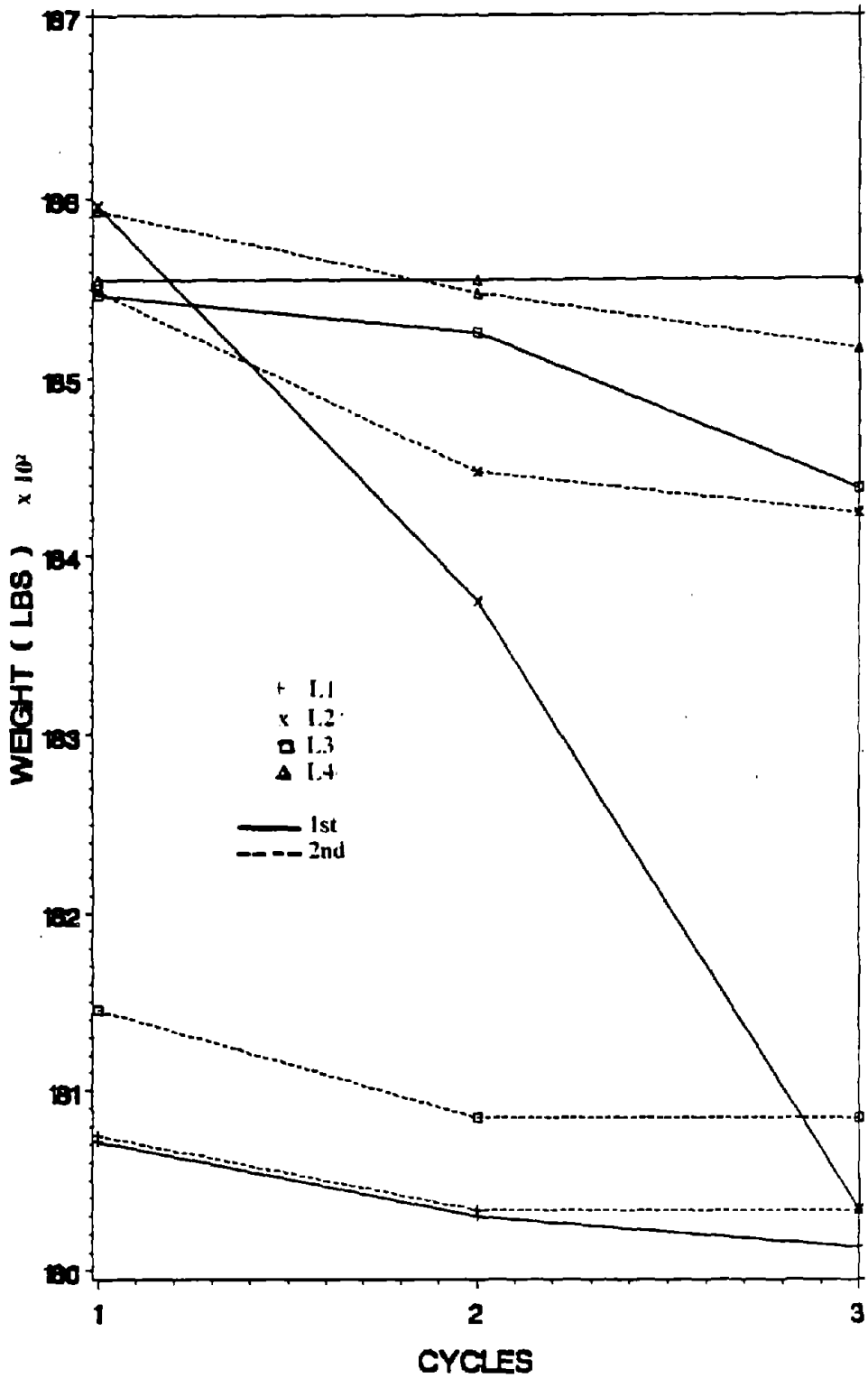

Figure 21. Optimum Weight for Various Live Load Models with N and D + L + E Case. (1 lb = 4.45 N)

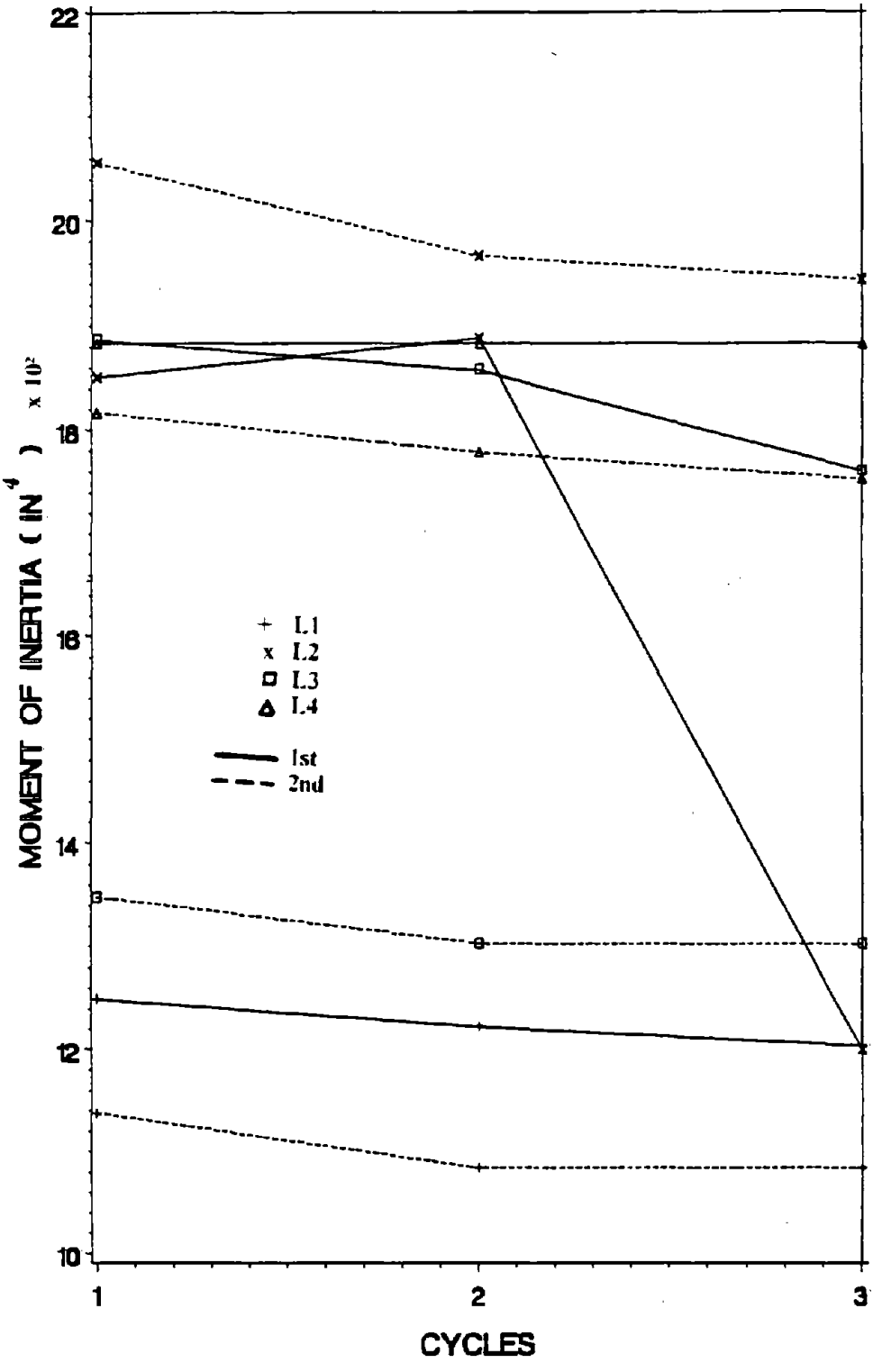

Figure 22. I_1 for Various Live Load Models with N and D + L + E Case.(1 in^4 = 41.62 cm^4)

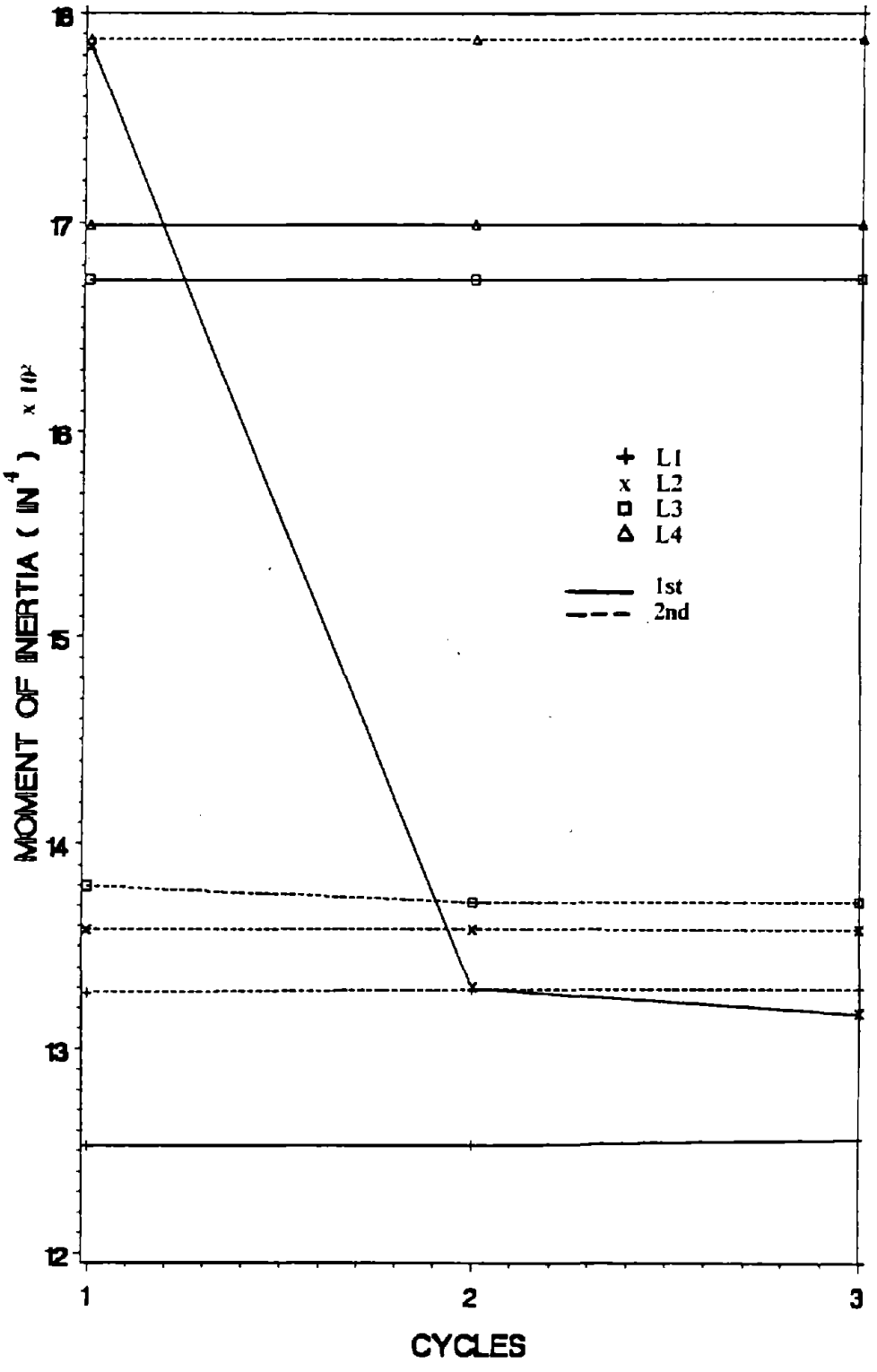

Figure 23. I_4 for Various Live Load Models with N and D + L + E Case.(1 in^4 = 41.62 cm^4)

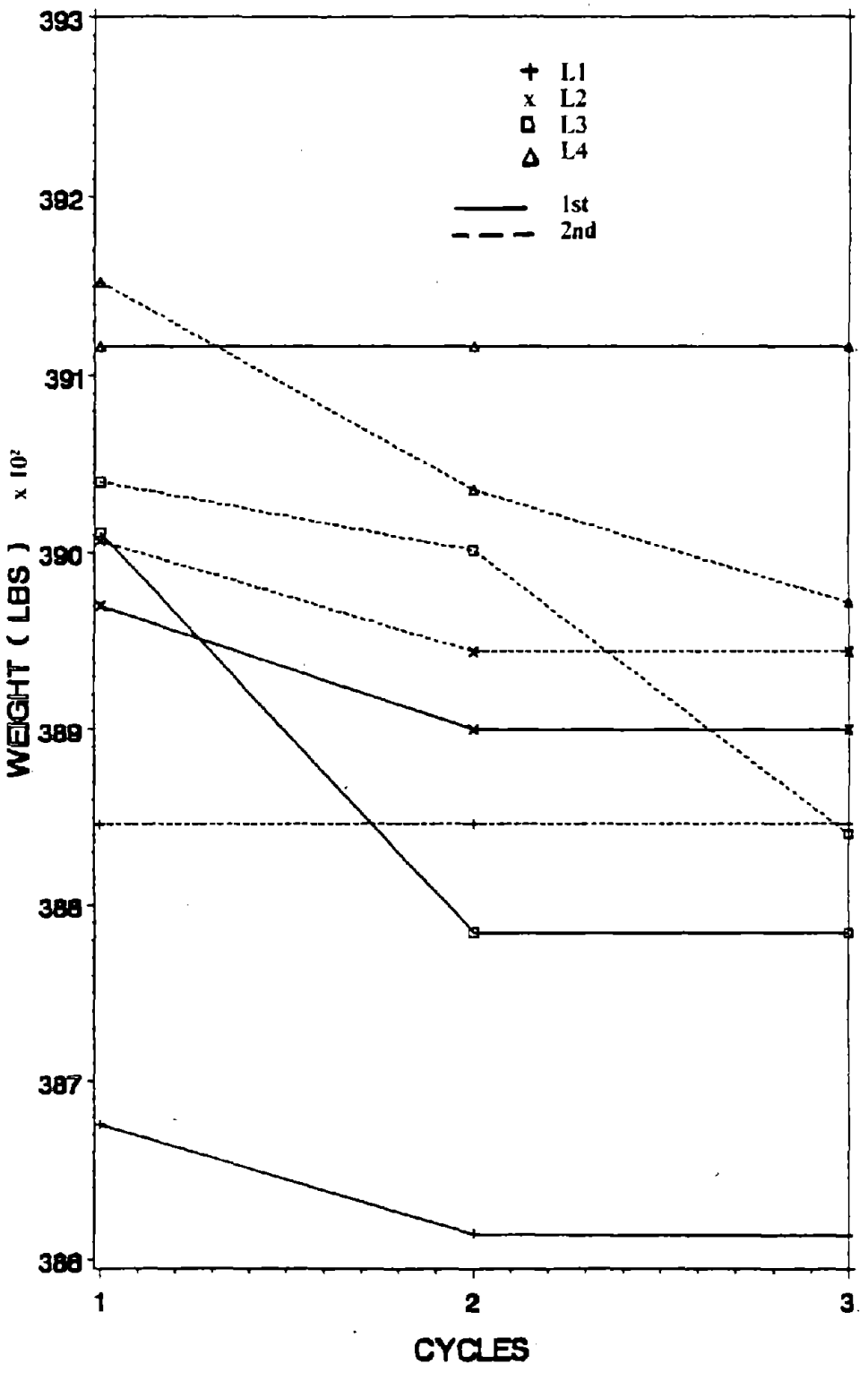

Figure 24. Optimum Weight for Various Live Load Models with LN and D + L + E Case.(1 lb = 4.45 N)

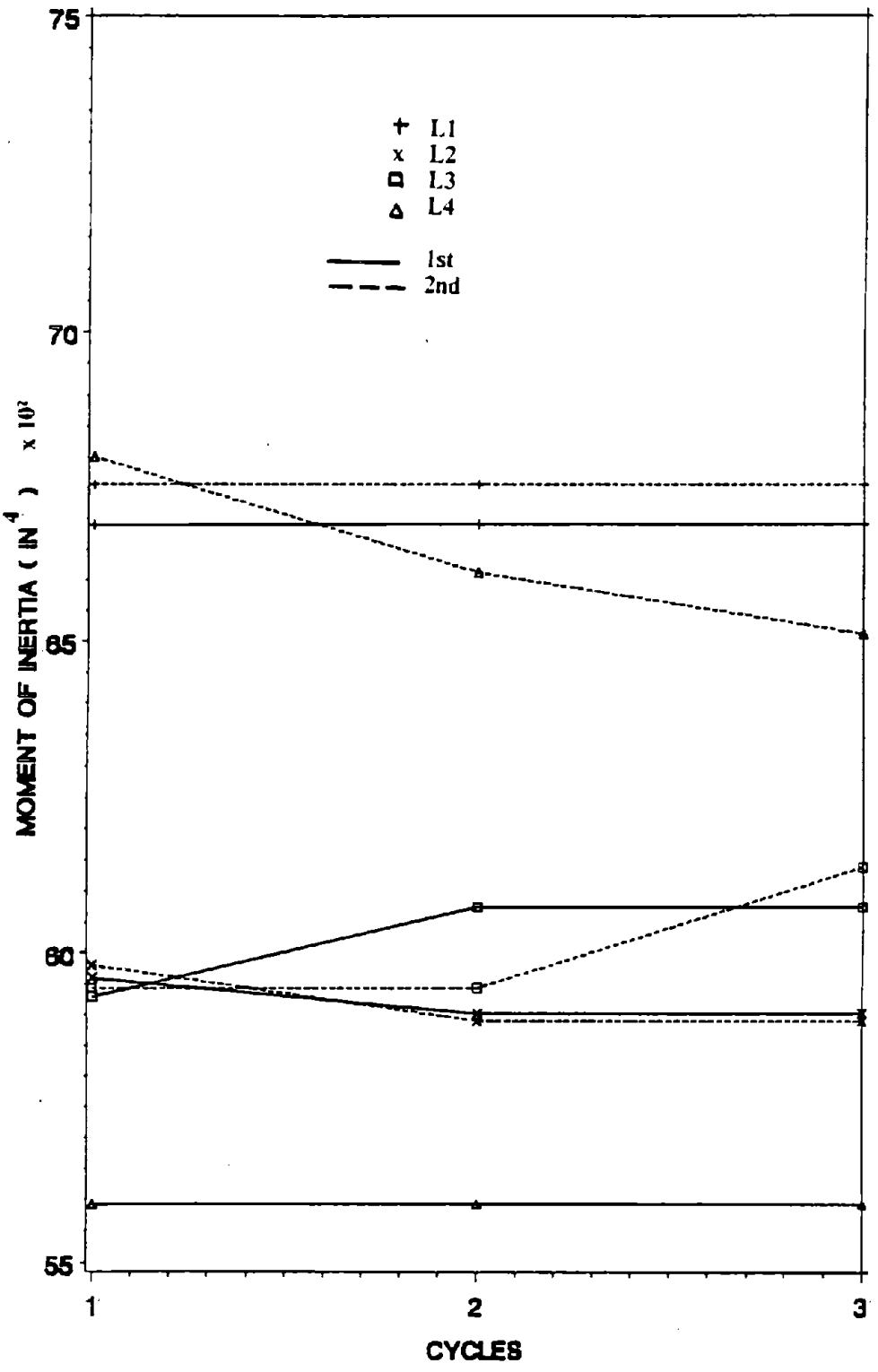

Figure 25. I_1 for Various Live Load Models with LN and D + L + E Case.(1 in^4 = 41.62 cm^4)

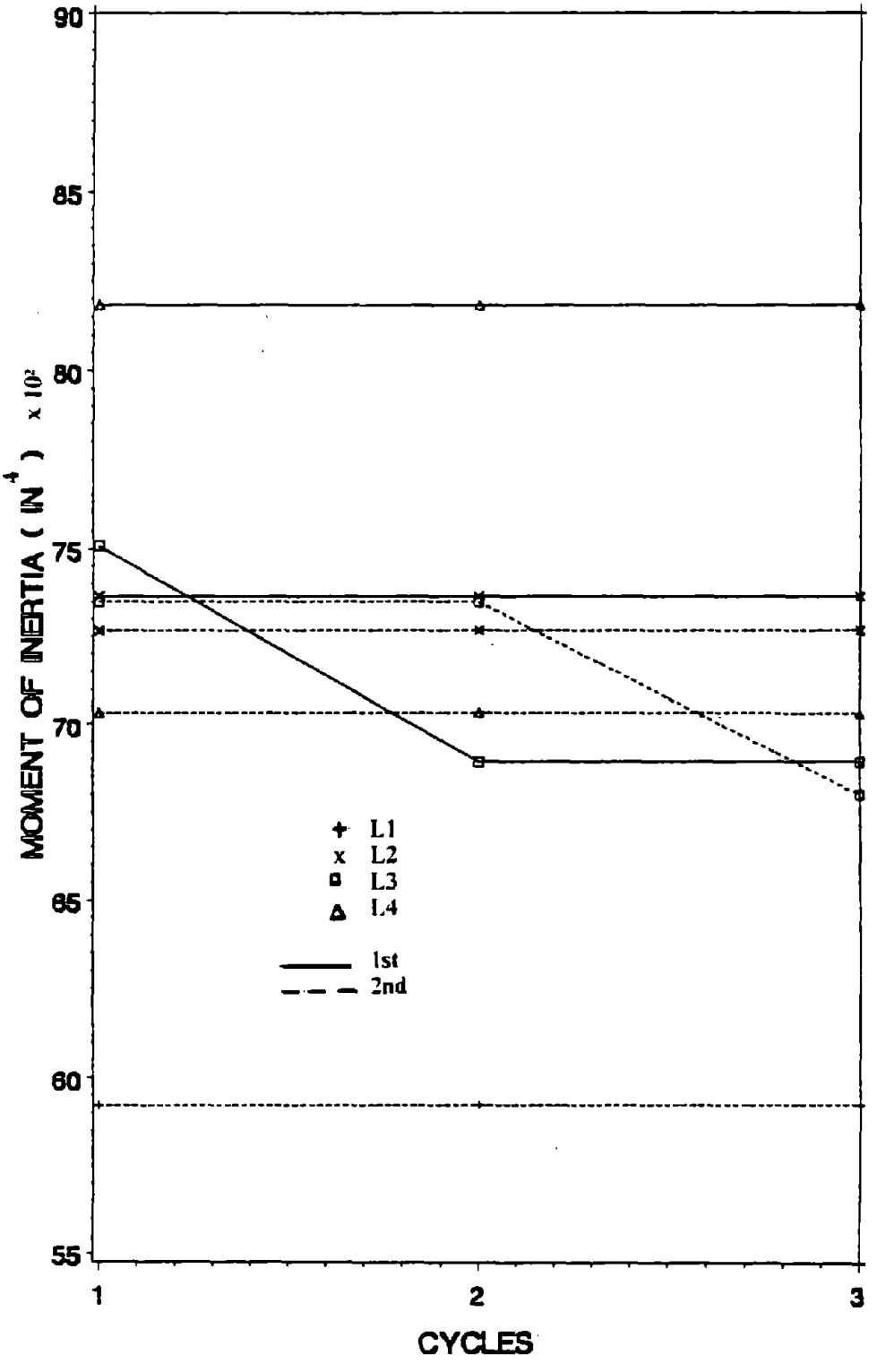

Figure 26. I_4 for Various Live Load Models with LN and D + L + E Case.(1 in^4 = 41.62 cm^4)

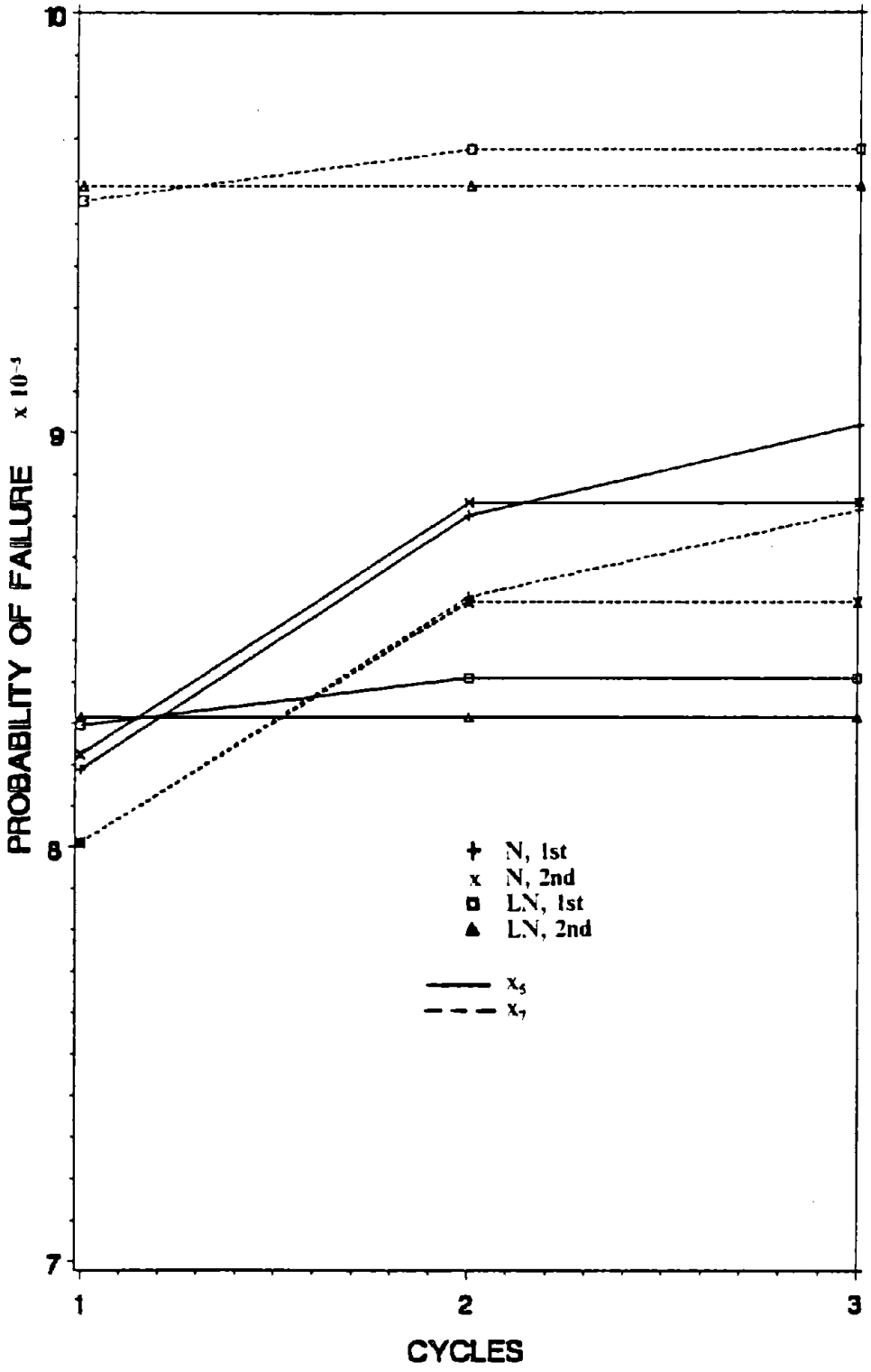

Figure 27. Probability of Failure for ANSI Live Load Model with D + L + E Case.

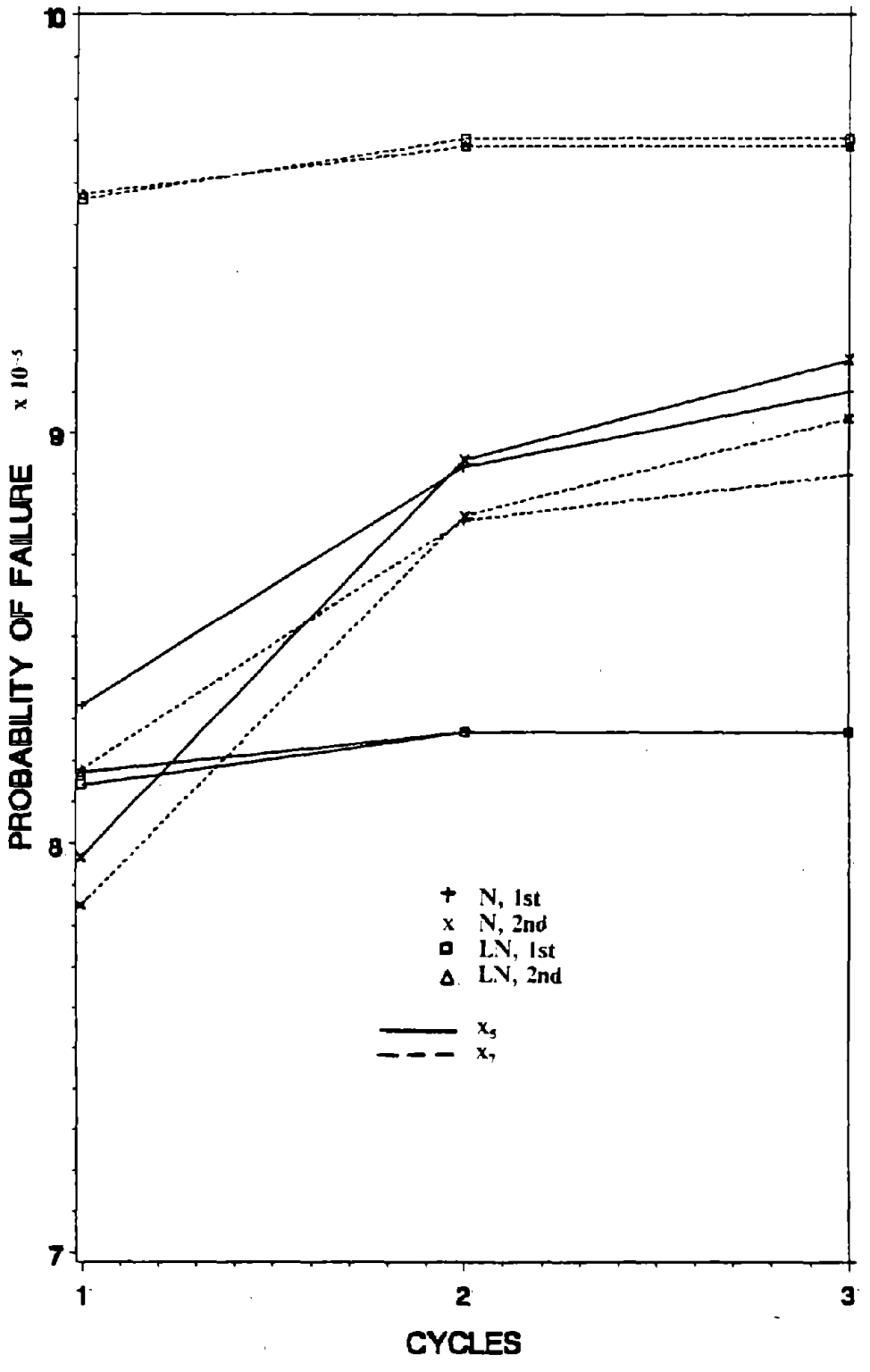

Figure 28. Probability of Failure for NBS Live Load Model with D + L + E Case.

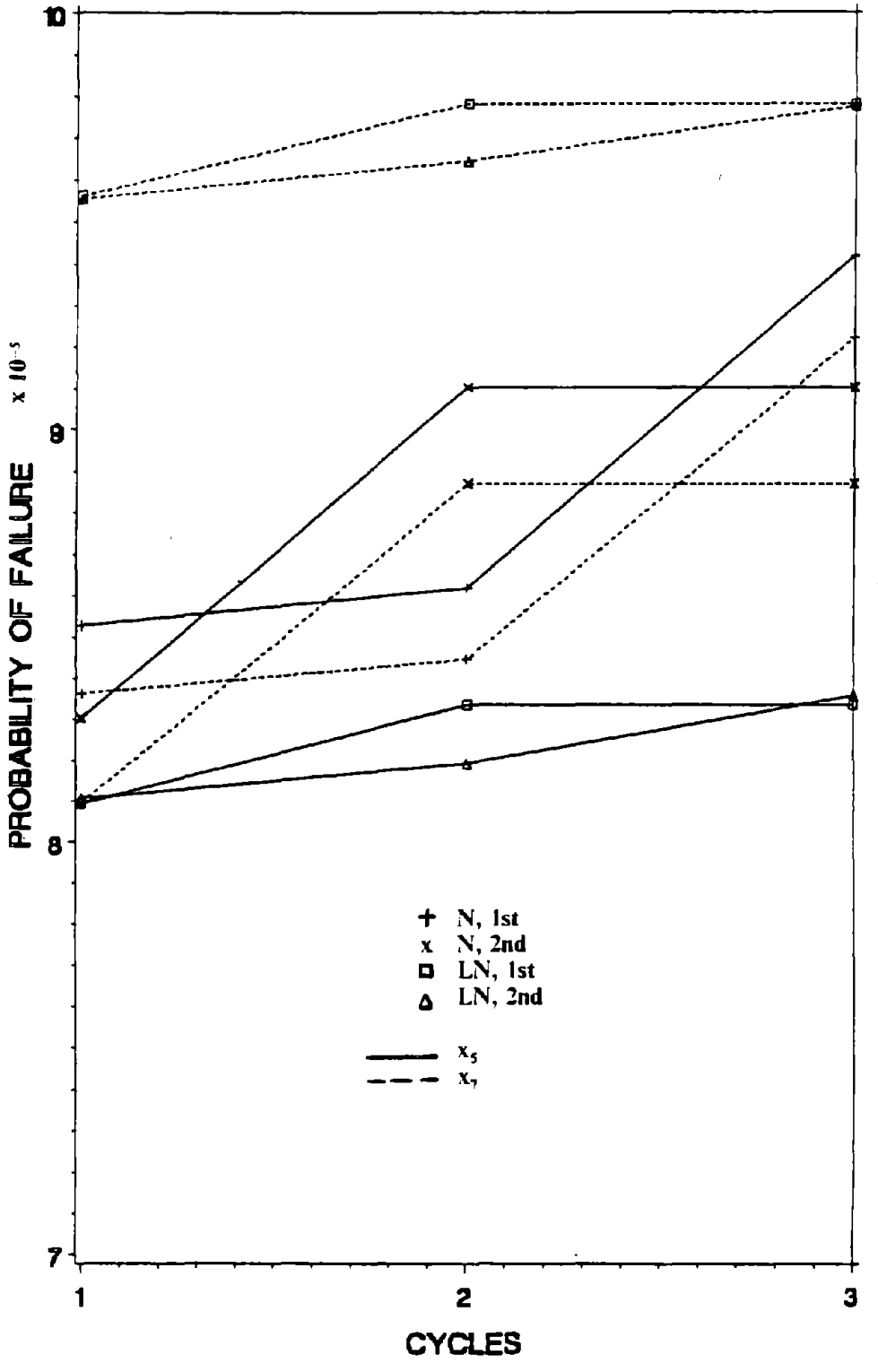

Figure 29. Probability of Failure for UK Live Load Model with D + L + E Case.

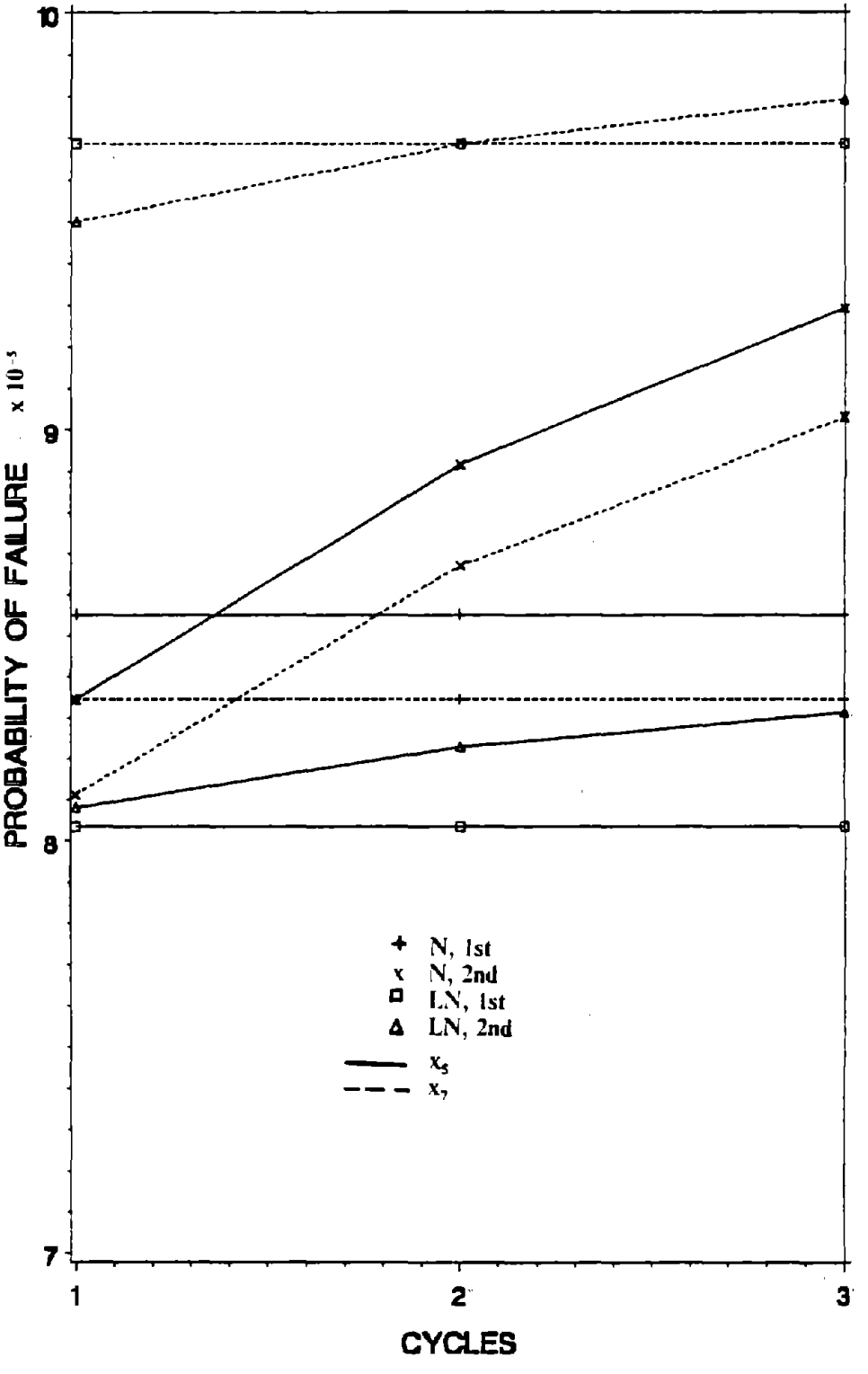

Figure 30. Probability of Failure for UNREDUCED Live Load Model with D + L + E Case.

3. For the D + L case, the 2nd variance approach yields heavier structural design than 1st variance approach for both normal and lognormal distribution.

4. For the D + L case, the structural failures are mainly due to the failures of beams and the top column.

5. For the D + L + E case, the magnitude of optimum weight from large to small is not in the consistent order as the D + L case. For the 1st variance approach, the orders are UNREDUCED, UK, NBS, ANSI, for normal distribution and UNREDUCED, NBS, UK, ANSI, for lognormal distribution; for the 2nd variance approach, the orders are UNREDUCED, NBS, UK, ANSI, for normal distribution and UNREDUCED, NBS, ANSI, UK, for lognormal distribution. The structural failures are mainly due to the failures of lateral displacement on the top floor.

VIII. COMPARISON BASED ON OPTIMALITY CRITERION AND PENALTY FUNCTION METHOD.

Two structural systems of a truss and a frame are used to illustrate the application of optimality criterion method and to show the close agreement of design results obtained by using the optimality criterion method and the penalty function method.

A. TRUSS STRUCTURES

The unsymmetric three bar truss in Figure 31 is used to illustrate the optimum design problem by using both the optimality criterion method and the penalty function method. The design variables are areas of members 1 (A1), 2 (A2), 3 (A3). The random parameters are areas, elastic modulus (E_m), magnitude of applied load (P), and direction angle of applied load (θ). The mean values of random parameters are $\bar{P} = 20$ kips (89 kN) , $\bar{\theta} = \pi/4$, $\bar{E}_m = 10000.$ ksi (6.89×10^7 kPa) . The coefficients of variation of these parameters are $V_{A1} = V_{A2} = V_{A3} = 0.05$, $V_p = 0.05$, $V_\theta = 0.05$, and $V_{E_m} = 0.015$. The allowable mean displacements are 0.5 in (1.27 cm) and 0.125 (0.3175 cm) in corresponding to x and y directions, respectively. The allowable mean stresses for three members are assumed to be 36 ksi (2.448×10^5kPa). The variance of allowable displacements and stresses are zero. The optimum design problem is to find the minimum weight subjected to displacement and stress constraints. Based on optimality criterion method presented in Chapter VI, the mean displacement, $\bar{u}$, and its variance of displacement σ_u^2 (Equation (2.18)), can be expressed as

mean,

$$\bar{u} = \sum_{i=1}^{3} \frac{\bar{T}'_i \bar{t}'_i \bar{\ell}_i}{\bar{E}_m \bar{A}_i} \tag{8.1}$$

and

$$\sigma_u^2 = \sum_{r=1}^{6} \left(\frac{\partial u}{\partial \tau_r}\right)_r^2 V_{\tau_r}^2 \bar{\tau}_r^2$$

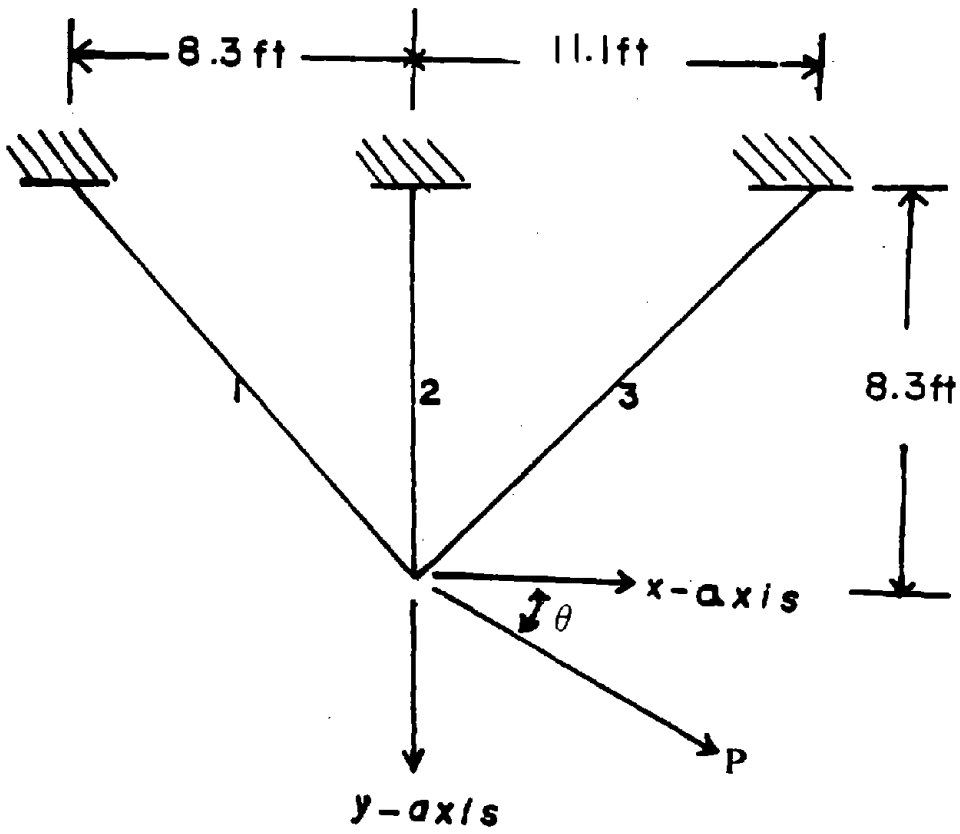

Figure 31. Unsymmetric Three Bar Truss. (1 ft = 30.48 cm)

$$= \sum_{i=1}^{3} \left(\frac{\partial u}{\partial A_i}\right)^2 \bar{r}^2 V_{A_i}^2 \bar{A}_i^2 + \left(\frac{\partial u}{\partial E_m}\right)^2 \bar{r}^2 V_{E_m}^2 \bar{E}_m^2 + \left(\frac{\partial u}{\partial P}\right)^2 \bar{r}^2 V_P^2 \bar{P}^2 + \left(\frac{\partial u}{\partial \theta}\right)^2 \bar{r}^2 V_{\bar{\theta}}^2 \bar{\theta}^2 \tag{8.2}$$

in which T'_i = the internal force of ith member; t'_i = the virtual internal force of ith member; ℓ_i = the length of ith member; and the other terms are expressed in Equations (8.3) through (8.6) as

$$\frac{\partial u}{\partial A_i} = \frac{T'_i t'_i \ell_i}{E_m A_i^2}, \tag{8.3}$$

$$\frac{\partial u}{\partial E_m} = \sum_{i=1}^{3} \frac{-T'_i t'_i \ell_i}{E_m^2 A_i}, \tag{8.4}$$

$$\frac{\partial u}{\partial P} = \frac{\partial(\{P\}^T \{S\})}{\partial P} = S_x \cos\theta + S_y \sin\theta, \tag{8.5}$$

$$\frac{\partial u}{\partial \theta} = \frac{\partial(\{P\}^T \{S\})}{\partial \theta} = -P \sin\theta S_x + P \cos\theta S_y \tag{8.6}$$

In Equations (8.5) and (8.6), $\{P\}^T$ = transponse of column matrix of external forces = $[P\cos\theta, P\sin\theta]$; $\{S\}$ = the column matrix of external virtual displacements due to the virtual load applied at x or y direction = $[S_x, S_y]^T$.

Using the above equations and the derivatives of uncertainties of displacement with respect to design variables (Equations (8.1) through (8.6)), one can determine the scaling factors (Equation (6.43)), Largrangian multipliers (Equation (6.49)), and recurrence equations (Equation (6.47)). For the optimum solution, Figures 32 and 33 show the optimum weights and the cross sectional areas of the truss based on the optimality criterion method and the penality fuction method. The solutions obtained by these two methods are very close.

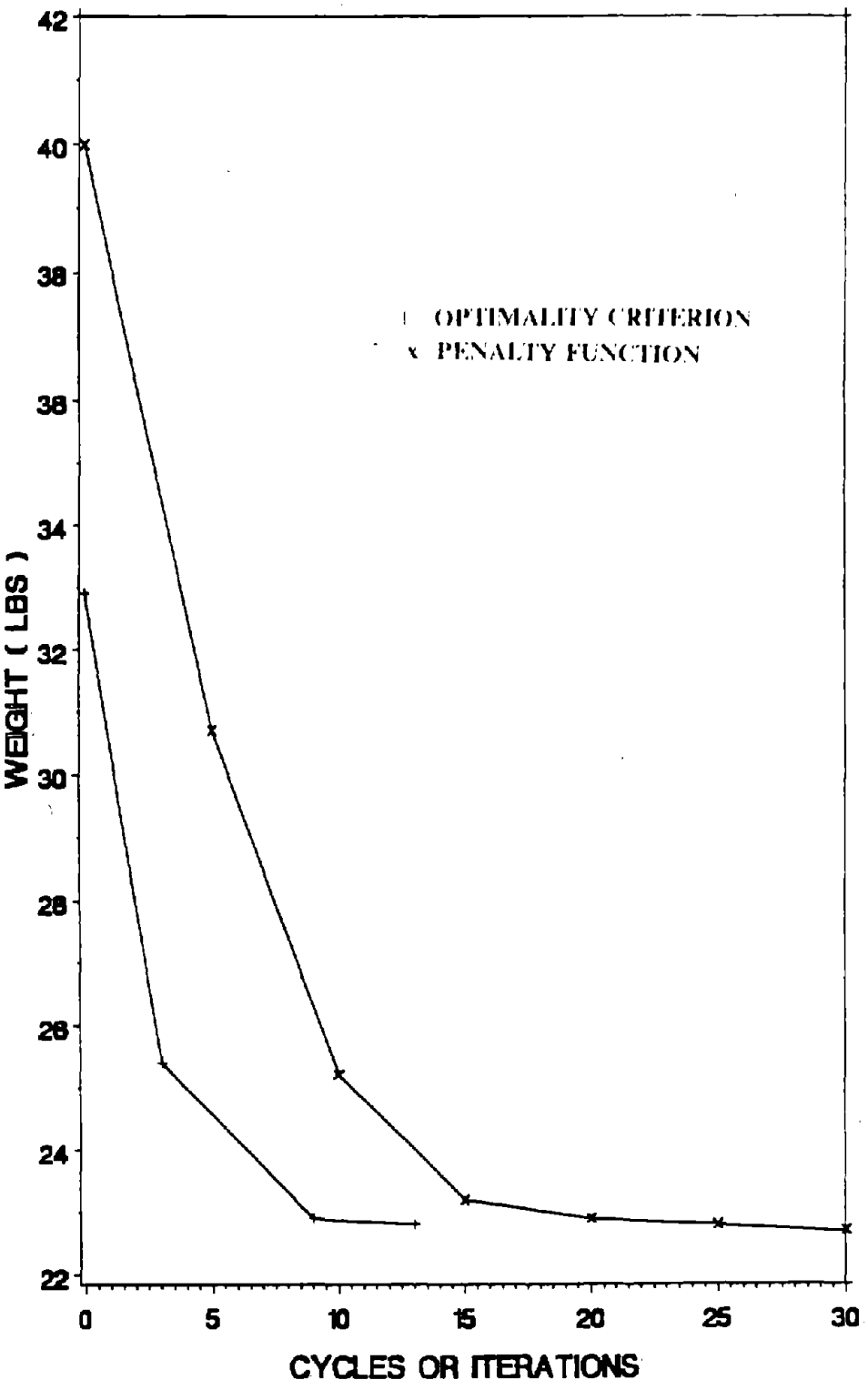

Figure 32. Optimum Weight of Unsymmetric Three Bar Truss Based on Optimality Criterion Method and Penalty Function Method. (1 lb = 4.45 N)

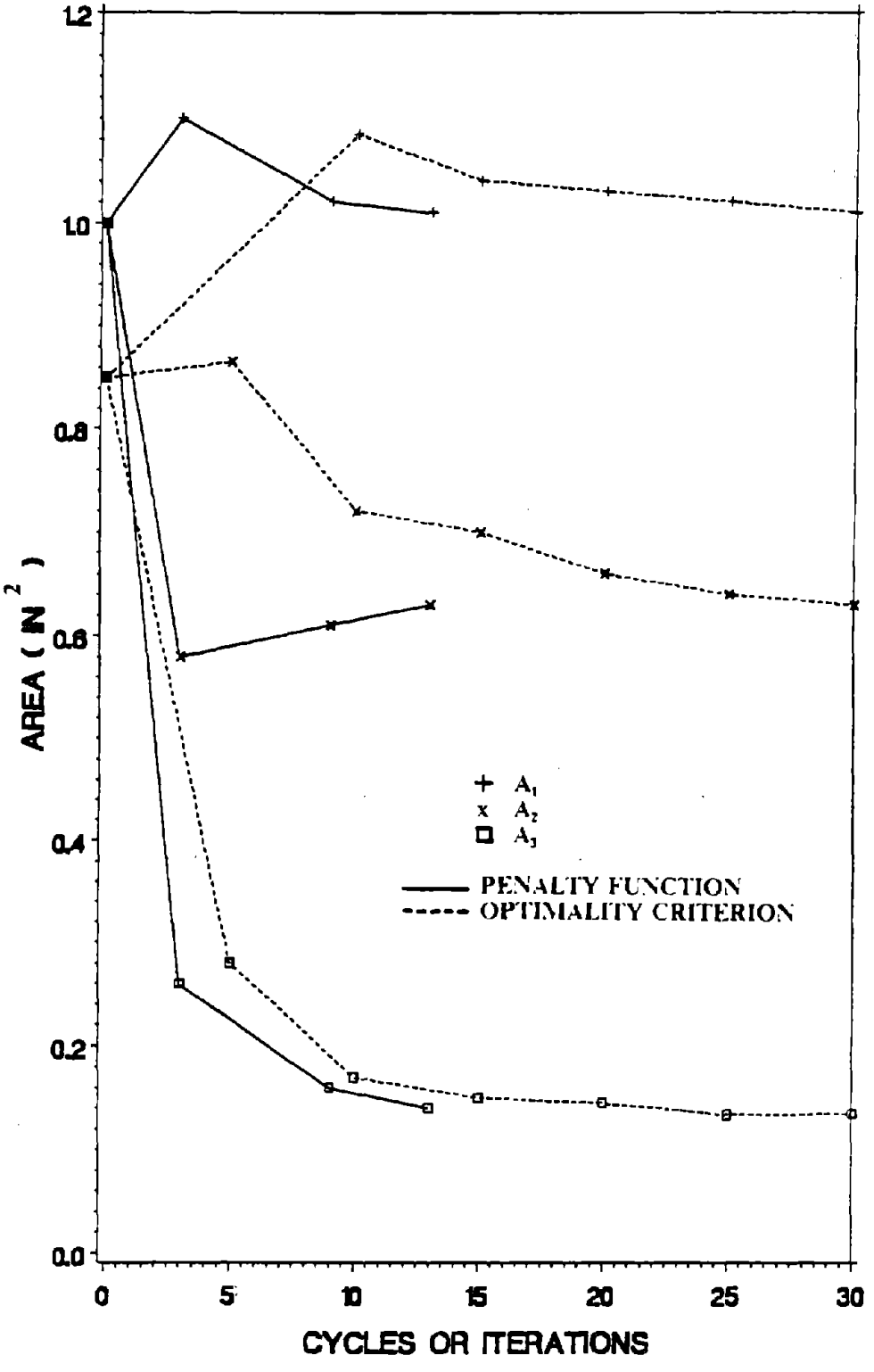

Figure 33. Areas of Unsymmetric Three Bar Truss Based on Optimality Criterion Method and Penalty Function Method. (1 in = 2.54 cm)

B. FRAME STRUCTURES

Two-story building shown in Figure 6 and five-story building in Figure 34 are used to demonstrate the application of optimality criterion method for cost objective function. The structural parameters for the two-story building are the same parameters used in previous chapter. The NBS live load model (L2) is used here. The cost function is assumed as $C_T = C_I + L_f P_{fT}$. The initial cost is C_I = 1.55 (dollars / volume) times structural volume and the expected loss is L_f = 1.15 (2.5 C_I + 3194100) dollars for the two-story building. 3194100 is the combination of the liability due to death ($ 700000 for 1 person of annual income 20000 dollars), serious injuries ($1400000 for 4 persons), minor injuries ($75000 for 15 persons), and the business interruption ($1019100). For the five-story building, the initial constructure cost is C_I = 1.55 (dollars/ volume) times structural volume and expected loss is L_f = 1.15 (2.5 C_I + 14362500) dollars. 14362500 is the combination of the liability due to death ($3500000 for 5 persons of annual income 20000 dollars), serious injuries ($3500000 for 10 persons), minor injuries ($375000 for 75 persons), and the business interruption ($6987500). The calculations of liability cost due to death, serious injuries, and minor injuries for each person are described in Section VIA. The business interruption has been calculated in the remaining amount of 3194100 or 14362500 excluding the liability cost.

The problem with the given cost function may be constrained or unconstrained depending on the location of optimal solution fallen on the boundary or within feasible region. It can be decided to check whether the allowable failure probabilities are reached on the optimal solution. The algorithm is explained in Appendix I for the application of optimality criterion method to this type of problem. Figures 35 and 36 reveal the optimum cost of the two-story building subjected to D + L and D + L + E. The solution first approaches the unconstrained solution and then jumps up to converge to the constrained solution based on the allowable probability of failure, $P_{f0} = 10^{-7}$. For the D + L case, because the unconstrained solution violated the given constraints, the unconstrained and constrained results of the penalty function method are around 1.57×10^4 dollars and 1.6×10^4 dollars, respectively, which are close to the results of

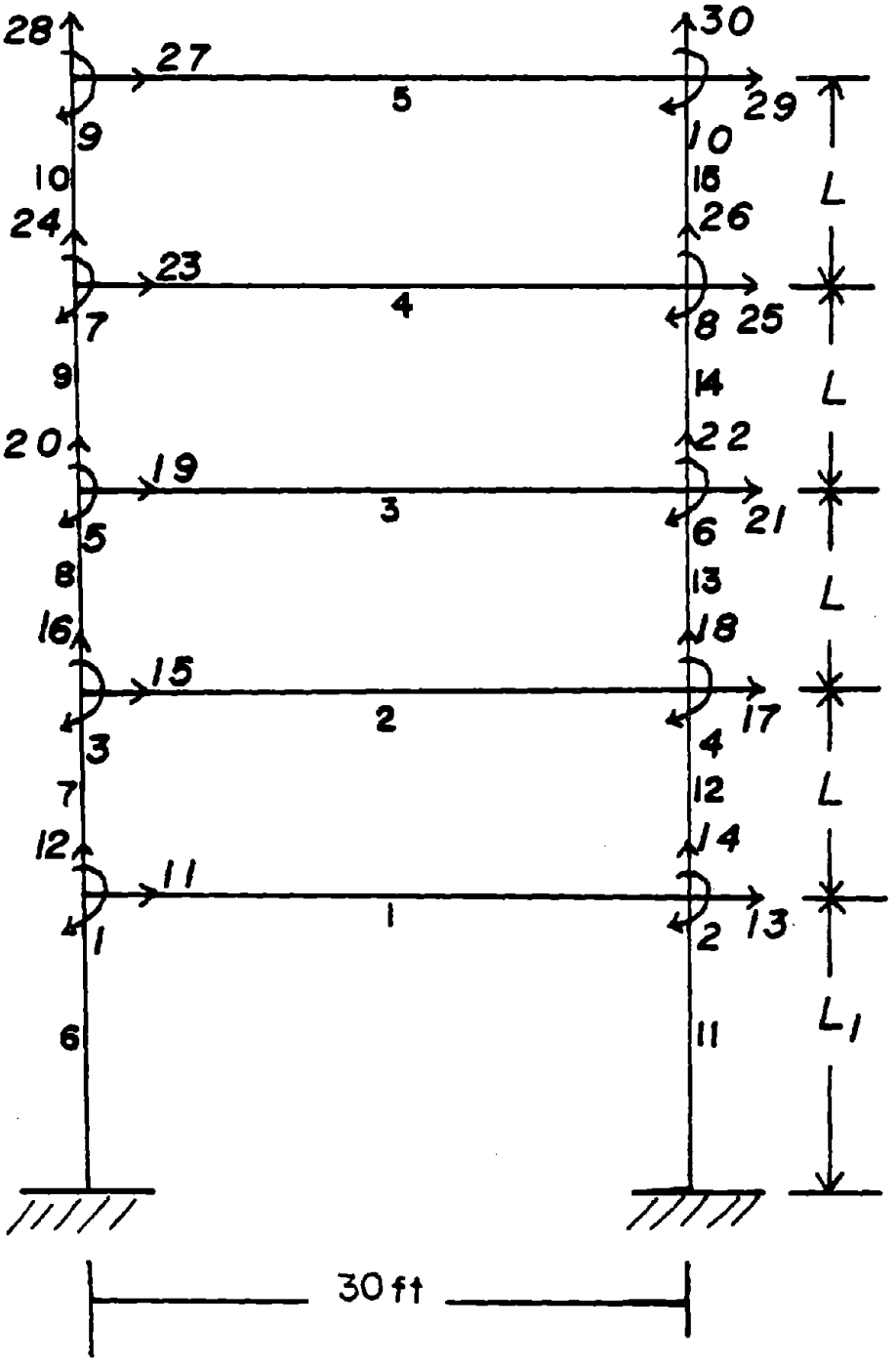

Figure 34. 5-Story Building Structure.(L_1 = 15 ft, L = 12 ft, 1 ft = 30.48 cm)

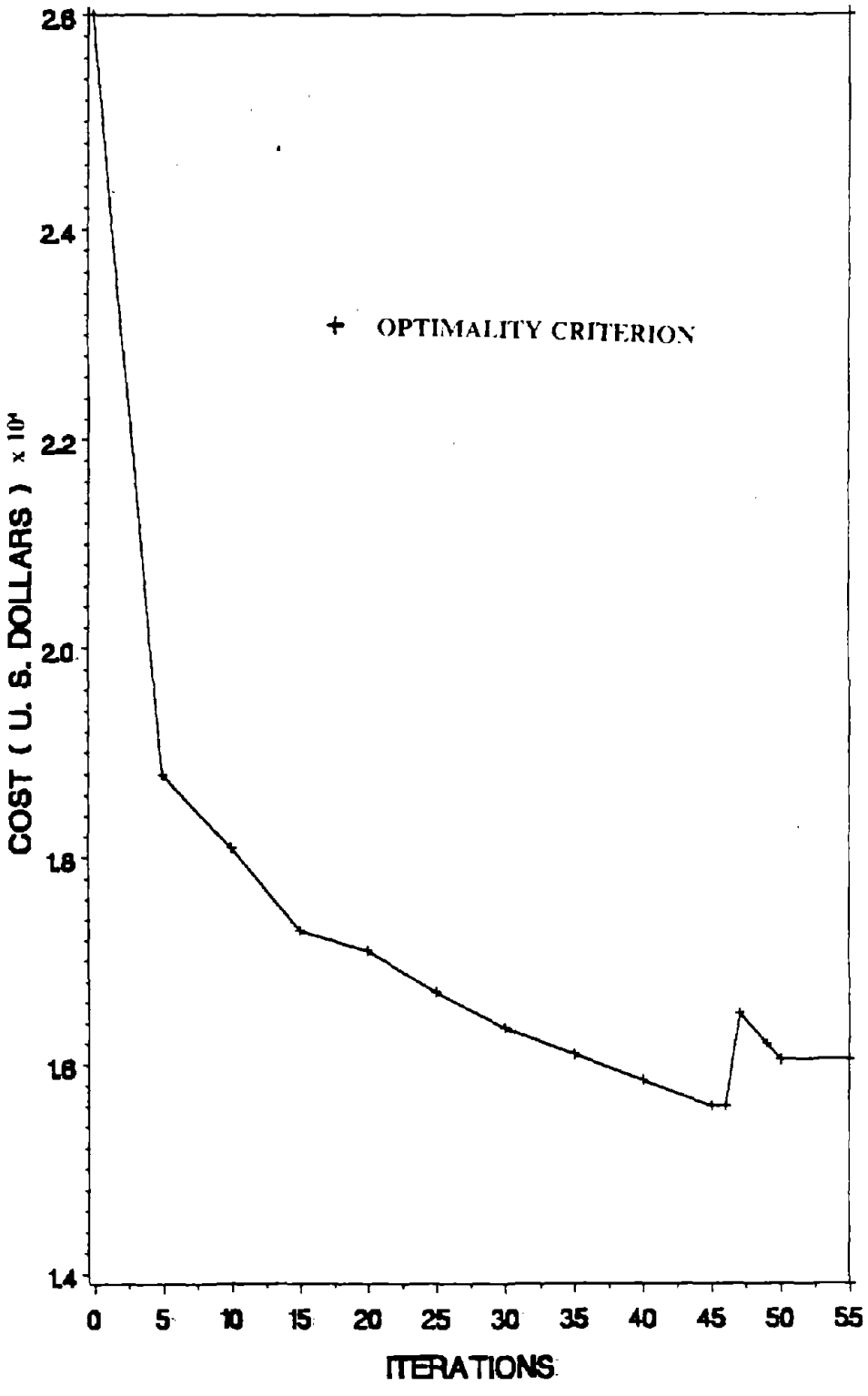

Figure 35. Optimum Cost of 2-Story Structure with N and D + L Case.

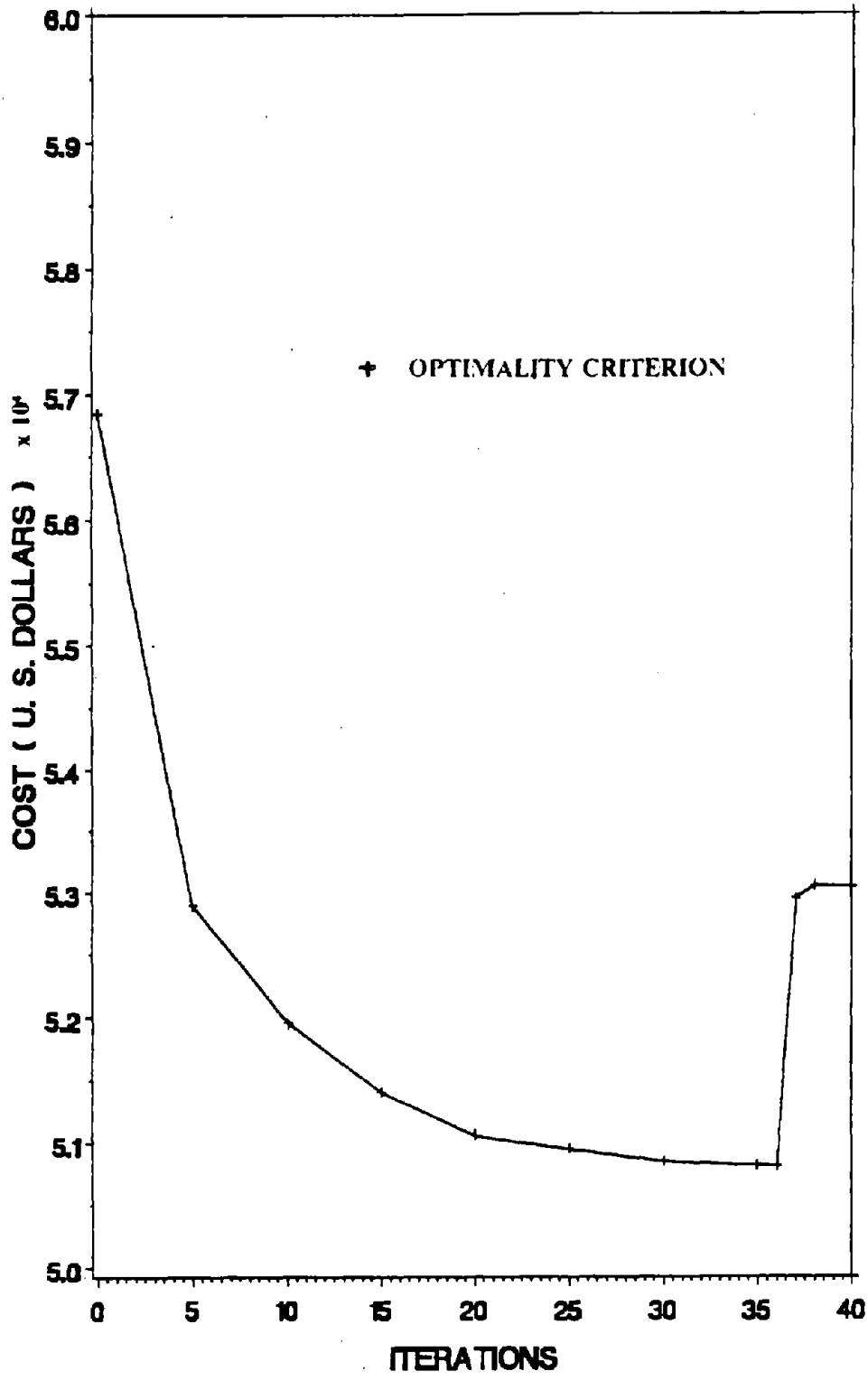

Figure 36. Optimum Cost of 2-Story Structure with N and D + L + E Case.

1.56×10^4 dollars (unconstrained) and 1.605×10^4 dollars (constrained) based on the optimality criterion method as shown in Figure 35. For the D + L + E case, the unconstrained and constrained results of the penalty function method are around 5.0×10^4 dollars and 5.3×10^4 dollars, respectively, which are close to the results of 5.08×10^4 dollars (unconstrained) and 5.34×10^4 dollars (constrained) based on the optimality criterion method as shown in Figure 36.

In Figure 37, the solution is based on the optimality criterion fo the five-story building. The structural parameters used are the same parameters as in previous chapter. The unconstrained optimum total cost is 4.46×10^6 dollars and the constrained optimum total cost is 5.39×10^6 dollars for the allowable failure probability = 10^{-7}.

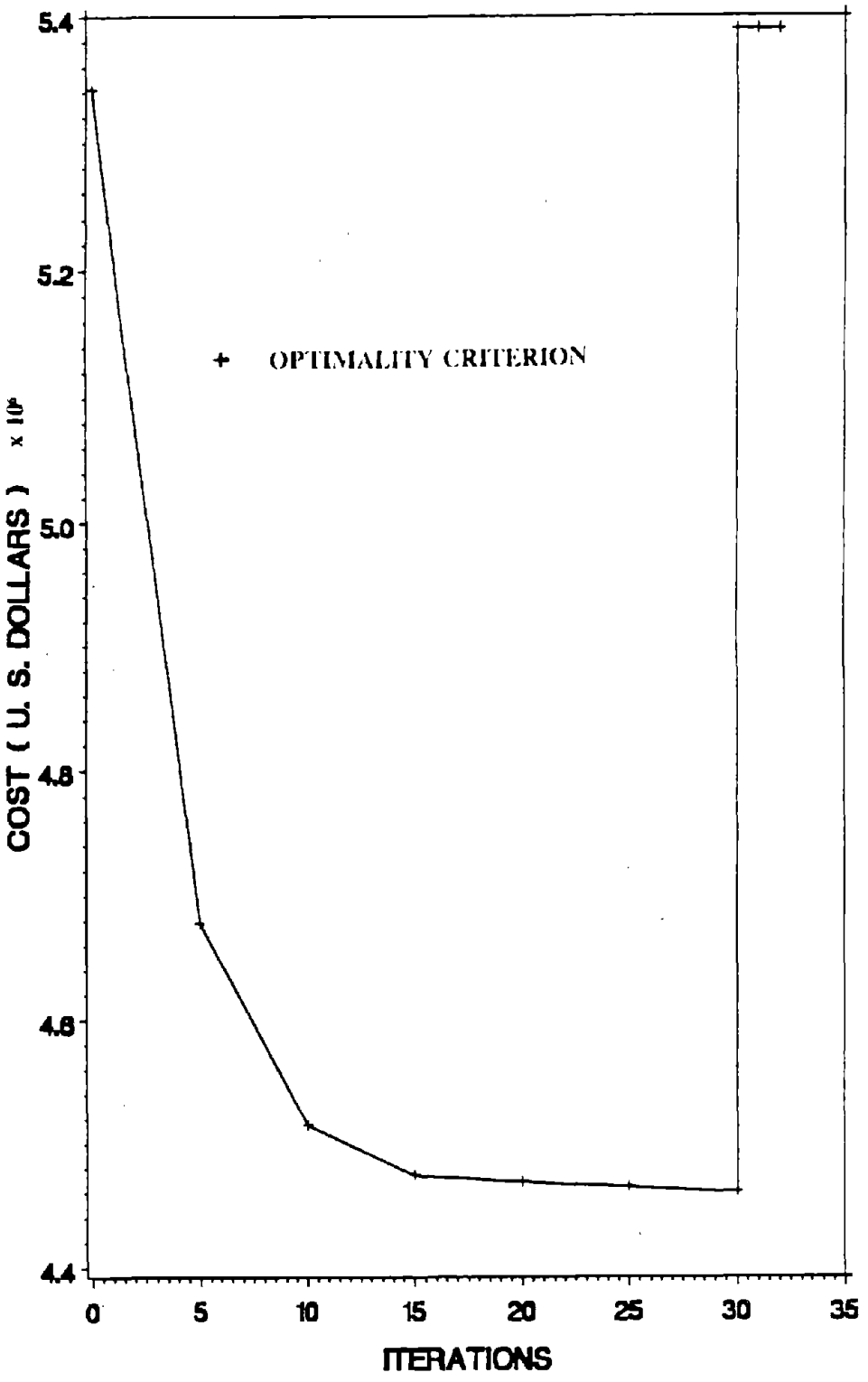

Figure 37. Optimum Cost of 5-Story Structure with N and D + L + E Case.

IX. OPTIMUM DESIGNS FOR UBC LOAD

The earthquake load recommended in the Uniform Building Code (UBC) is utilizied here to study the sensitivities of coefficients of variation of structural resistance parameters, the sensitivities of coefficients of variation of UBC load, the sensitivities of two probability distributions of structural resistance and response, and those of the zone coefficient in UBC on the optimum design results. The two-story and ten-story symmetrical shear buildings shown in Figures 38 and 39 are used to study the optimum solutions. The parameters used in the examples are : A_I = 900 ft^2 (83.61 m^2) for each floor; $\overline{D}$ = 80 psf (3.82 kPa); V_D = 0.12; the allowable displacements = 0.005 times the corresponding height relative to the base; the allowable variance of displacements = 0; the mean yielding strength, $\overline{F}_y$ = 36 ksi (2.448 x 10^5 kPa); the mean elastic modulus, $\overline{E}_m$ = 30000 ksi (2.067 x 10^8 kPa); the coefficient of variation of elastic modulus, $V_{I;m}$ = 0.06; and the coefficient of variation of moment of inertia, V_I = 0.05. The parameters for the base shear in UBC are: I_I = 1.0, K_I = 1.0, S_I = 1.5, C_I = 1/(15$\sqrt{T}$), hn = 27 ft (8.23 m), and Dn = 30 ft (9.14 m).

A. VARIATION OF COLUMN RESISTANCE PARAMETERS.

The column resistance parameters of shear building structures considered may be yielding moment and critical moment. The coefficients of variation of these parameters have been estimated and reported in Reference 76. However, these values were determined by experimental works or experienced assumptions, the exact values can not clearly be known. Therefore, the investigation for sensitivities of variation of these parameters is necessary.

Two individual failure modes, yielding and torsional buckling, may exist appear at each column. The uncertainties of the interaction equation of yielding may be expressed in mean and coefficient of variation as

$$\overline{f}_I = \overline{M}/\overline{M}_y \tag{9.1}$$

and

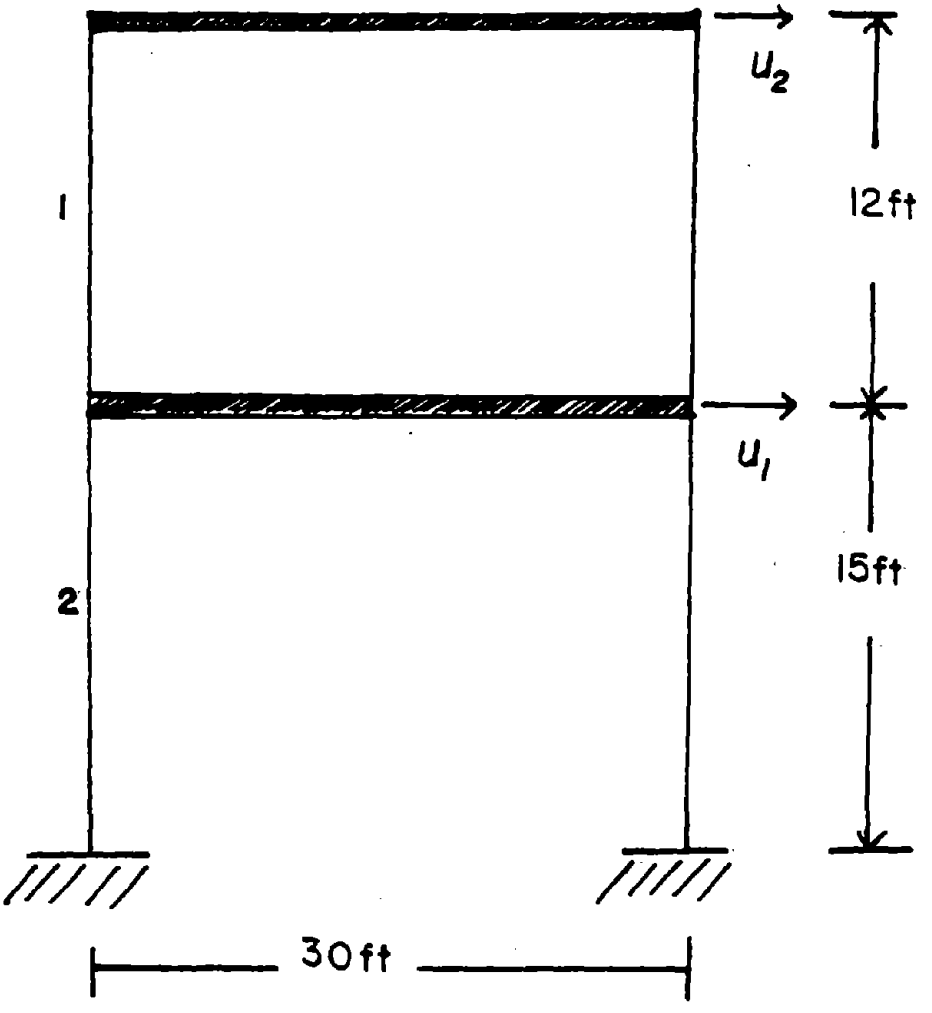

Figure 38. 2-Story Shear Building Structure (1 ft = 30.48 cm)

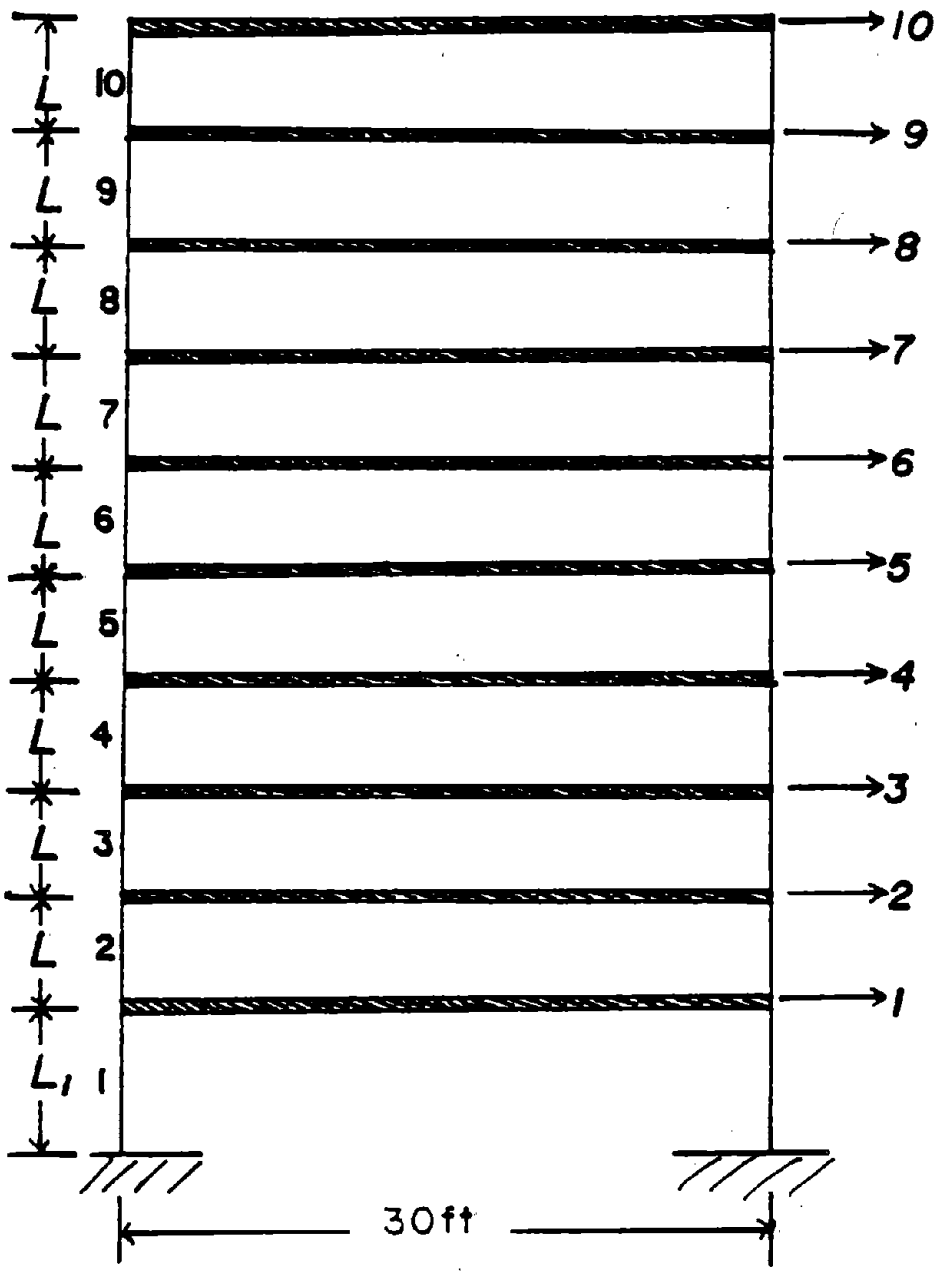

Figure 39. 10-Story Shear Building Structure.(L_1 = 15 ft, L = 12 ft, 1ft = 30.48 cm)

$$V_{f_1}^2 = V_M^2 + V_{M_y}^2 \tag{9.2}$$

in which V_M = coefficient of variation of applied moment and V_{M_y} = coefficient of variation of yielding moment. The mean and the coefficient of variation of the interaction of torsional buckling are

$$\bar{f}_2 = \overline{M}/\overline{M}_{cr} \tag{9.3}$$

and

$$V_{f_2}^2 = V_M^2 + V_{M_{cr}}^2 \tag{9.4}$$

in which $V_{M_{cr}}$ = coefficient of variation of critical moment.

1. Sensitivity of Variation of Yield Moment. The numerical values of V_{M_y} are assumed to vary from 0.05 to 0.2 to investigate the sensitivity of coefficient of variation of yield moment in this study. The value of 0.12 is recommended in Reference 76. For the purpose of studying the sensitivity of V_{M_y} alone, the coefficient of variation of critical moment is kept constant as 0.2 which is also recommended in that reference. The study is based on the two variance approaches in both normal and lognormal distribution for various allowable probability failures. Two coefficients of variation of earthquake are assumed to be zero and 1.38 in the study, and the value of 1.38 is recommended by NBS.

a. No Variation of UBC. In Figures 40 through 43, the optimum solutions of weight and moments of inertia are not sensitive to the change of variation of yield moment for 1st and 2nd variance approach with normal distribution and lognormal distribution when V_{p_y} is less than 0.15. When V_{p_y} is larger than 0.15, the design results increase as allowable reliability criteria increase. When the values of V_{p_y} vary from 0.15 to 0.2, the increases of optimum weight with normal distribution are about 2% and 4% at $P_{f0} = 10^{-5}$ and 10^{-7}, respectively.

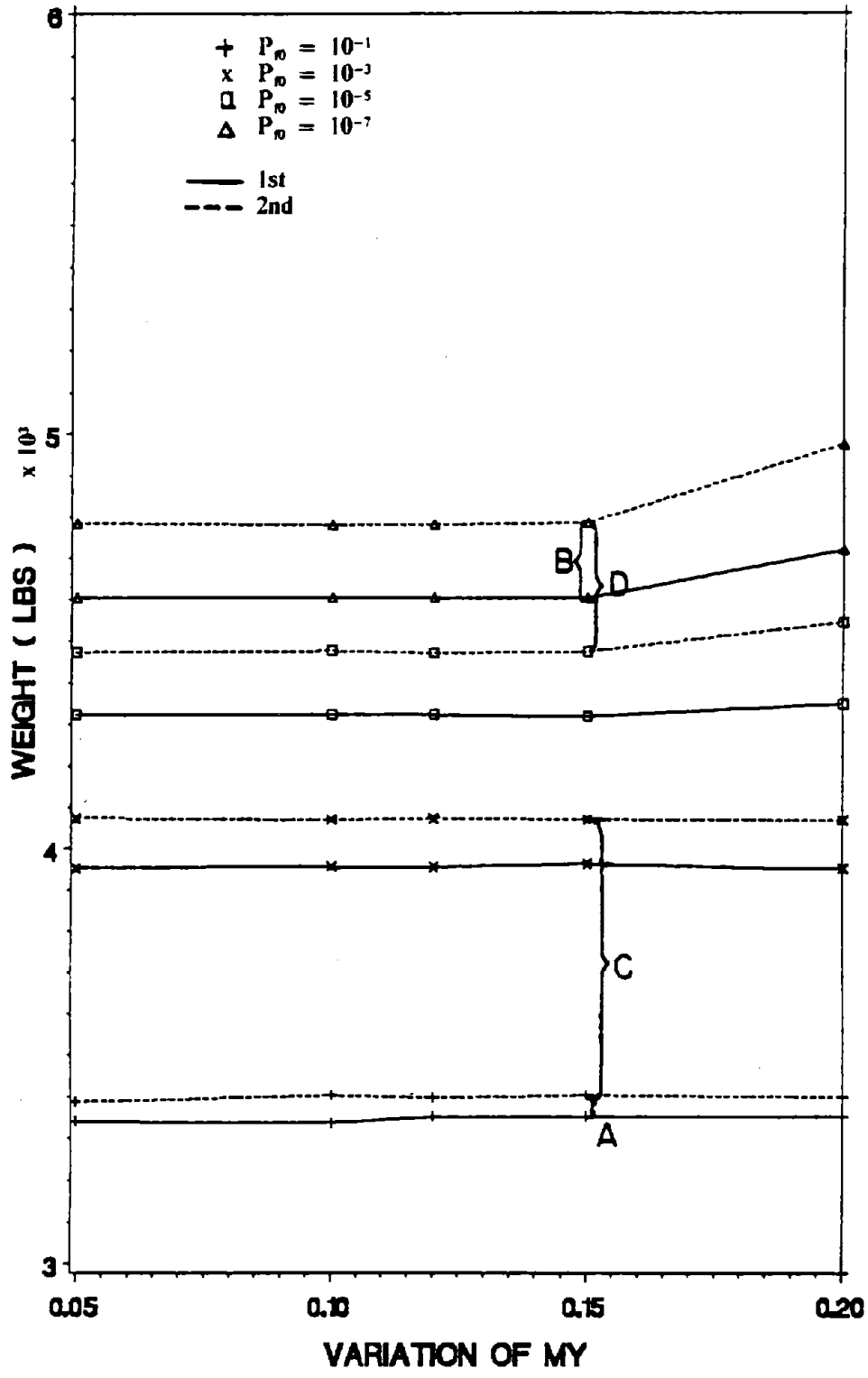

Figure 40. Optimum Weight for Various V_{M_y} with N and V_E = 0 of 2-Story Building,(1 lb = 4.45 N)

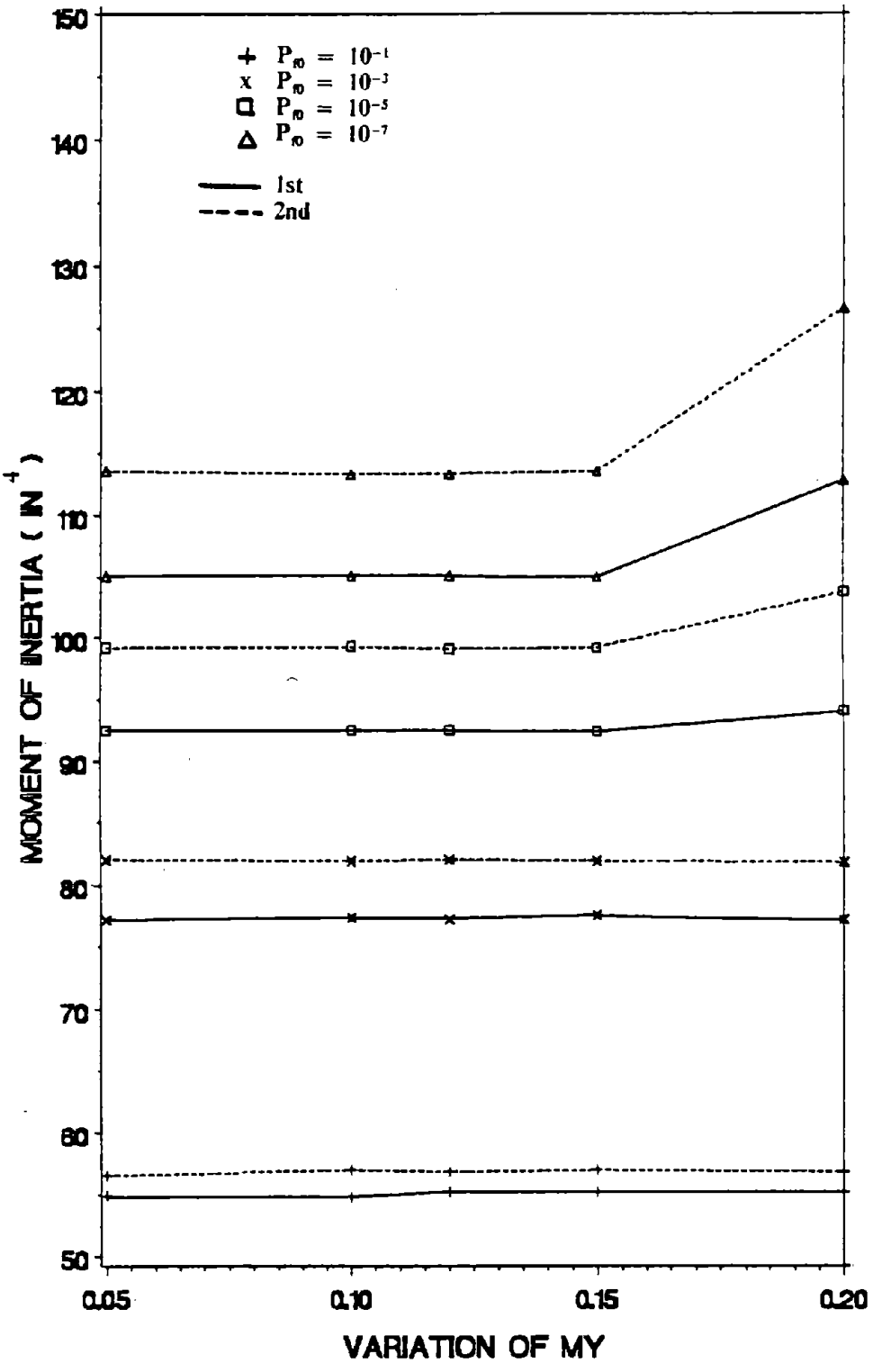

Figure 41. I_1 for Various V_{M_y} with N and V_E = 0 of 2-Story Building.(1 in^4 = 41.62 cm^4)

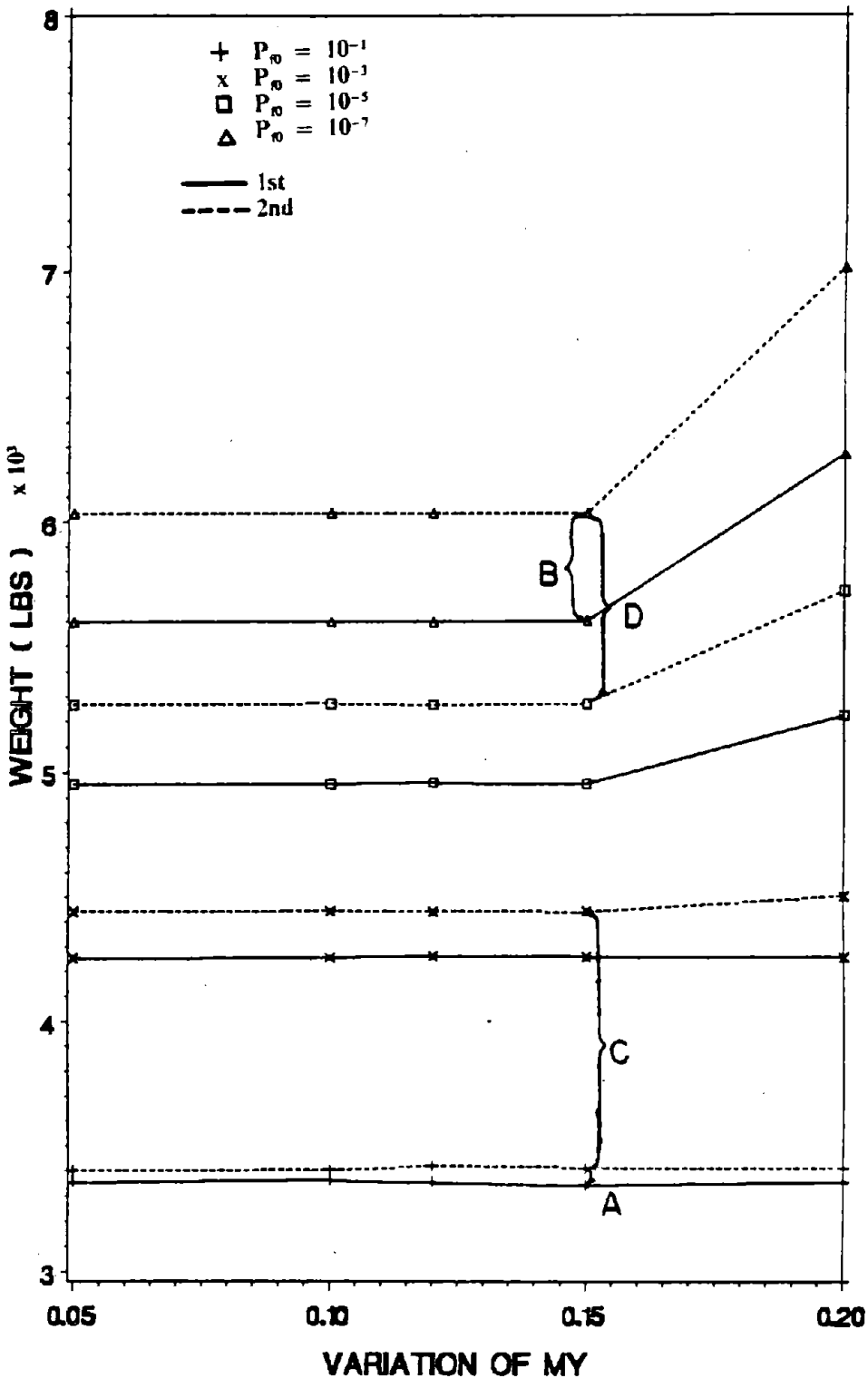

Figure 42. Optimum Weight for Various V_{M_y} with LN and $V_E = 0$ of 2-Story Building. (1 lb = 4.45 N)

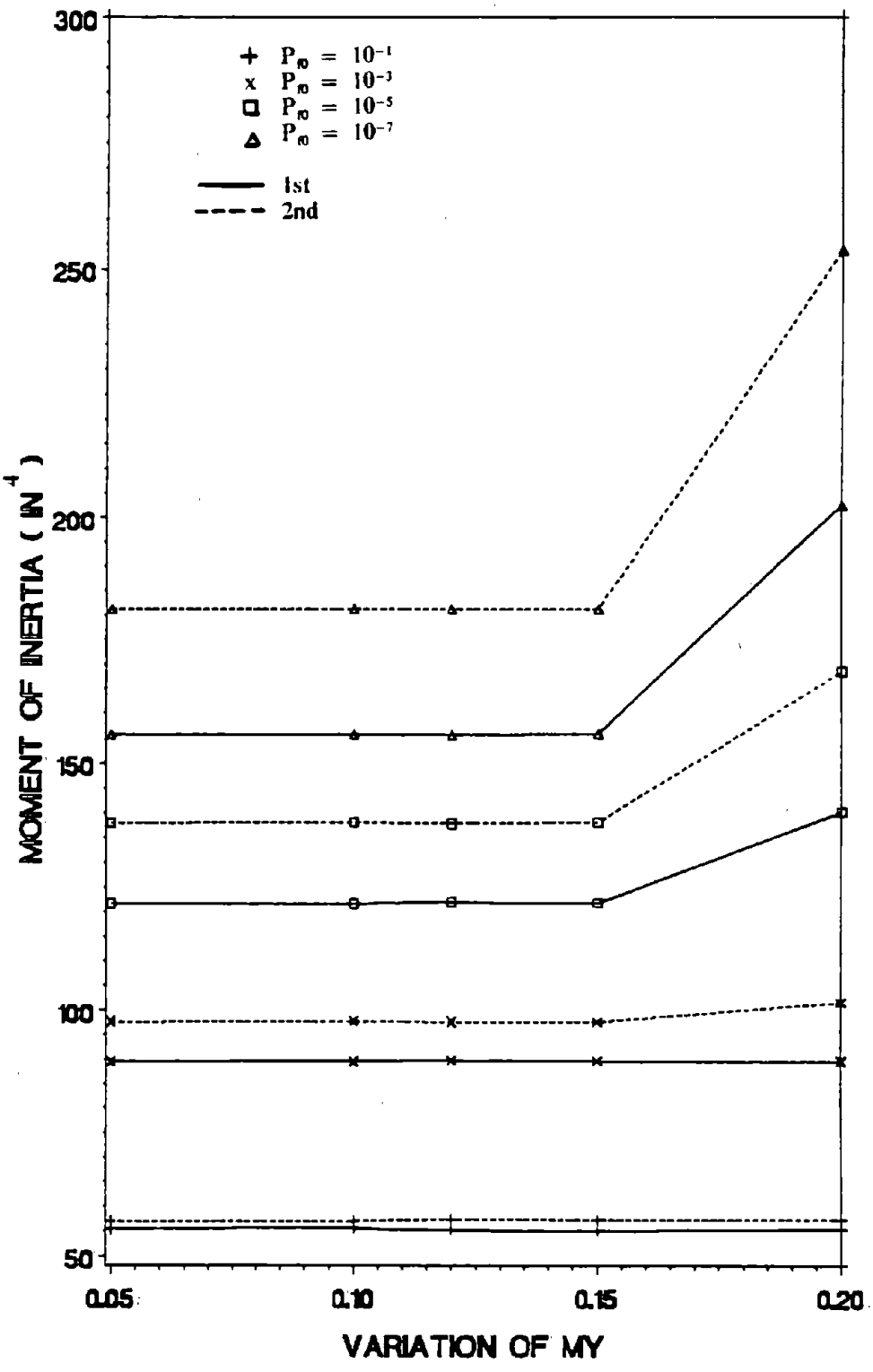

Figure 43. I_1 for Various V_{M_y} with LN and V_E = 0 of 2-Story Building.(1 in^4 = 41.62 cm^4)

The increases associated with lognormal distribution are about 8% at $P_{f0} = 10^{-5}$ and 16% at $P_{f0} = 10^{-7}$. No noticeable increases for $P_{f0} = 10^{-1}$ and 10^{-3}.

Figures 40 through 43 show that the 2nd variance approach demands a heavier weight and larger sections than the 1st variance approach for all V_{p_y} values with both the normal and lognormal distributions. The difference between two approaches increases as reliability increases. In Figures 40 and 42, at $V_{p_y} = 0.15$ the weight differences are from 52.6 lbs (234.1 N) at reliability of 10^{-1} to 181.3 lbs (806.7 N) at reliability of 10^{-7} with normal distribution (A and B in Figure 40) and 67.8 lbs (301.7 N) at reliability of 10^{-1} to to 432.7 lbs (1925.5 N) at reliability of 10^{-7} with lognormal distribution (A and B in Figure 42). The weight difference between two reliabilities decreases as reliability increases. For a given $V_{p_y} = 0.15$ value associated with the 2nd variance approach, the optimum weight difference is about 667.4 lbs (2969.9 N) between two reliabilities of 10^{-1} and 10^{-3} and 311.0 lbs (1383.9 N) between 10^{-5} and 10^{-7} with normal distributions (C and D in Figure 40); about 1026.7 lbs (4568.8 N) between 10^{-1} and 10^{-3}, and 762.4 lbs (3392.6 N) between 10^{-5} and 10^{-7} with lognormal distribution (C and D in Figure 42).

b. Variation of 1.38 for UBC. Due to the highly complicated earthquake phenomina, NBS recommended a value of 1.38 as the variation of UBC in Reference 66. In Figures 44 and 45, one may observe that, at various reliabilities, the optimum weights obtained by using 1st and 2nd variance approach are close for both the normal and lognormal distributions and that V_{M_y} is not sensitive to the solution at all. The reason is mainly due to the high value of variation of earthquake; when 1.38 is used, the variations of structural response and resistance do not influence the design results any more.

2. Sensitivity of Variation of Critical Moment. The numerical values of $V_{M_{cr}}$ are varied from 0.1 to 0.3 for investigating the sensitivity of the coefficient of variation of critical moment; the value of 0.2 is recommended in Reference 76. In the sensitivity study, the other parameters are based on 0.12 of the coefficient of variations of yield moment, zero and 1.38 of the variations of UBC, normal and lognormal distributions, and the two variance formulations.

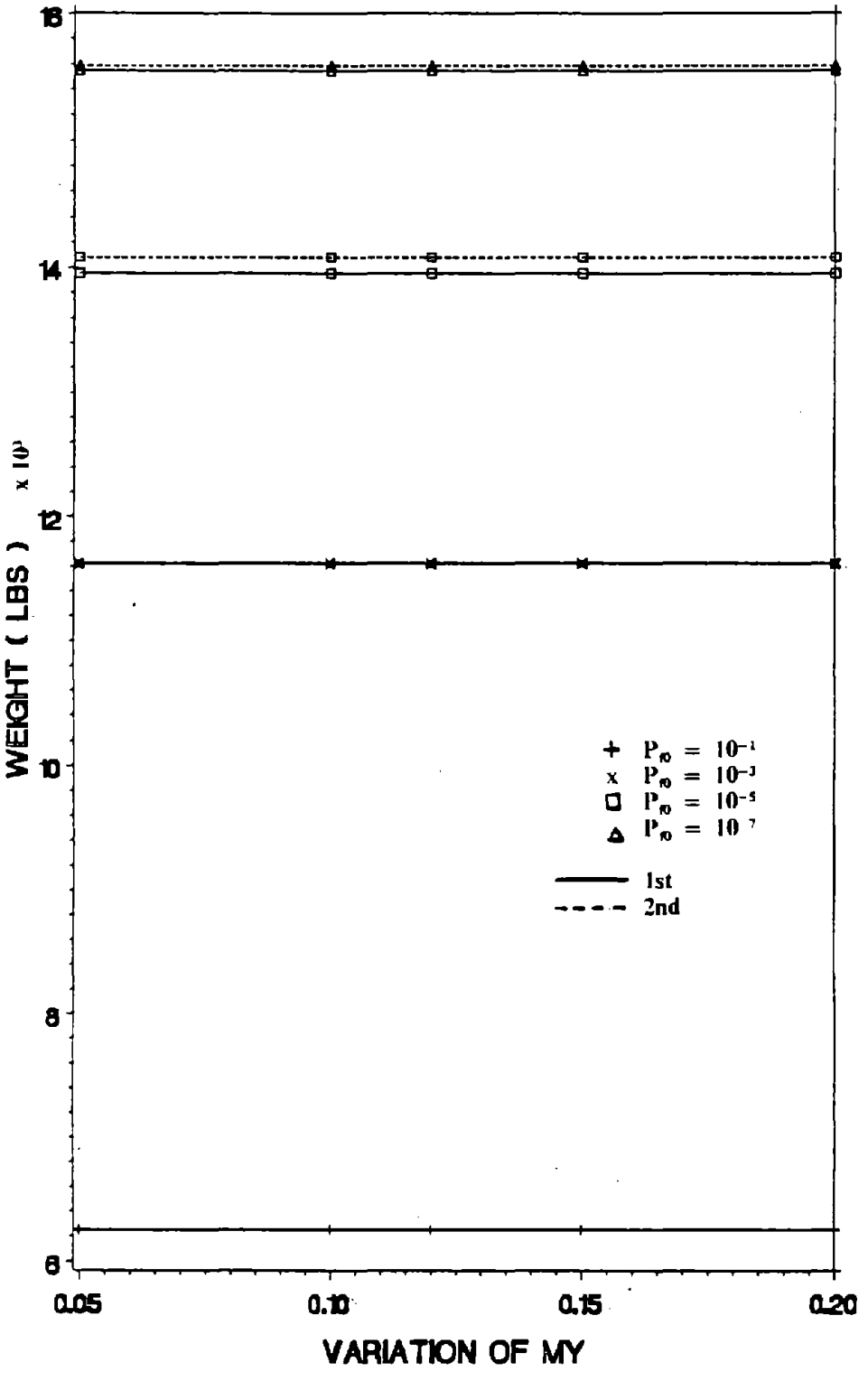

Figure 44. Optimum Weight for Various V_{M_y} with N and V_E = 1.38 of 2-Story Building. (1 lb = 4.45 N)

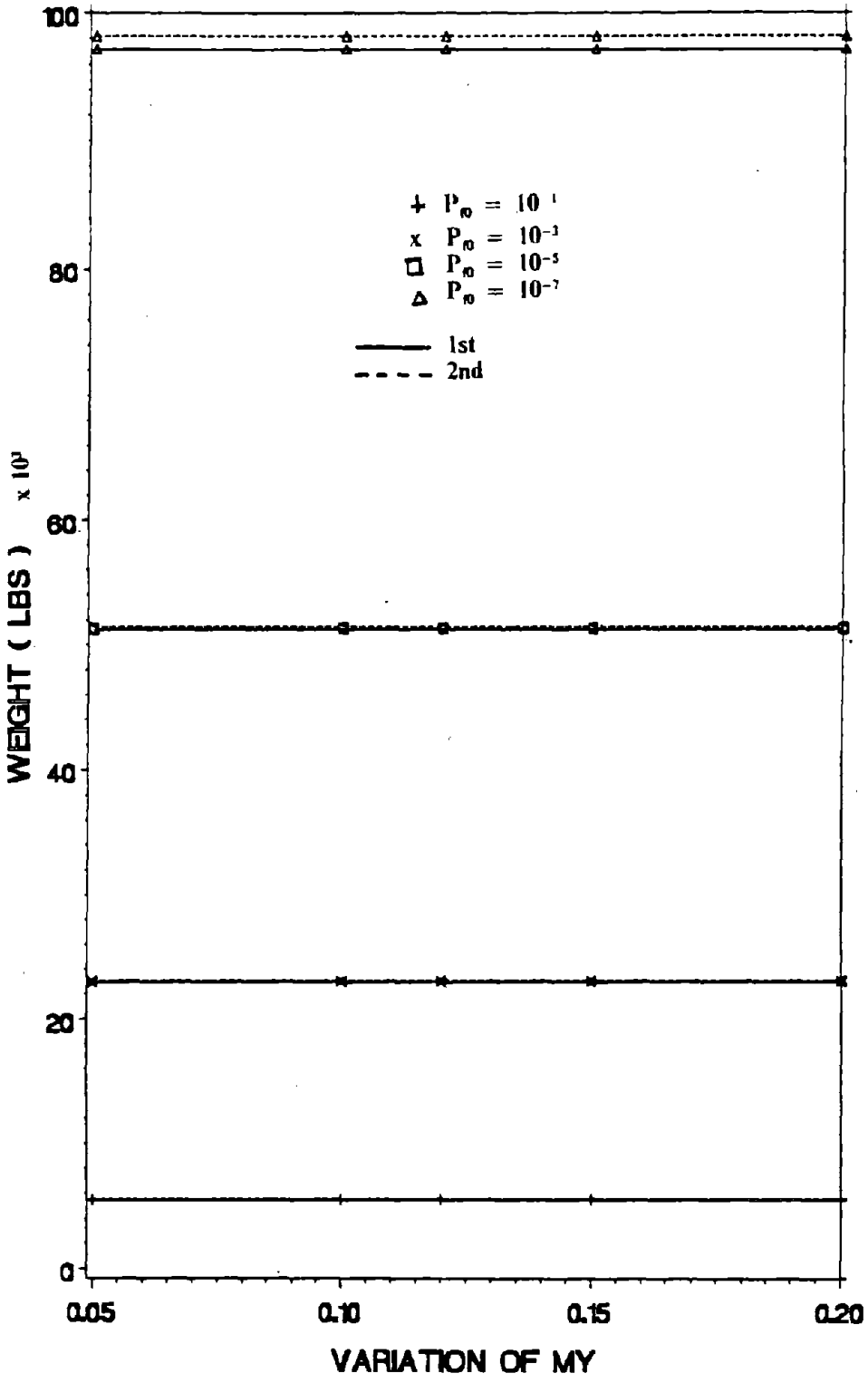

Figure 45. Optimum Weight for Various V_{M_y} with LN and V_E = 1.38 of 2-Story Building. (1 lb = 4.45 N)

a. No Variation of UBC. The influence of the variation of critical moment on the optimum design parameters is shown in Figures 46 through 49. From these figures one may observe that the optimum weight of the building increases as $V_{M_{cr}}$ increases for both normal and lognormal distributions and for both the 1st and 2nd variance approaches. The same observation may be concluded for the optimum moment of inertia. Observing Figures 46 through 49 indicates that the difference of design results between the 1st and the 2nd variance approach increases as the reliability increases and that the difference of the design results between two reliabilities for 2nd variance approach decreases as the reliability increases. For instance, the difference of the optimum weight between the reliabilities of 10^{-1} and 10^{-3} is 677.4 lbs (3014.4 N); and the weight difference between 10^{-5} and 10^{-7} is 309.6 lbs (1377.7 N) with normal distribution. These are signified by A and B in Figure 46. In the same figure, C and D signify 46.2 lbs (205.6 N) at 10^{-1} and 177.0 lbs (787.6 N) at 10^{-7} for the difference between the two approaches. The difference of the optimum weight between 10^{-1} and 10^{-3} is 1021.2 lbs (4544.4 N); and 767.5 lbs (1377.7 N) between 10^{-5} and 10^{-7} with lognormal distribution. These are signified by A and B in Figure 48 in which C and D indicate 60.9 lbs (271 N) and 438.3 lbs (1950.4 N) associated with the difference between the two approaches.

b. Variation of 1.38 for UBC. When $V_{U} = 1.38$ is used in the design, the optimum weight is not sensitive to the variation of critical moment for both normal and lognormal distributions and for both the 1st and 2nd variance approaches. The observation is drawn from Figures 50 and 51. The same observation has been concluded for the moments of inertia which are not shown here. It is believed that the high variations of earthquake overdominate the structural response behavior, the variations of other parameters in structural response and resistance can not therefore reflect their influences on the design results.

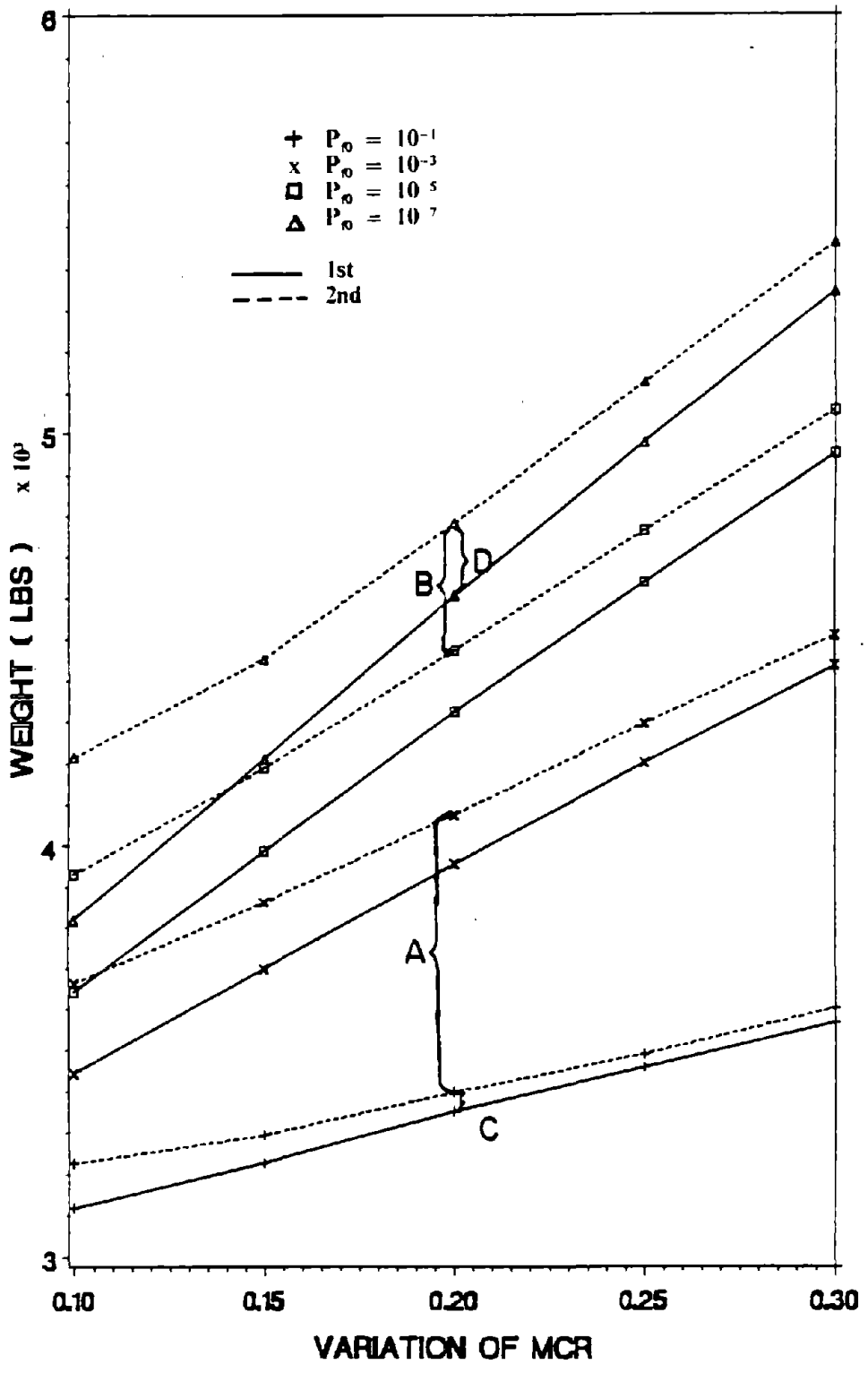

Figure 46. Optimum Weight for Various $V_{M_{cr}}$ with N and $V_E = 0$ of 2-Story Building. (1 lb = 4.45 N)

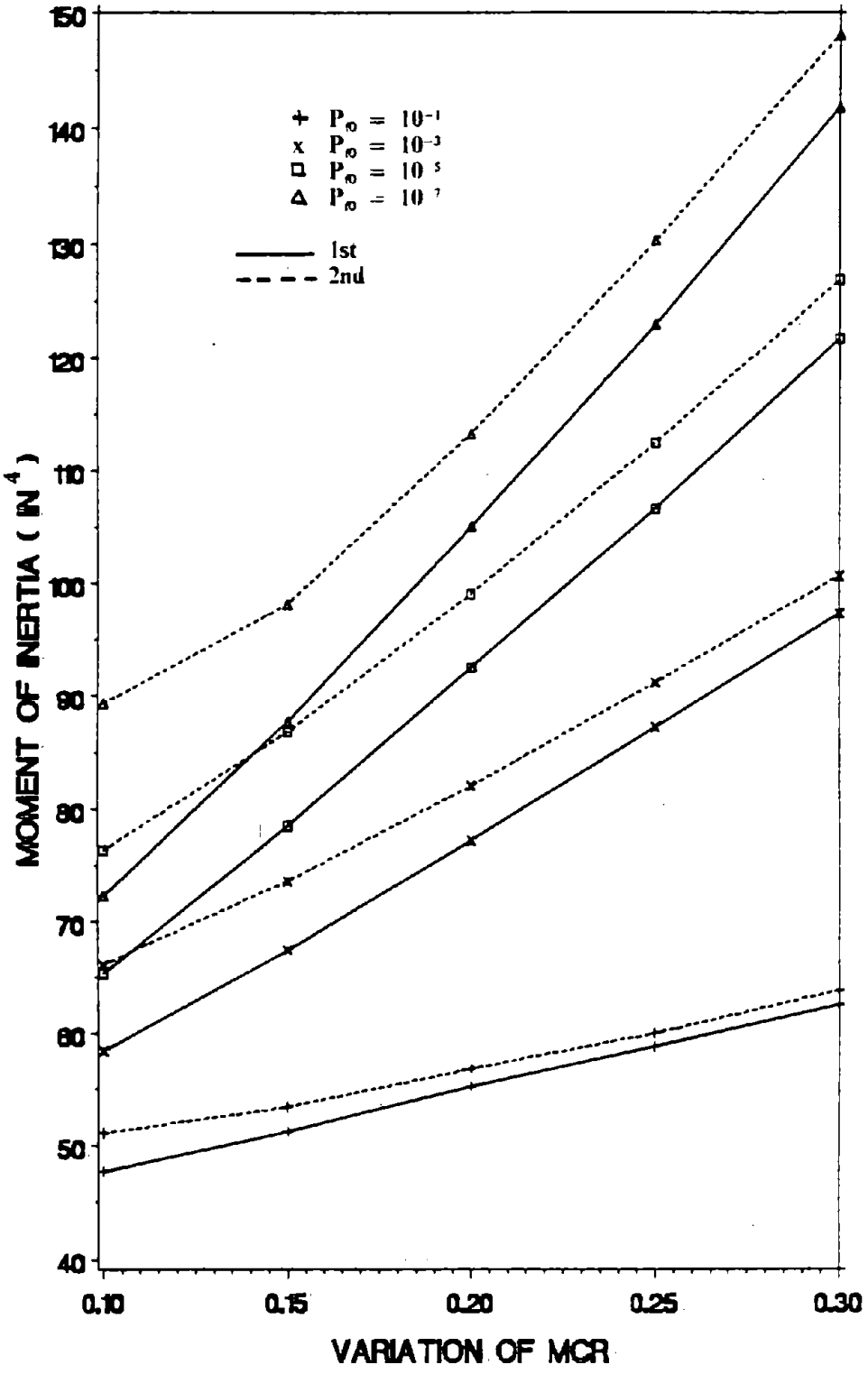

Figure 47. I_1 for Various $V_{M_{cr}}$ with N and $V_E = 0$ of 2-Story Building. (1 in^4 = 41.62 cm^4)

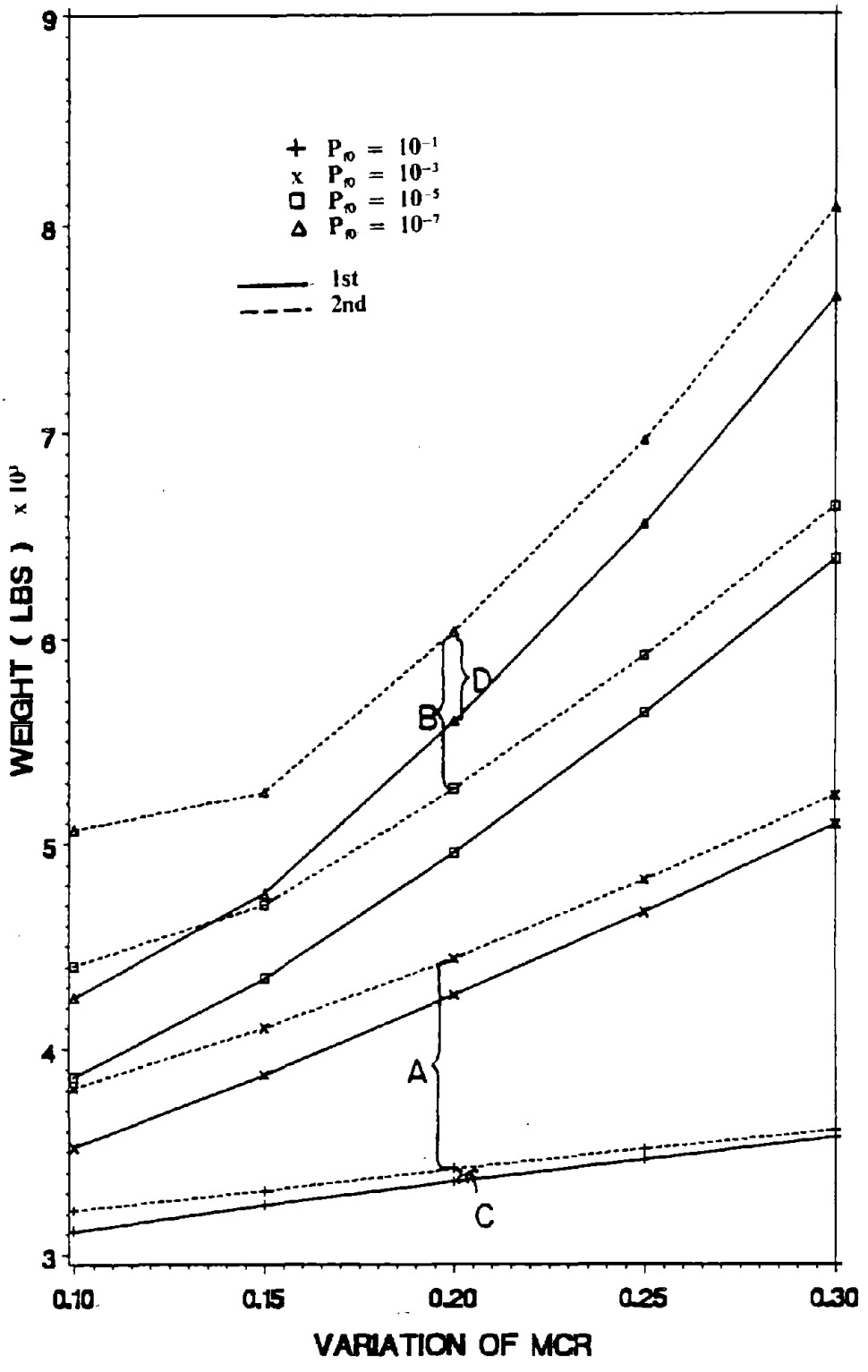

Figure 48. Optimum Weight for Various $V_{M_{cr}}$ with LN and $V_E = 0$ of 2-Story Building. (1 lb = 4.45 N)

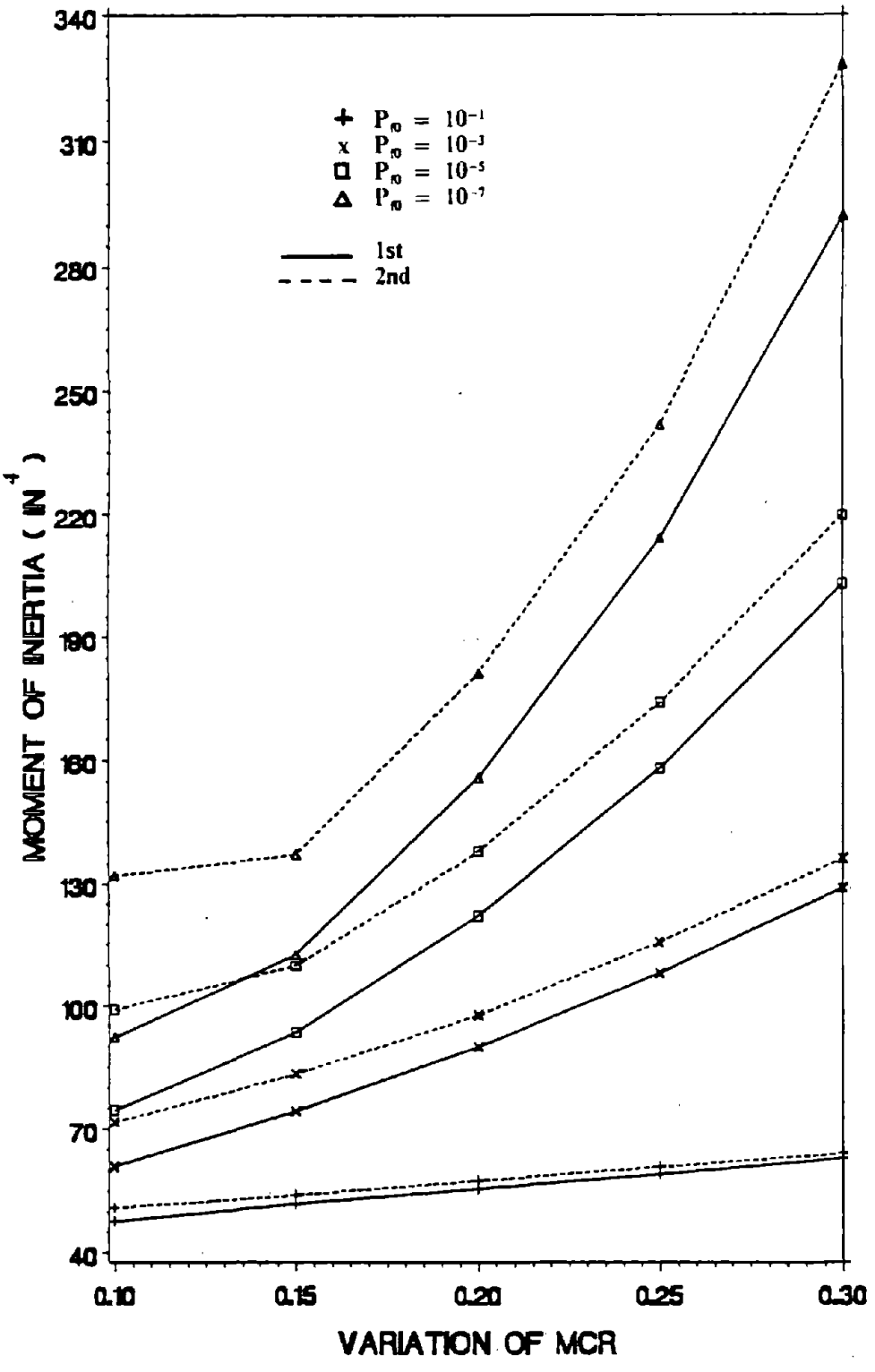

Figure 49. I_1 for Various $V_{M_{cr}}$ with LN and $V_E = 0$ of 2-Story Building.(1 in^4 = 41.62 cm^4)

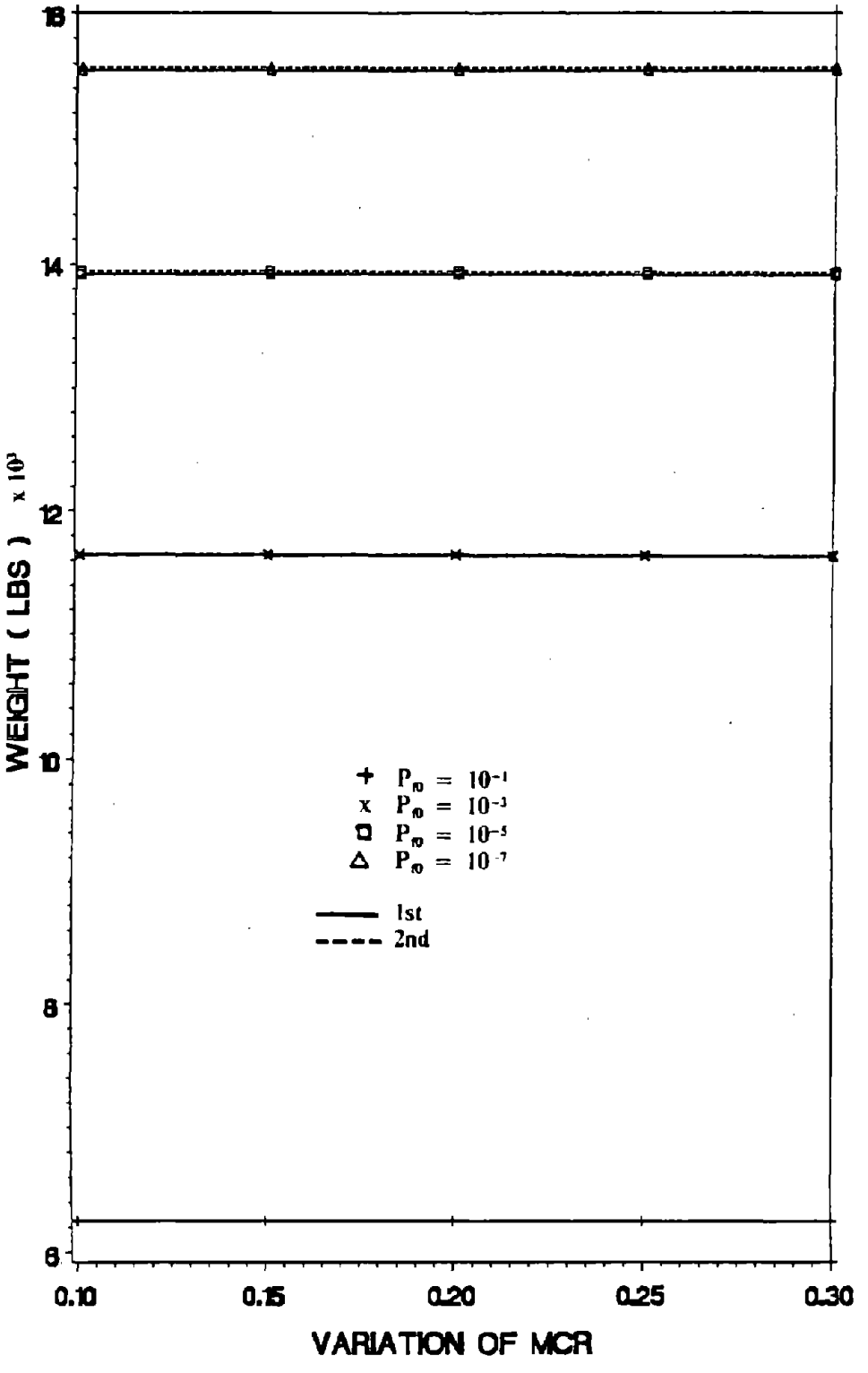

Figure 50. Optimum Weight for Various $V_{M_{cr}}$ with N and V_{E} = 1.38 of 2-Story Building. (1 lb = 4.45 N)

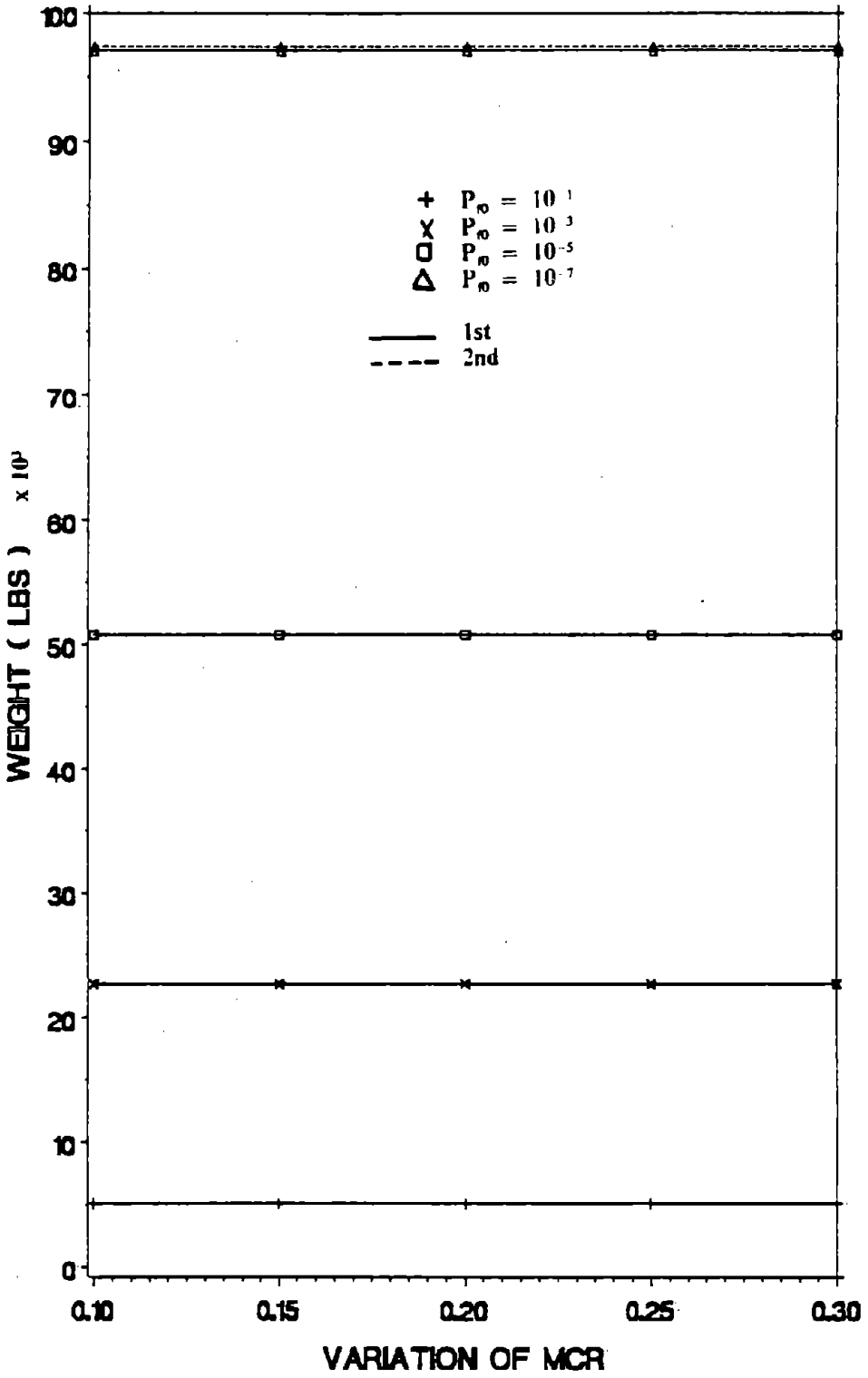

Figure 51. Optimum Weight for Various $V_{M_{cr}}$ with I.N and V_E = 1.38 of 2-Story Building. (1 lb = 4.45 N)

B. SENSITIVITY OF VARIATION OF UBC LOAD.

Since the accuracy of the coefficient of variation of UBC is questionable, a sensitivity study is performed by varying V_E from 0 to 1.38 for the two-story building design. The failure modes considered for the design are displacement failures at the floors and two column failure modes (Equations (9.1) through (9.4)) for each column member. The coefficients of variation of yield moment and critical moment are the values of 0.12 and 0.2, respectively.

The results are shown in Figures 52 through 55 from which one may observe that the changes of optimum weight and moments of inertia increase rapidly, when V_E varies from 0 to 1.38. The change is more significant at high reliability than at low reliability for both the 1st and 2nd variance approach. Also the increases are especially faster for lognormal distribution than for normal distribution. For instance the weight differences between $P_{f0} = 10^{-1}$ and 10^{-5} are 884.5 lbs (3936.0 N) at $V_E = 0$ and 6137.0 lbs (27.309 kN) at $V_E = 1.38$ with normal distribution (A and B in Figure 52) and 1144.8 lbs (5.094 kN) at$V_E = 0$ to 42.628 kips (189.694 kN) at $V_E = 1.38$ with lognormal distribution (A and B in Figure 54). The weight differences for $P_{f0} = 10^{-5}$ are 9370.5 lbs (41698.7 N) between $V_E = 0$ and 1.38 with normal distribution (C in Figure 52) and 44.686 kips (198.854 kN) between $V_E = 0$ and 1.38 with lognormal distribution (C in Figure 54).

The weight differences between two variance approaches, which may be illustrated for $P_{f0} = 10^{-5}$, are 473.9 lbs (2108.8 N) at $V_E = 0$ and 56.8 lbs (252.7 N) at $V_E = 0.5$ with normal distribution (D and E of Figure 52), and 637.8 lbs (2838.2 N) at $V_E = 0$ and 150 lbs (667.5 N) at $V_E = 0.5$ with lognormal distribution (D and E of Figure 54). The discrepancy between 1st and 2nd variance approach gradually reduces as the variation of earthquake increases. After $V_E = 0.5$ the designs based on the two approaches are practically the same. Apparently the high values of variation of earthquake control the designs.

The ten-story building shown in Figure 39 was studied for further investigating the optimum design parameters. The data for the design are the same as those used for the

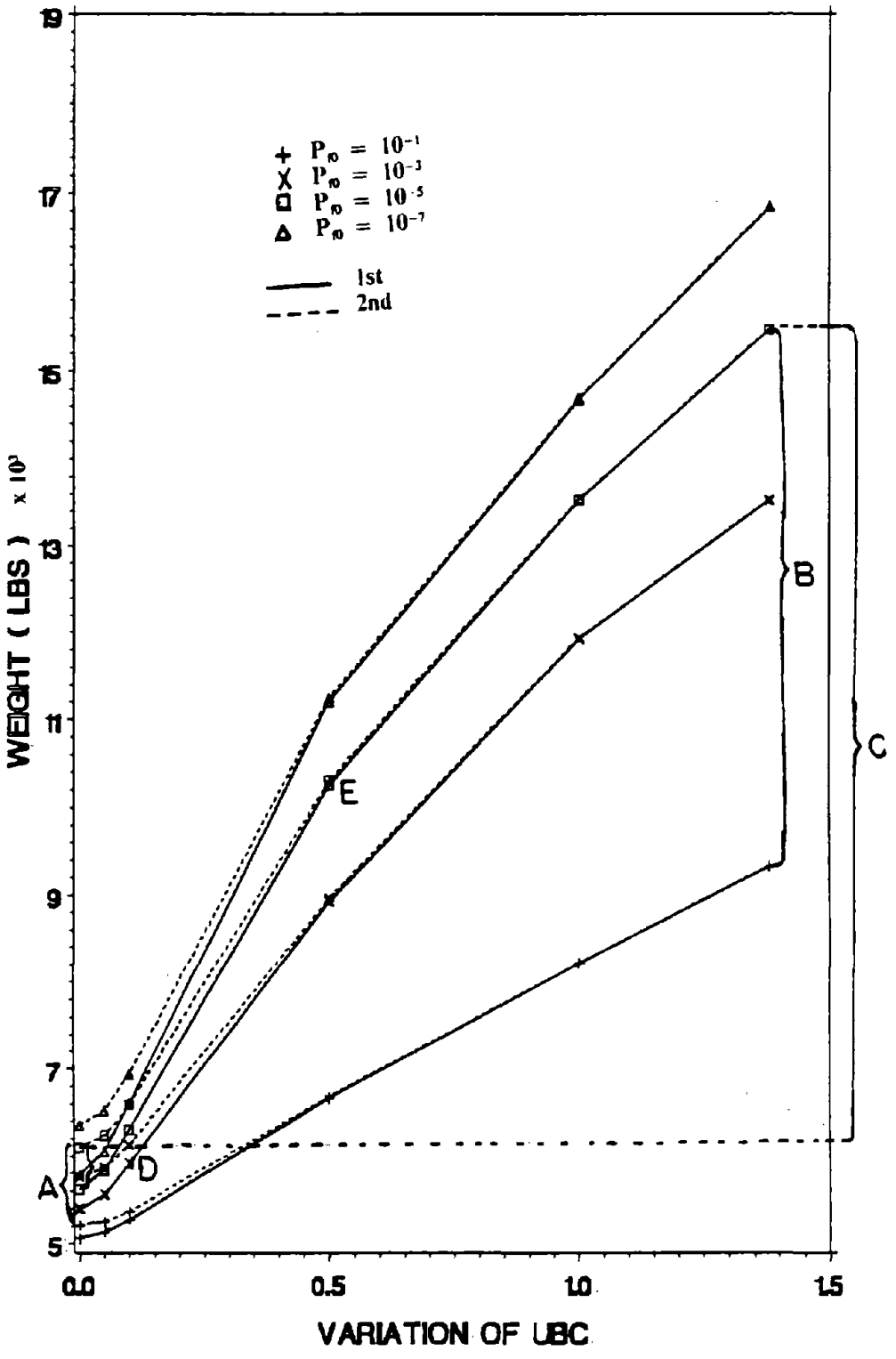

Figure 52. Optimum Weight for Various V_E with N of 2-Story Building. (1 lb = 4.45 N)

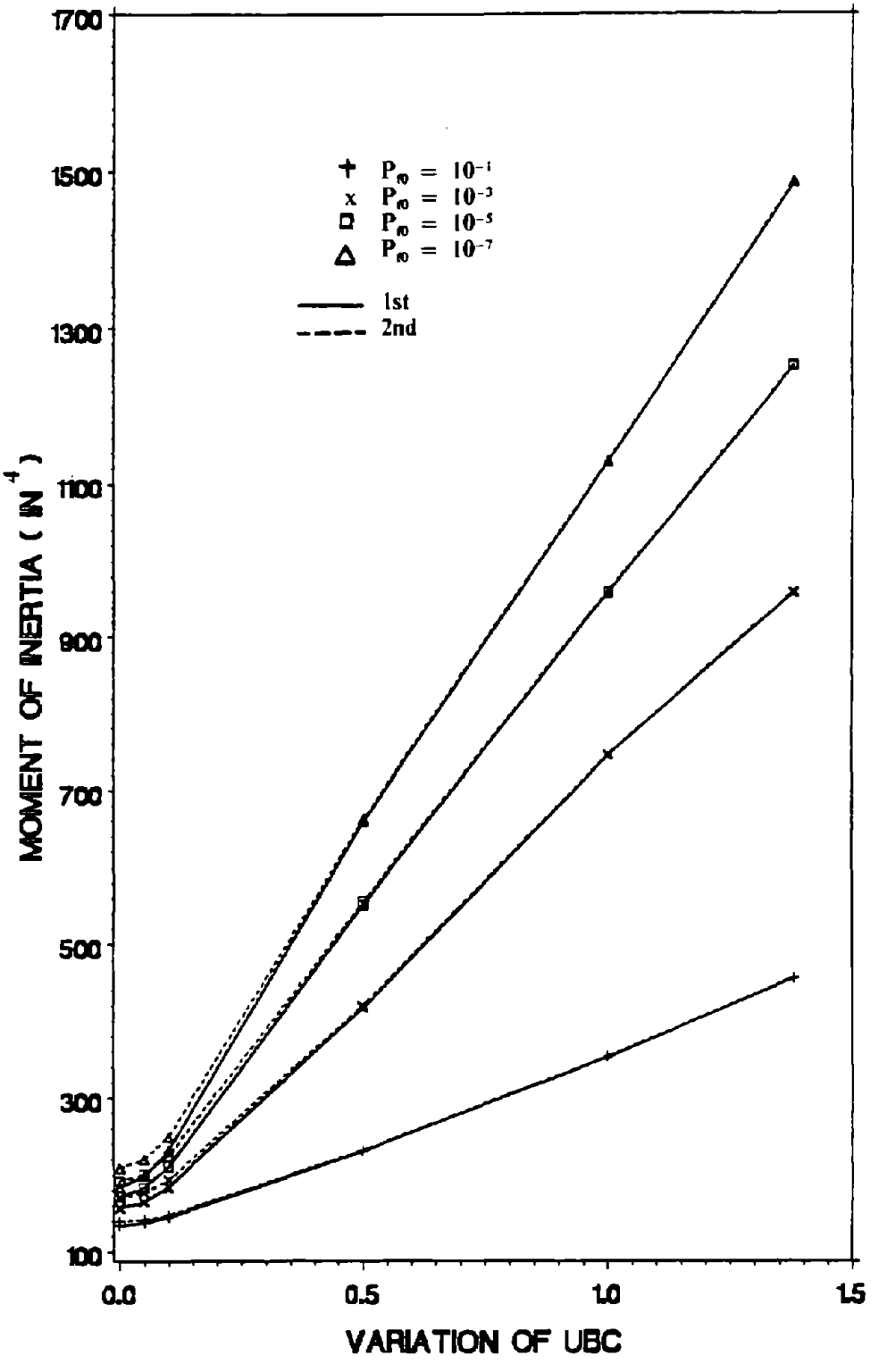

Figure 53. I_1 for Various V_E with N of 2-Story Building.(1 in^4 = 41.62 cm^4)

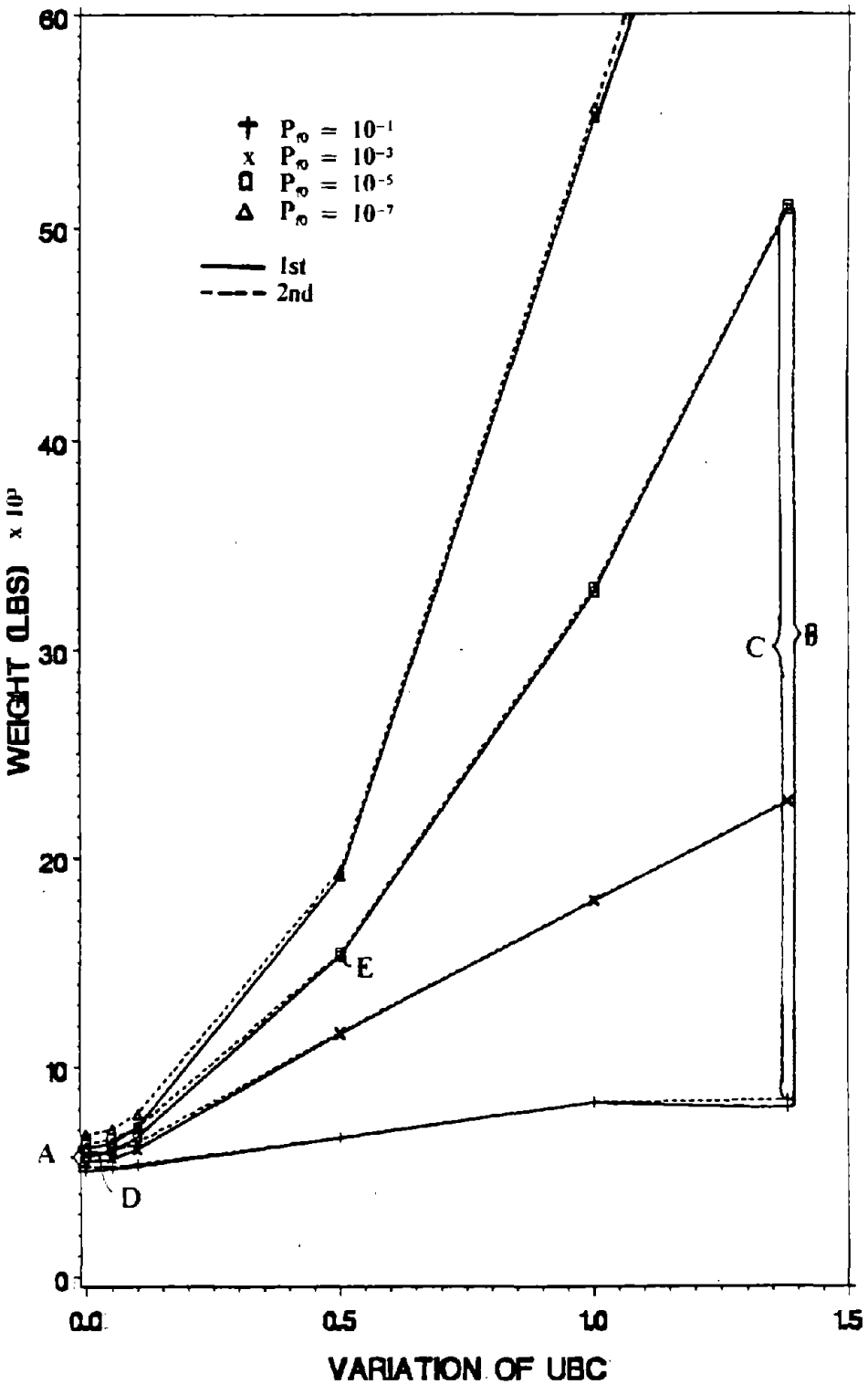

Figure 54. Optimum Weight for Various V_E with LN of 2-Story Building. (1 lb = 4.45 N)

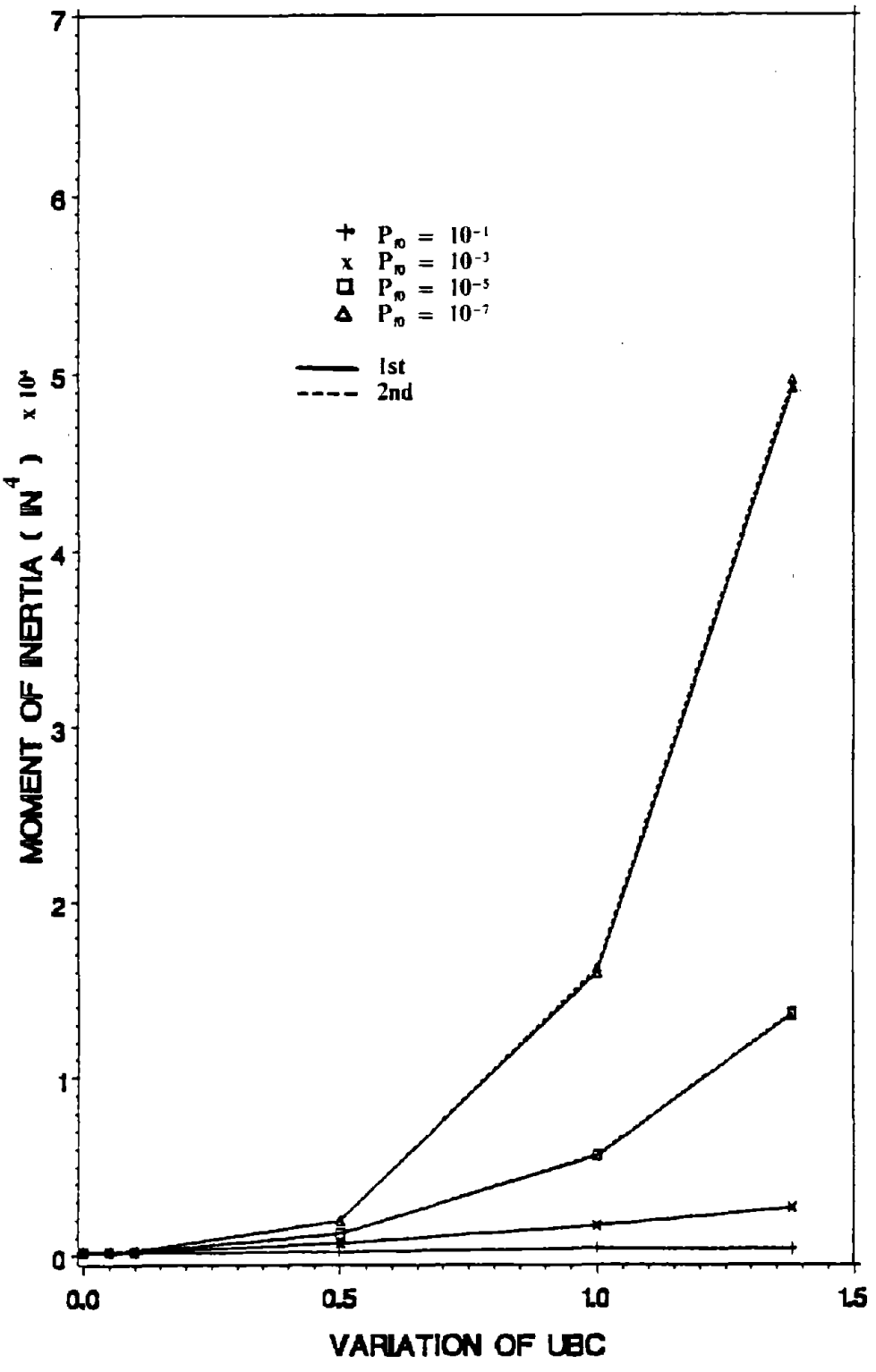

Figure 55. I_1 for Various V_E with LN of 2-Story Building.(1 in^4 = 41.62 cm^4)

two-story building structure. In this study the design results of nondeterminstic cases are compared with deterministic case. The nondeterministic cases are based on two extreme probability failures of $P_{f0} = 10^{-1}$ and $P_{f0} = 10^{-7}$. The optimum weight and the moments of inertia vs the coefficients of earthquake variation are shown in Figures 56 through 61 for the 2nd approach with normal and lognormal distribution. As observed previously, the discrepancies of the design results increase as V_E increases. The results of the deterministic design are the lower bound of all the designs.

C. COMPARISON BASED ON NORMAL AND LOGNORMAL DISTRIBUTION.

The influences of the probability of normal and lognormal on the design are studied for the 2-story building for which the design data are the same as used previously, the variation of UBC is assumed to be 1.38. The optimum weight and the moment of inertia vs the probability failure levels are shown in Figures 62 and 63. It is interesting to note that at low reliability the design for normal distribution is higher than that for lognormal distribution. Approximately after $P_f = 10^{-3}$, the design for normal distribution is lower than that for lognormal, the discrepancy increses as the reliability increases. The optimum weight differences between normal and lognormal distribution are 1256.7 lbs (5592.3 N) at $p_{f0} = 10^{-1}$ and 80.069 kips (356.308 kN) at $p_{f0} = 10^{-7}$ for the 1st variance approach; 906.2 lbs (4032.6 N) at $p_{f0} = 10^{-1}$ and 80.502 kips (358.235 kN) at $p_{f0} = 10^{-7}$ for the 2nd variance approach. The differences are symbolically signified by A and B in Figure 62. Because $V_E = 1.38$ is used, the difference between the two variance approaches are very small.

D. COMPARISON OF ZONE COEFFICIENTS IN UBC.

In Equation (3.14), the coefficients, Z, represent the zone the structure is located. The values of 3/16, 3/8, 3/4, and 1 correspond to zone I, II, III, and IV, respectively. It is to investigate how the zone coefficients affect the design results for different reliability levels based on two variance approaches and normal and lognormal distribution. It is also to find how the UBC variation coefficient ($V_E = 1.38$) affects the design. The two-story shear building shown in Figure 6 is used for this study. The solutions are shown in Figures 64 through 67.

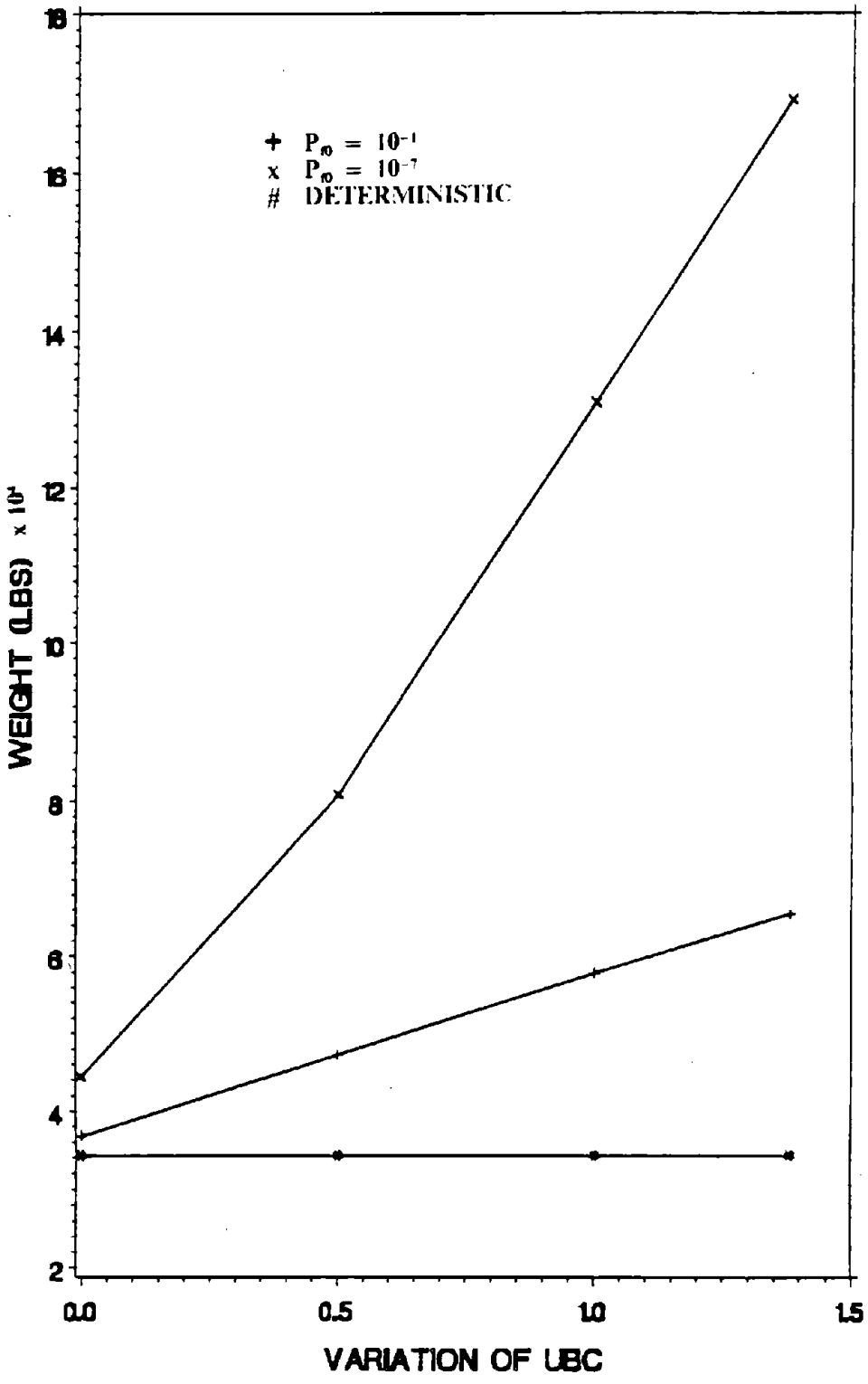

Figure 56. Optimum Weight for Various V_E with N of 10-Story Building. (1 lb = 4.45 N)

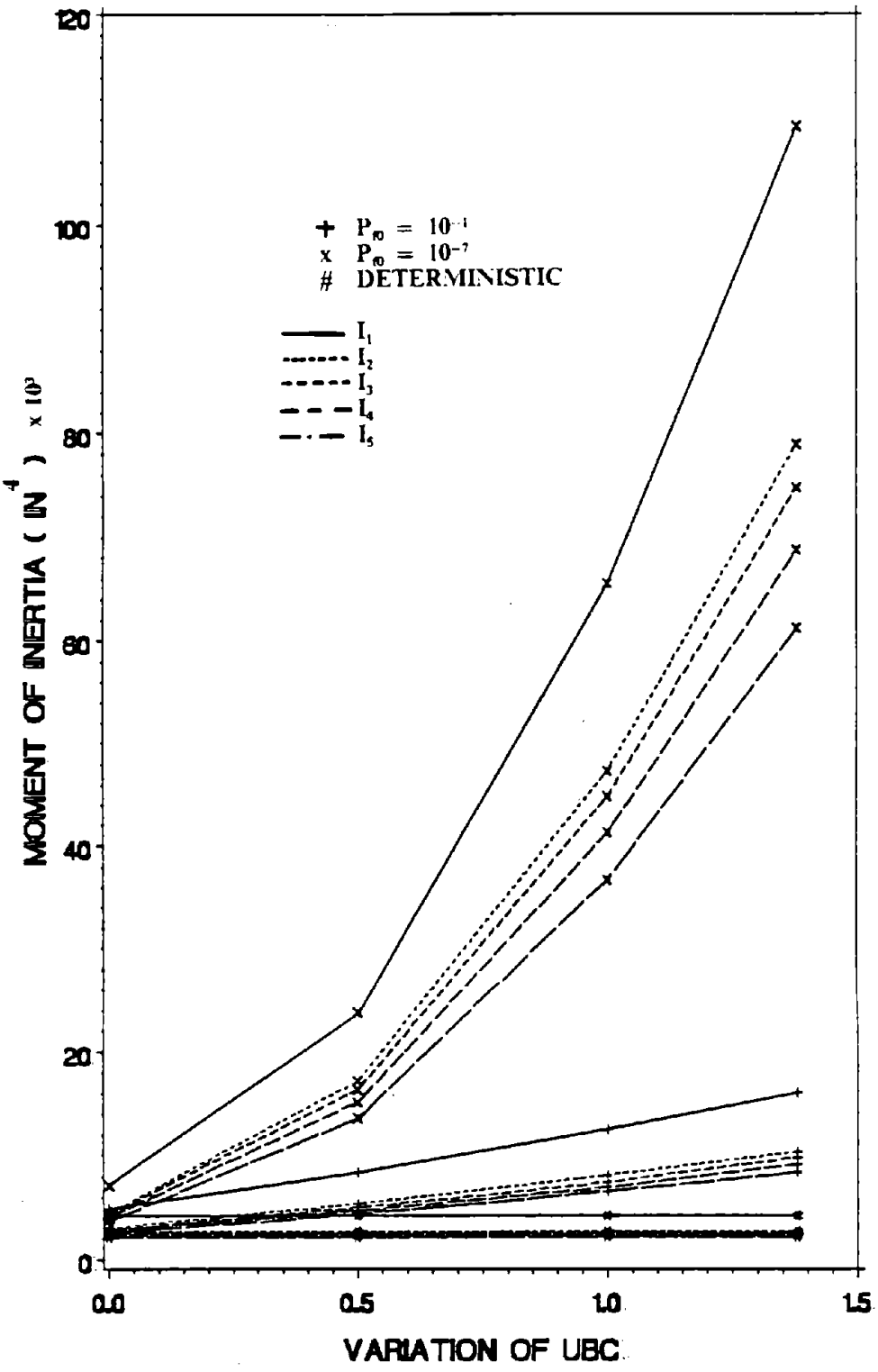

Figure 57. I_1 - I_5 for Various V_E with N of 10-Story Building.(1 in^4 = 41.62 cm^4)

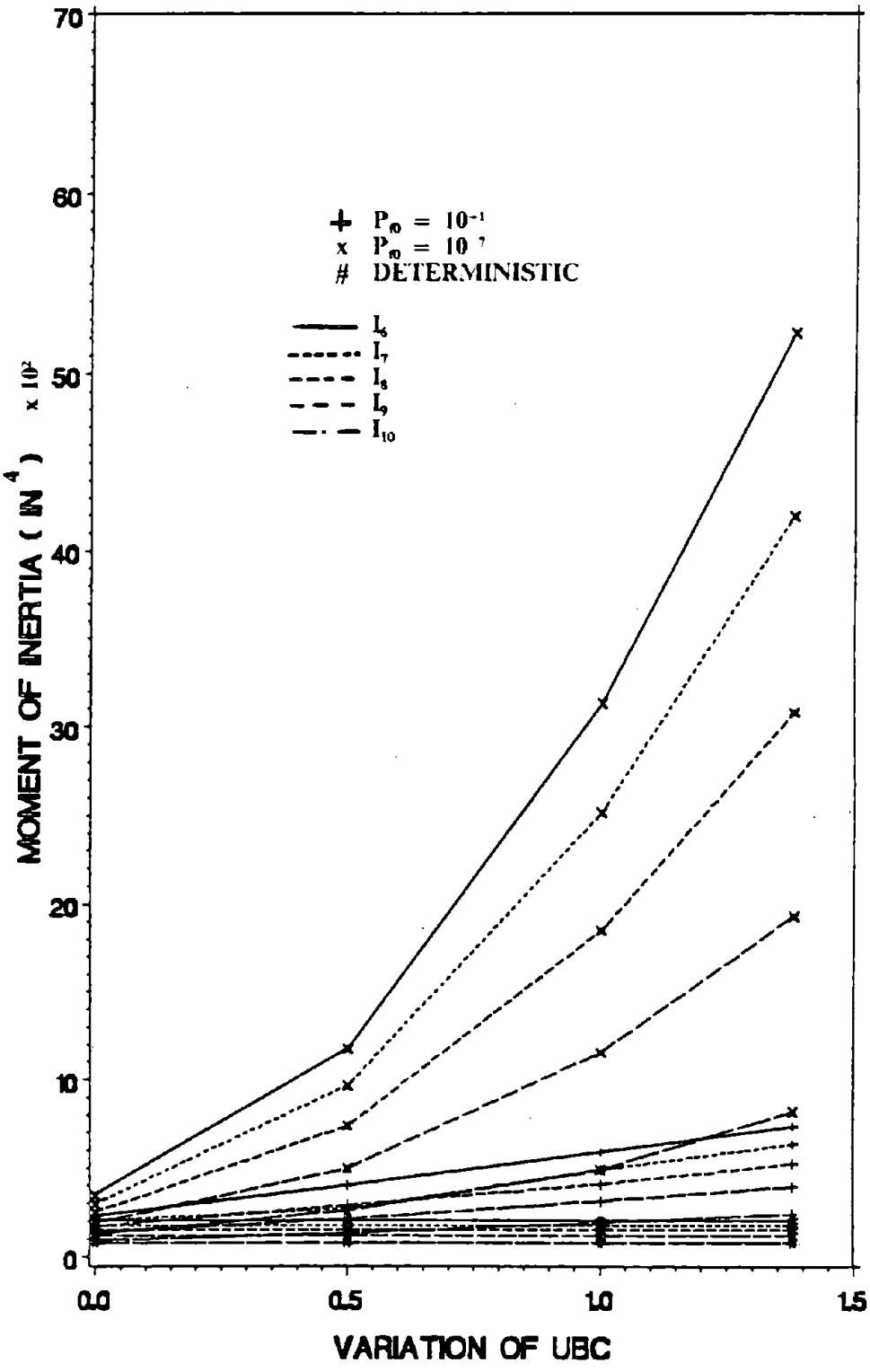

Figure 58. I_6 - I_{10} for Various V_E with N of 10-Story Building. (1 in^4 = 41.62 cm^4)

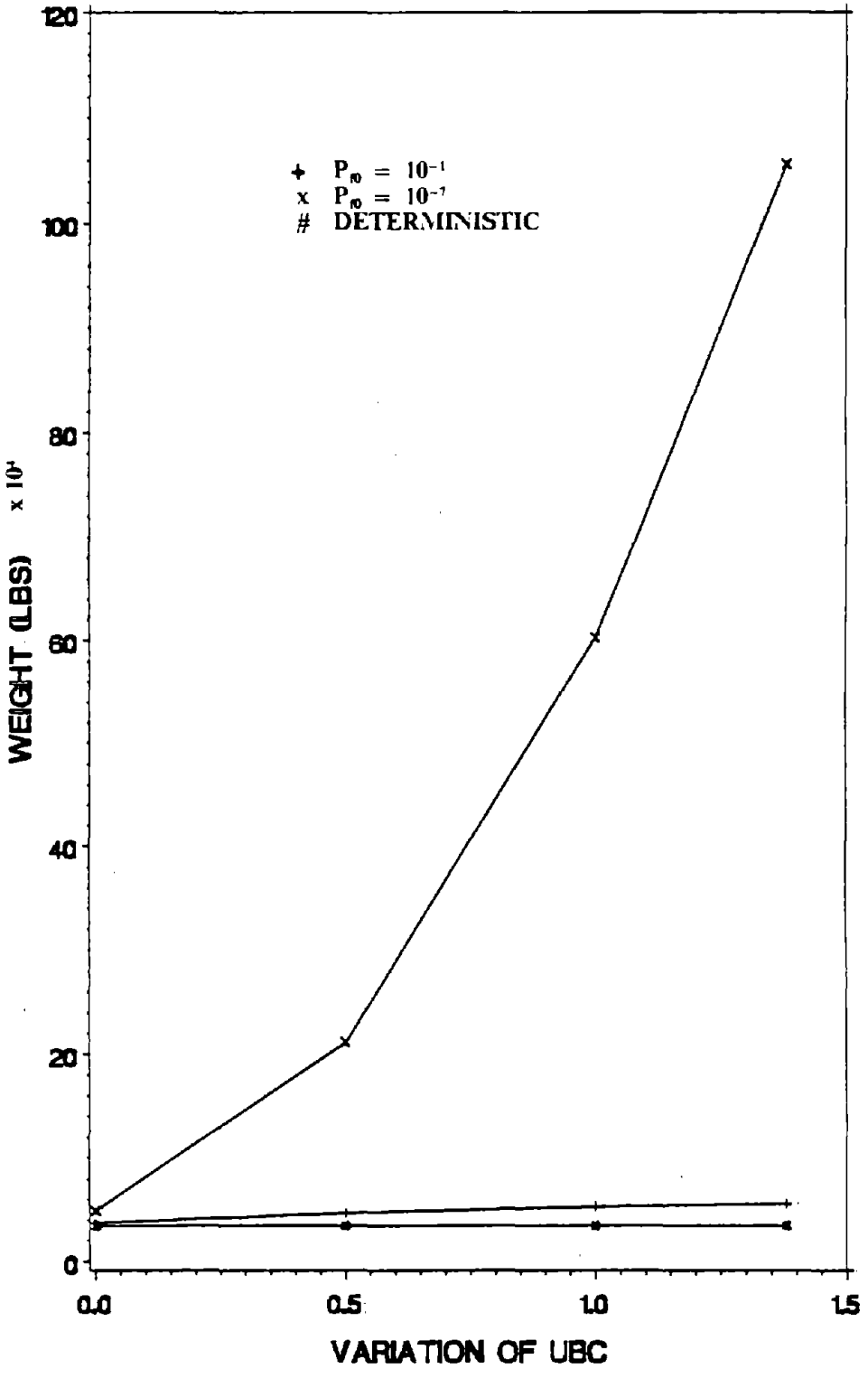

Figure 59. Optimum Weight for Various V_E with LN of 10-Story Building. (1 lb = 4.45 N)

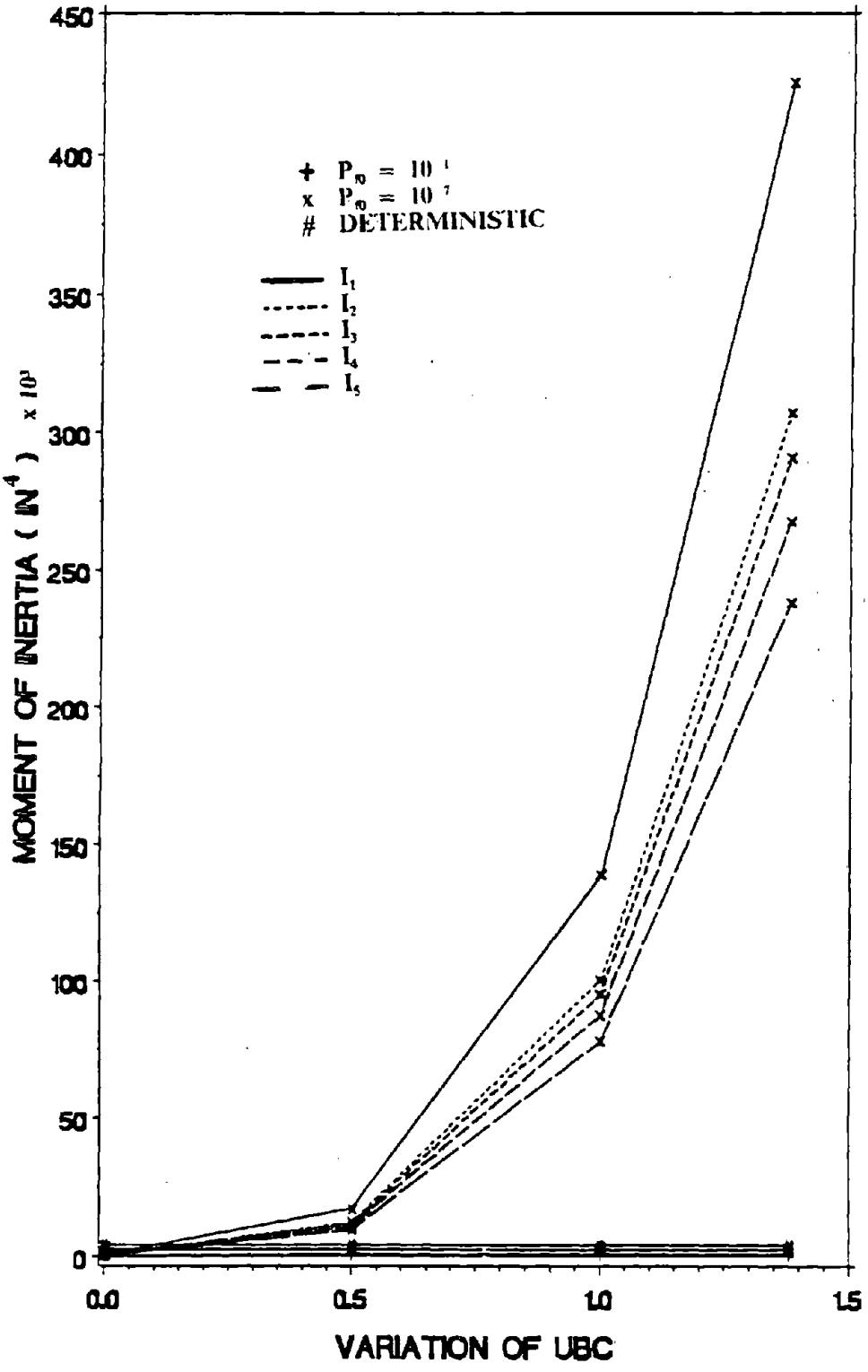

Figure 60. I_1 - I_5 for Various V_E with LN of 10-Story Building.(1 in^4 = 41.62 cm^4)

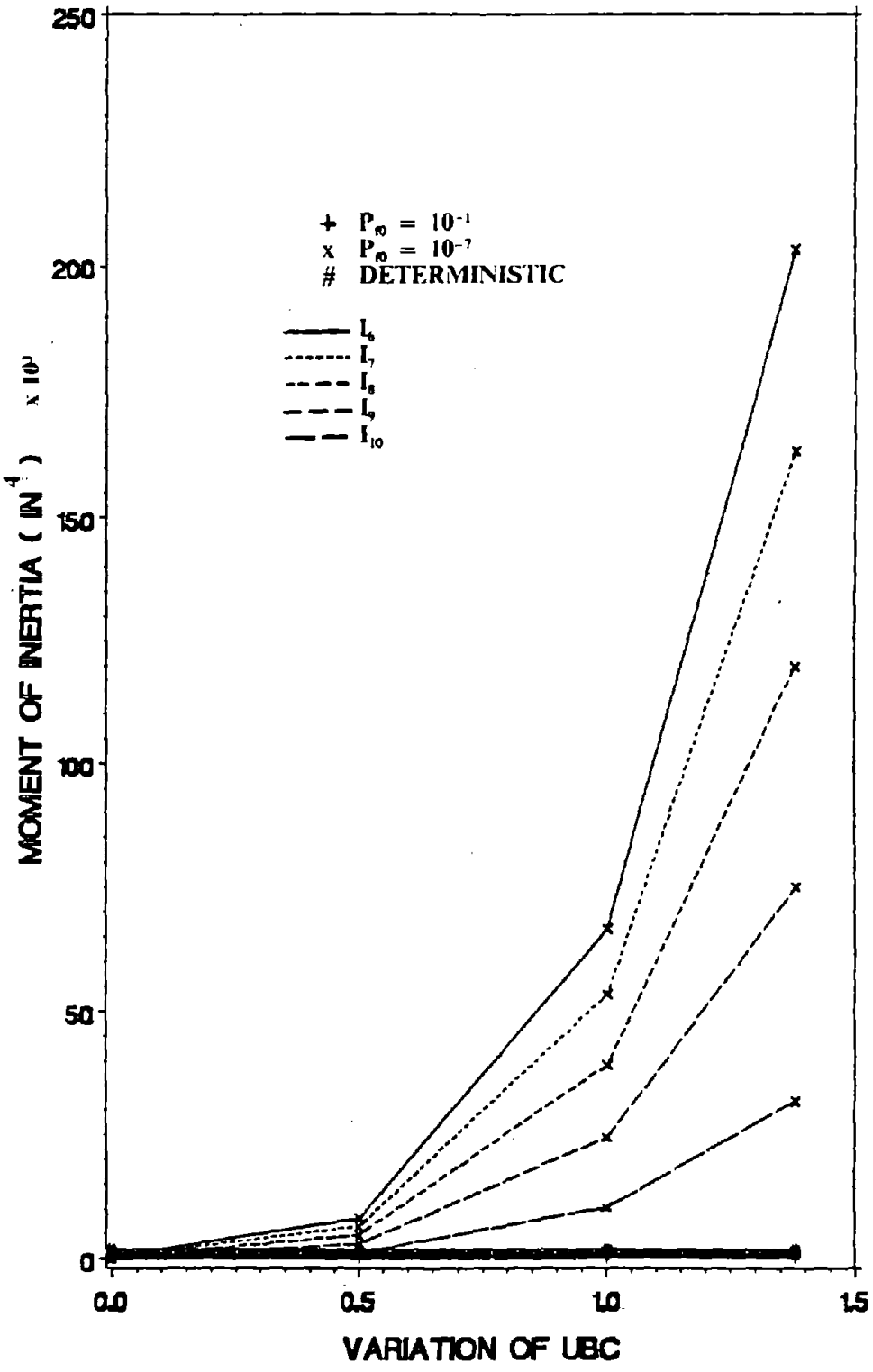

Figure 61. I_6 - I_{10} for Various V_E with LN of 10-Story Building.(1 in^4 = 41.62 cm^4)

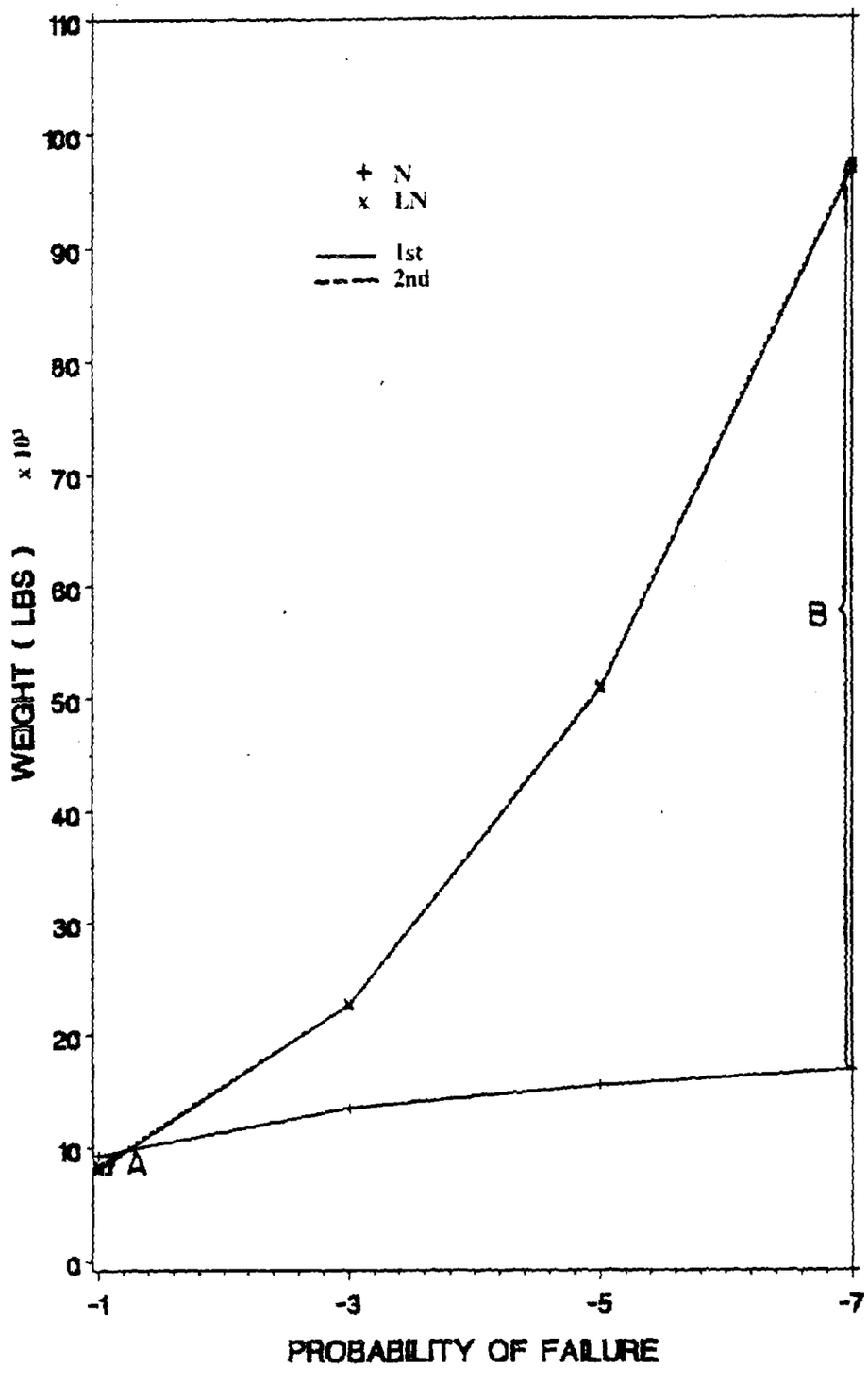

Figure 62. Optimum Weight at V_E = 1.38 of 2-Story Building. (1 lb = 4.45 N)

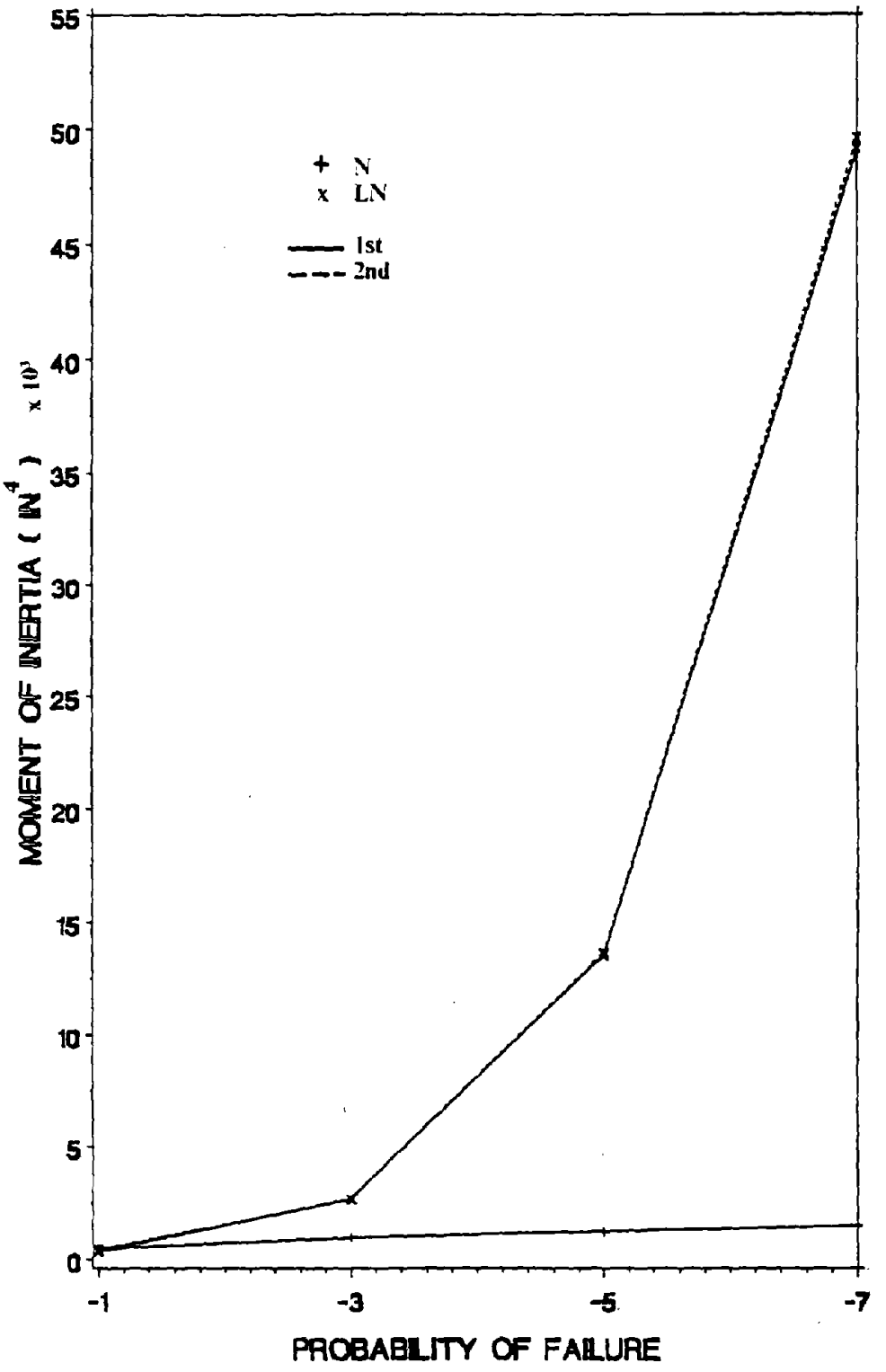

Figure 63. I_1 at V_E = 1.38 of 2-Story Building. (1 in^4 = 41.62 cm^4)

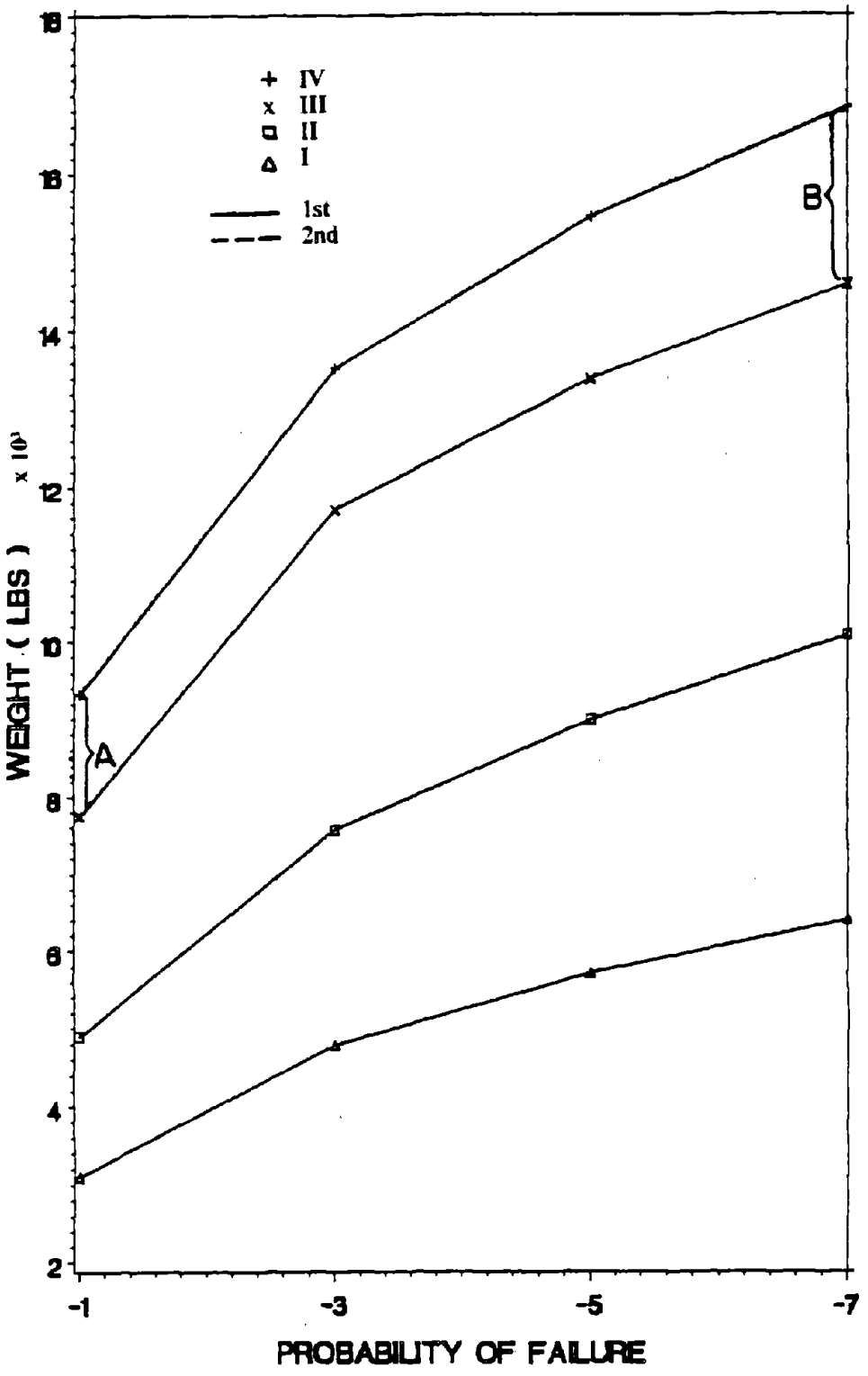

Figure 64. Optimum Weight for Various Zone Coefficients at V_E = 1.38 and N of 2-Story Building. (1 lb = 4.45 N)

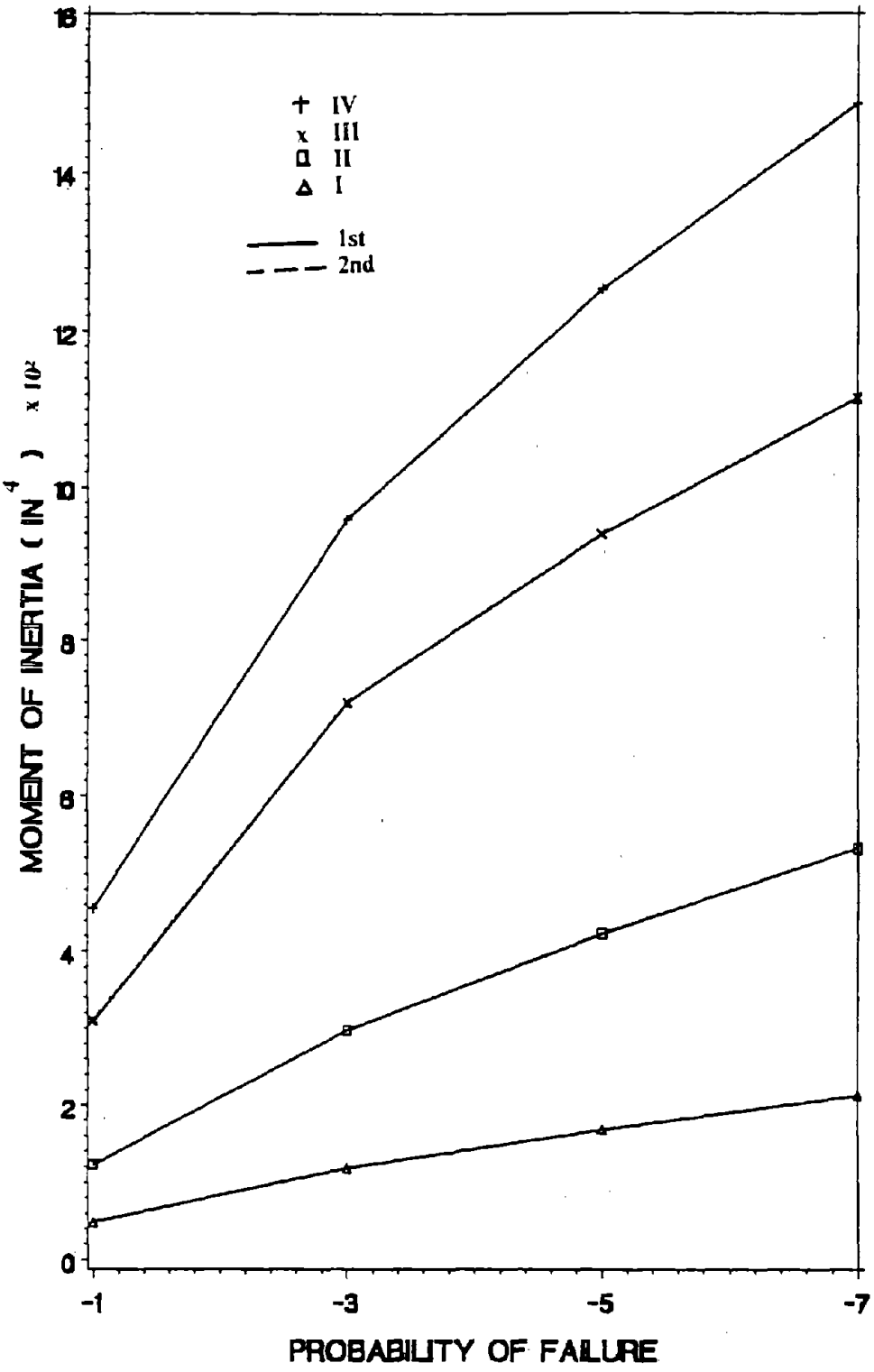

Figure 65. I_1 for Various Zone Coefficients at V_E = 1.38 and N of 2-Story Building. (1 in^4 = 41.62 cm^4)

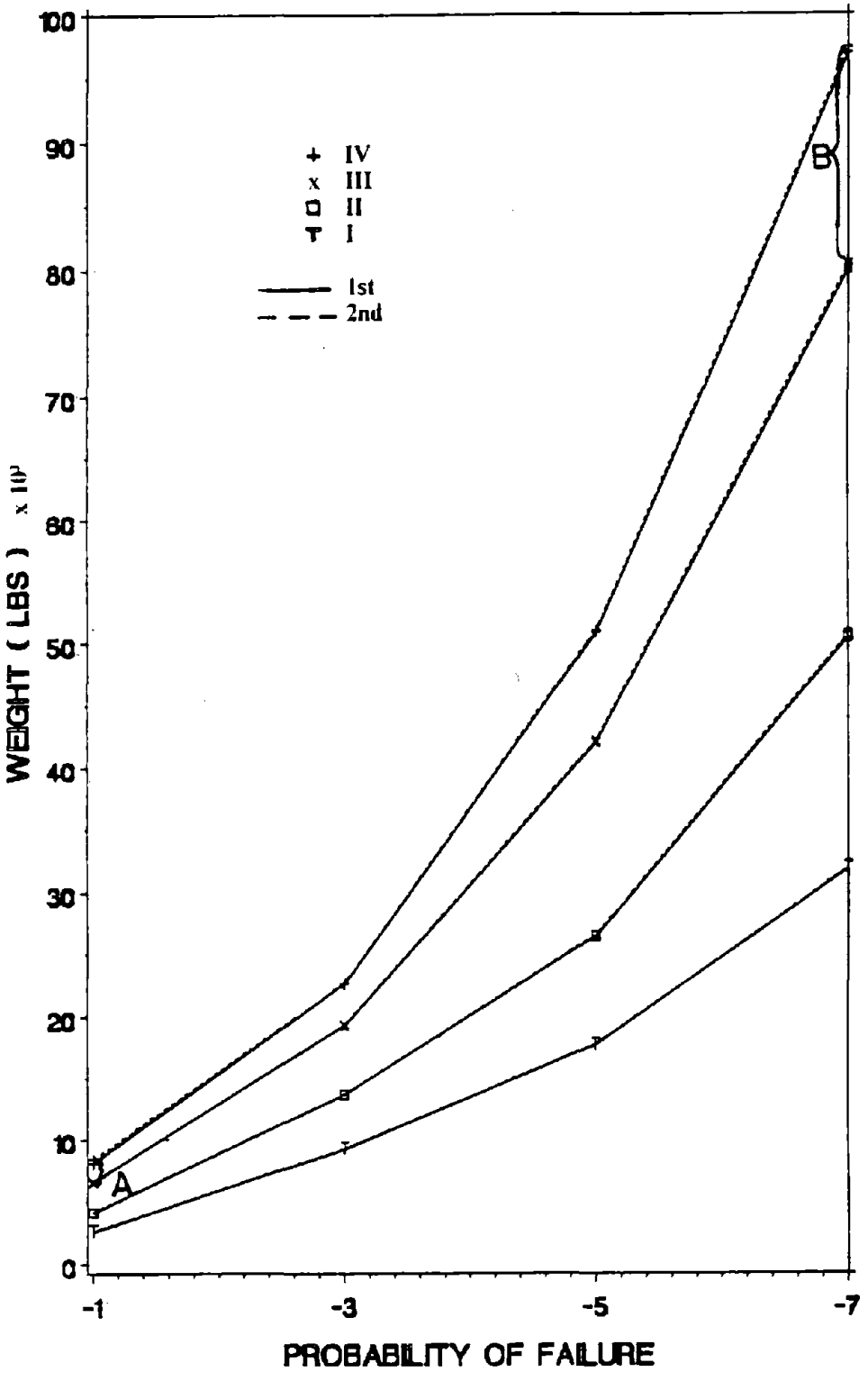

Figure 66. Optimum Weight for Various Zone Coefficients at V_E = 1.38 and LN of 2-Story Building. (1 lb = 4.45 N)

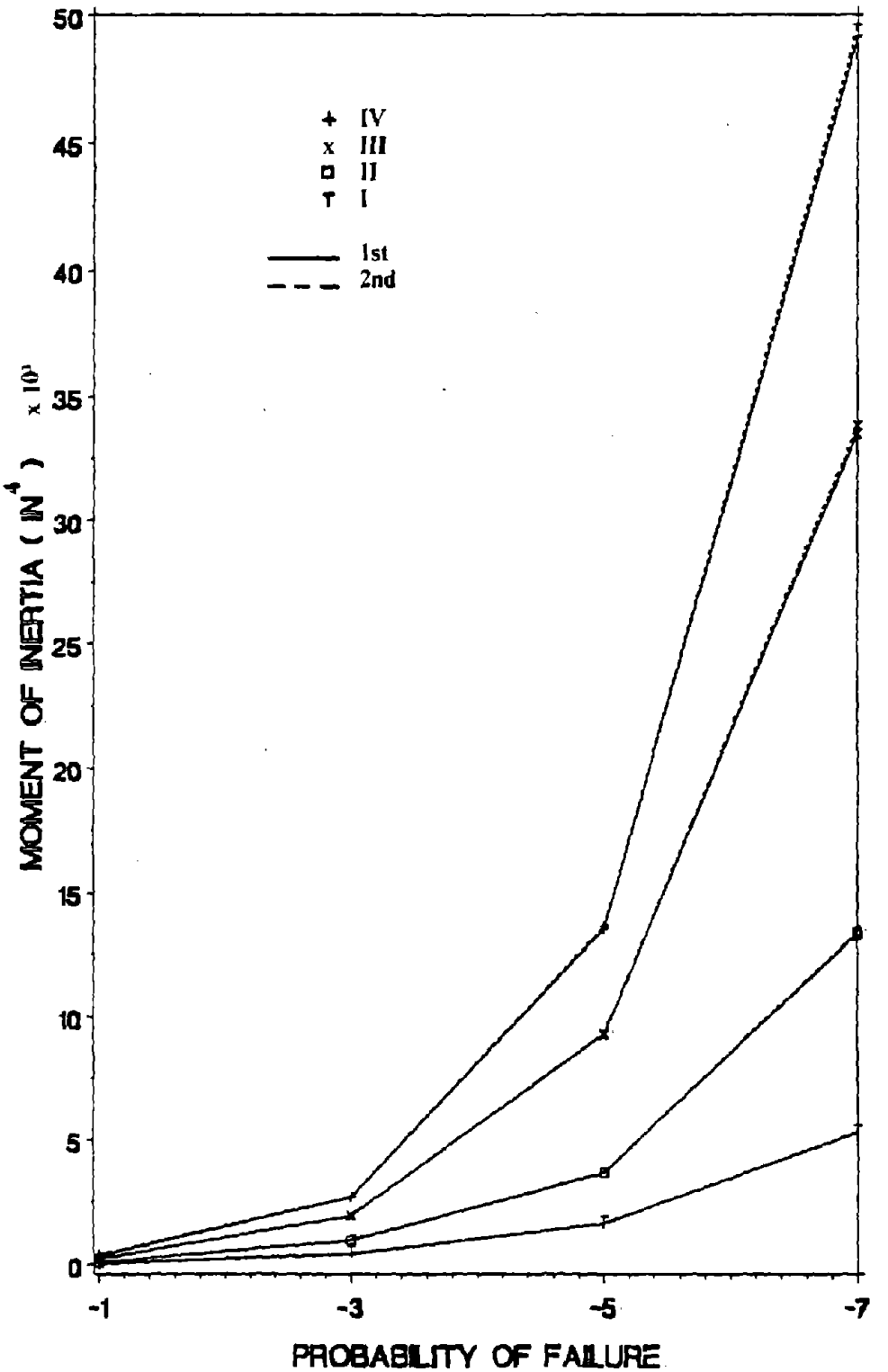

Figure 67. I_1 for Various Zone Coefficients at V_E = 1.38 and LN of 2-Story Building. (1 in^4 = 41.62 cm^4)

As shown in Figures 64 and 66, the weight differences increase as reliability increase. The differences between zone III and IV are 1577.6 lbs (7020.3 N) at $P_{f0} = 10^{-1}$, and 2257.3 lbs (10.044 kN) at $P_{f0} = 10^{-7}$ with normal distribution (A and B in Figure 64); and 1831.0 lbs (8147.9 N) at $P_{f0} = 10^{-1}$, 16.993 kips (75.621 kN) at $P_{f0} = 10^{-7}$ with lognormal distribution (A and B in Figure 66). Because $V_E = 1.38$ is used, the two variance approaches yield practically the same design.

E. EFFECTS OF COST FUNCTION ON SENSITIVITY STUDIES.

The cost objective function in Section VIA may have three components: initial construction cost (C_I), future failure cost (L_f), and system probability of failure (P_{f_T}). They are expressed as

$$C_T = C_I + L_f P_{f_T} \tag{9.5}$$

in which

$C_I = C_u \sum_i L_i A_i + C_n$,

C_u = an unit steel volume cost,

C_n = nonstructural members cost,

$L_f = C_V C_I + C_L$,

C_V = a coefficient to describe the ratio of repair cost to initial cost,

C_L = the business and human losses,

P_{f_T} = system probability of failure.

Although initial construction cost and future failure cost can be classified into many items, these quantities are difficult to estimate. Therefore two coefficients of the ratio of initial cost to members cost (C_{in}) and the ratio of future failure cost to initial cost (C_{VL}) are used to represent the various magnitudes of initial construction cost and future failure cost which may now be expressed as:

$$C_I = C_{in} C_u \sum_i L_i A_i \tag{9.6}$$

$$L_f = C_{VL} C_I \tag{9.7}$$

Through these two coefficients, the influences of nonstructural cost and future failure on the optmium cost design may be observed. The two-story and ten-story shear building shown in previous examples are used for this study. The failure modes are displacements failures of the structure, and yielding and torsional buckling failures of columns.

1. The Ratio of Initial Cost to Structural Member Cost. The initial cost has two components which are structural member cost and nonstructural member cost. Since the terms involved in the nonstructural member cost are not clear, it is reasonable to assume that the structural member cost may be a percentage of initial cost. That means the initial cost is assumed as the product of C_{in} and member cost. Three values of C_{in} in the amount of 2, 5, and 10, are used to investigate the relationship between the structural and nonstructural costs. The value of C_{VL} is assumed to be constant as 1.0.

Figures 68 through 71 show the optimum solution of the two-story building and Figures 72 through 77 reveal the design results of the ten-story building. All the design are based on the 2nd variance approach with normal and lognormal distribution. The unit cost is 0.15 dollars/in^3. From all the figures, one may observe that there are some differences between total cost and initial cost at low reliability ($P_{f0} < 10^{-3}$); the differences practically become zero as the reliability levels increase. The total costs increase as C_{in} increases. But the moments of inertia are not much different for different C_{in} values. It is because the change of nonstructural member cost does not affect the change of structural responses under the same safety criterion. Therefore, the increase of nonstructural member cost does not influence the design of structural members. The differences between total costs and initial costs decrease for higher reliability levels because the increase of reliability results the decrease of future failure losses.

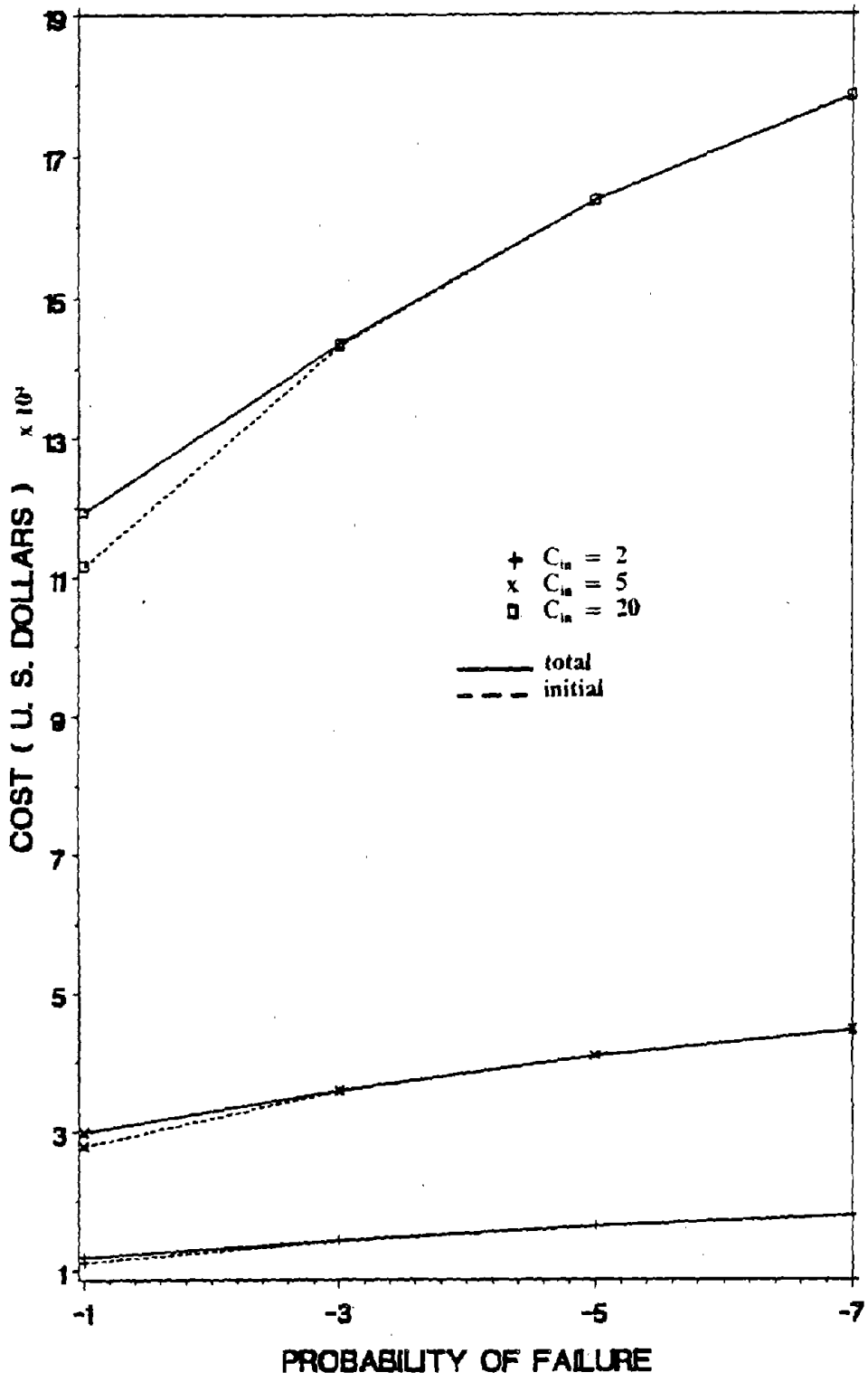

Figure 68. Optimum Cost for Various C_{in} with N of 2-Story Building.

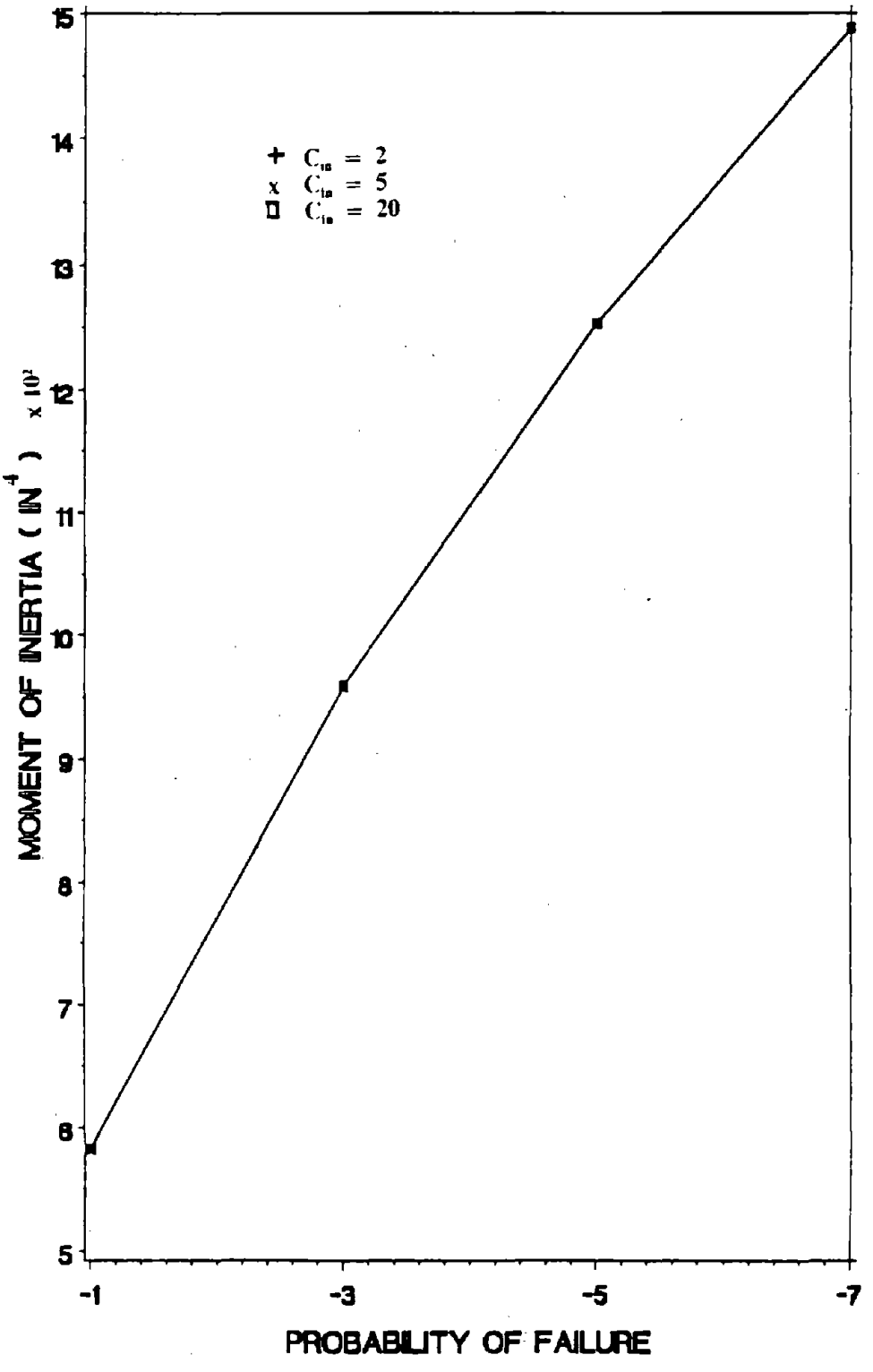

Figure 69. I_1 for Various C_{in} with N of 2-Story Building. (1 in^4 = 41.62 cm^4)

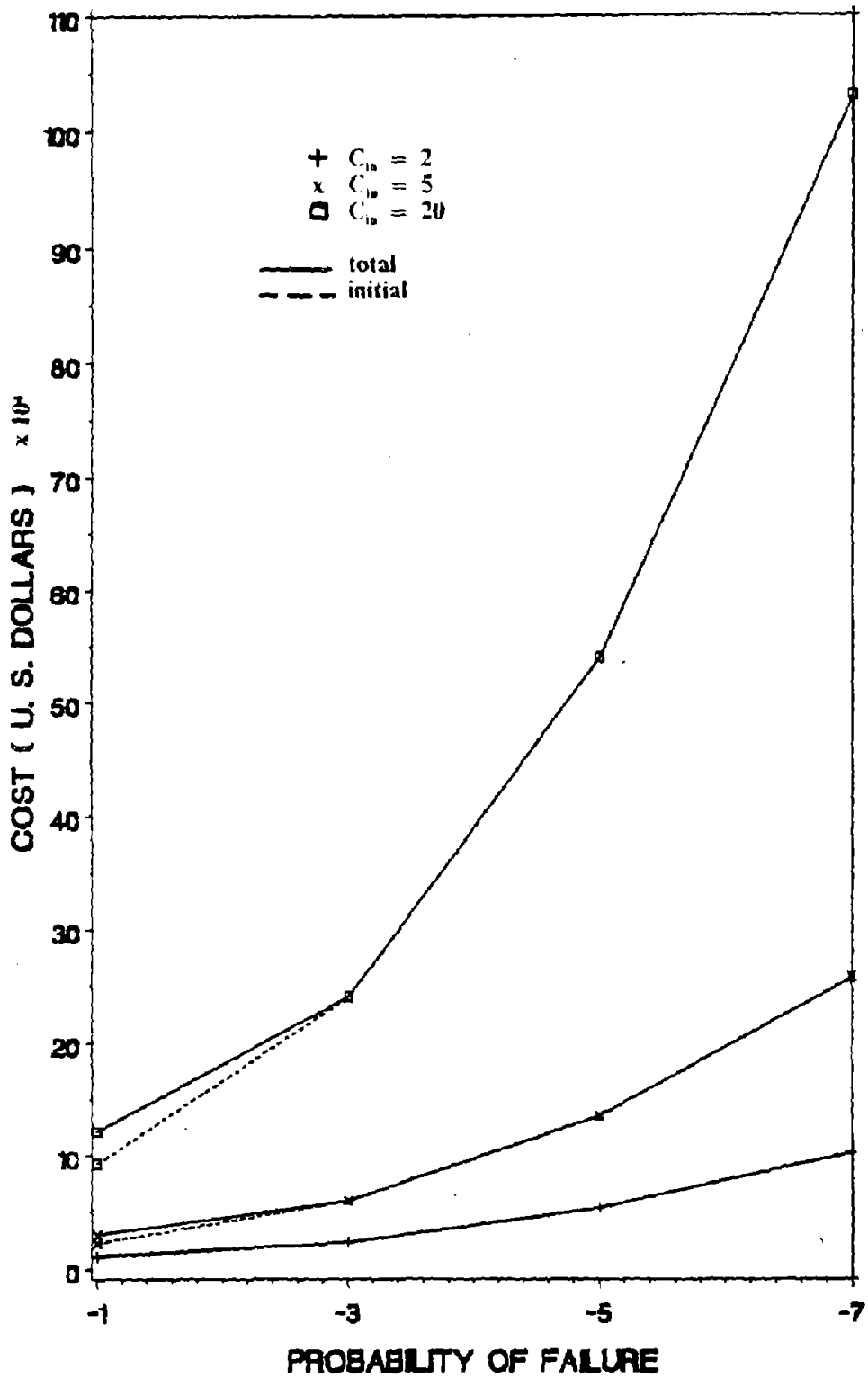

Figure 70. Optimum Cost for Various C_{in} with LN of 2-Story Building.

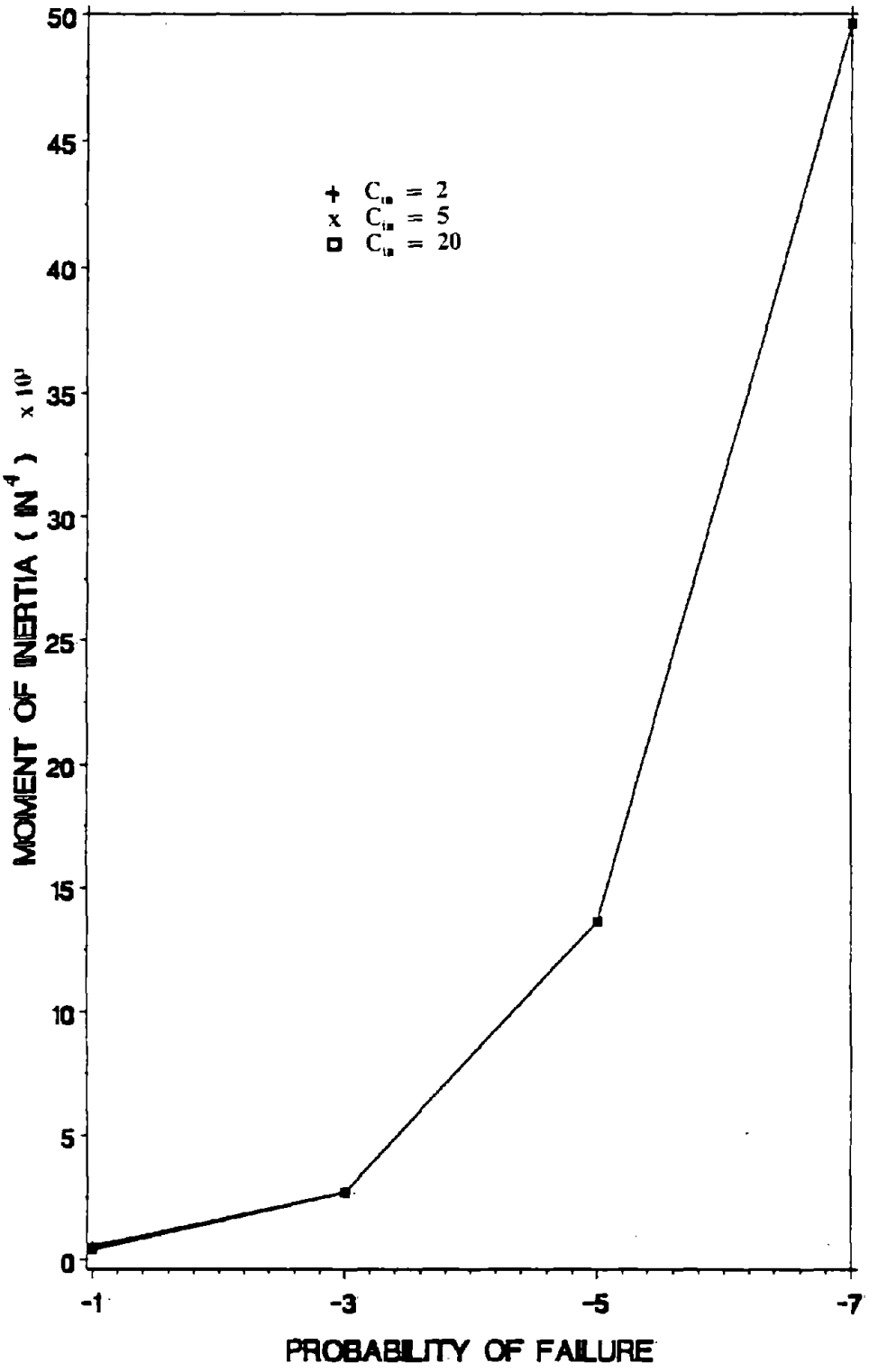

Figure 71. I_1 for Various C_{in} with LN of 2-Story Building.(1 in^4 = 41.62 cm^4)

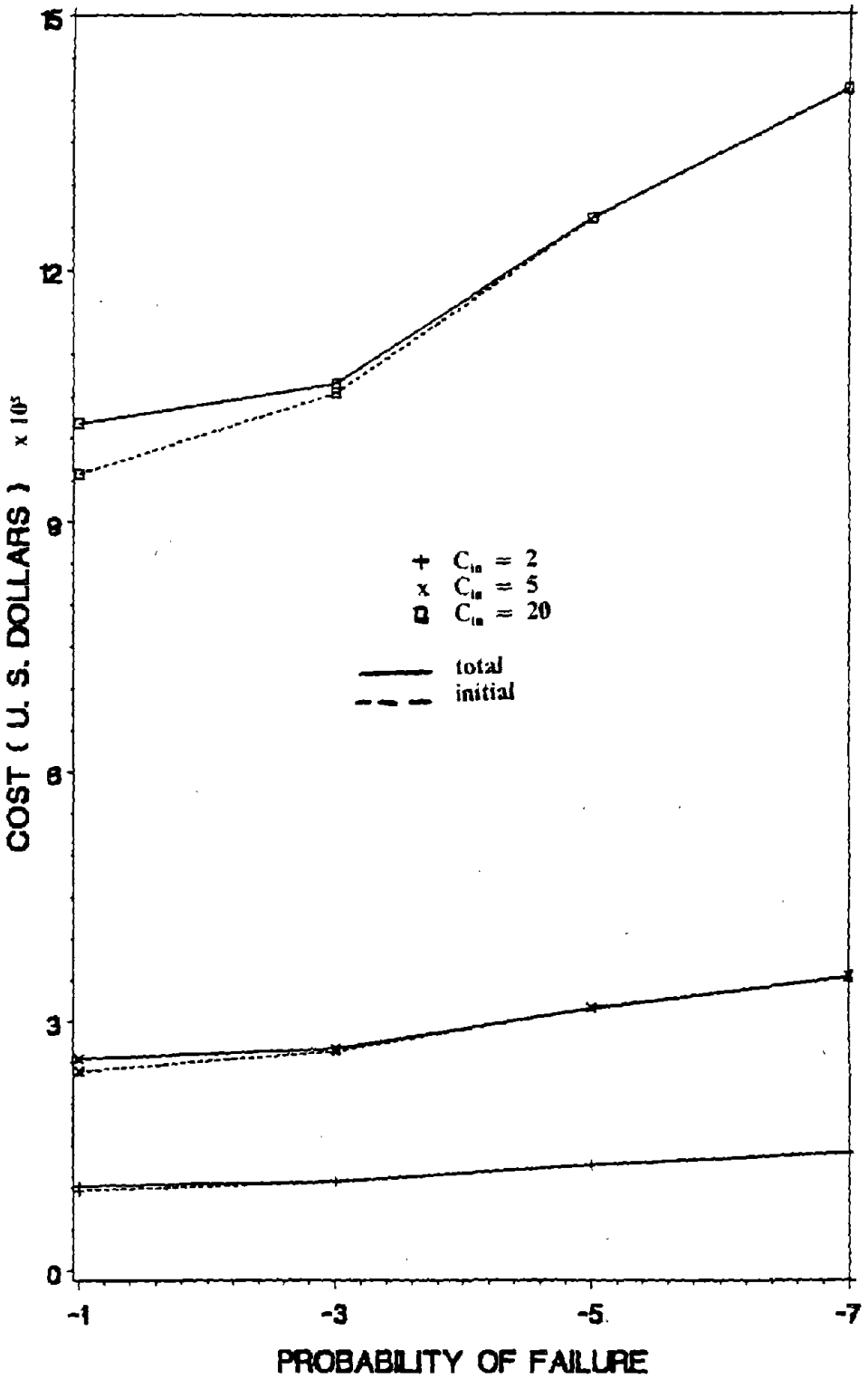

Figure 72. Optimum Cost for Various C_{in} with N of 10-Story Building.

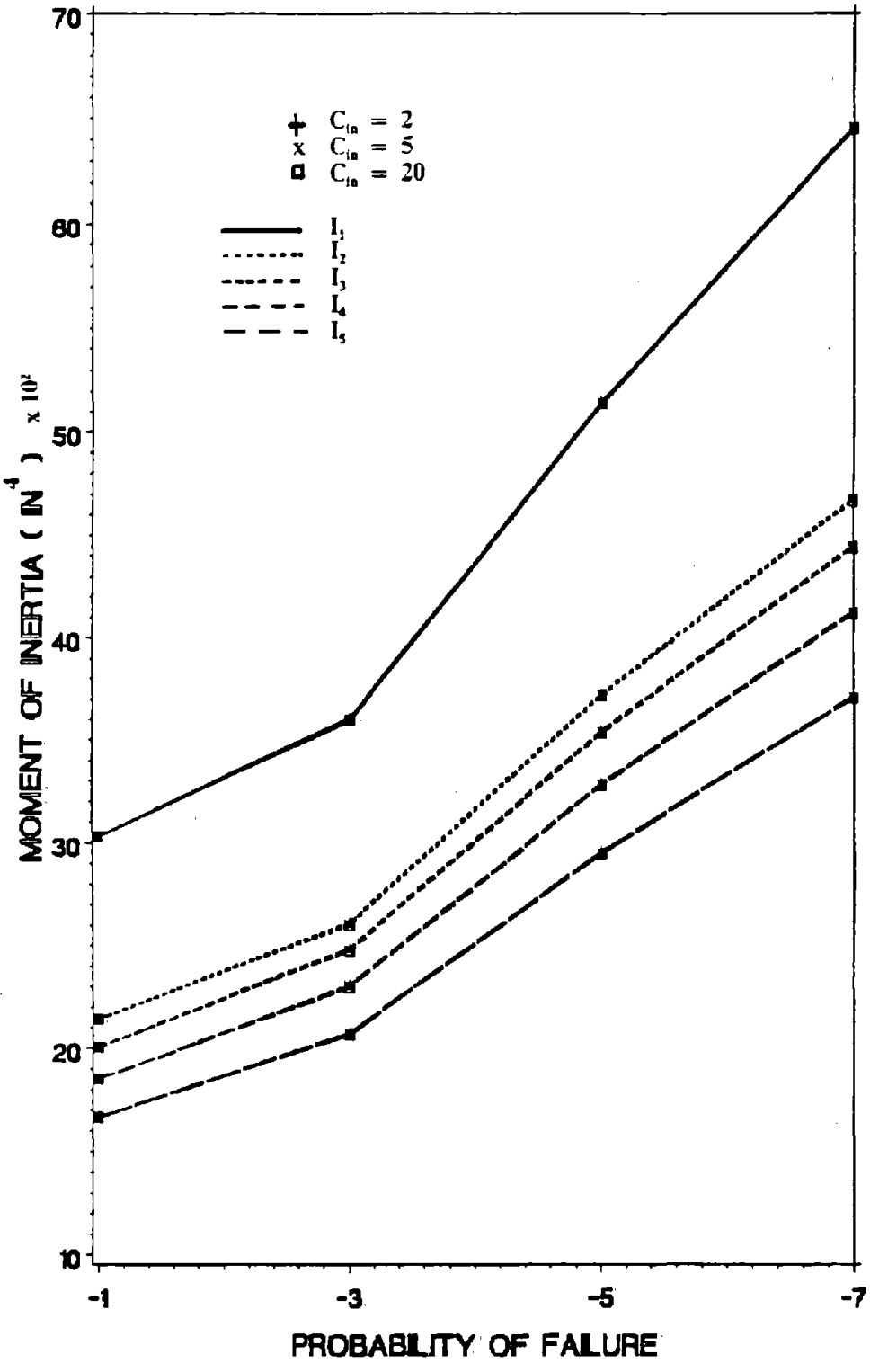

Figure 73. I_1 - I_5 for Various C_{in} with N of 10-Story Building.(1 in^4 = 41.62 cm^4)

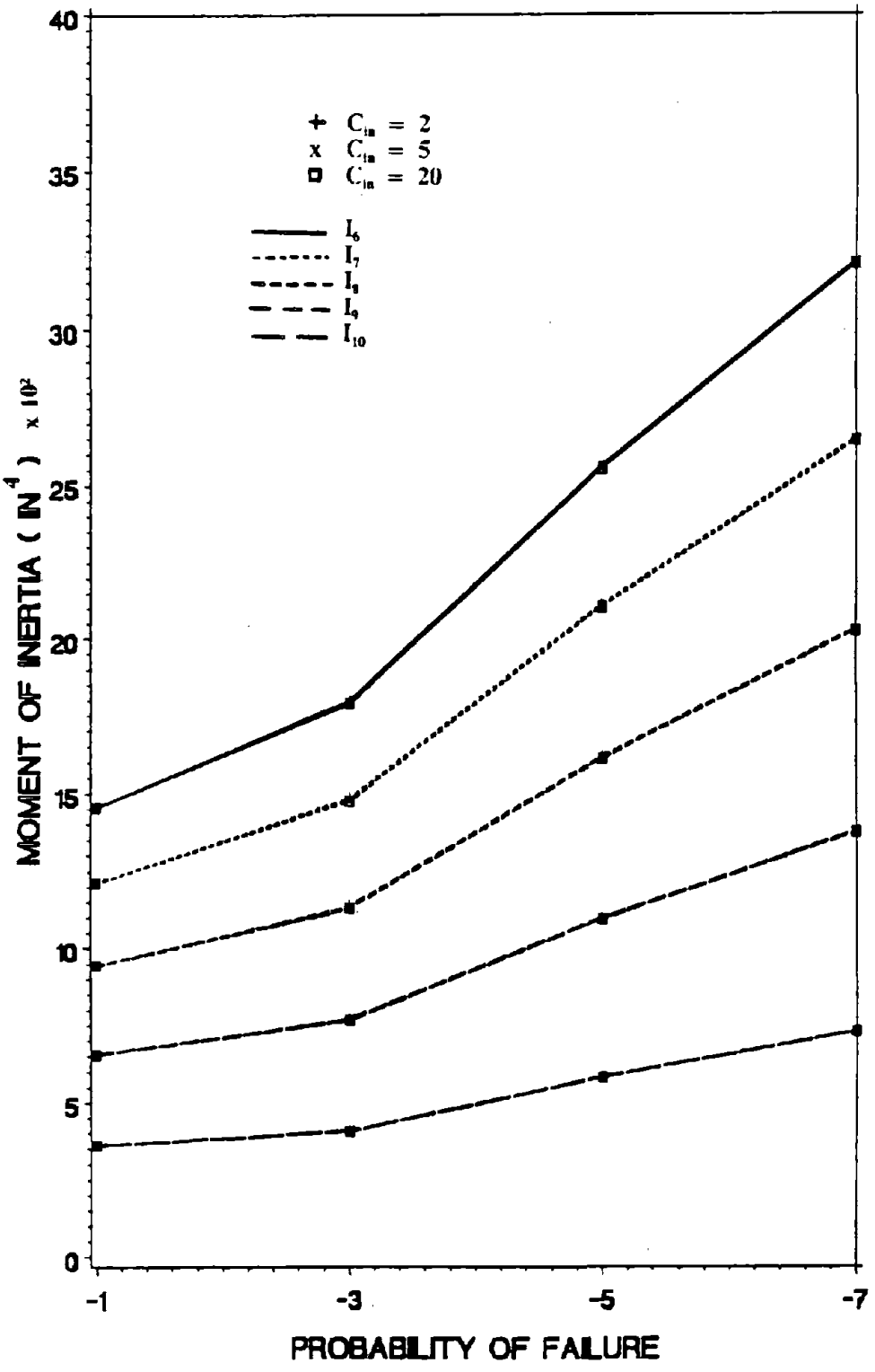

Figure 74. I_6 - I_{10} for Various C_{in} with N of 10-Story Building. (1 in^4 = 41.62 cm^4)

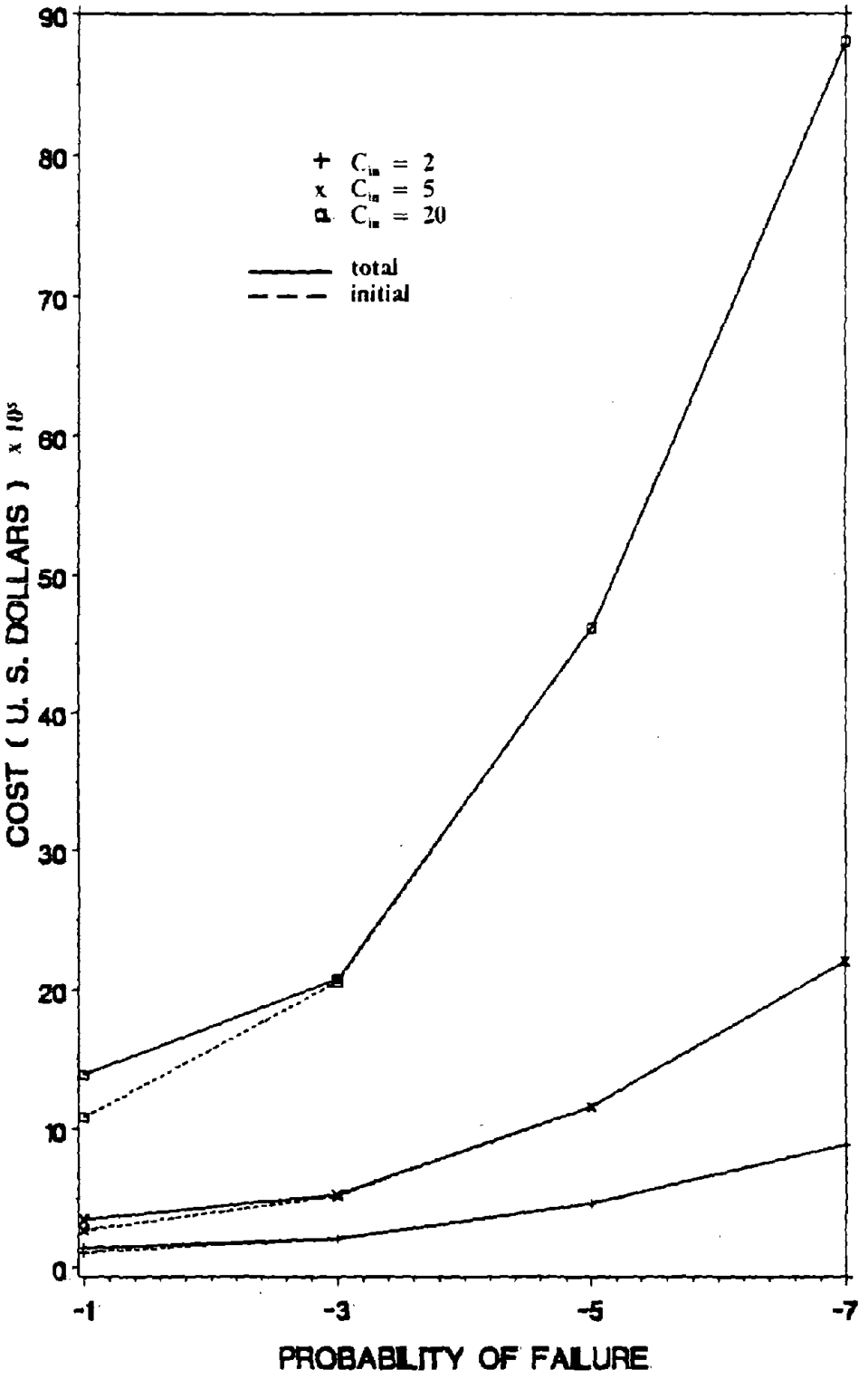

Figure 75. Optimum Cost for Various C_{in} with *LN* of 10-Story Building.

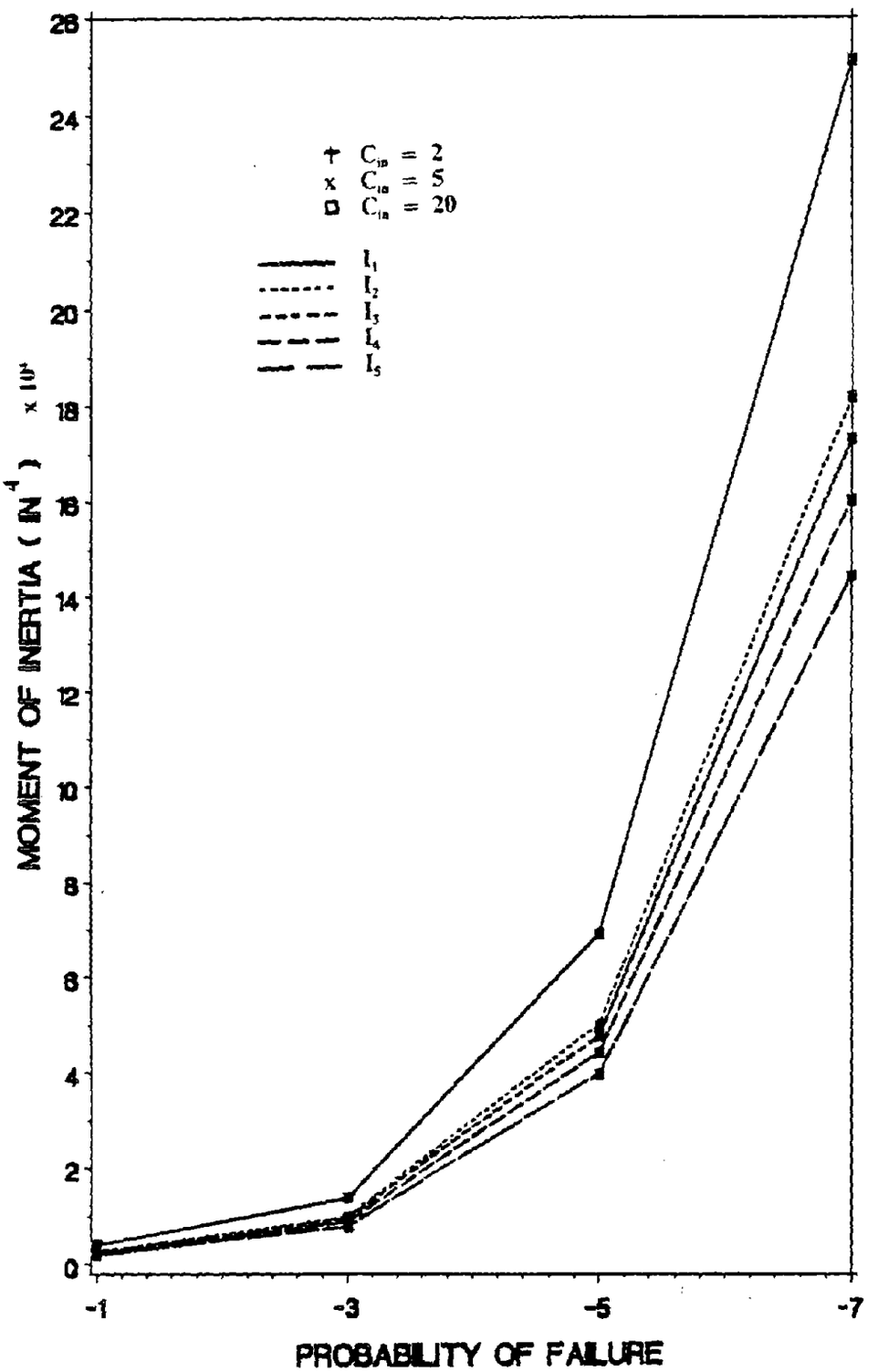

Figure 76. I_1 - I_5 for Various C_{in} with LN of 10-Story Building. (1 in^4 = 41.62 cm^4)

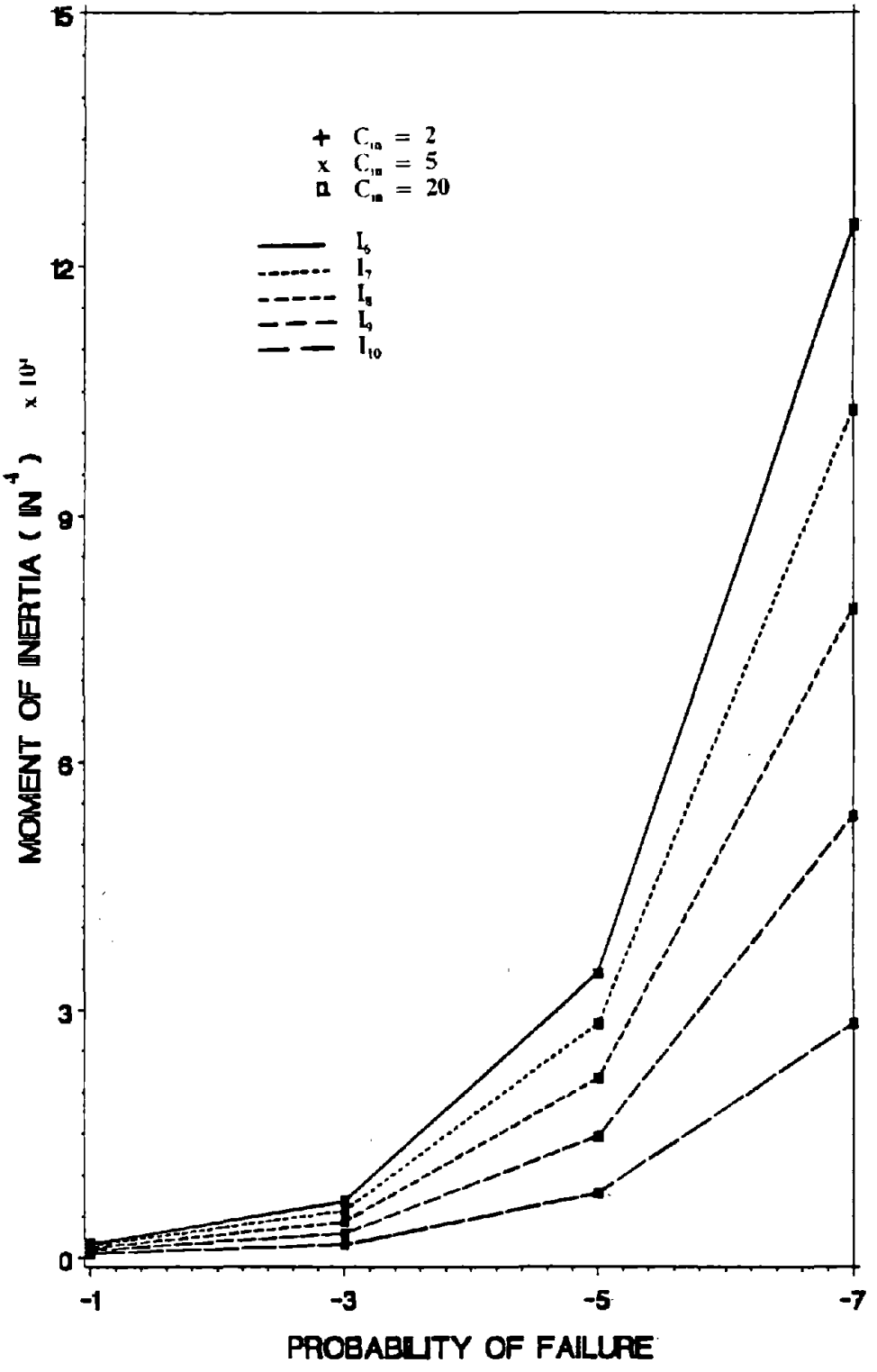

Figure 77. I_6 - I_{10} for Various C_{in} with I.N of 10-Story Building.(1 in^4 = 41.62 cm^4)

2. The Ratio of Expected Failure Cost to Initial Cost. The expected failure cost has two components which are structural losses (repair costs) and nonstructural losses (business or human losses). However, this cost is also not clearly to be defined. So in this section the expected failure costs are all assumed to have a relationship with initial cost. Three values of C_{VL} in the amount of 0.5, 1.0, and 10. are used to investigate the influence of different expected failure costs on the optimum solutions. The value of C_{in} is assumed to be constant as 5.

Figures 78 through 81 show the optimum solution of the two-story building and Figures 82 through 87 reveal the design results of the ten-story building. All the design are based on the 2nd variance approach with normal and lognormal distribution. The unit cost is 0.15 dollars/in^4. From all the figures, one may observe that there are some differences between total cost and initial cost at low reliability ($P_{f0} < 10^{-5}$); the differences practically become zero as the reliability levels increase. The total costs increase as C_{VL} increases at low reliability ($P_{f0} < 10^{-5}$). But the differences are not much different for different C_{VL} values as reliability increases. It is because the values of future failure losses are small at high reliability; therefore, the increase of future failure cost does not change the design of structural members signifcantly. The differences between total costs and initial costs decrease for higher reliability levels because the increase of reliability results the decrease of future failure losses.

F. SUMMARIES

1. For no variation of UBC and for 1st and 2nd variance approach with normal and lognormal distribution, the optimum solutions do not change with different V_{M_y} values while these values are less than 0.15. The results between V_{M_y} = 0.15 and 0.2 for lognormal distribution increase while allowable failure probabilities are larger than 10^{-5}.

2. For no variation of UBC, and for 1st and 2nd variance approach with normal and lognormal distribution, the optimum solutions change as the values of $V_{M_{cr}}$ change.

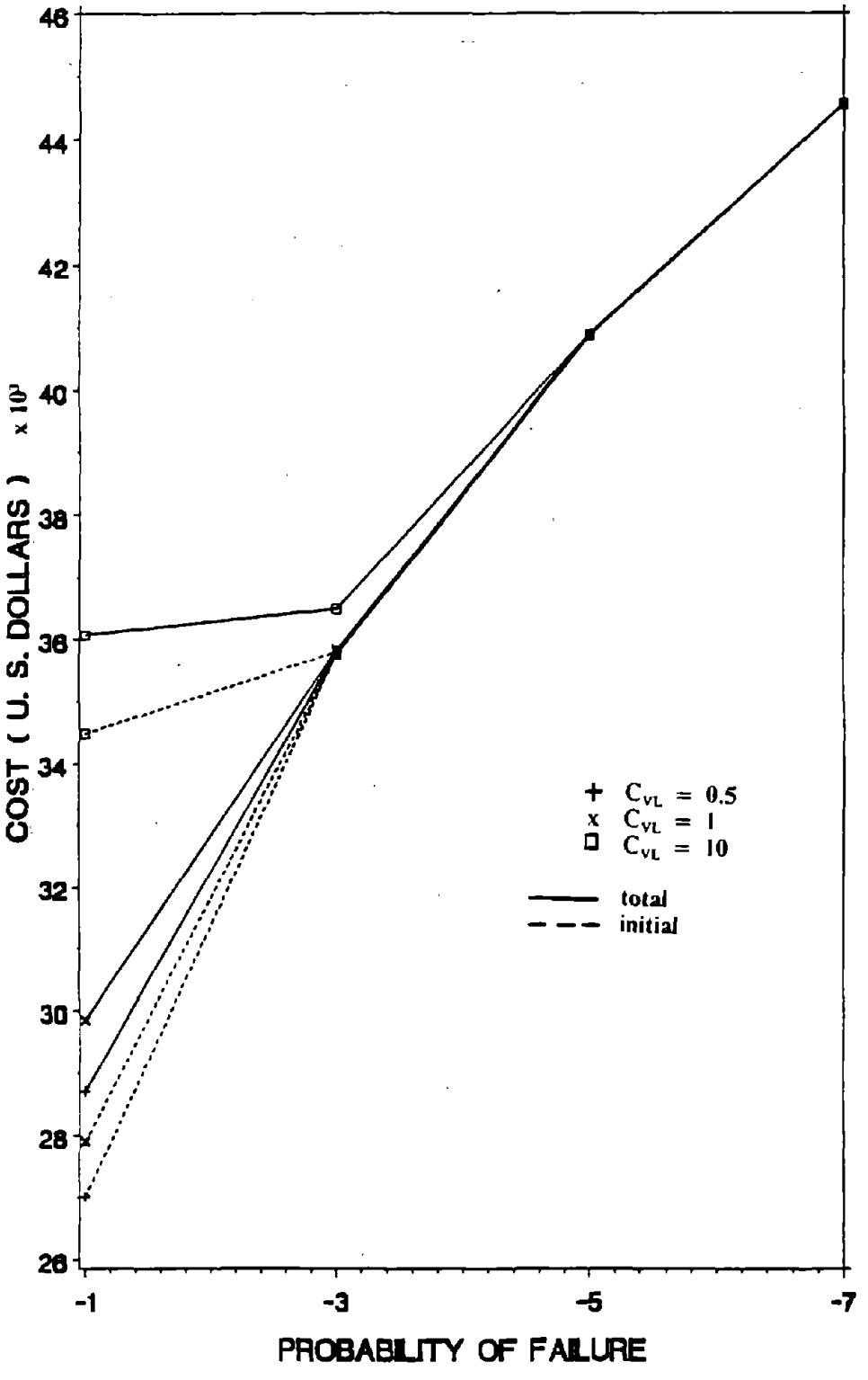

Figure 78. Optimum Cost for Various C_{VL} with N of 2-Story Building.

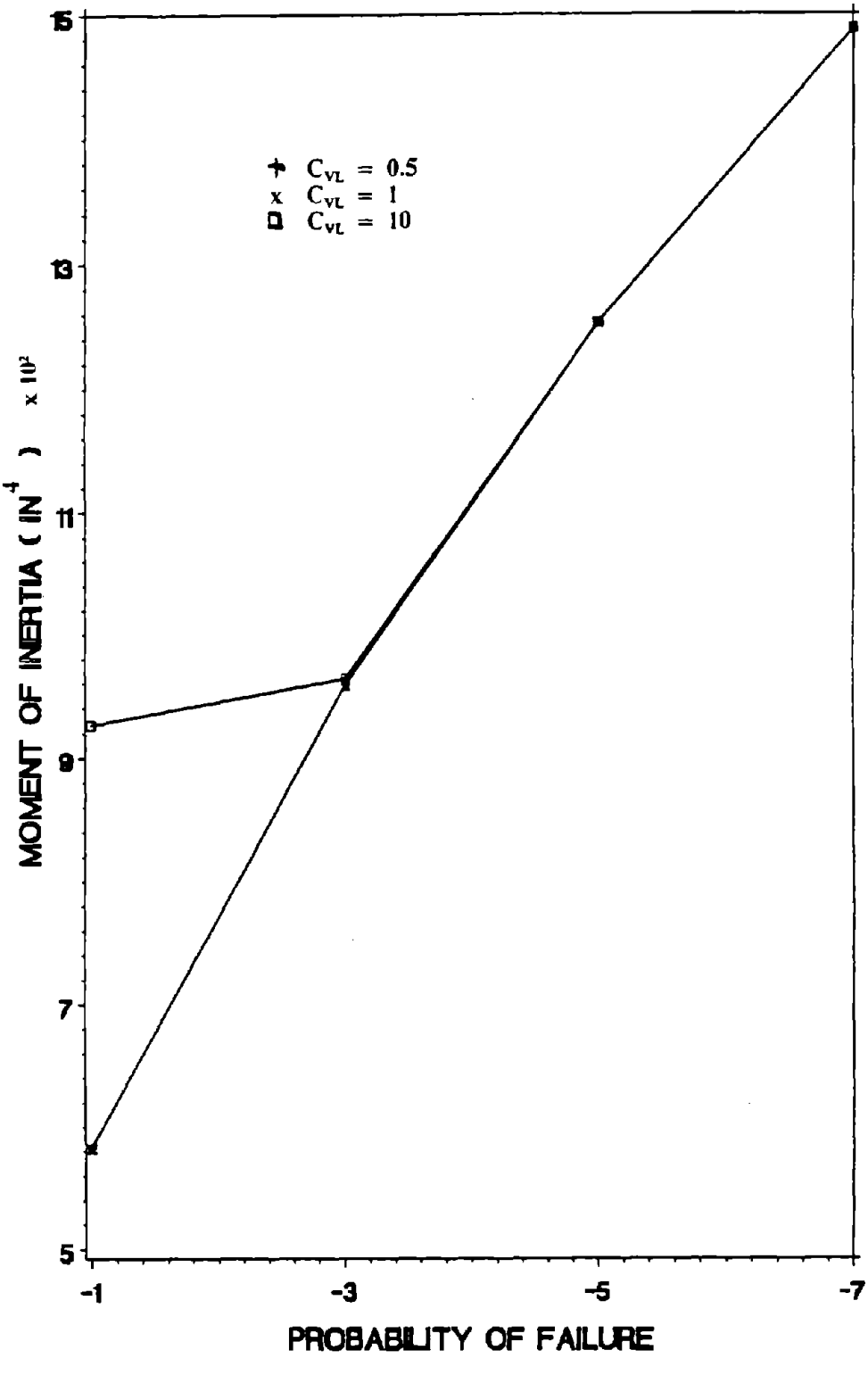

Figure 79. I_1 for Various C_{VL} with N of 2-Story Building.(1 in^4 = 41.62 cm^4)

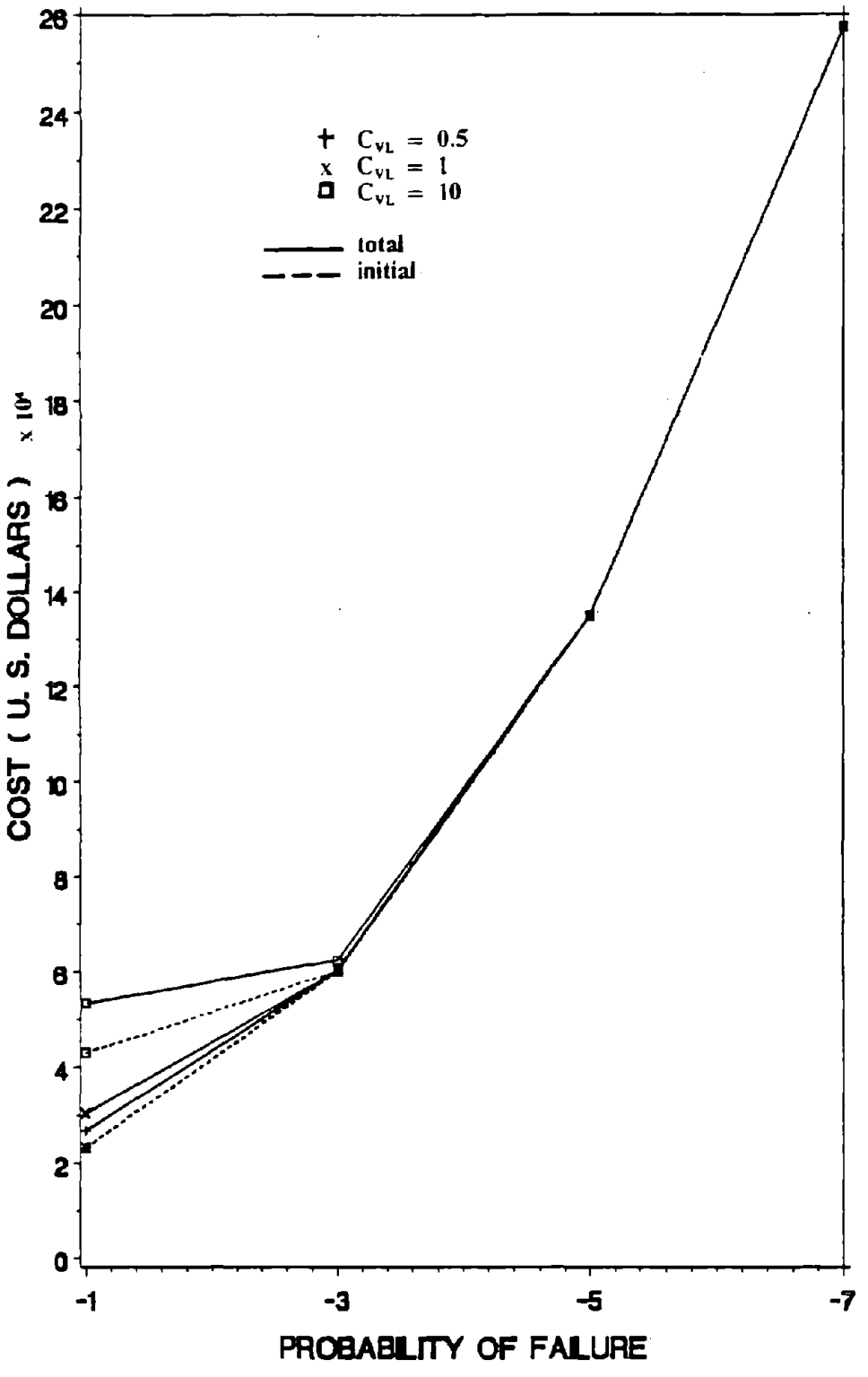

Figure 80. Optimum Cost for Various C_{VL} with LN of 2-Story Building.

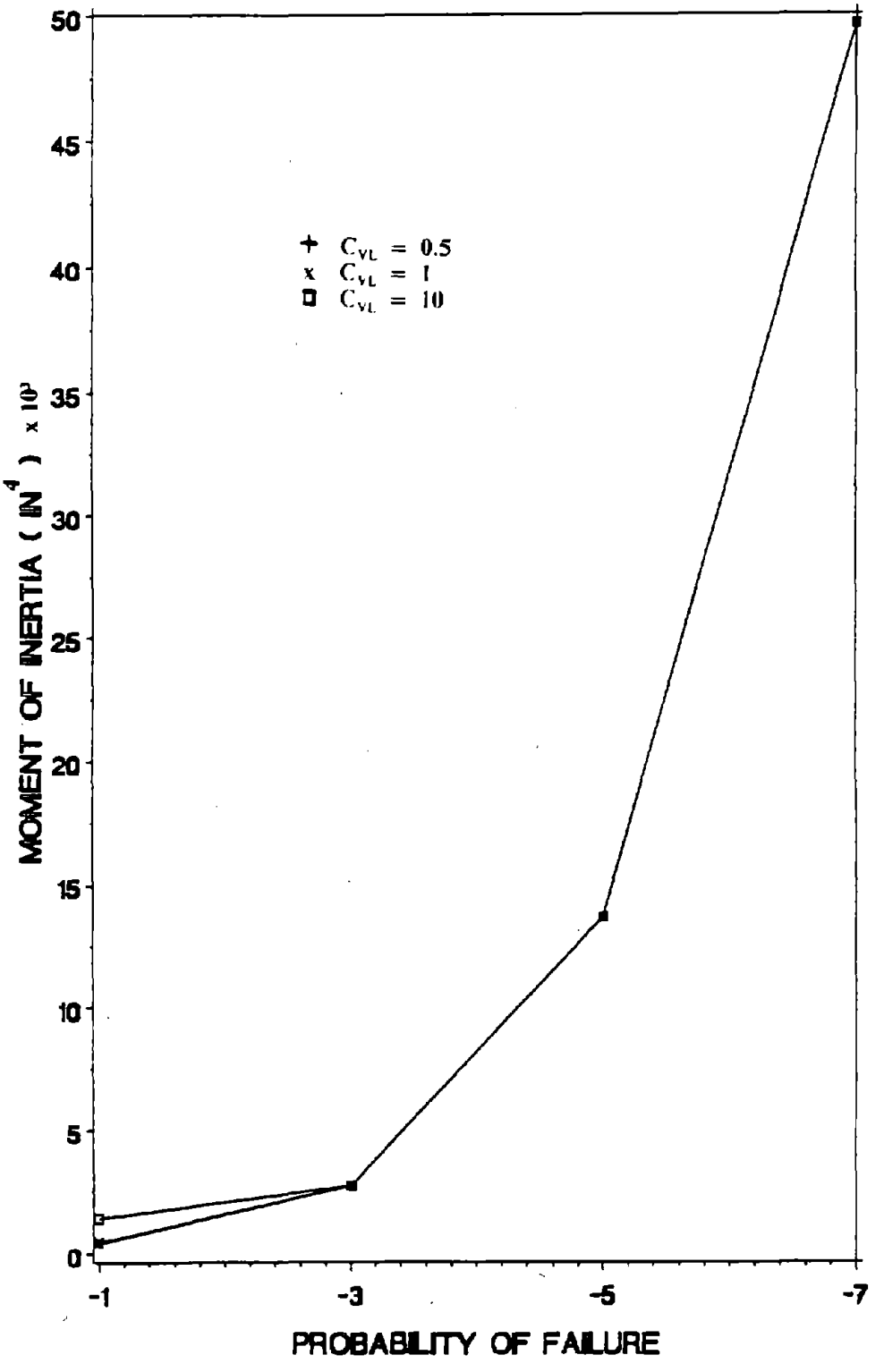

Figure 81. I_1 for Various C_{VL} with LN of 2-Story Building. (1 in^4 = 41.62 cm^4)

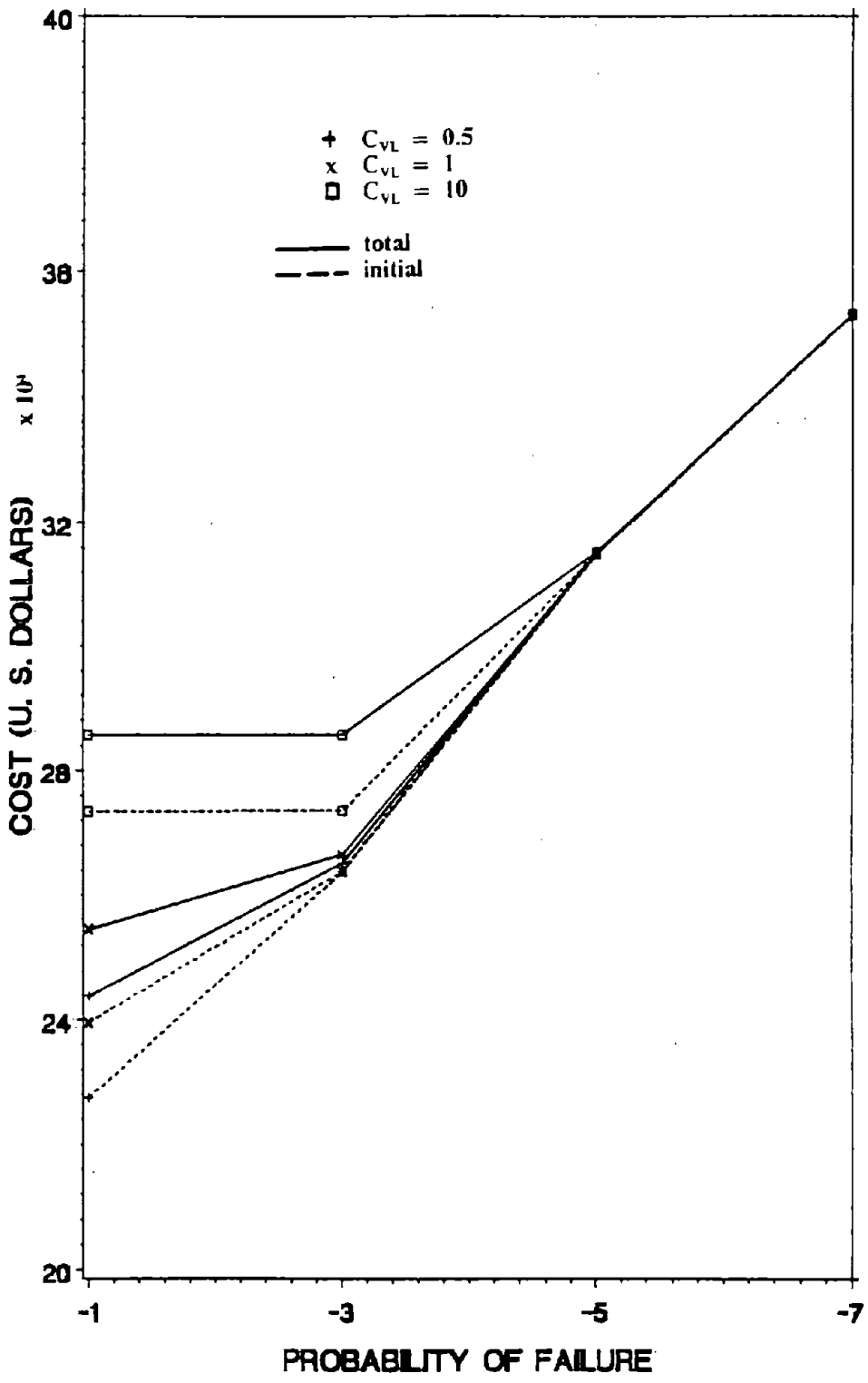

Figure 82. Optimum Cost for Various C_{VL} with N of 10-Story Building.

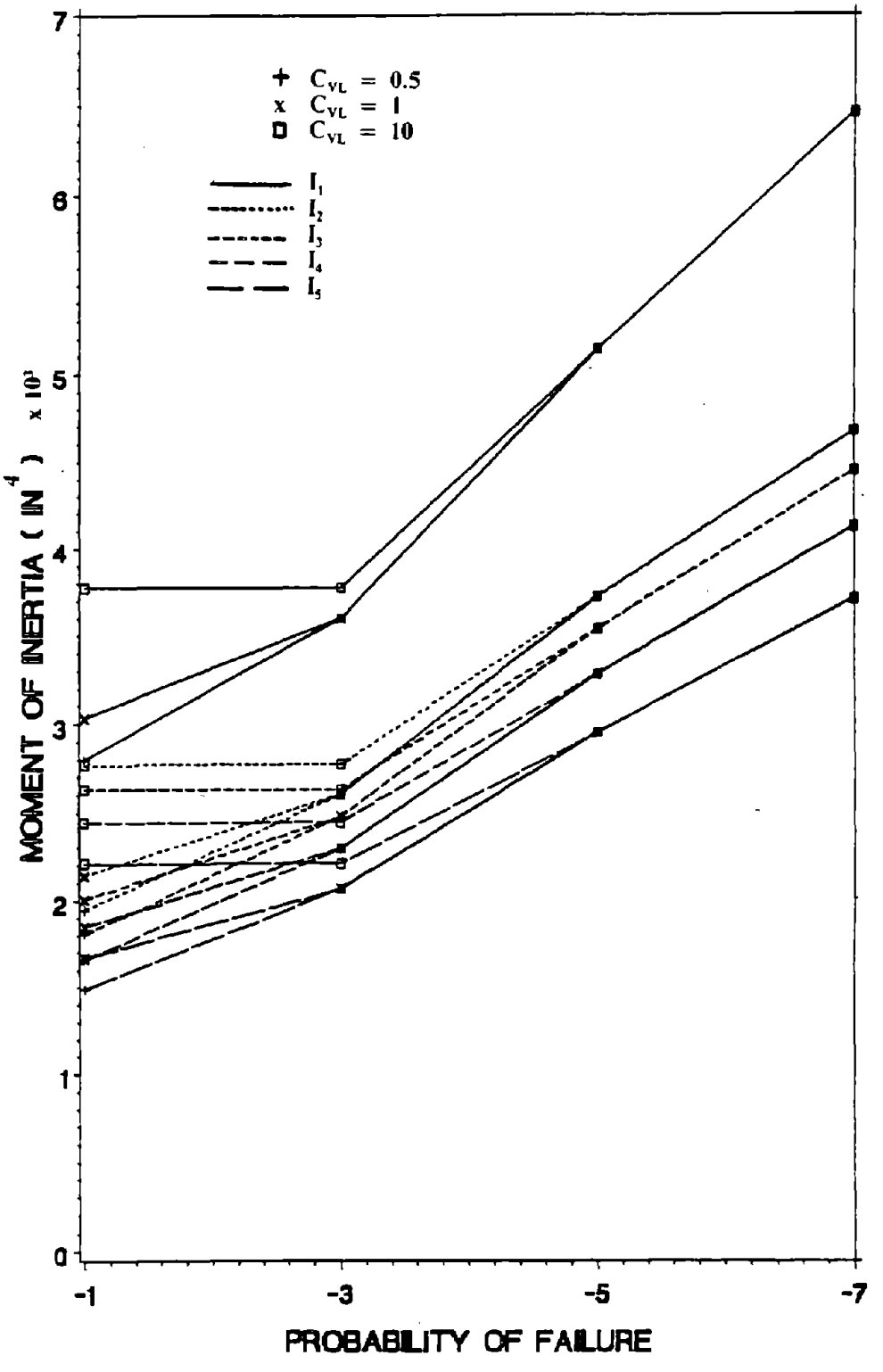

Figure 83. I_1 - I_5 for Various C_{VL} with N of 10-Story Building.(1 in^4 = 41.62 cm^4)

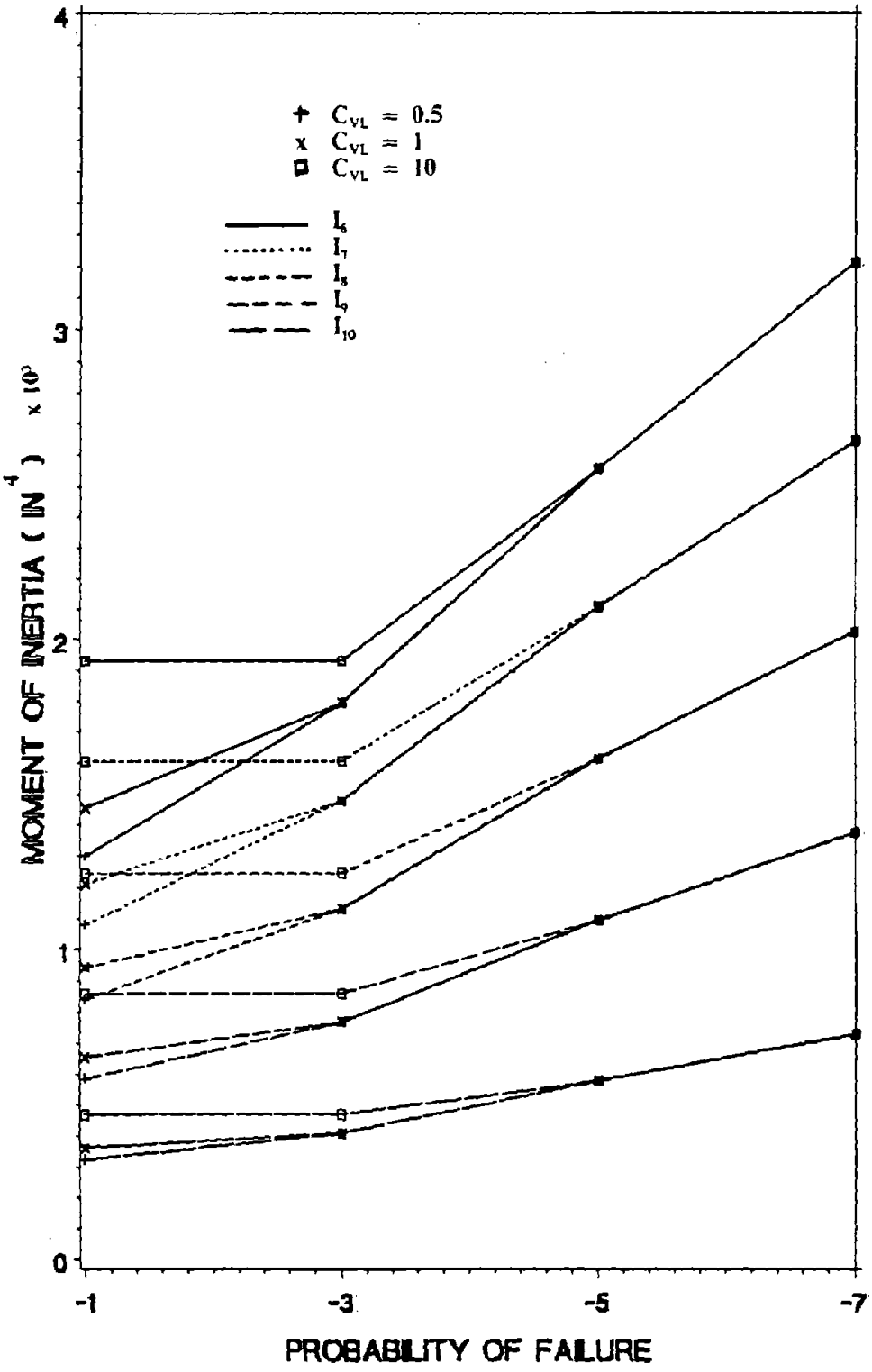

Figure 84. I_6 - I_{10} for Various C_{VL} with N of 10-Story Building. (1 in^4 = 41.62 cm^4)

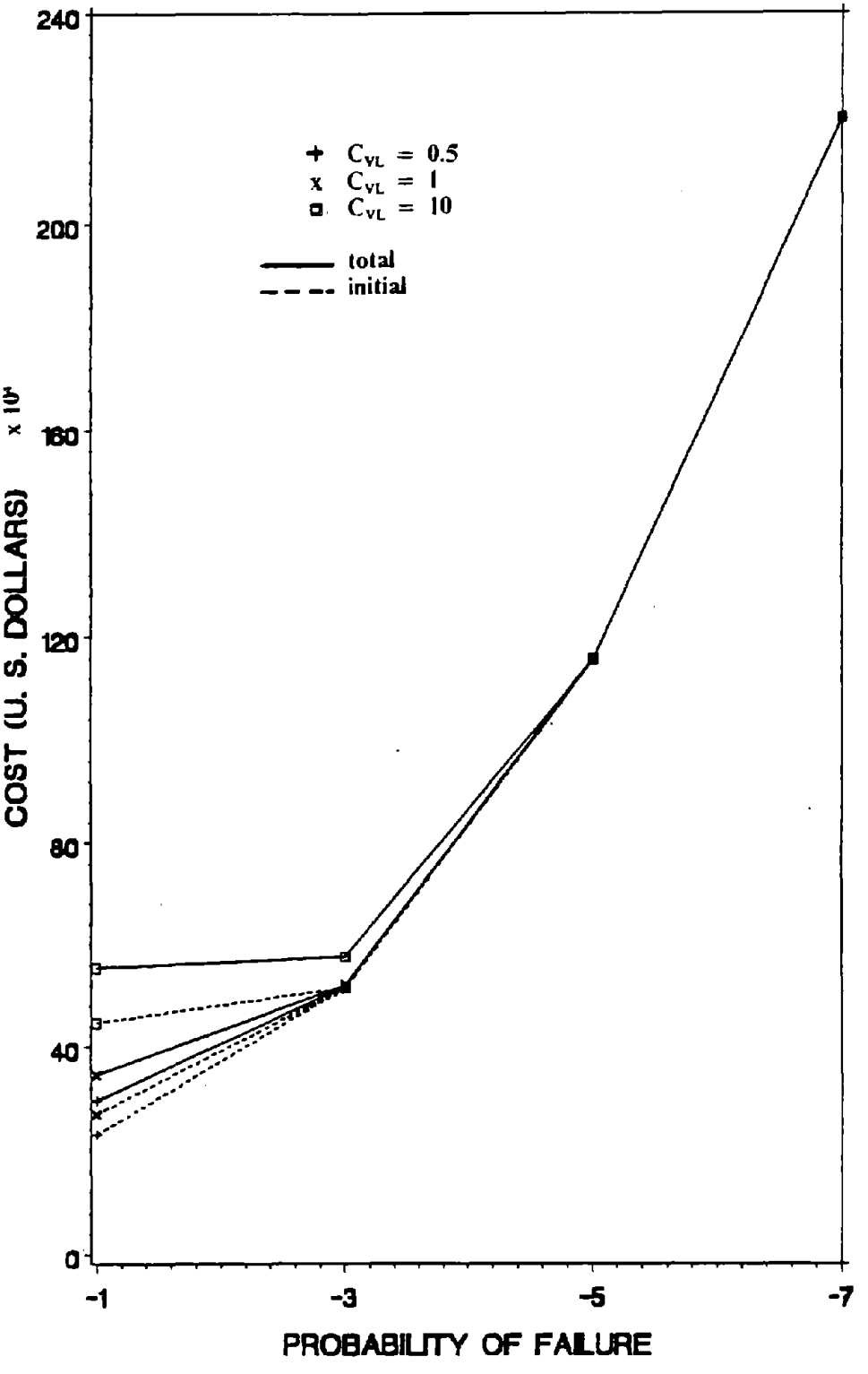

Figure 85. Optimum Cost for Various C_{VL} with LN of 10-Story Building.

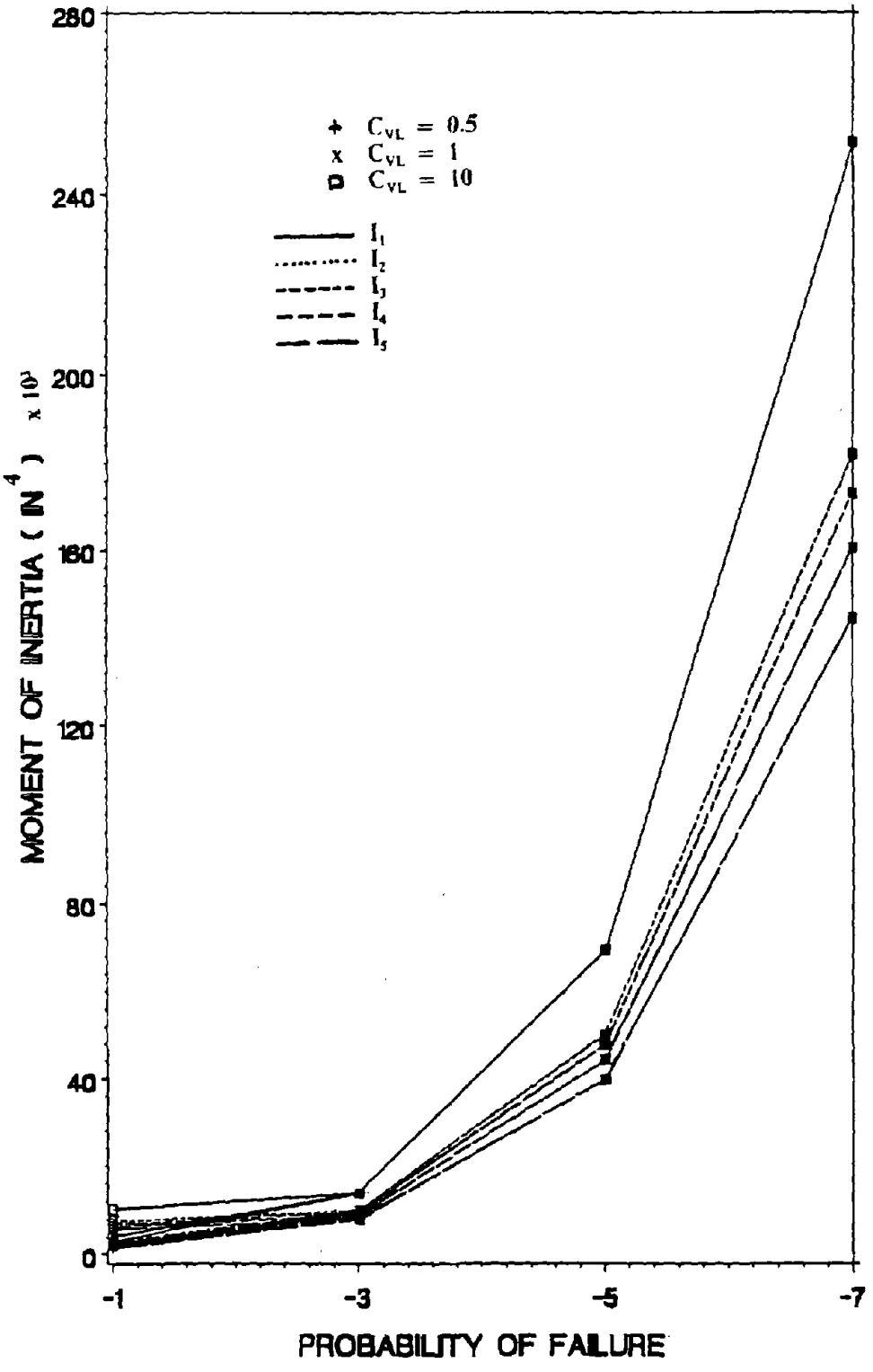

Figure 86. I_1 - I_5 for Various C_{VL} with LN of 10-Story Building.(1 in^4 = 41.62 cm^4)

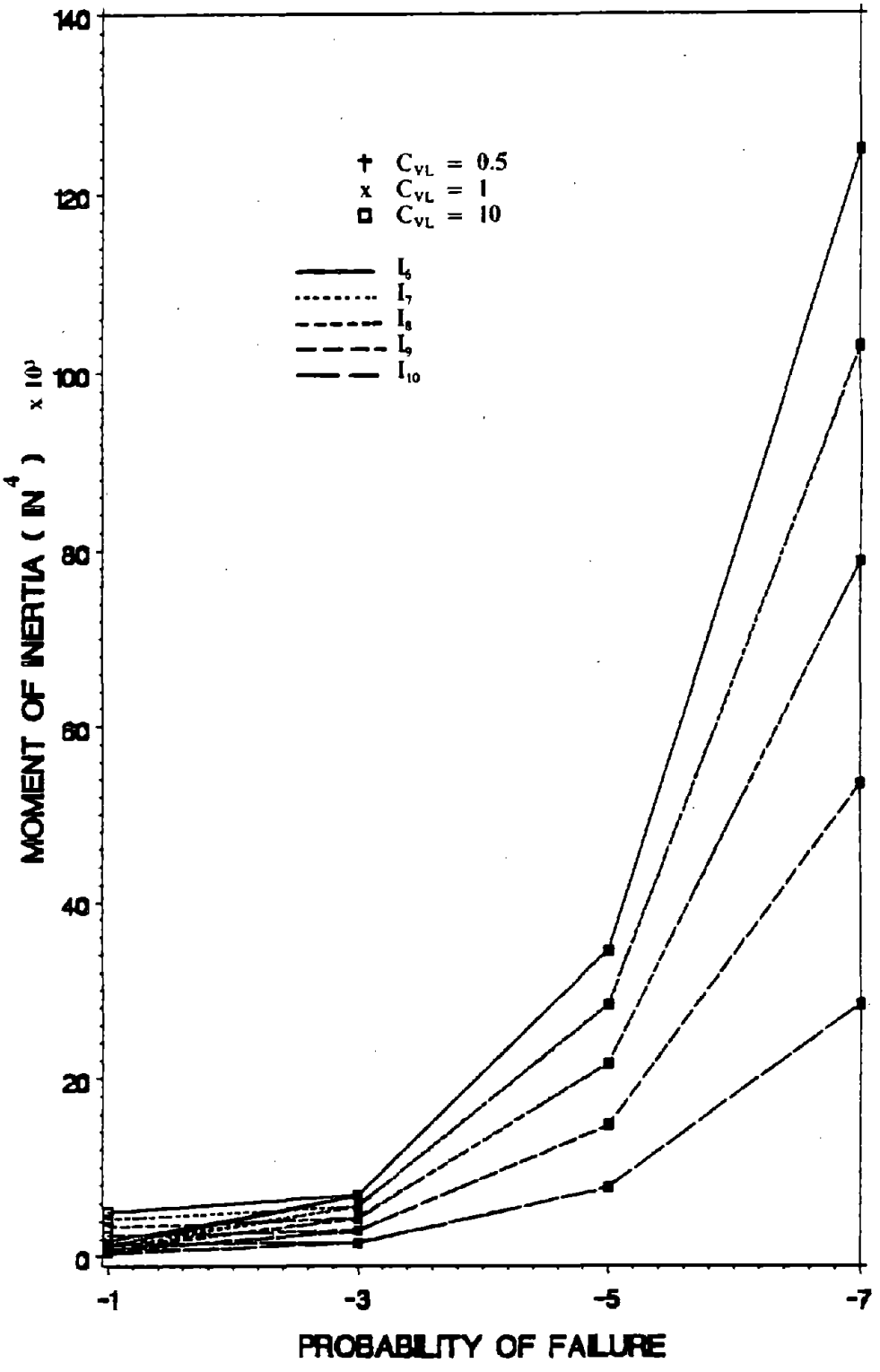

Figure 87. I_6 - I_{10} for Various C_{VL} with LN of 10-Story Building.(1 in^4 = 41.62 cm^4)

3. For NBS recommended variation of UBC, and for 1st and 2nd variance approach with normal and lognormal distribution, the optimum solutions do not change as the values of V_{M_y} or $V_{M_{cr}}$ change.

4. The change of optimum design due to the change of V_{I_E} are faster at high reliability for 1st and 2nd variance approach with normal and lognormal distribution. This change is especially fast for lognormal distribution and high variance of earthquake.

5. The optimum solutions between 1st and 2nd variance approach are very close, while the values of V_E are larger than o.5.

6. At high reliability level, the optimum designs with lognormal distribution are higher than those with normal distribution. However it reverses the order at low reliability level.

7. The optimum designs among the zone coefficients increases as the reliability increases for 1st and 2nd variance approach with normal and lognormal distribution.

8. The total cost changes as values of C_{in} change. However, the moments of inertia do not change noticeably.

9. The differences of total cost among various values of C_{VL} reduce as the reliability increases.

10. The difference between total cost and initial cost reduces as the reliability increases.

XI. OPTIMUM DESIGNS FOR NNSRS LOAD

In this chapter, the Newmark's nondeterministic seismic response spectrum (NNSRS) is used to investigate the sensitivities of coefficients of structural resistance parameters, the comparison of 1st and 2nd variance approach, and the coefficient of variation of peak ground acceleration. The statistics of amplification factors for Newmark's nondeterminisitic response spectrum in the 50 percentile are adopted here. These statistics for horizontal ground acceleration are $\tilde{f}_{\omega 1} = 0.4$, $\tilde{f}_{\omega 2} = 2.0$, $\tilde{f}_{\omega 3} = 6.0$, $\tilde{f}_{\omega 4} = 20.0$, $\bar{\alpha}_d = 1.4$, $\bar{\alpha}_v = 1.66$, $\bar{\alpha}_a = 2.11$, $\bar{\alpha}_{(ad/v^2)} = 6.04$, $\bar{\alpha}_{(v/a)} = 48/g$, $\sigma_{\alpha_d} = 0.64$, $\sigma_{\alpha_v} = 0.66$, $\sigma_{\alpha_a} = 0.56$, $V_{(ad/v^2)} = 0.65$, $V_{(v/a)} = 0.45$, $V_{\alpha_d} = \sigma_{\alpha_d}/\bar{\alpha}_d$, $V_{\alpha_v} = \sigma_{\alpha_v}/\bar{\alpha}_v$, $V_{\alpha_a} = \sigma_{\alpha_a}/\bar{\alpha}_a$. The statistics for vertical ground acceleration are $\tilde{f}_{\omega 1} = 0.3$, $\tilde{f}_{\omega 2} = 3.0$, $\tilde{f}_{\omega 3} = 10.0$, $\tilde{f}_{\omega 4} = 50.0$, $\bar{\alpha}_d = 1.4$, $\bar{\alpha}_v = 1.51$, $\bar{\alpha}_a = 2.05$, $\bar{\alpha}_{(ad/v^2)} = 10.11$, $\bar{\alpha}_{v/a} = 29/g$, $\sigma_{\alpha_d} = 0.61$, $\sigma_{\alpha_v} = 0.67$, $\sigma_{\alpha_a} = 0.77$, $V_{(ad/v^2)} = 0.7$, $V_{v/a} = 0.53$, $V_{\alpha_d} = \sigma_{\alpha_d}/\bar{\alpha}_d$, $V_{\alpha_v} = \sigma_{\alpha_v}/\bar{\alpha}_v$, $V_{\alpha_a} = \sigma_{\alpha_a}/\bar{\alpha}_a$. The peak ground accelerations are assumed to be 0.2g in Sections A, B, and C, and 0.4g in Section D. The two-story strucure shown in Figure 38 and the ten-story structure shown in Figure 39 have lumped mass for each story of 0.27 k-sec^2/ in (0.47 kN-sec^2 / cm). The parameters used in the examples are: the allowable displacements = 0.005 times the corresponding height relative to the structural base; the allowable variance of displacements = 0; the mean yielding strength, $\bar{F}_y$ = 36 ksi (2.448 x 10^5 kPa); the mean elastic modulus, $\bar{E}_m$ = 30000 ksi (2.067 x 10^8 kPa); the coefficient of variation of elastic modulus, V_{E_m} = 0.06; and the coefficient of variation of moment of inertia, V_I = 0.05. The coefficients of variation of yield moment and critical moment are 0.12 and 0.2, respectively.

A. SENSITIVITIES OF VARIATION OF COLUMN RESISTANCE PARAMETERS.

In order to see the sensitivities of coefficients of variation of yield moment and critical moment, no variation of peak ground acceleration will be assumed. The failure modes considered are the yielding or torsional buckling failures for each column member.

1. Sensitivity of Variation of Yield Moment. The coefficient of variation of yield moment is varied from 0.05 to 0.2, and the coefficient of variation of critical moment is constant at 0.2. The optimum weights in Figures 88 and 90, and the moments of inertia in Figures 89 and 91 change when the coefficient of variation of yield moment varies. However, these changes with normal distribution are not as sensitive as those associated with lognormal distribution. The weight percentage increase for 2nd variance approach between $V_{M_y} = 0.05$ and $V_{M_y} = 0.2$ are 6.8% at $P_{f0} = 10^{-5}$ and 7.3% at $P_{f0} = 10^{-7}$ with normal distribution and 14.5% at $P_{f0} = 10^{-5}$ and 18.3% at $P_{f0} = 10^{-7}$ with lognormal distribution.

The discrepancies of weights and moments of inteia between 1st and 2nd variance approach are not sensitive to the change of V_{M_y}. The weight differences between 1st and 2nd variance approaches at $P_{f0} = 10^{-5}$ for V_{M_y} varies from 0.05 to 0.2 are changing 230.2 lbs (1024.4 N) to 185.2 lbs (824.1 N) with normal distribution and from 587.7 lbs (2615.2 N) to 540.3 lbs (2404.3 N) with lognormal distribution.

2. Sensitivity of Variation of Critical Moment. The coefficient of variation of critical moment is varied from 0.1 to 0.3. The coefficient of variation of yield moment used is constant at 0.12. The optimum weights given in Figures 92 and 93, with normal and lognormal distributions for two variance approaches, show that they are not sensitive to the change of coefficient of variation of critical moment. The moments of inertia are consequently not given.

B. COMPARISON OF 1ST AND 2ND VARIANCE APPROACH.

In 2nd variance approach, the recommended value of coefficient of variation of natural frequency, V_ω, is 0.16. [50] The determination of this value is based on the following equation. Since $\omega = (M/K)^{1/2}$, then

$$V_\omega = \sqrt{(0.1)^2 + \frac{1}{\bar{\omega}^2}\left[\left(\frac{\partial \omega}{\partial K}\right)^2 \bar{K}^2 V_K^2 + \left(\frac{\partial \omega}{\partial M}\right)^2 \bar{M}^2 V_M^2\right]}$$

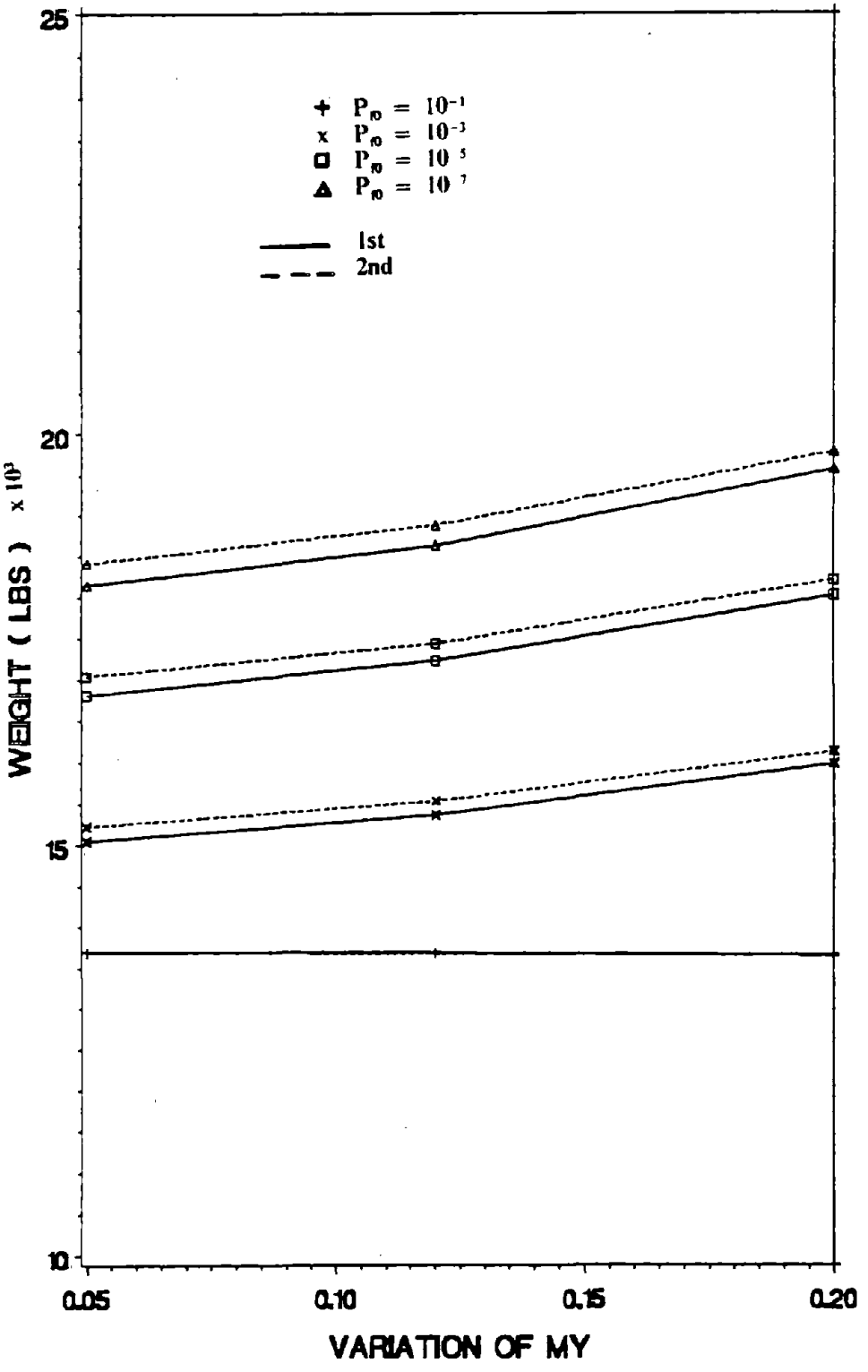

Figure 88. Optimum Weight for Various V_{M_y} with N of 2-Story Building. (1 lb = 4.45 N)

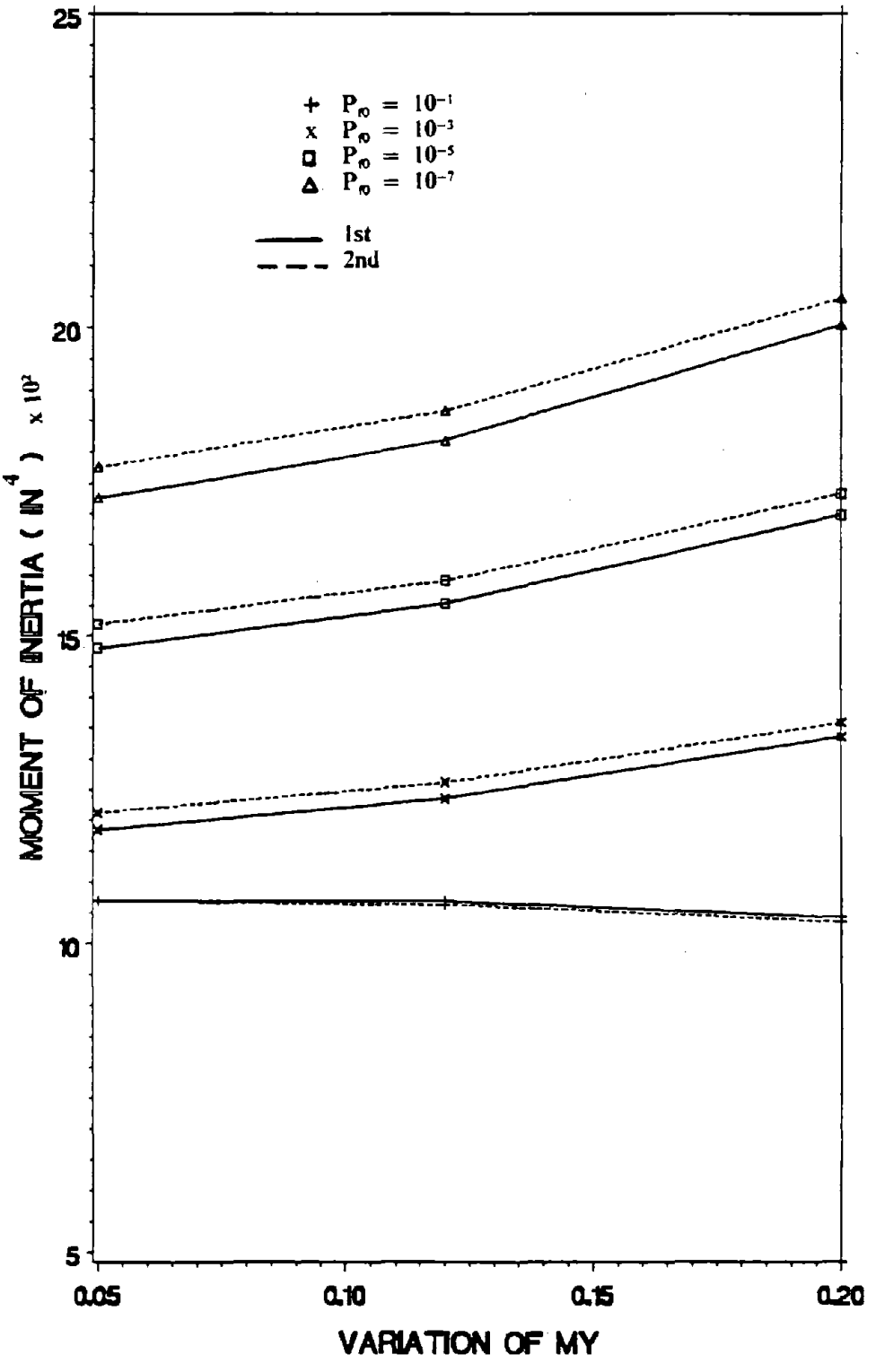

Figure 89. I_1 for Various V_{M_y} with N of 2-Story Building. (1 in = 2.54 cm)

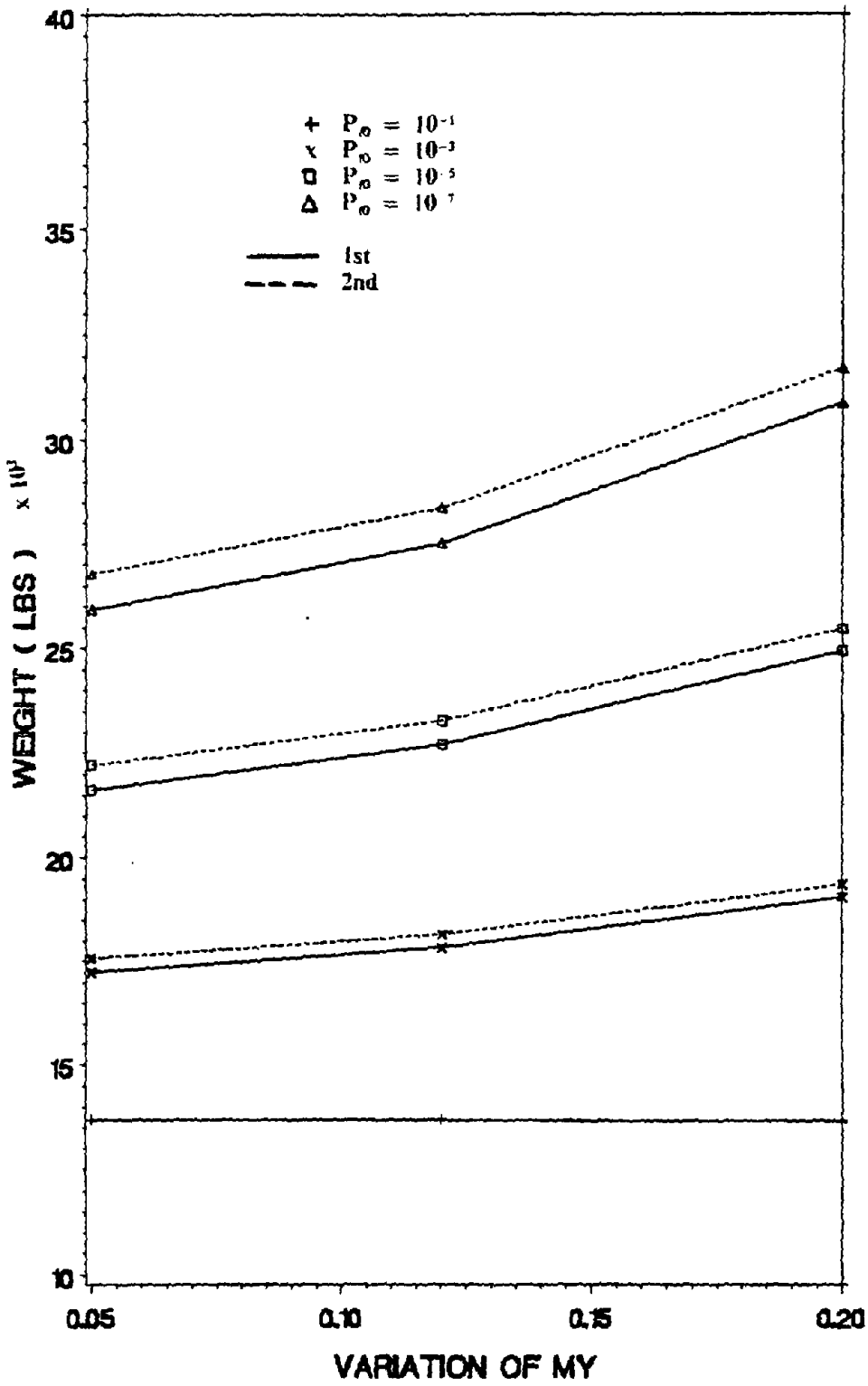

Figure 90. Optimum Weight for Various V_{M_y} with LN of 2-Story Building. (1 lb = 4.45 N)

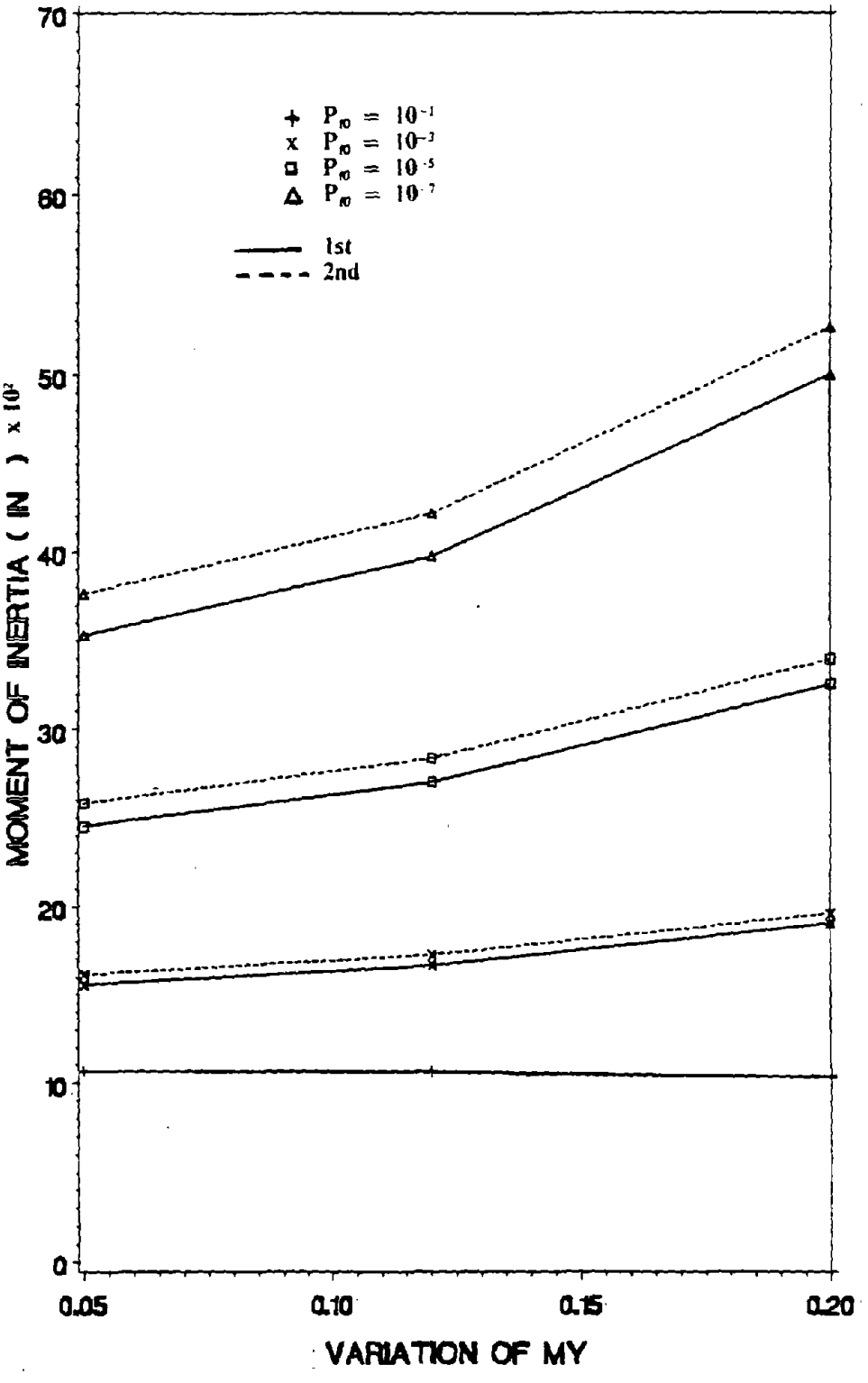

Figure 91. I_1 for Various V_{My} with LN of 2-Story Building. (1 in = 2.54 cm)

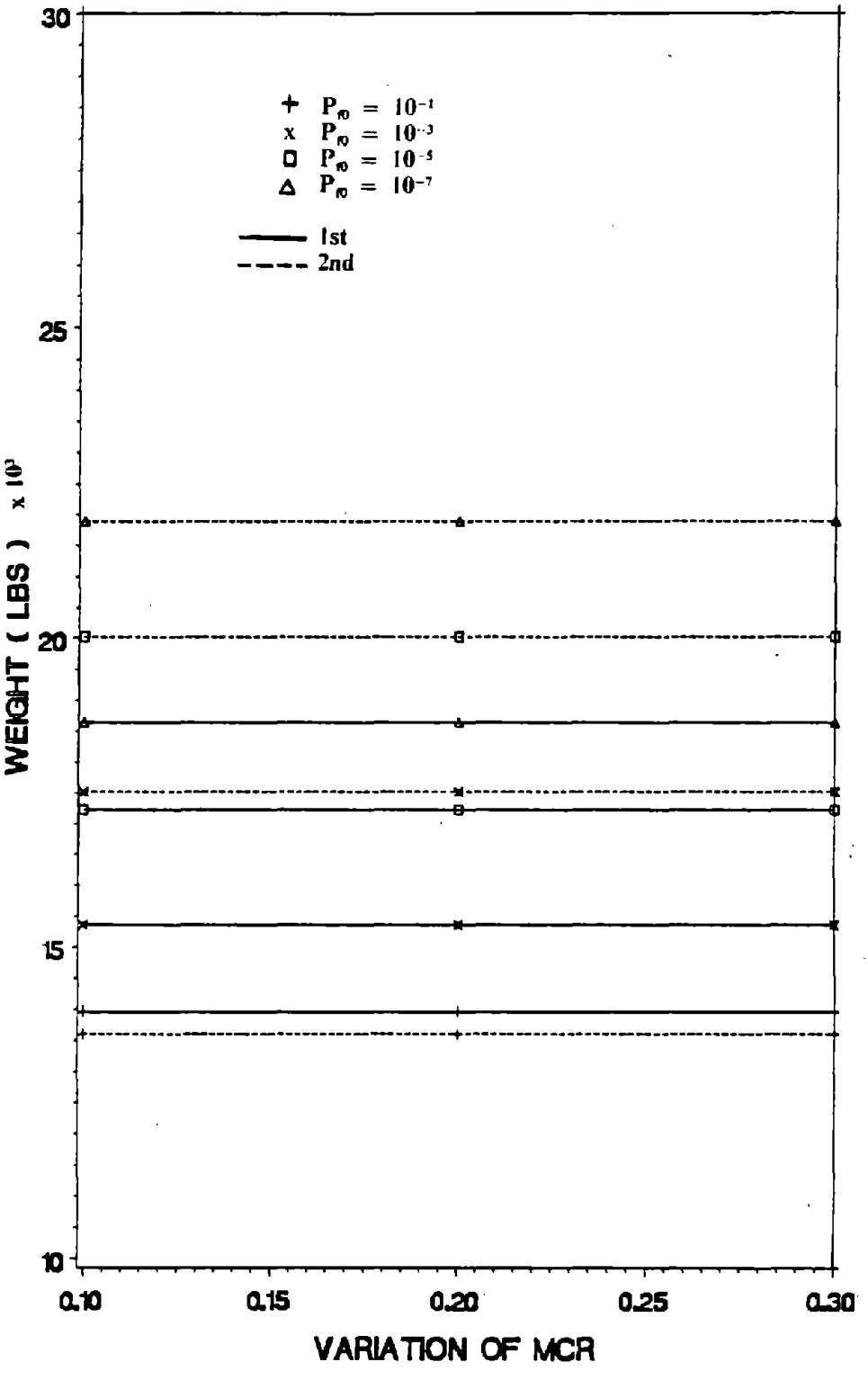

Figure 92. Optimum Weight for Various $V_{M_{cr}}$ with N of 2-Story Building. (1 lb = 4.45 N)

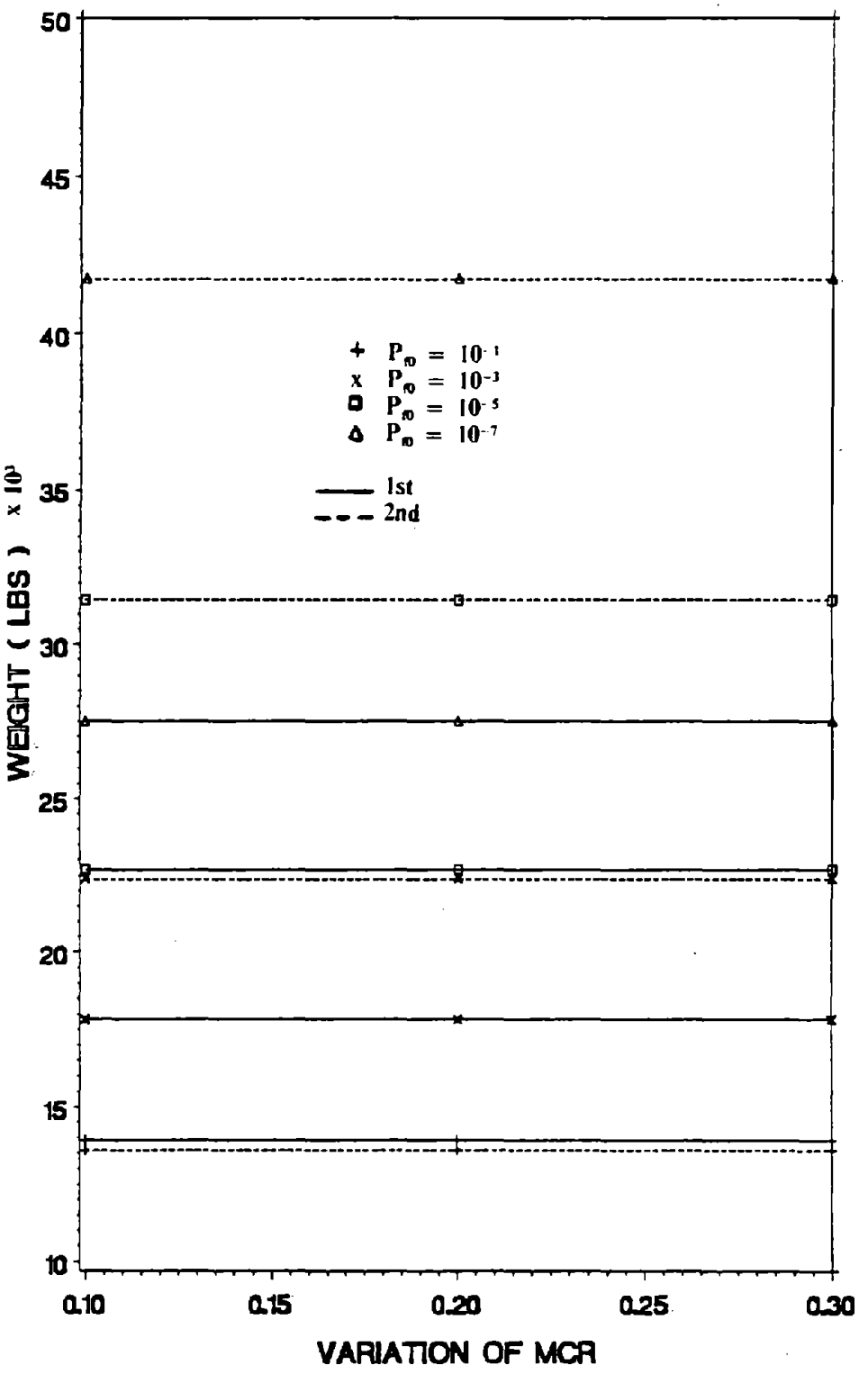

Figure 93. Optimum Weight for Various $V_{M_{cr}}$ with LN of 2-Story Building. (1 lb = 4.45 N)

$$= \sqrt{(0.1)^2 + \frac{1}{\bar{\omega}^2}\{[\frac{1}{2}(\frac{K}{M})^{-1/2}\frac{1}{M}]^2\bar{K}^2V_K^2 + [\frac{1}{2}(\frac{K}{M})^{-1/2}\frac{K}{M^2}]^2\bar{M}^2V_M^2\}}$$

$$= \sqrt{(0.1)^2 + \frac{1}{4}(V_K^2 + V_M^2)} = 0.16$$

where 0.1 is the estimation of natural frequency which may reflect the influence of non-structural elements, soil-structure interaction; $\bar{\omega}, V_\omega$ = the mean and coefficient of variation of natural frequency; V_M = the coefficient of variation of mass = 0.12; V_K = the coefficient of variation of stiffness value and is assumed to be

$$V_K = \sqrt{(0.2)^2 + V_{E_m}^2 + V_I^2} = 0.21$$

in which 0.2 is the stiffness formulation error, V_{E_m} = the coefficient of variation of elastic modulus = 0.06, V_I = the coefficient of variation of moment of inertia = 0.05. [76]

Therefore, there are three assumed values for formulation errors which are not clearly defined for 2nd variance approach. The first value, 0.2, is the stiffness formulation error. The second value, 0.1, is the natural frequency formulation error. The third is a value of 0.15, C_f, in Equation (4.37) which is a coefficient of variation of dynamic analysis error.

If the first one is excluded,the coefficient of variation of stiffness becomes

$$V_K = \sqrt{V_{E_m}^2 + V_I^2} = 0.08.$$

If the second one is also excluded,the coefficient of variation of natural frequency is given to be

$$V_\omega = \{\frac{1}{4}(V_K^2 + V_M^2)\}^{1/2} = 0.072.$$

In addition to the recommended values of 0.16 for the coefficient of variation of natural frequency and 0.15 for the coefficient of variation of dynamic analysis error, C_f, two other assumed values for the 2nd variance approach can be used to see the comparison of the 1st and 2nd variance approach. One assumes the value of 0.072 for the coefficient of variation of natural frequency and zero value for the dynamic analysis error. The other assumes the zero value for the coefficient of variation of natural frequency and 0.15 for the coefficient of variation of dynamic analysis error.

The optimum weights in Figures 94 and 96, and the moments of inertia in Figures 95 and 97 reveal that the 1st variance approach is close to the 2nd variance approach with $V_\omega = 0.072$ and $C_E = 0$, and the 2nd variance approach with $V_\omega = 0$ and $C_E = 0.15$ at low reliability with normal and lognormal distributions. When reliability increases, the differences among them increase. The 2nd variance approach with $V_\omega = 0.16$ and $C_E = 0.15$ has the largest optimum design results.

C. SENSITIVITY OF VARIATION OF PEAK GROUND ACCELERATION.

Similar to the assumption of variation of UBC load, the peak ground acceleration can be assumed to follow a type II extreme distribution. Equation (3.18) can still be applied to compute the coefficient of variation of peak ground acceleration. Since the exact value of this coefficient is difficult to determine, the various values of coefficient of variation of peak ground acceleration from zero to 1.38 are used to investigate the sensitivity of this coefficient. The optimum weights in Figures 98 and 100, and the moments of inertia in Figures 99 and 101 show that results with lognormal distribution increase faster than those with normal distribution when the variation of peak ground acceleration increases. The optimum weights for variations of peak ground acceleration from 0 to 1.38 with 2nd variance approach and normal distribution are from 14.754 kips (65.655 kN) to 19.859 kips (88.374 kN) at $P_{f0} = 10^{-1}$ and from 21.891 kips (97.417 kN) to 40.639 kips (180.847 kN) at $P_{f0} = 10^{-7}$. The optimum weights for variations of peak ground acceleration from 0 to 1.38 with 2nd variance approach and lognormal distribution are from 14.751 kips (65.641 kN) to 17.375 kips (77.318 kN) at $P_{f0} = 10^{-1}$ and from 41.754 kips (185.807 kN) to 154.808 kips (688.895 kN) at $P_{f0} = 10^{-7}$.

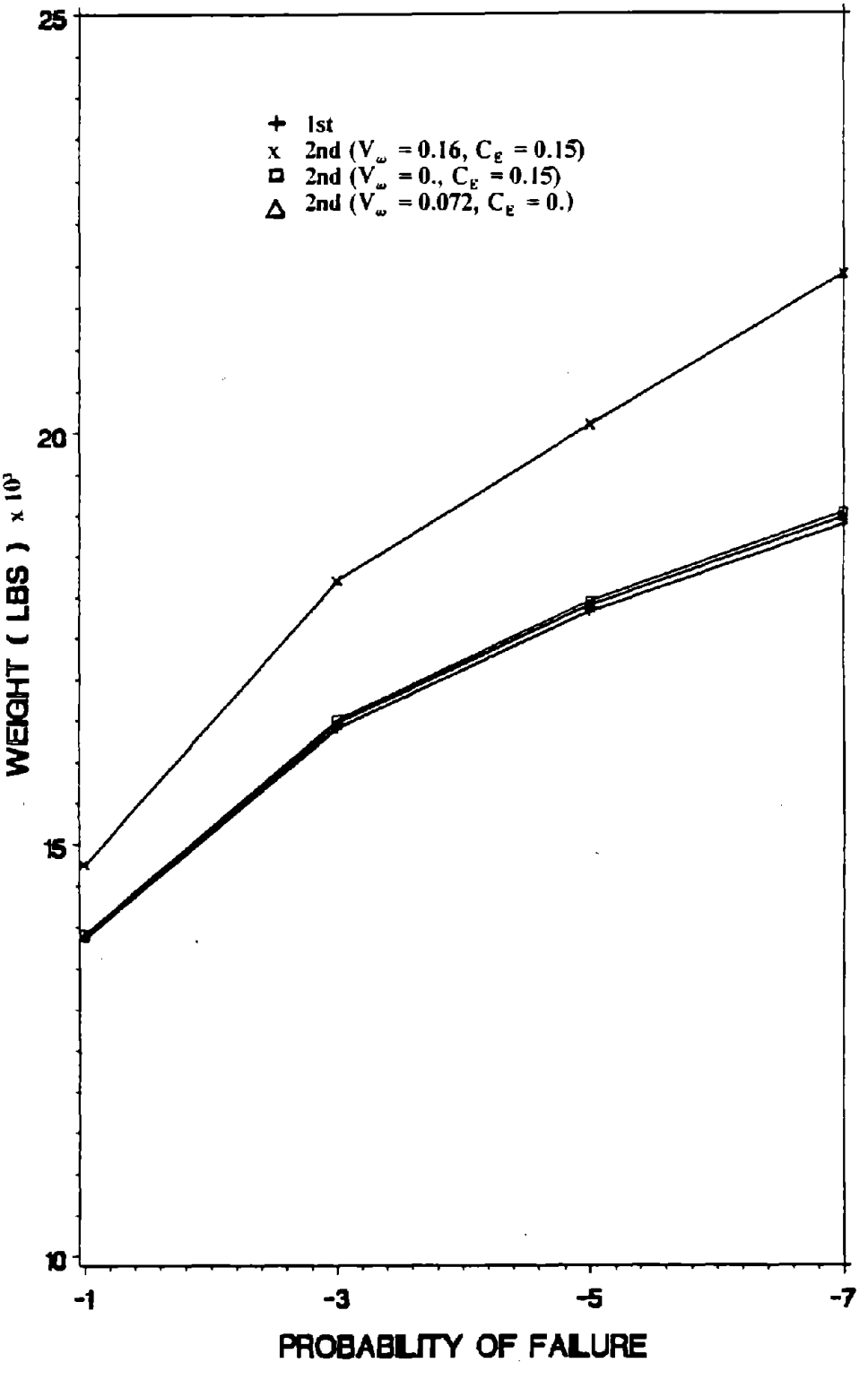

Figure 94. Optimum Weight for Various Variance Expressions with N of 2-Story Building. (1 lb = 4.45 N)

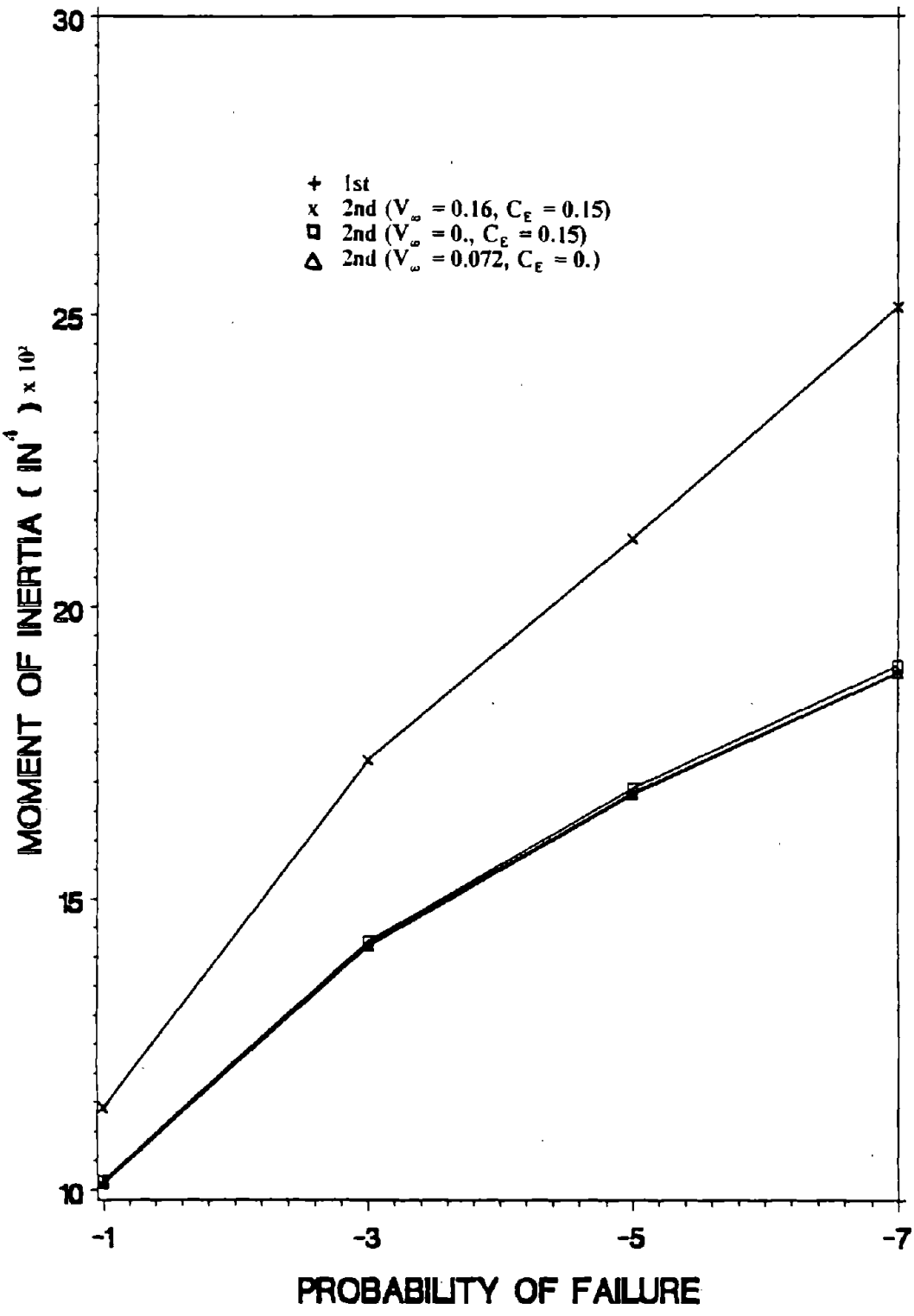

Figure 95. I_1 for Various Variance Expressions with N of 2-Story Building. (1 in = 2.54 cm)

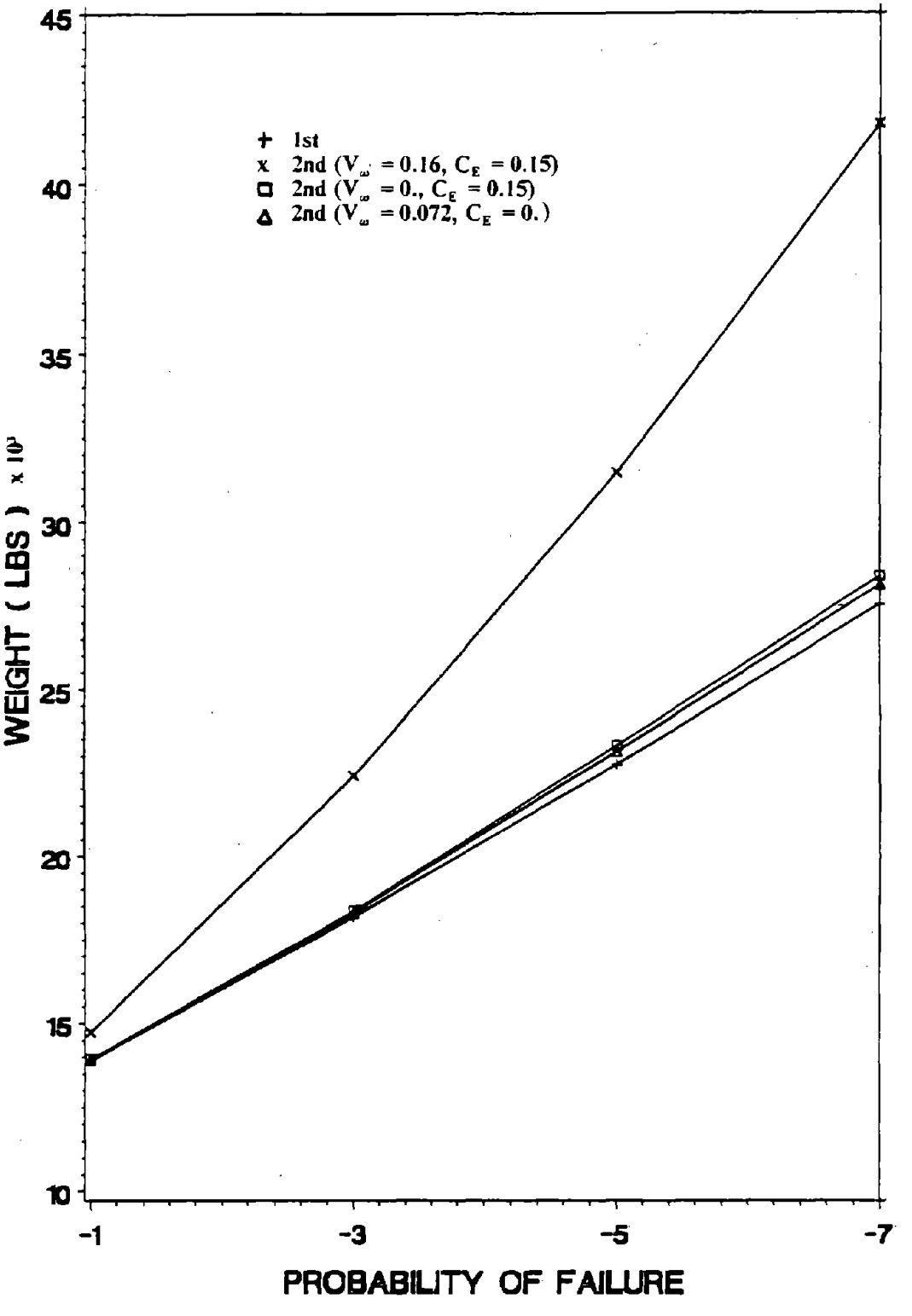

Figure 96. Optimum Weight for Various Variance Expressions with LN of 2-Story Building. (1 lb = 4.45 N)

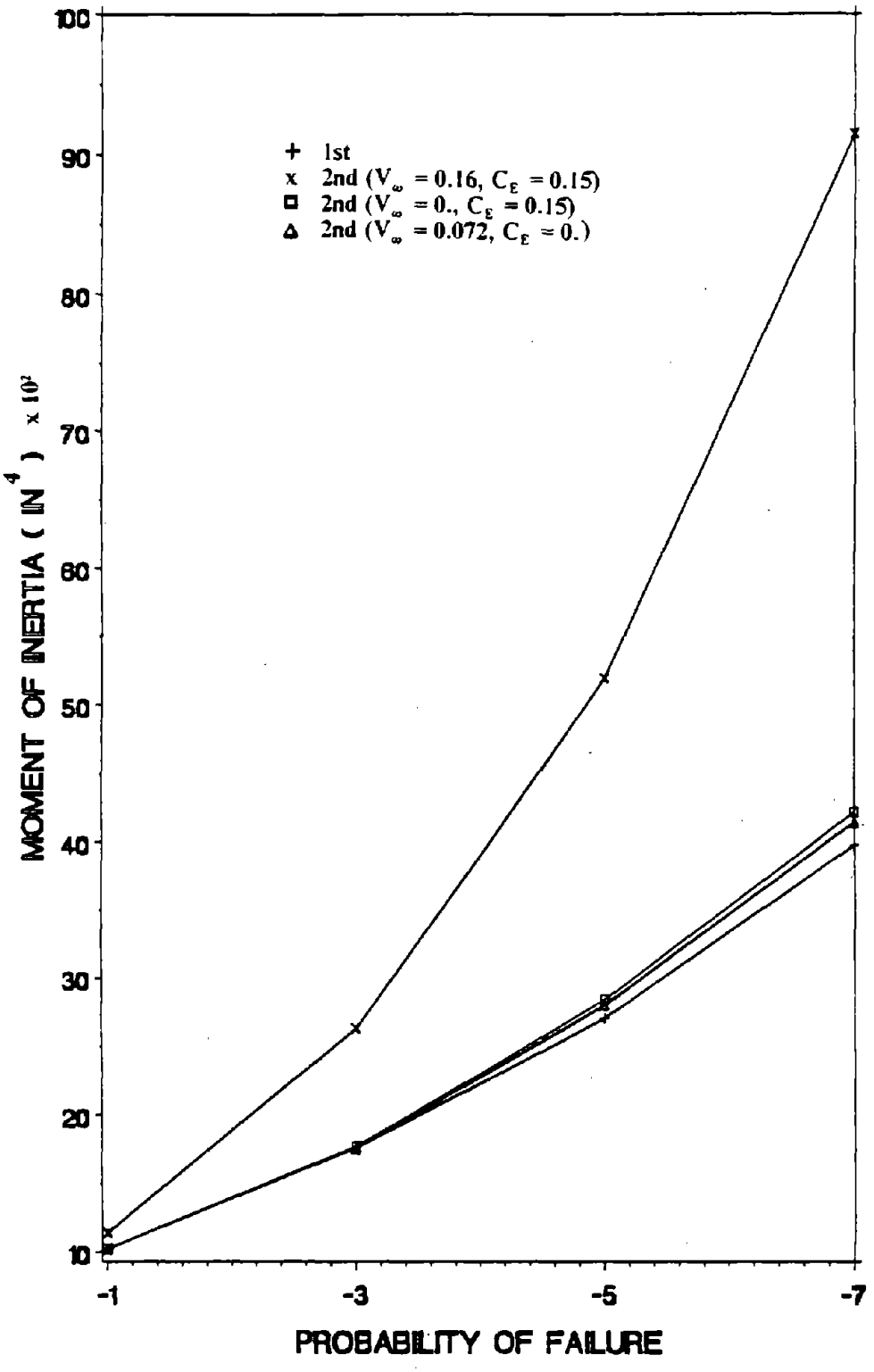

Figure 97. I_1 for Various Variance Expressions with LN of 2-Story Building. (1 in = 2.54 cm)

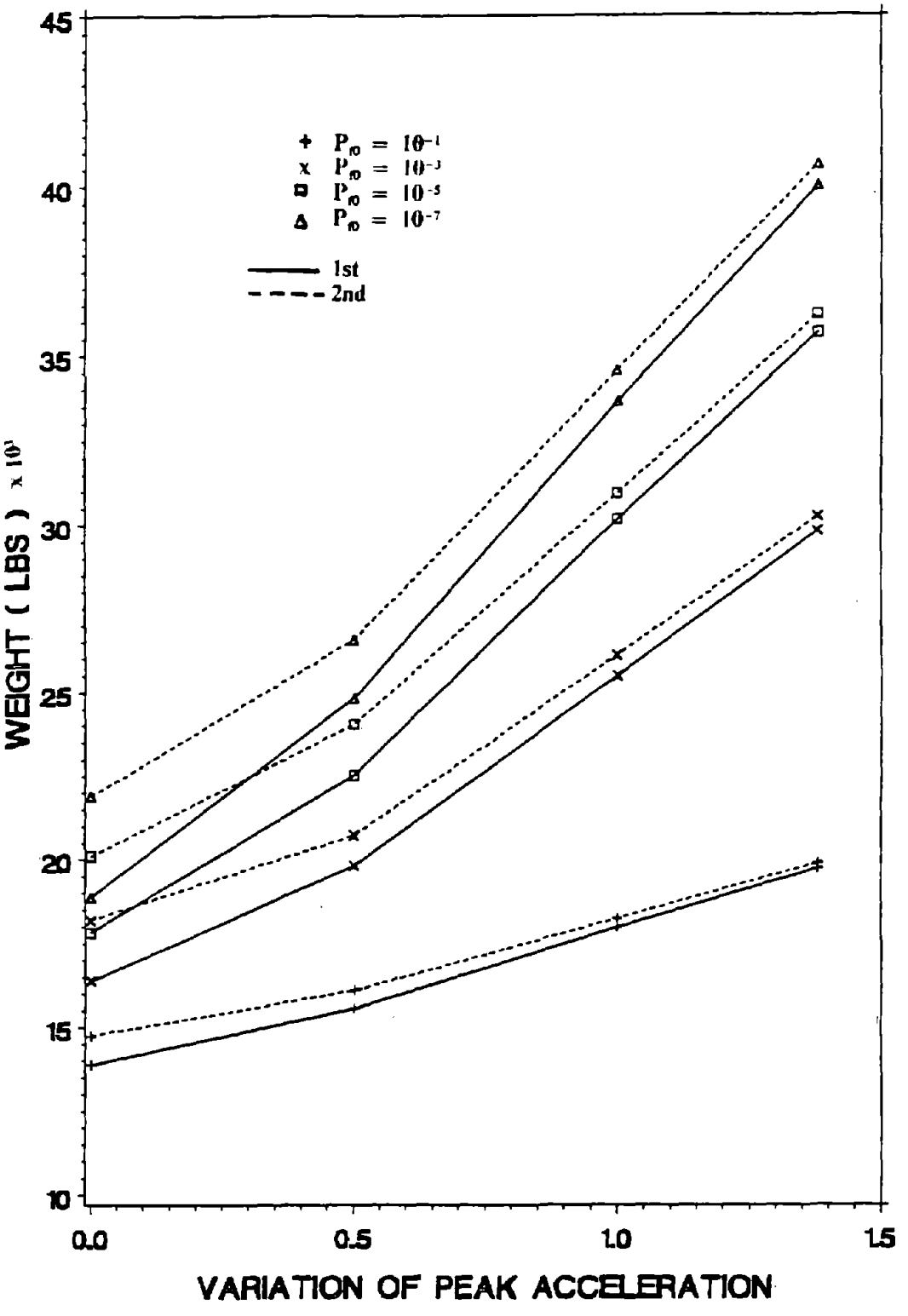

Figure 98. Optimum Weight for Variation of Peak Acceleration with N of 2-Story Building. (1 lb = 4.45 N)

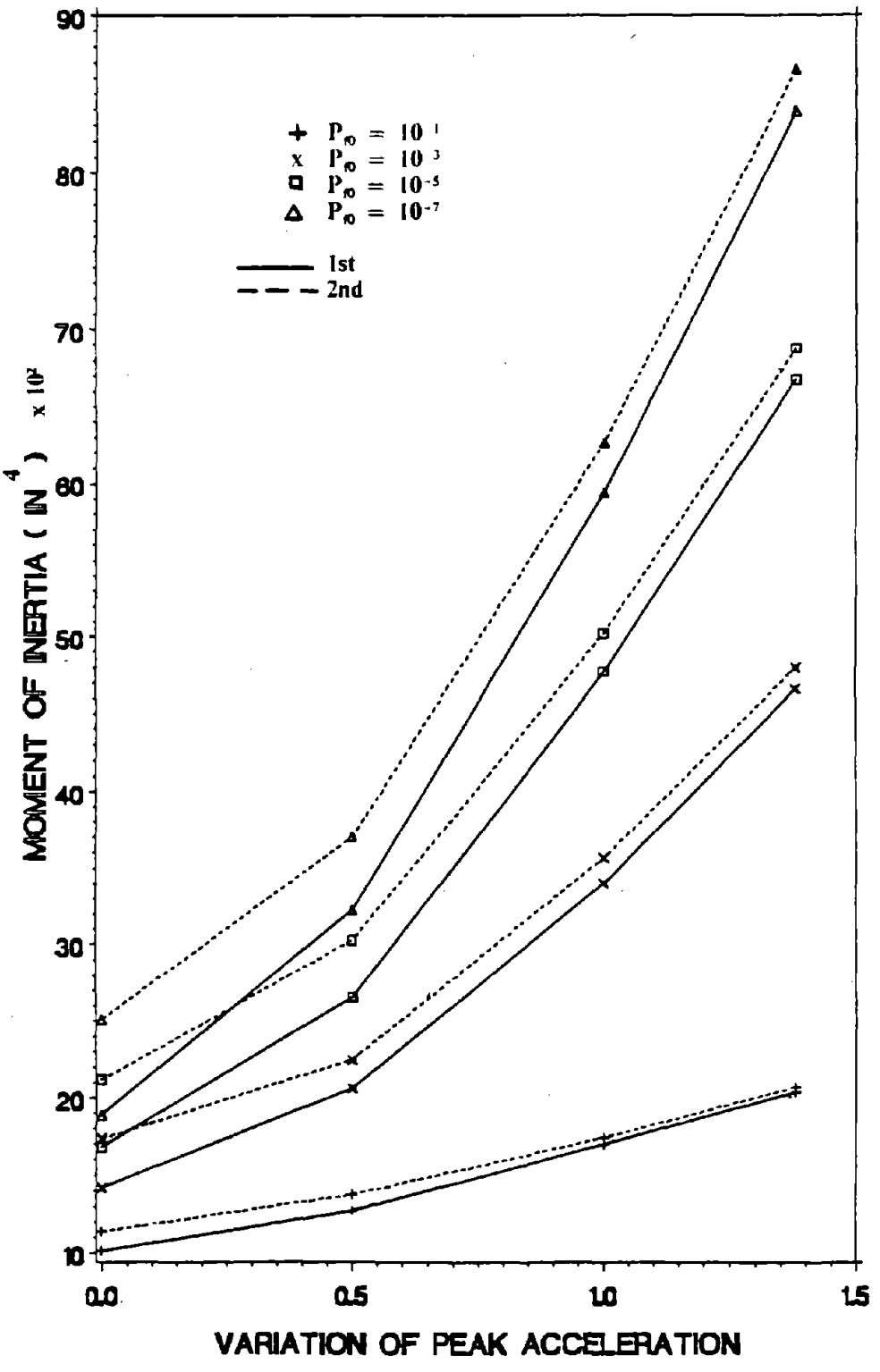

Figure 99. I_1 for Variation of Peak Acceleration with N of 2-Story Building. (1 in = 2.54 cm)

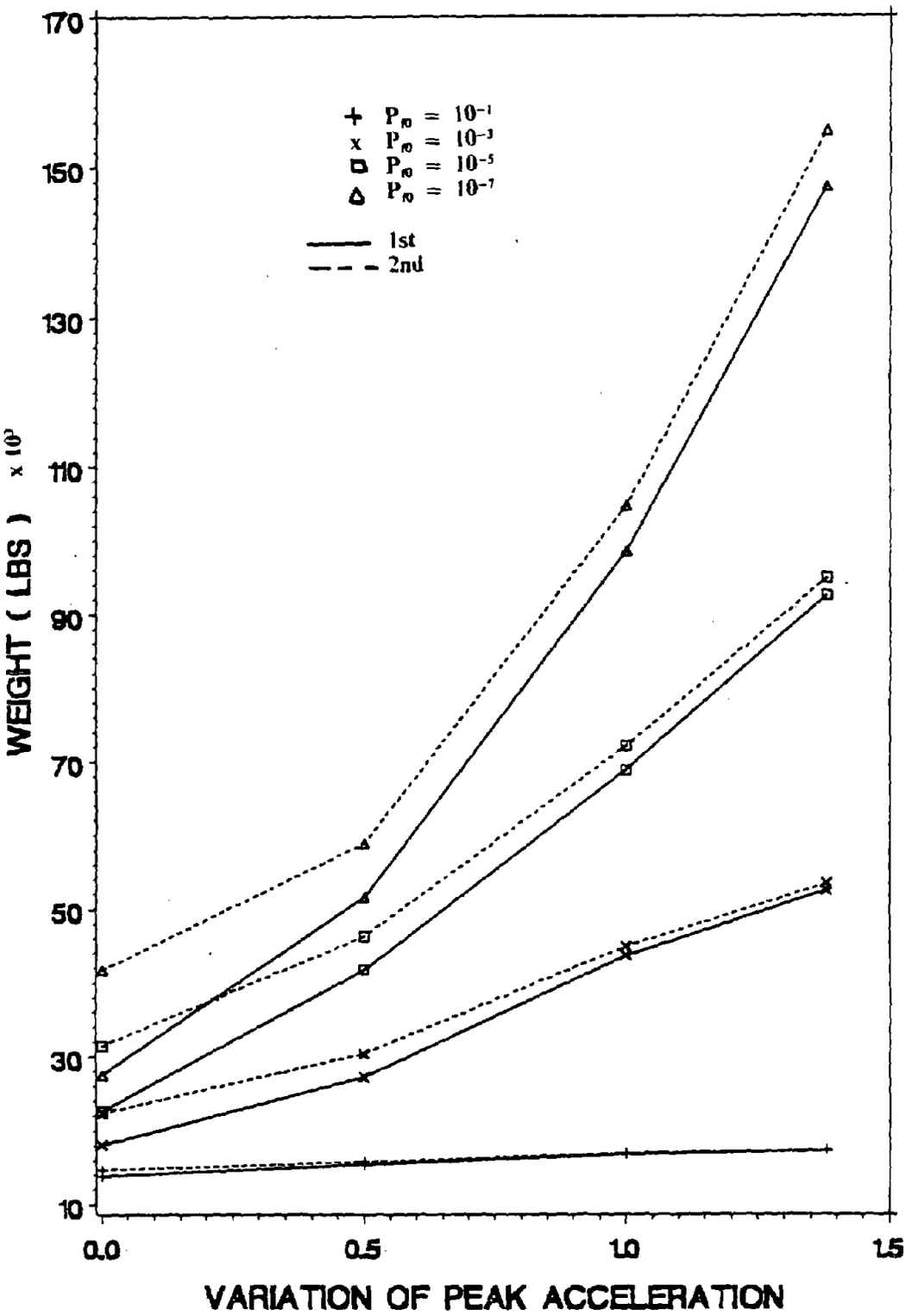

Figure 100. Optimum Weight for Variation of Peak Acceleration with LN of 2-Story Building. (1 lb = 4.45 N)

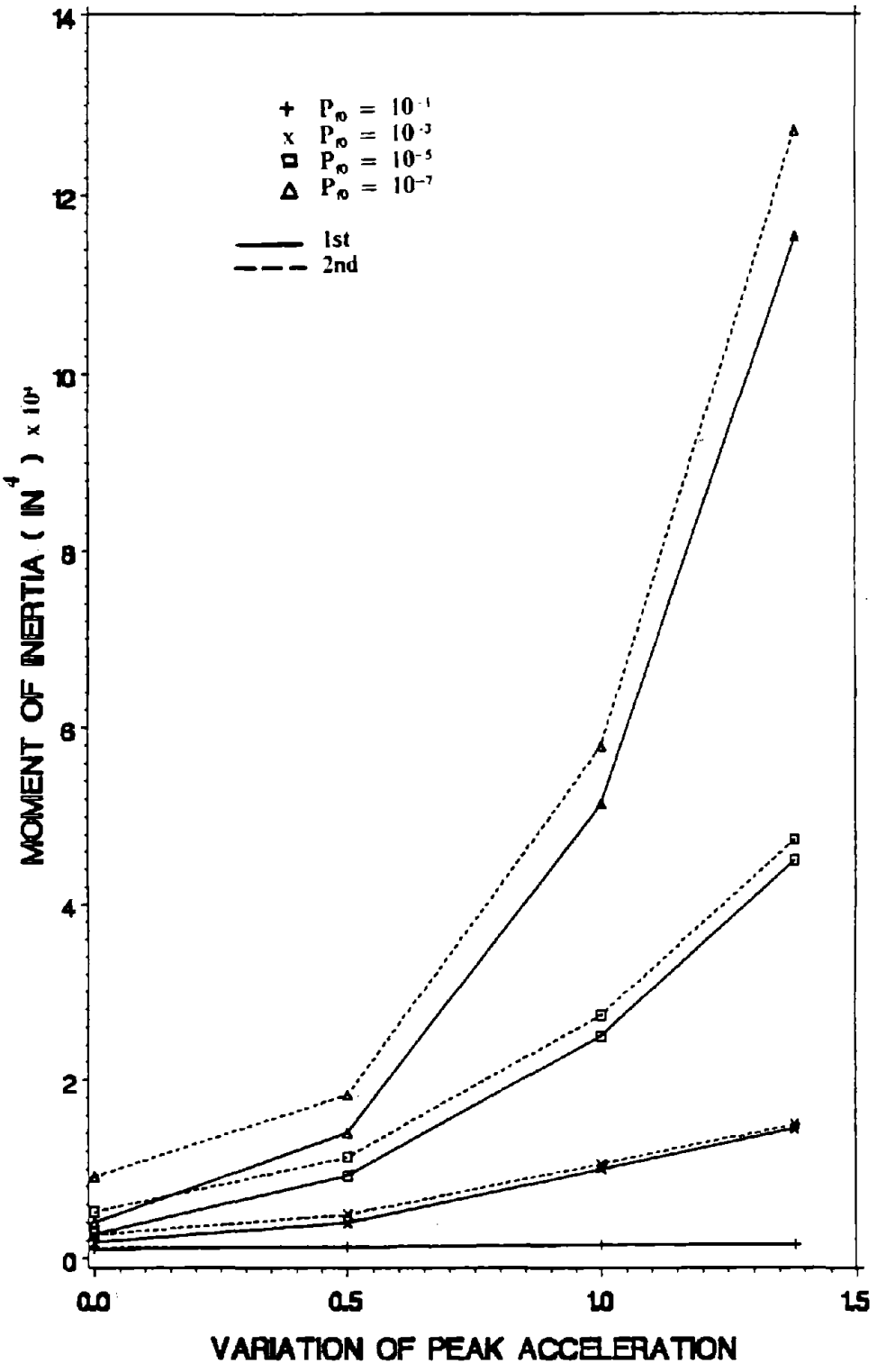

Figure 101. I_1 for Variation of Peak Acceleration with LN of 2-Story Building. (1 in = 2.54 cm)

D. COMPARISON OF RESPONSES DUE TO HORIZONTAL AND HORIZONTAL-COUPLED-WITH-VERTICAL GROUND ACCELERATIONS.

The earthquake forces are three dimensional in nature, they are two from the horizontal and one from vertical directions. However, due to complexity in analysis, the vertical acceleration is sometimes neglected in design. In this section the influence of this vertical earthquake force is studied. The relationship between area and moment of inertia, section modulus and moment of inertia are used as [33]

$I_x < 9000$,

$A = 0.465\sqrt{I_x}$; $\quad \frac{\partial A}{\partial I_x} = 0.2325\, I_x^{-1/2}$

$S = \sqrt{60.6I_x + 84100} - 290$; $\quad \frac{\partial S}{\partial I_x} = \frac{1}{2}(60.6I_x + 84100)^{-1/2}(60.6)$

$I_y = \frac{4}{9} I_x$

$I_x > 9000$,

$A = (I_x + 2300)/256$; $\quad \frac{\partial A}{\partial I_x} = \frac{1}{256}$

$S = (I_x - 8056.3)/1.876$; $\quad \frac{\partial S}{\partial I_x} = \frac{1}{1.876}$

$I_y = \frac{4}{9} I_x$

The ten-story shear building shown in Figure 102 has a lumped mass for each story of 0.27 k-sec^2/ in (0.47 kN-sec^2/ cm). The ratio of vertical to horizontal ground acceleration is assumed to be 4/3. When the structure is subjected to horizontal and vertical ground accelerations, the axial internal forces which are neglected in the design associated with horizontal ground accelerations only, become an additional part of the structural responses. Then the column failure modes are yielding failure (f_1), lateral buckling failure (f_2), and torsional buckling failure (f_3) for horizontal coupled with vertical ground acceleration instead of yielding failure (f_1) and torsional buckling (f_3) in horizontal ground acceleration only. The P - Δ effects due to vertical forces are not considered. The optimum solution against cycle for horizontal or combination of horizontal and vertical ground accelerations is shown in Figures 103 through 106. The notations given in the figures are H (horizontal ground acceleration) and V (vertical ground acceleration). The results for 2nd variance approach with normal distribution are

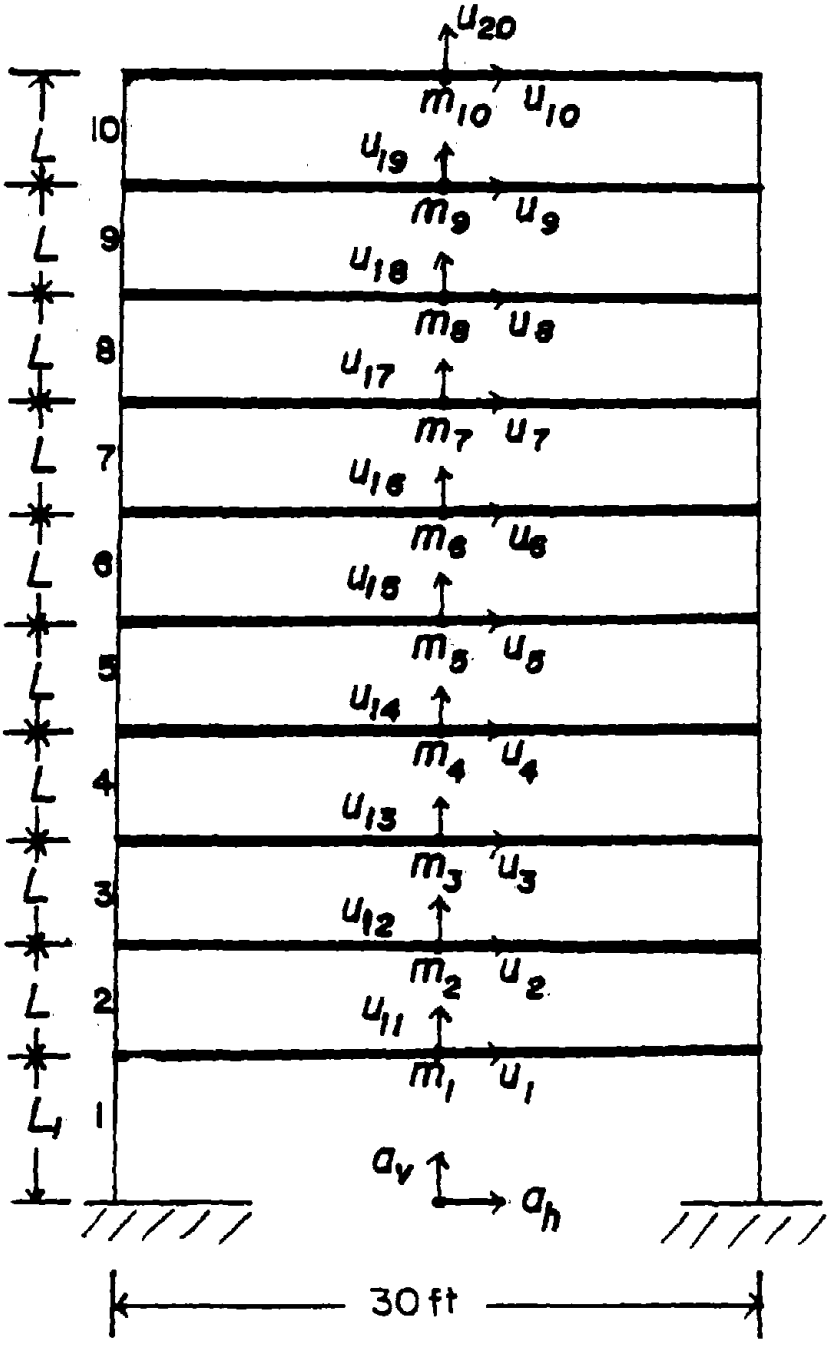

Figure 102. 10-Story Shear Building Subjected to Horizontal and Vertical Ground Acceleration. (L_1 = 15 ft, L = 12 ft, 1 ft = 30.48 cm)

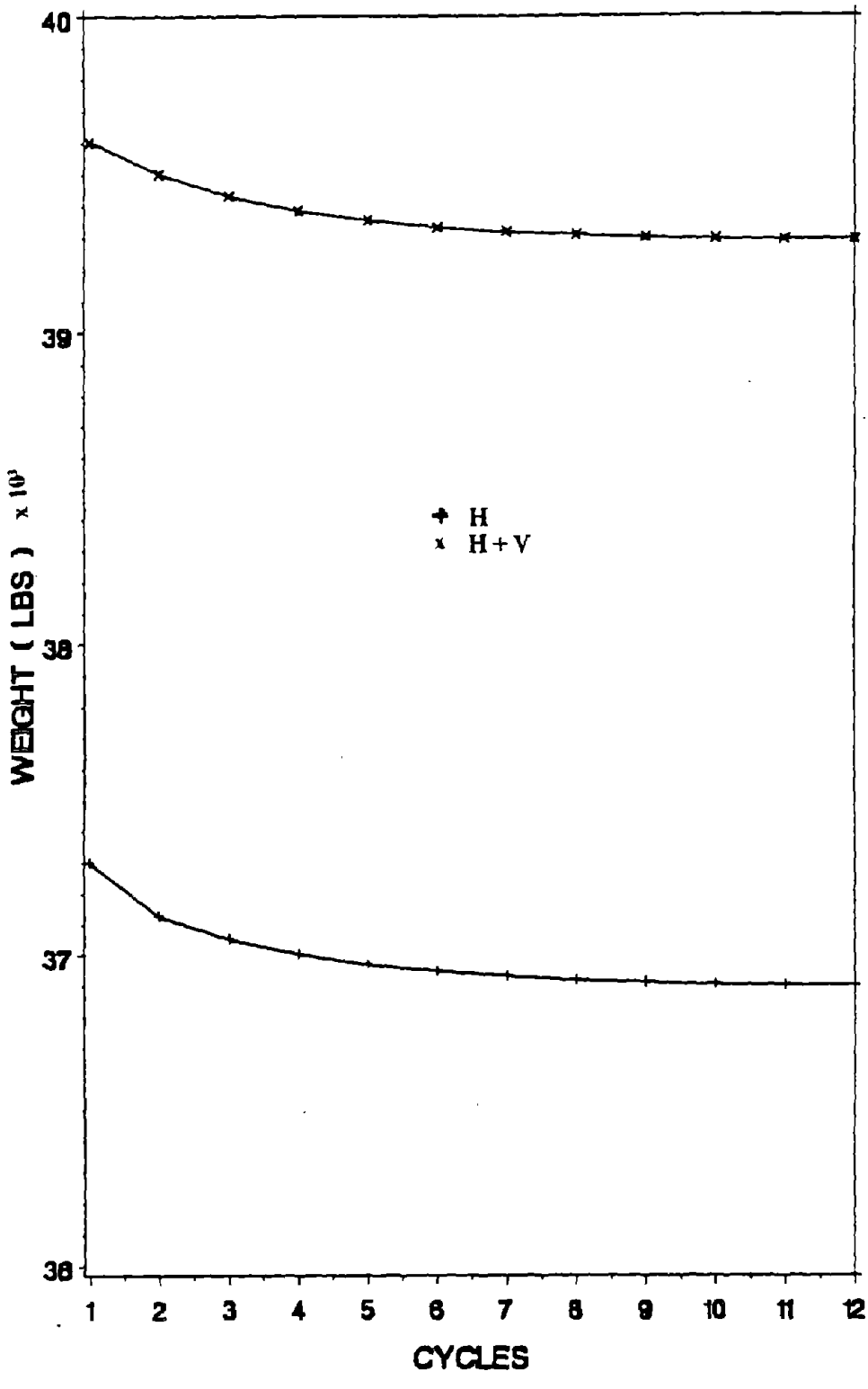

Figure 103. Optimum Weight vs Cycle with N and 2nd of 10-Story Building. (1 lb = 4.45 N)

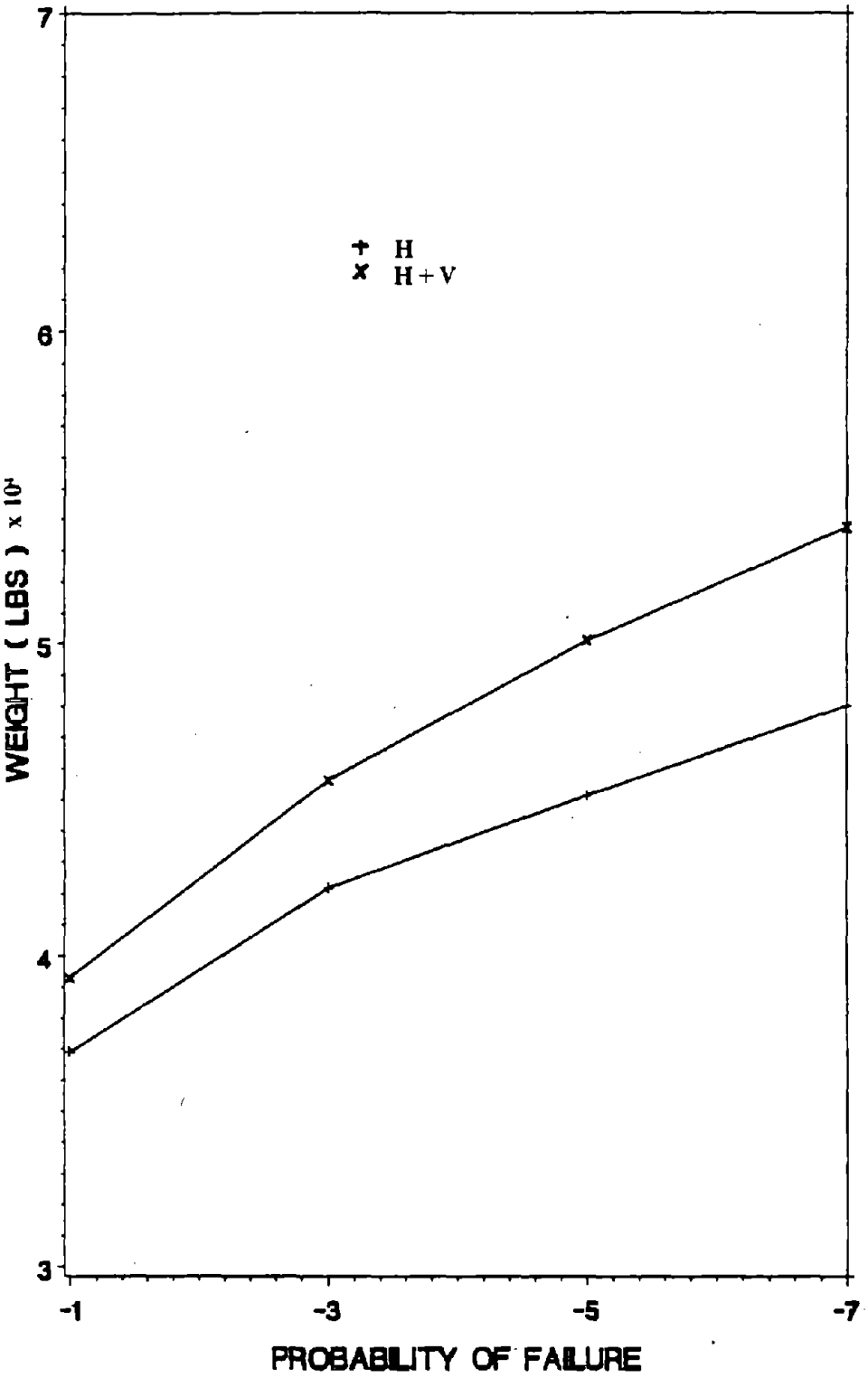

Figure 104. Optimum Weight with N and 2nd of 10-Story Building. (1 lb = 4.45 N)

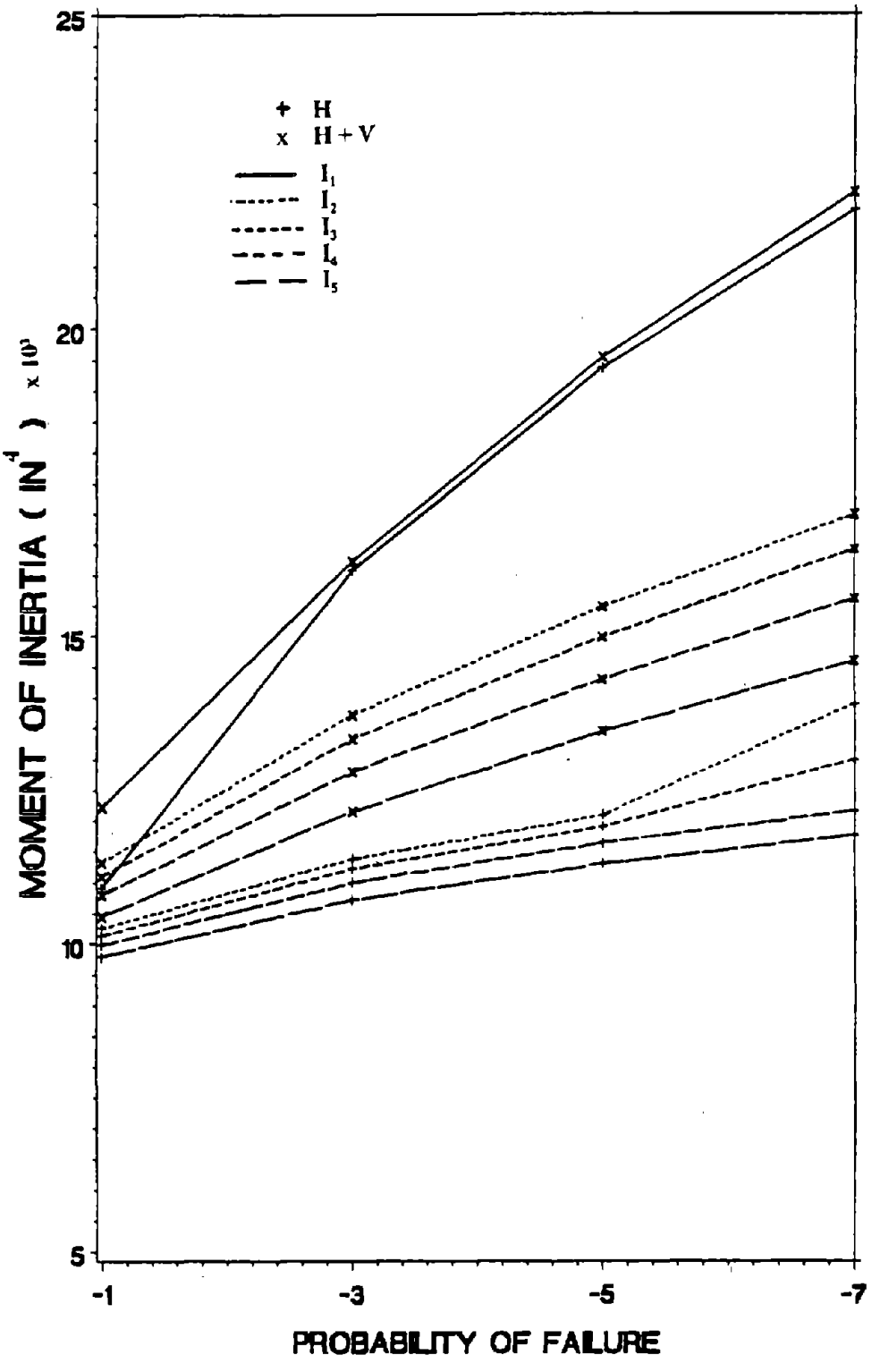

Figure 105. I_1 - I_5 with N and 2nd of 10-Story Building. (1 in = 2.54 cm)

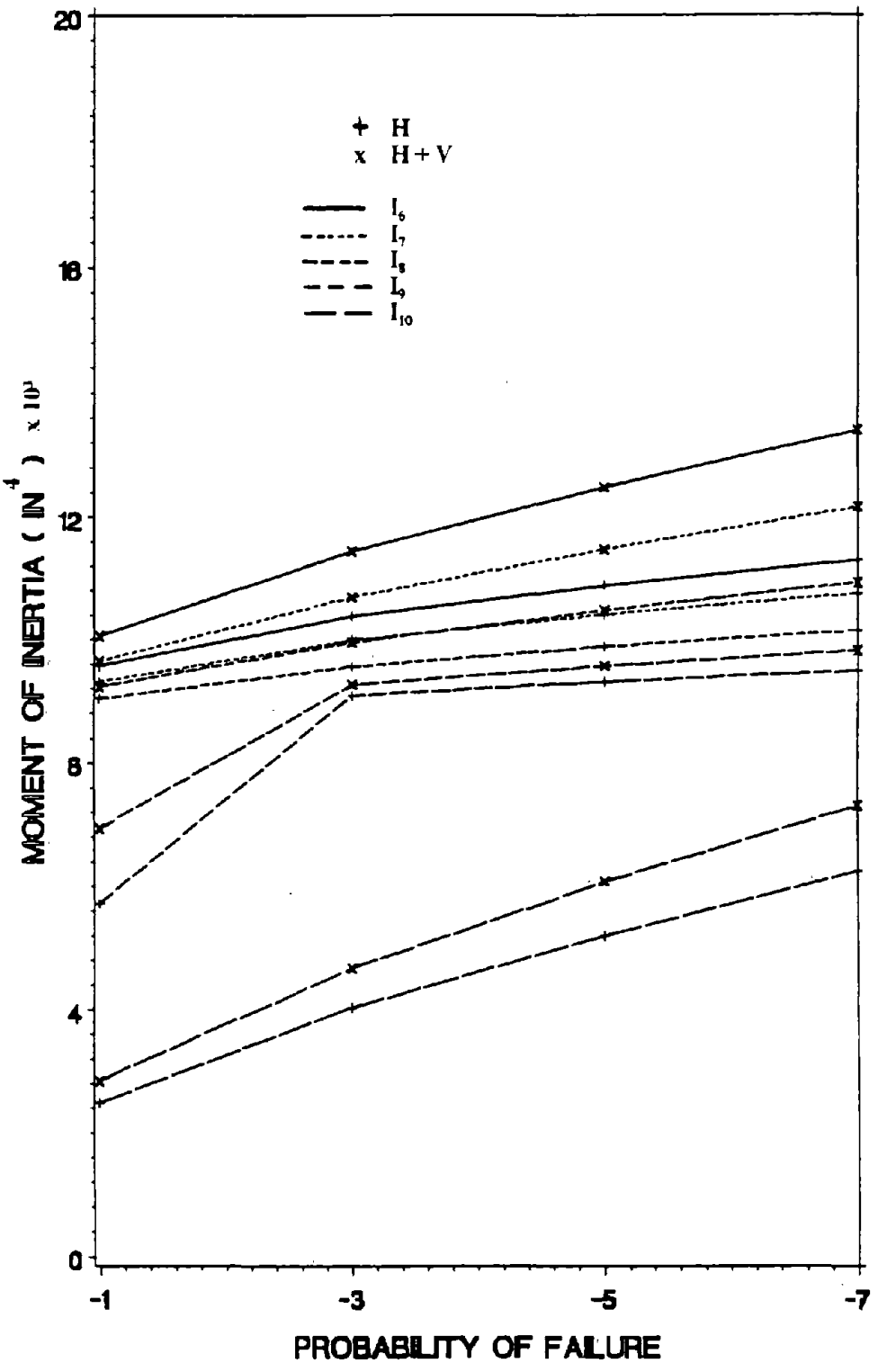

Figure 106. I_6 - I_{10} with N and 2nd of 10-Story Building. (1 in = 2.54 cm)

considered here. In Figure 104 the weight difference between horizontal and horizontal coupled with vertical ground acceleration increases with the reliability level. It shows the weight increases due to the appearance of vertical ground acceleration are 6.59 % at $P_{f0} = 10^{-1}$ and 11.07 % at $P_{f0} = 10^{-5}$. In Figures 105 and 106, the moments of inertia for combination of horizontal and vertical ground acceleration are heavier than those for horizontal ground acceleration.

The mode shapes from first to 10th modes are the horizontal vibration modes, and from 11th to 20th modes are the vertical vibration modes. In Figures 107 and 108, the natural frequencies increases with the reliability levels. The natural frequencies of the structure subjected to horizontal coupled with vertical ground acceleration are higher than those associated with the horizontal ground acceleration.

In Figures 109 and 110, the mean and variance of displacement subjected to horizontal and vertical ground acceleration are less than those subjected to horizontal ground acceleration. In Figure 111, for horizontal ground acceleration only, the active constraints are the lateral displacement at lowest level at $P_{f0} = 10^{-1}$ and $P_{f0} = 10^{-3}$, at the 1st and 2nd level at $P_{f0} = 10^{-5}$, and at 1st, 2nd, 3rd, and 4th level at $P_{f0} = 10^{-7}$. For horizontal coupled with vertical ground acceleration, the active constraints are the lateral displacements at the 1st level at $P_{f0} = 10^{-1}$ to 10^{-7}. The reason for active constraints at the lower levels is that the differences between allowable and actual displacements at lower levels are smaller than those at higher levels.

In Figures 112 and 113, the mean values of interaction equations for horizontal and vertical ground acceleration are higher than those for horizontal ground acceleration at $P_{f0} = 10^{-3}$. However, the variance values for f_1 are in reverse order. In Figure 114, the active constraints at $P_{f0} = 10^{-3}$ are f_1 of column 2 to column 10 for horizontal ground acceleration, f_1 of column 10 and f_2 of column 2 to column 10 for combination of horizontal and vertical ground acceleration.

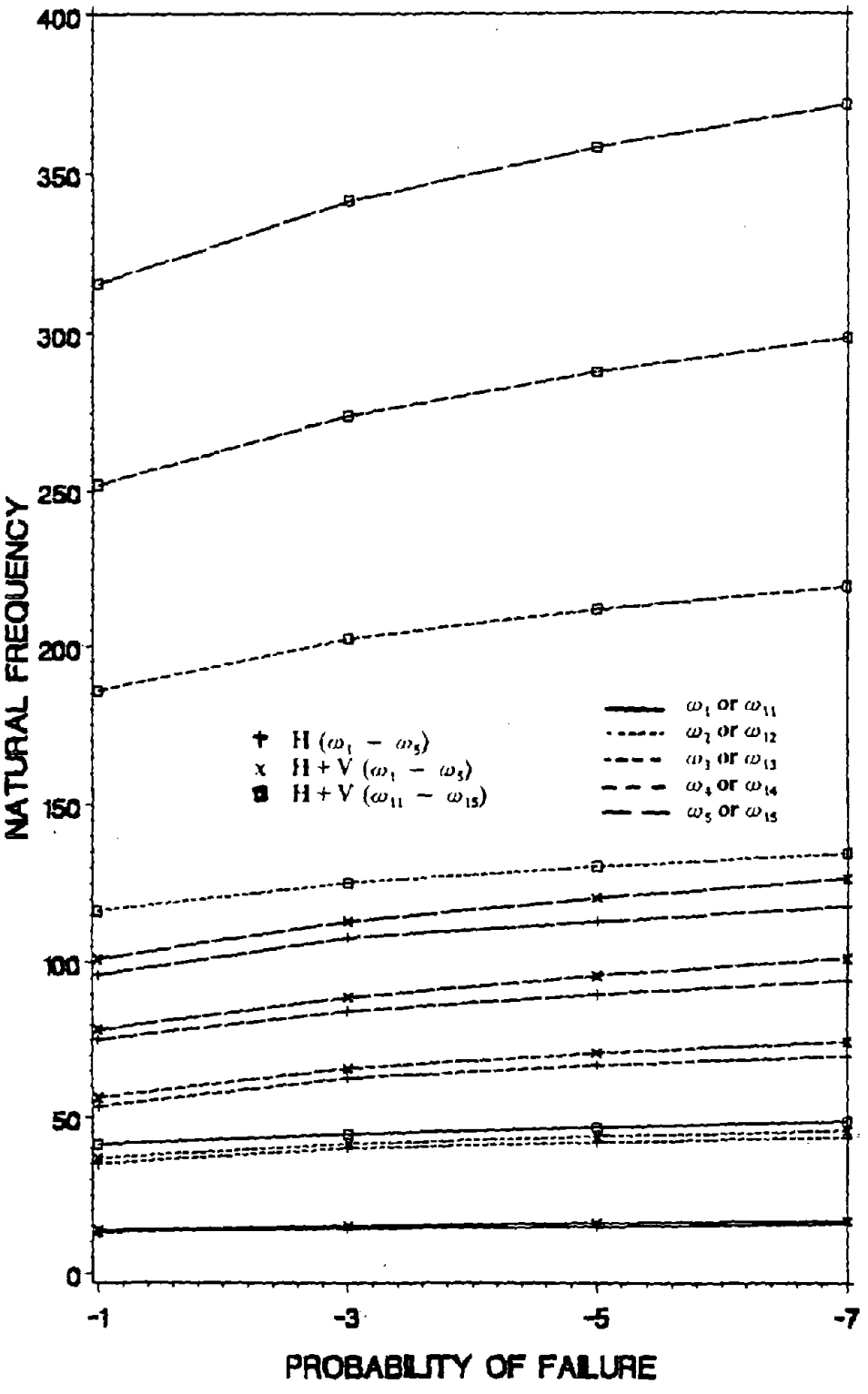

Figure 107. ω_1 - ω_5 with N and 2nd of 10-Story Building.

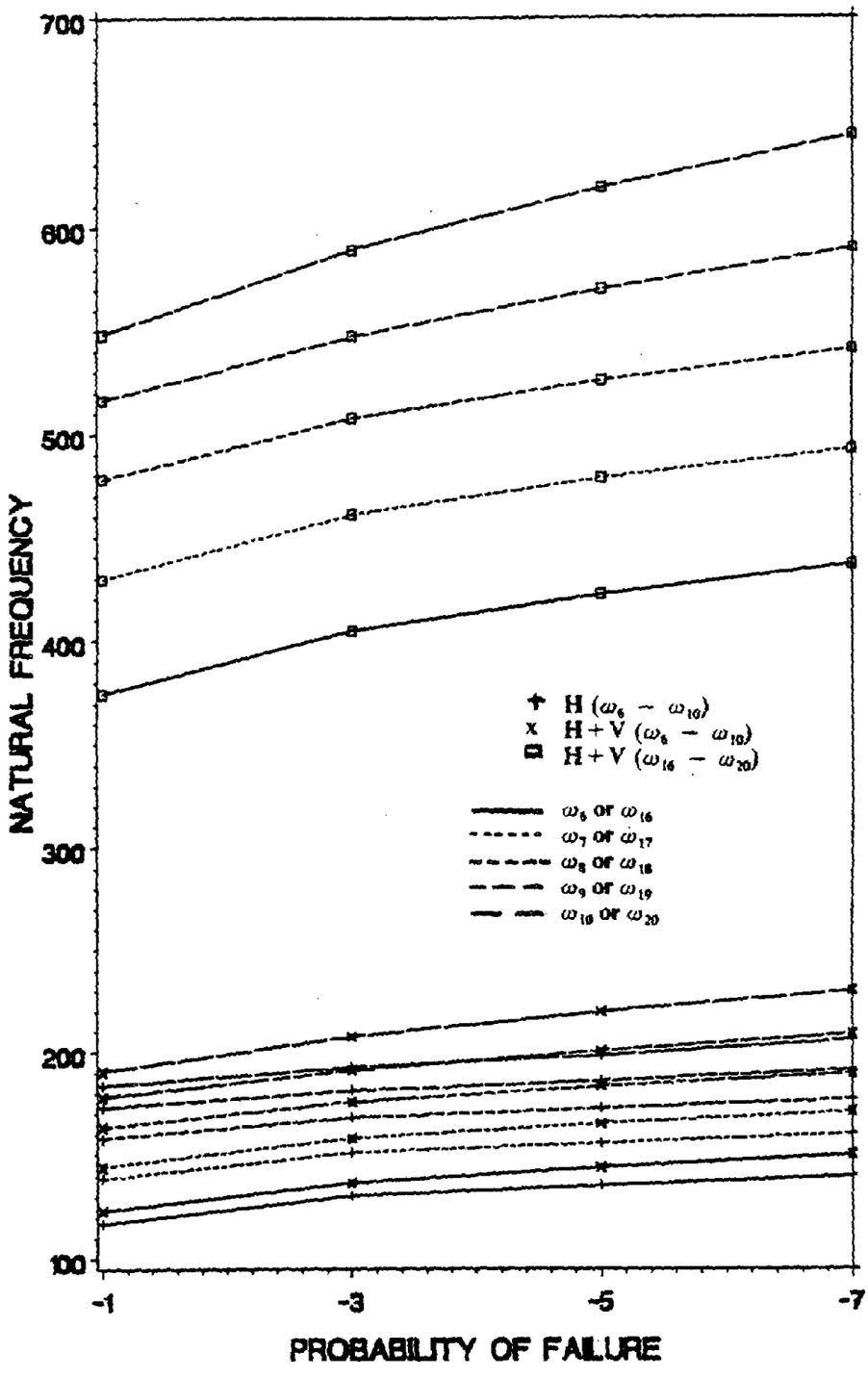

Figure 108. ω_6 - ω_{10} with N and 2nd of 10-Story Building.

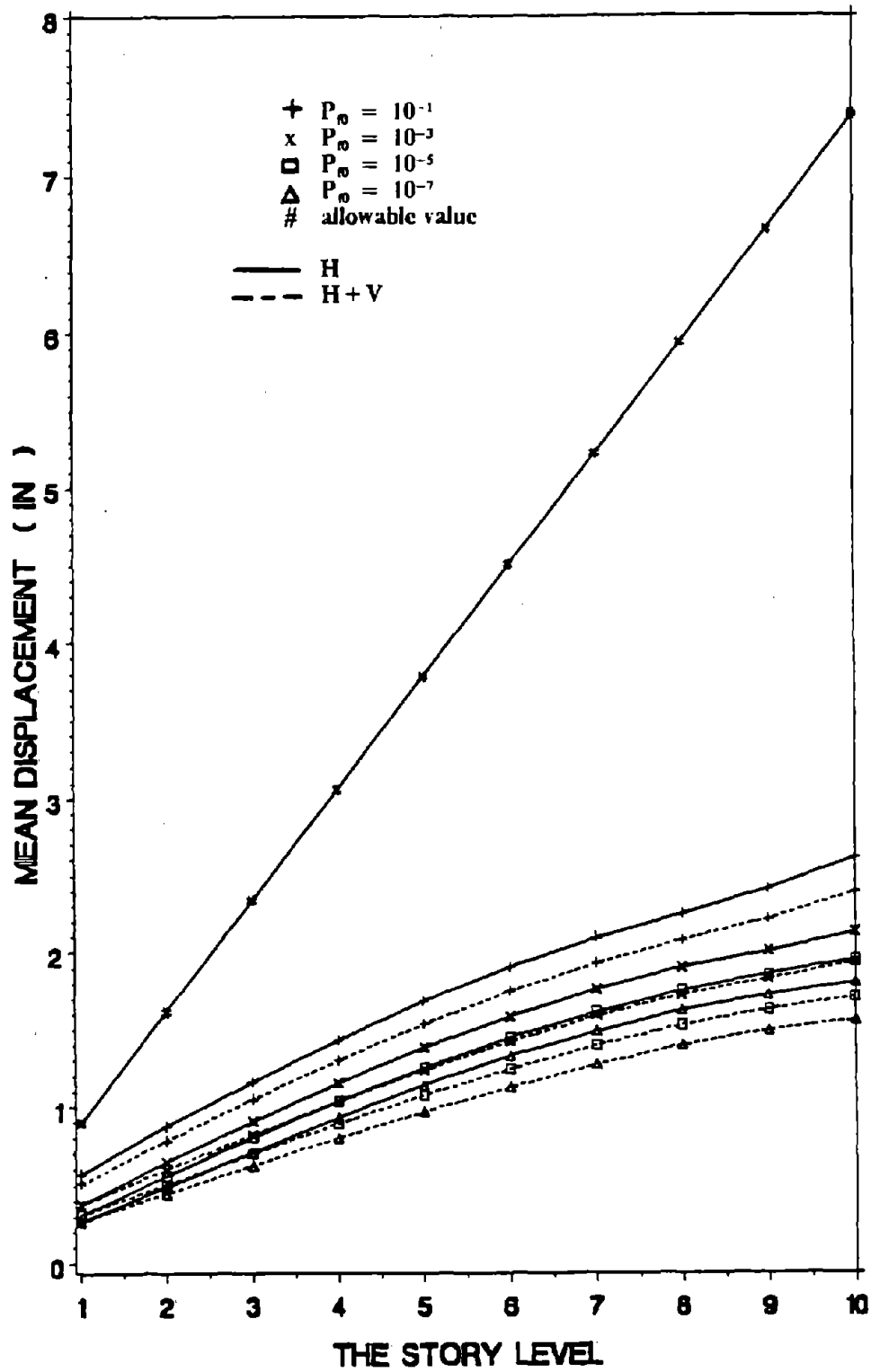

Figure 109. Mean Displacement with N and 2nd of 10-Story Building. (1 in = 2.54 cm)

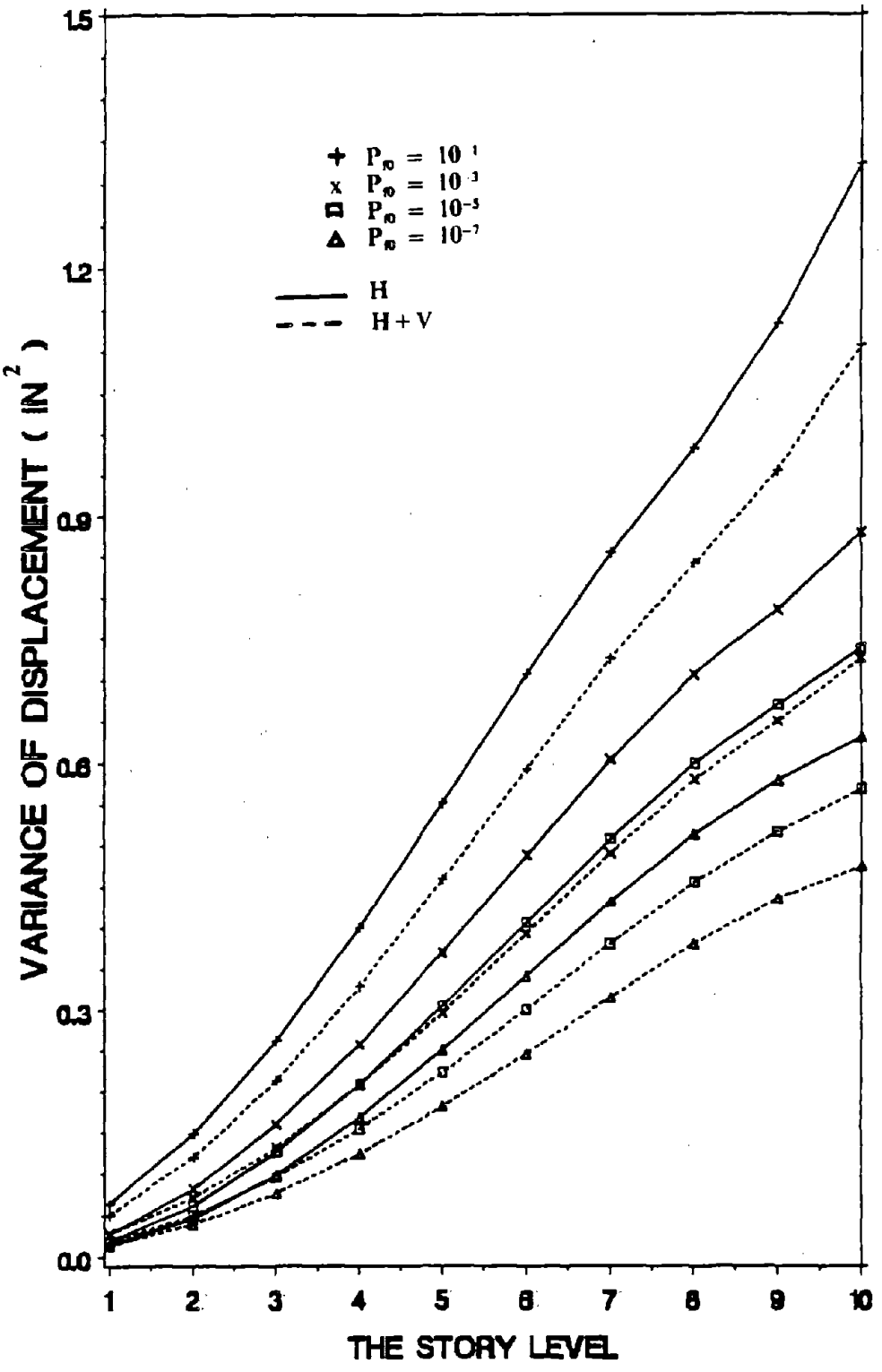

Figure 110. Variance of Displacement with N and 2nd of 10-Story Building. (1 in = 2.54 cm)

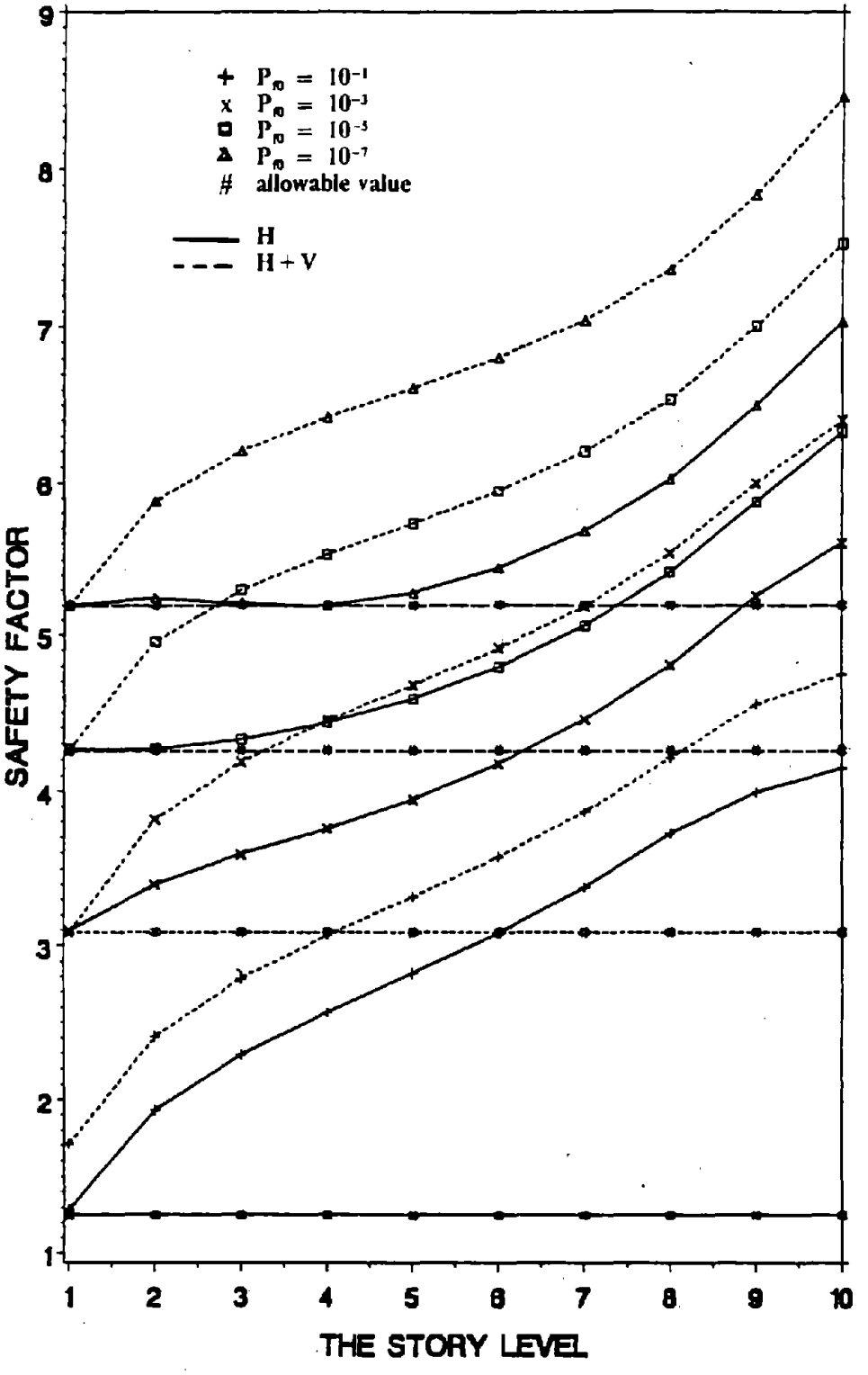

Figure 111. Safety Factor of Displacement with N and 2nd of 10-Story Building.

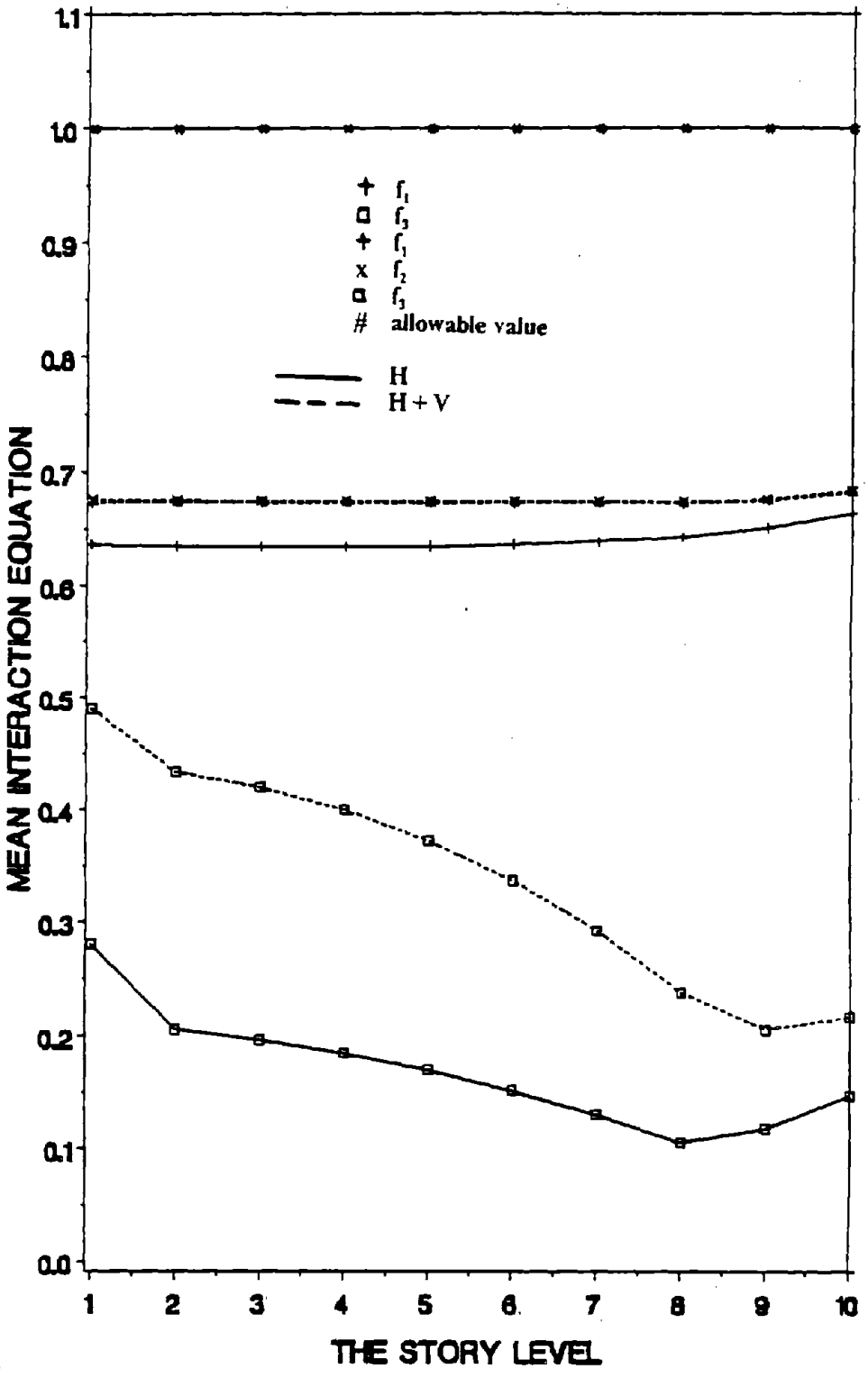

Figure 112. Mean Interaction Equation with N and 2nd of 10-Story Building.

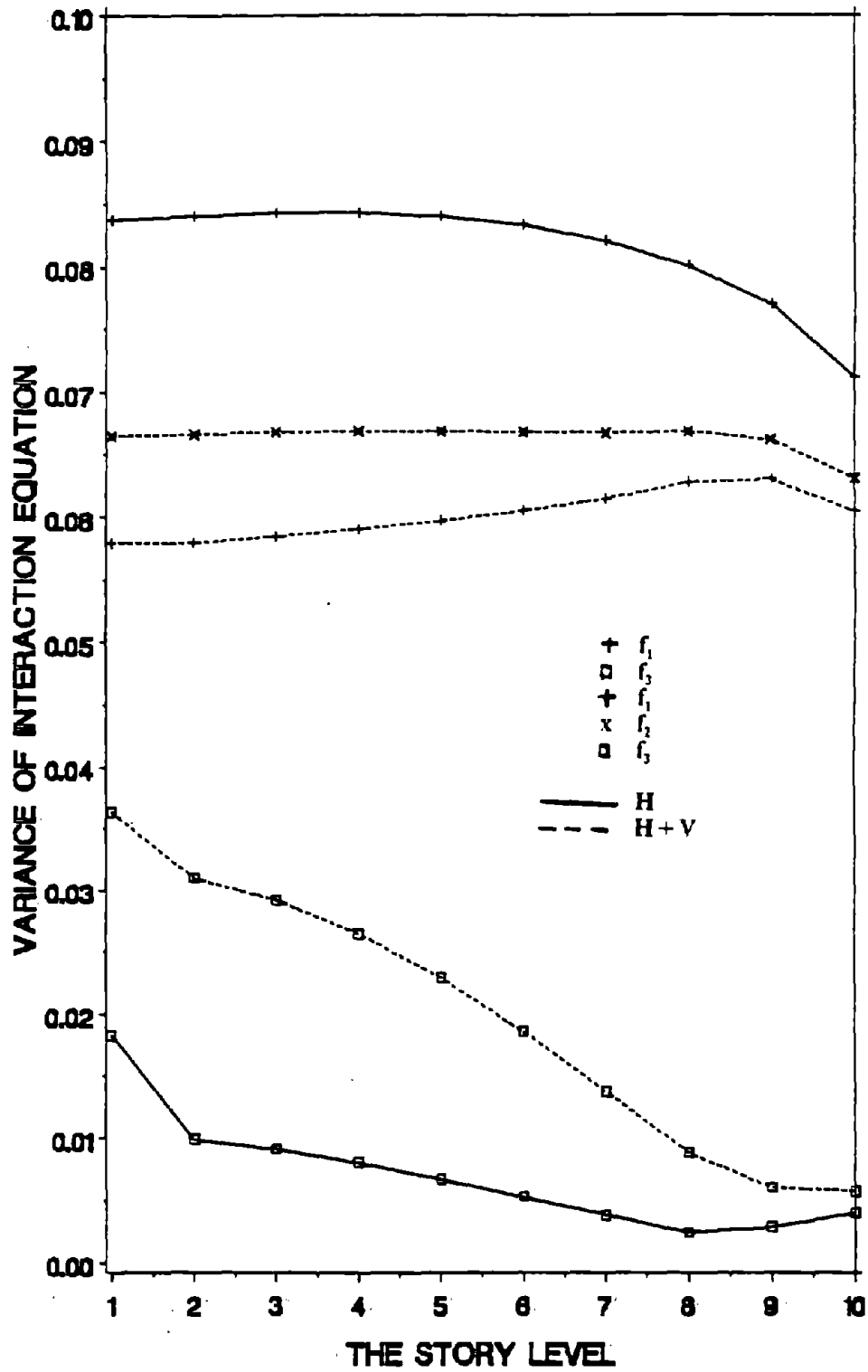

Figure 113. Variance of Interaction Equation with N and 2nd of 10-Story Building.

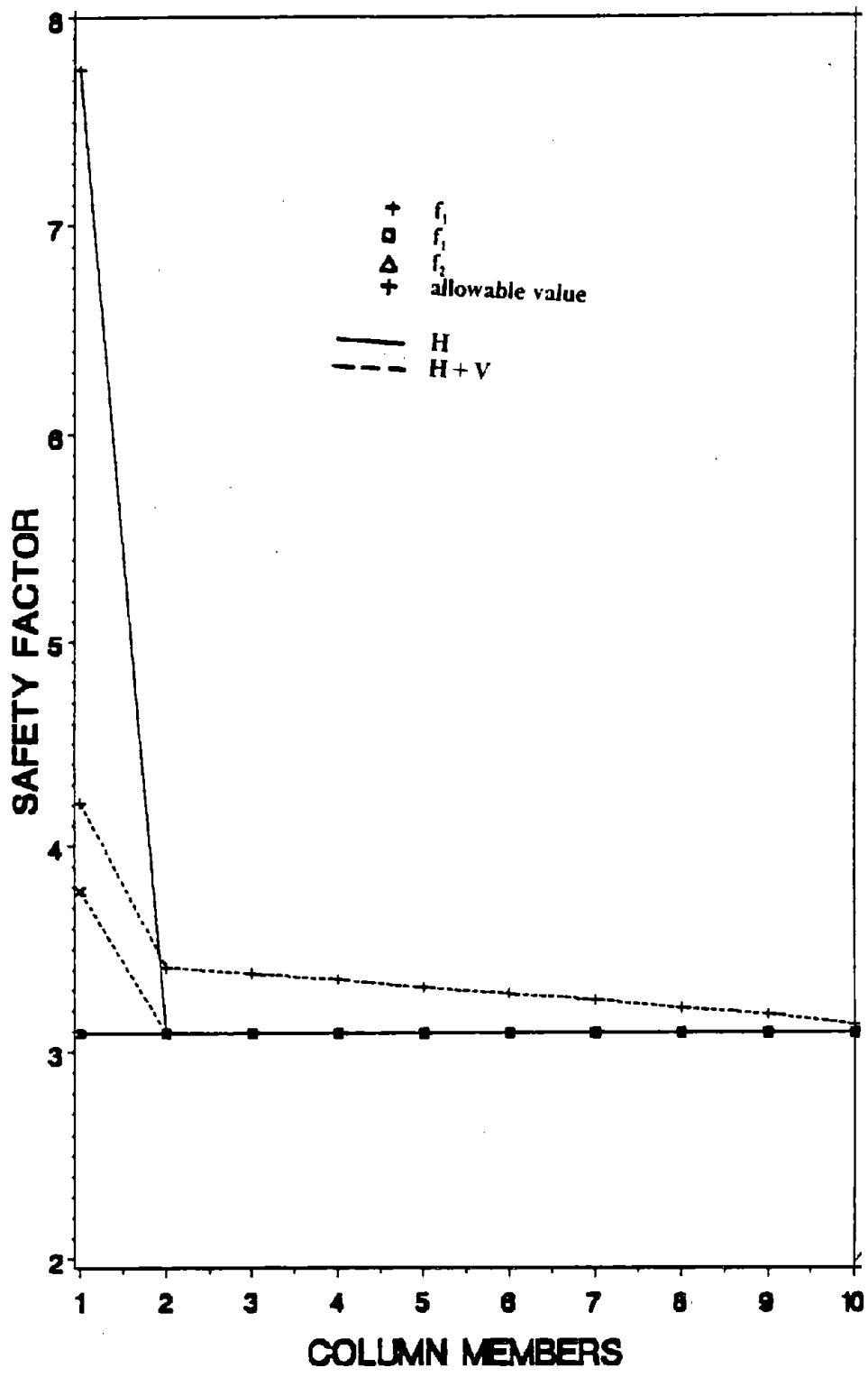

Figure 114. Safety Factor of Interaction Equation with N and 2nd of 10-Story Building.

E. SUMMARIES

1. The optimum designs change as the values of V_{My} change; however, the changes with normal distribution are not large.

2. The differences between 1st and 2nd variance approach are not sensitive to the change of V_{M_y}.

3. The optimum designs are not sensitive to the change of $V_{M_{cr}}$.

4. When the coefficient of variation of peak ground acceleration increases, the optimum design results with lognormal distribution increase faster than those with normal distribution.

5. The optimum design results for 1st variance approach are close to those for 2nd variance approach with $V_\omega = 0.072$ and $C_E = 0$, and 2nd variance approach with $V_\omega = 0$, $C_E = 0.15$ at low reliability level; the differences among them increase with reliability level; the optimum design results for 2nd variance approach with recommended values of coefficients of variation of natural frequency and C_E are the heaviest designs.

6. The vertical ground acceleration can noticeably affect the optimum solution.

XI. OPTIMUM DESIGN FOR STATIONARY SEISMIC PROCESSES.

The earthquake load based on stationary seismic process is also used to investigate the comparison for various random seismic spectra, for various failure probability expressions, and for three types of loading. The comparisons also include cost design for two cost ratios, and two system failure bounds. The two-story and ten-story shear buildings used previously are investigated in this study. The parameters for stationary seismic process are $G_{0_g} = 1.0\ in^3/sec^3$, $(16.38\ cm^3/sec^3)$, $\omega_g = 15.6\ rad/sec$, $\zeta_g = 0.6$. The deterministic allowable displacements are 0.005 times the corresponding height relative to the structural base. The yielding strength is $F_y = 36$ ksi (2.448×10^5 kPa), and the elastic modulus is 30000 ksi (2.067×10^8 kPa). The notations given in the figures are first passage expression (FP), safety factor expression with normal distribution and Davenport's equation (SND), safety factor expression with lognormal distribution and Davenport's equation (SLND), safety factor expression with normal diatribution and Kiureghian's equation (SNK), safety factor expression with normal distribution and Kiureghian's equation (SLNK).

A. COMPARISON OF VARIOUS SEISMIC SPECTRA.

The stochastic seismic spectrum may be white noise spectrum (WN), Kani-Tajimi filter white noise spectrum (FW), or modified white noise spectrum (MW). These spectra are used to investigate their effects on optimum weights and moments of inertia.

The optimum weights and moments of inertia subjected to three stochastic seismic spectra for five failure probability expressions of FP, SND, SLND, SNK, and SLNK are shown in Figures 115 to 124. The results subjected to modified white noise spectrum are the largest among these spectra. However, the differences of the results between modified white noise spectrum and filter white noise spectrum are small. The results for white noise spectrum are the smallest among these spectra. The weight differences between modified white noise spectrum and white noise spectrum are from 706.1 lbs (3142.1 N) at $P_{f0} = 10^{-1}$ to 1826.6 lbs (8128.3 N) at $P_{f0} = 10^{-7}$. The weight differences between modified white noise spectrum and filter white

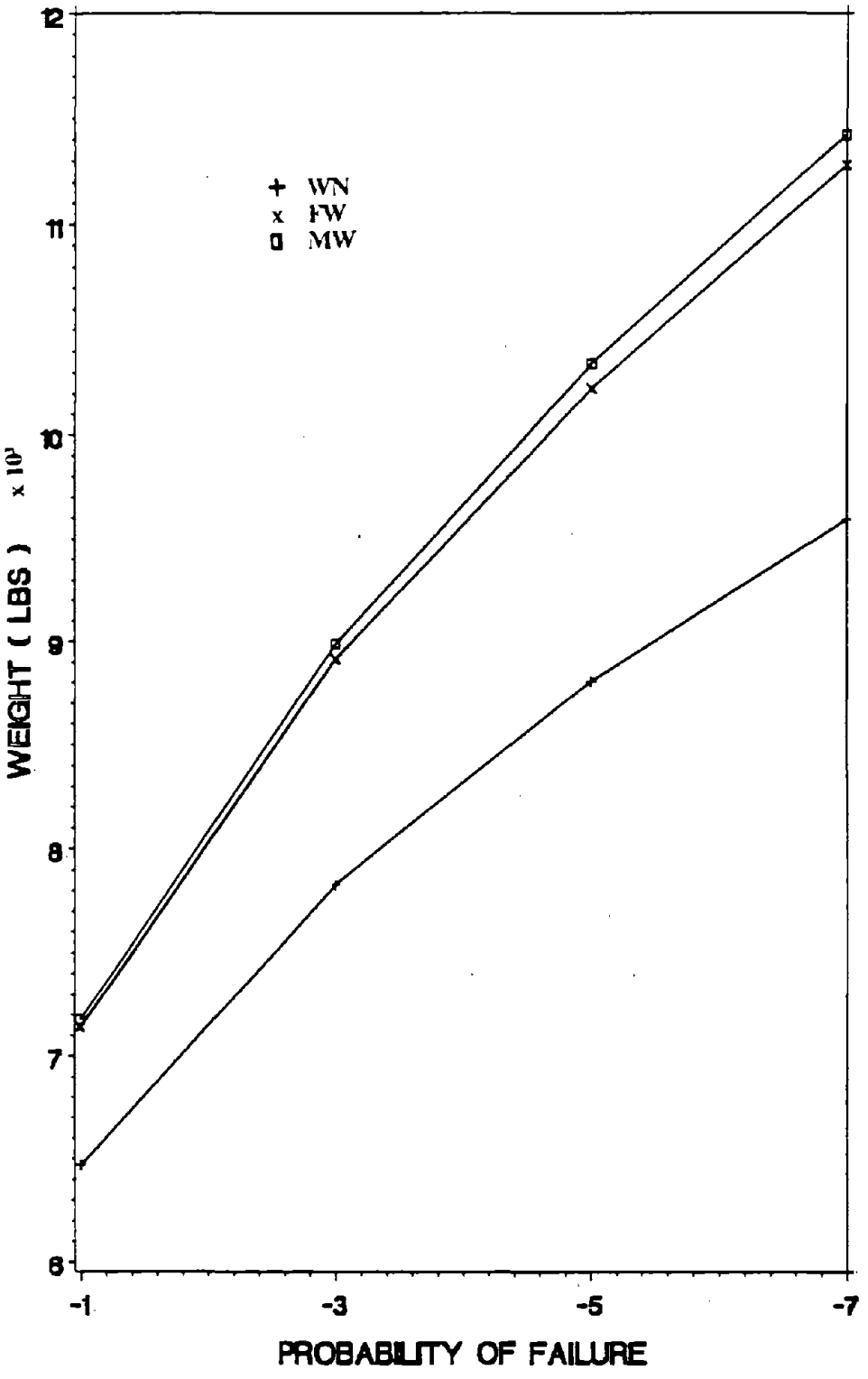

Figure 115. Optimum Weight for Three Seismic Input Spectra with FP of 2-Story Building. (1 lb = 4.45 N)

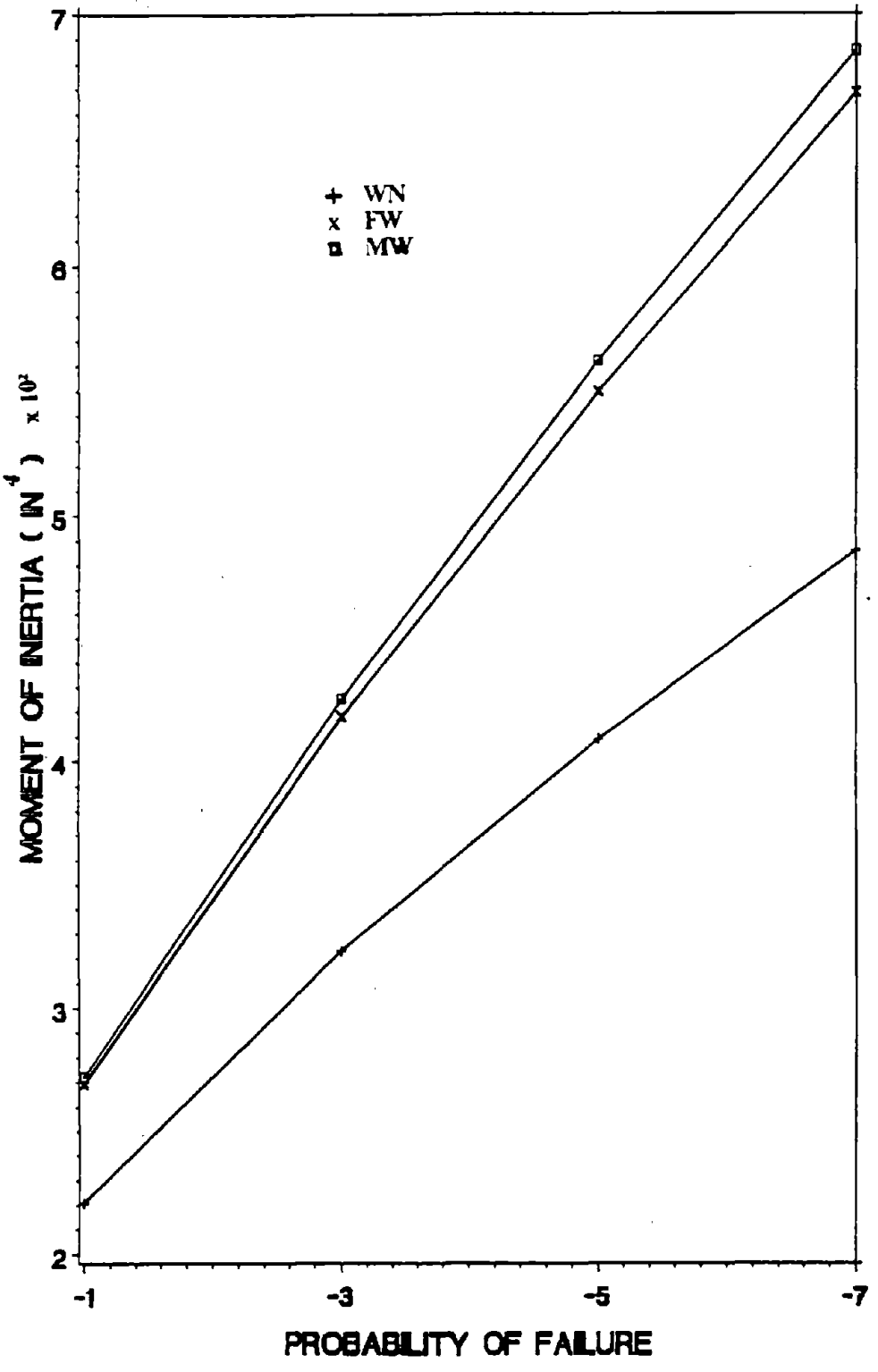

Figure 116. I_1 for Three Seismic Input Spectra with FP of 2-Story Building. (1 in = 2.54 cm)

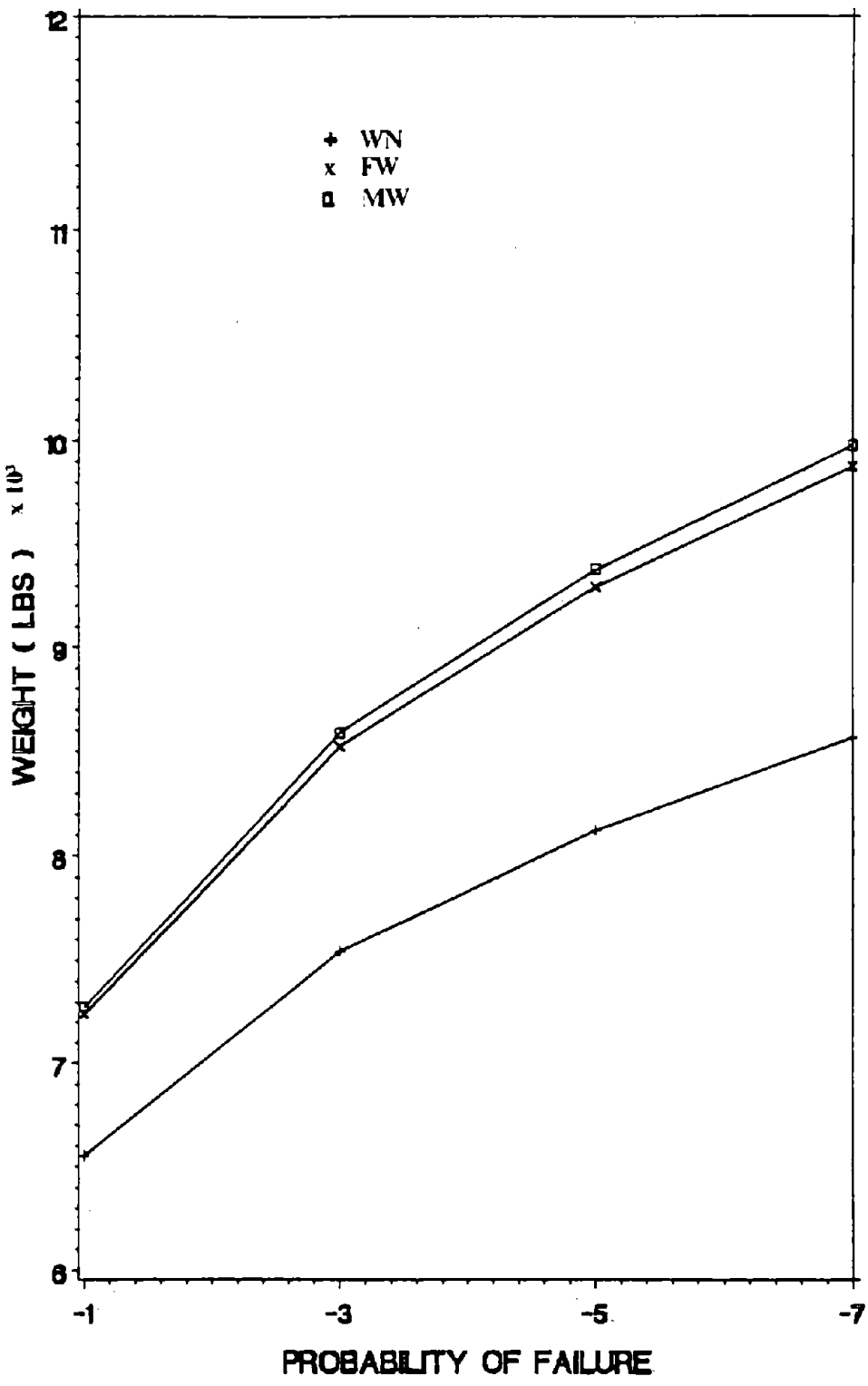

Figure 117. Optimum Weight for Three Seismic Input Spectra with SND of 2-Story Building. (1 lb = 4.45 N)

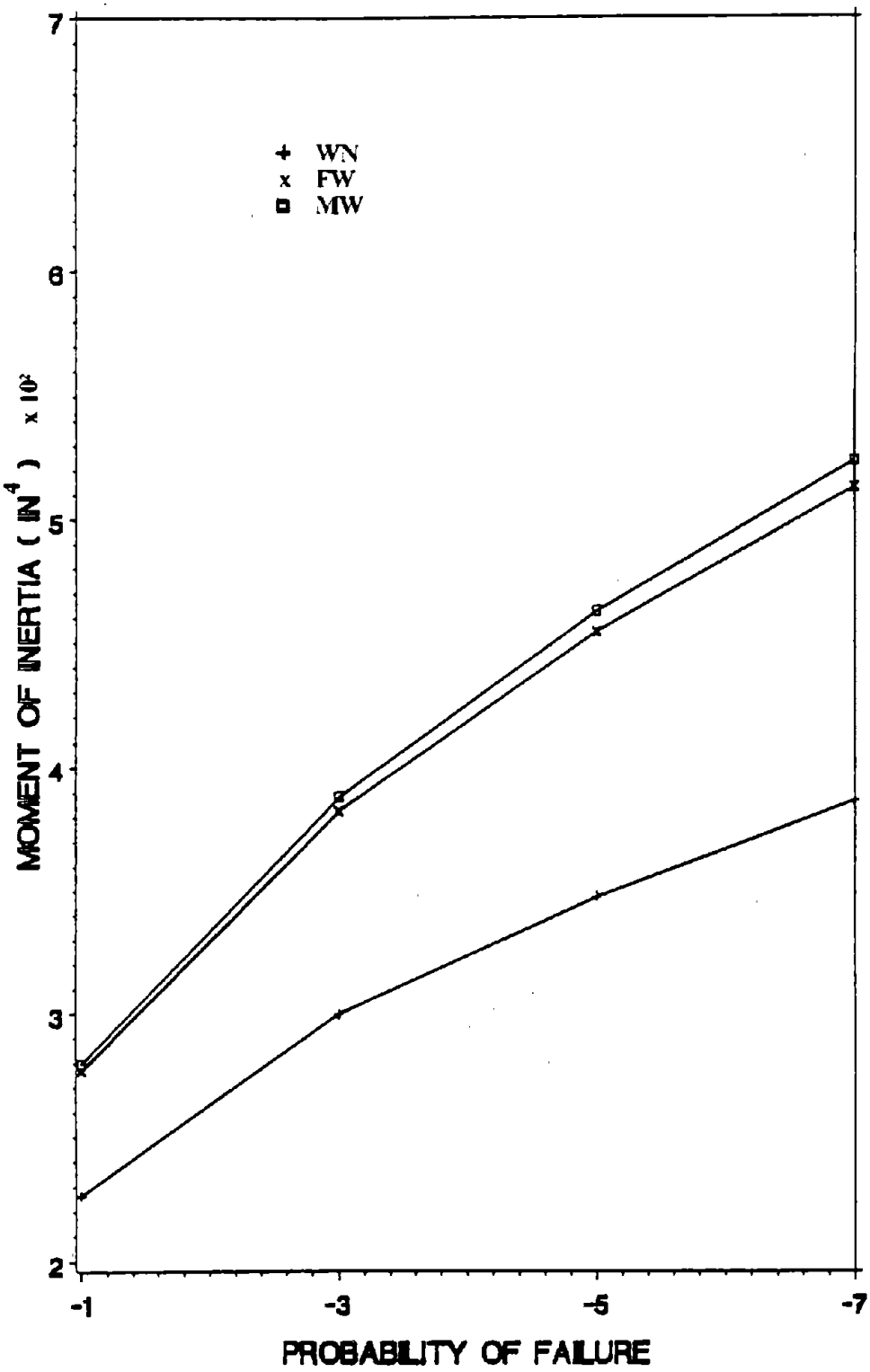

Figure 118. I_1 for Three Seismic Input Spectra with SND of 2-Story Building. (1 in = 2.54 cm)

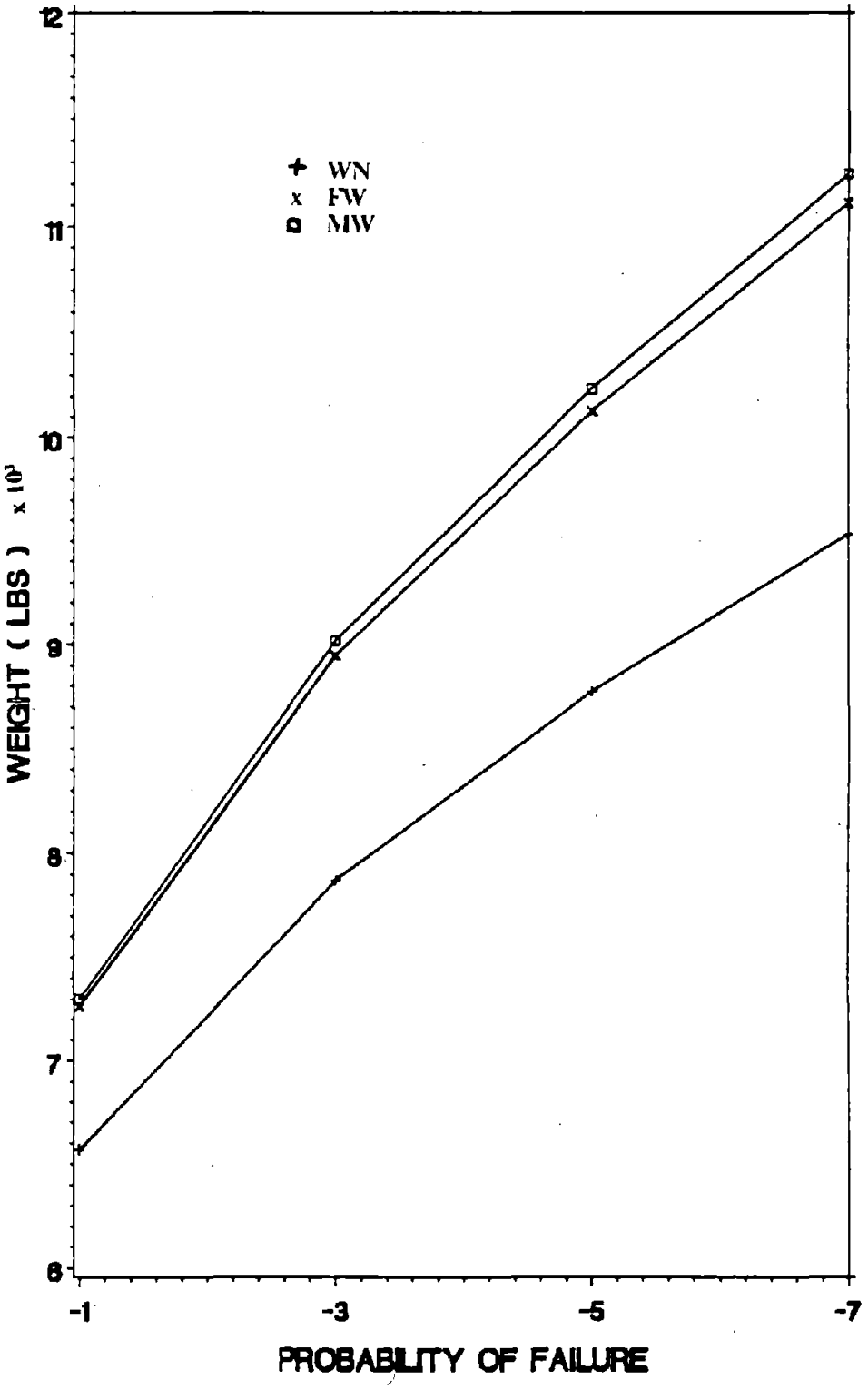

Figure 119. Optimum Weight for Three Seismic Input Spectra with SLND of 2-Story Building. (1 lb = 4.45 N)

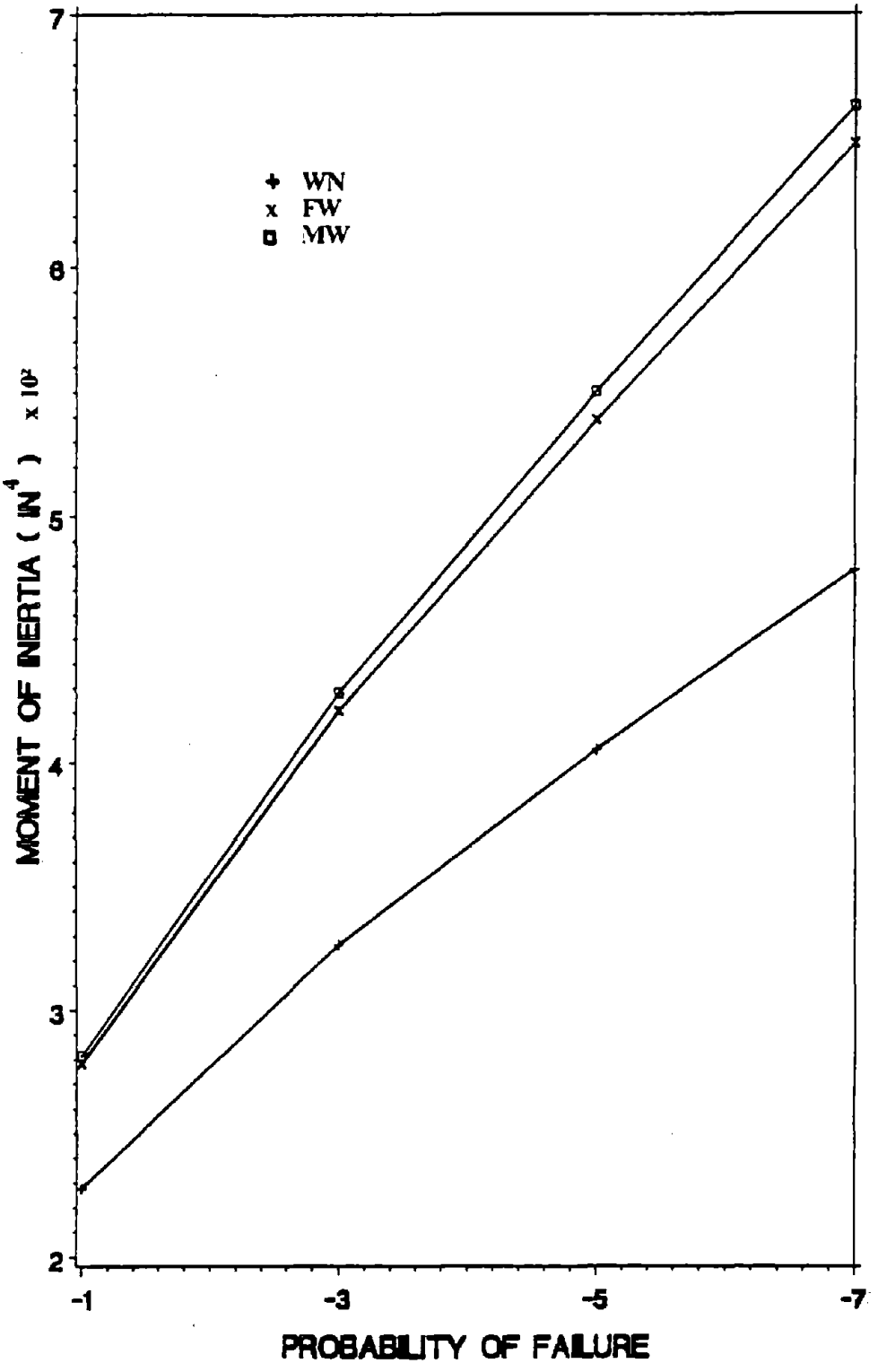

Figure 120. I_1 for Three Seismic Input Spectra with SLND of 2-Story Building. (1 in = 2.54 cm)

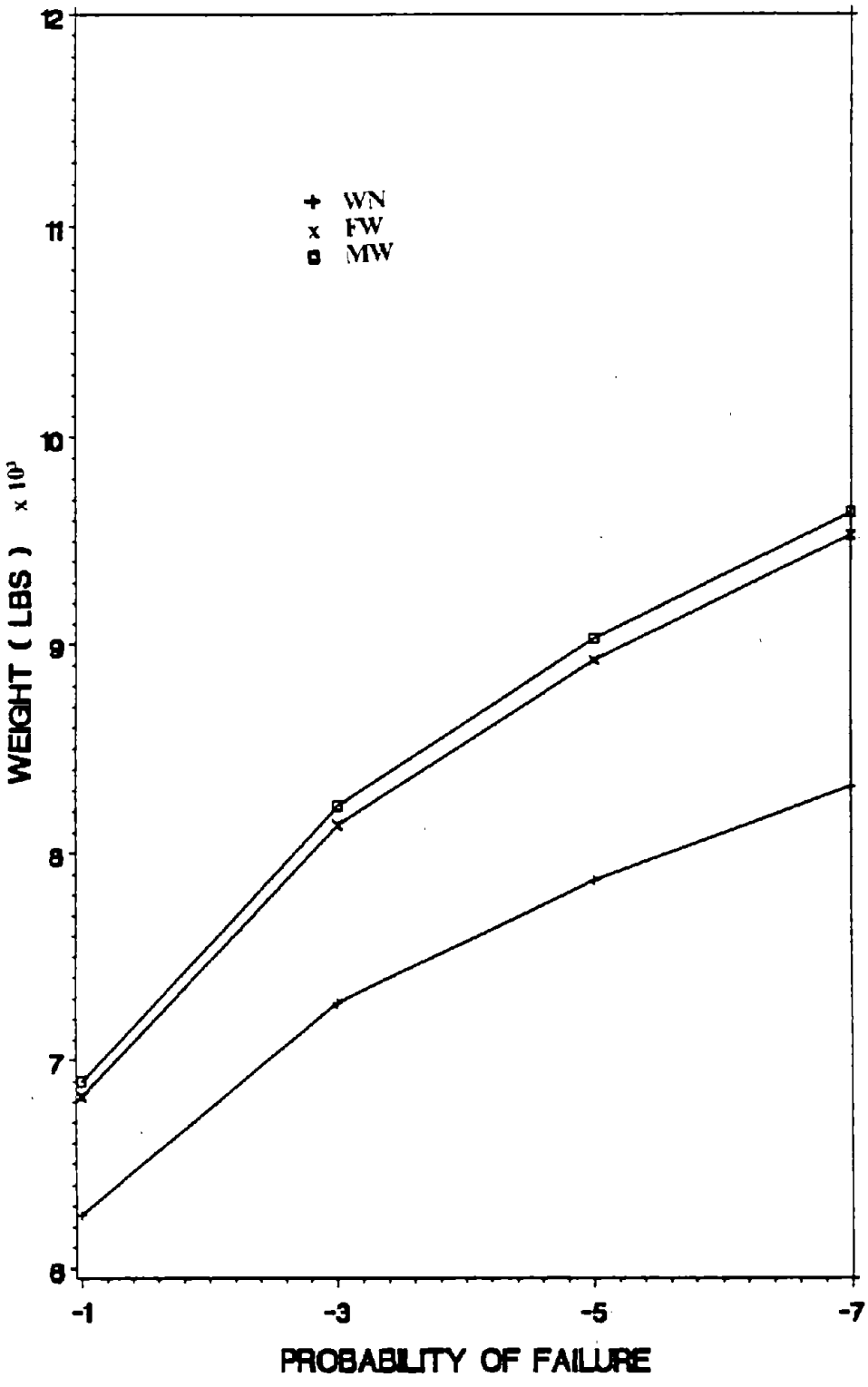

Figure 121. Optimum Weight for Three Seismic Input Spectra with SNK of 2-Story Building. (1 lb = 4.45 N)

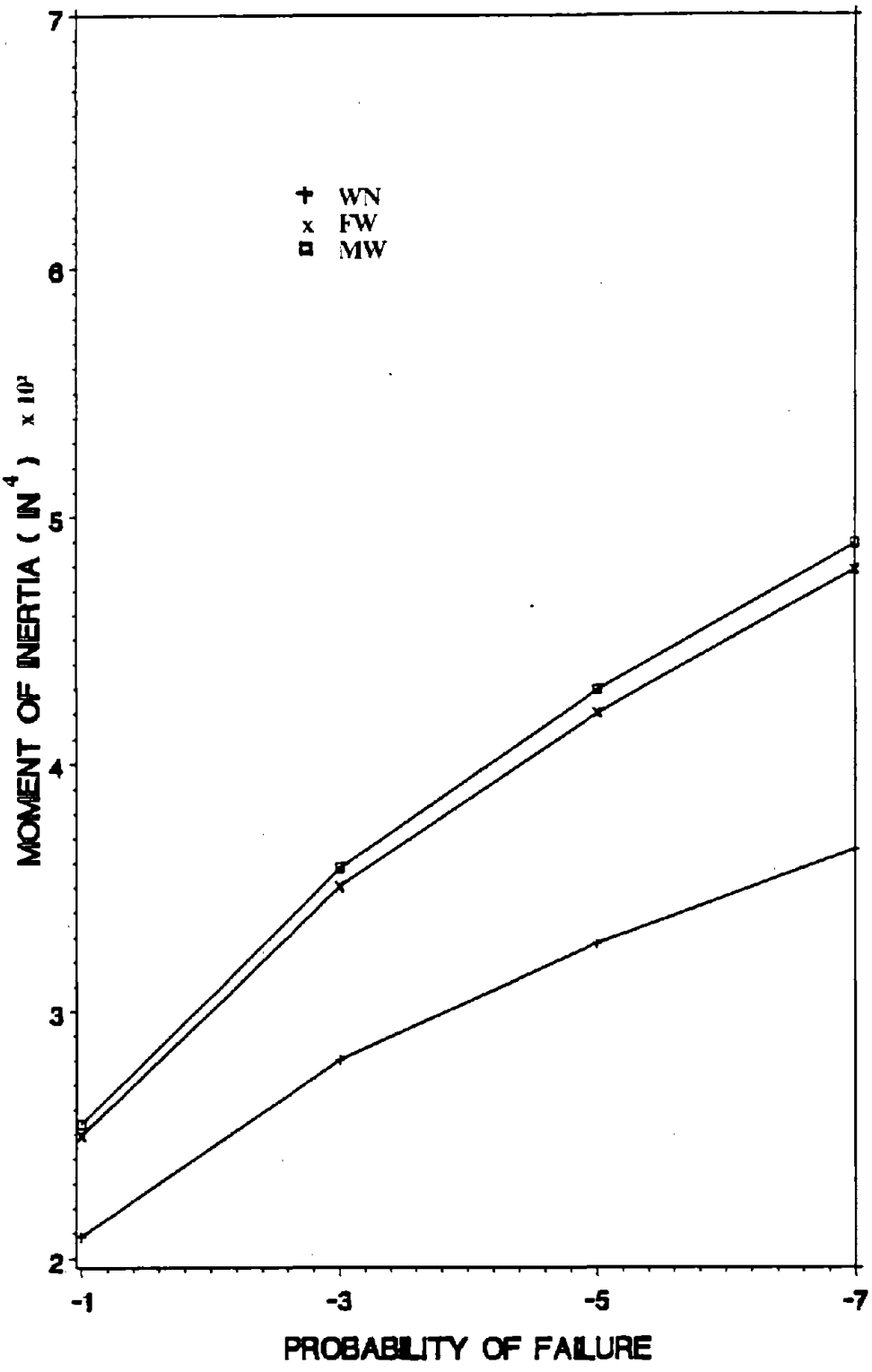

Figure 122. I_1 for Three Seismic Input Spectra with SNK of 2-Story Building. (1 in = 2.54 cm)

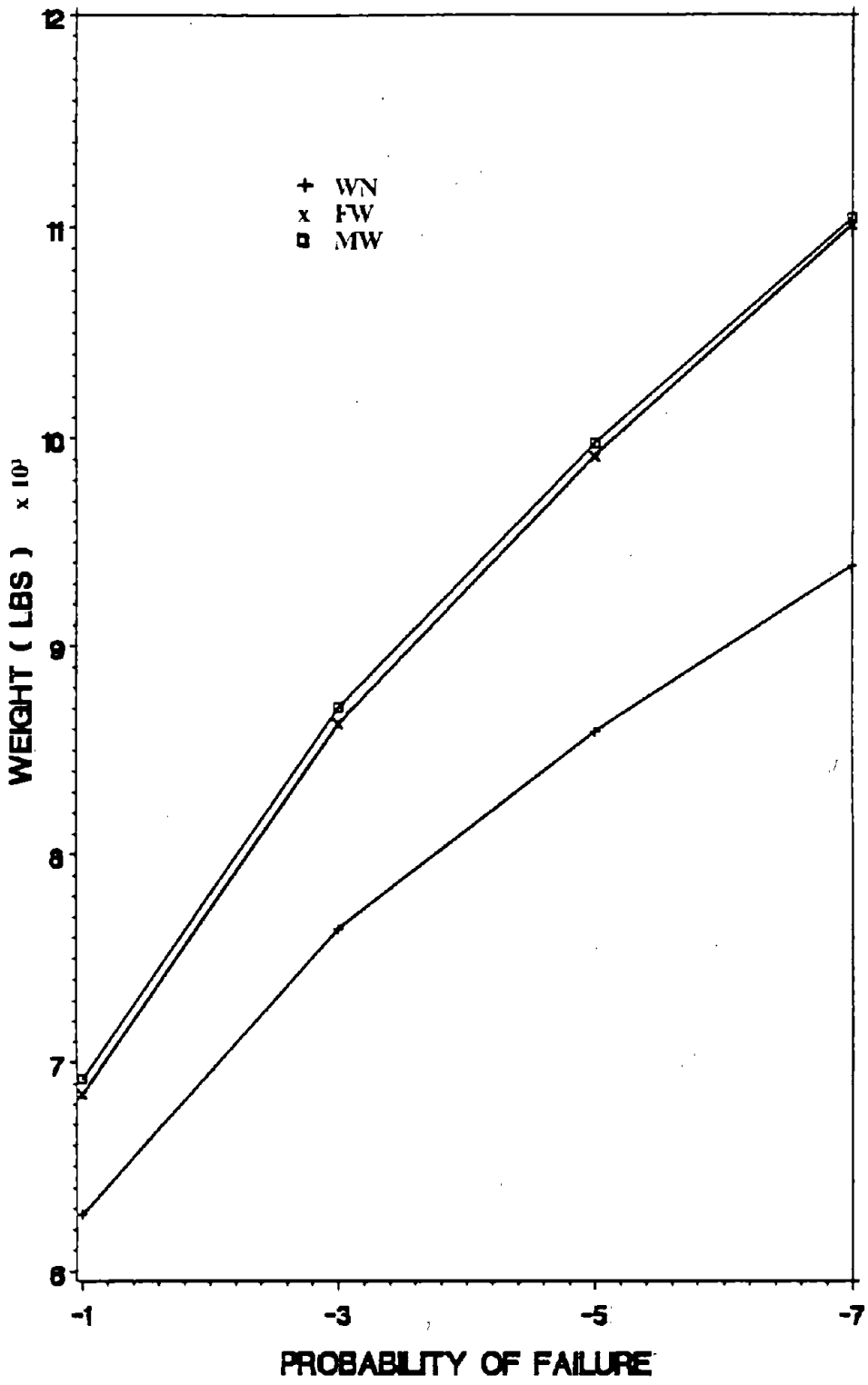

Figure 123. Optimum Weight for Three Seismic Input Spectra with SLNK of 2-Story Building. (1 lb = 4.45 N)

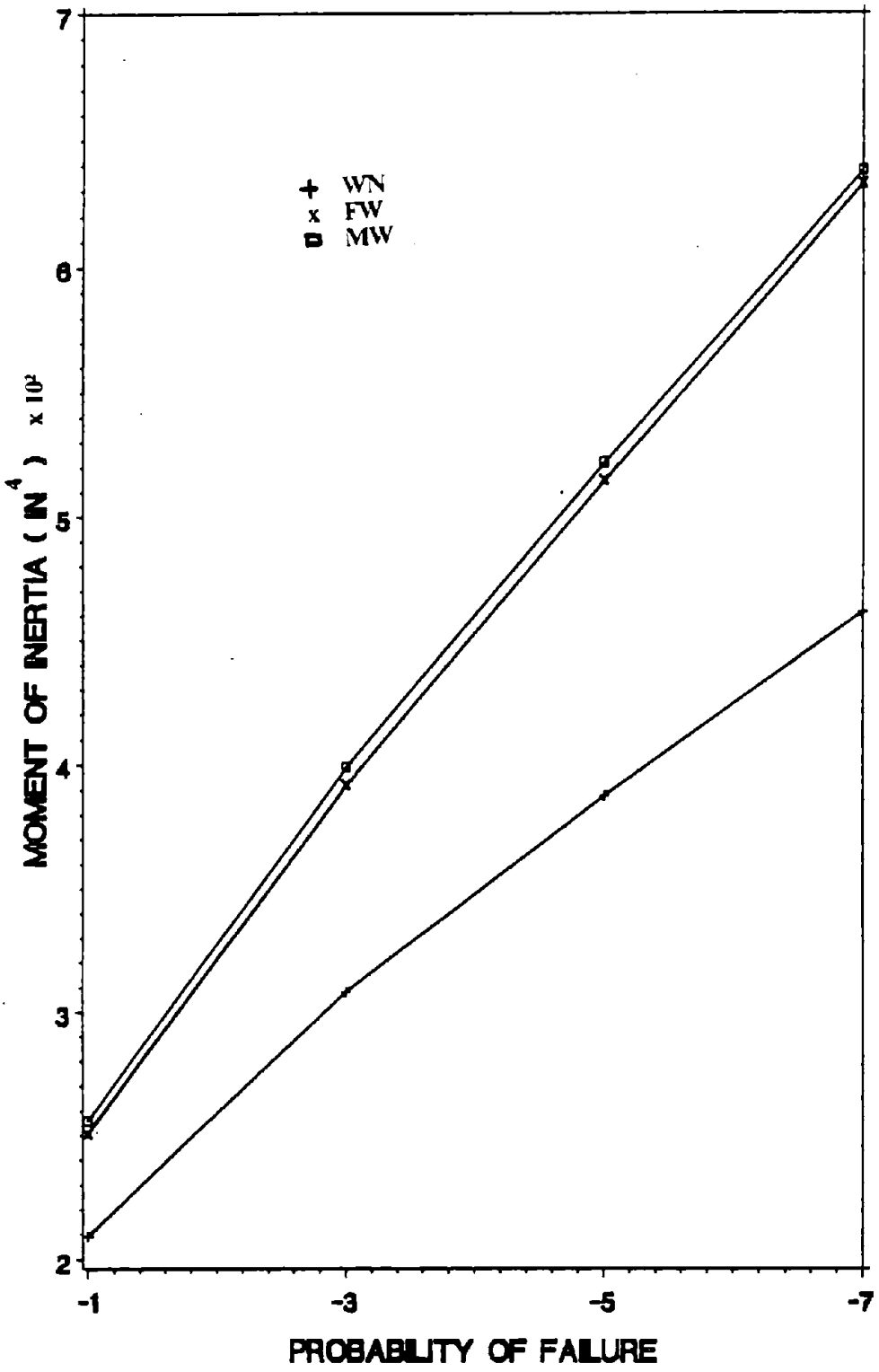

Figure 124. I_1 for Three Seismic Input Spectra with SLNK of 2-Story Building. (1 in = 2.54 cm)

noise spectrum are from 35.8 lbs (159.3 N) at $P_{f0} = 10^{-1}$ to 142.9 lbs (635.9 N) at $P_{f0} = 10^{-7}$.

The optimum weight in Figure 125 and the moments of inertia in Figures 126 and 127 of 10-story shear building for first passage expression show that the observations are the same as those for 2-story shear building. The deterministic designs in the figures are the optimum solutions which do not include the probabilities of failures in the constraints. The deterministic constraints used are

$\bar{u}_{max}$ – allowable displacement ≤ 0

$\bar{f}_{1max} - 1.0 \leq 0$

$\bar{f}_{2max} - 1.0 \leq 0$

$\bar{f}_{3max} - 1.0 \leq 0$

$\bar{f}_{4max} - 1.0 \leq 0$

where $\bar{u}_{max}$, $\bar{f}_{1max}$, $\bar{f}_{2max}$, $\bar{f}_{3max}$, $\bar{f}_{4max}$ can be obtained from Equations (5.42), (6.27), (6.29), (6.31), and (6.33).

The results show that the optimum weight and moments of inertia with reliability constraints are higher than those with deterministic constraints. The differences of optmium solutions between the designs including reliability constraints and the designs including deterministic constraints increase with reliability criteria.

B. COMPARISON OF VARIOUS EXPRESSIONS OF FAILURE PROBABILITY.

The failure probability expressions for stationary seismic processes may be the first passage expression and the safety factor expressions with two peak response equations of Davenport's and Kiureghian's equations and two probability distributions of normal and lognormal distributions. The optimum weights in Figures 128, 130, and 132, and the moments of inertia in Figures 129, 131, and 133 for different expressions of probabilities of failures with three spectra of white noise, filter white noise, and modified white noise are compared for two-story shear building.

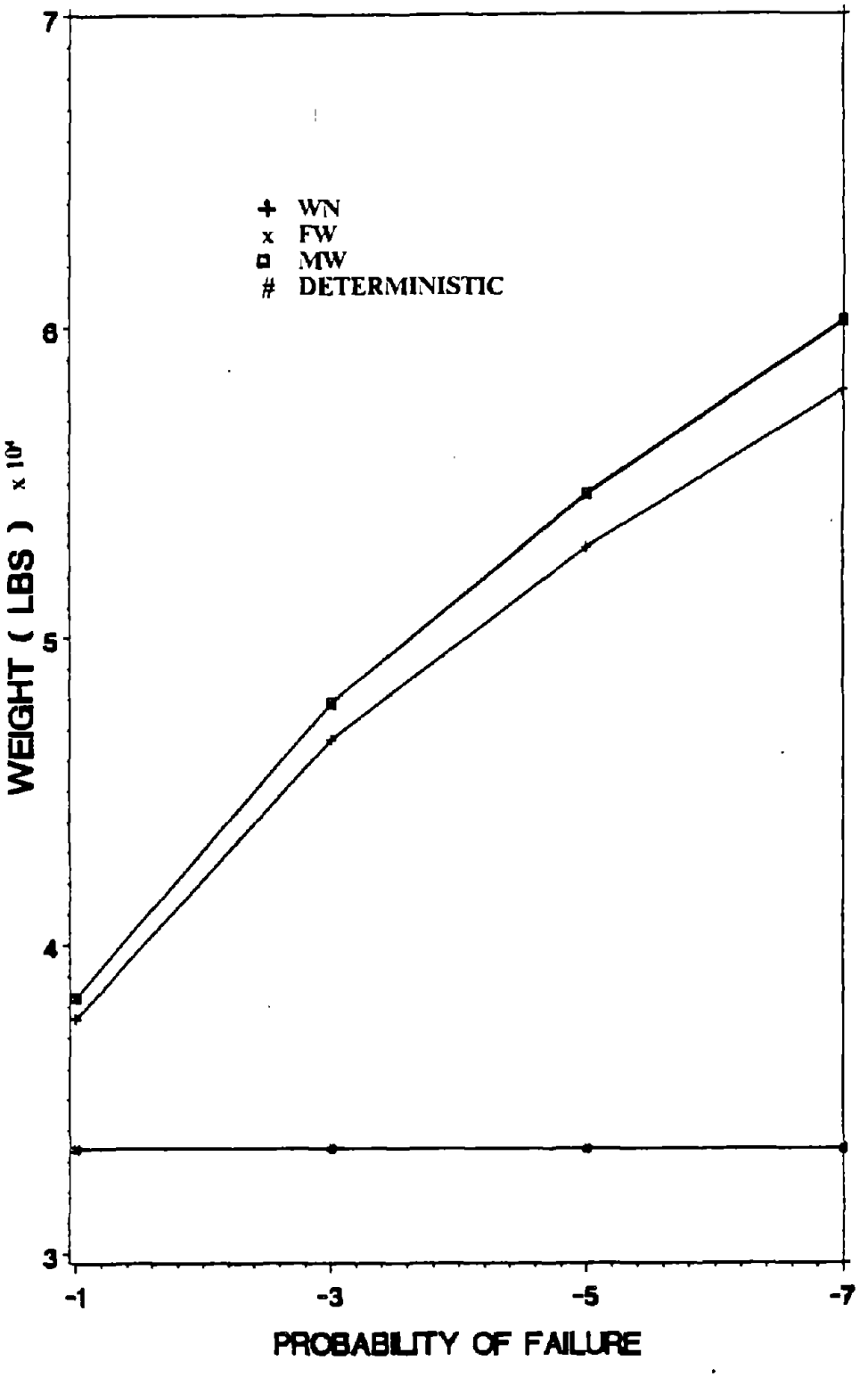

Figure 125. Optimum Weight for Three Seismic Input Spectra with FP of 10-Story Building. (1 lb = 4.45 N)

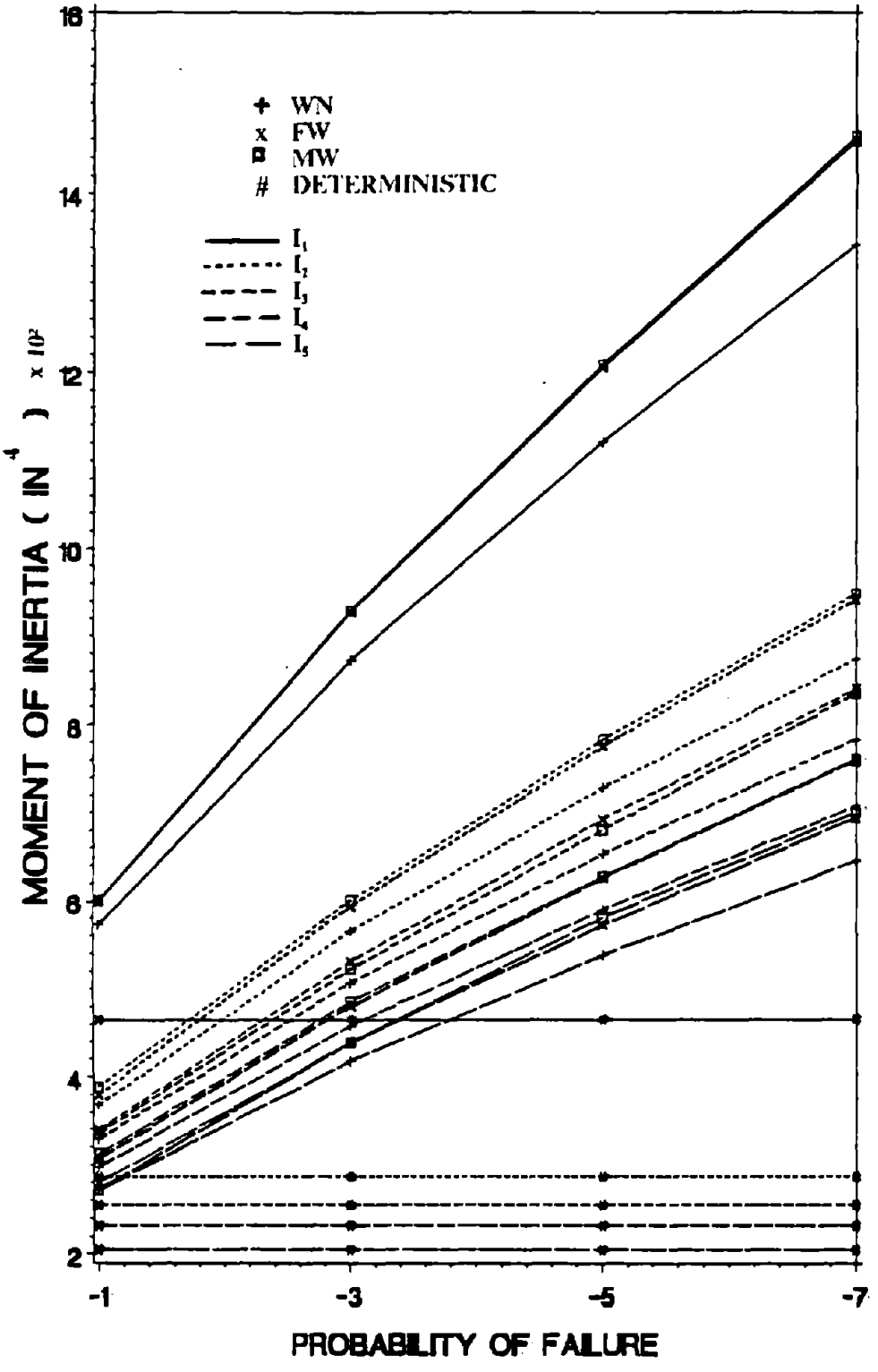

Figure 126. I_1-I_5 for Three Seismic Input Spectra with FP of 10-Story Building. (1 in = 2.54 cm)

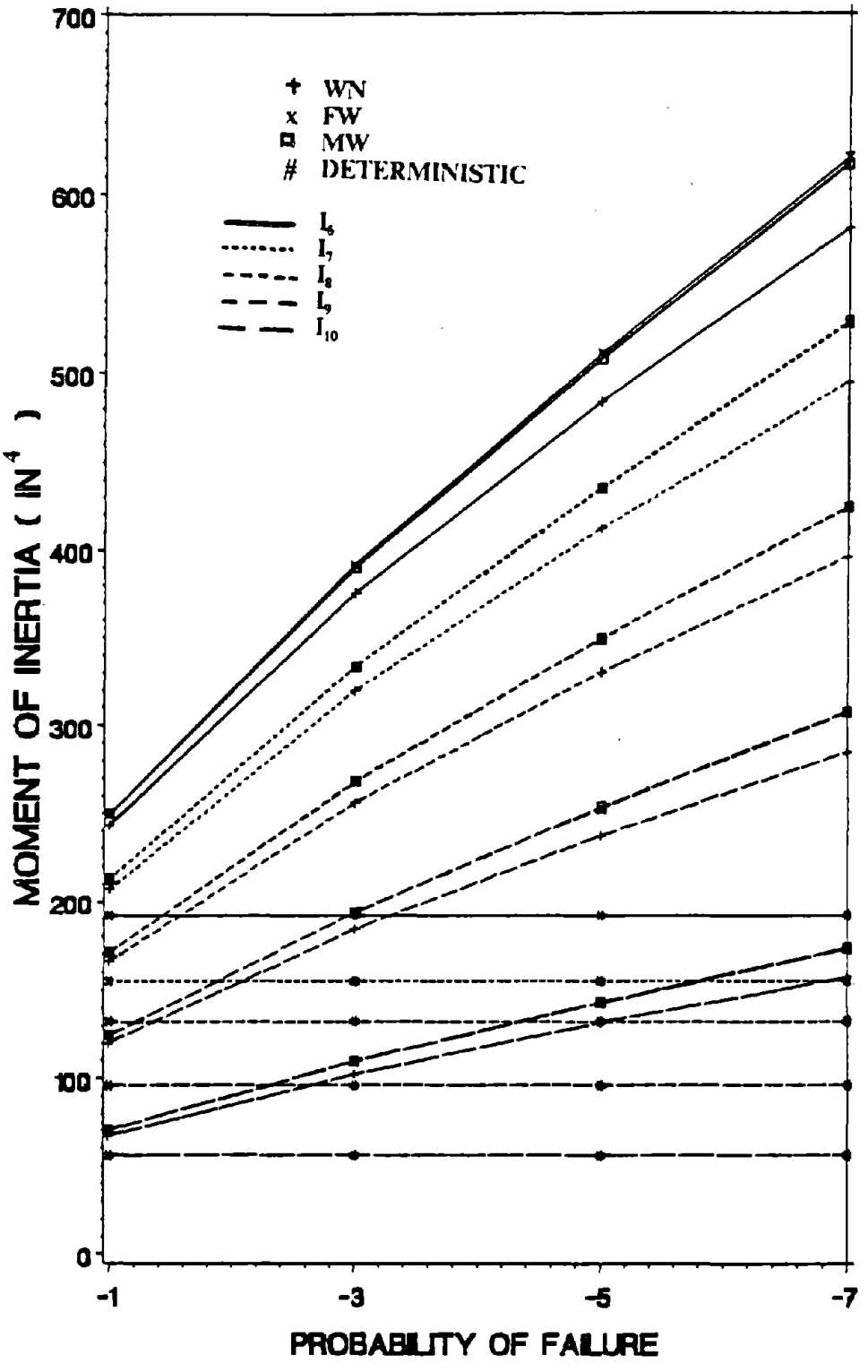

Figure 127. I_6-I_{10} for Three Seismic Input Spectra with FP of 10-Story Building. (1 in = 2.54 cm)

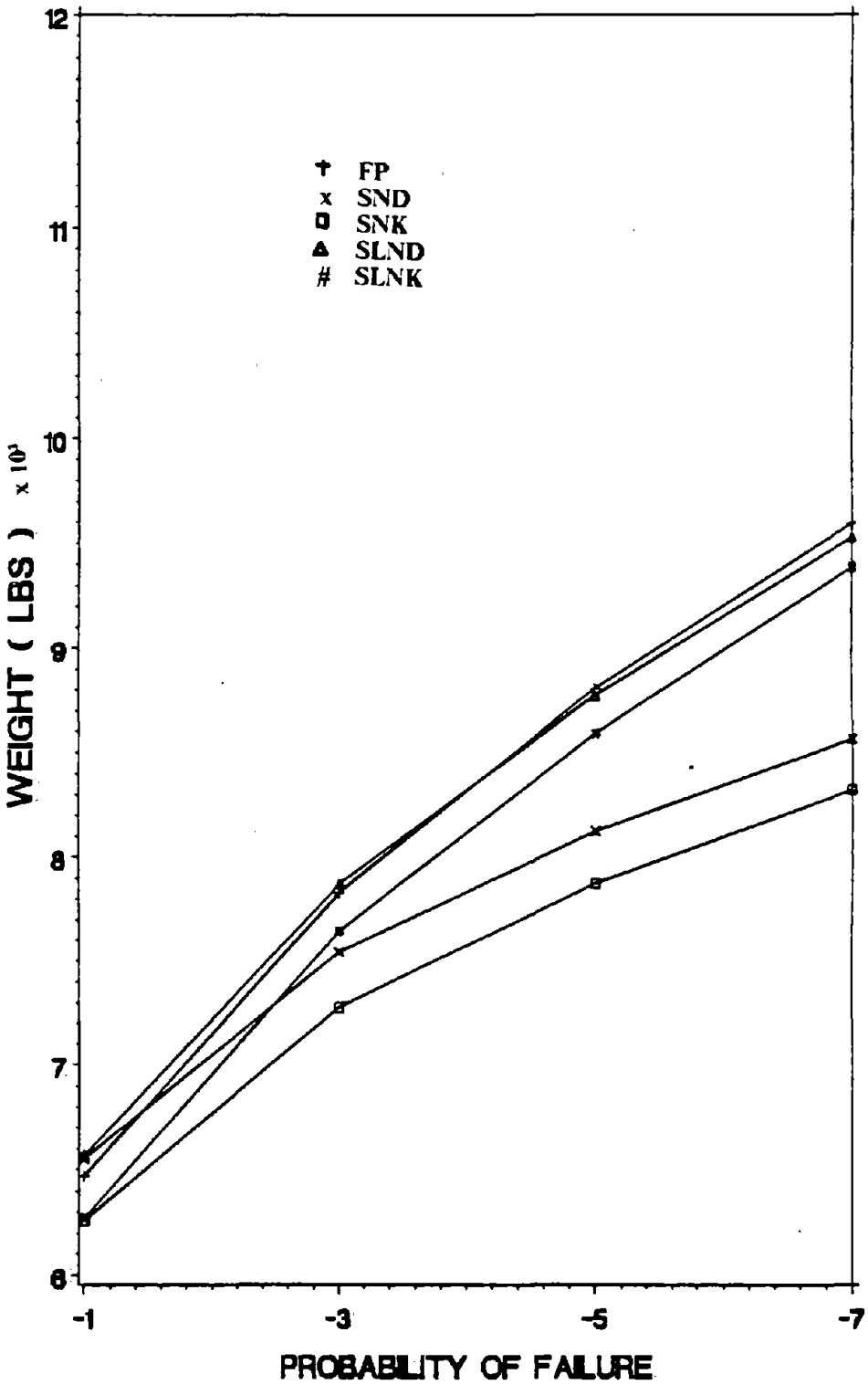

Figure 128. Optimum Weight for Various Failure Expressions with WN of 2-Story Building. (1 lb = 4.45 N)

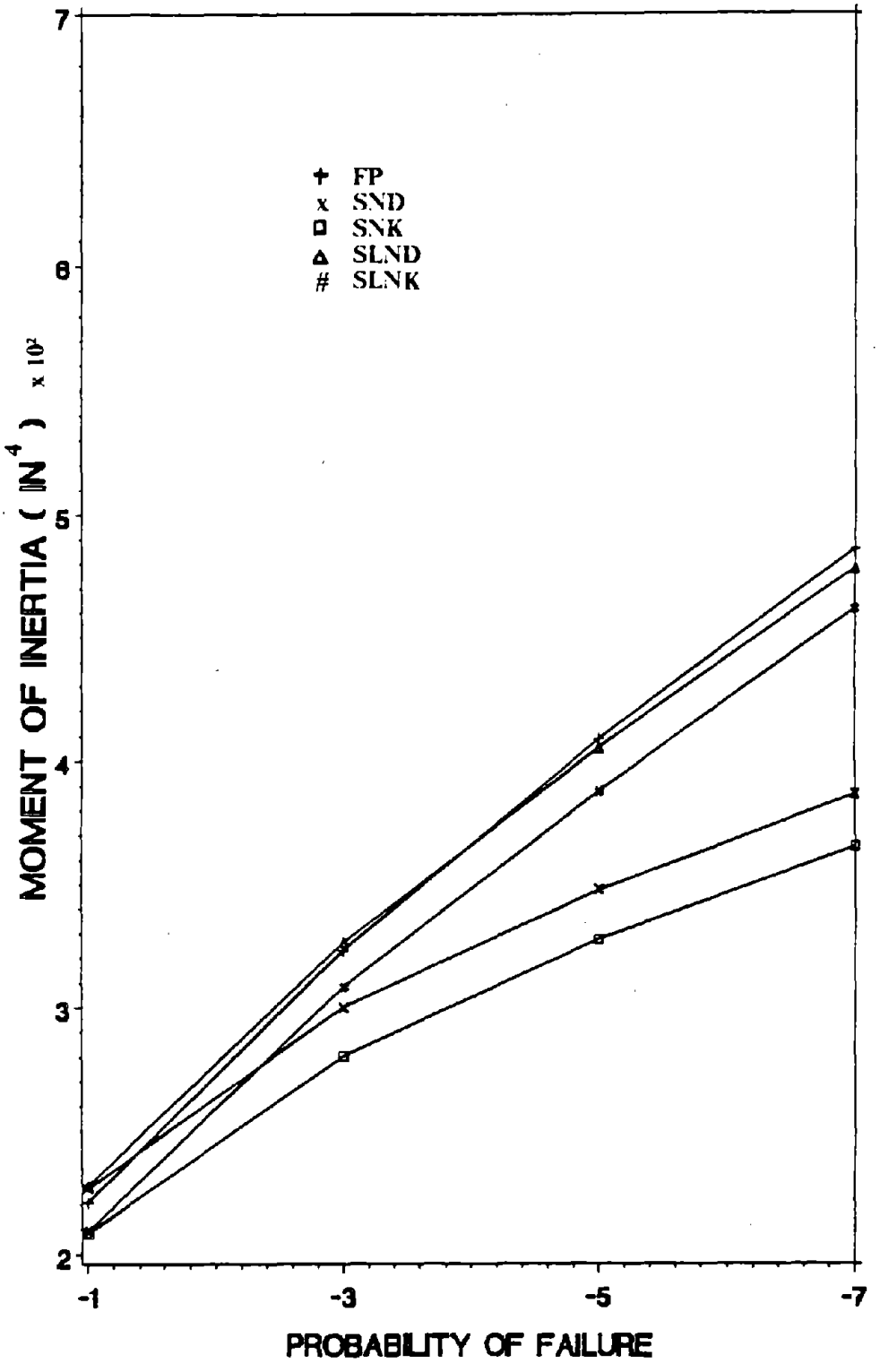

Figure 129. I_1 for Various Failure Expressions with WN of 2-Story Building. (1 in = 2.54 cm)

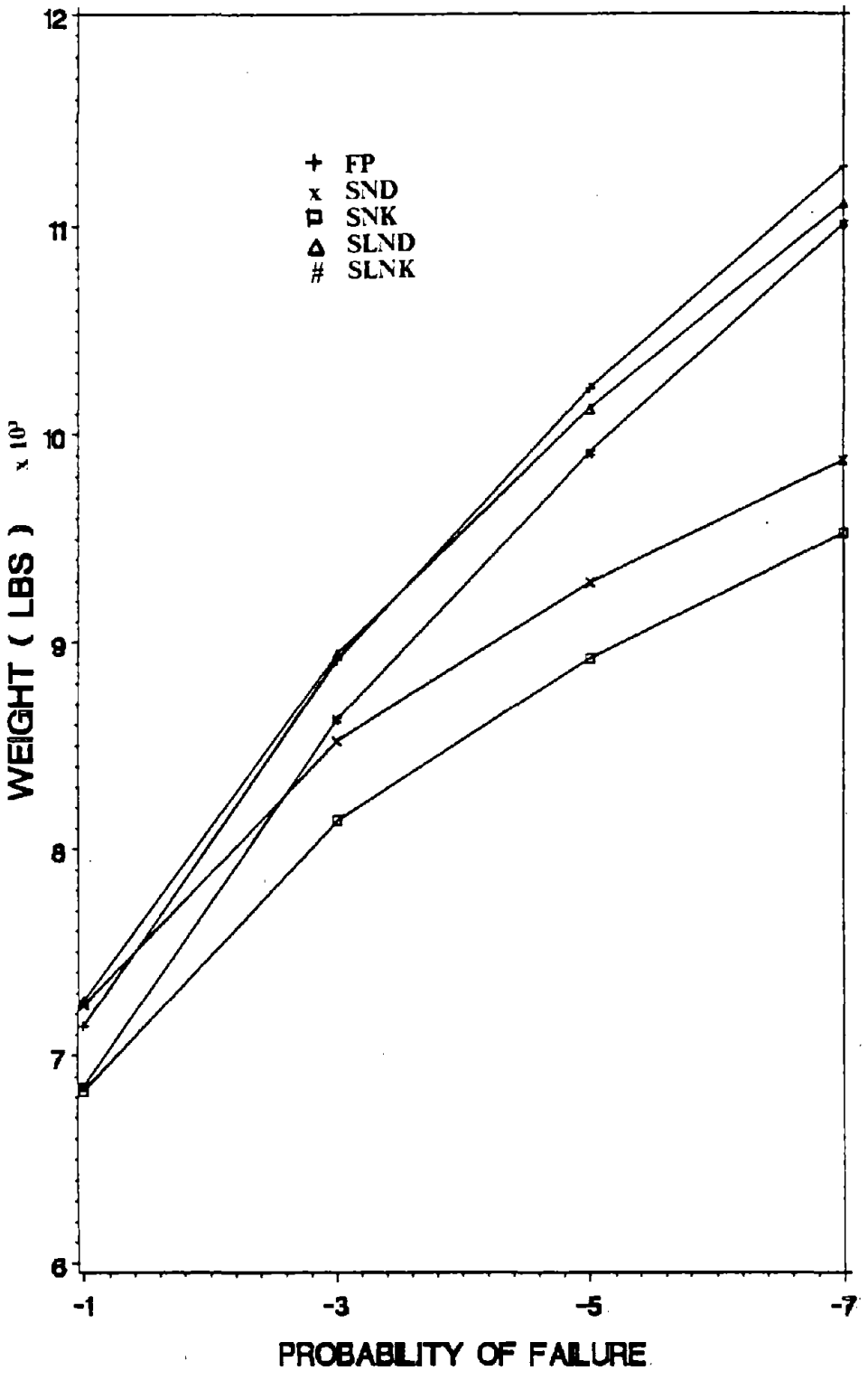

Figure 130. Optimum Weight for Various Failure Expressions with FW of 2-Story Building. (1 lb = 4.45 N)

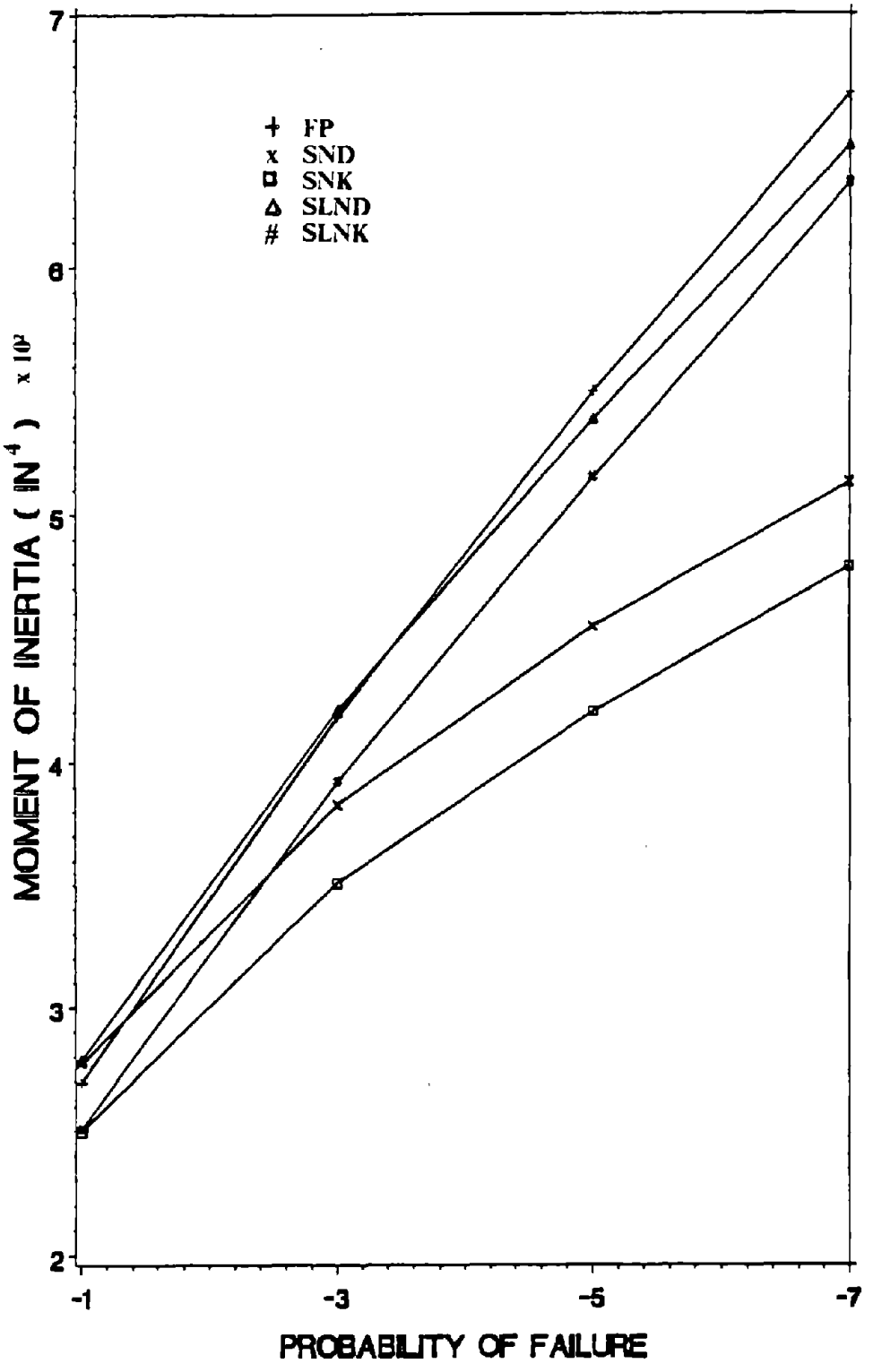

Figure 131. $I_{\perp}$ for Various Failure Expressions with FW of 2-Story Building. (1 in = 2.54 cm)

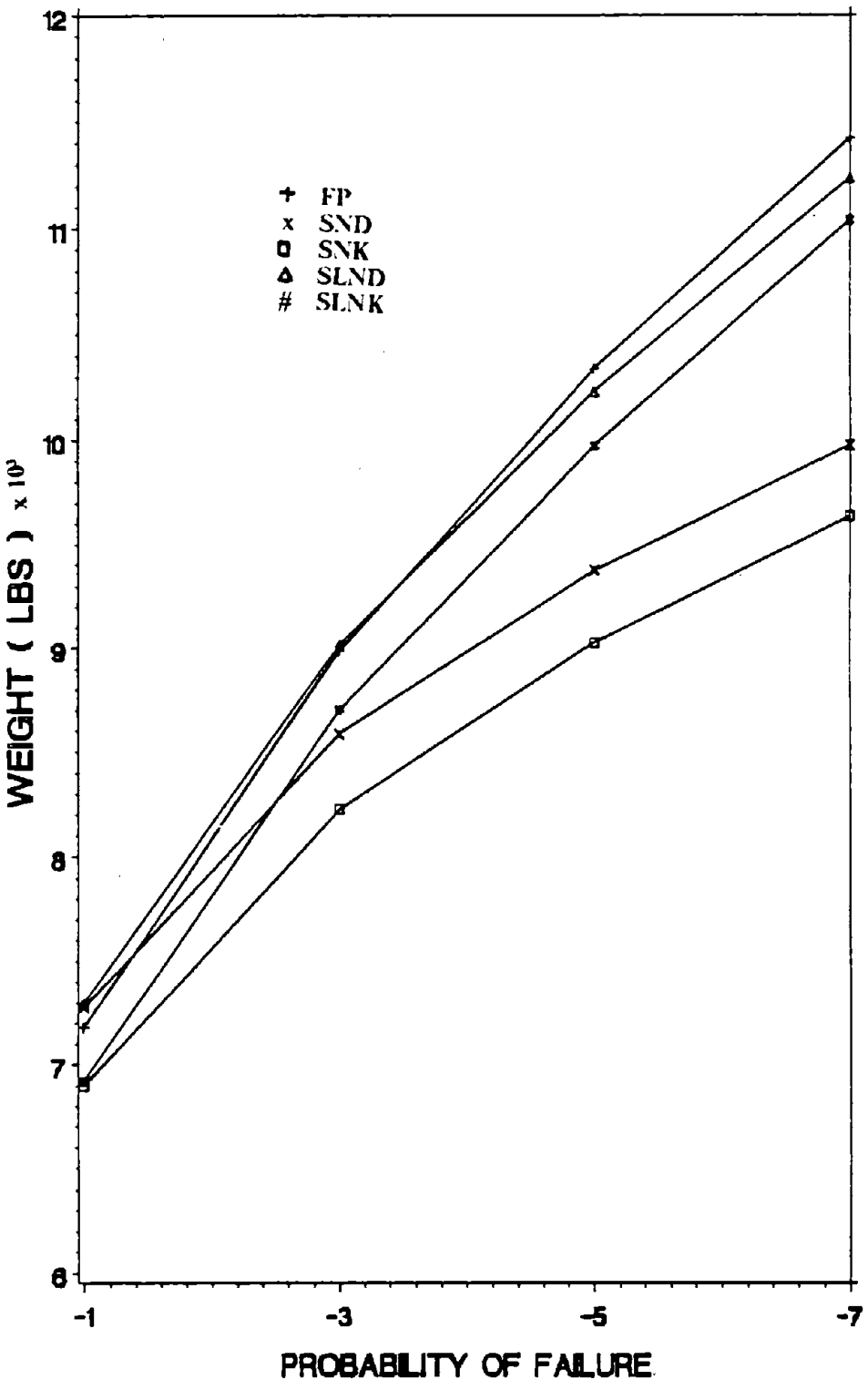

Figure 132. Optimum Weight for Various Failure Expressions with MW of 2-Story Building. (1 lb = 4.45 N)

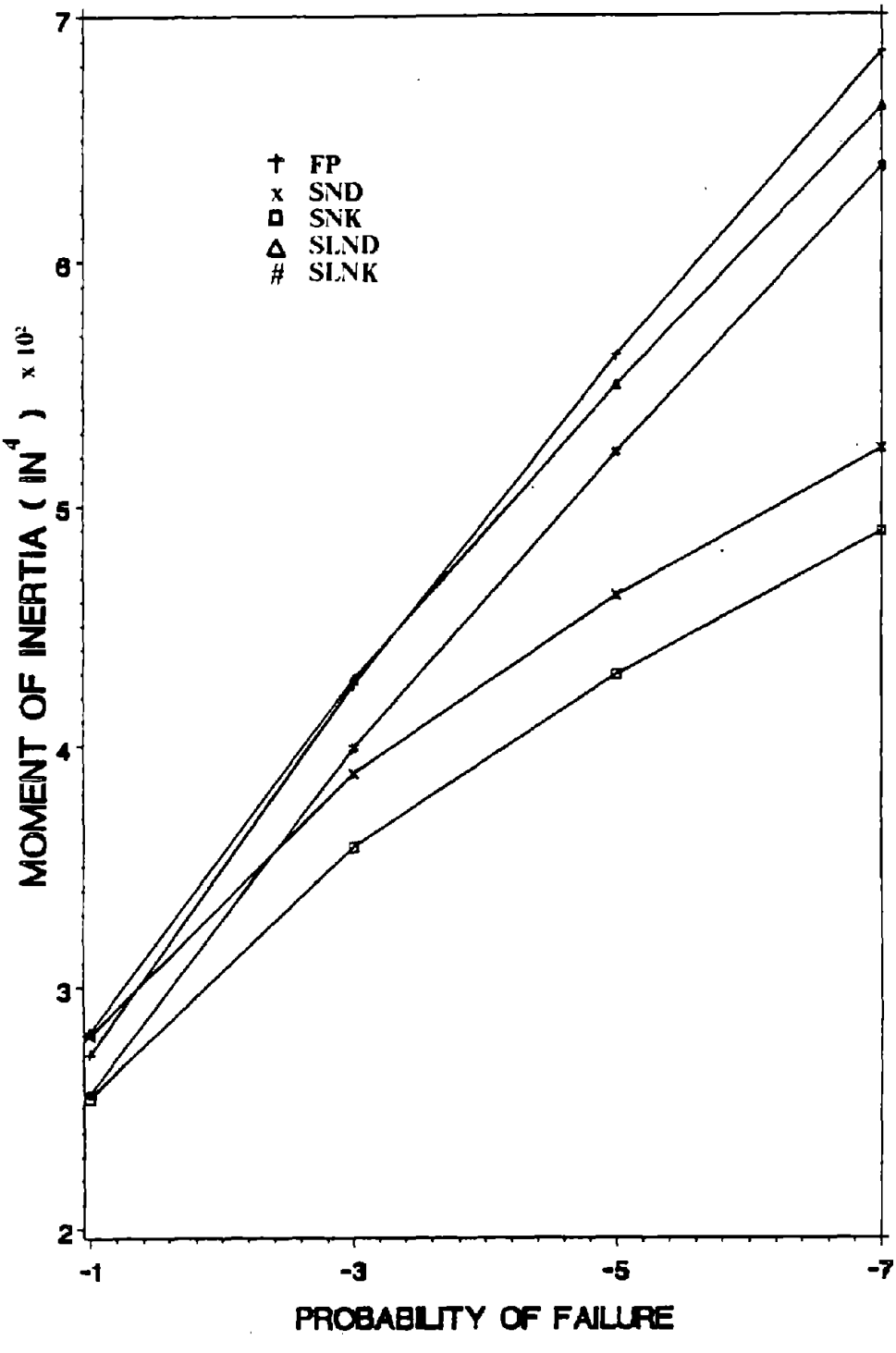

Figure 133. $I_{\perp}$ for Various Failure Expressions with MW of 2-Story Building. (1 in = 2.54 cm)

(1) at $P_{f0} = 10^{-1}$, the order of optimum solutions from large to small values in the following sequence is (a) safety factor expression with lognormal distribution and Davenport's equation (SLND), (b) safety factor expression with normal distribution and Davenport's equation (SND), (c) first passage equation (FP), (d) safety factor expression with lognormal distribution and Kiureghian's equation (SLNK), (e) safety factor expression with normal distribution and Kiureghian's equation (SNK).

(2) at $P_{f0} = 10^{-3}$, the order of optimum solutions from large to small values is in the sequence of (a) safety factor expression with lognormal distribution and Davenport's equation (SLND), (b) first passage equation (FP), (c) safety factor expression with lognormal distribution and Kiureghian's equation (SLNK), (d) safety factor expression with normal distribution and Davenport's equation (SND), (e) safety factor expression with normal distribution and Kiureghian's equation (SNK).

(3) at $P_{f0} = 10^{-5}$ and 10^{-7}, the order of optimum solutions from large to small values is in the sequence of (a) first passage equation (FP), (b) safety factor expression with lognormal distribution and Davenport's equation (SLND), (c) safety factor expression with lognormal distribution and Kiureghian's equation (SLNK), (d) safety factor expression with normal distribution and Davenport's equation (SND), (e) safety factor expression with normal distribution and Kiureghian's equation (SNK).

C. COMPARISON OF UBC, NNSRS, STATIONARY SEISMIC LOADS

Three types of loadings are used here for the comparison of their optimum design results. The loadings are the peak ground acceleration of 0.348g in NNSRS approach which can represent the 1940 El Centro earthquake;[1] the stationary modified white noise process of $G_0 = 1.0$, $\zeta_g = 0.6$, $\omega_g = 15.6$, with an amplification factor of 2.7 corresponding to the El Centro earthquake; [20] and UBC seismic load with zone IV and coefficient of variation of UBC = 1.38. The comparison of the optmum weight and moments of inertia for 1st and 2nd variance approach with normal and lognormal distributions of the two-story shear building is studied. Figures 134 to 137 show that optimum solutions indicate that the order of magnitude

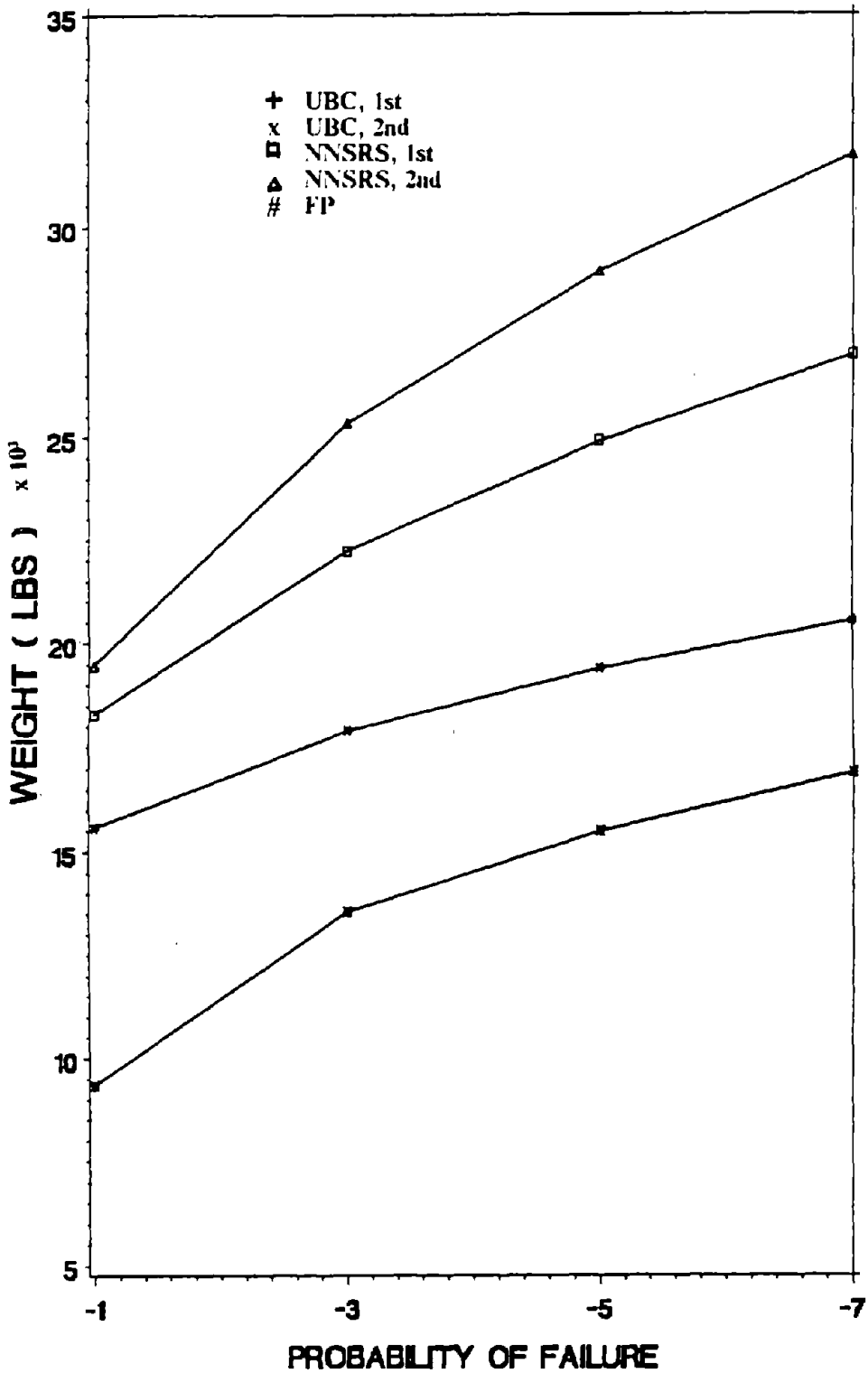

Figure 134. Optimum Weight for UBC, NNSRS, and Stationary with MW and N of 2-Story Building. (1 lb = 4.45 N)

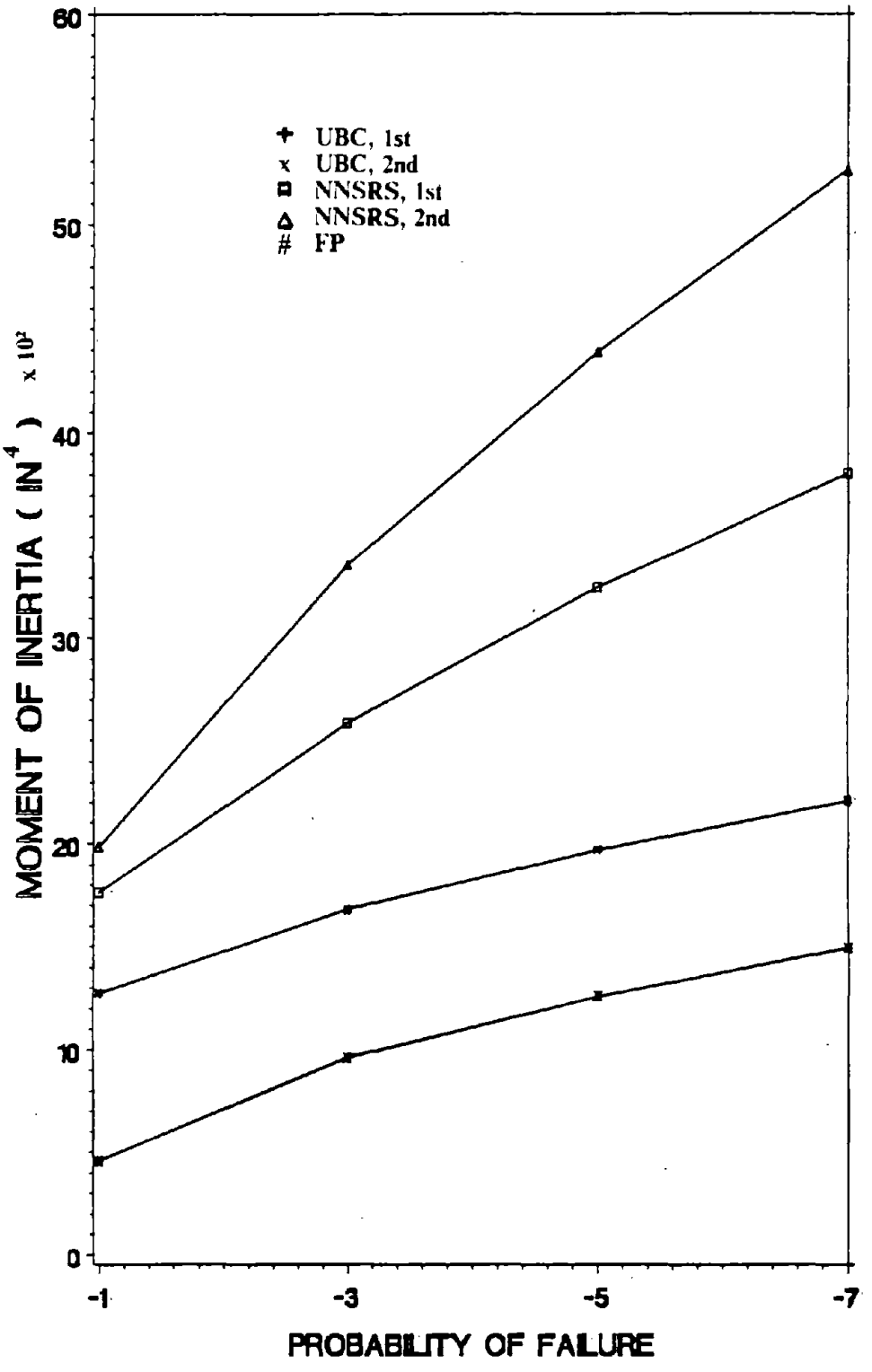

Figure 135. $I_{\perp}$ for UBC, NNSRS, and Stationary with MW and N of 2-Story Building. (1 in = 2.54 cm)

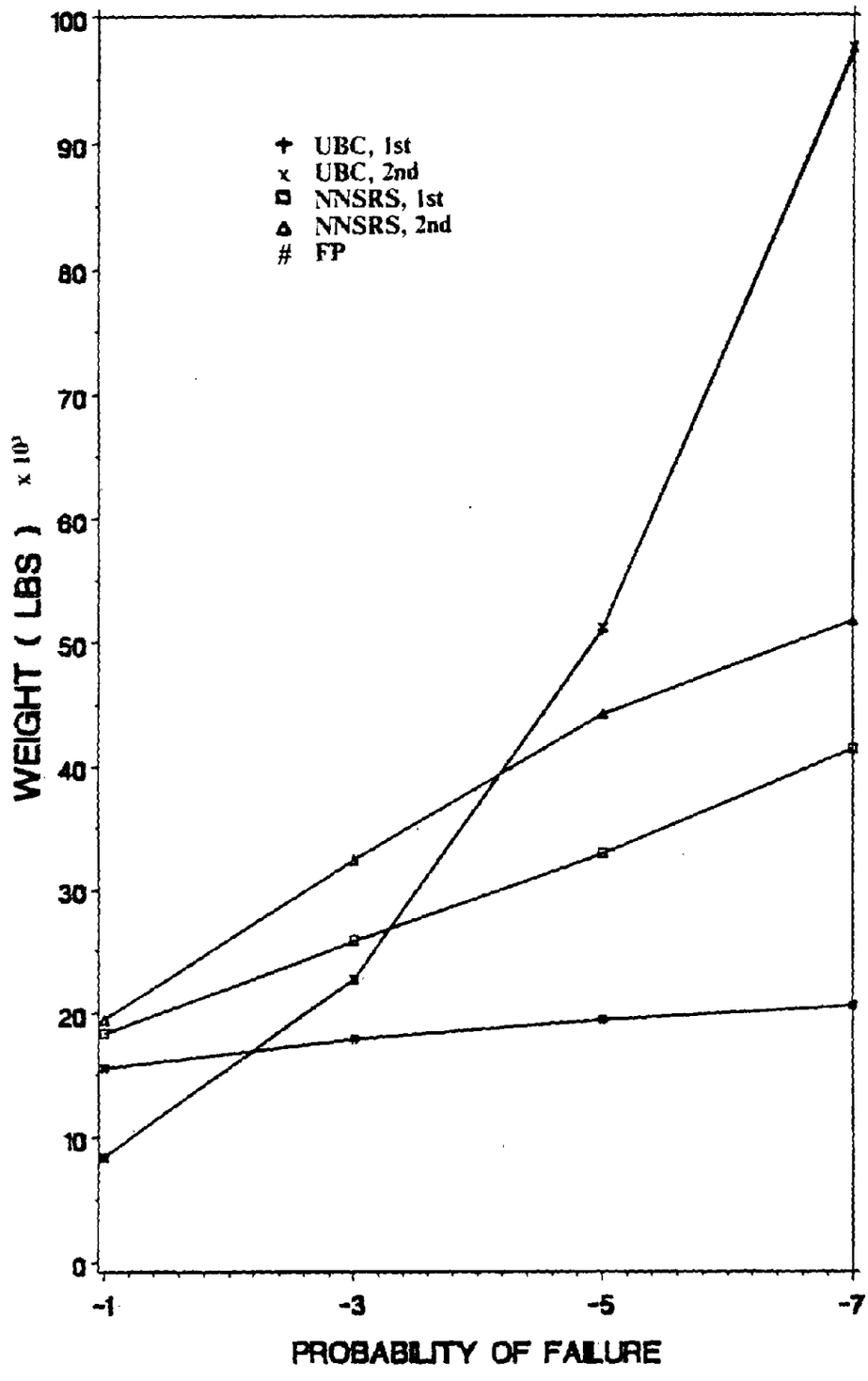

Figure 136. Optimum Weight for UBC, NNSRS, and Stationary with MW and LN of 2-Story Building. (1 lb = 4.45 N)

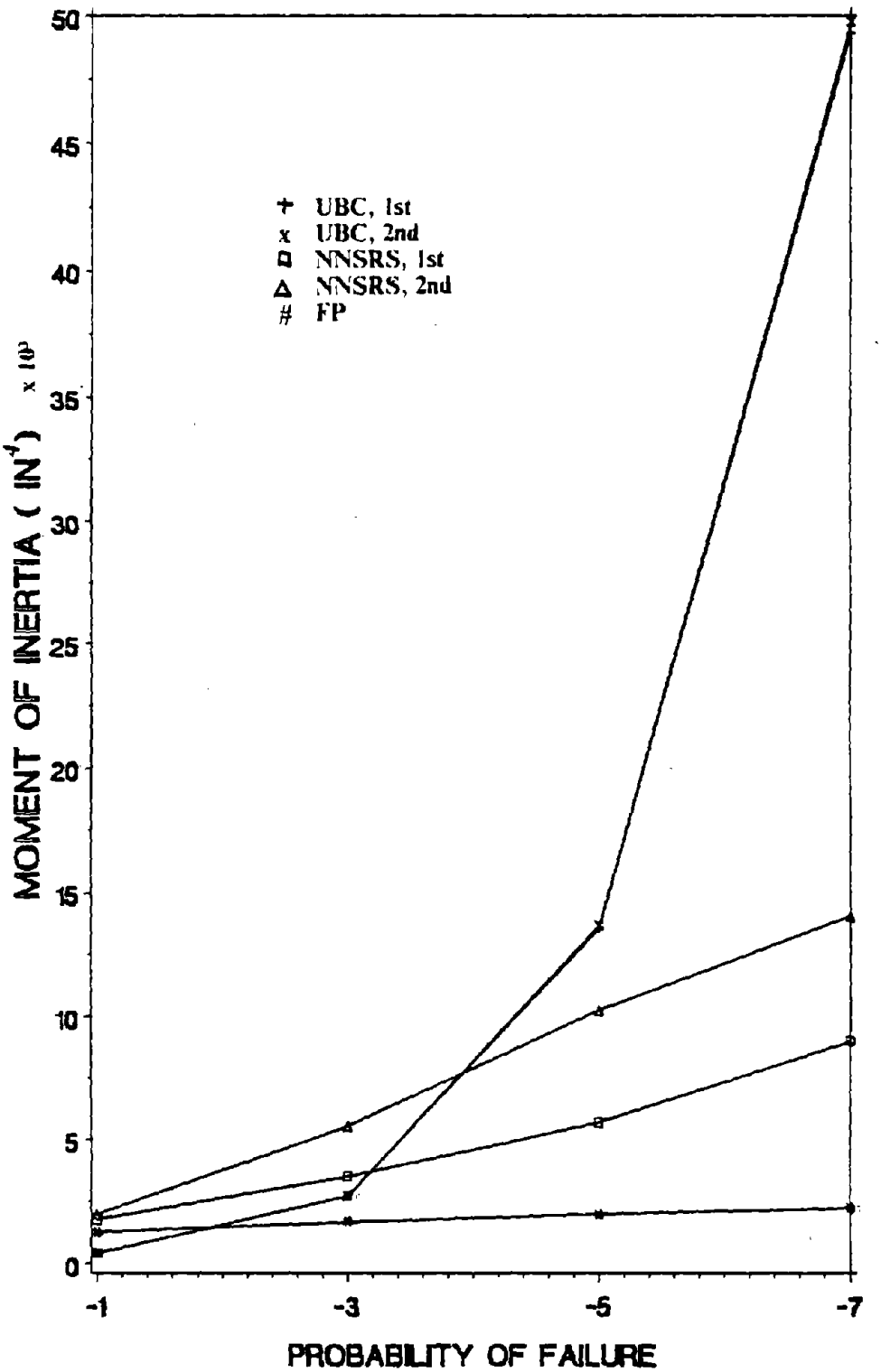

Figure 137. I_1 for UBC, NNSRS, and Stationary with MW and LN of 2-Story Building. (1 in = 2.54 cm)

with lognormal distribution from large to small values is in the sequence of NNSRS, Stationary, UBC at $P_{f0} = 10^{-1}$; of NNSRS, UBC, Stationary at $P_{f0} = 10^{-3}$; of NNSRS, UBC, Stationary at $P_{f0} = 10^{-5}$; and of UBC, NNSRS, Stationary at $P_{f0} = 10^{-7}$. The order of magnitude with normal distribution from large to small values is in the sequence of NNSRS, FP, UBC at $P_{f0} = 10^{-1}$ to 10^{-7}.

D. EFFECTS OF COST FUNCTION ON SENSITIVITY STUDY.

The same observations for sensitivy studies of two ratios, C_{in} and C_{VL}, employed in the study of UBC load are used herein. The optimum cost and the moments of inertia are shown in Figures 138 and 139 for the two-story shear building for three C_{in} values with modified white noise spectrum and first passage expression. The optimum costs and the moments of inertia are shown in Figures 140 to 142 for the ten-story shear building for the assumed C_{in}, seismic input spectrum, and failure expression used for the two-story shear building. The results on both structures reveal that the moments of inertia do not change for different values of C_{in}. Since nonstructural member cost is not involved in the computation of probabilities of failures and future failure losses, the change of nonstructural member cost does not affect the change of structural members.

The optimum cost given Figure 143 and the moment of inertia in Figure 144 for the two-story shear building are obtained for three C_{VL} values with modified white noise spectrum and first passage equation. The optimum costs given in Figure 145 and the moments of inertia in Figures 146 and 147 for the ten-story shear building are obtained for same C_{VL} values, seismic spectrum, and failure expression used for the two-story shear building. The results on both structures show that the optimum costs and moments of inertia do not change for different C_{VL} values at high reliability level. This is because that the future failure loss is small when high reliability criteria are employed in the design.

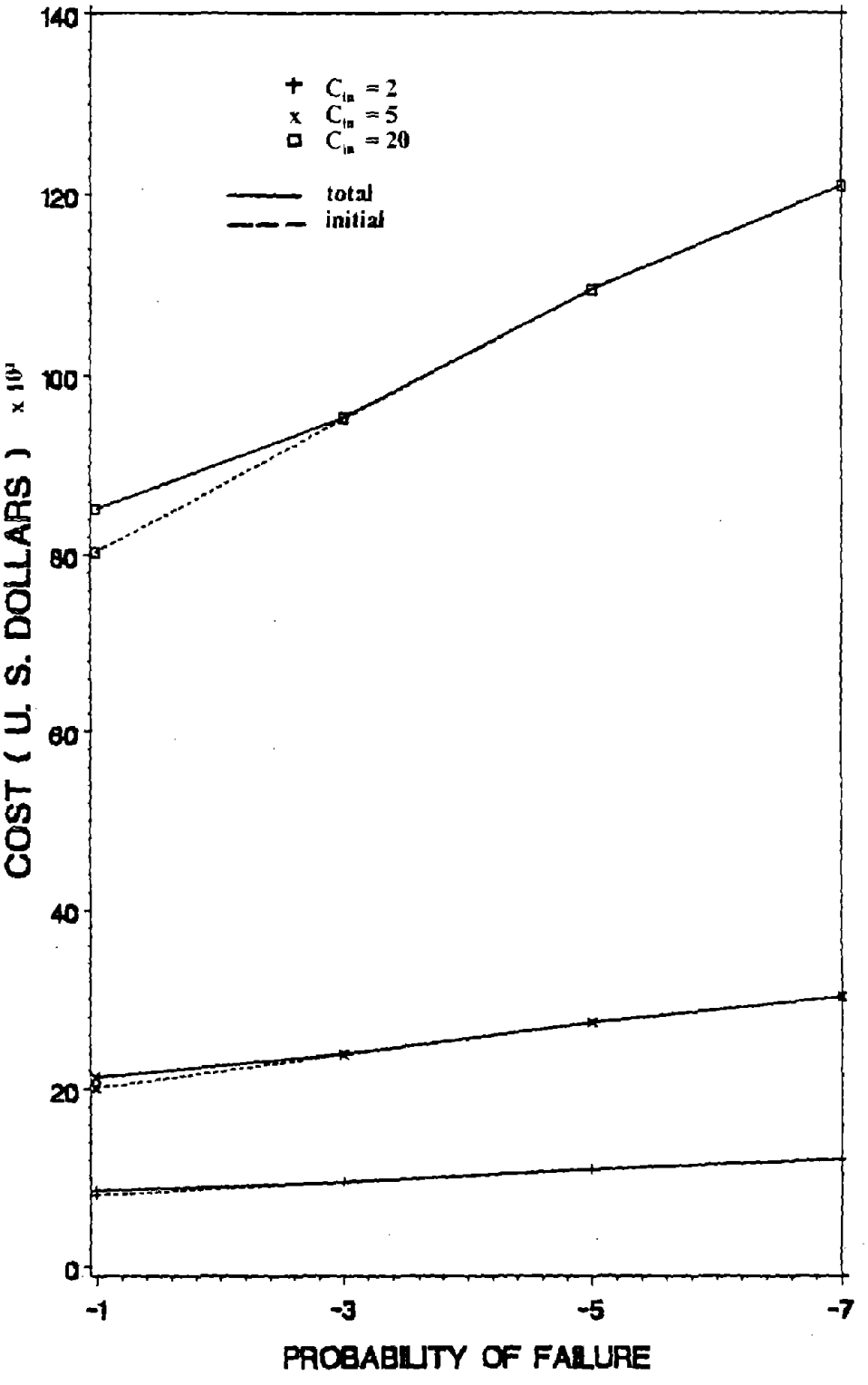

Figure 138. Optimum Cost for Various C_{in} with MW and FP of 2-Story Building.

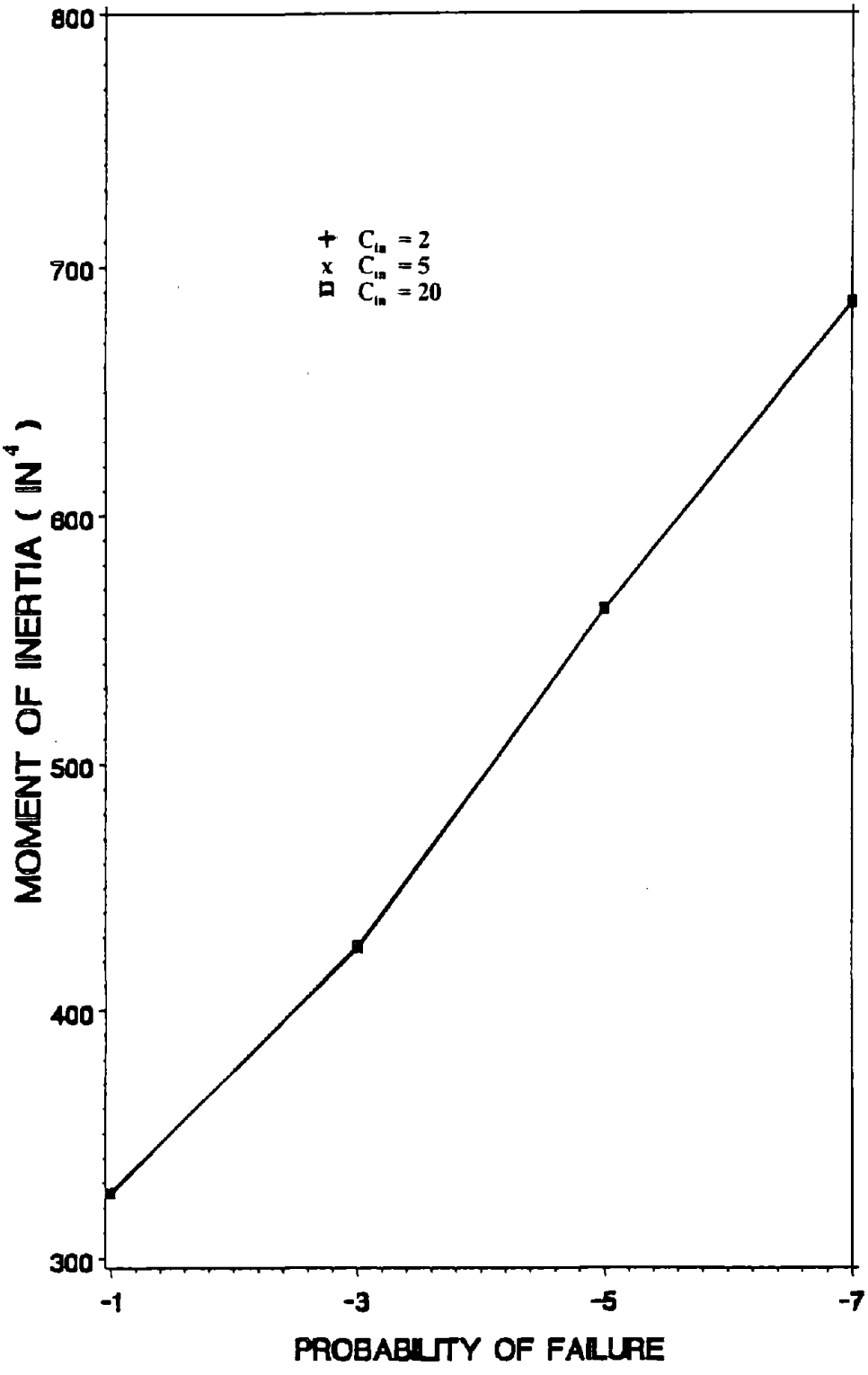

Figure 139. I_1 for Various C_{in} with MW and FP of 2-Story Building. (1 in = 2.54 cm)

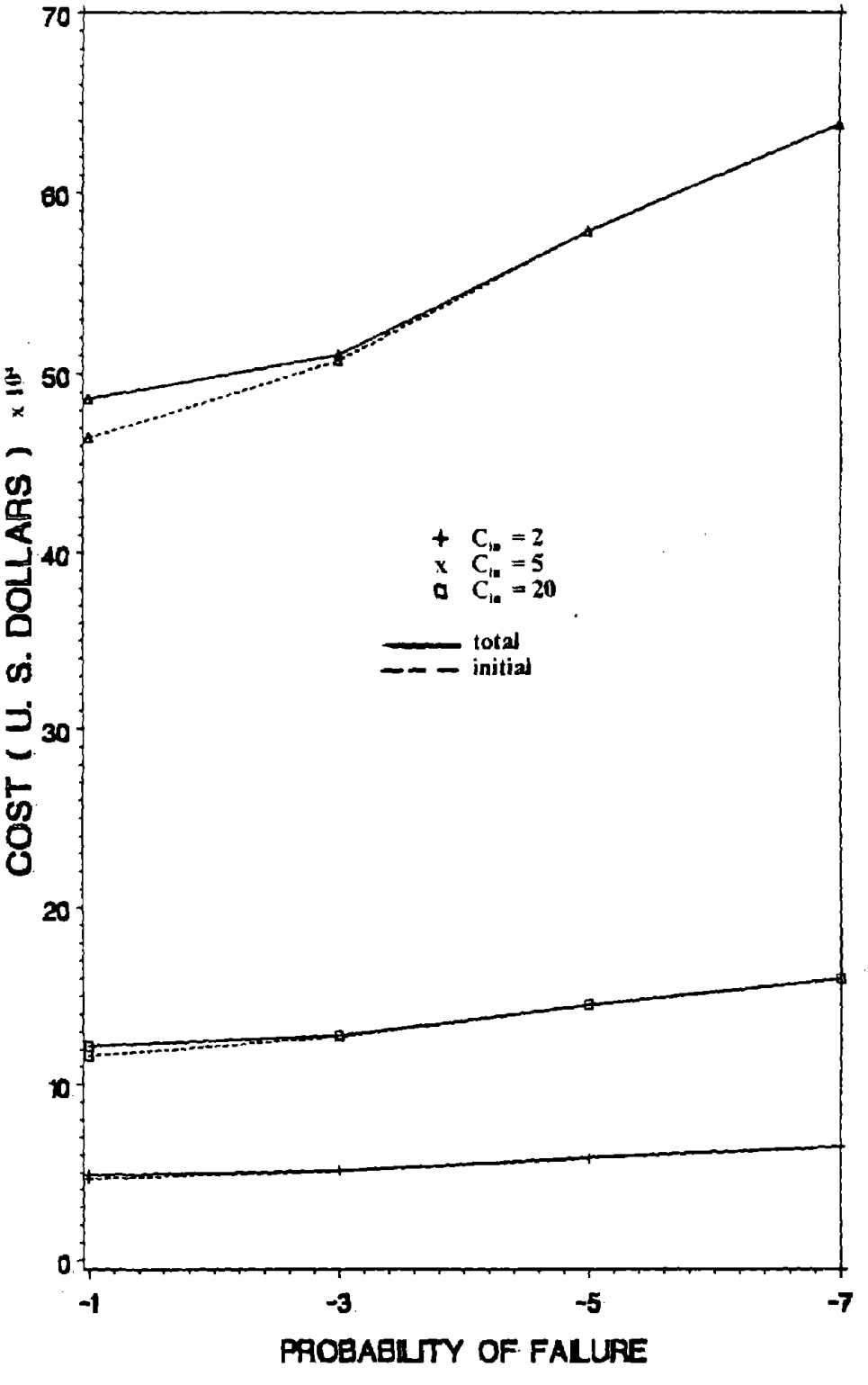

Figure 140. Optimum Cost for Various C_{in} with MW and FP of 10-Story Building.

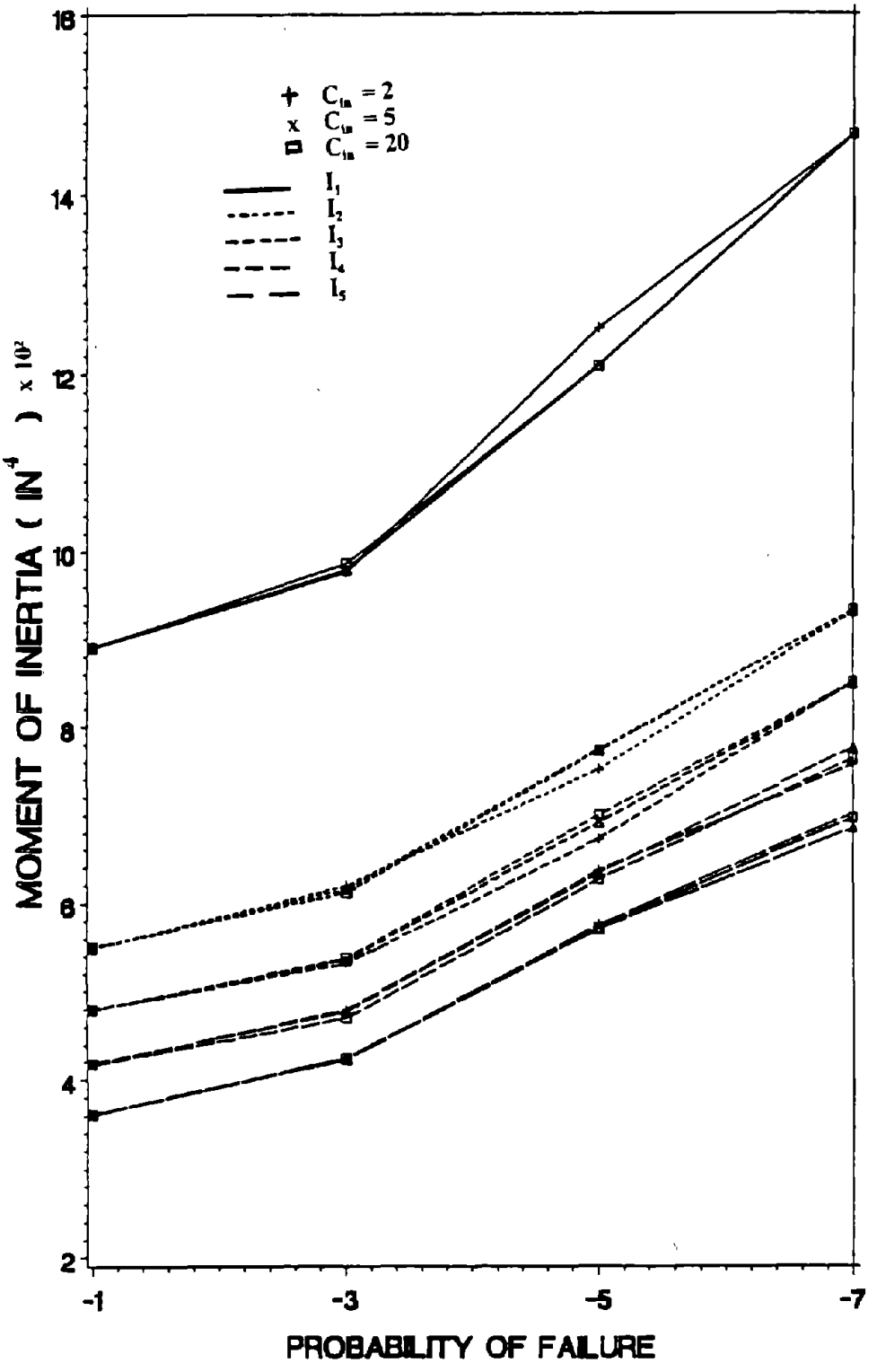

Figure 141. I_1 - I_5 for Various C_{in} with MW and FP of 10-Story Building. (1 in = 2.54 cm)

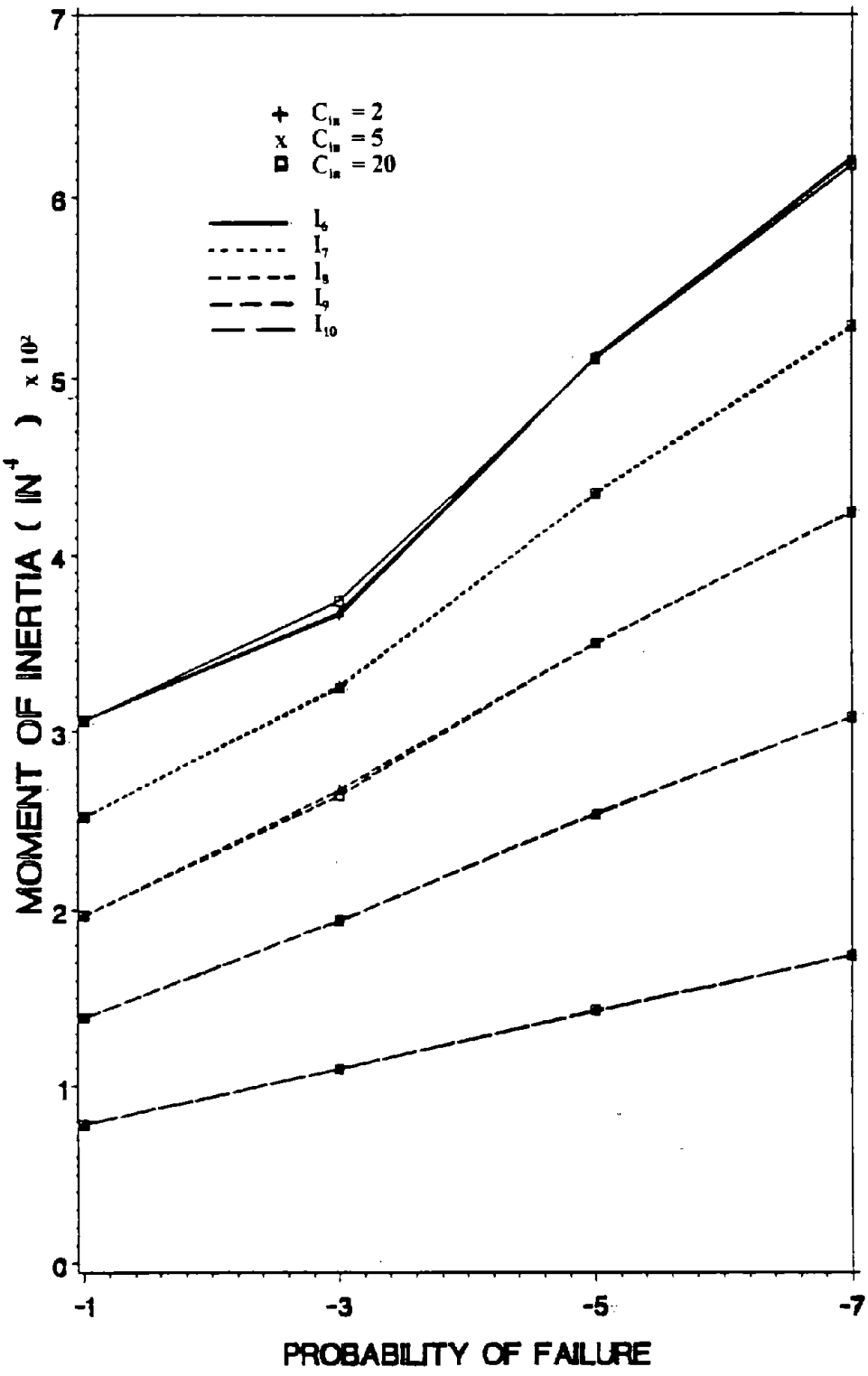

Figure 142. I_6 - I_{10} for Various C_{in} with MW and FP of 10-Story Building. (1 in = 2.54 cm)

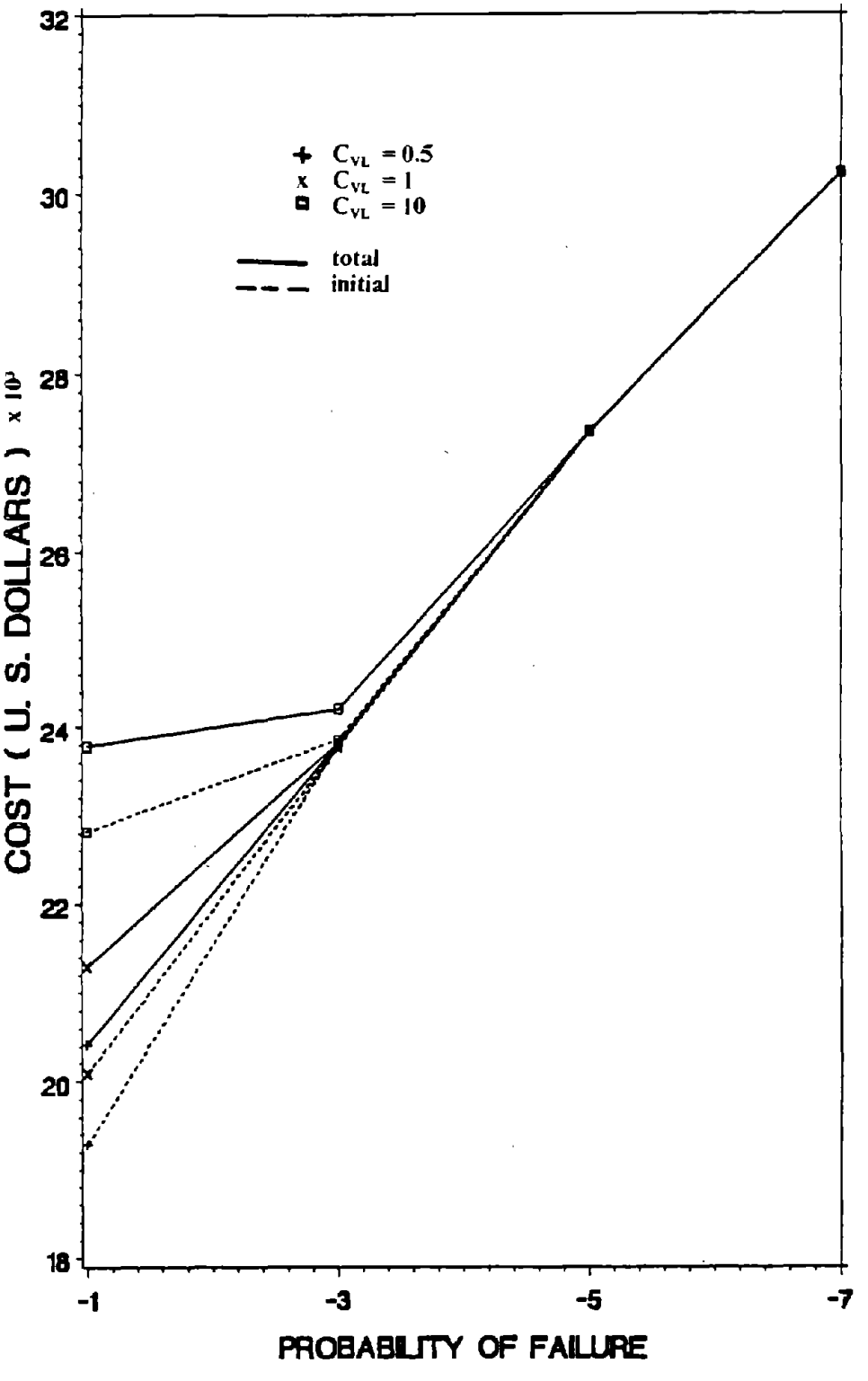

Figure 143. Optimum Cost for Various C_{VL} with MW and FP of 2-Story Building.

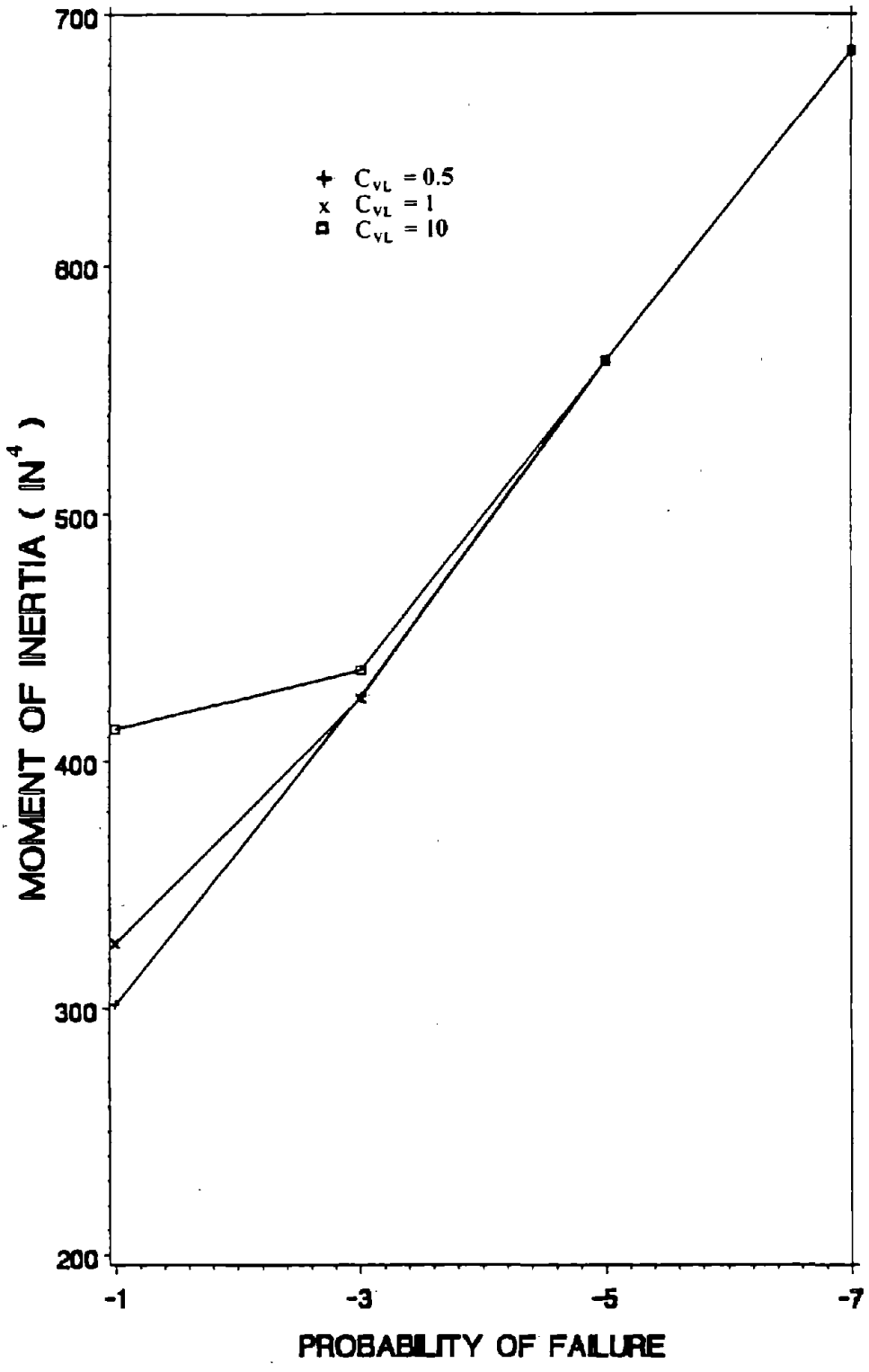

Figure 144. I_1 for Various C_{VL} with MW and FP of 2-Story Building. (1 in = 2.54 cm)

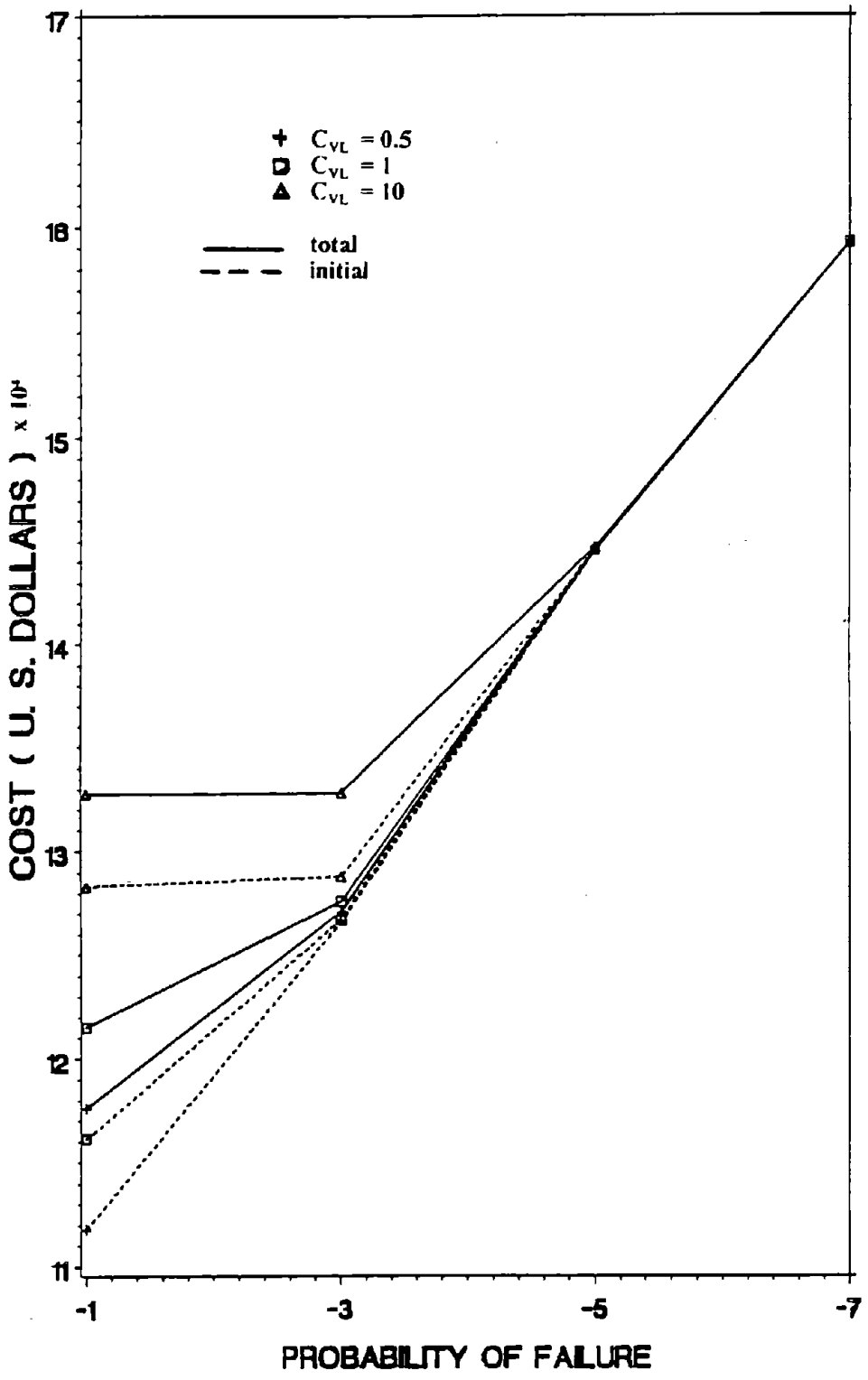

Figure 145. Optimum Cost for Various C_{VL} with MW and FP of 10-Story Building.

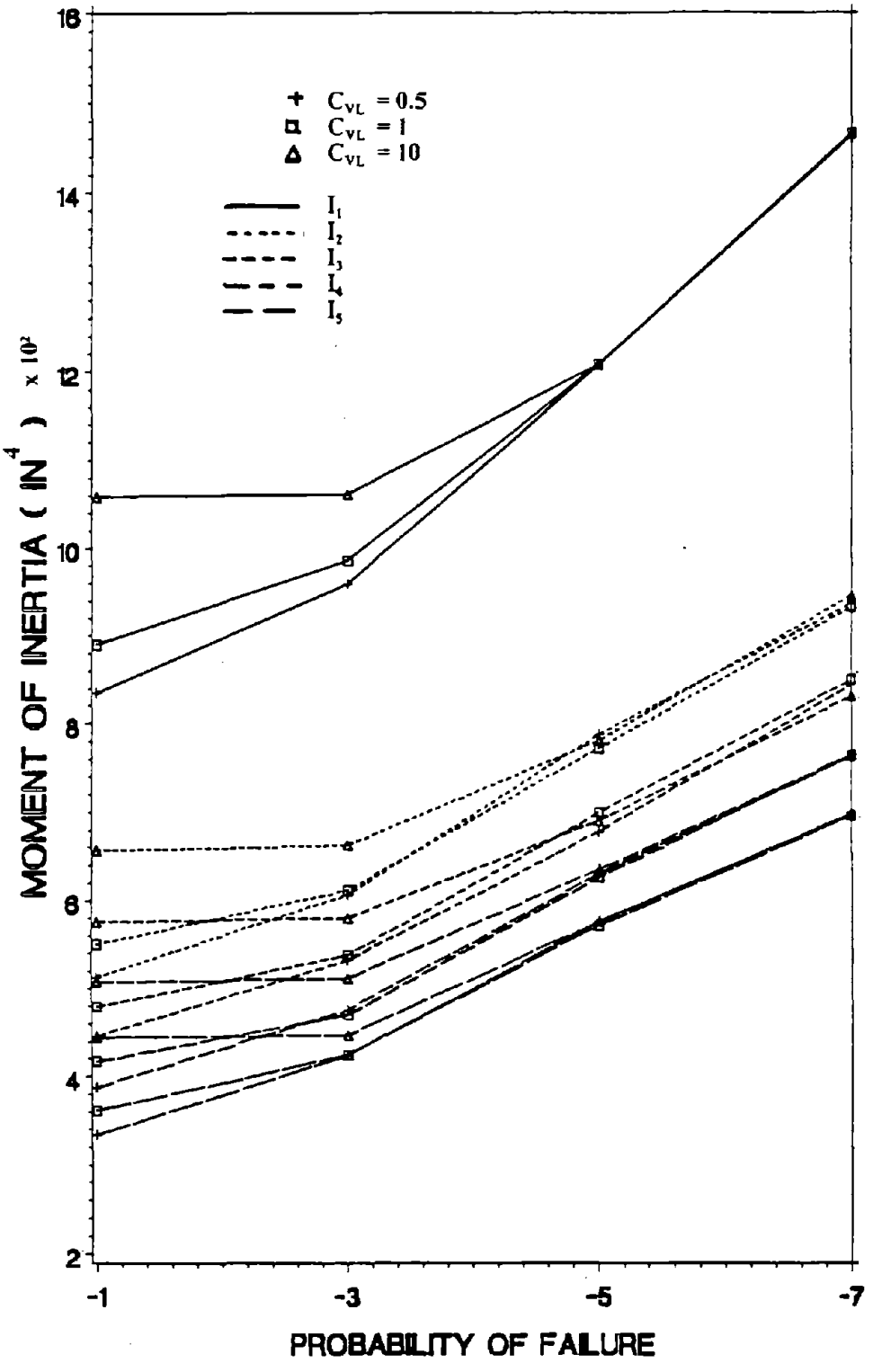

Figure 146. I_1 - I_5 for Various C_{VL} with MW and FP of 10-Story Building. (1 in = 2.54 cm)

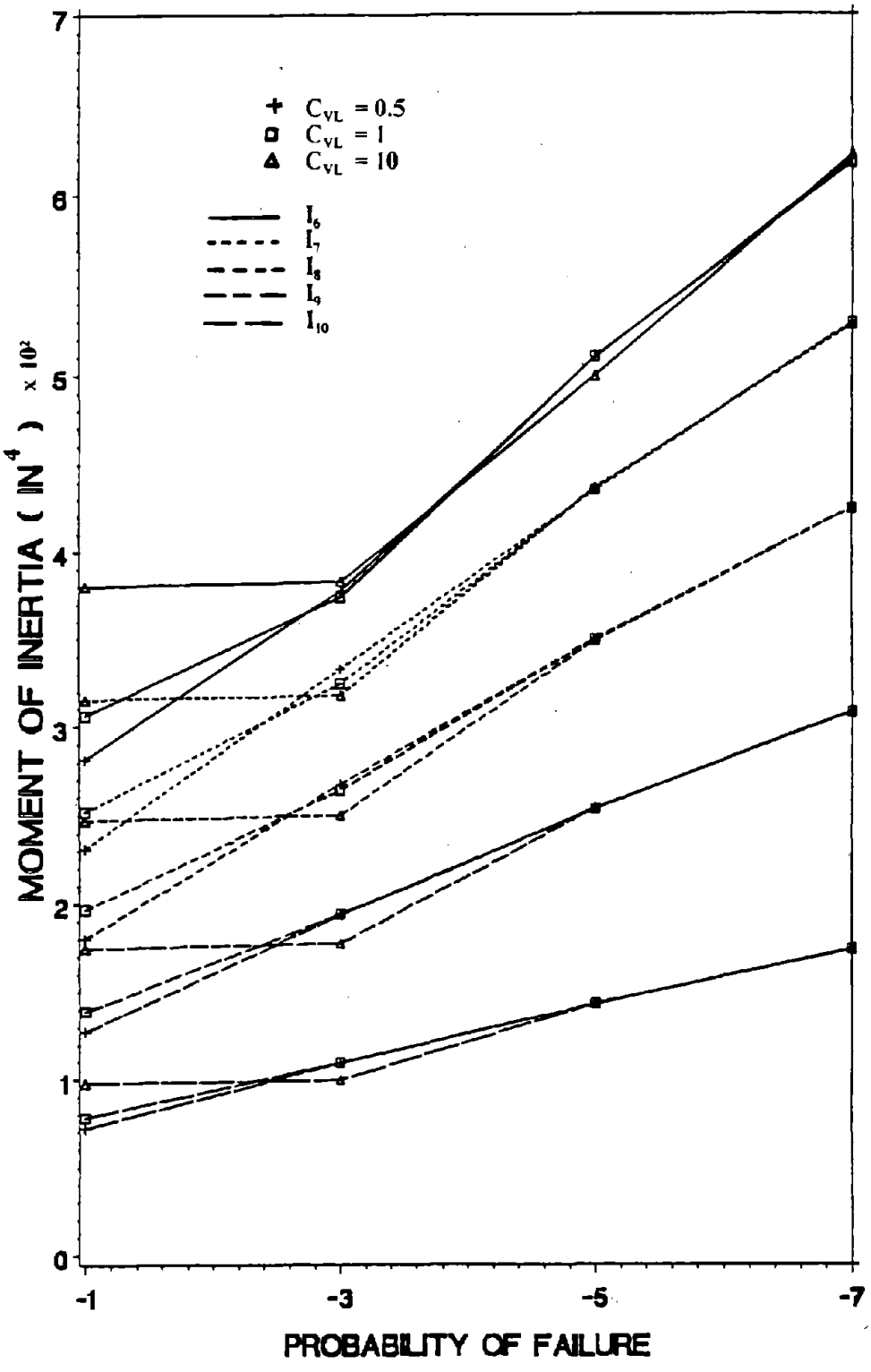

Figure 147. I_6 - I_{10} for Various C_{VL} with MW and FP of 10-Story Building. (1 in = 2.54 cm)

E. COMPARISON OF SYSTEM FAILURE PROBABILITY FORMULATION IN COST OPTIMIZATION.

In Section IID, the exact system probability of failure is too complicate to obtain. However the upper and lower bound for this probability can be obtained. In this section the upper bound, which is the sum of all individual failure modes, and the lower bound, which is the maximum value among all individual failure modes, are used to investigate the range of exact system probability of failure may lie. The ten-story shear building structure is used. The values of C_{in}, 5, and C_{VL}, 1, are assumed to represent the cost function. The unit cost is 0.15 dollars / in^3.

The total cost in Figure 148 and the moment of inertia in Figure 149 for modified white noise spectrum and first passage expression show that the differences between maximum and minimum bound are large at low reliability. These differences reduce when the allowable reliability increases. At $P_{f0} = 10^{-1}$ the optimum total costs are \$121528.7 in maximum bound system failure probability and \$111224.5 in minimum bound system failure probability. At $P_{f0} = 10^{-7}$ the optimum total costs are \$159248.1 in maximum bound system failure probability and \$159243.9 in minimum bound system failure probability.

F. COMPARISON OF MOMENT OF INERTIA IN COST AND WEIGHT OPTIMIZATION.

In spite of different objective functions between cost and weight, the comparison of moment of inertia for these two functions may be used to see the differences of optimum design sections. The ten-story shear building, modified white noise spectrum, and first passage expression are used. The values of C_{in}, 5, and C_{VL}, 1, are assumed to represent the cost function. The unit cost is 0.15 dollars / in^3.

In Figures 150 to 152, there are differences of moments of inertia between cost and weight optimization at low reliability. The differences reduce as reliabilities increase. At $P_{f0} = 10^{-1}$ the moments of inertia for column 1 is 606.4 in^4 (25240.2 cm^4) in weight optimization and

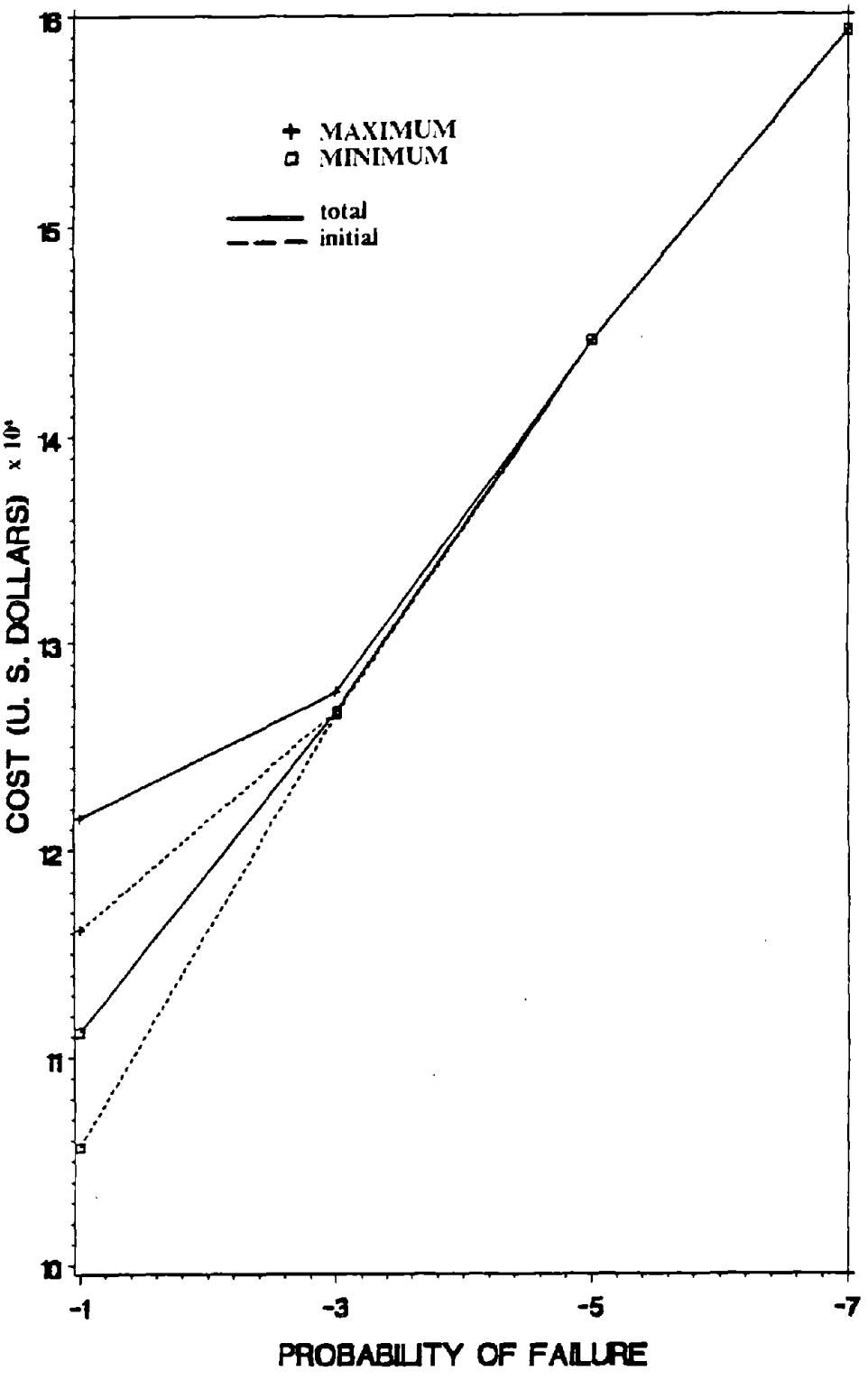

Figure 148. Cost for Maximum and Minimum System Failure with MW and FP of 10-Story Building.

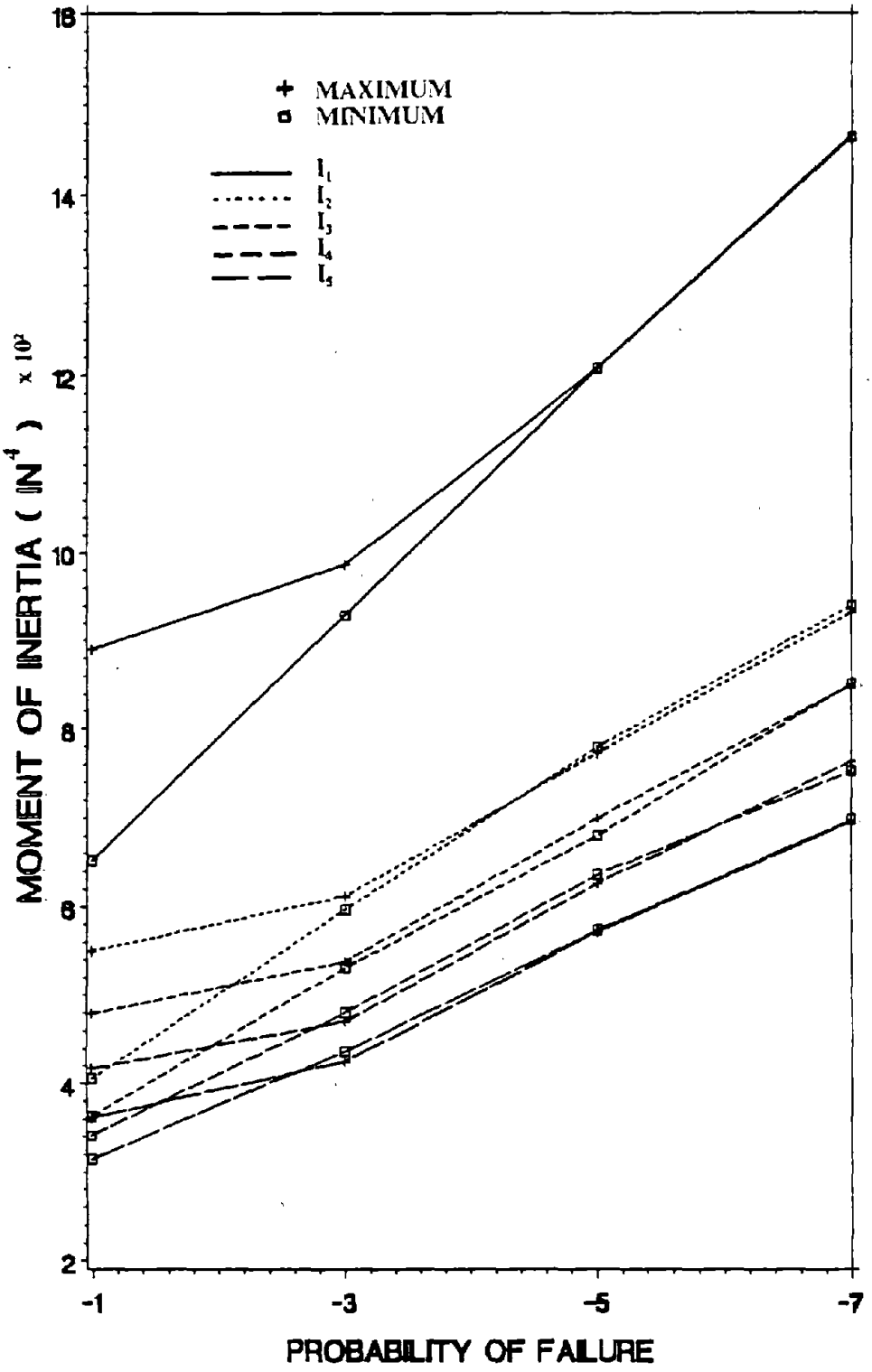

Figure 149. I_1 - I_5 for Maximum and Minimum System Failure with MW and FP of 10-Story Building. (1 in = 2.54 cm)

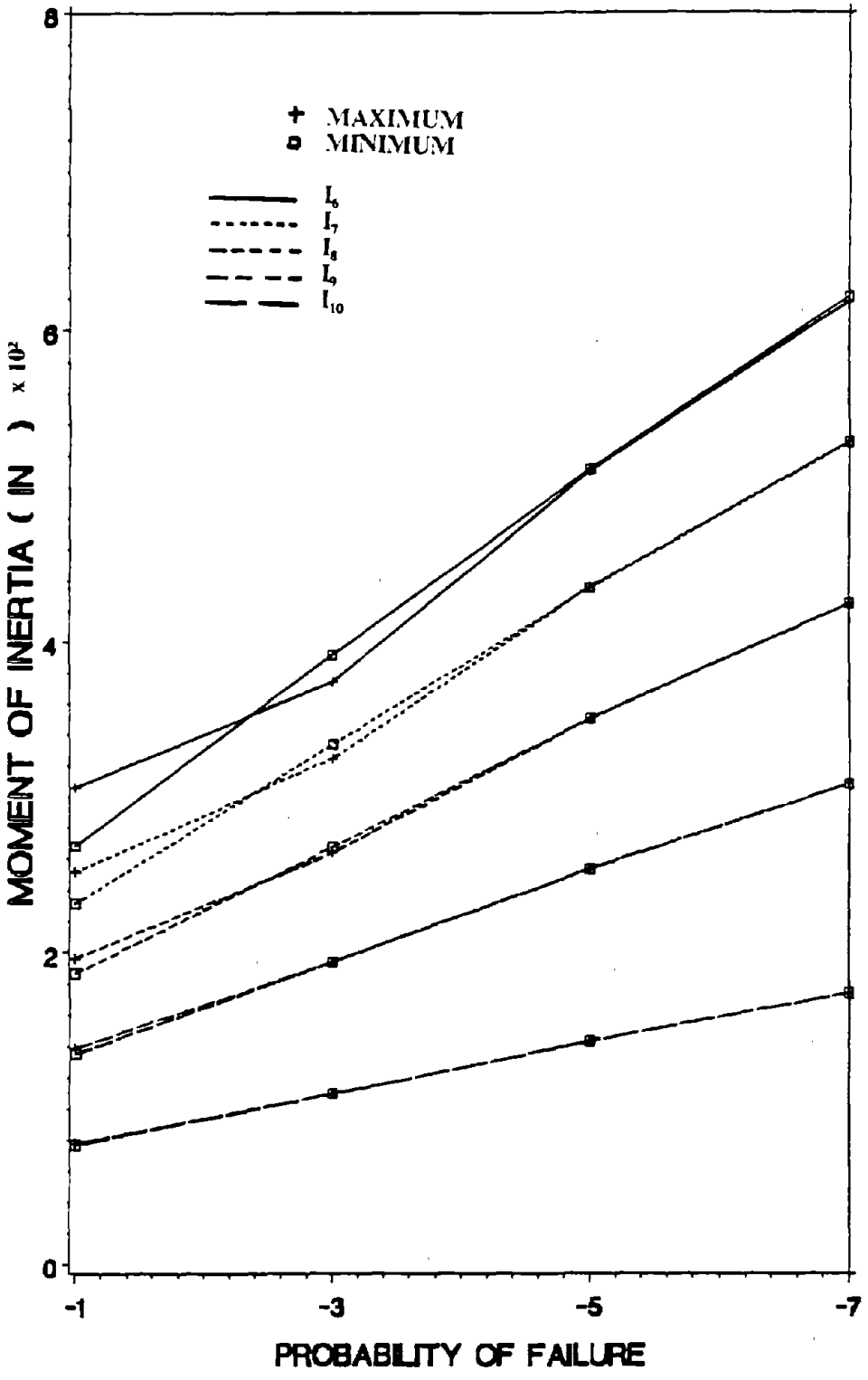

Figure 150. I_6 - I_{10} for Maximum and Minimum System Failure with MW and FP of 10-Story Building. (1 in = 2.54 cm)

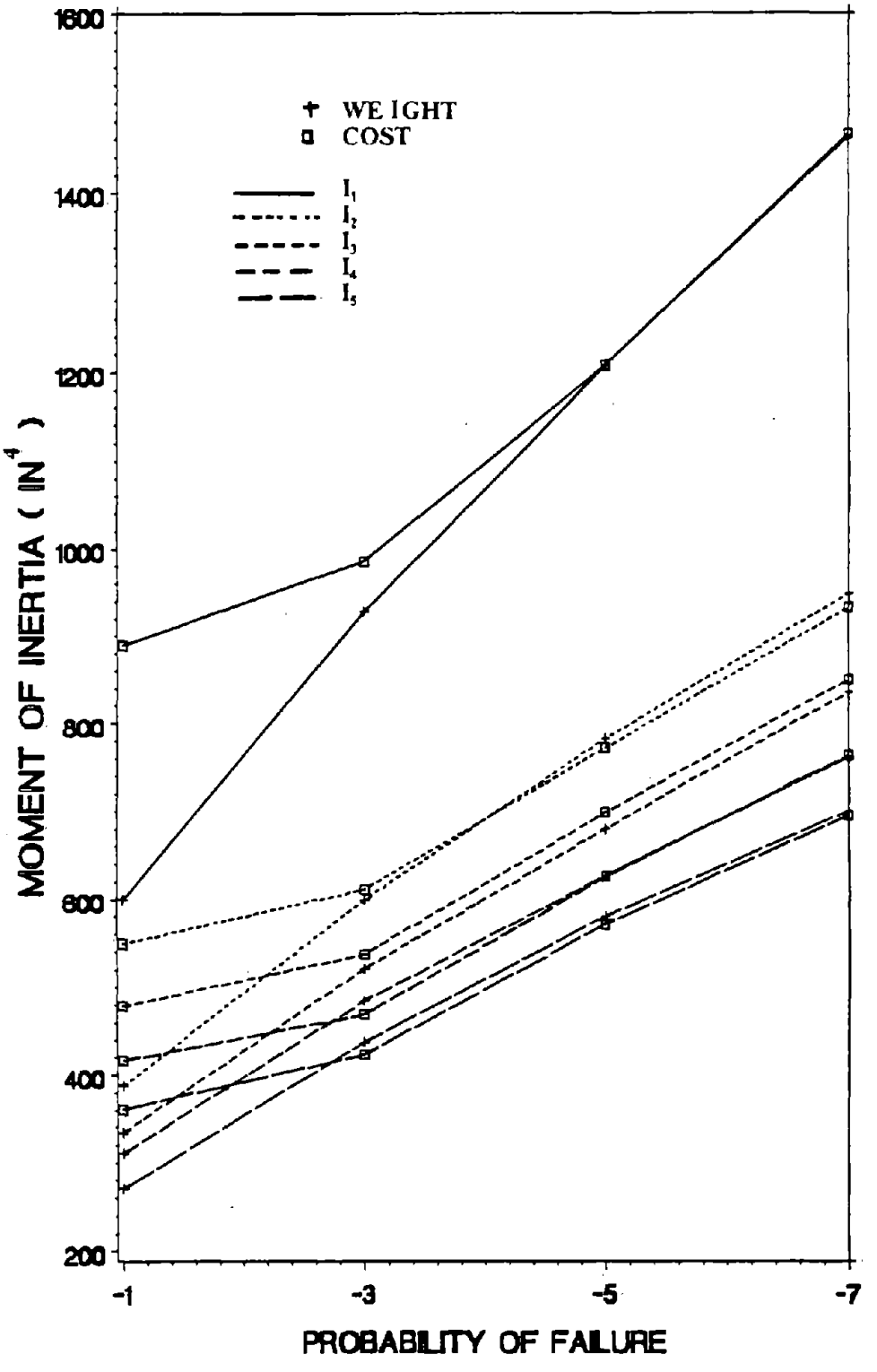

Figure 151. I_1 - I_5 for Weight or Cost Function with MW and FP of 10-Story Building. (1 in = 2.54 cm)

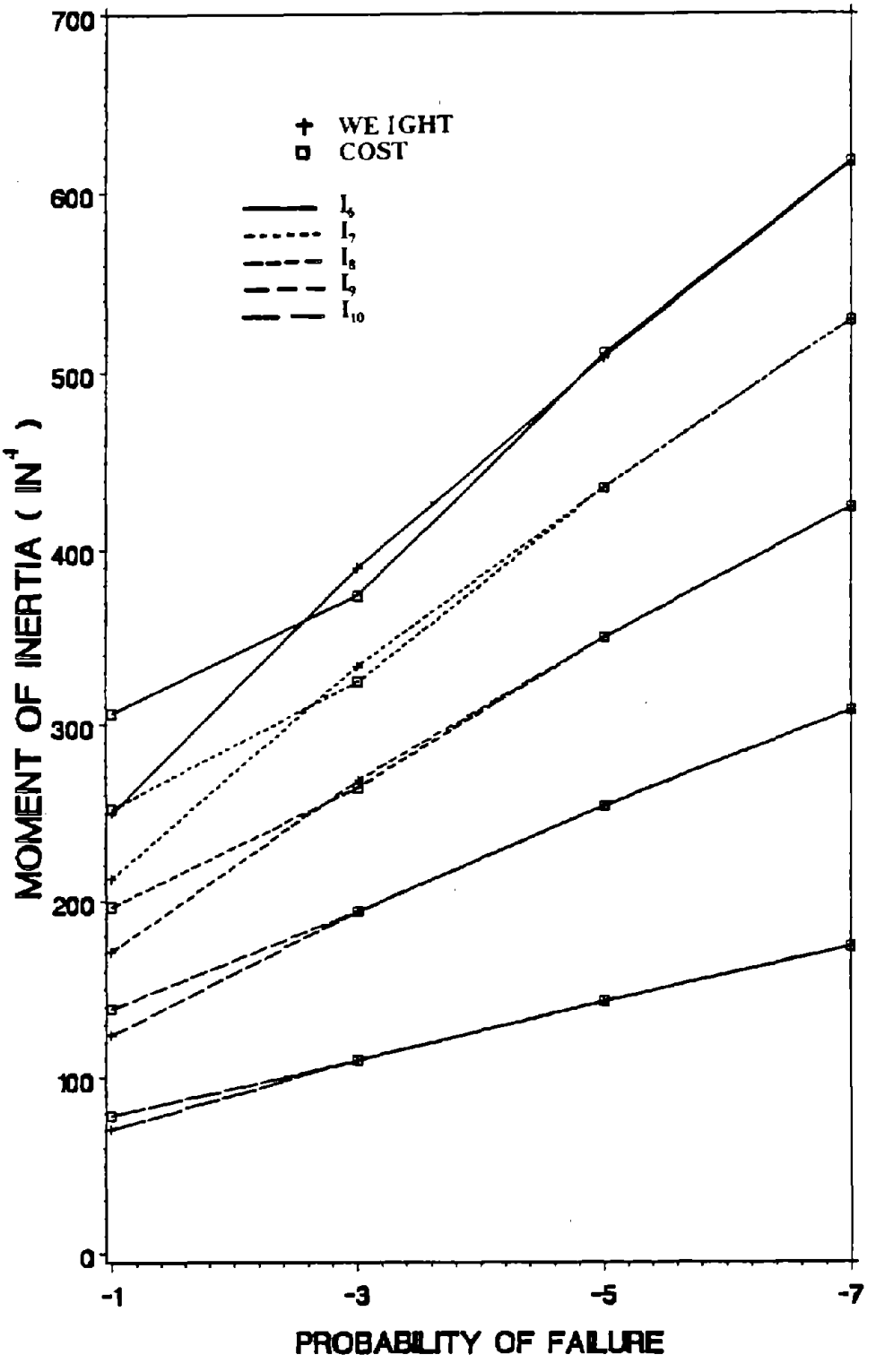

Figure 152. I_6 - I_{10} for Weight or Cost Function with MW and FP of 10-Story Building. (1 in = 2.54 cm)

889.3 in^4 (37015.4 cm^4) in cost optimization. At $P_{f0} = 10^{-7}$ the moments of inertia for column 1 are 1462.5 in^4 (60873.8 cm^4) in weight optimization and 1466.2 in^4 (61027.8 cm^4) in cost optimization.

G. SUMMARIES

1. The results for modified white noise seismic spectrum are the heaviest design.

2. The results for modified white noise spectrum and filtered white noise spectrum are close.

3. The order of optimum solution for five failure probability expressions from large to small is in different sequential order for different reliability levels.

4. The results of NNSRS at all reliabilities with normal distribution and at low reliabilities with lognormal distribution is the heaviest design among UBC, NNSRS, and stationary seismic process. The results of UBC at high reliability with lognormal distribution is the heaviest design among UBC, NNSRS, and stationary seismic process.

5. The moments of inertia do not change with C_{in} at all reliabilities and with C_{VI} at high reliabilities.

6. There is a difference of cost between system maximum and minimum bound at low reliability; the difference reduces as reliability increases.

7. There is a difference of moments of inertia between cost and weight objective function at low reliability; the difference reduces as reliability increases.

XII. CONCLUSIONS

Four live load models are used to investigate their optimum design results. The magnitude from large to small for dead load plus live load with two distributions and two variance approaches is in the sequential order of UNREDUCED, UK, NBS, and ANSI. The magnitude from large to small for dead load plus live and UBC loads is in different sequential order for different variance approaches and probability distributions.

The sensitivities of variations of yielding moment and critical moment are studied for UBC seismic load and NNSRS approach. For UBC seismic load with no variation, the optimum design results are not sensitive to the change of variation of yield moment when V_{M_y} is less than 0.15; the optimum designs change when $V_{M_{cr}}$ changes; no sensitivities of coefficient of variation of yield moment and critical moment can be observed for high variation of UBC. For NNSRS approach with no variation of peak ground acceleration, the optimum design results are sensitive to the variation of yield moment and not sensitive to the variation of critical moment.

For UBC loading, the demand of optimum design with lognormal distribution is heavier than that with normal distribution; the 2nd variance approach requires heavier design than the first variance approach; the optimum weight and moments of inertia are sensitive to the variation of UBC and the increase with lognormal distribution is very fast at high variation value. The optimum design discrepancy among four earthquake zone coefficients in UBC increases with allowable reliability level.

For NNSRS approach, the 2nd variance approach requires heavier design than the first variance approach; the optimum weight and moments of inertia are sensitive to the variation of peak ground acceleration and the increase with lognormal distribution is very fast at high variation. The vertical ground acceleration effects can significantly influence the optimum solutions.

Investigation of the structure subjected to stationary process with three seismic spectra and five failure expressions reveals that the optimum designs of modified white noise spectrum are the conservative designs and close to those of filter white noise spectrum. The optimum designs of the safety factor expression with Davenport's equation are the conservative designs at lower reliability levels and the optimum designs of the first passage expression are the conservative designs at higher reliabilities.

Comparing with three types of seismic loadings of UBC, NNSRS, and stationary process with seismic input spectrum, the designs for NNSRS approach are the conservative designs at low reliability.

For UBC and stationary seismic processes, the moments of inertia do not change for different ratios of C_{in} because the change of nonstructural members cost does not affect the computation of failure probabilities and future losses. The optimum cost is not sensitive to the ratio of C_{VL} at higher reliability because the value of future failure loss is small at high reliability criteria.

For stationary seismic processes, there are the differences of optimum designs between maximum and minimum bound of system failure probability at low reliability; and the differences decrease with reliability level. The designs for cost function require heavier sections than those for weight function at low reliability. At higher reliability level, this difference becomes very small.

BIBLIOGRAPHY

1. Ahmadi, G., "Bounds on Earthquake Response of Structures," J. of Engineering Mechanics Div., ASCE, Vol. 112, No. 4, April, 1986, pp. 351-369.

2. Ang, A. H-S. and Amin, M., "Reliability of Structures and Structural Systems," J. of Engineering Mechanics, ASCE, Vol. 94, No. EM2, April, 1968, pp. 671-691.

3. Ang, A. H-S., "Structural Risk Analysis and Reliability Based Design," J. of Structural Div., ASCE, Vol. 99, No. ST9, September, 1973, pp. 1891-1910.

4. Ang, A. H-S. and Cornell, C. A., "Reliability Bases of Structural Safety and Design," J. of Structural Div., ASCE.,Vol. 100, No. ST9, Sept.,1974, pp. 1755-1769.

5. Applied Technology Council, Tentative Provisions for the Development of Seismic Regulations for Buildings, ATC-3-06, National Bureau of Standards, Washington D. C., 1978; also BSSC (1985).

6. Arora, J. S. and Haug, E. J., "Methods of Design Sensitivity Analysis in Structural Optimization," AIAA J., Vol. 17, No. 9, September, 1979, pp. 970-974.

7. Austin, M. A., Pister, K. S., and Mabin, S. A., "Probabilistic Limit States Design of Moment-Resistant Frames Under Seismic Loading," Proc. of 3rd National Conf. on Earthquake Engineering, Vol. III, Charleston, S. Carolina, August 24-28, 1986, pp. 1709-1720.

8. Balling, R. J., Pister, K. S., and Polak, E., DELIGHT.STRUCT: A Computer-Aided Design Environment for Structural Engineering, Earthquake Engineering Research Center, Rept. UCB/EERC-81/19, Univ. California, Berkeley, Calif., December, 1981.

9. Balling, R. J., Ciampi, V., Pister, K. S., and Polak, E., Optimal Design of Seismic Resistant Planar Steel Frames, Earthquake Engineering Research Center, Rept. UCB/EER-81/20, Univ. California, Berkeley, Calif., December, 1981.

10. Balling R. J., Pister, K. S.,and Ciampi, V., "Optimal Seismic- Resistant Design of A Planar Steel Frame," Earthquake Eng. and Structural Dynamics, Vol. 11, 1983, pp. 541-556.

11. Batti, M. A. and Pister, K. S., "Application of Optimum Design to Structures Subjected to Earthquake Loading," in Optimization of Distributed Parameter Structural Systems, Vol. 1, Sijthoff and Hoordhoff International, 1981.

12. Bennett, J. and Botkin, M., "The Optimum Shape," Technology Illustrated, September 1983.

13. Belegundu, A. D. and Arora, J. S., "A Study of Mathematical Programming Methods for Structural Optimization Part I: Theory," Intl. J. for Num. Method in Engineering, Vol. 21, No. 9, Sept., 1985, pp. 1583-1599.

14. Belegundu, A. D. and Arora, J. S., "A Study of Mathematical Programming Methods for Structural Optimization Part II: Numerical Results," Intl. J. for Num. Method in Engineering, Vol. 21, No. 9 , Sept., 1985, pp. 1601-1623.

15. Blume, J. A. and Monroe, R. F., "The Spectral Matrix Method of Predicting Damage from Ground Motion," John A. Blume and Associates Research Div., Nevada Operations Office of the U.S. Atomic Energy Commission, Las Vegas, Nev., 1971.

16. Borges, J. F., "Qualification of Design Rules Based on the Assessment of Earthquake Risk," Proc. 5th World Conf. on Earthquake Engineering, Rome, Italy, 1973.

17. Botkin, M. E., "Shape Optimization of Plate and Shell Structures," Proc. 22nd Structures, Structural Dynamics, and Materials Conf., Sponsored by AIAA, ASME, ASCE, and AHS, Atlanta, Ga., April, 1981.

18. Bycroft, G. N., "White Noise Representation of Earthquakes," J. of Engineering Mechanics Div., ASCE, Vol. 86, No. EM2, April, 1960 , pp. 1-16.

19. Cartwrigit, D. and Longuet-Higgins, "Statistical Distribution of the Maxima of Random Function," Proc. Roy. Soc. A., Vol. 237, 1956.

20. Cheng, F. Y. and Botkin, M. E., "P-Δ Effect on Optimum Design of Dynamic Tall Buildings," Proc. ASCE-IABSE Joint Reg. Conf. on Tall Buildings, Bangkok, Thailand, January, 1974, pp. 621-632.

21. Cheng, F. Y., Venkayya, V. B., and Khachaturian, N., et al., Computer Methods of Optimum Structural Design, Vols. 1 and 2, University of Missouri-Ralla, Rolla, Mo., 1976.

22. Cheng, F. Y. and Botkin, M. E., " Nonlinear Optimum Design of Dynamic Damped Frames," J. of Structural Div., ASCE., Vol. 102, No. ST3 , March, 1976, pp. 609-628.

23. Cheng, F. Y. and Srifuengfung, D., "Earthquake Structural Design Based on Optimality Criterion," in Earthquake Resistant Design, Vol. 5, Proc. 6th World Conf. on Earthquake Engineering, New Delhi, India, January, 1977.

24. Cheng, F. Y., "Evaluation of Frame Systems Based on Optimality Criteria with Multicomponent Seismic Inputs, Performance Constraints, and P-Δ Effect," in Optimization of Distributed Parameter Structural Systems, Vol. 1, Sijthoff and Noordhoff International, 1981, pp. 650-684.

25. Cheng, F. Y. and Srifuengfung, D., "Optimum Design for Simultaneous Multicomponent Static and Dynamoc Input," Intl. J. Numerical Methods in Engineering, Vol. 13, 1981, pp. 353-371.

26. Cheng, F. Y., Srifuengfung, D., and Seng, L. H., ODSEWS -- Optimum Design of Static, Earthquake, and Wind Steel Structures, Natl. Sci. Found. Rept. U.S. Department of Commerce, NTIS, Springfield, Va., PB81-232738, January, 1981.

27. Cheng, F. Y., "Design Algorithms for Static and Dynamic Structures Based on Optimality Criteria," Proc. U.S.-China Workshop on Advances in Computational Engineering Mechanics, Dalian, China, 1983.

28. Cheng, F. Y. and Chang, C. C., "Optimality Criteria for Safety Based Design," Proc. of 5th ASCE Engineering Mechanics Div. Speciality Conf., Vol. 1, University of Wyoming, Laramie, Wyoming, Aug., 1984, pp. 54-57.

29. Cheng, F. Y. and Juang, D. S., "Assessment of ATC-03 for Steel Structures Based on Optimization Algorithm," Proc. of 8th World Conf. on Earthquake Eng., Vol. V, San Francisco, CA, July 21-28, 1984, pp. 435-442.

30. Cheng, F. Y. and Chang, C. C., "Optimum Design of Steel Building with Consideration of Reliability," Proceedings of the 4th International Conference on Structural Safety and Reliability, Kobe, Japan, Vol. 3, 1985, pp. 81-88.

31. Cheng, F. Y. and Truman, K. Z., Optimum Design of Reinforced Concrete and Steel 3-D Static and Seismic Building Systems with Assessment of ATC-03, Final Report Series 85-20 for the National Science Foundation, Available at U.S. Department of Commerce, National Technical Information Service, Springfield, Va 22151, NTIS Access No. PB87-168564/AS (414 pages).

32. Cheng, F. Y. and Chang, C. C., "Aseismic Structural Optimization with Safety Criteria and Code Provisions," Proc. of the US-Asia Conference on Engineering for Mitigating Natural Hazards Damage, Bangkok, Thailand, Dec., 1987, D8/1 - D8/12.

33. Cheng, F. Y. and Juang, D. S., "Assessment of Various Code Provisions Based on Optimum Design of Steel Structures," Journal of Earthquake Engineering and Structural Dynamics, Vol. 16, 1988, pp. 46-61.

34. Clough, R. W. and Penzien, J., Dynamics of Structures , New York, McGraw-Hill, 1975.

35. Cornell, C. A., "Bounds on the Reliability of Structural Systems," J. Structural Div., ASCE, Vol. 93, No ST1 ,Feb., 1967, pp. 171-200.

36. Cornell, C. A., "Engineering Seismic Risk Analysis," Bulletin of the Seismological Society of America, Vol. 58, 1968, pp. 1583-1600.

37. Cornell, C. A., "A Probability-Based Structural Code," J. of the American Concrete Institute, Vol. 66, No. 12, Dec., 1969, pp. 974-985.

38. Crandall, S. H. and Mark, W. D., Random Vibration in Mechanical Systems, Academic Press, New York and London, 1963.

39. Davenport, A. G., "Note on the Distribution of the Largest Value of a Random Value of a Random Function with Application to Gust Loading," Institution of Civil Engineers, Vol. 28, 1956.

40. Davidson, J. W., Felton, L. P., and Hart, G. C., "Optimum Design of Structures with Random Parameters," Computers & Structures, Vol. 7, 1977, pp. 481-486.

41. Davidson, J. W., Felton, L. P., and Hart, G. C., "Reliability-Based Optimization for Dynamic Loads," J. Structural Div., ASCE, Vol. 103, No. ST10, Oct., 1977, pp. 2021-2035.

42. Davidson, J. W., Felton, L. P., and Hart, G. C., "On Reliability -Based Optimization for Earthquake," Computers and Structures, Vol. 12, 1980, pp. 99-105.

43. 1978 Dodge Construction Systems Costs, McGraw-Hill Information Systems Company, 1978.

44. Ellingwood, B., and Ang, A. H-S., A Probabilistic Study of Safety Criteria for Design, Structural Res. Ser. No. 387, U. of Ill., 1972.

45. Ellingwood, B. and Culver, C., "Analysis of Live Loads in Office Buildings," J. of Structural Div., ASCE, Vol. 103, No. ST8, Aug., 1977, pp. 1551-1560.

46. Ellingwood, B. and Batts, M.E., "Characterization of Earthquake Forces for Probability-Based Design of Nuclear Structures," U.S. Regulatory Commission Report NUREG/CR-2945, Washington D.C., Sept., 1982.

47. Feng, T. T., Arora, J. S., and Haug, E. J., "Optimum Structural Design under Dynamic Loads," Intl. J. Num. Methods Eng., Vol. 11, 1977, pp. 39-52.

48. Fleury, C., "A Unified Approach to Structural Weight Minimization," Comp. Meth. Appl. Mech. Eng. 20(1), 1979, pp. 17-38; and Lecture on Modern Structural Optimization, NATO Advanced Study Institute, Belgium, 1981.

49. Freeman, J. R., Earthquake Damage and Earthquake Insurance, McGraw-Hill, N. Y., 1932.

50. Gallo, M. P., "Evaluation of Safety of Reinforced Concrete Buildings to Earthquakes," Ph.D. Thesis, Civil Eng. Dept., Univ. of Ill., 1971.

51. Grandori, G. and Benedetti, D., "On the Choice of the Acceptable Seismic Risk," in International Journal of Earthquake Engineering and Structural Dynamics, Vol. 2, No. 1, 1973, pp. 3-10.

52. Greene, M. R., Risk and Insurance, Southwestern Publishing, Cincinnati, Ohio, 1973.

53. Housner, G. W. and Jennings, P. C., "Generation of Artificial Earthquakes," J. of Engineering Mechanics Div., ASCE, Vol. 90, No. EM1, Feb., 1964, pp. 113-150.

54. Hwang, H., Kagami, S., Reich, M., Ellingwood, B., Shinozuka, and Kao, C. S., Probability Based Load Combination Criteria for Design of Concrete Containment Structures, U. S. Regulatory Commission Report NUREG/CR-3876, Washington D. C., March, 1985.

55. International Conference of Building Officials, Uniform Building Code, 1984 ed., Whittier, C. A., 1984.

56. Kanai, K., "Semi-empirical Formula for Seismic Characteristics of the Ground," Bull. of the Earthquake Research Institute, U. of Tokyo, 1957.

57. Kato, B., Nakamura, Y., and Anraku, H., "Optimum Earthquake Design of Shear Buildings," J. of Engineering Mechanics Div., ASCE, Vol. 98, No. EM4, 1972, pp. 891-910.

58. Kim, H. S. and Wen, Y. K., Reliability-Based Structural Optimization Under Stochastic Time Varying Loads, Civil Engineering Studies, Structural Research Series No. 533, University of Illinois at Urbana-Champaign, Urbana, Illinois, Feb., 1987.

59. Kiureghian, A. H. and Ang, A. H. S., "A Fault Rupture Model for Seismic Risk Analysis," Bull. Seis. Soc. Am., 1977.

60. Kiureghian, A. H., "Structural Response to Stationary Excitation," J. of Engineering Mechanics Div., ASCE, Dec., 1980.

61. Lev, O. E., (ed.), Structural Optimization: Recent Development and Applications, ASCE Publications, 1981.

62. Liu, S. C. and Neghabat, F., "A Cost Optimization Model for Seismic Design of Structures," Bell Tech. J., Vol. 51, 1972, pp. 2209-2225.

63. Liu, S. C., Dougherty, M. R., and Neghabat, F., "Optimal Aseismic Design of Building and Equipment," J. Engineering Mechanics Div., Am. Soc. Civil Engrs., Vol. 102, No. EM3, Proc. Paper 12208, June, 1976, pp. 395-414.

64. Mitchell, G. and Woodgate, R., "Floor Loadings in Office Buildings the Result of a Survey," Current Paper 3/71, Building Research Station, Garston, Watford, England, 1971.

65. Mohraz, B., Hall, W. ,and Newmark, N., "A Study of Vertical and Horizontal Earthquake Spectra," Div. of Reactor Standards, U. S. Atomic Energy Commission Washington, D. C., Dec., 1972.

66. NBS 577, Development of a Probability Based Load Criterion for American National Standard A58, National Bureau of Standards, June, 1980.

67. Noor, A. K., "Survey of Computer Programs for Solution of Nonlinear Structural and Mechanics Problems," in Computers and Structures, Vol. 13, 1981.

68. Pilkey, W., Saczalski, K., and Schaeffer, H., Structural Mechanics Computer Programs -- Survey, Assessment, and Availability, Univ. Press, Virginia, 1979.

69. Pister, K. S., "Optimal Design of Structures Under Dynamic Loading," NATO Advanced Study Institutes Series, Optimization of Distributed Parameter Structures, Vol. 1 (E. J. Haug and J. Cea, eds.), Sijthoff and Hoordhoff, 1981.

70. Portillo, M. and Ang, A. H. S., "Safety of Reinforced Concrete Buildings to Earthquakes," in Earthquake Resistant Design, Vol. 5, Proc. 6th World Conf. on Earthquake Engineering, New Delhi, India, January, 1977.

71. Prager, W. and Taylor, J. E., "Problems of Optimum Structural Design," J. Appl. Mech., Trans. Am. Soc. Mech. Engrs., Vol. 90, March, 1968, pp. 102-106.

72. Rao, S. S., "Reliability-Based Optimization Under Random Vibration Enviroment," Computers and Structures, Vol. 14, No. 5-6, March, 1981, pp. 345-355.

73. Ray, D., Pister, K. S., and Chopra, Optimal Design of Earthquake-Resistant Shear Building, Report EERC 74-3, Earthquake Engineering Research Center, Univ. of California, Berkeley, Calif., 1974.

74. Ray, D., Pister, K. S., and Polak, E., Sensitivity Analysis for Hysteretic Dynamic Systems: Theory and Applications, Report EERC 76-12, Univ. California, Berkeley, Calif., 1976.

75. Rice, S. O., " Mathematical Analysis of Random Noise, " Bell Tech., Vol. 18, 1944 and Vol. 19, 1945.

76. Rojiani, K. B., Evaluation of the Reliability of Steel Buildings to Wind Loadings, Ph. D. Thesis, Civil Eng. Dept., U. of Ill., 1978.

77. Roos, N. R. and Gerber, J. S., Governmental Risk Management Manual, Risk Management Publishing, Tucson, Arizon, 1976.

78. Rosenblueth, E. and Mendoza, E., "Optimum Seismic Design of Auditoriums," Proc. of 5th World Conf. on Earthquake Engineering , Vol. 2, Rome, Italy, 1973, pp. 2577-2585.

79. Rosenblueth, E., "Optimum Design to Resist Earthquakes," J. of Engineering Mechanics, ASCE, Vol. 105, No. EM1, Feb., 1979, pp. 159-176.

80. Rosenblueth, E., "Optimum Expenditures in Seismic Design," J. of Engineering Mechanics, ASCE, Vol. 105, No. EM1, Feb., 1979, pp. 177-187.

81. Rosenblueth, E., "On Computing Normal Reliabilities," Structural Safety, Vol. 2, No. 3, Jan., 1985, pp. 165-167.

82. Scawthorn, C., "Seismic Risk: State of Art," Proc. U.S.- Japan Cooperative Research on Seismic Risk Analysis and Its Application to Reliability-Based Design of Life-Line Systems, Honolulu, 1981, pp. 89-109.

83. Shinozuka, M. and Tan, R. Y., "Estimation and Optimization of the Serviceability of Underground Water Transmission Network Systems Under Seismic Risk," Proc. U.S.-Japan Cooperative Research on Seismic Risk Analysis and Its Application to Reliability-Based Design of Life-Line Systems, Honolulu, 1981.

84. Solnes, J. and Holst, O. L., "Optimization of Framed Structures under Earthquake Loads," Fifth World Conference on Earthquake Engineering, Rome, June, 1973.

85. Surahman, A. and Rojiami, K. B., "Reliability Based Optimum Design of Concrete Frames, " J. of Structural Div., ASCE, Vol. 109, No. 3, March, 1983, pp. 741-757.

86. Tajimi, H., "A Statistical Method of Determining the Maximum Response of a Building Structure During an Earthquake," Proc. 2nd world Conf. on Earthquake Engineering, Vol. 2, Tokyo, Japan, 1960.

87. Vanderplaats, G. N., "Comment on Methods of Design Sensitivity Analysis in Structural Optimization," AIAA J., Vol. 18, No. 11, November, 1980, pp. 1406-1407.

88. Vanmarcke, E. H., "Properties of Spectral Moments with Application to Random Vibration," J. of Engineering Mechanics Div., ASCE, Vol. 98, No. EM2, April, 1972, pp. 425-446.

89. Venkayya, V. B., "Design of Optimum Structures," Computers and Structures, Vol. 1, 1971, pp: 265-309.

90. Venkayya, V. B. and Cheng, F. Y., "Resizing of Frames Subjected to Ground Motion," Proc. of the International Symposium on Earthquake Structural Engineering, University of Missiouri-Rolla, Vol. 1, Aug., 1976, pp. 597-612.

91. Venkayya, V. B., Khot, N. S., and Berke, L., "Application of Optimality Criteria Approaches to Automated Design of Large Practical Structures," AGARD 2nd Symp. on Structural Optimization, No. 123, Milan, Italy, April 2-6, 1973; "Comparison of Optimality Criteria Algorithms for Minimum Weight Design of Structures," AIAA, J. 17, 1979; and Khot's paper on "Modern Structural Optimization," NATO Advanced Institute, Belgium, 1981.

92. Venkayya, V. B., "Structural Optimization: A Review and Some Recommendations," Intl. J. Num. Methods Eng., Vol. 13, 1978.

93. Walker, N. D. and Pister, K. S., Study of a Method of Feasible Directions for Optimal Elastic Design of Framed Structures Subjected to Earthquake Loading, Report EERC 75-39, University of California, Berkeley, Calif., 1975.

94. Whitman, R. V. et al., "Seismic Design Decision Analysis," J. Structural Div., ASCE, May, 1975, pp. 1067-1084.

APPENDICES

APPENDIX A

DERIVATION OF MEAN AND VARIANCE OF LNR OR LNS

If x and y are random variables, they have a relationship

$$x = \ln y \tag{A1}$$

and

$$dx/dy = 1/y \tag{A2}$$

For an one to one transformation, $f_y(y)dy = f_x(x)dx$, shown in Figure 153 it induces

$$f_y(y) = f_x(x)\frac{1}{y} \tag{A3}$$

where $f_x(x)$, and $f_y(y)$ are the probability density functions of x and y. Since x is normally distributed, $f_x(x)$ is

$$f_x(x) = \frac{1}{\sigma_x\sqrt{2\pi}} \exp\left[\frac{-1}{2}\left(\frac{x-\bar{x}}{\sigma_x}\right)^2\right] \tag{A4}$$

where $\bar{x}$ and σ_x are mean and standard deviation of x.

Substituting Equation (A4) into Equation (A3), it yields

$$f_y(y) = \frac{1}{y\sigma_x\sqrt{2\pi}} \exp\left[\frac{-1}{2}\left\{\frac{\ln y-\bar{x}}{\sigma_x}\right\}^2\right] \tag{A5}$$

Since

$$0.5 = P[y \le \hat{y}] = P[\ln y \le \ln \hat{y}] = P[x \le \ln \hat{y}] = F_x(\ln \hat{y}) = F_x(\hat{x}) \tag{A6}$$

where F ( ) = cumulative distribution function, $\hat{x}, \hat{y}$ = medians of x and y.

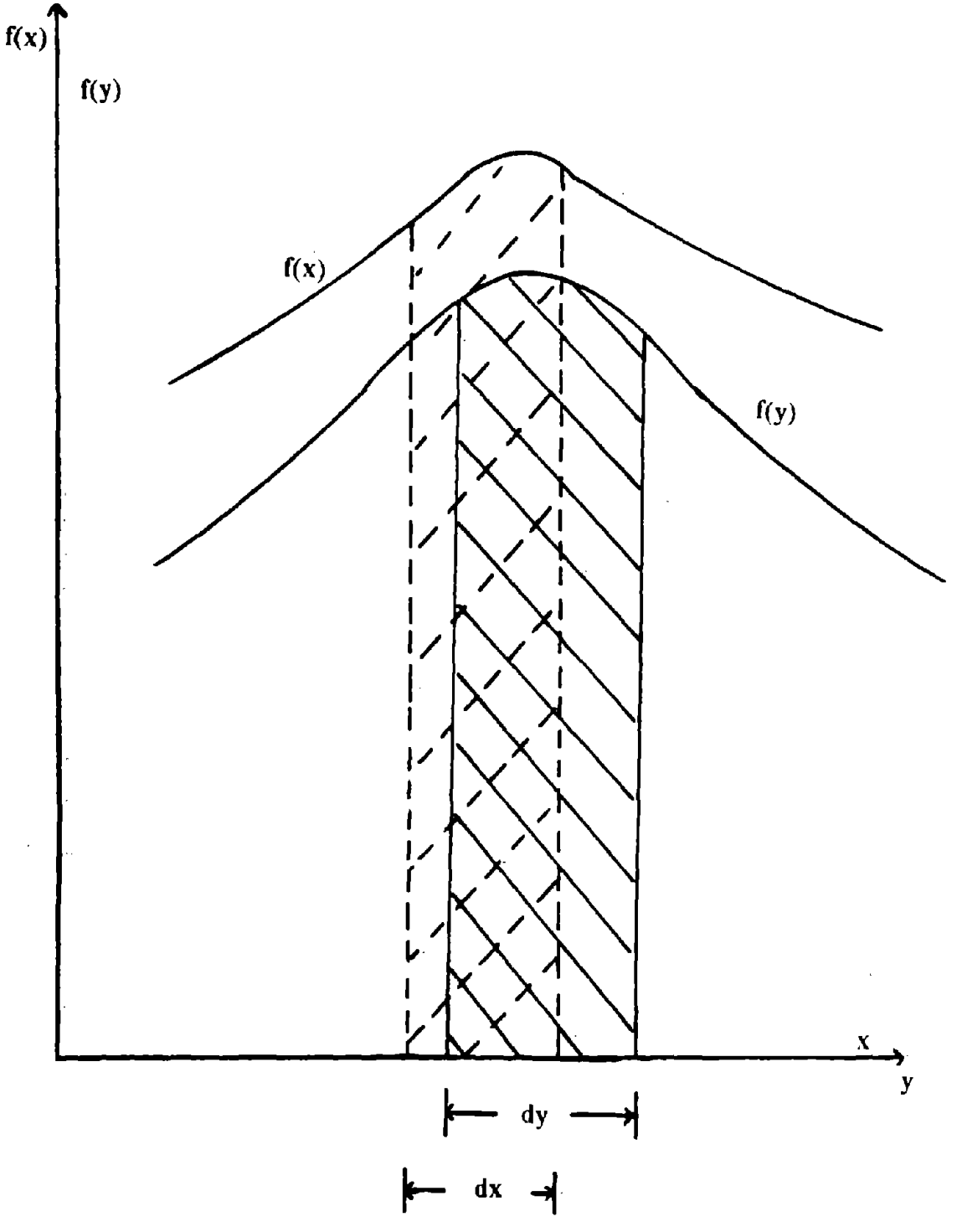

Figure 153. The Equal Area of f(x)dx and f(y)dy.

Since normal distribution is a symmetrical distribution, it resulta

$$0.5 = F_x(\hat{x}) = F_x(\bar{x}) \tag{A7}$$

Thus,

$$\ln \hat{y} = \bar{x} \tag{A8}$$

Substituting Equation (A5) into the following equation, it yields

$$E[y^r] = \int_0^\infty y^r f_r(y)dy = (\hat{y})^r \exp(\frac{1}{2}r^2\sigma^2_{\ln y}) \tag{A9}$$

The 1st and 2nd moment can be determined to be

$$\bar{y} = E[y] = \hat{y} \exp(\frac{1}{2}\sigma^2_{\ln y}) \tag{A10}$$

and $$\sigma^2_y = E[y^2] - \bar{y}^2 = \hat{y}^2 \exp(2\sigma^2_{\ln y}) - \hat{y}^2 \exp(\sigma^2_{\ln y})$$

$$= \hat{y}^2 \exp(\sigma^2_{\ln y})(\exp(\sigma^2_{\ln y}) - 1) = \bar{y}^2(\exp(\sigma_{\ln} y^2) - 1) \tag{A11}$$

Thus,

$$V^2_y = \frac{\sigma^2_y}{\bar{y}^2} = \exp(\sigma^2_{\ln y}) - 1 \tag{A12}$$

Therefore;

$$x \quad \overline{\ln y} \quad \ln \hat{y} \quad \ln[y \exp(\quad \sigma^2_{\ln y}/2)] \quad \ln y \; - 1/2\sigma^2_{\ln y} \tag{A13}$$

$$\sigma^2_{\ln y} = \ln(1 + V^2_y) \tag{A14}$$

If y = R or S, Equations (A13) and (A14) become Equations (2.10) or (2.11).

APPENDIX B

AN EXPECTED CROSSING RATE

An expected crossing rate $\nu_{\tilde{a}}^{+}$ is an expected frequency of crossing the level $s = \tilde{a}$ with positive slope. In what follows, the determination of this rate will be described.

In a geometry sketch shown in Figure 154, a point of a sample function at $t = t1$ will cross the given bound, $s = \tilde{a}$, during a very small time interval, dt, which is so small that the sample can be treated as a straight line in this interval. In order to cross the bound, the slope, $\dot{s}$, should have postive values such as curves (a) and (b). At $t = t1$ the curve (c) does not have chance to cross the given bound during dt since its slope is negative. Thus the combination of s, which is less than and equals to $\tilde{a}$, and $\dot{s}$, which has positive value, decides the process at $t = t1$ will cross the bound. The shaded area between the cureves $s = \tilde{a}$ and $\dot{s} = (\tilde{a} - s)/dt$ in Figure 155 are the combinations of s and $\dot{s}$ that result the crossing of the given bound.

Not only considering the combinations of s and $\dot{s}$ we also need to determine the probability of these combinations occured. This probability can be described by a joint probability of s and $\dot{s}$, $P_d(s, \dot{s})ds d\dot{s}$ which is the probability having s values between s and $s + ds$ and having $\dot{s}$ values between $\dot{s}$ and $\dot{s} + d\dot{s}$. Thus, the expected number of crossings of $s = \tilde{a}$ during dt is the cumulative probability distribution of combinations of s and $\dot{s}$ which result the crossings. That is

$$\int_0^{\infty} d\dot{s} \int_{\tilde{a} - \dot{s}dt}^{\tilde{a}} P_d(s, \dot{s}) ds$$

where the integration limits have been chosen to cover the shaded area in Figure 155.

Therefore, the value of $\nu_{\tilde{a}}^{+}$ which is expected number of crossings per unit time can be obtained to be

$$\nu_{\tilde{a}}^{+} = \frac{1}{dt} \int_0^{\infty} d\dot{s} \int_{\tilde{a} - \dot{s}dt}^{\tilde{a}} P_d(s, \dot{s}) ds$$

Finally letting $dt \to 0$, the desired expected crossing rate becomes

$$\nu_{\tilde{a}}^{+} = \int_0^{\infty} \dot{s} P_d(\tilde{a}, \dot{s}) d\dot{s}$$

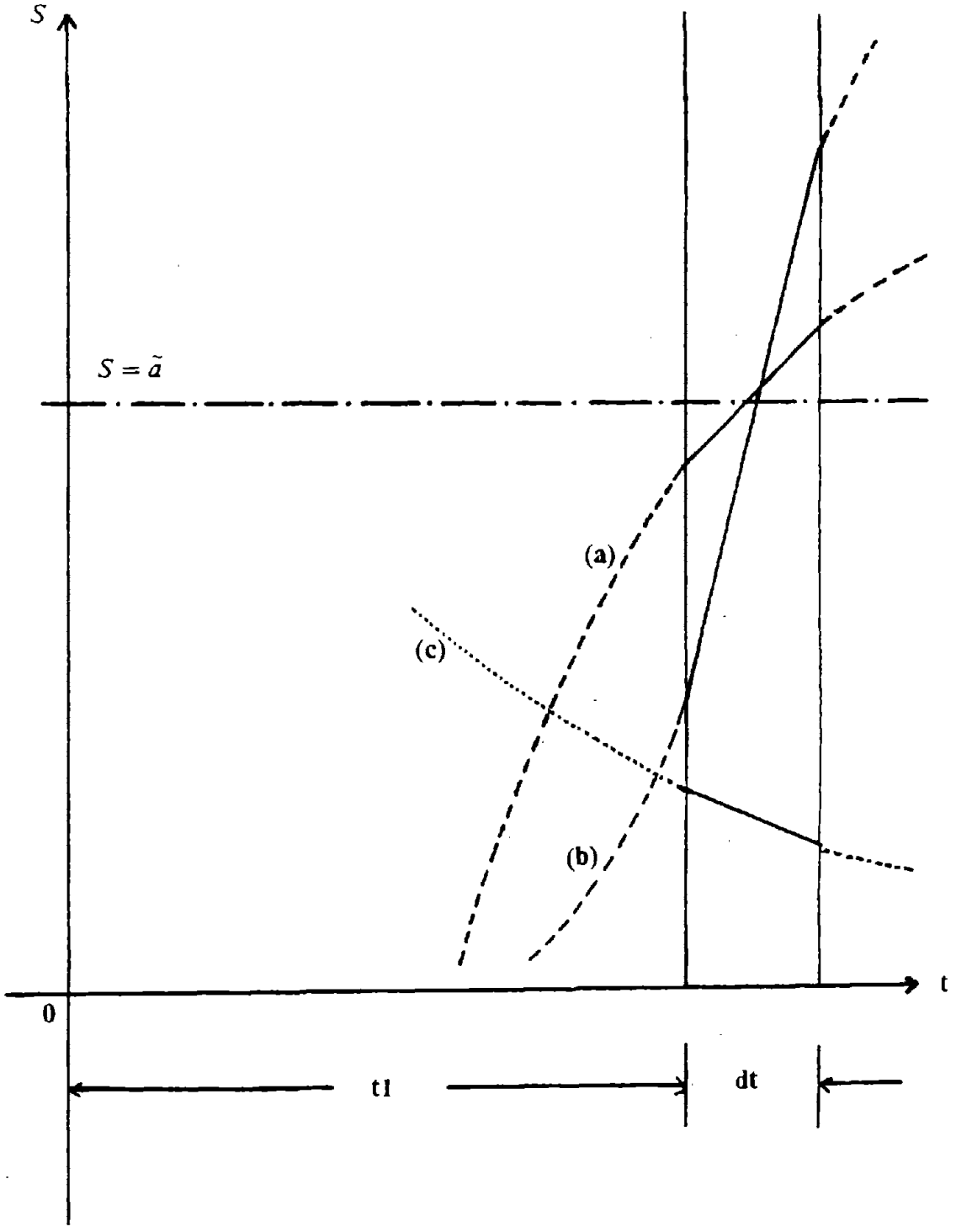

Figure 154. Sample Functions Cross s = $\tilde{a}$ During the Interval dt.

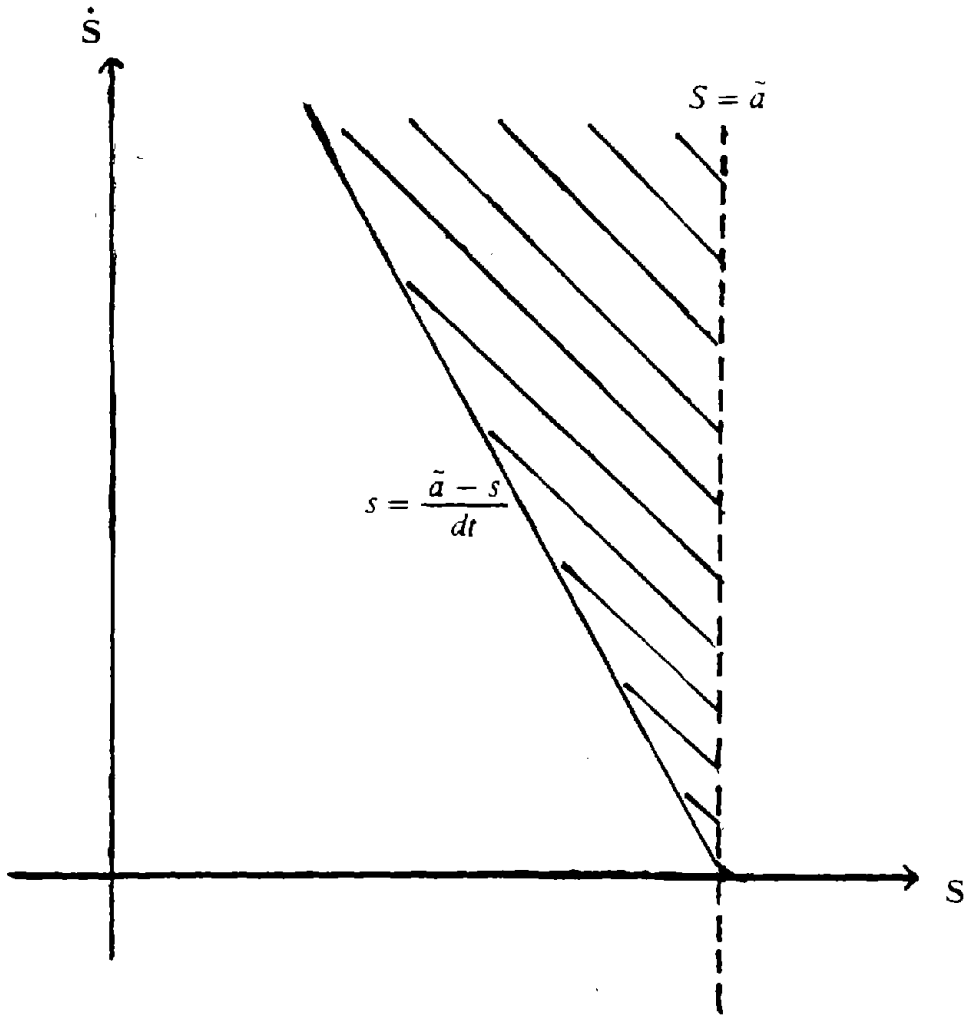

Figure 155. The Combinations of s and ṡ Which Cross the Specified Bound s = ã.

APPENDIX C

EQUIVALENT UNIFORM DISTRIBUTED LOAD

To derive an equivalent uniform distributed load (EUDL), an influence surface coefficient is needed. An influence surface coefficient is two-dimension extension of the principle of influence line. The ordinate I (x,y) of an influence surface at any point (x,y) is the influence on some desired load effect due to a unit load at (x,y). An influence surfaces may be constructed by multiplying appropriate influence lines.

For example, a desired load effect is an axial load on a typical interior column (one story). From the principle of influence line, this axial load will be determined by assuming a unit displacement at one corner of a panel. In Figure 156 a panel subjected to a unit displacement at one corner will be the product of two influence lines in X and Y axes. The determination of this influence surface is as follows.

Assuming a deflection curve in X axis is $U_z = a + bx + cx^2 + dx^3$, the deflection in terms of nondimensional variable, $x' = x / \ell$ is solved by substituting boundary conditions $U_z = 0, U_z = 0$ at $x' = 0$, and $U_z = 1, U_z = 0$ at $x' = 1$. Therefore the influence line along x axis has the form:

$$U_z = 3x'^2 - 2x'^3 , \qquad 0 \le x' \le 1$$

In a similar manner, the influence line along Y axis which has the same boundary conditions is

$$U_z = 3y'^2 - 2y'^3 , \qquad 0 \le y' \le 1$$

where $y' = y/\ell$. Thus, the influence surface I (x,y) is approximately the product of the influence lines in X and Y axes.

$$I(x', y') = (3x'^2 - 2x'^3)(3y'^2 - 2y'^3) , \qquad 0 \le x' \le 1 \text{ and } 0 \le y' \le 1$$

In the design, the maximum EUDL shown in Figure 157 is our concern. The statistics of this maximum EUDL can be assumed to be

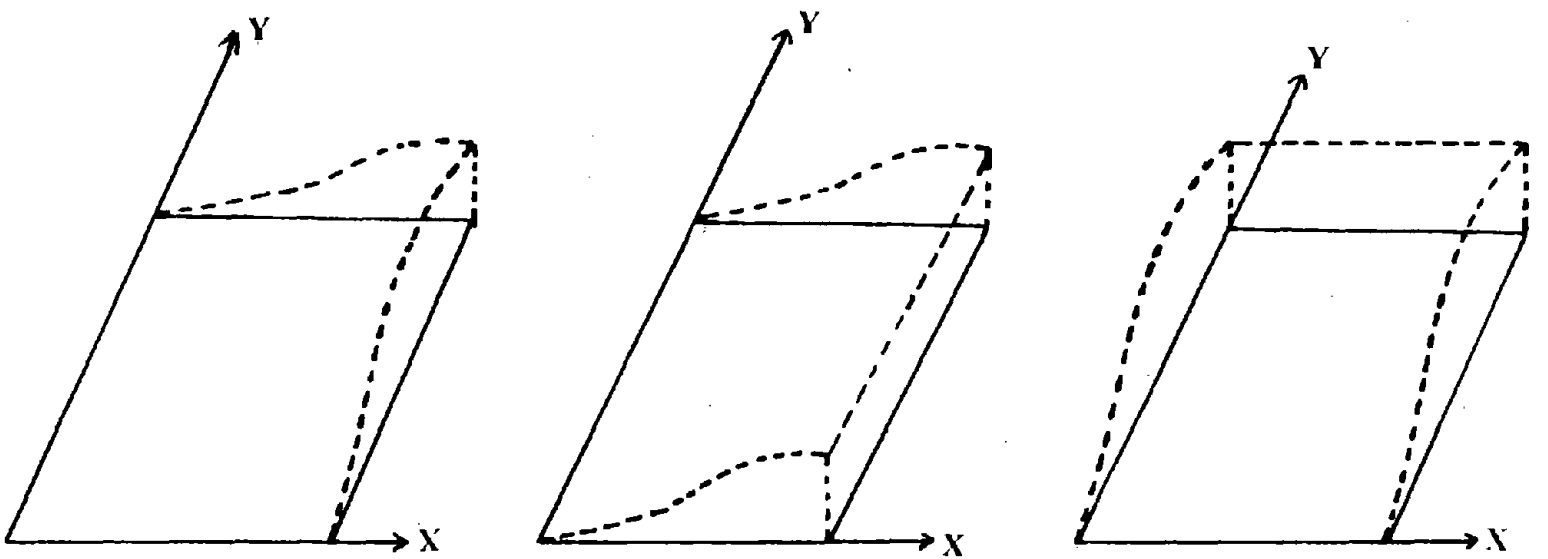

Figure 156. Panal Subjected to a Unit Displacement at One Corner.

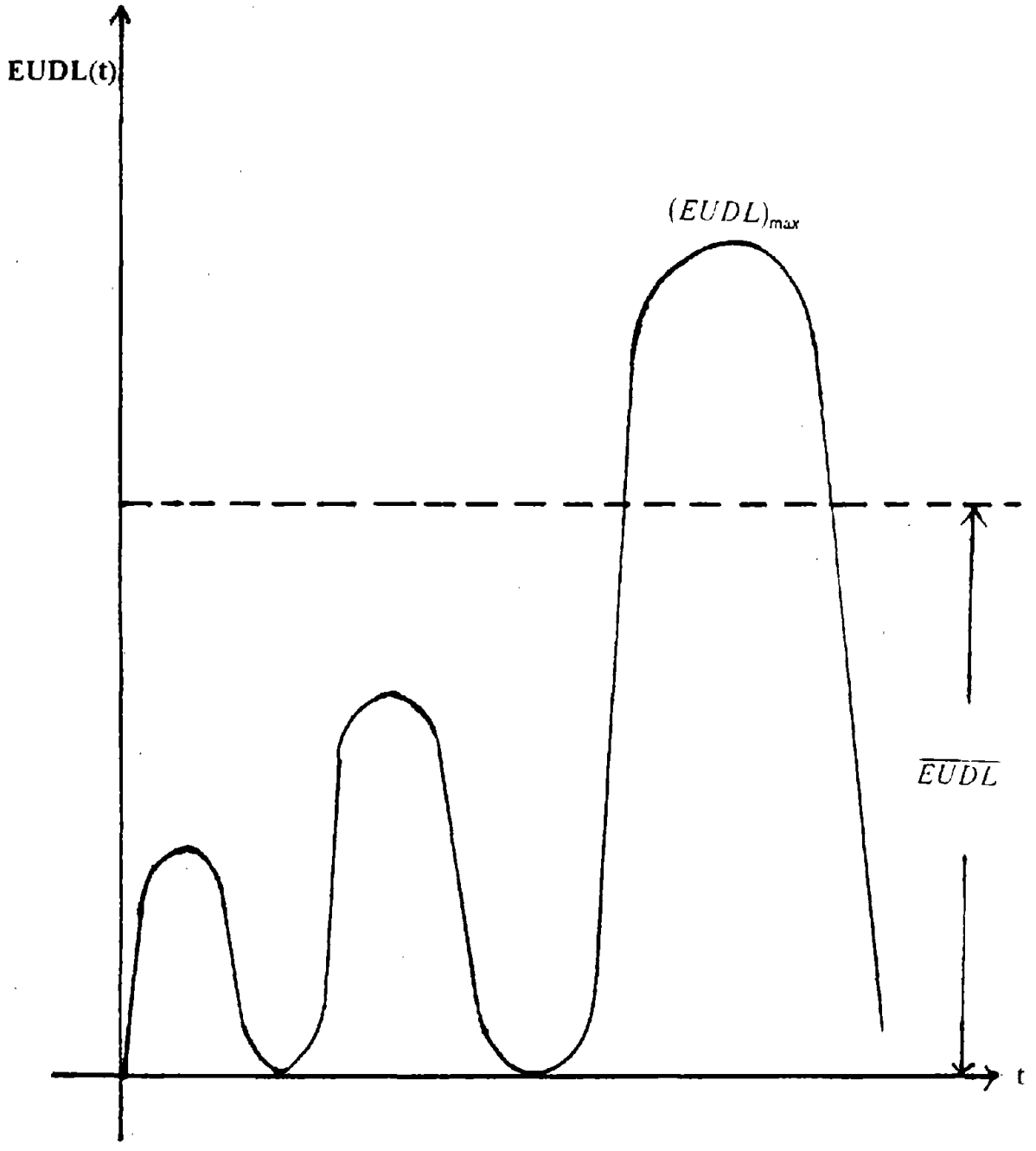

Figure 157. The Time History of EUDL.

$$(\overline{EUDL})_{max} = \overline{EUDL} + r_1(\sigma^2_{EUDL})^{1/2} \quad (C1)$$

and

$$\sigma^2_{(EUDL)_{max}} = r_2\sigma^2_{EUDL} \quad (C2)$$

where $\overline{EUDL}$, σ_{EUDL} = mean and variance of EUDL; r_1, r_2 are constants.

Substituting Equations (3.4) and (3.5) into Equations (C1) and (C2). They become

$$(\overline{EUDL})_{max} = \overline{L}_y + r_1(\sigma_r^2 + \frac{\sigma_t^2}{A_I}K_L)^{1/2} = C_1 + \frac{C_2}{A_I^{1/2}} \quad (C3)$$

and

$$\sigma^2_{EUDL} = r_2(\sigma_r^2 + \frac{\sigma_t^2}{A_I}K_L) = C_3 + \frac{C_4}{A_I} \quad (C4)$$

where C_1, C_2, C_3, C_4 are constants which can be determined from live load survey. Equation (C4) is corresponding to Equation (3.5).

APPENDIX D

A PROBABILITY DISTRIBUTION OF PEAK ACCELERATION

To determine the mean and variance of maximum peak ground acceleration, the probability distribution of this accelaration has to be known. In 1968 Cornell showed that this probability distribution is a type II extreme distribution. In what follows his derivation will be described.

Since the energy, E, released by earthquake has the relationship $\log_{10}E = a_0 + b_0 M$ which was proposed by Ritcher, some researchers such as Kanai, Esteva, and Rosenblueth, suggested the following relationship among peak ground acceleration (A), magnitude (M), and focal distance (R) is determined to be

$$A = b1e^{b2M}R^{-b3} \tag{D1}$$

where b1, b2, b3 are constants which are obtained from field data. Esteva and Rosenblueth used b1 = 2000, b2 = 0.8, and b3 = 2 with unit of A (cm/sec^2) and R (kilometers) to represent southern California condition as shown in Figure 158.

The formulation of Equation (D1) may be explained as follows: since E = mass (m) acceleration (A) distance (R) = $a_0 + b_0 M$, then $m\ A\ R = e^{a_0 \ln 10} + e^{M b_0 \ln 10}$. Consequently, A is exponentially proportional to M but inversely proportional to R.

From Equation (D1), the alternative relationship is

$$M = \frac{-\ln b1}{b2} + \frac{b3}{b2}\ln R + \frac{\ln A}{b2} \tag{D2}$$

The conditional probability of lnA of actual A which is greater than any number lna of allowable peak ground acceleration at focal distance R = r is

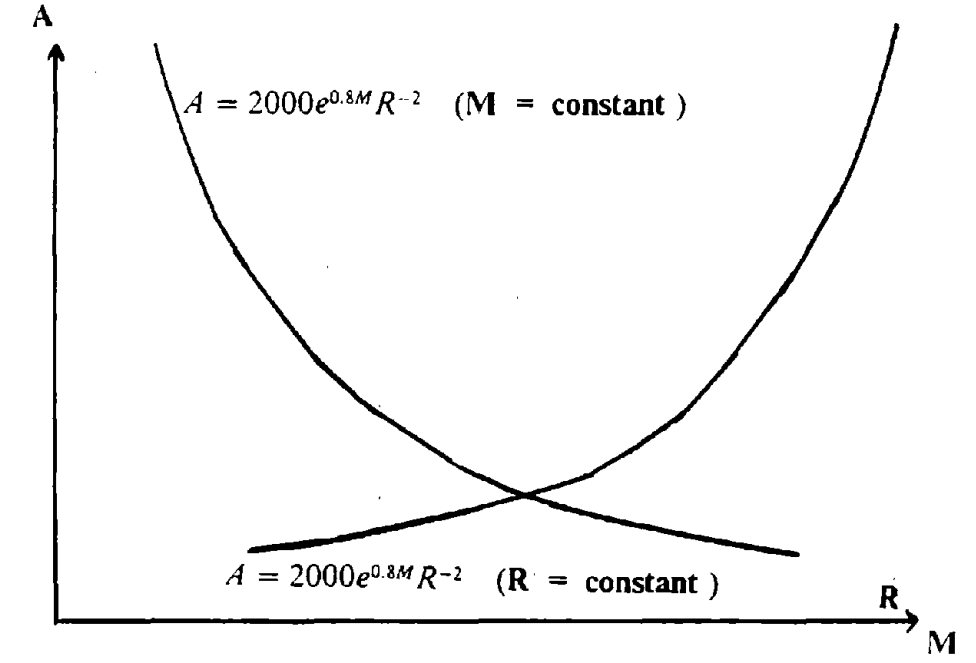

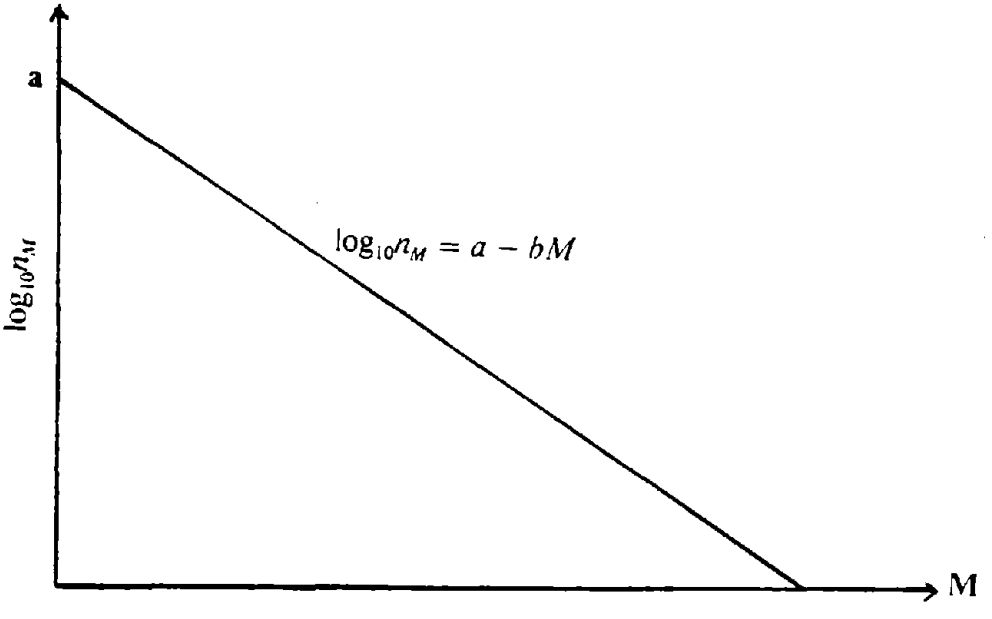

Figure 158. The Relationship of A and M, A and R, n and M.

$$P[\ln A \geq \ln a | R = r] = P[M \geq \frac{\ln a + b3 \ln r - \ln b1}{b2}]$$

$$= 1 - F(\frac{\ln a + b3 \ln r - \ln b1}{b2}) \qquad (D3)$$

where F(M) = the cumulative probability distribution function of M.

Since Ritcher also suggested the following relationship which is shown in Figure 158

$$\log_{10} n_M = a - b\ M \qquad (D4)$$

where n_M = frequency of earthquake, a and b are constants obtained from field data, the frequency of earthquake can be expressed to be the form

$$n_M = \exp[a \ln 10 - b \ln 10\ M] = \exp[-b \ln 10\ (M - \frac{a}{b})] \qquad (D5)$$

Thus 1-F(M) is computed as

$$1 - F(M) = e^{-\beta(M - M_0)} \qquad (D6)$$

where $\beta = b \ln 10$ and M_0 is the smallest magnitude will be considered for the design.

Therefore, from Equation (D3)

$$P[\ln A \geq \ln a | R = r] = \exp\ [-\beta\ (\frac{\ln a + b3 \ln r - \ln b1}{b2} - M_0\ )] \qquad (D7)$$

Based on Equation (D7) and Figure 159 the cumulative distribution of lnA for the distance of site to central point of line fault source (d) and to the farthest point of line fault source (r_0) yields

$$1 - F_{\ln A}(\ln a) = P[\ln A \geq \ln a] = \int_d^{r_0} P[\ln A \geq \ln a | R = r]\ f_R(r) dr \qquad (D8)$$

where $f_R(r)$ is the probability density function of R. The cumulative distribution of focal distance R is

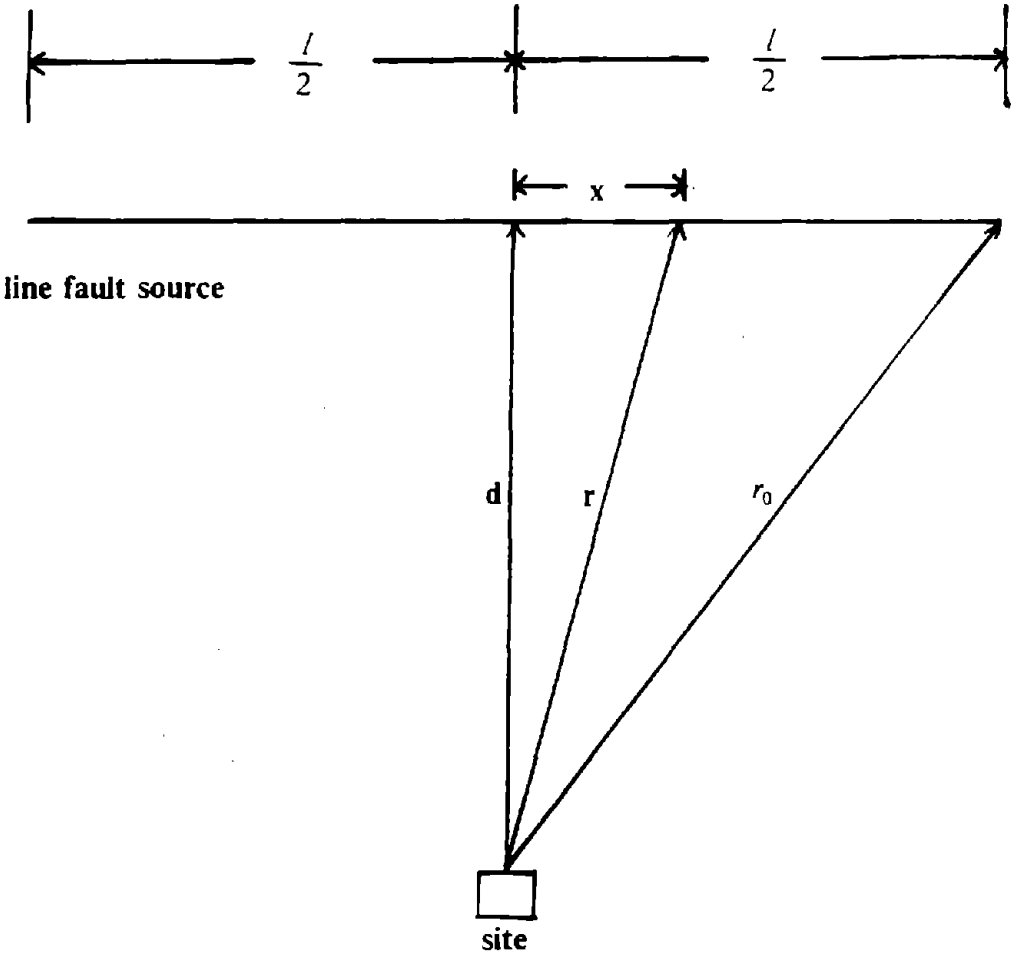

Figure 159. The Configuration of Site and Line Earthquake Source.

$$F_R(r) = P[R \le r] = P[R^2 \le r^2]$$
$$= P[X^2 + d^2 \le r^2] = P[|X| \le \sqrt{r^2 - d^2}\,]$$

Since the cumulative distribution is the probability of focal length from 0 to $\sqrt{r^2 - d^2}$ in half length of line source ($\ell/2$), then

$$F_R(r) = \frac{2\sqrt{r^2 - d^2}}{\ell}, \qquad d \le r \le r_0 \tag{D9}$$

the probability density function of R is

$$f_R(r) = \frac{dF_R(r)}{dr} = \frac{2\,r}{\ell\sqrt{r^2 - d^2}} \qquad d \le r \le r_0 \tag{D10}$$

Substituting Equation (D10) into Equation (D8), its integration is very complicated. However, in the region of greatest interest, namely larger values of lna the results is [36]

$$1 - F_{\ln A}(\ln a) = \frac{1}{\ell} C\,G\,\exp[-\frac{\beta}{b2}\ln a] \tag{D11}$$

where C = a constant = $\exp[\beta(\frac{b1}{b2}) + m_0]$,

G = a constant = $\frac{2\pi}{(2d)^{r1}} \frac{\Gamma(r1)}{[\Gamma(\frac{r1+1}{2})]^2}$,

$r1 = \beta\frac{b3}{b2} - 1.$

$\Gamma(\ )$ = Gamma function

Equation (D11) is also the probability of earthquake event in which A is larger than a. This probability can be substituted into the following equation to determine a probability distribution of random number, N, of this earthquake event which is assumed to be a Poisson process in a time interval of length t years with average occurence rate of ν per year.

$$P_N(n) = P[N = n] = \frac{e^{-P_i \nu t}\,(P_i \nu t)^n}{n!}, \qquad n = 0, 1, 2, 3, \ldots\ldots \tag{D12}$$

where $P_i = 1 - F_A(a)$

If the zero number of an earthquake event which is less than an allowable value, the probability becomes

$$F_A(a) = P[N=0] = \exp[-\tilde{\nu} C G t a^{-\beta/b2}] \tag{D13.}$$

where $\tilde{\nu} = \nu/\ell$

Comparing Equation (D13) with a type II distribution

$$F_A(a) = e^{-(\frac{a}{u1})^{-K1}} \tag{D14}$$

the coefficients of u1 and K1 will be determined to be

$$u1 = (\tilde{\nu} CGt)^{b2/\beta} \tag{D15}$$

$$K1 = \frac{\beta}{b2} \tag{D16}$$

which are used in Equation (3.17)

APPENDIX E

A WHITE NOISE PROCESS

Considering a periodic function f(t) of period T, it can be respresented as a superposition of sinusoids in the following exponent Fourier series

$$f(t) = \sum_{-\infty}^{\infty} C_n \exp(i n \omega_0 t) \tag{E1}$$

where $\omega_0 = 2\pi/T$ is the fundamental frequency. The coefficients C_n can be evaluated directly from the relation

$$C_n = \frac{1}{T}\int_{-T/2}^{T/2} f(t) \exp(-i n \omega_0 t)dt \tag{E2}$$

If f(t) is considered to be a nonperiodic function from $t = -\infty$ to ∞, Equations (E1) and (E2) become the following relations which are called Fourier integral.

$$f(t) = \int_{-\infty}^{\infty} F(\omega) \exp(i \omega t)d\omega \tag{E3}$$

and

$$F(\omega) = \frac{1}{2\pi}\int_{-\infty}^{\infty} f(t) \exp(-i \omega t)dt \tag{E4}$$

To illustrate, considering the rectangular pulse function f(t) shown in Figure 160, it yields

$$F(\omega) = \frac{1}{2\pi}\int_{-T/2}^{T/2} A \exp(-i \omega t)dt = \frac{A}{\pi\omega} \sin\frac{\omega T}{2} \tag{E5}$$

where the function is sketched in Figure 160.

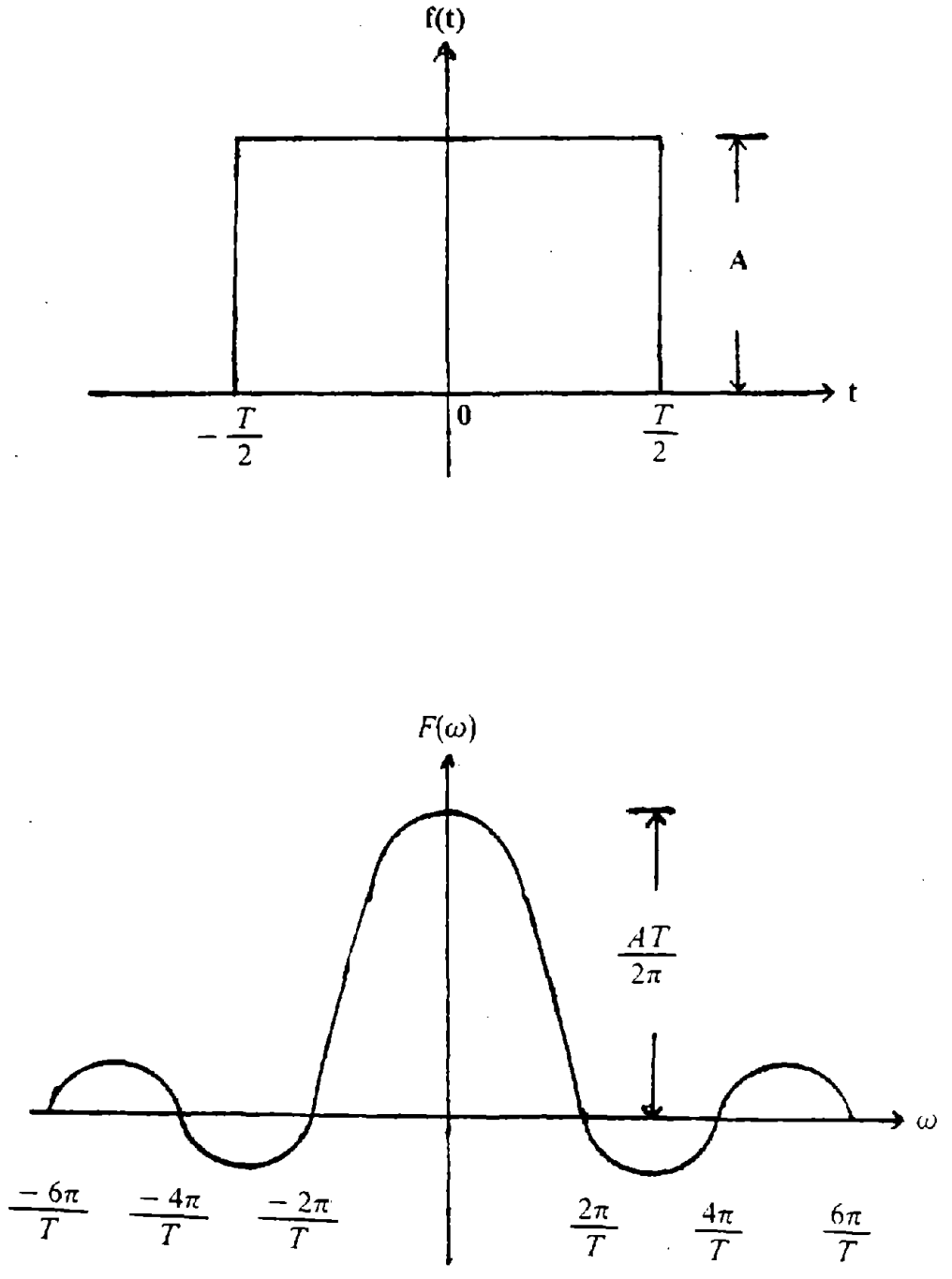

Figure 160. Rectangular Pulse Function and Its Spectral Fourier Transform.

If a random process s(t) is considered, the previous relations for autocorrelations of this process which is also a nonperiodic function become

$$E[s(t)\ s(t+\tau)] = R(\tau) = \int_{-\infty}^{\infty} G(\omega)\ \exp(i\,\omega\,t)d\omega \tag{E6}$$

and

$$G(\omega) = \frac{1}{2\pi}\int_{(-)}^{\infty} R(\tau)\ \exp(-i\,\omega\,\tau)d\tau \tag{E7}$$

where τ = a time difference and $G(\omega)$ is called a spectral density function.

For a special case where $\tau = 0$,Equations (E6) and (E7) become

$$R(0) = \int_{-\infty}^{\infty} G(\omega)d\omega \tag{E8}$$

and

$$G(\omega) = \frac{1}{2\pi}\int_{-\infty}^{\infty} R(0)\ d\tau \tag{E9}$$

Therefore each stationary process has a corresponding spectral density function to describe it. The process with an uniform spectral density value G_0 shown in Figure 161(a) is called a white noise process in analogy with white light which has the constant uniform spectrum. The white noise process will result the autocorrelation becomes

$$R_s(\tau) = 2\pi G_0\delta(\tau) \tag{E10}$$

where $\delta(\tau)$ is a Dirac delta function which has unit area concentrated at $\tau = 0$ and zero values for $\tau \neq 0$. The zero correlation of s(t) and $s(t+\tau)$, $R_s(\tau)$, for $\tau \neq 0$ results that the process has random behavior. A sample function of this random process is shown in Figure 161(b).

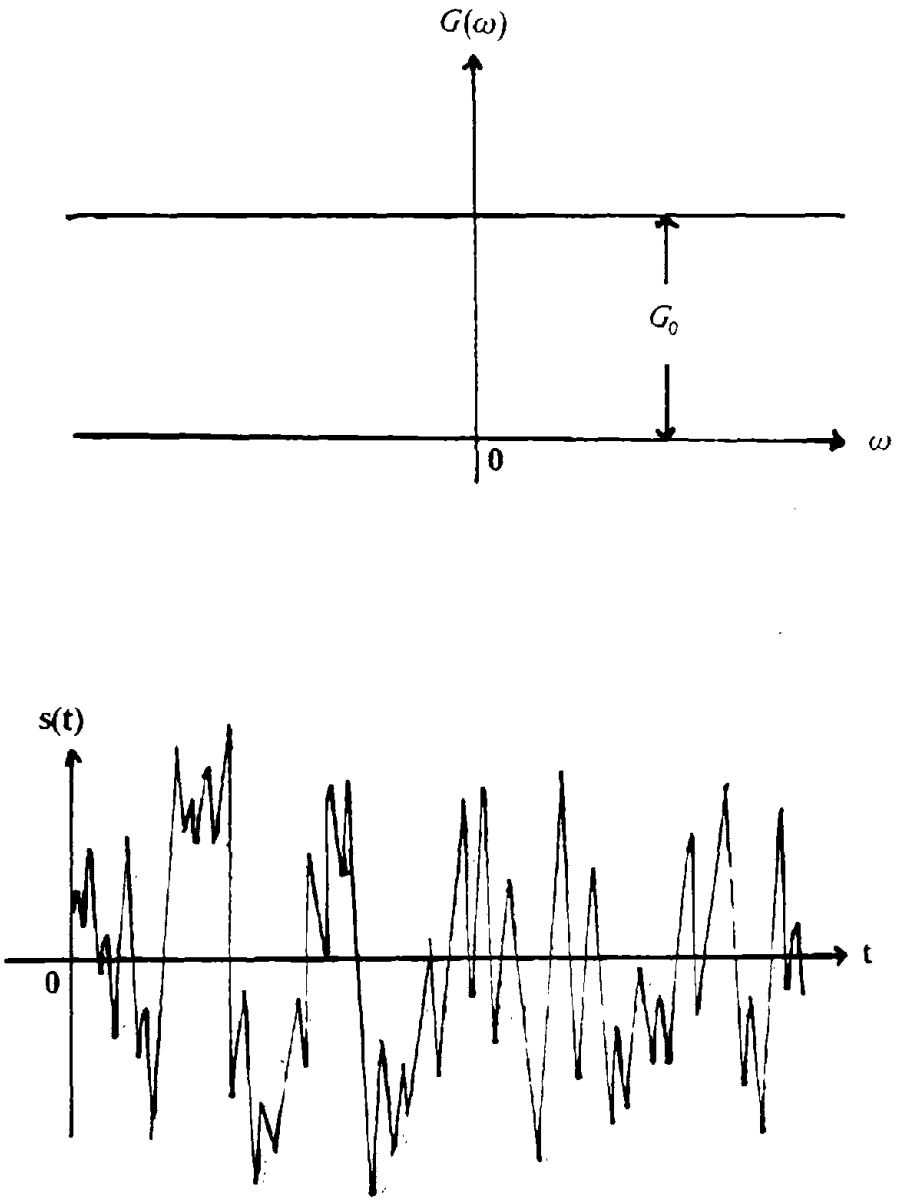

Figure 161. The Spectral Density Function and Time History of a Sample Function for a White Noise Process.

APPENDIX F

MOMENTS OF FILTER WHITE NOISE PROCESS

$$\lambda_{s0} = \frac{\pi G_0}{2\zeta\omega_n^3}\frac{A}{F} + \frac{\pi G_0}{2\zeta_g\omega_g^3}\frac{B}{F} \tag{F1}$$

$$\lambda_{s1} = \frac{\pi G_0}{2\zeta\omega_n^2}\frac{1 - 2/\pi \tan^{-1}(\zeta/\sqrt{1-\zeta^2})}{\sqrt{1-\zeta^2}}\frac{A'}{F} + \frac{\pi G_0}{2\zeta\omega_g^2}\frac{1 - 2/\pi \tan^{-1}(\zeta_g/\sqrt{1-\zeta_g^2})}{\sqrt{1-\zeta_g^2}}\frac{C}{F} - \frac{2G_0}{\omega_g^2}\frac{D}{F}\ln r \tag{F2}$$

$$\lambda_{s2} = \frac{\pi G_0}{2\zeta\omega_n}\frac{A''}{F} + \frac{\pi G_0}{2\zeta_g\omega_g}\frac{E}{F} \tag{F3}$$

where $r = \omega_0/\omega_g$; $A = A_0 + 4\zeta^2 r^2 [2 - 4\zeta_g^2 - (3 - 4\zeta^2) r^2 - 4\zeta_g^2 r^4]$; $A' = A_0 + 4\zeta^2 r^2 [1 - 4\zeta_g^2 - 2(1 - \zeta^2) r^2 - 2\zeta_g^2 r^4]$; $A'' = A_0 + 4\zeta^2 r^2 [-4\zeta_g^2 - r^2]$; $B = 1 - 8\zeta_g^2 - 2(1 - 2\zeta^2) r^2 + (1 + 4\zeta_g^2) r^4$; $C = 1 - 4\zeta_g^2 - 2(1 - 2\zeta^2 + 2\zeta_g^2 - 4\zeta^2\zeta_g^2) r^2 + (1 + 4\zeta_g^2 - 8\zeta_g^4) r^4$; $D = 1 - (1 - 2\zeta^2) r^2 - 2\zeta_g^2 r^4$; $E = 1 - 2(1 - 2\zeta^2 + 4\zeta_g^2 - 8\zeta^2\zeta_g^2) r^2 + (1 + 4\zeta_g^2 - 16\zeta_g^4) r^4$; $F = F_0 + 8\zeta^2 r^2 [1 - 2\zeta_g^2 - 2(1 - \zeta^2) r^2 + (1 - 2\zeta_g^2) r^4]$; $A_0 = 1 - 2(1 - 4\zeta_g^2) r^2 + (1 + 4\zeta_g^2) r^4$; and $F_0 = 1 - 4(1 - 2\zeta_g^2) r^2 + 2(3 - 8\zeta_g^2 + 8\zeta_g^4) r^4 - 4(1 - 2\zeta_g^2) r^6 + r^8$.

APPENDIX G

SUPPLIMENTS OF PENALTY FUNCTION METHOD

1. A simple illustration example

Assume a linear optimization problem formulated as

$$\text{min.,} \quad x_1 + x_2$$

$$\text{S.T.,} \quad g_1 = 3 - x_1 \le 0$$

$$g_2 = 2 - x_2 \le 0$$

For interior penalty function method, the penalty function is

$$P_p(x, r_p) = x_1 + x_2 + r_p\left(\frac{1}{3 - x_1} + \frac{1}{2 - x_2}\right)$$

As we know, the solution of $\partial P_p / \partial x_1 = 0, \partial P_p / \partial x_2 = 0$, will be the minimum solution of P_p. Therefor these two conditions yield

$$x_1 = 3 - r_p^{1/2} \quad \text{or} \quad 3 + r_p^{1/2}$$

and $$x_2 = 2 - r_p^{1/2} \quad \text{or} \quad 2 + r_p^{1/2}$$

The values $x_1 = 3 + r_p^{1/2}$ and $2 + r_p^{1/2}$ which are the feasible points are the desired solutions. As r_p approaches to zero value, the optimum solutions $x_1 = 3, x_2 = 2$ are obtained.

APPENDIX H

FLOWCHART OF PENALTY FUNCTION ALGORITHM

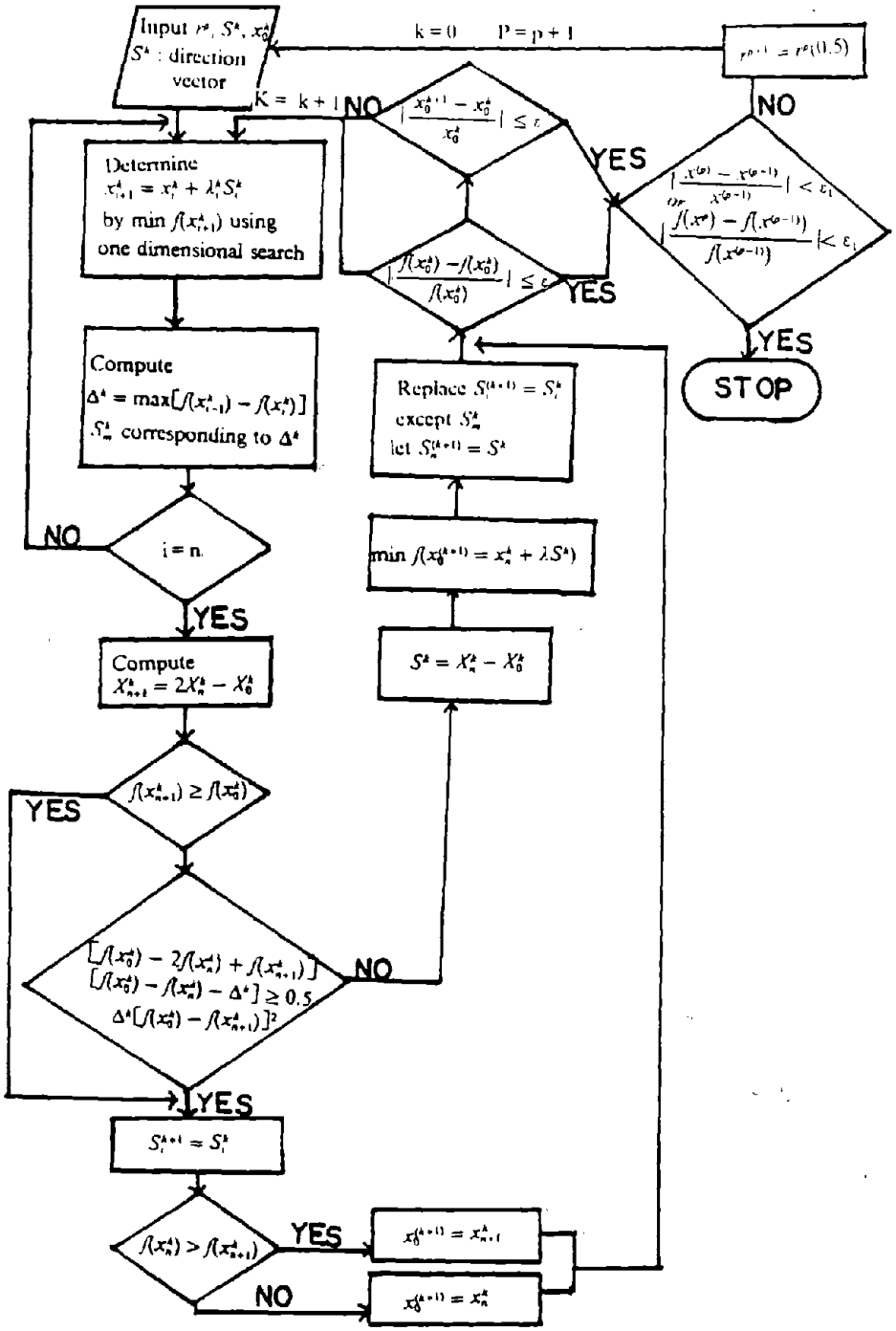

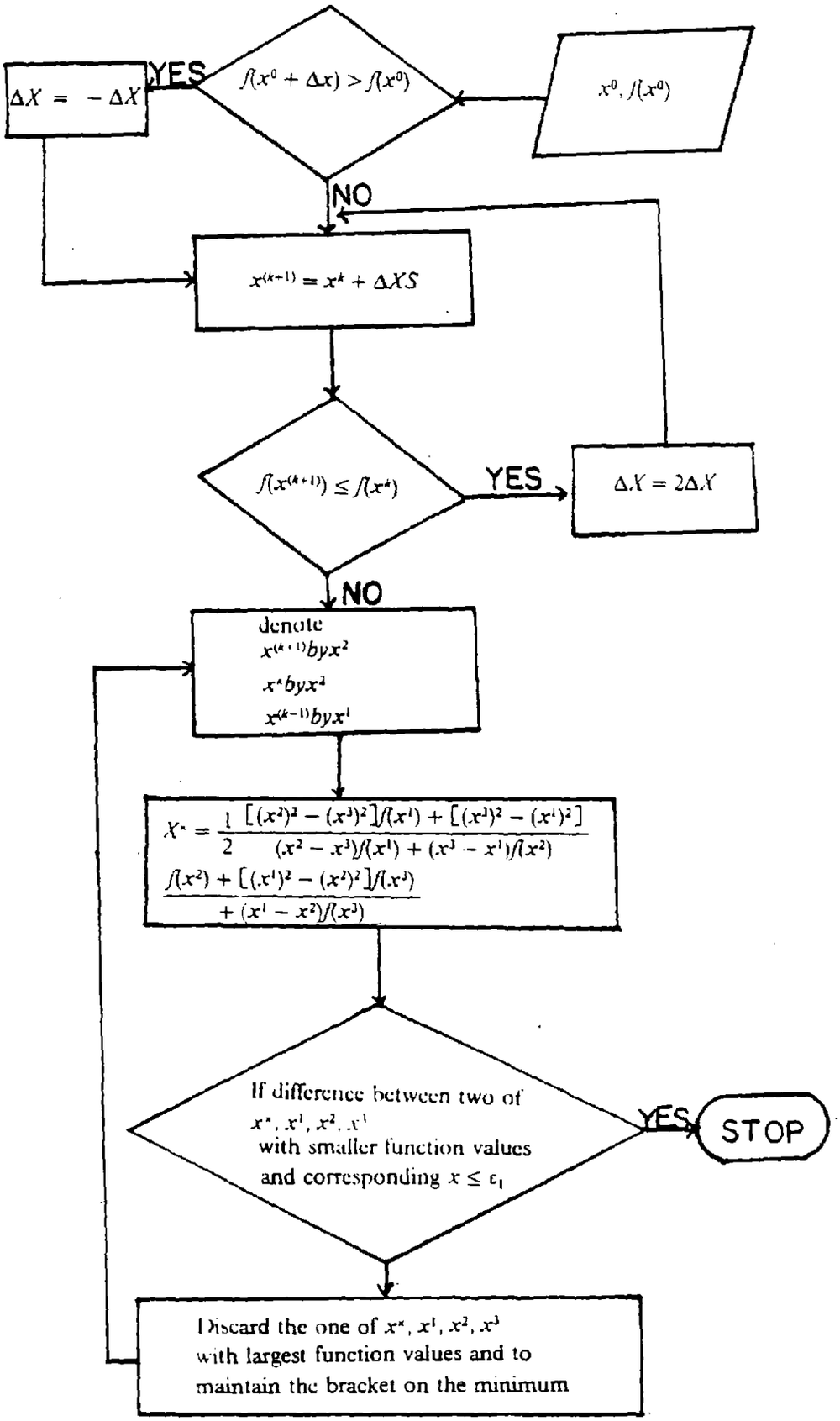
$x^0, f(x^0)$
$f(x^0 + \Delta x) > f(x^0)$
YES
$\Delta X = -\Delta X$
NO
$x^{(k+1)} = x^k + \Delta XS$
$f(x^{(k+1)}) \leq f(x^k)$
YES
$\Delta X = 2\Delta X$
NO
denote
$x^{(k+1)}$ by x^2
x^k by x^2
$x^{(k-1)}$ by x^1
$X^* = \frac{1}{2} \frac{[(x^2)^2 - (x^3)^2]f(x^1) + [(x^3)^2 - (x^1)^2]f(x^2) + [(x^1)^2 - (x^2)^2]f(x^3)}{(x^2 - x^3)f(x^1) + (x^3 - x^1)f(x^2) + (x^1 - x^2)f(x^3)}$
If difference between two of x^*, x^1, x^2, x^3 with smaller function values and corresponding $x \leq \varepsilon_1$
YES
STOP
Discard the one of x^*, x^1, x^2, x^3 with largest function values and to maintain the bracket on the minimum

APPENDIX I

FLOWCHART OF OPTIMALITY CRITERION ALGORITHM

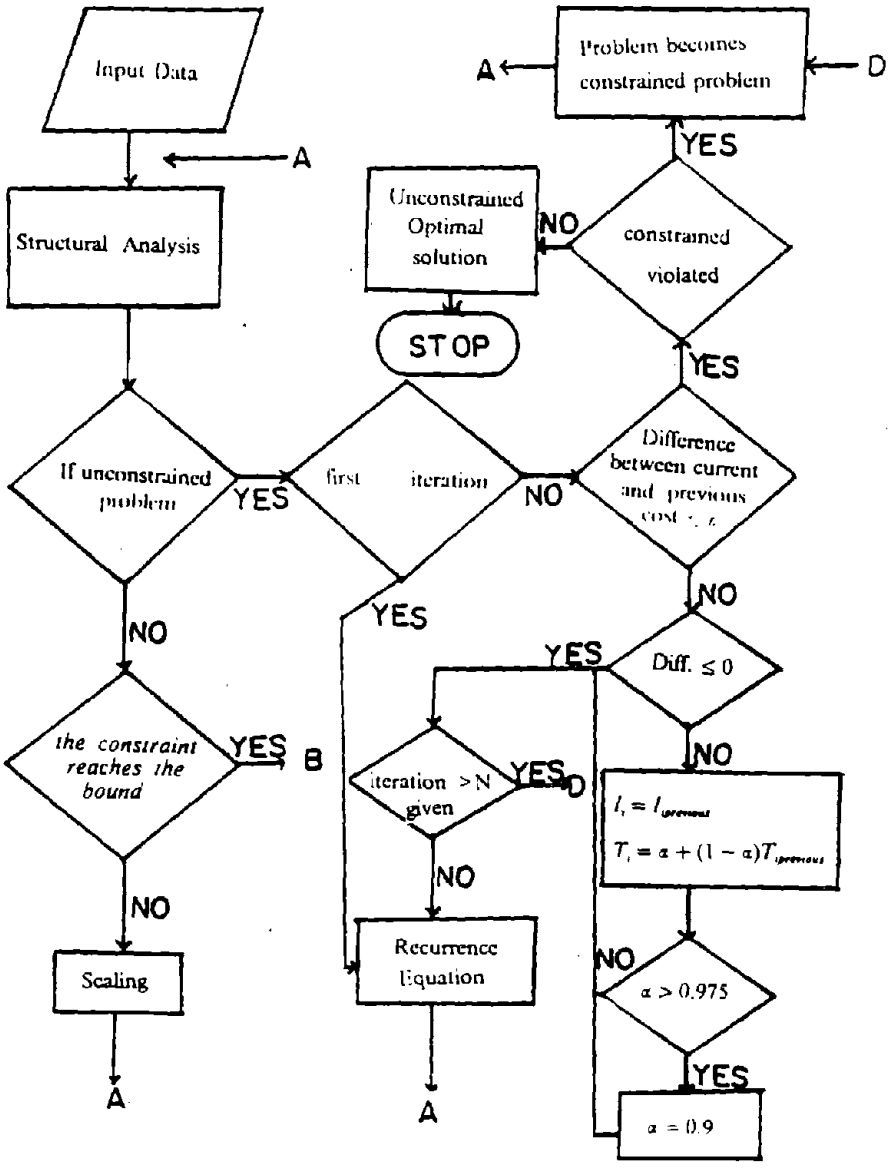

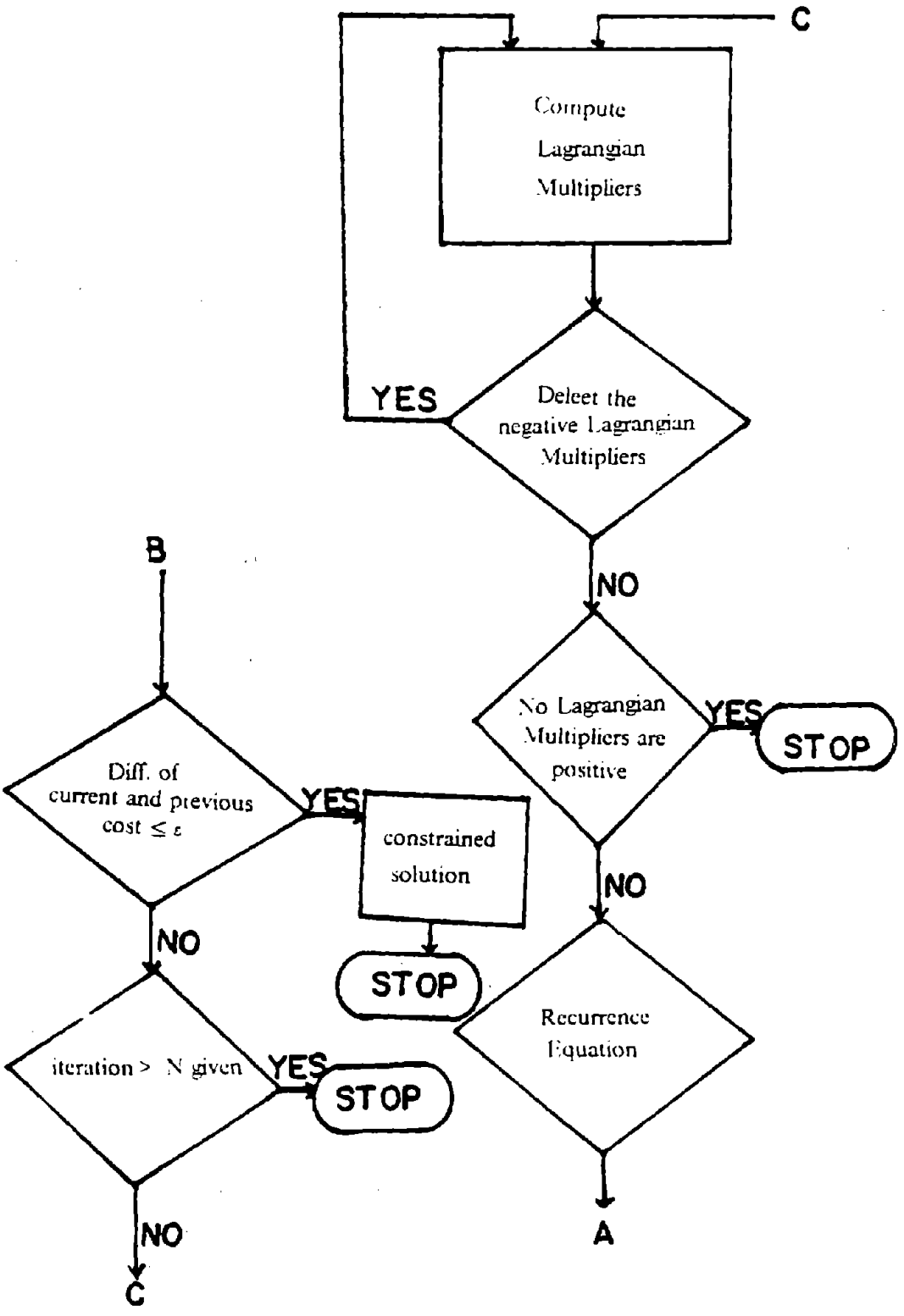
C
Compute
Lagrangian
Multipliers
YES
Deleet the
negative Lagrangian
Multipliers
NO
B
No Lagrangian
Multipliers are
positive
YES
STOP
NO
Diff. of
current and previous
cost ≤ ε
YES
constrained
solution
STOP
NO
Recurrence
Equation
iteration > N given
YES
STOP
NO
C
A